Universitat de Girona

[2+2+2] CYCLOADDITION REACTIONS INVOLVING ALLENES CATALYSED BY RHODIUM

Ewelina HARABURDA

Dipòsit legal: Gi. 2077-2015
http://hdl.handle.net/10803/328439

Universitat de Girona

DOCTORAL THESIS:

[2+2+2] Cycloaddition reactions involving allenes catalysed by rhodium

Ewelina Haraburda

2015

Universitat de Girona

Doctoral thesis:

[2+2+2] Cycloaddition reaction involving allenes catalysed by rhodium

Ewelina Haraburda

2015

Doctoral Programme in Chemistry

Supervised by: Anna Pla Quintana

Tutor: Anna Roglans Ribas

This manuscript has been presented to opt for the doctoral degree from the

University of Girona

Universitat de Girona

Dr Anna Pla-Quintana, of Universitat de Girona

I DECLARE:

That the thesis entitled “[2+2+2] Cycloaddition reaction involving allenes catalysed by rhodium”, presented by Ewelina Haraburda to obtain a doctoral degree, has been completed under my supervision.

For all intents and purposes, I hereby sign this document.

Dr Anna Pla-Quintana

Girona, 29/06/2015

Publications:

This doctoral thesis has resulted in the following publications:

- *Stereoselective rhodium- catalysed [2+2+2] cycloaddition of linear allene-ene/yne-allene substrates.* Haraburda, E.; Torres, Ò.; Parella, T.; Solà, M.; Pla-Quintana, A. *Chem. Eur. J.* **2014**, *20,* 5034.

- *Dehydrogenative [2+2+2] Cycloaddition of Cyano-yne-allene Substrates: Convienient Access to 2,6–Naphthyridine Scaffolds.* Haraburda, E.; Lledó, A.; Roglans, A.; Pla-Quintana, A. *Org. Lett*. **2015**, *17*, 2882.

Abbreviations

v (in IR):	Frequency (units: cm^{-1})
Ar:	Aryl
ATR (in IR):	Attenuated Total Refractance
Bn:	Benzyl
Boc:	*tert*-butyloxycarbonyl
Bu:	Butyl
CID:	Collision Induced Dissociation
cod:	1,5-cyclooctadiene
Cp:	Cyclopentadiene
DFT:	Density Functional Theory
DMF:	Dimethylformamide
EA:	Elemental Analysis
ee:	Enantiomeric excess
equiv.:	Equivalent
ESI-MS:	Electrospray Ionization-Mass Spectrometry
ESI-HRMS:	Electrospray Ionization-High Resolution Mass Spectrometry
Et:	Ethyl
et al.:	Collaborators
EtOH:	Ethanol
GC:	Gas Chromatography
h:	Hours
HPLC:	High Performance Liquid Chromatography

***i*Pr:**	*iso*-propyl
IR:	Infrared Spectroscopy
LC:	Liquid Chromatography
***m*-:**	*Meta*-
min.:	Minutes
***m/z*:**	Mass to charge ratio
m.p:	Melting point
Me:	Methyl
MeOH:	Metanol
Mes:	Mesityl or 2,4,6-trimethylphenyl
M.W.:	Molecular Weight
***o*-:**	*Orto*-
***p*-:**	*Para*-
Ph:	Phenyl
r.t.:	Room temperature
t:	time
T:	Temperature
***t*Bu:**	*tert*-butyl
TFA:	Trifluoroacetic acid
THF:	Tetrahydrofuran
TLC:	Thin Layer Chromatography
Ts:	Tosyl or 4-methylphenylsulfonyl
Tr:	Triphenylmethyl
Mes:	2, 4, 6 –trimethylphenyl
Tripp:	2, 4, 6 –tris(isopropyl)phenyl

Abbreviations used in Nuclear Magnetic Resonance (NMR)

δ:	Chemical shift (units: ppm)
^{13}C-NMR:	Nuclear magnetic resonance of carbon (13)
^{1}H-NMR:	Nuclear magnetic resonance of proton
^{31}P-NMR:	Nuclear magnetic resonance of phosphorous (31)
abs.:	Absorption
d:	Doublet
dd:	Double doblet
dt:	Double triplet
***J*:**	Coupling constant
m:	Multiplet
q:	Quadruplet
s:	Singlet
t:	Triplet

Graphical summary

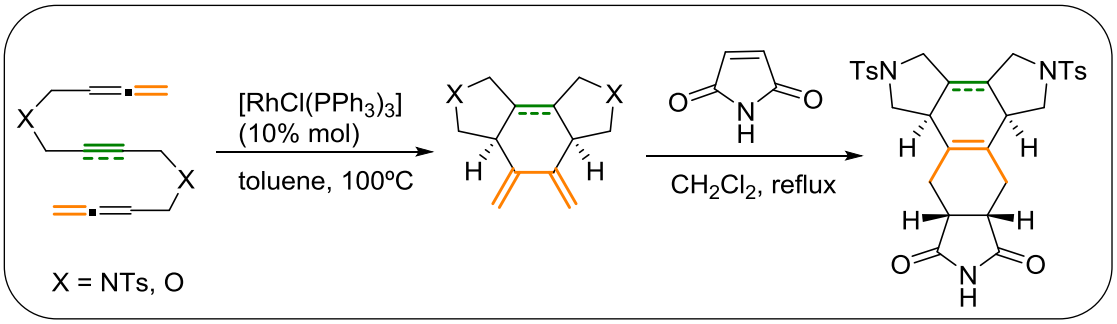

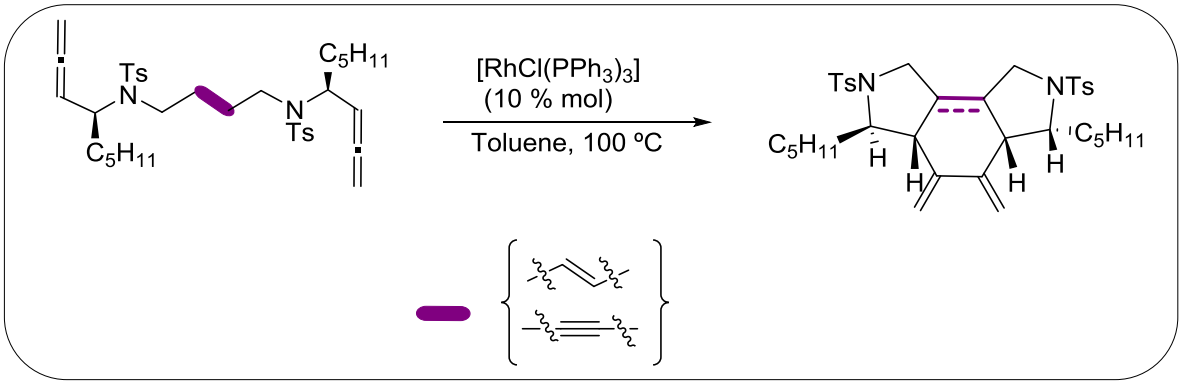

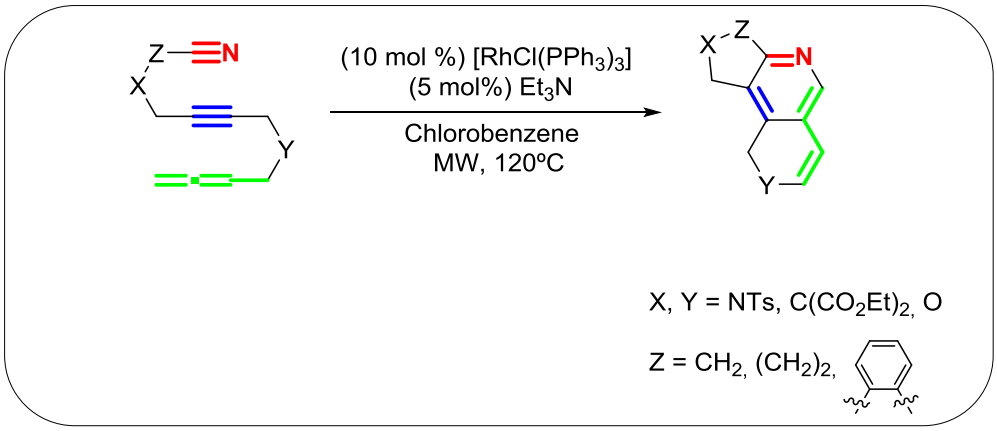

Supplementary data

The material listed below is attached as supplementary data on the CD included in the thesis:

- **Thesis:** Memory of the thesis in .pdf format.

- **Chapter 3**:

  C3_Spectra: selection of the ^{1}H NMR, ^{13}C NMR, IR and MS spectra of the products synthesised in pdf format.

- **Chapter 4**:

  C4_Spectra: selection of the ^{1}H NMR, ^{13}C NMR, IR and MS spectra of the products synthesised in pdf format.

  C4_HPLC: HPLC chromatograms HPLC of the products obtained with enantiomeric excess in pdf format.

- **Chapter 5**:

  C5_Spectra: selection of the ^{1}H NMR, ^{13}C NMR, IR and MS spectra of the products synthesised in pdf format.

Acknowledgements

This work would not have been possible without the following collaborations:

- Universitat de Girona for the PhD Grant BR-UdG-2012.
- AGAUR of Generalitat de Catalunya for financial support through the projects SGR2009-637 and 2014SGR-931.
- MINECO of Spain for financial support through the project CTQ2011-23121.
- Serveis Tècnics de Recerca from Univeritat de Girona for technical support.

List of figures

Chapter 1.

Chapter 3.

Chapter 4.

Chapter 5.

List of schemes

Chapter 1.

Chapter 3.

Chapter 4.

List of tables

Chapter 3.

Chapter 5.

Table of Contents

Summary

The development of new chemical processes for the formation of carbon-carbon bonds is an important topic in organic chemistry. In particular, the transition metal catalysed [2+2+2] cycloaddition reaction is a highly efficient synthetic tool that allows six-membered polysubstituted carbo- and heterocyclic derivatives to be obtained in an atom economy process. Allenes are versatile substrates for cycloaddition reactions that provide a good reactivity profile together with the ability to increase the stereochemical complexity of the cycloadducts obtained.

This doctoral thesis, divided into seven different chapters, is based on the methodological study of the rhodium(I)-catalysed [2+2+2] cycloaddition reaction involving allenes. Chapter 1 contains a general introduction to the structural and reactivity particularities of allenes and to the [2+2+2] cycloaddition reactions, making reference to the main examples found in the literature. Chapter 2 sets out the general objectives of the thesis. In Chapters 3 and 4 the reactivity of linear chiral and non-chiral allene-ene/yne-allene substrates in totally intramolecular rhodium-catalysed [2+2+2] cycloaddition is evaluated. In Chapter 5, a dehydrogenative [2+2+2] cycloaddition of cyano-yne-allene substrates is developed which allows for the synthesis of the 2,6-naphthyridines core found in biologically relevant products. Chapter 6 draws general conclusions from the results of these studies. Finally, Chapter 7 contains the experimental procedure and the characterization data for the compounds synthesised in this thesis.

Resumen

El desarrollo de nuevos procesos químicos para la formación de enlaces carbono-carbono es un campo importante en química orgánica. Concretamente, la reacción de cicloaddición [2+2+2] catalizada por metales de transición es una herramienta muy eficiente que permite la formación de derivados carbo- y heterocíclicos polisustituidos de seis miembros en un proceso de economía atómica. Por otro lado, los alenos son sustratos versátiles en reacciones de cicloadición que además de poseer un buen perfil de reactividad tienen la habilidad de incrementar la complejidad estructural en los cicloaductos que permiten sintetizar.

La presente tesis doctoral, dividida en siete capítulos, se ha basado en el estudio metodológico de cicloadiciones [2+2+2] catalizadas por rodio(I) involucrando alenos. El Capítulo 1 contiene una introducción general a las particularidades estructurales y de reactividad de los alenos y a las reacciones de cicloadición [2+2+2] haciendo referencia a los principales ejemplos descritos en la bibliografía. El Capítulo 2 presenta los objetivos generales de la tesis. En los Capítulos 3 y 4 se describe la reactividad de sustratos lineales aleno-eno/ino-aleno en forma aquiral o quiral en la reacción totalmente intramolecular de la cicloadición [2+2+2] catalizada por rodio(I). El Capítulo 5 desarrolla una reacción de cicloadición [2+2+2] deshidrogenativa de sustratos ciano-ino-aleno que permite la síntesis de la unidad estructural de 2,6-naftiridina presente en distintos productos biológicamente relevantes. El Capítulo 6 incluye las conclusiones generales que se extraen de la tesis. Por último, el Capítulo 7 contiene el procedimiento experimental y la caracterización de todos los compuestos sintetizados en esta tesis.

Resum

El desenvolupament de nous processos químics per a la formació d'enllaços carboni-carboni és un tema rellevant en química orgànica. Concretament, la reacció de cicloaddició [2+2+2] catalitzada per metalls de transició és una eina molt eficient que permet obtenir derivats carbo- i heterocíclics de sis membres polisubstituïts en un procés d'economia atòmica. D'altra banda, els al·lens són substrats versàtils per reaccions de cicloaddició que a més de tenir un bon perfil de reactivitat tenen l'habilitat d'incrementar la complexitat estructural dels cicloadductes que es poden obtenir mitjançant la seva reacció.

Aquesta tesis doctoral, dividida en set capítols, es basa en l'estudi metodològic de les cicloaddicions [2+2+2] catalitzades per rodi(I) involucrant al·lens. El Capítol 1 conté una introducció general a les particularitats estructurals i de reactivitat dels al·lens i a les reaccions de cicloaddició [2+2+2], fent referència als principals exemples descrits a la bibliografia. El Capítol 2 presenta els objectius generals de la tesi. En els Capítols 3 i 4 es descriu la reactivitat de substrats lineals al·lè-è/í-al·lè en forma aquiral o quiral en la reacció totalment intramolecular de la cicloaddició [2+2+2] catalitzada per rodi(I). En el Capítol 5 es desenvolupa una reacció de cicloaddició [2+2+2] deshidrogenativa de substrats ciano-í-al·lè que permet la síntesi de la unitat estructural de 2,6-naftiridina present en varis productes biològicament rellevants. El Capítol 6 conté les conclusions generals que s'han extret de la tesi. Per últim, el Capítol 7 inclou els procediments experimentals i la caracterització estructural de tots els compostos sintetitzats en aquesta tesi.

Chapter 1. General introduction

1.1. *Allenes as versatile substrates in transition-metal catalysed cycloaddition reactions*

Allenes are a class of compounds which have always fascinated chemists because of the intriguing features of the cumulated diene function. The *sp*-hybridization of the central carbon atom causes that the two CH_2 groups of the parent allene are perpendicular to each other and consequently the two π orbitals are roughly orthogonal (Figure 1.1).

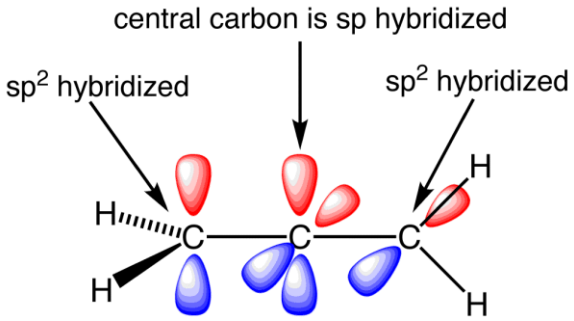

Figure 1. 1 Hybridization and π bond in allene structure

The interest in this class of the IUPAC is the stereoisomerism resulting from the non-planar arrangement of four groups in pairs about a chirality axis. In allenes, axial chirality arises when the terminal ends of the cumulative π-system contain different substituents (Figure 1.2). This property provide additional bonus from the synthetic point of view.

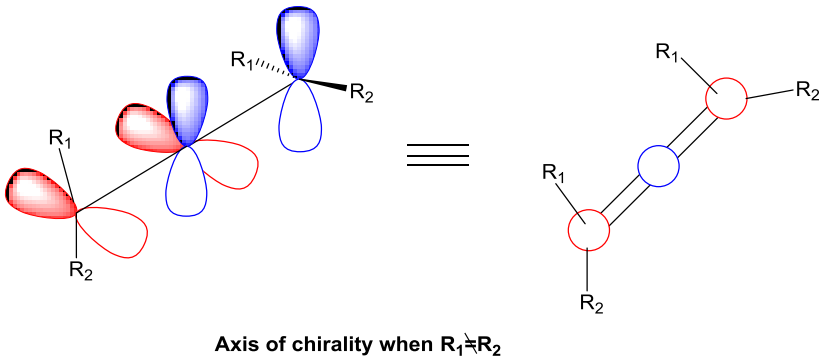

Figure 1. 2 Axial chirality shown on allene structure

For a long period, allenes were considered chemical curiosities and unstable unsaturated moieties, a fact that greatly retarded the development both of their preparation and synthetic applications. However, over the last thirty years the chemistry of allenes has experienced a great advancement.[1] It is also noteworthy that at the same time, isolation and characterisation of allenic natural compounds have been pursued and about 150 natural products containing an allenic or a cumulenic structure are now known.[2]

Alkenes and alkynes have a prominent position among the organic substrates for transition metal catalysed reactions and specially cycloaddition reactions. From a general reactivity point of view, allenes can often be considered as hybrids of alkenes and alkynes with characteristic

features that makes them appealing substrates for cycloaddition and cyclization reactions.[3] The two orthogonal double bonds in the allene retain the linear geometry of alkynes, but possess only a single *sp* hybridized atom. So regardless of which terminus reacts a new sp^3 centre will be formed. Therefore, replacing alkynes with allenes should allow the development of cycloadditions that produce a greater number of sp^3-hybridized stereocenters relative to the isomeric alkyne substrates. Furthermore, one of the allene double bonds remains in the product and is useful for further chemistry. It is also important to note that the allene isomer of a given alkyne is generally 3 – 5 kcal/mol less stable due to strain energy.[2] This energy provides an additional thermodynamic driving force for the reaction. Finally, the ability to possess axial chirality is another clear advantage both compared to alkenes and alkynes.

On the other hand, the control of the selectivity in cycloadditions involving allenes is more complex than with the alkene or alkyne counterparts. Apart from controlling the chemoselectivity, regioselectivity (leading to constitutional isomers) and stereoselectivity (leading to stereoisomers), in the cycloadditions that involve allenes the positional selectivity (which of the two orthogonal double bonds reacts, thus again leading to constitutional isomers) needs also to be mastered (Figure 1.3).

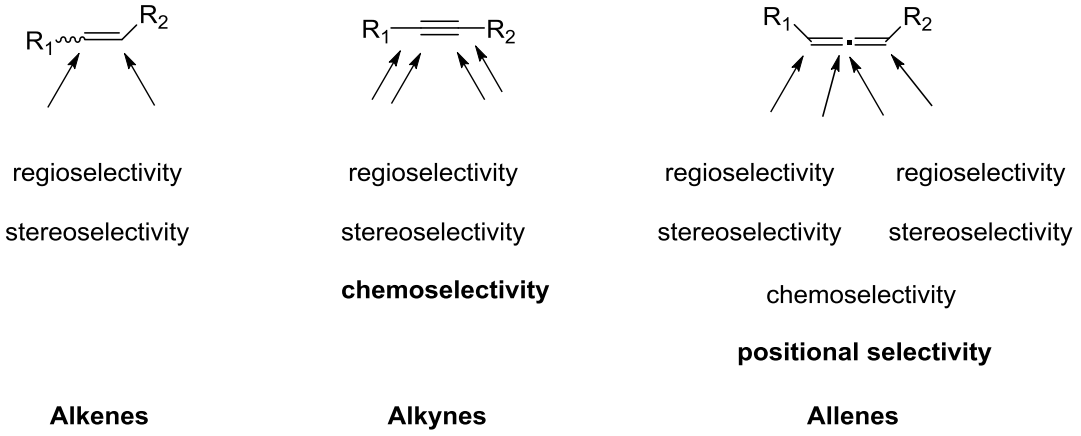

Figure 1. 3 Selectivity problems in different types of unsaturated substrates

1.2. Transition metal-catalysed [2+2+2] cycloaddition reactions

The development of chemical processes to enable the formation of carbon-carbon bonds is an important topic in organic chemistry. In particular, reactions where cyclic systems with high structural complexity are formed from simple precursors are of great importance. One of these processes is the transition metal-catalysed [2+2+2] cycloaddition reaction where a wide range of six-membered carbon and heterocyclic compounds with different functionalities can be obtained.

The first substrates involved in this reaction were alkynes. In 1948, Reppe et al.[4] described the first transition metal-catalysed version of this transformation under nickel catalysis to obtain substituted benzene derivatives upon reaction of three alkynes. Nowadays this reaction represents one of the most elegant methods for the construction of aromatic compounds due to the fact that three carbon-carbon bonds are formed in a single reaction step in an atom economy process (Scheme 1.1).

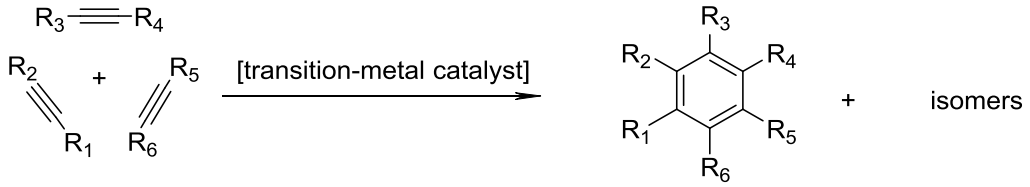

Scheme 1. 1 Transition metal-catalysed [2+2+2] cycloaddition reaction of three alkynes

Since the first study by Reppe, many examples of [2+2+2] alkyne cycloaddition catalysed by different transition metals have been described. The metals which have been more often used are Ni, Co, Pd, Rh, Ru, Zr, and Ir.[5] Over the last few years, the reaction, which originally required stoichiometric amounts of the transition metal and harsh reaction conditions, has become a highly efficient catalytic process which can be performed in mild conditions and with quite low catalyst loads.

There are many aspects of this kind of reactions which are worth of study. These include the study of catalysts with high levels of activity, the mechanistic aspects that govern these processes, the type of unsaturated substrates that can participate in the cycloaddition, the chemo- and regioselectivity, at times the enantioselectivity, and the application of these reactions especially in the synthesis of natural products. All of these aspects will be discussed here. Given that this thesis is based on Rh-catalysed [2+2+2] cycloaddition reactions, the precedents described will be mainly focused on such catalytic systems.

1.2.1. The mechanism

Progress in computational chemistry has allowed a breakthrough in the knowledge of the mechanistic rationale of the transition metal-catalysed [2+2+2] cycloaddition reaction.[6] The specific reaction mechanism depends on the nature of the metal, ligands and substrate partners, but the most generally accepted pathway is shown in Scheme 1.2.

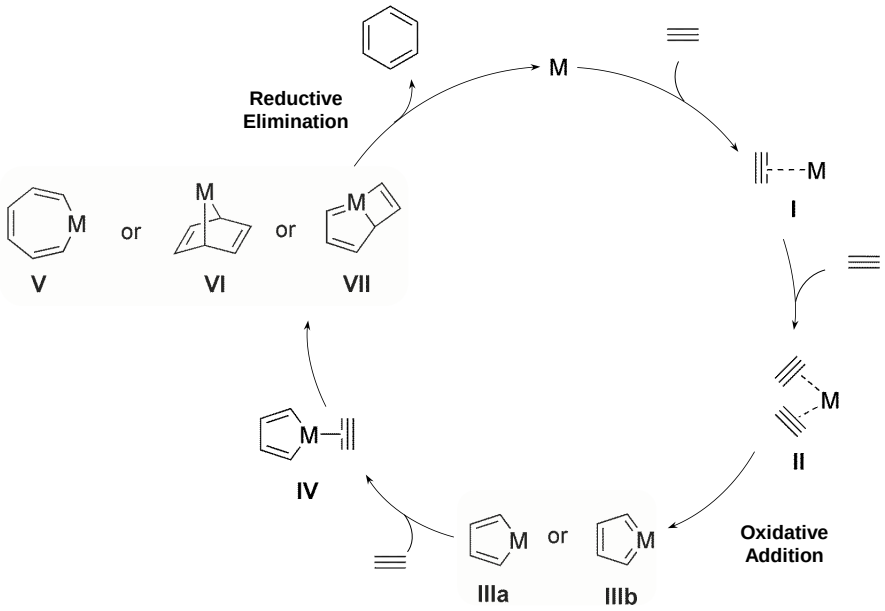

(M = transition metal catalyst)

Scheme 1. 2 Postulated general mechanism of the transition-metal catalysed [2+2+2] cycloaddition reaction involving three alkynes (M = transition metal catalyst)

In a first step, the coordination of one alkyne partner to the metal takes place leading to species **I**, followed by a second alkyne coordination to form species **II**. There is then an oxidative addition of the metal to afford the metallacyclopentadiene **IIIa** or the metallacyclopentatriene **IIIb** with a biscarbene type structure (when M = Ru) in which the metal adopts an oxidation state two units higher than in its precursor **II**. This has been found to be the rate-determining step.[6j-l] It should be noted that a myriad of rodacyclopentadiene complexes of type **IIIa** have to date been experimentally isolated and characterized, supporting the structure of this intermediate.[7] The subsequent coordination of the third alkyne to intermediates **IIIa** or **IIIb** results in the formation of species **IV** and proceeds to either an alkyne insertion to form the metallacycloheptatriene **V** (the so-called Schore mechanism[8]), or by a metal-mediated [4+2] cycloaddition to afford the bicyclic complex **VI**, or by a formal [2+2] cycloaddition giving rise to metallabicyclo[3.2.0] heptatriene **VII**. Finally, reductive elimination of the metal results in the benzene ring formation and catalyst (M) being recovered. The whole process is highly exothermic as the thermodynamic driving force is provided by the new σ bonds formed and the aromaticity that is gained. Unlike the uncatalysed [2+2+2] cycloaddition of acetylenes, which presents a prohibitive energy barrier,[9] the barriers for the transition metal-catalysed [2+2+2] cycloaddition are relatively low. This agrees with the fact that this reaction typically occurs under mild conditions.

Our group has studied the mechanism of the rhodium-catalysed [2+2+2] cycloaddition reaction using both experimental[7a,b] and computational[6j-l,7a] techniques. In a collaboration with Prof. A. Jutand we described for the first time kinetic data for the catalytic cycle of the [$RhCl(PPh_3)_3$]-catalysed [2+2+2] cycloaddition al alkynes. The oxidative addition and the insertion of the third alkyne where kinetically characterized by monitoring electrochemically the formation and further reaction of the oxidative addition intermediate.[7b] The mechanism of the Rh-catalysed [2+2+2] cycloaddition reaction of diynes with monoynes was also examined using ESI-MS and ESI-CID-MS analysis. For the first time ESI-MS online monitoring allowed the detection of all the intermediates in the catalytic system, and the data collected was further supported by DFT calculations.[7a] This mass spectrometric study provided new insight into the reactivity of cationic rhodacyclopentadienes, which should facilitate the design of related rhodium-catalysed carbon-carbon couplings.

1.2.2. Participation of other unsaturated partners

The transition-metal catalysed [2+2+2] cycloaddition has been modified to involve not only alkynes but also other unsaturated substrates such as olefins, allenes, nitriles, aldehydes, ketones, carbon dioxide, carbon disulfide, isocyanates, and isothiocyanates, which can react with two alkynes to afford the corresponding cyclohexadienic or heterocyclic compounds (Scheme 1.3).[5e-h,l-s] Among the multiple possibilities the use of allenes that constitutes the core of the present thesis will be highlighted in each of the different subsections that follow. The involvement of nitriles as unsaturated partners that is developed in chapter 5 is revised below.

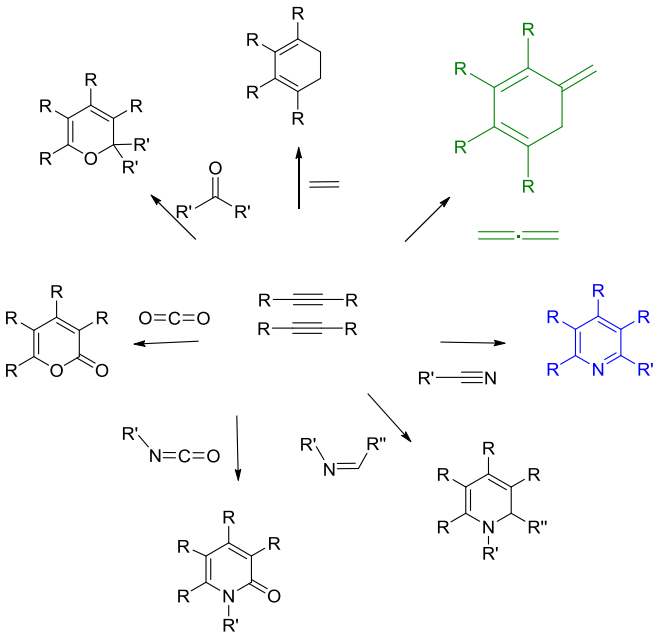

Scheme 1. 3 Transition metal-catalysed [2+2+2] cycloaddition between two alkynes and other unsaturations

1.2.2.1. Synthesis of pyridine cores by transition-metal catalysed [2+2+2] cycloaddition

The pyridine ring plays a crucial role in chemical and biological catalysis. The potent activity of this heteroaromatic ring in biologic systems is evident from its presence in the NADP nucleotide and in many important vitamins such as niacin (B3 vitamin) and piridoxin (B6 vitamin), but also in highly toxic alkaloids such as nicotine. The demand for pyridine derivatives has notably increased in the last years due to the discovery of various natural products and bioactive compounds that have as a basic unit the pyridine ring. In the pharmaceutical industry, the pyridine ring constitutes the core of thousands of drugs. But the pyridine ring is also a fundamental component in agrochemical products due to the fungicide properties that some pyridine derivatives show. Apart from biological applications, pyridine containing compounds have shown great utility in organic synthesis. A classic example is the 4-dimethylaminopyridine (DMAP) which is generally used in the activation of carboxylic acids and has found a particular important use in acylation reactions. Pyridine rings have also been widely used in coordination chemistry. In summary, the development of synthetic methods for the synthesis of pyridine derivatives has attracted considerable attention due to the diverse uses that these derivatives show.

The transition-metal catalysed [2+2+2] cycloaddition reaction of two alkynes and a nitrile is an elegant and efficient option for the synthesis of the pyridine ring.[10] This reaction was first described at the beginning of 1970s, when Wakatsuki and Yamazaki reported the synthesis of pyridine derivatives by reaction of two acetylene molecules and one nitrile using a stoichiometric quantity of a cobalt catalyst.[11] Some years later, Vollhardt[12] demonstrated that pyridines can be synthesised by the [$CpCo(CO)_2$]-catalysed [2+2+2] cycloaddition reaction of alkynenitriles and exogenous alkynes. However, high temperature and visible light irradiation were required to activate the catalyst.

Although [$CpCo(CO)_2$] is the most commonly used catalyst for pyridine synthesis by [2+2+2] cycloaddition reaction,[13] other complexes based on ruthenium,[14] rhodium,[15] and iron,[16] have also been able to catalyse such a process.

Our research group studied the synthesis of polycylic pyridines and bipyridines with high functionality from cyanodiynes using the Wilkinson's catalyst under microwave heating (Scheme 1.4).[17] The choice of the solvent proved to be crucial for the success of the reaction.

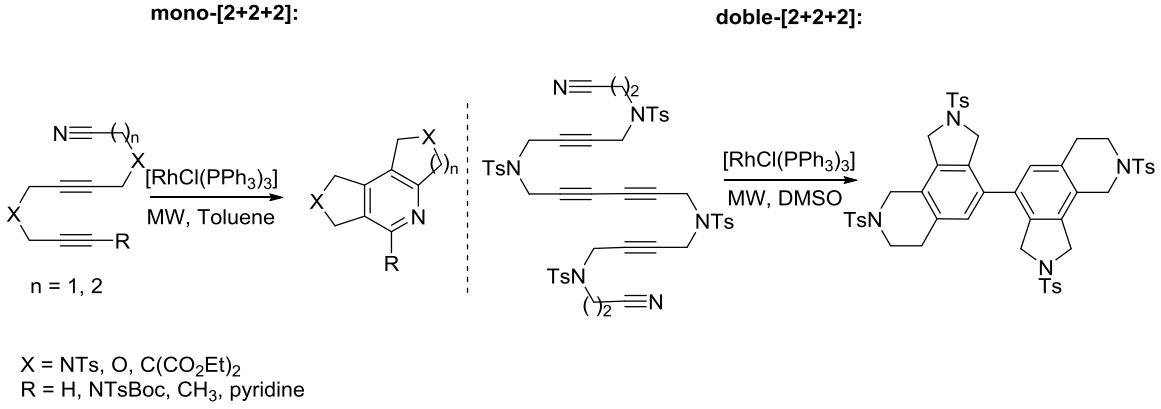

Scheme 1. 4 Synthesis of pyridines and bipyridines from cyanodiynes

Strategies to access cyclic compounds with multiple nitrogen atoms have recently been developed by the groups of Louie[18] and Liu[19]. Louie et al. reported that a variety of cyanamides and alkynenitriles can be effectively involved in cycloaddition reactions using a catalytic amount of FeI_2 ^{iPr}PDAI and Zn affording bicyclic 2-aminopyrimidines (Scheme 1.5).

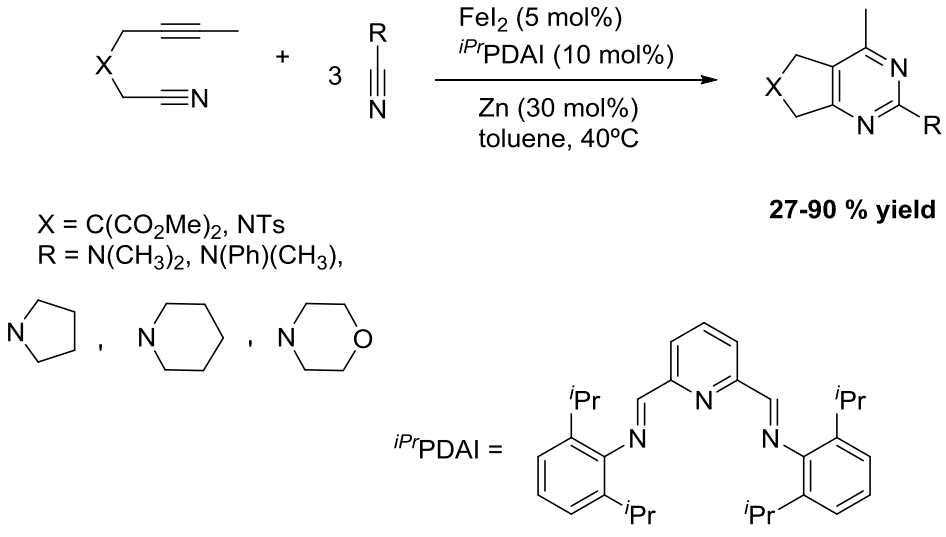

Scheme 1. 5 Iron-catalysed [2+2+2] cycloaddition between alkynenitrile and other alkyne

Aminopyrimidine cores can also be synthesized through a gold-catalysed [2+2+2] cycloaddition reaction between ynamides and nitriles, as shown by a recent work by Liu et al. It is worthy to note that gold is not often used as catalyst in the [2+2+2] cycloaddition reaction (Scheme 1.6).[19]

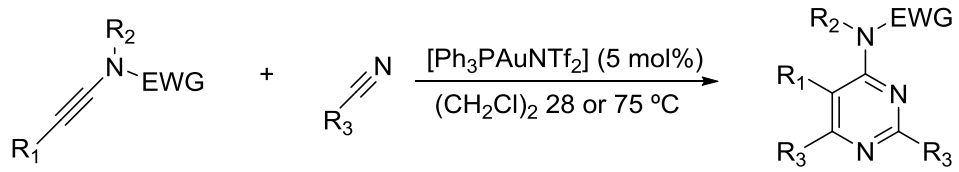

53-93 % yield

R_1 = Ph, *p*-$OMeC_6H_4$cyclopropan, thiophene, $CH_2CH_2CH_3$, styrene

R_2 = CH_3, CH_2Ph

R_3 = *p*-MeC_6H_4, *p*-ClC_6H_4, *p*-$CO_2C_6H_4$, $C(CH_3)_3$

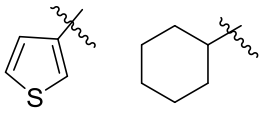

Scheme 1. 6 Gold-catalysed [2+2+2] cycloaddition of alkynes with nitriles leading to aminopyrimidine cores

1.2.3. Chemoselective and regioselective features

Due to the atom economy and convergent nature of the [2+2+2] cycloaddition reaction, this process represents a useful tool for the preparation of polysubstituted hetero- and carbocyclic compounds and is considered as an example of *de novo* synthesis of this kind of products. As an advantage over conventional strategies for the construction of such derivatives, this approach enables the introduction of high functionality in a single reaction step. Despite its synthetic potential, controlling the chemo- and regioselectivity of this process still remains an important goal in most cases.

The transition-metal catalysed [2+2+2] cycloadditions reaction can be classified into the approaches shown in Scheme 1.7 using three alkynes as generic substrates.

Completely Intermolecular:

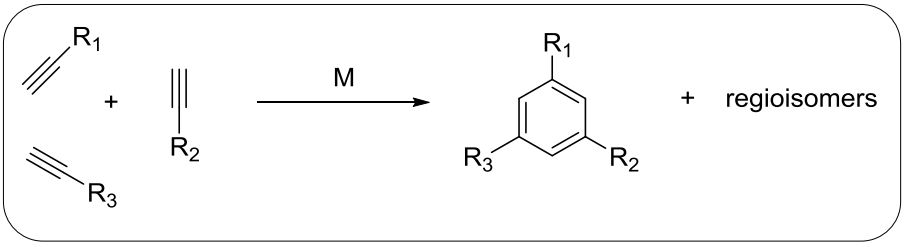

Partially intramolecular:

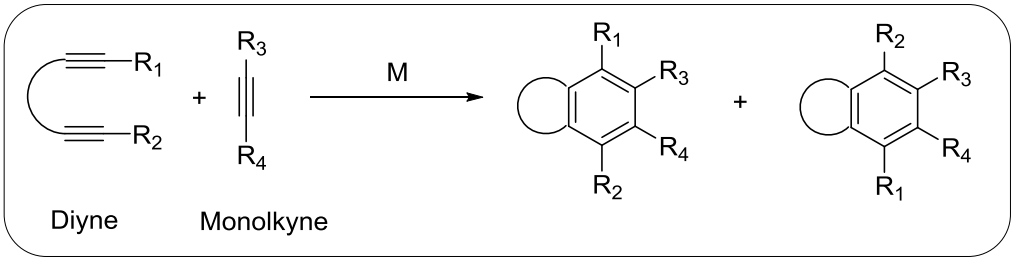

Totally intramolecular:

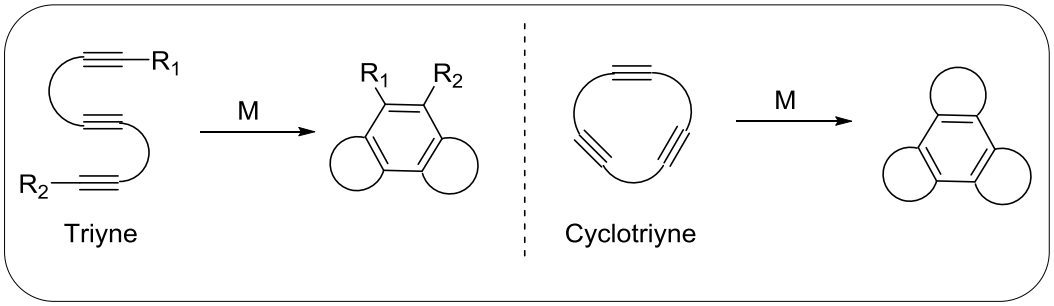

Scheme 1. 7 [2+2+2] cycloaddition versions (M = transition metal catalyst)

The totally intramolecular reactions are the ones in which the chemo- and regioselectivity is most easily controlled. Polycyclic systems can be efficiently build up with such an strategy[5g,20] although the preparation of starting materials that possess the necessary substituents or functional groups at the desired positions can be quite complex. This method has been used as a key step in the preparation of natural products containing polycyclic fused systems.[21] As an example, the synthesis of alcyopterosin E[22] and Herbindole A[23] that make use of the Wilkinson's catalyst are shown below (Scheme 1.8).

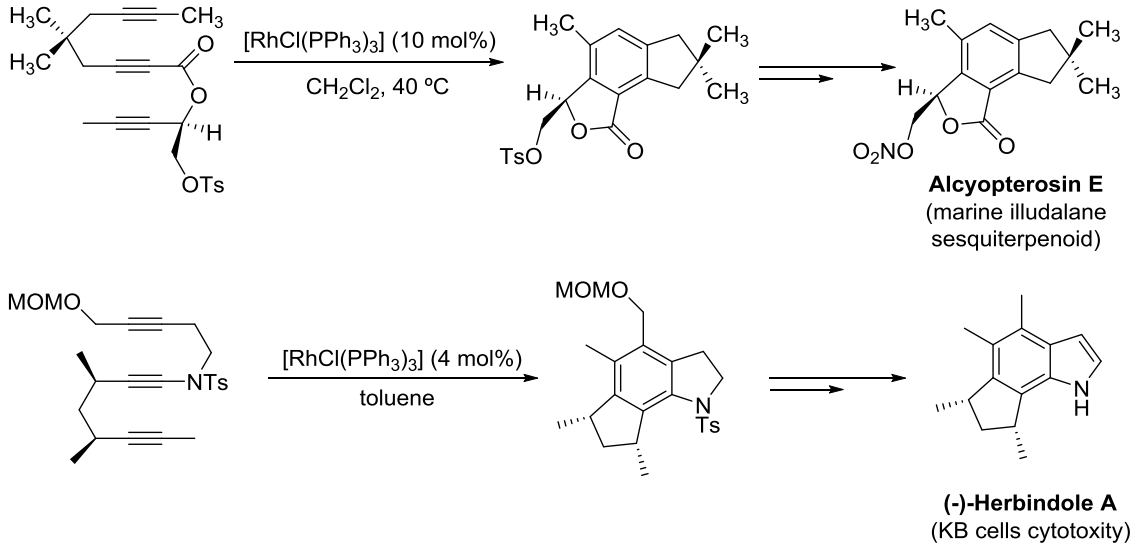

Scheme 1. 8 Synthesis of Alcyopterosin E and (-)-Herbindole A by totally intramolecular [2+2+2] cycloaddition reaction (MOMO = methoxy methyl protecting group)

Partially intramolecular methods have the advantage of using readily accessible diynes and monoalkynes but the dimerization of the diyne component is a serious drawback. Thus, a considerable excess of monoalkyne or the slow addition of diyne is generally required to prevent such a side reaction. Partially intramolecular [2+2+2] cycloadditions between diynes and monoynes have been thoroughly studied using different transition metal complexes as the catalyst, where rhodium complexes are one of the most widely used.[24] This partially molecular version has also been used for the synthesis of natural products. Estrone was synthesized by a

cobalt mediated [2+2+2] cycloadditions in a classic example of the use of this cycloaddition in total synthesis of the Vollhardt's group.[25] During this synthesis, a [2+2+2] cycloaddition was used to generate a benzocyclobutane, which undergoes subsequent 4-π electrocyclic ring opening to generate a diene, and terminates with a Diels-Alder cycloaddition with the tethered alkene. Remarkably, this transformation occurs in a single synthetic manipulation (Scheme 1.9).

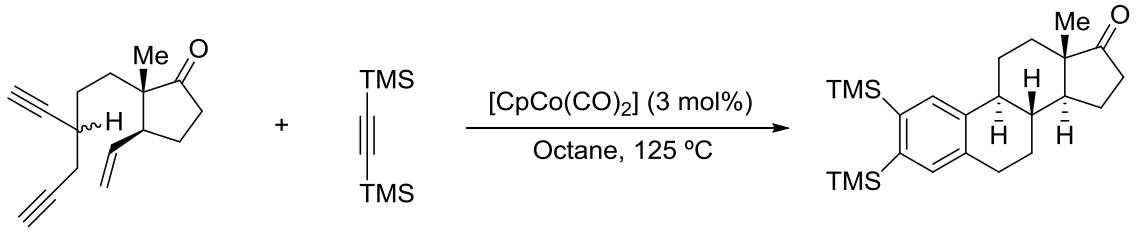

Scheme 1. 9 Vollhardt's synthesis of estrone based on a [2+2+2] cycloaddition reaction

The completely intermolecular version of [2+2+2] cycloaddition reactions is the most problematic approach in terms of regio- and chemoselectivity.[5c,k] Several strategies have been attempted to control the chemo- and regioselectivity such as to the use of electronically different alkyne components,[26] alkyne surrogates, regiodirecting groups or temporary tethers,[27] but a precise control of the selectivity of these reactions is still a challenge.

1.2.3.1. Intra- and intermolecular [2+2+2] cycloaddition using allenes

[2+2+2] cycloadditons of substrates including an allene as a coupling partner is still limited to several precedents. Some of them will be commented below classified as completely intramolecular and partially or totally intermolecular.

Pioneer work on the involvement of allenes in a completely intramolecular [2+2+2] cycloaddition reaction was done by Malacria et al. The first work investigating this reaction demonstrated the efficient regio- and diastereoselective cyclization of various allenediynes.[28] Later, the pronounced effect of phosphine oxides on the outcome of enediyne cycloadditions[29] was applied in the special case of a chiral allenediyne.[30] This method represents a convenient route to the family of 11-β-steroid cores (Scheme 1.10).[31]

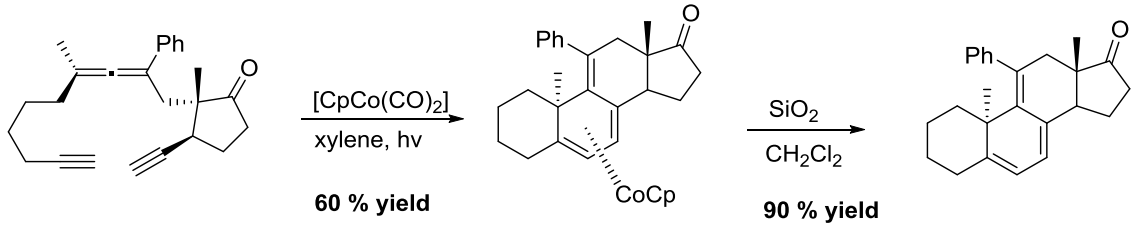

Scheme 1. 10 Cobalt-catalysed [2+2+2] cycloaddition of allenediynes leading to the synthesis of 11-β-stereoid scaffolds

Sato and his group reported a completely intramolecular cyclization of an allene-yne-ene substrate catalysed by a ruthenium catalyst as a powerful method to construct fused tricyclic skeletons.[32] The reaction proceeds to give a ruthenacycle intermediate, and subsequent reductive elimination afford the product as a single diastereisomer (Scheme 1.11). It was proved that the progress of the cyclization was strongly affected by the type of substituent on the unsaturated bonds. One year later the same group reported a novel Rh-catalysed

cycloaddition between alkyne, allene and aldehyde, giving a tricyclic compound containing a pyran ring (Scheme 1.12).[33]

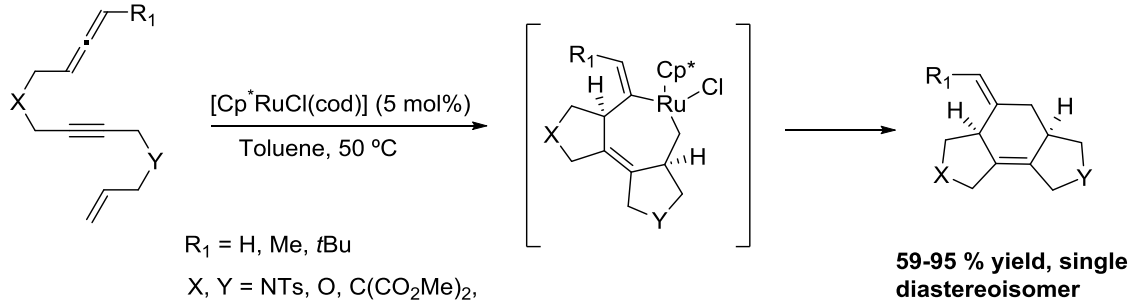

Scheme 1. 11 Ruthenium-catalysed cyclization of allene-yne-ene through ruthenacycle

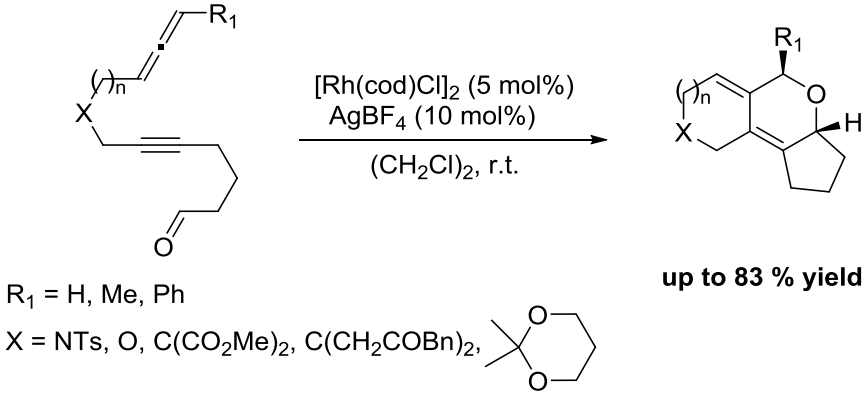

Scheme 1. 12 Rhodium-catalysed cyclization of allenynes with tethered aldehydes

Oxygen heterocycles were also synthesized by Tanaka et al. using a partially intramolecular strategy (Scheme 1.13).[34] The enantioselective [2+2+2] cycloaddition reaction of tosylamide-linked 5-allenal and 5-allenone with internal alkynes using cationic rhodium(I)-binap complex was reported leading to bicyclic heterocycles.

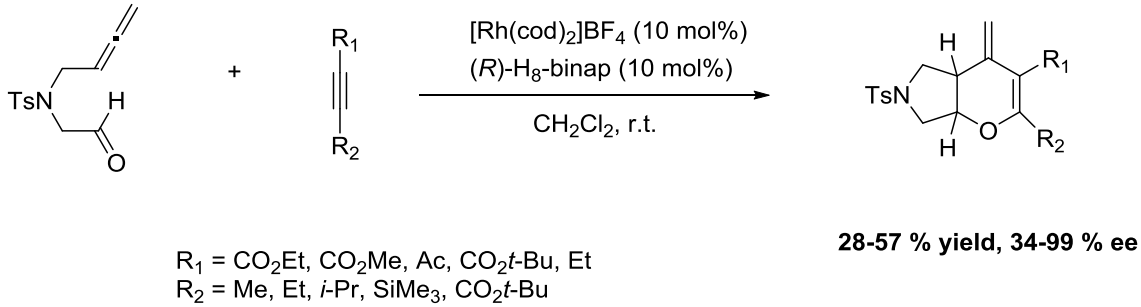

Scheme 1. 13 Rhodium(I) catalysed cycloaddition of tosyl-linked 5-allenal with internal alkynes leading to oxygen heterocycles

Cheng et al. also reported a partially intramolecular [2+2+2] cycloaddition reaction of electron-deficient diynes[35] or electron neutral diynes[36] with allenes (Scheme 1.14). The reactions, which tolerate a variety of functional groups in the diynes, proceed in a highly regio- and chemoselective fashion. However, the cycloadduct initially formed tautomerizes to the corresponding benzene derivative. Therefore, it was proved that allenes are synthetically equivalent to monosubstituted alkynes, but are superior in terms of regioselectivity.

Additionally, it was shown that the $CoI_2(PPh_3)_2$/Zn system, which is used for the electron neutral diynes, is much more active and selective than the $NiBr_2$(dppe)/Zn system that works for the electron deficient dyines.

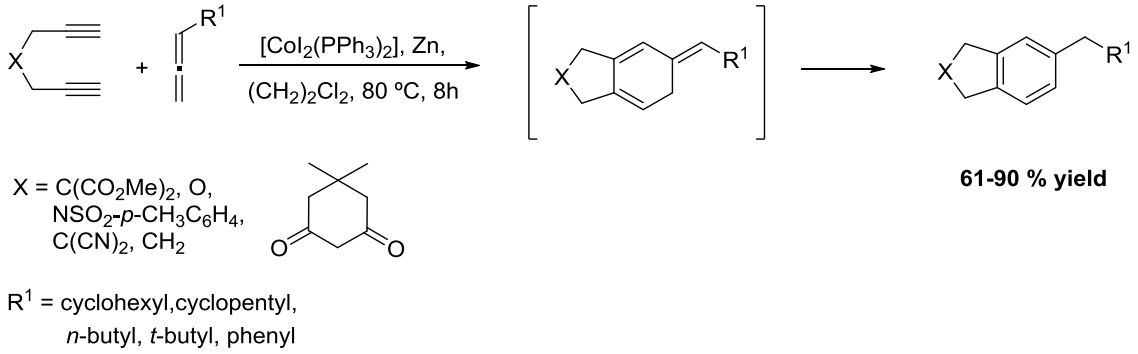

Scheme 1. 14 Cobalt-catalysed cocyclotrimerization of electronically neutral diynes with allenes

Cheng et al. also reported the first intermolecular alkyne-allene-alkyne cocyclotrimerization ever studied. The synthesis of polysubsituted benzenes in a highly regio- and chemoselective reaction was achieved using a nickel catalytic system.[37] Again, the final product was formed by isomerisation of the cyclohexadiene initially formed (Scheme 1.15). Remarkably, reactions produced single regioisomeric products as only the unsubstituted terminal carbon-carbon double bonds of allenes are involved in the cycloaddition. The reaction proceeds without the need for excess substrates or slow addition of either reaction component.

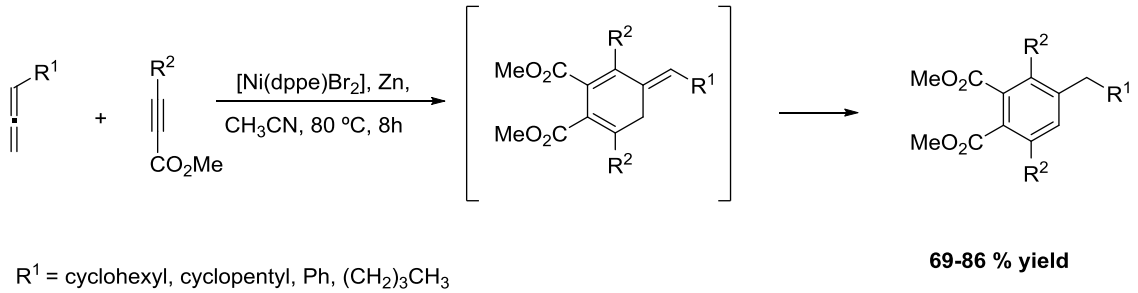

Scheme 1. 15 Nickel-catalysed cocyclotrimerization of propiolates with allenes

Further extension of this work into the cocyclotrimerization reaction involving arynes with allenes has been reported by the same group.[38] The $NiBr_2$(dppe)-Zn system effectively catalysed the [2+2+2] cycloaddition reaction of two benzynes and an allene, providing a method to the synthesis of 10-methylene-9,10-dihydrophenanthrene derivatives in a highly selective fashion (Scheme 1.16). Noteworthy the final product is not isomerized at the end of the reaction.

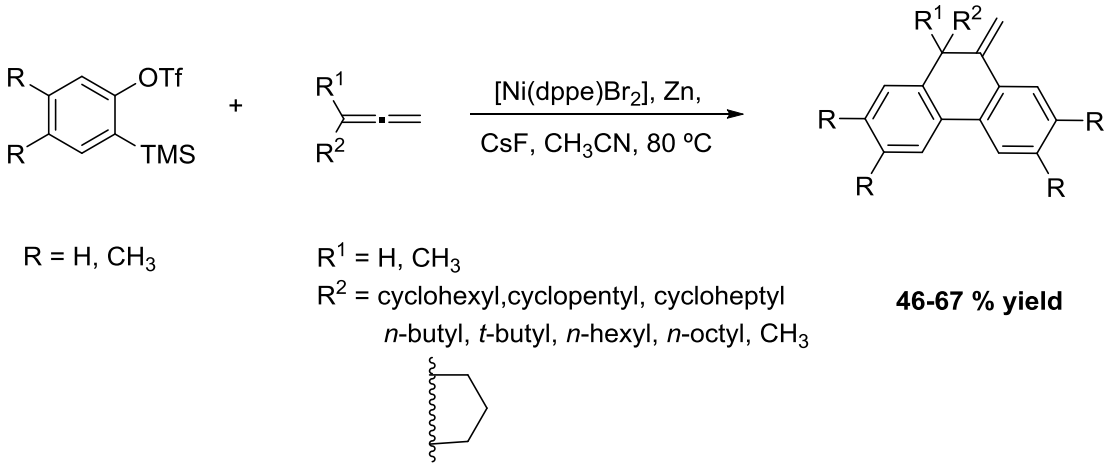

Scheme 1. 16 Nickel-catalysed cocyclotrimerization of benzynes with allenes

The gold(I)-catalysed [2+2+2] cycloaddition of allenamides, alkenes and aldehydes for the synthesis of tetrahydropyrans has recently been reported by Mascareñas, López et al.[39] The use of a phosphite gold complex in catalytic amounts proved crucial for this efficient transformation of three different π-unsaturated components, which is postulated to occur through carbocations stabilized by the gold atom (Scheme 1.20).

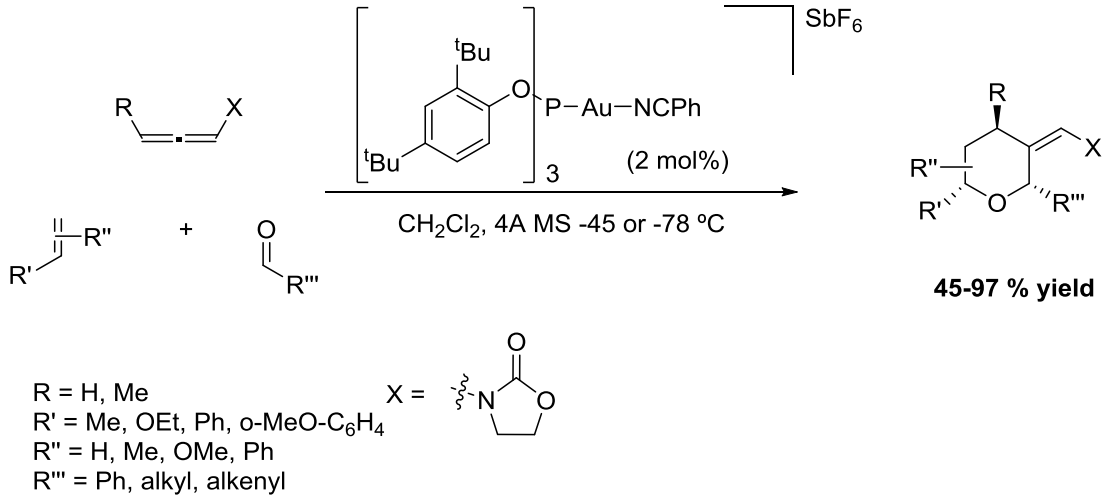

Scheme 1. 17 Gold-catalysed [2+2+2] intermolecular cycloaddition for the synthesis of tetrahydropyrans

1.2.4. Enantioselective features

The production of enantiomerically pure compounds is one of the most desirable goals in modern organic synthesis. Single enantiomers of a chiral compound are highly sought as they are active molecules in many drugs. Among numerous strategies for the production of chiral molecules, asymmetric synthesis which is defined as the conversion of an achiral starting material to a chiral product in a chiral environment is currently the most valuable option.[40] Although most of the processes developed are devoted to the installation of central chirality, achieving the stereoselective formation of compounds having other type of chirality is also an important goal.[41] Indeed, whereas the properties of biologically or pharmaceutically compounds are often associated with central chirality, derivatives displaying planar, axial, or

helical chirality have played a crucial role in asymmetric catalysis, as for example essential chiral ligands.

The majority of [2+2+2] cycloadditions published prior until 1995 generated benzenoid products. Because sp^3 stereocenters were not commonly produced in [2+2+2] cycloadditions, ways to affect enantioselective catalysis are non-obvious. The Mori group reported the first example of enantioselective [2+2+2] cycloaddition using a nickel catalyst generated *in situ* from [Ni(cod)$_2$] and a chiral monodentate phosphine. The reaction produces a stereocentre *via* the desymmetrization of a triyne with acetylene (Scheme 1.18).[42] Although the isoquinoline cycloadducts were formed with moderate enantioselectivity, this reaction served as proof-of-principle for enantioselective [2+2+2] cycloadditions.

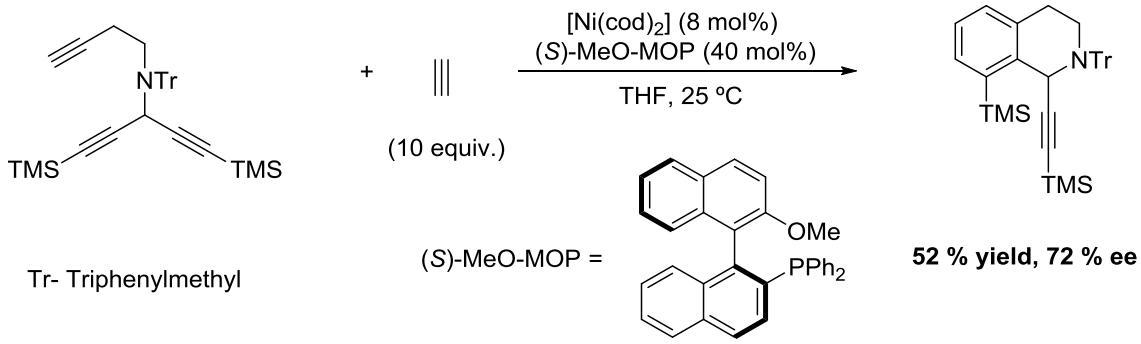

Scheme 1. 18 Mori's pioneer work on catalytic asymmetric [2+2+2] cycloaddition reaction

After this first example, subsequent works have focused their attention not only to the formation of products with central chirality, but also with planar, axial and helicoidal chirality (Figure 1.4). Among the transition metals employed in the [2+2+2] cycloaddition reaction, rhodium has emerged as one of the most effective and general catalyst to promote these processes with high enantioselectivities.

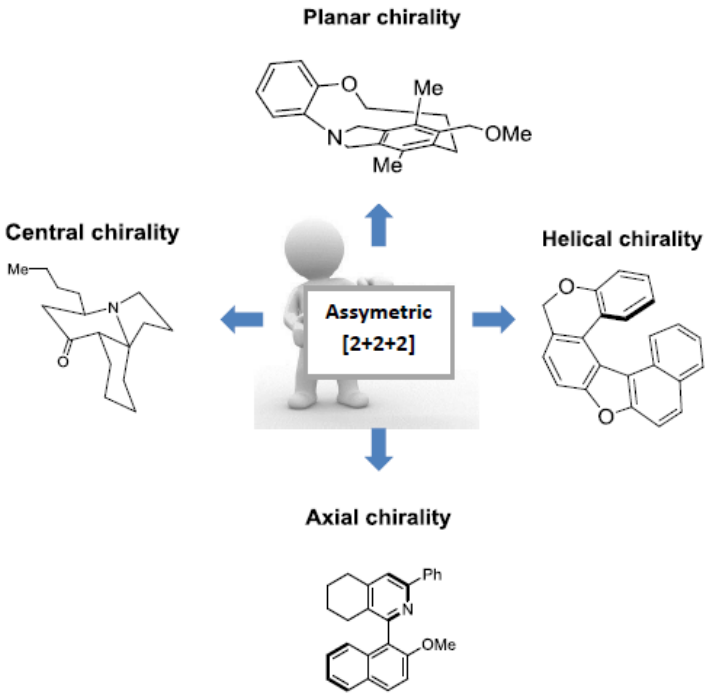

Figure 1. 4 Access to various chirality modes through asymmetric [2+2+2] cycloaddition

1.2.4.1. Construction of Central Chirality

1.2.4.1.1. Totally intramolecular cycloadditions

The use of polyunsaturated substrates with the presence of at least one double bond is an excellent option to construct fused and bridged tricyclic systems with central chirality. The totally intramolecular nature of these reactions dictates the chemo- and regioselectivity of the reaction, which allows multiple alkenes to be used in the presence of significantly more reactive alkynes. The effective concentration of the tethered alkene is always substantially higher than that of another molecule of substrate and geometric constrains prohibit the formation of regioisomeric products.

Shibata et al. reported the enantioselective intramolecular [2+2+2] cycloaddition of different (*E*)-enediynes catalysed by $[Rh(cod)_2]BF_4$ complex and the chiral phosphine (*S*)-H_8-binap for the synthesis of chiral 1,3-cyclohexadienes (Scheme 1.19).[43] The study involved internal and terminal alkynes as well as carbo- and heteroatom-linked unsaturations and showed that the process was very sensitive to the nature of substrates and phosphine used.

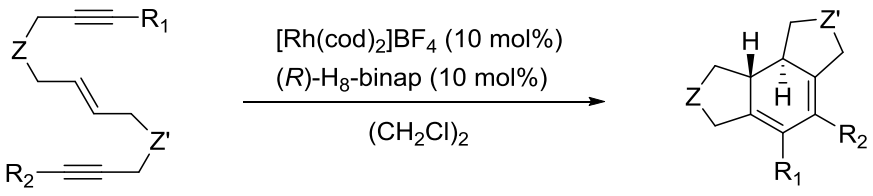

R_1, R_2 = H, Me, Bu, Br, Ph, CO_2Me, CH_2OBn
Z = $C(CO_2Me)_2$, NTs, $C(SO_2Ph)_2$
Z' = $C(CO_2Me)_2$, NTs, $C(SO_2Ph)_2$, O

15-98 % yield,
41-99 % ee

Scheme 1. 19 Intramolecular enantioselective [2+2+2] cycloadditions generating 1,3-cyclohexadienes with two stereocentres

More recently our group in collaboration with Prof. Riera's group at the University of Barcelona have also contributed to the topic by reporting the Rh(I)-catalysed intramolecular [2+2+2] cycloaddition of enediynes. Two sets of hemilabile S-stereogenic (PNSO) and P-stereogenic ligands which are capable to induce chirality were described. The formation of chiral 1,3-cyclohexadienes from terminal (*E*)-enediynes resulted in the highest enantioselectivities ever reported and thus highlight their utility in catalysis (Scheme 1.20).[44]

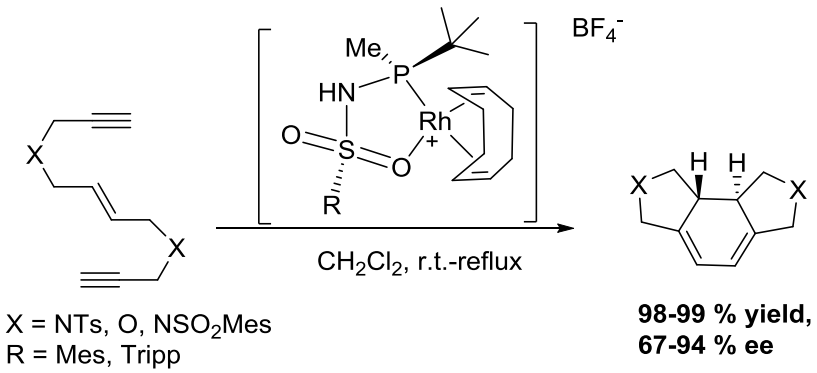

Scheme 1. 20 Enantioselective Rh-catalysed [2+2+2] cycloaddition using P-stereogenic ligands

The two examples just showed reaction of two alkynes and one alkene to form polycyclic hexadienes. Cyclohexenes can be obtained by reaction of one alkyne and two alkenes. Tanaka et al. described the [2+2+2] cycloaddition of unsymmetrical oxygen-linked (*E*)-ene-yne-enes systems using the same cationic rhodium complex as Shibata although with various chiral phosphines. The best results were again obtained with (*R*)-H_8-binap. Products were obtained with good yields and excellent enantiomeric excesses that reached 99 % (Scheme 1.21).[45]

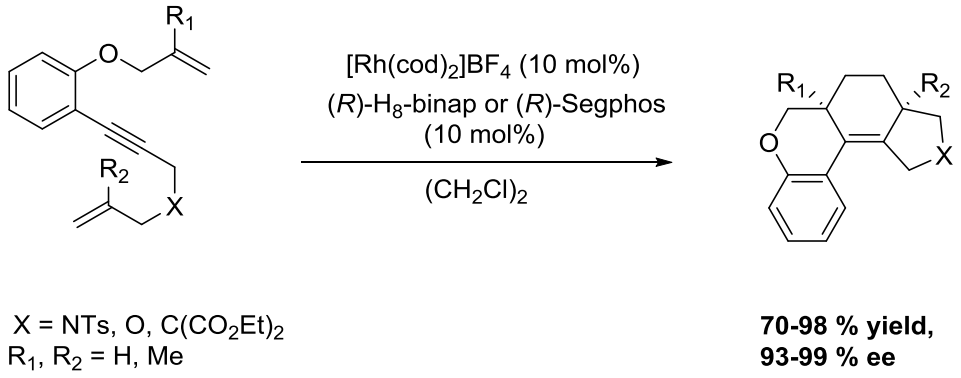

Scheme 1. 21 Intramolecular enantioselective Rh-catalysed [2+2+2] cycloaddition leading to cyclohexenes

In 2006, Shibata and co-workers focused their effort on the cycloaddition of 1,4-diene-ynes, in which the order of unsaturations in the polyunsaturated substrate is changed.[46] Under mild

reaction condition, strained polycyclic compounds containing a pair of quaternary centres were formed with great efficiency (Scheme 1.22).

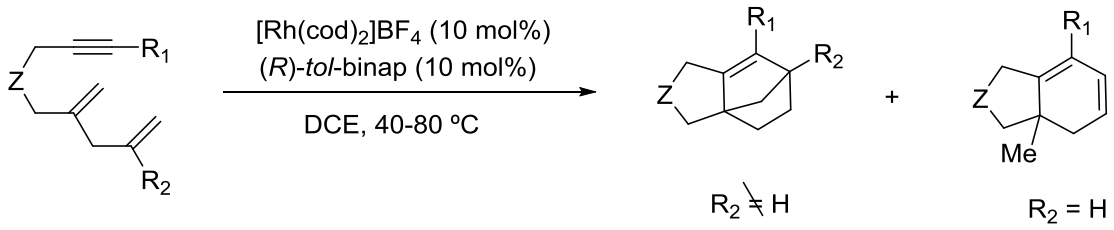

Z = NTs, O, $C(CO_2Bn)_2$
R_1 = H, Bu, Ph, $BnOCH_2$
R_2 = Me, Ph

40-83 % yield, 91-99 % ee

Scheme 1. 22 Synthesis of enantioenriched bicyclo[2.2.1]heptane derivatives

1.2.4.1.2. Partially intramolecular cycloadditions

Tanaka reported the construction of polycyclic cyclohexadienes featuring one or two newly formed stereogenic centres through the reaction between diynes and alkenes under rhodium catalysis. This represents a versatile new method for the synthesis of enantioenriched C_2 symmetric cyclohexadiene derivatives (Scheme 1.23).[47]

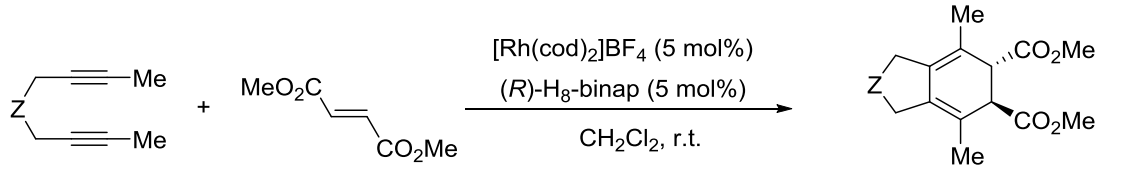

Z= O, NTs, $C(CO_2Me)_2$

35-96 % yield, 82-98 % ee

Scheme 1. 23 Cationic rhodium-catalysed enantioselective [2+2+2] cycloaddition of 1,6-diynes and dimethyl fumarate

Protected dehydroamino acids[48] and sulfonimines[49] are suitable partners for these reactions as well.

The partially intramolecular cycloadditions involving one alkene unsaturation has also been proven to be highly effective for the synthesis biologically interesting compounds such as (+)-lasubine II, which is a polycyclic aromatic compound that is difficult to prepare by conventional synthetic routes. Rovis and his group described the first regio- and enantioselective Rh(I)-catalysed [2+2+2] cycloaddition between alkenyl isocyanates and alkynes in the presence of chiral phosphoramidites. In the course of the reaction, a carbonyl group migration occurs, unexpectedly leading to vinylogous amides together with the corresponding lactams (Scheme 1.24).[50]

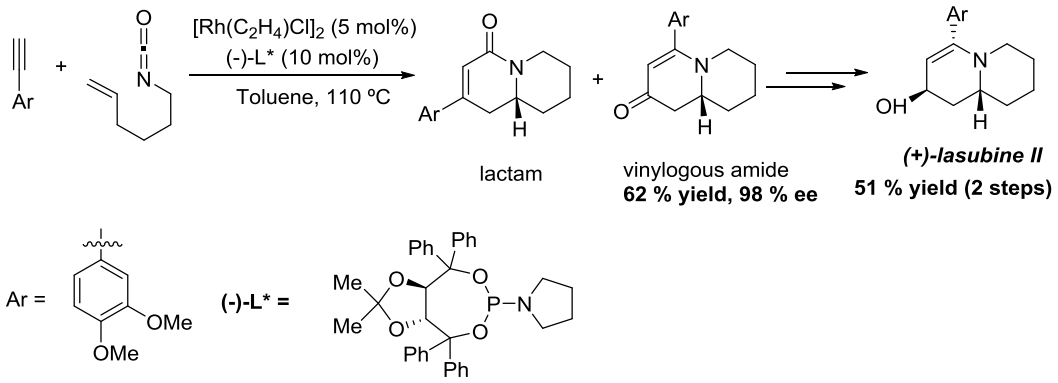

Scheme 1. 24 Enantioselective synthesis of (+)-lasubine II from isocyanates

1.2.4.1.3. Completely intermolecular cycloadditions

There are not many examples of enantioselective completely intermolecular [2+2+2] cycloaddition reactions. Since the precise control of the chemo- and regioselectivity of these reactions is still a challenge few authors have attempted to control the stereoselectivity. Only very recently did Tanaka and co-workers describe the first efficient asymmetric cross-cycloaddition of two alkynes and an alkene (Scheme 1.25).[51] Interestingly, in this process, a large excess of at least one unsaturated partner is not required in order for high reaction efficiency, chemo-, regio-, and enantioselectivities to be observed. The use of silylacetylene derivatives appears to be crucial for the success of the reaction, favouring the final reductive elimination step to form the desired cyclohexa-1,3-diene.

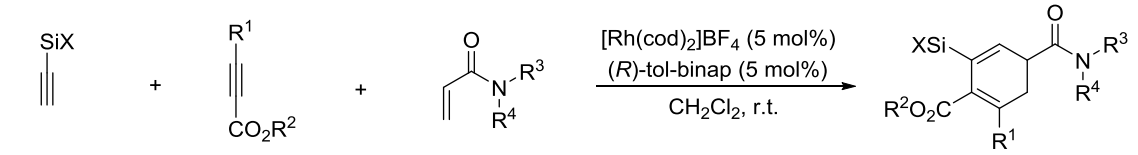

X = Me_3, Et_3, $BnMe_2$, *t*$BuMe_2$,
R^1 = Me, CF_3, CH_2OMe, CO_2*t*Bu
R^2 = Me, Et, *t*Bu
R^3, R^4 = Me, Ph, OMe, *n*Bu,

Scheme 1. 25 Enantioselective [2+2+2] cross-trimerization of two alkynes with an alkene

1.2.4.2. Construction of other types of chirality

1.2.4.2.1. Axial chirality in transition-metal catalysed [2+2+2] cycloaddition reactions

The [2+2+2] cycloaddition reaction has developed to an extremely efficient tool to synthesize axially chiral biaryl molecules. Pioneering works devoted to the synthesis of biarylic patterns through [2+2+2] cycloaddition have been reported by Mori et al.,[52] who used $[Ni(acac)_2]$ as precatalyst. Two main strategies (totally intermolecular or partially intermolecular) were envisaged for the formation of the desired biaryl compounds in high yields (Scheme 1.26).

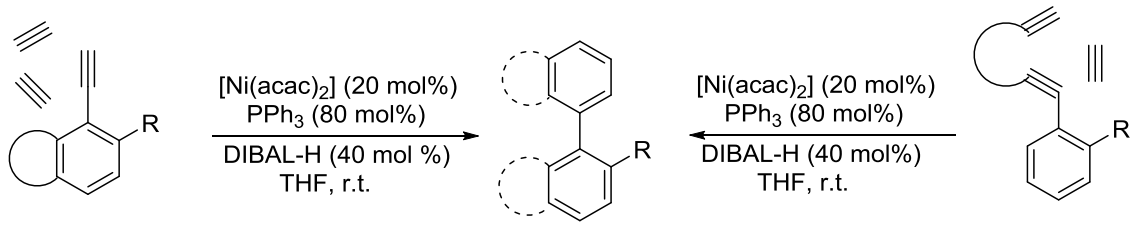

Scheme 1. 26 Strategies for biaryl synthesis through nickel-catalyzed [2+2+2] cycloaddition

Because of the potential benefits of these reactions, several attempts were made to apply this strategy to an asymmetric version. Chiral catalysts based on cobalt, iridium and rhodium have been successfully used. Chiral biaryl molecules can arise both from fully intramolecular cycloaddition and from partially intramolecular version.

An asymmetric synthesis of axially chiral biaryl biphosphine compounds by the Rh-catalysed intramolecular double [2+2+2] cycloadditions of hexayne diphosphine oxides has been reported by Tanaka et al. (Scheme 1.37).[53] The new chiral compounds were obtained in low to moderate yields but with good enantiomeric excesses. Furthermore, the diphenylphosphine oxide derivative was reduced to the corresponding phosphine and was tested as a ligand in catalytic asymmetric hydrogenations of disubstituted alkenes and in enantioselective partially intramolecular [2+2+2] cycloadditions providing good ee values in both cases.

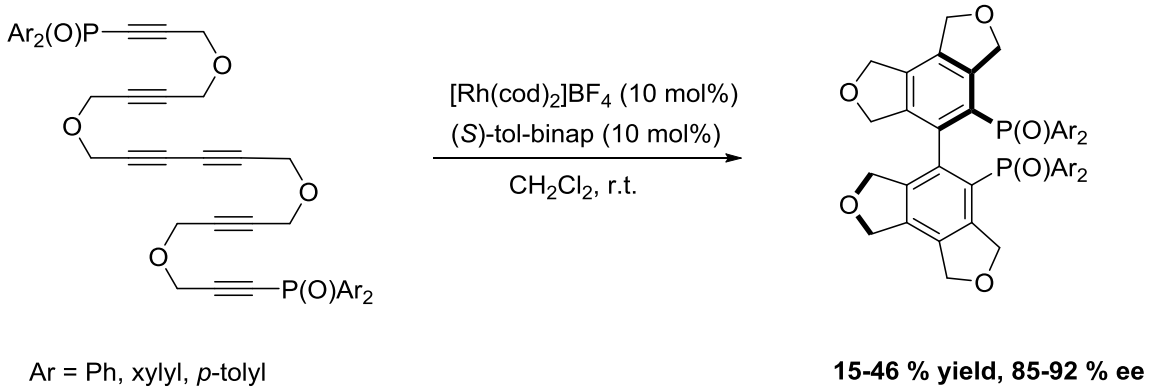

Scheme 1. 27 Synthesis of axially chiral biaryl diphosphine oxides

Tanaka's and Doherty's groups developed the partially intermolecular version. They tested the reactivities of several catalytic combinations based on cationic rhodium for the asymmetric cycloaddition of 1,6-diynes or buta-1,3-diynes.[54] Chiral biaryl phosphonates, diphosphonates, and even carboxylates were smoothly obtained under mild conditions with excellent enantioselectivities (Scheme 1.28).

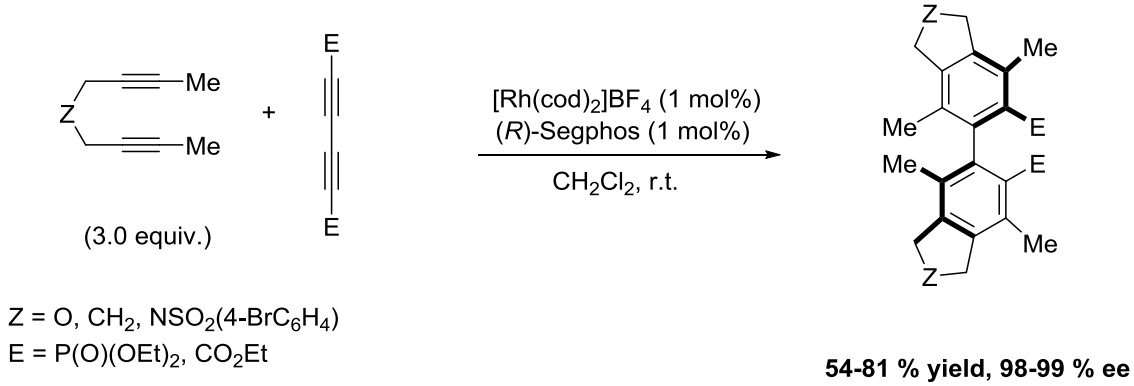

Scheme 1. 28 Enantioselective double cycloaddition of 1,6-diyne with phosphinobuta-1,3-diynes

1.2.4.2.2. Helical chirality in transition-metal catalysed [2+2+2] cycloaddition reactions

As unique nonplanar polycyclic aromatic compounds, helicenes find use as chiral auxiliaries. The steric hindrance existing at the terminal rings endows a helicene with an inherent C_2-symmetric axis perpendicular to its formal helical axis. This phenomenon is demonstrated by the fact that helicene can wind in opposite direction depending on their helicity.[55] Important efforts have been made towards the construction of helical chirality through a [2+2+2] cycloaddition process in the presence of various transition metals. Once again, application of the reactivity of cationic rhodium complexes to this end has been envisaged. In 2007, Tanaka and co-workers described the first enantioselective synthesis of [7]helicene-like compounds under rhodium catalysis conditions.[56] The same authors then applied this strategy to the rapid synthesis of longer helicenes by reaction of tetraynes and dialkynylketones to obtain enantioenriched fluorenone-[9]helicenes (Scheme 1.29).[57]

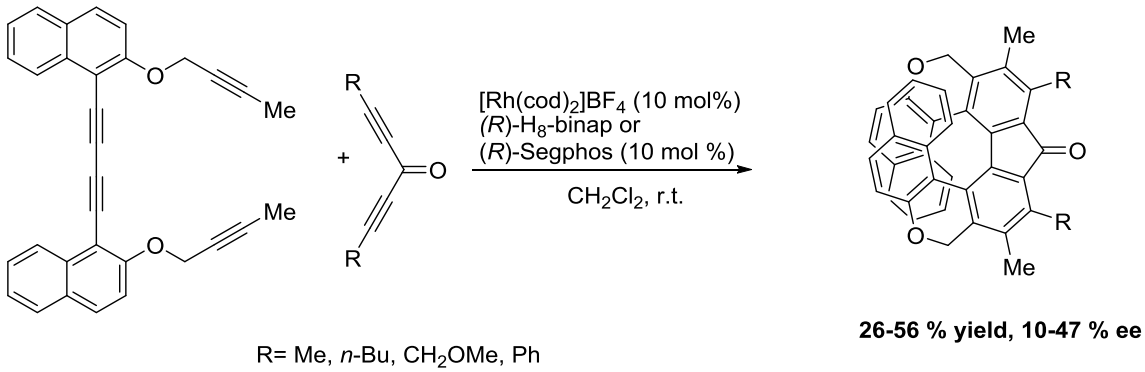

Scheme 1. 29 Rhodium-catalysed partially intramolecular double [2+2+2] cycloaddition leading to enantioenriched [9]helicene-like derivatives

Similarly, dialkynyl phosphorus oxide derivatives can also be employed as substrates for rhodium-mediated cycloaddition with tetraynes, leading to helical phosphafluorenes.[58] Later, enantioselective syntheses of fluorenone- and phosphafluorene-type helicenes were optimized, giving access to a general and efficient method for the formation of 1,1'-bis-triphenylene products (Scheme 1.30).[59]

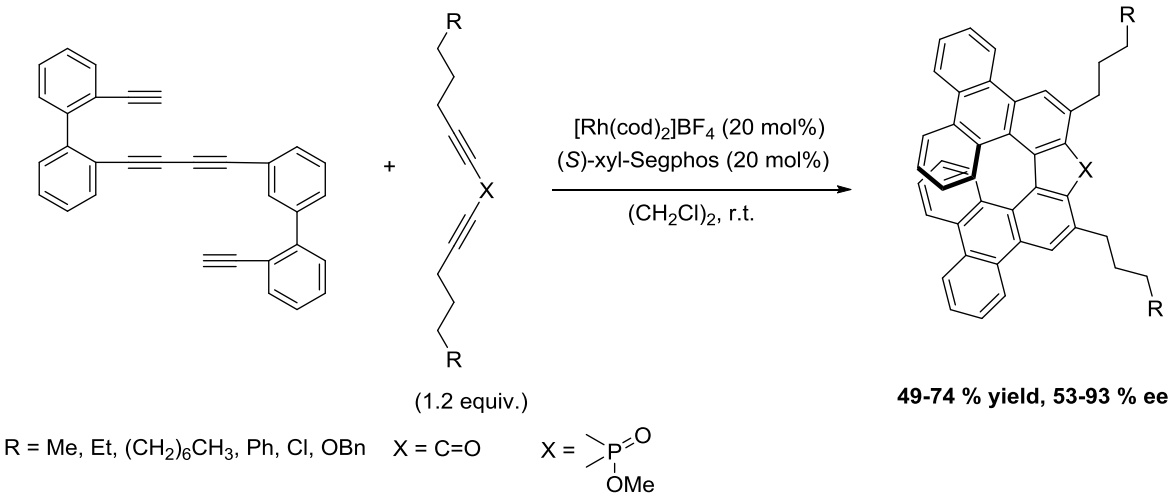

Scheme 1. 30 Optimized asymmetric synthesis of fluorenone helicenes and phosphahelicenes

1.2.4.2.3. Planar chirality in transition-metal catalysed [2+2+2] cycloaddition reactions

Planar chirality is mainly associated with cyclophanes possessing short *ansa* chains, thus preventing the possibility of rotation of the aromatic ring (Scheme 1.31).[60] The transition-metal catalysed [2+2+2] cycloaddition reaction has also been shown to be a suitable method for the enantioselective synthesis of cyclophanes by controlling the regioselectivity of the intramolecular version.

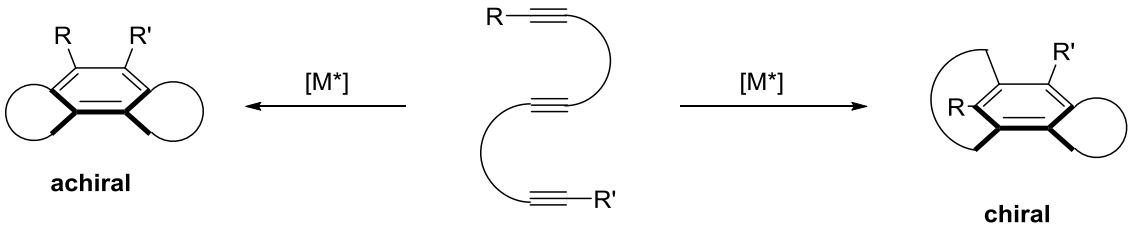

Scheme 1. 31 Access to cyclophanes through [2+2+2] cycloaddition reaction

The first asymmetric synthesis of planar chiral [7]–[10]*meta*-cyclophanes through intramolecular alkyne cyclotrimerization was completed in 2007 and exhibited moderate yields but excellent enantioselectivities (Scheme 1.32).[61] This reaction then opened the way to the development of the corresponding intermolecular version.[62] The strong asymmetric induction observed in the course of these reactions would be the result of a favoured pathway involving the sterically less hindered rhodacyclopentadiene (with regard to the ligand substituents and the *ansa* chain) formed after oxidative coupling of the more reactive 1,6-diyne moiety.

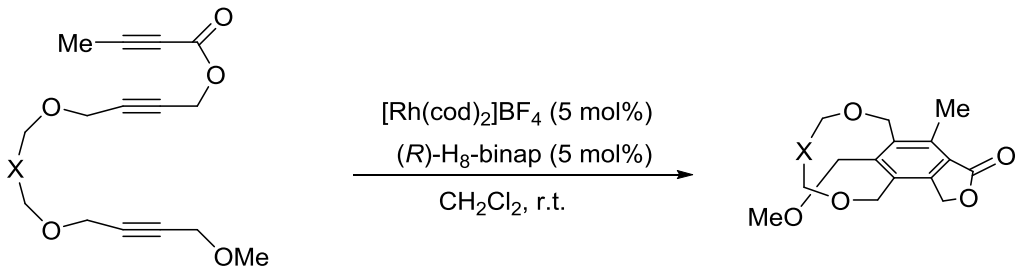

10-31 % yield, 88-98 % ee

X = CH_2, C_2H_4, C_3H_6, C_4H_8, CH_2OCH_2

Scheme 1. 32 First asymmetric synthesis of planar-*meta*-cyclophanes

1.2.4.3. Stereoselectivity in cycloaddition reactions using allenes

A general strategy to increase the number of stereocenters formed in a [2+2+2] cycloaddition product is to replace *sp* hybridized carbons in the reactive unsaturations by sp^2 ones. Indeed, functionalized cyclohexanes incorporating up to six stereogenic centers can in principle be generated by a [2+2+2] cycloaddition involving three alkenes. However, this ideal case remains unsolved. Another alternative is to replace the alkynes not by alkenes but allenes.

Ma et al.[63] showed that three allenes can be efficiently involved in the [2+2+2] cycloaddition reaction. They show that 1,5-bis-allenes can undergo a [2+2+2] cycloaddition with an additional molecule of an allene to generate unsaturated decalin derivatives possessing new stereocenters (Scheme 1.33) although the authors did not attempt the stereoselective version of the reaction.

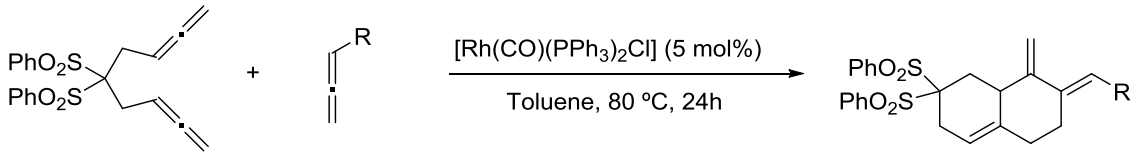

50-56 % yield

R = $CH_2C(CO_2Me)_2$, Ph, CH_2NTsBoc, $(CH_2)_2$NTsBoc, $(CH_2)_2$OH, CH_2phthalimide, $(CH_2)_2$phthalimide,

Scheme 1. 33 Bimolecular cyclization of 1,5-bis-allene with an allene

Alexanian group has directed their efforts towards the stereoselective cyclotrimerization of ene-allenes and allenoates.[64] These reactions exhibit good regio-, chemo-, diastereo-, and enantioselectivities, a plausible mechanism involves a first enantioselective rhodacyclopentane formation through the oxidative coupling of the two allene moieties and subsequent insertion of the final alkene (Scheme 1.34).

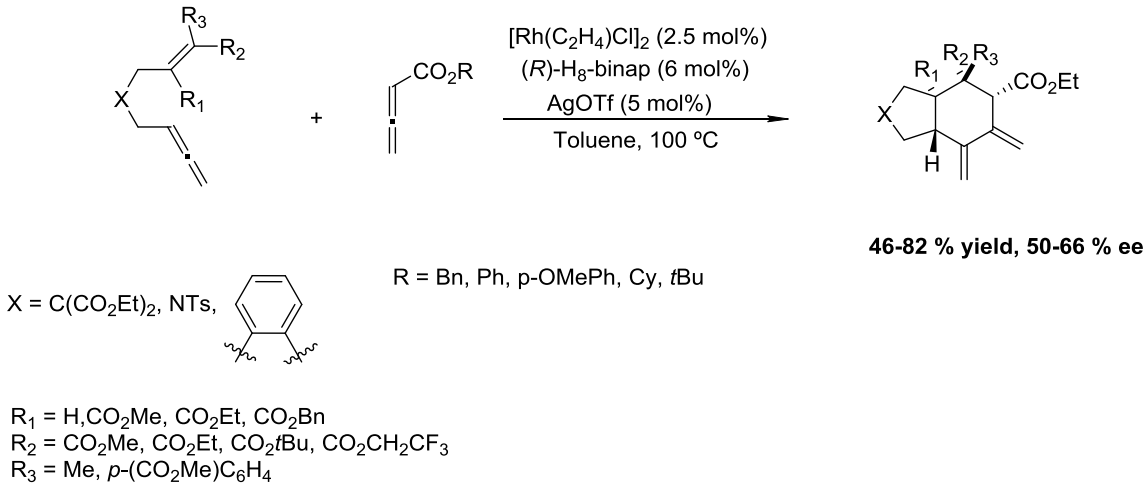

Scheme 1. 34 Enantioselective formation of *trans*-fused carbocycles

Murakami and co-workers described an efficient route to enantioenriched dihydropyrimidine-2,4-diones by intermolecular nickel-catalysed [2+2+2] cycloaddition of two isocyanate units with an allene moiety (Scheme 1.35).[65]

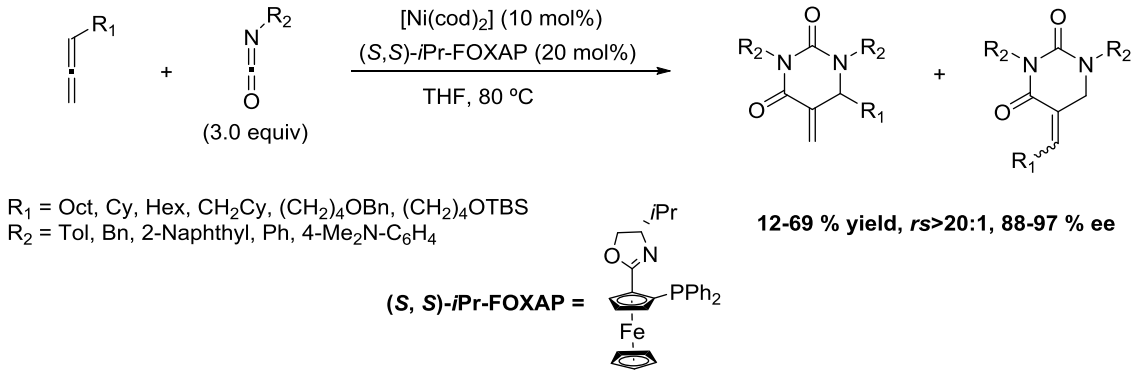

Scheme 1. 35 Enantioselective synthesis of dihydropyrimidine-2,4-diones under nickel catalysis

The examples commented so far on the enantioselective [2+2+2] cycloaddition reaction use the asymmetric synthesis strategy. Chirality transfer and chirality induction are other strategies that can afford an enantiopure product through a [2+2+2] cycloaddition reaction. The precedents on this topic are detailed in chapter 4.

Chapter 2. General objectives

Inspired by the versatility and particularities of allenes in cycloaddition reactions we set out the objectives of the present dissertation that aim to make a contribution to the research field of the rhodium(I)-catalysed [2+2+2] cycloaddition reaction involving allenes.

In the first part of this thesis (Chapter 3 and 4) we aim to explore the intramolecular [2+2+2] cycloaddition reaction as an efficient way to rapidly increase complexity. Our group had evaluated both methodologically and mechanistically the [2+2+2] cycloaddition reaction as an efficient entry to tetracycles by the reaction of macrocyclic substrates, and to tricyclic skeletons starting from linear triunsaturated substrates. Our interest in the construction of topologically new polycyclic structures, prompted us to set up as a first objective of the present thesis, to explore the [2+2+2] cycloaddition reaction of linear allene-ene-allene and allene-yne-allene derivatives. The introduction of allene moieties in the reaction is expected to modify the reactivity and due to the presence of the two orthogonal double bonds selectivity issues will need to be controlled. As highlighted in the introduction, cycloadditions involving allenes have particularities that will also need to be taken into account. The cycloadducts obtained have unreacted double bonds which are amenable for further reactivity. The reactivity of these double bonds will be exploited to further functionalize the cycloadducts obtained. A second important advantage on the use of allenes is the increased stereochemical complexity of the cycloadducts as compared to the analogous reactions involving alkynes. Once the methodology for the racemic version will be established, procedures to obtain the products in an enantiopure form will be sought. Strategies based both on asymmetric catalysis and chiral pool synthesis will be attempted.

Mechanisms that account for the observed reactivity have been proposed for [2+2+2] cycloaddition reactions involving allenes but, to the best of our knowledge, a mechanistic study for such a transformation has not been described. The reaction developed will be studied in order to propose a mechanism which rationalizes the reactivity of allenes in the [2+2+2] cycloaddition reaction, and helps to understand the particularities related to their reactivity.

In the second part of the thesis (Chapter 5) the focus will be set on the involvement of a cyano unsaturation on the cycloadditions reaction. [2+2+2] cycloaddition reactions involving allenes and π-components other than alkynes or alkenes have only been the focus of research in the last few years. Allenes have been reacted with isocyanates and carbonyl derivatives but to the best of our knowledge no example combining in a single [2+2+2] cycloaddition and allene and a nitrile is described, despite the excellent synthesis of pyridines which have been described by cycloaddition of alkynes and nitriles. Therefore we aim to develop reaction conditions that allow the synthesis of nitrogen-containing polycyclic scaffolds by [2+2+2] cycloaddition reactions that combine at the same time an allene and a nitrile.

Chapter 3.

Stereoselective rhodium catalysed [2+2+2] cycloaddition of linear allene-ene/yne-allene substrates

This chapter has been published in:

Haraburda, E.; Torres, Ò.; Parella, T.; Solà, M.; Pla-Quintana, A. *Chem. Eur. J*, **2014**, *20,* 5034.

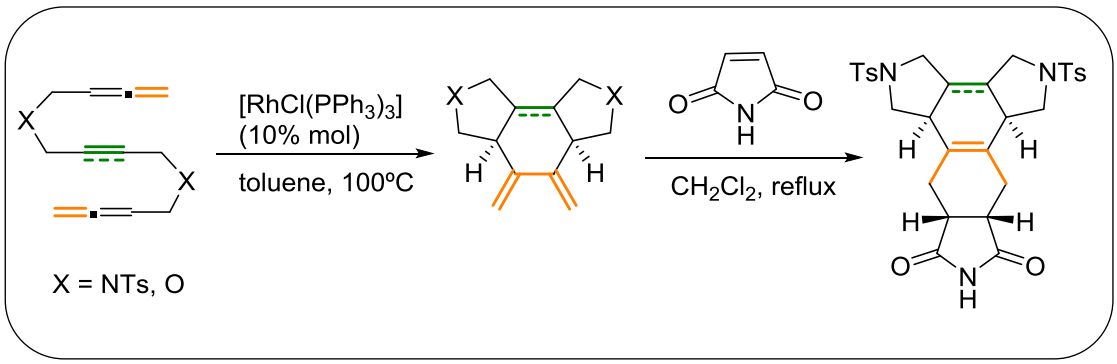

3.1. Results and discussion

After surveying the precedents found in the literature on the use of allenes in the [2+2+2] cycloaddition reaction that have been highlighted in chapter 1, we set out as main objective of this chapter to study the [2+2+2] cycloaddition involving two allene units and either an alkene or an alkyne. In order to decrease the regio- and chemoselectivity problems we decided to attempt the completely intramolecular version, so that the study could focus on the positional selectivity of the double bond and also the stereoselectivity.

3.1.1. Synthesis of the substrates

In order to evaluate the reactivity of allene-ene-allene and allene-yne-allene systems in the completely intramolecular [2+2+2] cycloaddition reaction, four model substrates bearing either and *N*-tosyl (*N*Ts) or *O*-tether were designed (Figure 3.1).

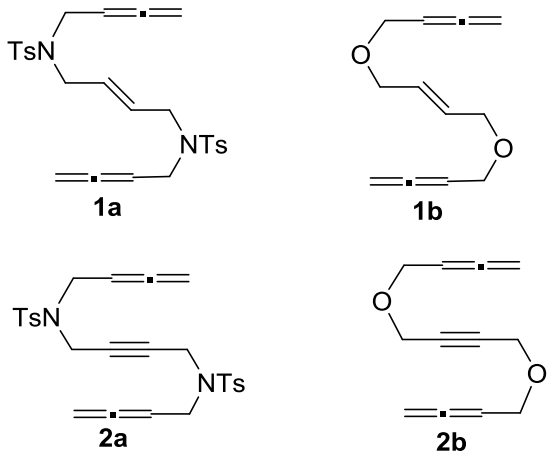

Figure 3. 1 Four model substrates tested in this study

Two different synthetic pathways were envisaged depending on the tether used. The retrosynthetic route proposed for the compounds with *N*Ts-linkage is represented in Scheme 3.1.

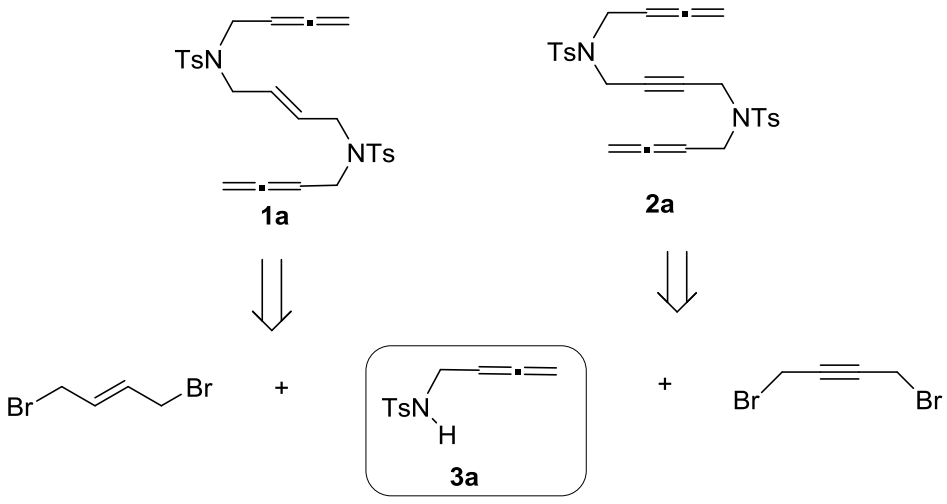

Scheme 3. 1 Retrosynthetic analysis of *N*Ts-linked substrates

Allene-ene/yne-allene substrates **1a** and **2b** could both be prepared through the nucleophilic substitution of either (*E*)-1,4-dibromo-2-butene or 1,4-dibromobutyne with the common intermediate *N*-tosylbuta-2,3-dien-1-amine (**3a**).[66] A different retrosynthetic route was envisaged for the *O*-linked allene-ene/yne-allene substrates (Scheme 3.2):

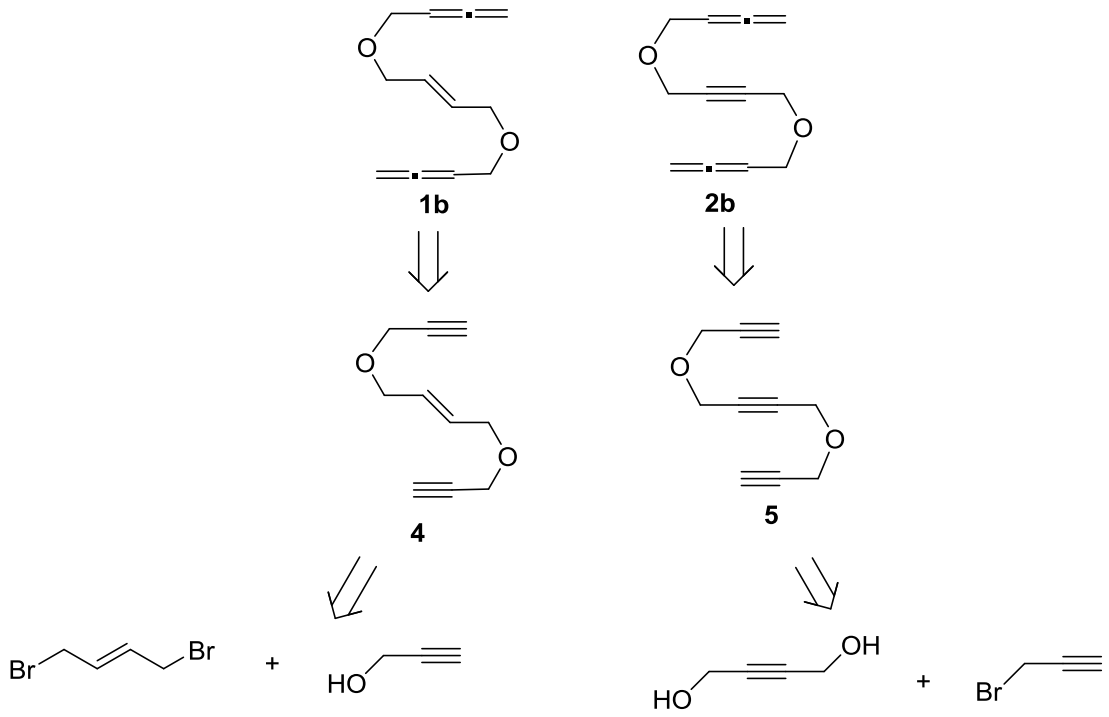

Scheme 3. 2 Retrosynthetic analysis of *O*-linked substrates

It could be possible to prepare *O*-tethered allene-yne/ene-allene compounds **1b** and **2b** by Crabbé-homologation[67] of the corresponding enediyne **4** and triyne **5** compounds that have terminal alkynes. Enediyne **4** and triyne **5**, which have previously been synthesised in our laboratory,[68] could be easily prepared by Williamson ether synthesis from commercially available starting materials. In this case the synthesis of the allenic motif has been planned for the last step of the synthesis mainly to avoid manipulation of highly volatile low molecular weight allenic derivatives bromobuta-1,2-diene **6** and buta-2,3-dien-1-ol **7** (Figure 3.2).[69]

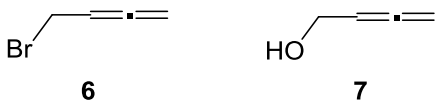

Figure 3. 2 Low molecular weight monosubstituted allenes

3.1.1.1. Synthesis of the NTs-tethered substrates

Compound **3a** was prepared in two steps from 4-toluenesulfonyl chloride, as previously described in the literature.[66] Reaction of the sulfonyl chloride and propargylamine in diethyl ether at room temperature afforded a good yield of 4-methyl-*N*-(prop-2-yn-1-yl)benzenesulfonamide (Scheme 3.3).

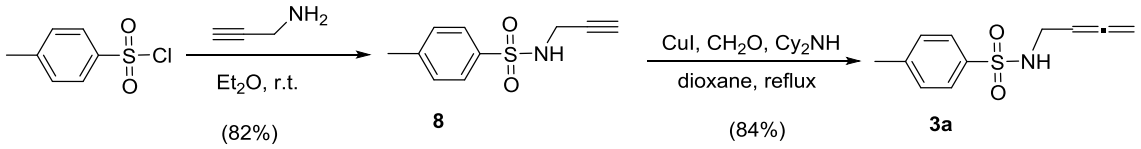

Scheme 3. 3 Preparation of *N*-tosylbuta-2,3-dien-1-amine **3a**

The next step consisted in the construction of the allene by Crabbé homologation. This procedure is often used to obtain allene compounds via homologation of acetylene precursors in the presence of diisopropylamine and formaldehyde under copper catalysis. The reaction proceeds via the stepwise formal retro-imino-ene reaction of the Mannich base intermediate initially formed. The main role of the Cu(I) catalyst is the alkyne activation toward nucleophilic attack by a formal hydride and the stabilization of the incipient formation of a vinyl carbanion at the transition state[70] (Scheme 3.4).

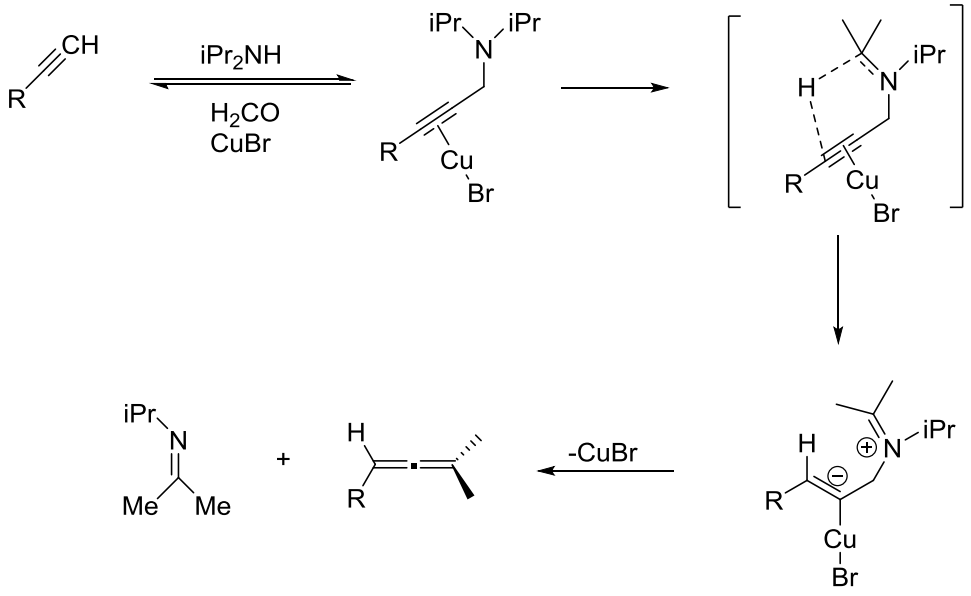

Scheme 3. 4 Mechanism of allene formation in Crabbé homologation

It is important to note that when using diisopropylamine as a secondary amine in the transformation of the terminal alkyne **8** to the allene following the original Crabbé homologation conditions, the reaction took place in only 59 % yield. Using dicyclohexylamine the yield of the reaction improved, and the allene intermediate **3a** was isolated with an 84 % yield. The use of dicyclohexylamine and CuI is an improved methodology of the Crabbé reaction reported by Ma et al.[71]

The next step was the nucleophilic substitution of the corresponding dibromide. Whereas (*E*)-1,4-dibromobutene is commercially available, 1,4-dibromobut-2-yne[72] was prepared from but-2-yne-1,4-diol by an Appel reaction. The two alcohol groups of but-2-yne-1,4-diol were readily converted to bromides using triphenylphosphine and bromine as a halide source in acetonitrile, furnishing a 61 % yield of the desired product (Scheme 3.5).

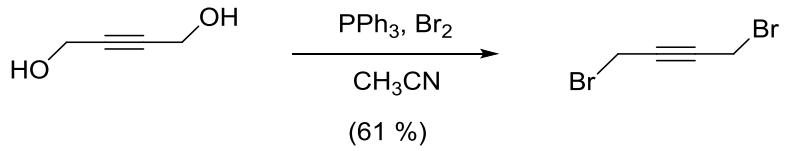

Scheme 3. 5 Preparation of (*E*)-1,4-dibromobut-2-yne

Once the substrates were prepared, compounds with the *N*Ts-tether and either an alkene or alkyne in the centre could be prepared by reacting the respective dibromoderivative with two equivalents of *N*-tosylbuta-2,3-dien-1-amine **3a**. Using potassium carbonate as a base, allene-ene-allene **1a** was obtained with a good yield (56 %), whereas a moderate yield of allene-yne-allene **2a** was afforded (35 %) (Scheme 3.6).

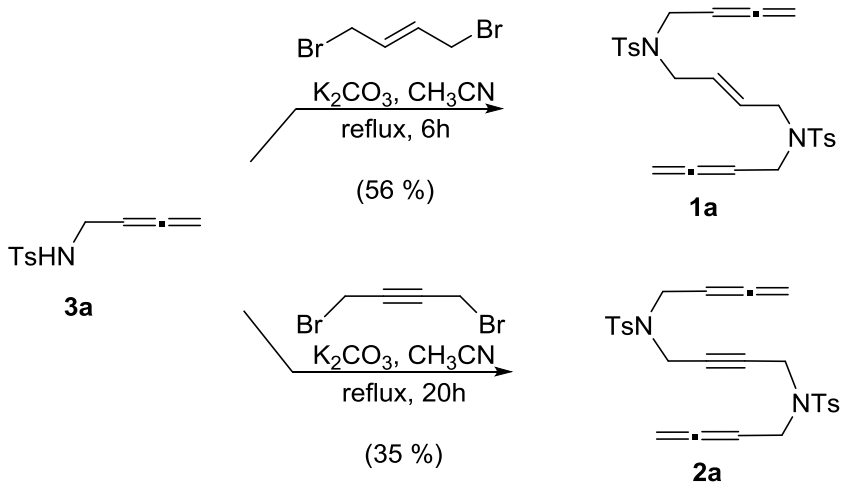

Scheme 3. 6 Preparation of *N*Ts-tethered substrates

3.1.1.2. Synthesis of the O-tethered substrates

In order to gain access to the substrates bearing an oxygen atom in the tether, enediyne **4** or triyne **5** substates were synthesized.[68]

Compound **4** was prepared by a nucleophilic substitution reaction of commercially available (*E*)-1,4-dibromobut-2-ene and prop-2-yn-1-ol. Using sodium hydride as a base in anhydrous tetrahydrofuran the reaction took place affording a good yield of enediyne **4** (Scheme 3.7).

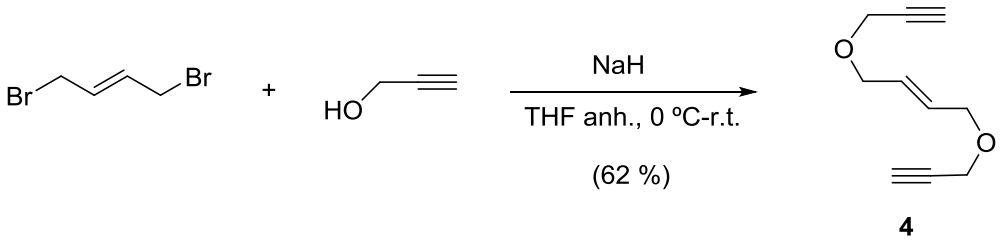

Scheme 3. 7 Synthesis of the *O*-tethered enediyne

Compound **5** was analogously prepared using as an electrophile 3-bromoprop-1-yne, which was attacked by but-2-yne-1,4-diol yielding *O*-linked triyne in 54 % yield (Scheme 3.8).

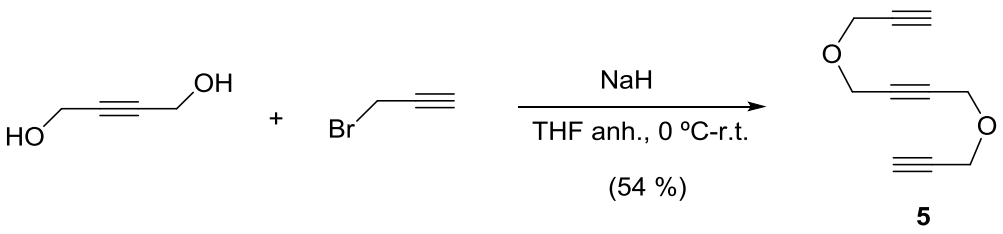

Scheme 3. 8 Synthesis of the *O*-tethered triyne

The terminal alkynes were converted to terminal allenes by Crabbé homologation. When the reaction was performed using diisopropylamine as a secondary amine, the transformation of terminal alkynes **4** and **5** took place with only 32 % and 15 % yields, respectively. When the reaction was carried out with paraformaldehyde in the presence of dicyclohexylamine and copper iodide in dioxane, following the improved methodology of Ma et.al,[71] the desired bisallenic products were obtained in greatly improved yields (Scheme 3.9).

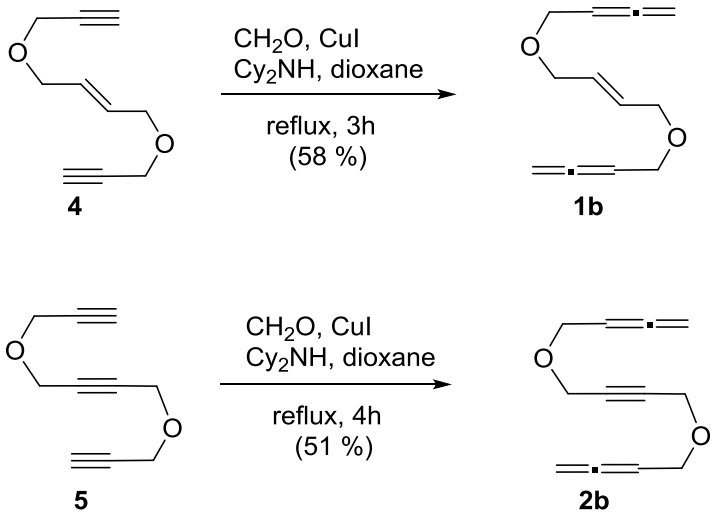

Scheme 3. 9 Synthesis of the *O*-tethered substrates

3.1.2. Structural study of compounds 1a, 1b, 2a and 2b.

Allenic compounds **1a**, **1b**, **2a** and **2b** were fully characterized using the common spectroscopic techniques. Among them, proton and carbon-13 nuclear magnetic resonance and mass spectroscopy were the most informative. A summary of the most relevant data obtained is shown in Table 3.1.

The four different allene-ene/yne-allene compounds were analysed by high resolution mass spectrometry with electrospray ionization (ESI-HRMS) in the positive ion mode. In all cases the spectra obtained gave signals which corresponded to adducts of the molecular peak with sodium that matched well with the theoretically predicted mass and isotopic pattern.

Table 3. 1 Spectroscopic data of compounds **1** and **2**

Allene-ene/yne-allene	ESI-HRMS (m/z)	^{1}H NMR δ(ppm)			^{13}C NMR δ (ppm)		
		-CH_2-	$-\overset{}{\underset{H}{C}}=$	$=C=CH_2$	-CH_2-	$-\overset{}{\underset{H}{C}}=$	$=\overset{1}{C}=\overset{2}{CH_2}$
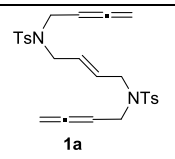 1a	521.1557[M+Na]$^+$	3.77-3.81 (8H)	4.79 (2H)	4.69 (4H)	45.7 47.8	85.4	^{1}209.5 ^{2}76.6
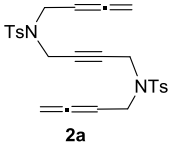 2a	519.1401[M+Na]$^+$	3.68 (4H) 3.94 (4H)	4.90 (2H)	4.72 (4H)	35.9 45.5	85.3	^{1}209.6 ^{2}76.4
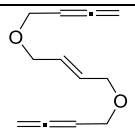 1b	215.1053[M+Na]$^+$	4.00-4.04 (8H)	5.23 (2H)	4.78 (4H)	67.8 69.7	87.6	^{1}209.3 ^{2}75.7
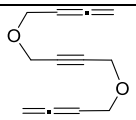 2b	213.0899[M+Na]$^+$	4.10 (4H) 4.22 (4H)	5.23 (2H)	4.81 4H)	57.1 67.4	87.1	^{1}209.6 ^{2}75.9

The nature of the tether used and central unsaturation in these compounds have a clear influence on the chemical shift of the signals in the NMR spectra (Table 3.1). For example, the methylene protons next to the *N*Ts-tether appear around δ 3.8 ppm, whereas when oxygen is used, they are shifted downfield up to a chemical shift of around 4.1 ppm. The same happens with the methine proton of the allene, which varies from δ 4.79 and 4.90 ppm for the *N*Ts-tether substrates to δ 5.23 ppm for the *O*-tether ones. In the ^{13}C NMR spectra, the same methine carbons are observed at δ 85 ppm for the *N*Ts-tethered substrates **1a** and **2a** and at around 87 ppm for the ones with an *O* as a tether. Carbon signals are shifted slightly downfield in *O*-linked substrates when compared to the analogous signals for the *N*Ts-tethered compounds.

3.1.3. Reactivity studies

3.1.3.1. [2+2+2] cycloaddition reaction using allene-ene-allene substrates

Wilkinson's catalyst, named after G. Wilkinson[73] who discovered it in 1964, was the first highly active homogeneous catalyst to be reported. This coordination compound whose formula is $[RhCl(PPh_3)_3]$, is a 16e-complex with the metal in the +1 oxidation state. It is very simply prepared by reacting rhodium(III) trichloride with an excess of triphenylphosphine in absolute ethanol. The use of Wilkinon's catalyst is particularly attractive due to its commercial availability and relatively low cost. Furthermore, it is a catalyst that is very robust, versatile and easy to handle and which has shown an excellent performance in [2+2+2] cycloaddition reactions, as it has been described by our and other groups. For these reasons, Wilkinson's catalyst was selected as the catalytic species to start the reactivity study.

The allene-ene-allene with *N*Ts-tether substrate was chosen to perform the optimization studies. Reactions were carried out in different solvents, such as dichloroethane (DCE), methanol or toluene, at different temperatures (Table 3.2).

Table 3. 2 [2+2+2] cycloaddition reaction using Wilkinson's catalyst

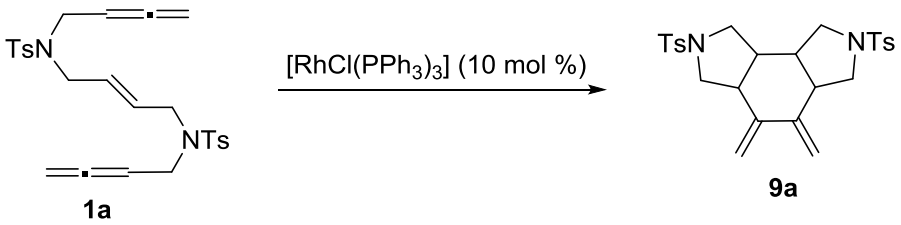

1a **9a**

Entry	Solvent	Reaction temp/ reaction time	Product, yield %
1	DCE	8h, 40˚C	30
2	MeOH	8h, 40˚C	35
3	Toluene	8h, 40˚C	32
4	MeOH	2.5h, 65˚C	38
5	Toluene	6.5h, 100˚C	41

When the reaction was run at 40˚C for 8 h, a new product was formed in the three different solvents (Entry 1-3, Table 3.2). The moderate yields of aroun d 30% in which the product is obtained can be explained by the starting material not being fully consumed and also by the decomposition of either the starting material or some intermediate in the reaction conditions.

The product was isolated and purified by column chromatography and afterwards analysed by NMR spectroscopy. An analysis of the olefinic region of the ^{1}H NMR spectra (Figure 3.3) clearly revealed that a tricyclic cycloadduct with two exocyclic double bonds was formed, indicating that the internal double bonds of the allene have reacted regioselectively in the process (Scheme 3.10). The four singlets observed correspond to the two methylenic units. As inferred from the HSQC spectra the two signals labelled with a green triangle belong to one exocyclic bond whereas the other two marked with the green rectangle belong to the other one.

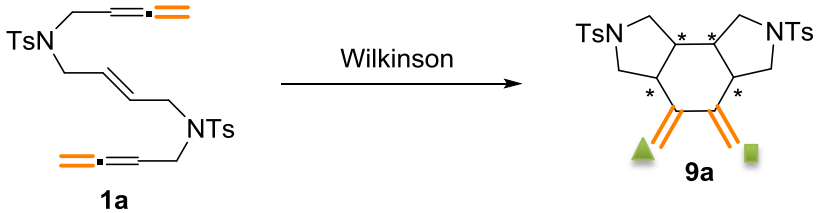

1a **9a**

Scheme 3. 10 Product formed in the [2+2+2] cycloaddition of substrate **1a**

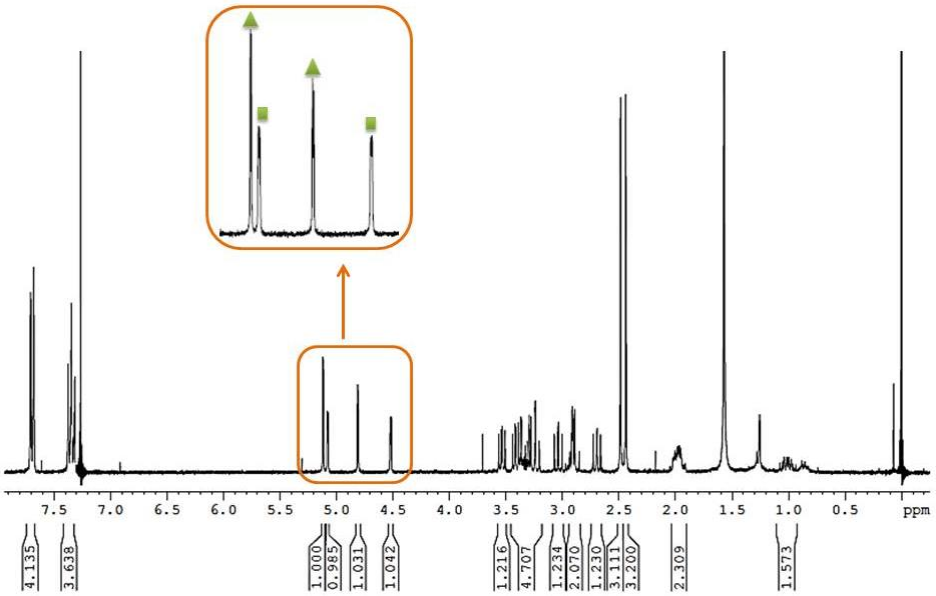

Figure 3. 3 ^{1}H NMR spectrum of the product formed showing olefinic proton signals

Furthermore, a single diastereoisomer with four stereogenic centres was formed. It is well known that [2+2+2] cycloaddtion reactions involving double bonds are stereospecific.[5g,20a,32,64b] So having started from a *trans* double bond, only products with a relative *trans* disposition of the two protons H^a and H^b in the cyclohexanic ring were considered as possible products for the [2+2+2] cycloaddtion reaction (Figure 3.4).

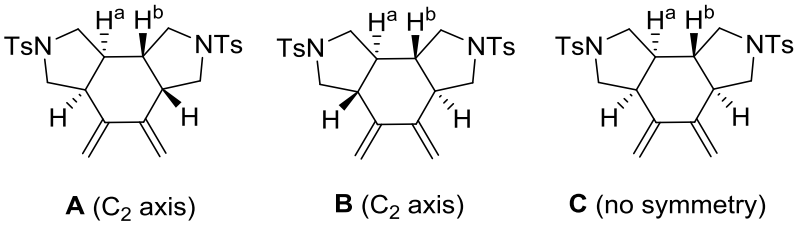

Figure 3. 4 Three possible diastereoisomers with *trans* protons coming from the alkene

The ^{1}H NMR spectra did not show a symmetrical product, so **A** and **B**, which both featured a C_2 axis, were discarded. Thus, diastereisomer **C** was considered to be the more likely diastereisomer formed as was later confirmed by 2D NMR. After a complete chemical shift assignment of the signals, the dipolar couplings observed in the NOESY spectrum (Figure 3.5) were analysed and compared with the distances obtained in the modelled structure of diastereoisomer **C** for cycloadduct **9a**.

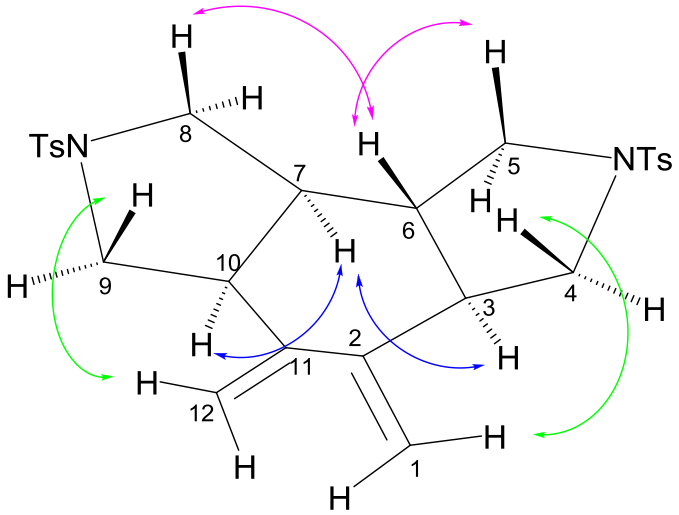

Figure 3. 5 Representation of cycloadduct **9a** showing the major NOESY correlations that were observed, helping to confirm the proposed geometry

Olefinic proton signals on C1 and C12 were used to differentiate the diastereotopic protons in proximal methylenic units C4 and C9 (green arrows). Intense dipolar couplings between the axial protons on C5 and C8 and the H6 proton were observed (pink arrows), whereas no NOE cross-peaks were observed between the H6 proton with any of the H3, H7 and H10 protons, confirming its relative *anti* conformation with the abovementioned protons. On the other hand, the H7 proton shows strong NOE with the H3 and H10 protons (blue arrows) indicating their relative *cis* relationship. The scalar couplings could not be completely determined due to the overlapping of signals.

Once the structure of the product was known, we next proceeded to further optimize the reaction conditions. Reaction with Wilkinson's catalyst was repeated using toluene and methanol as a solvent at 65˚C and 100˚C, respectively. In both cases, by applying a higher temperature we were able to complete the starting material and increase the yield of the reaction (compare entries 2 and 4, and 3 and 5 in Table 3.2). Since a slightly higher yield was obtained with toluene, this solvent was selected to continue with the optimization. It became obvious during the optimization studies that the reaction time and temperature were having a significant influence on the yield. The reaction at temperatures lower than 100˚C did not reach completion and degradation increased when the temperature was raised further or the reaction time was increased.

The optimized conditions set as for toluene at 100˚C were applied to the allene-ene-allene substrate with oxygen tethers (Table 3.3). The reaction was again diastereoselective, giving a 44 % yield of cycloaduct **9b** (Entry 2, Table 3.3).

It is noteworthy that the reaction proceeded satisfactorily without the need for the electron withdrawing CO_2R group, which has proven crucial in other [2+2+2] cycloaddition reactions involving allenes.[35,37,63,64]

Table 3. 3 [2+2+2] cycloaddition of allene-ene-allene substrates

Entry	Substrate	Time [h]	Product	Yield %
1	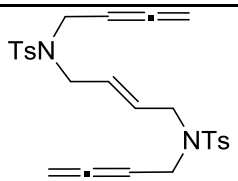 **1a**	6.5	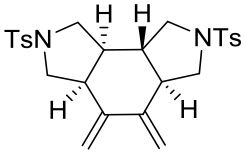 **9a**	41
2	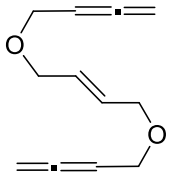 **1b**	2	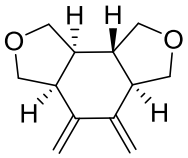 **9b**	44

3.1.3.2. [2+2+2] cycloaddition reaction using allene-yne-allene substrates

With the reaction conditions established in the optimization studies, the substrates with a central triple bond were evaluated (Scheme 3.11).

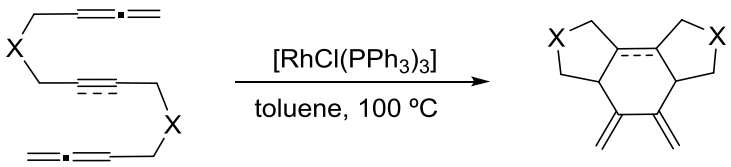

2a (X=Ts)
2b (X=O)

10a (X=Ts)
10b (X=O)

Scheme 3. 11 [2+2+2] cycloaddition of allene-yne-allene substrates

The allene-yne-allene substrates were treated with Wilkinson's catalyst in toluene, heating at 100˚C. We were pleased to find again that the reaction was completely regioselective with cycloaddition taking place only with internal double bonds of the allene furnishing tricyclic dienes. Furthermore, the reaction was diastereoselective and just one of the possible diastereisomers for each product was obtained in a moderate yield (Table 3.4).

Table 3. 4 [2+2+2] cycloaddition of allene-yne-allene substrates

Entry	Substrate	Time [h]	Product	Yield %
1	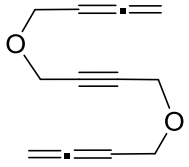 **2a**	2	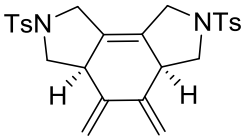 **10a**	32

2	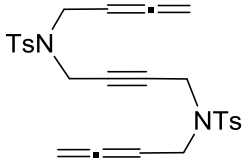 **2b**	1	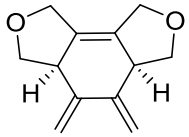 **10b**	27

Two different diastereoismers can be formed in the cycloaddition showing either a symmetry plane or a C_2 axis (Figure 3.6). 1D and 2D NMR experiments were examined to determine the product formed but since both are symmetric isomers, it was not possible to obtain an unambiguous answer at this point.

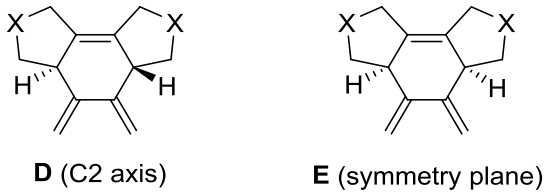

D (C2 axis) **E** (symmetry plane)

Figure 3. 6 The two diastereoismers which can be formed upon [2+2+2] cycloaddition of allene-yne-allene substrates

3.1.4. Diels-Alder reaction

Since the [2+2+2] cycloaddition reactions studied formed regio- and diastereoselectively tricyclic structures with a diene, we decided to test them in Diels-Alder reaction in order to increase the molecular complexity. [37,63,64] Cycloadducts **9a** and **10a** bearing the *N*Ts-tether were treated with maleimide in dichloromethane at reflux (Scheme 3.12). Pentacyclic adducts were afforded in good to excellent yields in short reaction times. The two scaffolds differ in the central cyclohexanic ring. Compound **11a** contains a cyclohexene ring, whereas the other compound (**12a**) has a 1,4-cyclohexadiene central ring. The process was again diastereoselective and only one diastereoisomer was formed in each of the reactions.

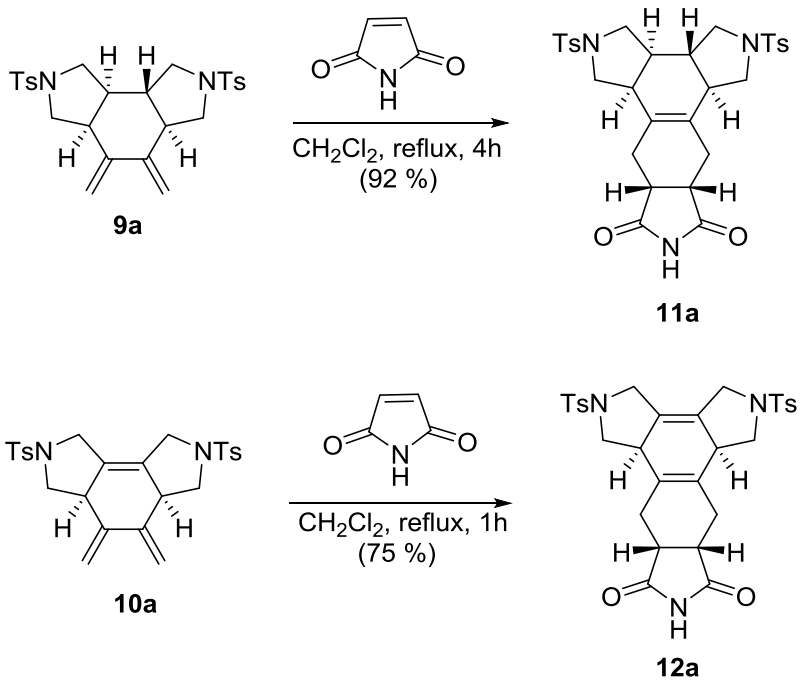

Scheme 3. 12 Diels-Alder reaction of the tricyclic diene cycloadducts

Analysis of the NMR spectroscopic data allowed us to determine the diastereoisomer formed in the [2+2+2] cycloaddition of the allene-yne-allene substrate (Figure 3.7). Cycloadduct **12a** is a symmetrical product proving that compound **10a** also had a symmetrical plane allowing us to conclude that diastereoisomer **E** had been formed for compound **2a** with the two hydrogens in *syn* position.

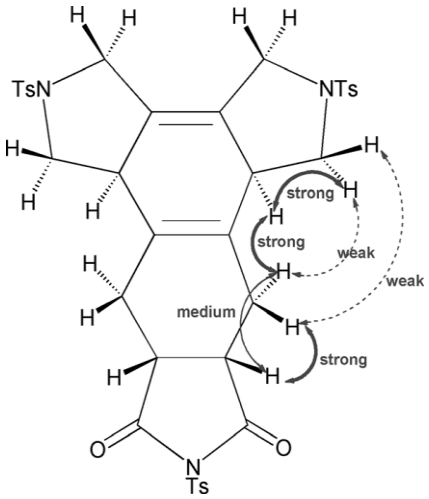

Figure 3. 7 Representation of cycloadduct **12a** showing the major NOESY correlations that are observed

3.1.5. Enantioselectivity study

The cycloadducts obtained from the [2+2+2] cycloaddition of allene-ene-allene substrates have four contiguous stereogenic centres, so we decided to look for conditions to achieve an enantioselective process.

Rh(I) complex $[Rh(cod)_2]BF_4$, due to its ability to produce *in situ* complexes with different chiral ligands, has been shown to form very efficient and versatile transition metal catalyst for stereoselective reactions. Tanaka,[74,75,79] whose group has made the greatest contribution in the field of stereoselective [2+2+2] cycloaddition reactions, developed a methodology involving the use of a catalytic system formed by the cationic rhodium complex $[Rh(COD)_2]BF_4$ and binap-type chiral diphosphines (Figure 8). This has enabled the preparation of compounds with axial,[52,53,74] helical,[54,56,75a] planar,[61,62,75] and central[43,44,45,51] chirality with excellent enantiomeric excesses.

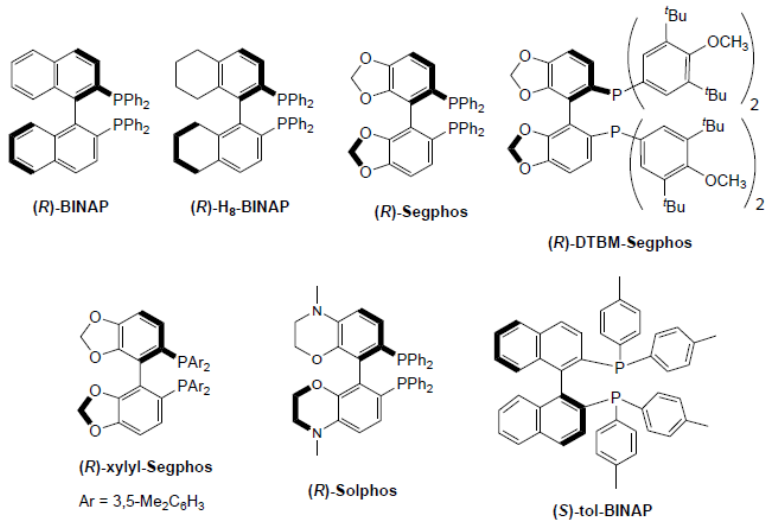

Figure 3. 8 Selected examples of chiral binap-type diphosphines used in enantioselective Rh-catalysed [2+2+2] cycloaddition reactions

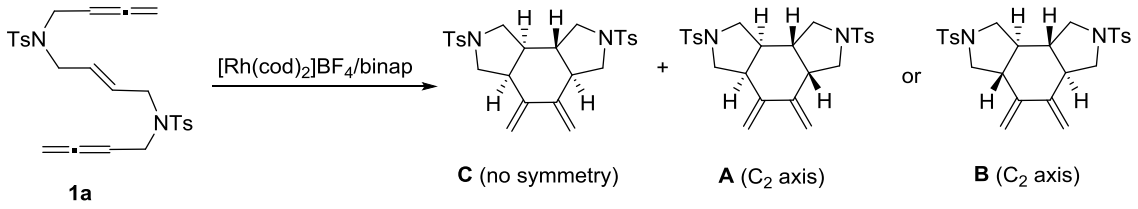

Scheme 3. 13 [2+2+2] cycloaddition reaction using cationic rhodium catalyst

Table 3. 5 [2+2+2] cycloaddition reaction using cationic rhodium catalyst

Entry	Rhodium source	Ligand/Additive	Solvent	Reaction time/temperature	Product ratio[a]/Yield[b]
1	$Rh(cod)_2BF_4$	(*R*)-H_8-binap / -	MeOH	72h / r.t.	4:1 /35%
2	$Rh(cod)_2BF_4$	(*R*)-H_8-binap / -	DCM	42h / r.t.	1:1 / 46%[c]
3	$Rh(cod)_2BF_4$	(*R*)-H_8-binap / -	Toluene	18h / r.t.	3:1 / 34%
4	$Rh(cod)_2BF_4$	(*R*)-binap / -	DCM	72h / r.t.	4:1 / 35%
5	$Rh(cod)_2BF_4$	(*R*)-binap / -	Toluene	72h / r.t.	2:1 /32%
6	$[RhCl(C_2H_4)_2]_2$	(*R*)-H_8-binap/ $AgBF_4$	Toluene	24 h / 50˚C	2:1 / 24%
7	$[RhCl(C_2H_4)_2]_2$	(*R*)-H_8-binap/ $AgBF_4$	Toluene	19 h / 100˚C	2:1 / 47%

[a] Ratio of the non-symmetric to the symmetric diastereoisomers calculated by ^{1}H-NMR analysis of the reaction mixture. [b] The yield refers to the mixture of the two diastereoisomeric products. [c] The mixture was separated to give two products in 24 % and 22 % yield, respectively.

Initially, combinations of (*R*)-binap or (*R*)-H_8-binap with $Rh(cod)_2]BF_4$ were tested as the catalytic system (Scheme 3.13 and Table 3.5). The catalyst was generated *in situ* by hydrogenation of a mixture of the cationic rhodium source and the biphosphine in dichloromethane for 30 minutes. After this time, both the hydrogen and solvent were removed from the flask and the appropriate solvent was added. The diallene substrate was then introduced, dissolved in the reaction media, and the reaction mixture was stirred at room temperature. In all cases, even though the starting material could not be completely consumed, two new products were formed in different ratios as determined by ^{1}H NMR analysis of the crude reaction mixture. As an example, the ^{1}H NMR spectrum of the reaction crude for the reaction run using (*R*)-H_8-binap as a ligand and dichloromethane as a solvent (Entry 2, Table 3.5) is shown in Figure 3.9. In the olefinic region, the signals of exocyclic protons of the products formed are observed. A symmetric and a non-symmetric product can be clearly distinguished. The four signals marked with a green rectangle belong to the four olefinic protons of the non-symmetric product (**5a**), which was obtained and characterised when the Wilkinson's was used as a catalyst. In the other product, only two signals labelled with an orange triangle are observed corresponding to a symmetric cycloadduct, which may correspond to either diastereoismer **A** or **B**.

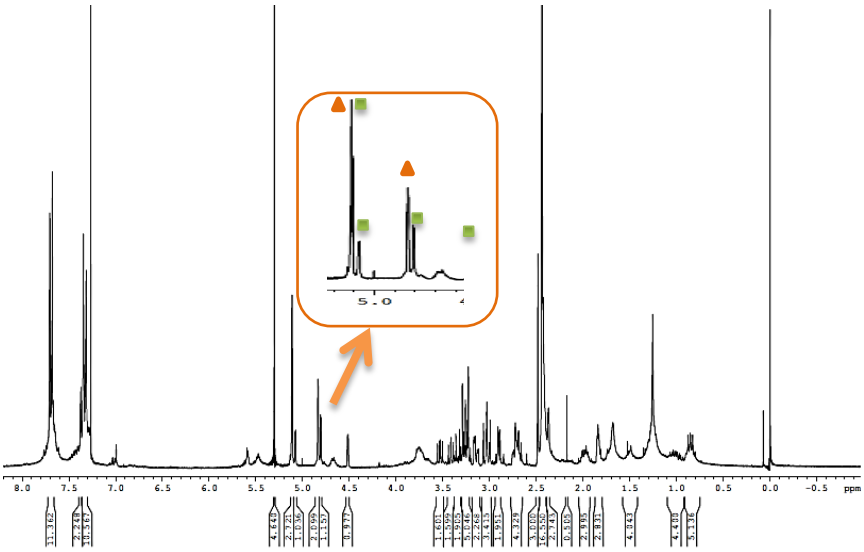

Figure 3. 9 ^{1}H NMR spectrum of mixture of products showing olefinic protons signals

When using (*R*)-H_8-binap as the ligand, the reaction run using dichloromethane as solvent gave the best yield but the lower diastereoisomeric ratio (compare entries 1-3 in Table 3.5). In fact the two regioisomers could be isolated in 24 % and 22 % yield, respectively. When MeOH was used as a solvent, the diastereisomers were formed in a 4:1 ratio of the non-symmetric to the symmetric one (Entry 1, Table 3.5) but the yield was moderate (35 %). Changing the phosphine to (*R*)-binap (Entries 4 and 5, Table 3.5) improved the diastereoisomeric ratio when dichloromethane was used as the reaction media, but the yield was erased. In the case of the

reaction run in toluene the yield could not be improved and the regioisomeric ratio was slightly decreased.

Then, the reaction was tested in the conditions described by Alexanian et al. for the intermolecular [2+2+2] cycloaddition of allene-ene substrates and an allene[64a] (Entries 6 and 7, Table 3.5). The reaction was run using the neutral rhodium dimer $[RhCl(C_2H_4)_2]_2$, (*R*)-H_8-binap and silver tetrafluoroborate as an additive to render the catalytic system cationic. The reaction was run both at 50˚C and 100˚C. Arriving to higher temperature, we could get the consumption of starting material and an increased yield, but analysis of the reaction mixture invariably showed a mixture of diastereoisomers.

The enantioselectivity study was aborted, as in all cases, the combination of a biphosphine ligand and cationic rhodium source although being a more active catalytic system that could in most cases be used at room temperature, could not catalyse the process in a diastereoselective way.

3.1.6. Computational calculations

After exploring the reactivity of our model systems in the laboratory, computational calculations were approached by another member of our group, Òscar Torres under the supervision of Prof. Miquel Solà. Whereas the mechanism for the [2+2+2] cycloaddition has been studied computationally by several groups including ours, the involvement of allenes had not been adressed. We turned our attention to unravel the reaction mechanism of the intramolecular [2+2+2] cycloaddition reaction involving two allenes. With this aim, density functional theory (DFT) calculations at the M06-2X/cc-pVTZ//B3LYP/cc-pVDZ level of theory were performed on the substrate with *O* as a tether, i.e. substrate **1b**, and considering $[RhClPPh_3]$ as the catalytically active species derived from the Wilkinson's catalyst. The use of this active species in the [2+2+2] cycloaddition reaction is justified by a previous study from our group which concluded that the catalytically active species in the oxidative addition process catalysed by Wilkinson's catalyst is the $[RhClPPh_3]$ complex.[7b,6k,l]

[2+2+2] cycloaddition reactions involving unsaturations other than alkynes are postulated as following the same general mechanistic scheme, with some particularities. In the case of reactions involving allenes, such as the ones presented here, there are three aspects that deserve special attention. Firstly, it is necessary to determine the order in which the unsaturations take part in the catalytic cycle (i.e. if the oxidative addition takes place between the two allene moieties or between an allene and the double bond). Secondly, due to the fact that the allenes have two contiguous double bonds, we must determine which of the double bonds is reacting and why. Finally, it is important to explain why the reaction under study is diastereoselective.

To address these three concerns we undertook a DFT study to evaluate the energies involved in the oxidative addition step leading to the rhodacyclopentane intermediate. Of the many possibilities for the oxidative cycloaddition, we decided to study not only the ones which could explain the formation of the carbon skeleton obtained in the experimental results (**1b.2A**-**D**, **1b.2F**, Figure 3.10), but also three cycloadditions involving the terminal double bond of the

allene which did not lead to the observed product (**1b.2E**, **1b.2G**, and **1b.2H**, Figure 3.10). The oxidative addition intermediates involving the ene and the internal double bond of the allene **A**-**D** differ either in the relative disposition of the PPh_3 ligand (**A** and **B**) or the faces of the double bond that had reacted giving different ring fusion of the newly formed bicyclic structure (*cis* for **A** and **B**, *trans* for **C** and **D**).

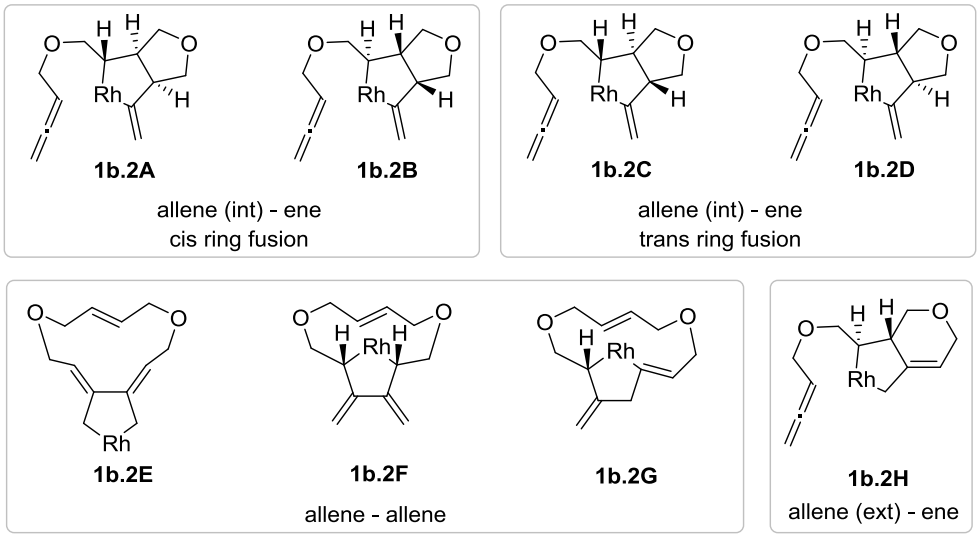

Figure 3. 10 Structure of the different oxidative coupling products modelled in the present study. The rhodacyclopentane compounds **1b.2A-H** has one PPh_3 and a Cl attached to the rhodium which has been omitted in the scheme for clarity

First, the allene (internal double bond) – alkene couplings were analysed (Scheme 3.14). Rhodacyclopentane **1b.2A** is the second most stabilized and has the lowest barrier of formation ($\Delta G^{\ddagger}$=18.7 kcal/mol). The barrier transforming **1b.1B** to **1b.2B**, which differs from **5.2A** by the location of the coordinated PPh_3 and Cl has the highest barrier ($\Delta G^{\ddagger}$=38.2 kcal/mol) showing the importance of the coordination sphere of the metal on the outcome of the reaction (see Figure 3.11). Formation of *trans*-fused bicyclic rhodacyclopentadienes **1b.2C** and **1b.2D** showed significantly higher Gibbs free energy barriers than the formation of **1b.2A**, and were therefore ruled out as possible reaction pathways.

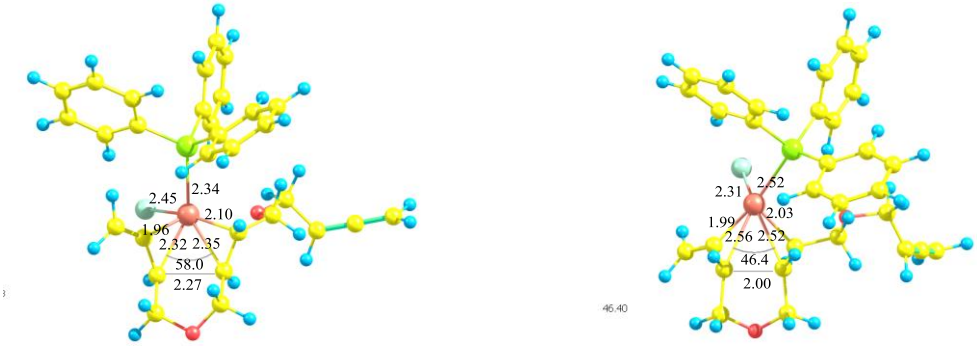

Figure 3. 11 Optimised structures (B3LYP/cc-pVDZ) for **TS(1b.1A, 1b.2A)** (left) and **TS(1b.1B, 1b.2B)** (right)

Next, the allene-allene coupling was evaluated. Only rhodacyclopentane **1b.2F**, which has the two hydrogens in *syn*, and its corresponding transition state were located when the two

internal bonds of the two allenes were considered as reacting unsaturations. All attempts to locate the *anti* stereoisomer were unsuccessful. Oxidative addition involving the internal double bonds of the allene (**1b.2F**) shows a higher Gibbs free energy barrier than when the external double bonds are involved (**1b.2E**) ($\Delta G^{\ddagger}$=19.6 kcal/mol for **1b.2E** and $\Delta G^{\ddagger}$=31.7 kcal/mol for **1b.2F**). The difference in Gibbs energy barriers for the formation of **1b.2A** (allene-ene) and **1b.2E** (allene-allene) is favourable to the allene-ene oxidative addition by only about 1 kcal/mol. However, **1b.2E** is endergonic by 15.5 kcal/mol and, therefore, thermodynamically disfavoured. The reason for the low stability of **1b.2E** has to be ascribed to the fact that it is the only oxidative coupling product having two trisubstituted *Z* double bonds. Finally, although the **1b.2G** species that result from the allene (external double bond)–ene is the most exergonic addition, it has a barrier that is about 8 kcal/mol higher than the one leading to **1b.2A**. Therefore, we conclude that the preferred oxidative coupling pathway was the alkene–allene (internal double bond) coupling furnishing a *cis* ring fusion yielding **1b.2A**. The larger reactivity of the internal double bond of the allene (compare **1b.2A** and **1b.2H**, Scheme 3.14) concurs with the fact that the occupied π molecular orbital (MO) corresponding to this internal double bond is 0.4 eV destabilized as compared to the occupied MO of the external double bond.

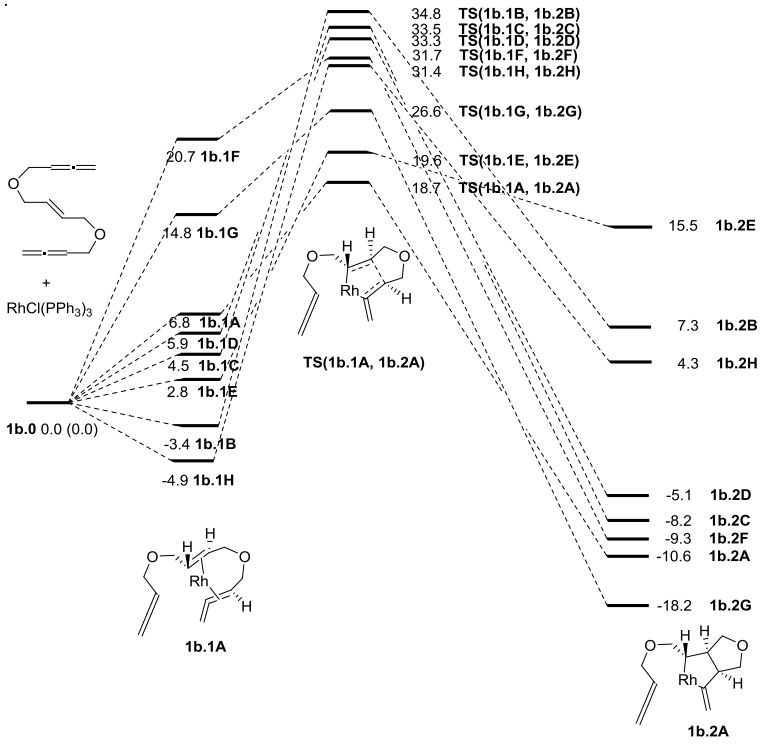

Scheme 3. 14 Gibbs energy profile for the different oxidative coupling products modelled in the present study. Gibbs energies at 298 K are given in kcal/mol. The rhodacyclopentane compounds **1b.1A-H** and **1b.2A-H** have one PPh_3 and a Cl attached to the rhodium which have been omitted in the scheme for clarity

Following the study from the 16-electron complex **1b.2A**, several possibilities emerge for the insertion of the internal double bond of the second allene. We have considered only the internal double bond of the allene for two reasons. First, we have seen in the previous step that the external allene double bond is less reactive than the internal one. Second, addition to the external double bond does not lead to the experimentally observed products. The

insertion of the internal double bond of the allene can take place to give a rhodacycloheptane or a rhodabicyclo [3.2.0]heptane by insertion into one of the Rh-C bonds of the rhodacyclopentane (**I**,**J**,**L**,**M**) or to give a rhodanorbornane (**K**,**N**) by a Diels-Alder like transition state (Scheme 3.14 and Figure 3.12). In the case of the insertion, the rhodacyclopentane is not symmetric, so two possibilities emerge, i.e. insertion on the Rh-Csp^3 (**I**,**L**) or Rh-Csp^2 (**J**,**M**) bond of the rhodacyclopentane. Moreover, the two double bond faces of the internal allene need to be considered. The insertion can take place with the hydrogen on the allene pointing inside the rhodacyclopentane (**I**,**J**,**K**) or outside the rhodacyclopentane (**L**,**M**,**N**). All these different attacks are schematically represented in Figure 3.12. It is worth noting here that just one of the faces of the rhodium catalyst is free to react, since the other one is hindered by the presence of the PPh_3 and the chloride.

Neither the transition state nor the rhodanorbornane intermediate for the Diels-Alder mechanism (**K**,**N**) could be located. This is not surprising taking into account the absence of double bonds in the attacked rhodacyclopentane. However the four other possibilities for the insertion were modelled and the results are represented in Figure 3.12. As can be seen in this Scheme, the barriers for the insertion of the internal allene double bond with the approaches **J** (42.9 kcal/mol) and **L** (29.7 kcal/mol) are too high to be competitive and, therefore, these two attacks were discarded. The approaches **I** (24.0 kcal/mol) and **M** (19.7 kcal/mol) are more favourable and, for this reason, we have continued analysing the reaction path for these two attacks.

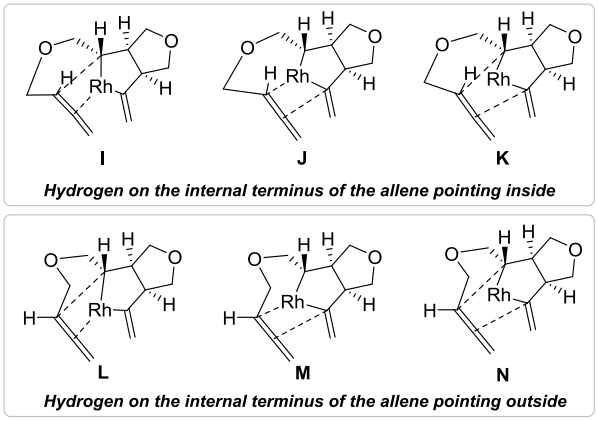

Figure 3. 12 Structure of the different aproximations for the insertion of the internal double bond of the allene to the rhodacyclopentane modelled in the present study. In all cases **(I-N)** the rhodium has one PPh_3 and a Cl attached on the upper face which have been omitted in the scheme for clarity

Next step corresponds to the formation of the C–C bond that generates the final cyclohexane ring. This process takes place through **TS(1b.7, 1b.8)**. The barrier corresponding to the **1b.7M**→**1b.8M** transformation is 25.7 kcal/mol while that of the **1b.7I**→**1b.8I** process is only 12.5 kcal/mol. The main difference comes from the different stability of the **1b.7M** and **1b.7I** intermediates. In particular, **1b.7M** is 11.6 kcal/mol more stable than **1b.7I** because in the former there is an interaction of the Rh with the allene terminal double bond that stabilizes this 16-electron complex (Figure 3.13).

When one depicts the whole Gibbs energy profile of the **1b.0** → **9bC** via approach **M** one finds that the turnover frequency (TOF) determining transition state (TDTS) is **TS(1b.7M, 1b.8M)** corresponding to the ring-closing step (Figure 3.14) and the TOF determining intermediate (TDI), the most abundant reaction intermediate, is **1b.7M** with an energetic span of 25.7 kcal/mol.[76] On the other hand, for approach **I**, the TDTS is **(TS 1b.5I, 1b.6I)** corresponding to the insertion of the second allene (Figure 3.14), the TDI is **1b.2A**, and the energetic span is 24.0 kcal/mol. From these energetic span values and using the Kozuch and Shaik approximation to compute the TOFs,[76] we find that the TOF for the **I** approach leading to the experimentally found product **9bC** is about 18 times higher than that of the **M** approach generating the non-observed product **9bA** (**C** and **A** refer to the corresponding diastereisomers depicted in Scheme 3.13). Although this is not a big difference, it seems enough to justify the exclusive formation of **9bC**. Having different reaction paths in relatively close proximity might possibly explain the decreased selectivity observed when changing the catalytic system from Wilkinson's catalyst to combinations of biphosphines and cationic rhodium complexes.

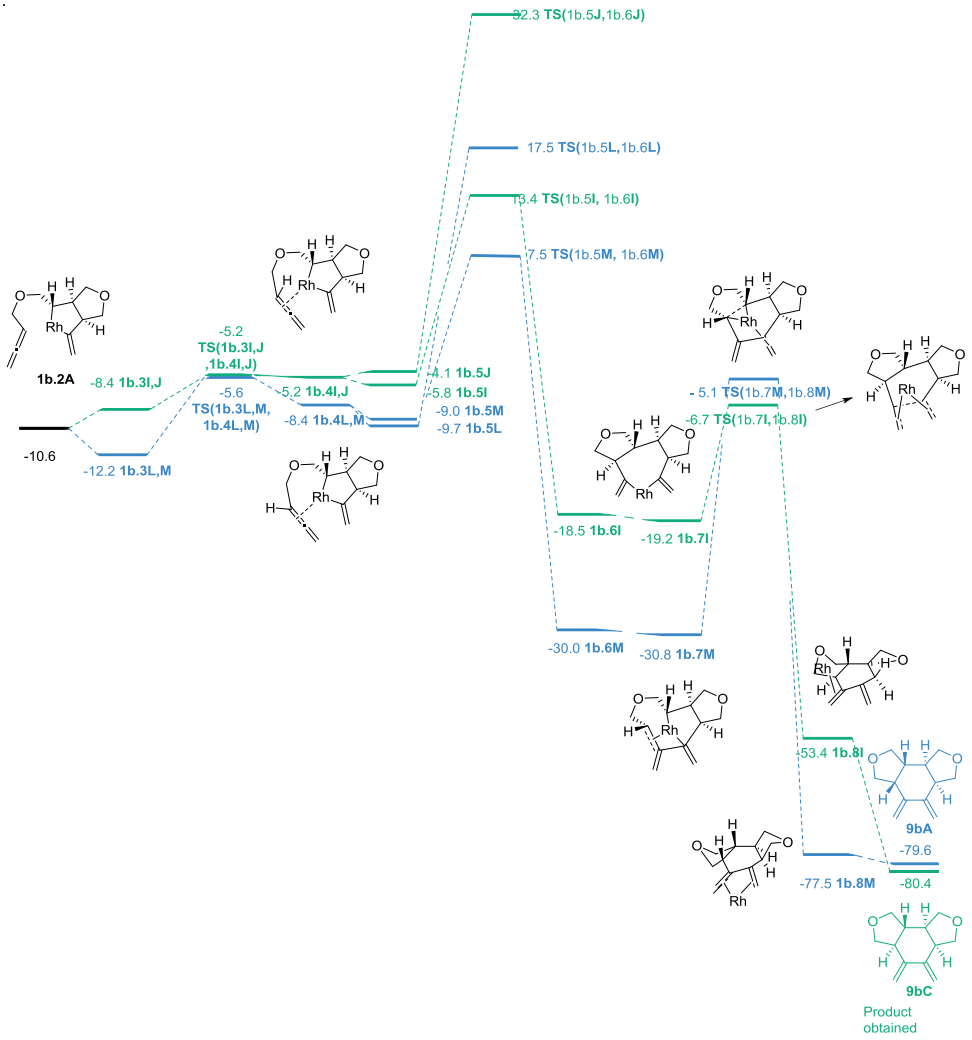

Scheme 3. 15 Gibbs energy profile for the different alkyne insertion and ring closing steps modelled in the present study. Gibbs energies at 298 K are given in kcal mol^{-1}. All intermediates and transition states have one PPh_3 and a Cl attached to the rhodium atom. These ligands have been omitted in the scheme for clarity

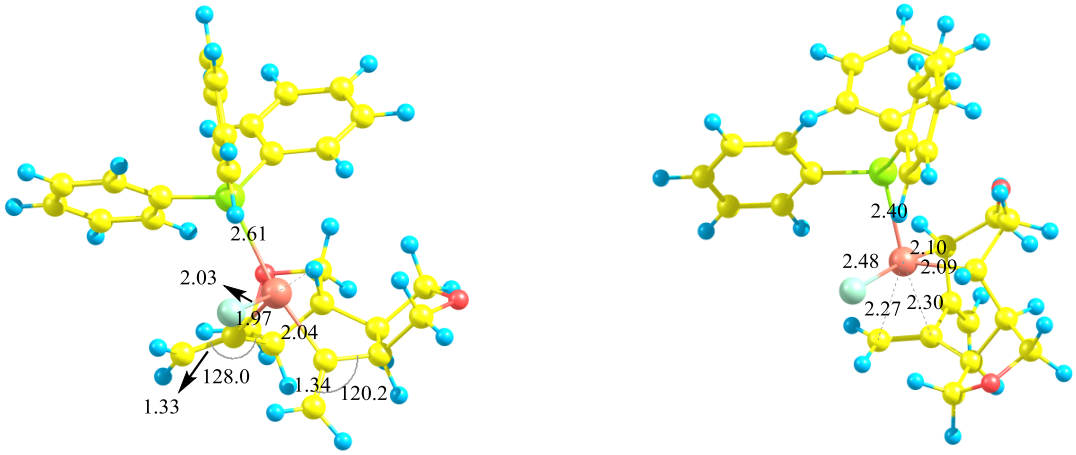

Figure 3. 13 Optimised structures (B3LYP/cc-pVDZ) for **1b.7I** (left) and 1b**.7M** (right)

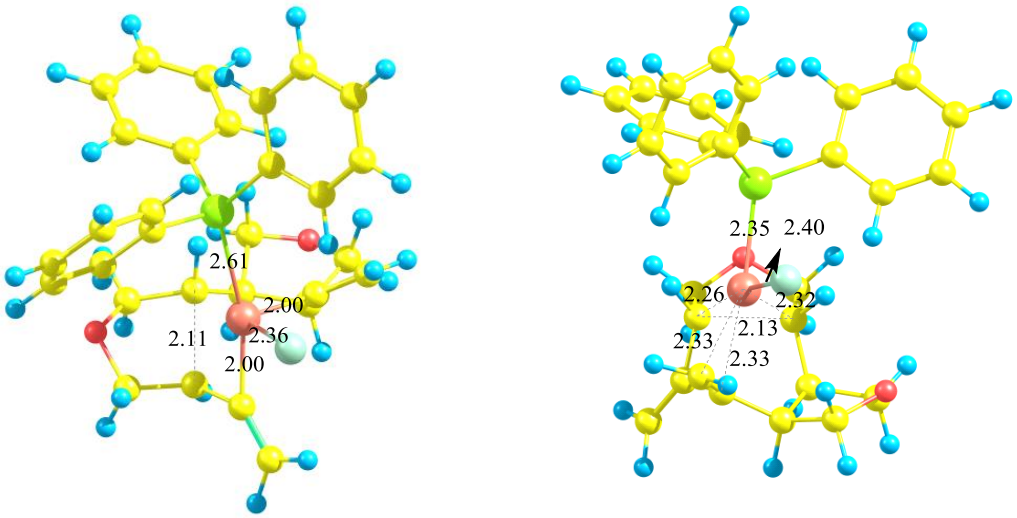

Figure 3. 14 Optimised structures (B3LYP/cc-pVDZ) for **TS(1b.5I, 1b.6I)** (left) and **TS(1b.7M, 1b.8M)** (right)

The complete reaction mechanism for the Rh-catalyzed reaction of allene-ene-allene **1b** that derives the present study is shown in Scheme 3.16. The overall reaction corresponding to **1b.0** to **9bC** transformation is exergonic by 80.4 kcal/mol and the energetic span between TDI and TDTS is 24.0 kcal/mol.

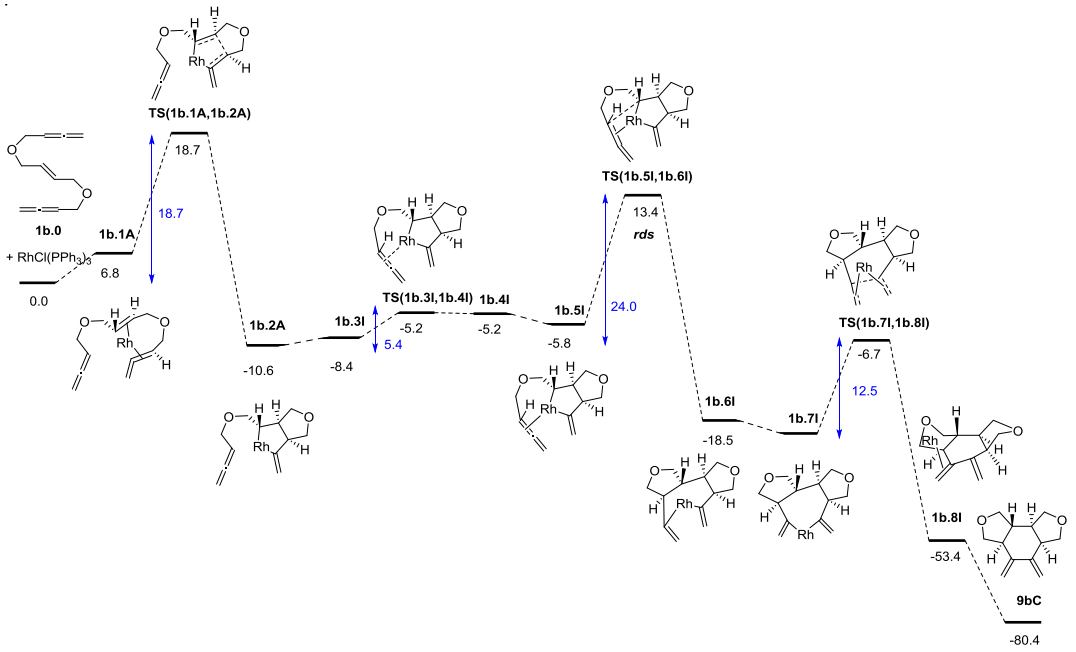

Scheme 3. 16 Gibbs energy profile for the [2+2+2] cycloaddition of allene-ene-allene **1b** where the catalytic species is [$RhClPPh_3$]

A comparative analysis can be performed at this point between linear allene-ene-allene and yne-ene-yne systems[6j] when submitted to a rhodium-catalyzed [2+2+2] cycloaddition reaction. Comparing the corresponding postulated mechanisms, several qualitative differences arise. First of all, the oxidative addition step takes place between the two triple bonds in the yne-ene-yne systems, whereas the allene-ene-allene substrate preferentially reacts by allene-ene oxidative addition. This might be ascribed to the decreased reactivity of the allenes as compared to the triple bonds. On the other hand, the rate determining step also varies for the two systems. Whereas the oxidative addition is the rate-determining step for yne-ene-yne systems, when two allenes are involved in the place of the alkynes, insertion of the third unsaturation becomes the rate-determining step.

Chapter 4.

Chirality induction in totally intramolecular [2+2+2] cycloaddition reaction of a bisallenic substrate

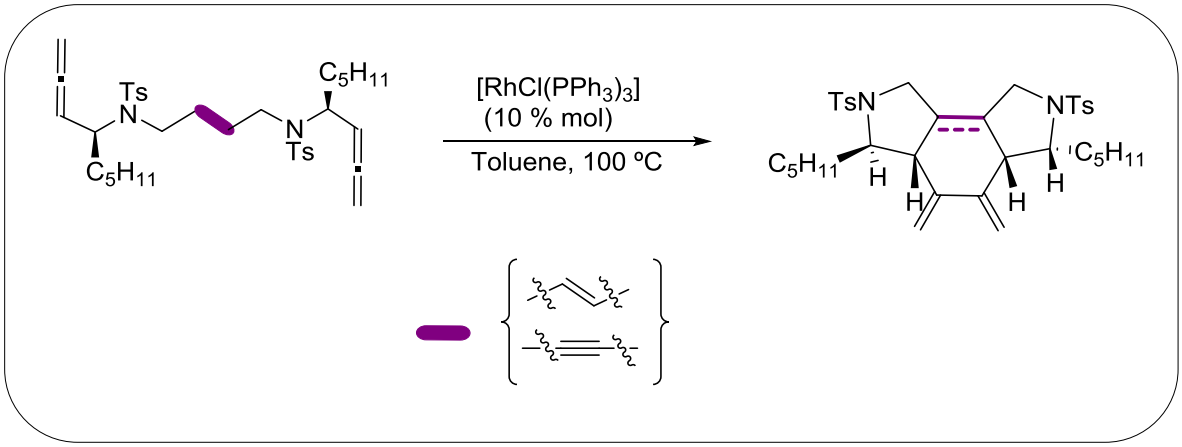

4.1. Precedents

The development of stereoselective methodologies for the introduction of chirality in complex molecules is one of the most significant challenges nowadays. A number of asymmetric syntheses of complex polycyclic (and heterocyclic) compounds using as a key step the transition-metal-catalysed enantioselective [2+2+2] cycloaddition have been reported[40a], as has already been detailed in the introduction section (1.2.4) of this manuscript. These examples clearly demonstrate that the enantioselective [2+2+2] cycloaddition reaction is a powerful tool for the construction in one-step fashion of central, axial, planar and helical chiralities. In most of the cases, the enantiomerically pure compounds are obtained by an asymmetric catalysis strategy, that uses an optimized combination of a transition metal and a chiral ligand that promote the reaction in an enantioselective manner. The majority of the catalytic systems that have been developed so far are based on rhodium(I), iridium(I), and cobalt(I) catalytic systems and the most active catalytic system is based on cationic rhodium complexes and axially chiral biphosphine ligands.

However, there are also a few examples which have used strategies other than the use of a chiral catalyst to obtain an asymmetric synthesis involving the [2+2+2] cycloaddition reaction. Malacria's group described the axial-to-central chirality transfer from an enantioenriched allenediyne.[30] The cobalt catalysed [2+2+2] cycloaddition reaction yielded the cyclohexadiene-cobalt complex almost quantitatively with total axial-to-central chirality transfer due to a highly selective approach on the less hindered allene face (Scheme 4.1).

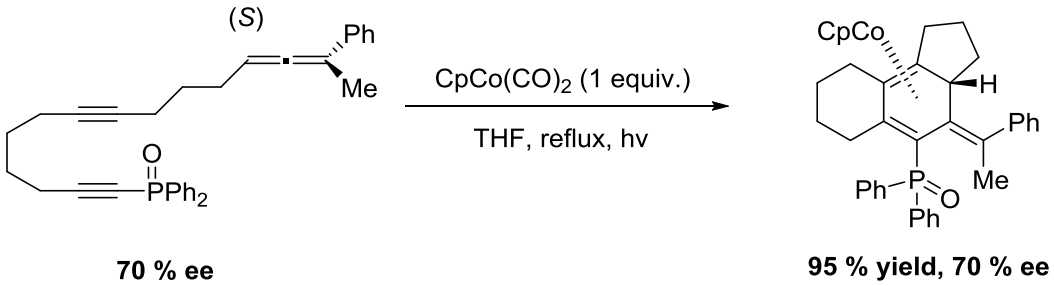

Scheme 4. 1 Axial-to-central chirality transfer in cobalt-catalysed cycloaddition of allenediynes

Whereas in chirality transfer processes a new chiral element is created while the chirality of the original element is lost, another possibility to synthesize an enantiopure compound is a diastereoselective process in which the initial inducing stereogenic element is maintained in the final product.[77] This strategy, referred to as chirality induction has also been applied in the [2+2+2] cycloaddition reaction. Hapke and co-workers reported in 2012 the cobalt(I) catalysed [2+2+2] cycloaddition of chiral proline-derived diynes with nitriles, which led to the formation of both atropoisomers of the axially chiral arylpyridines.[78] No large selectivity effects were observed, presumably due to the distance of the proline moiety to the reaction center, and both atropoisomers were obtained (*dr* ranging from 1:1.05 to 1:1.75). However, this strategy provided access to both diastereisomeric atropisomers which could be easily separated by

column chromatography without the need for chiral catalysts, offering a chiral platform for further manipulations towards ligands and chiral backbones for synthetic purposes (Scheme 4.2).

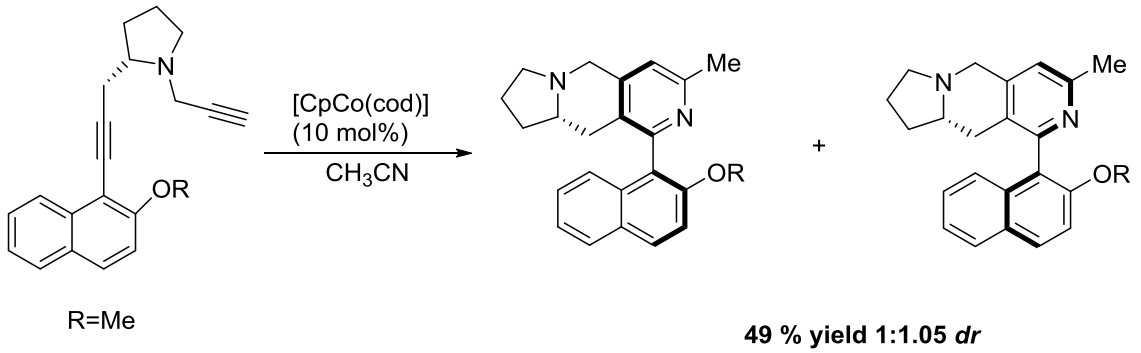

Scheme 4. 2 Selected example of central-to-axial chirality induction in the cobalt-catalysed formation of pyridines described by Hapke et al.

On the other hand, Tanaka *et.al* reported the rhodium(I)-catalysed diastereoselective [2+2+2] cycloaddition of chiral tetraynes with functionalised monoynes to achieve C_2-symmetric axially chiral biaryls (Scheme 4.3).[79] In this case, the reaction was completely diastereoselective leading to enantiopure compounds. Interestingly, the authors demonstrated that the diastereoselectivity of the reaction is under substrate control and not induced even when a chiral ligand is used in the catalytic system.

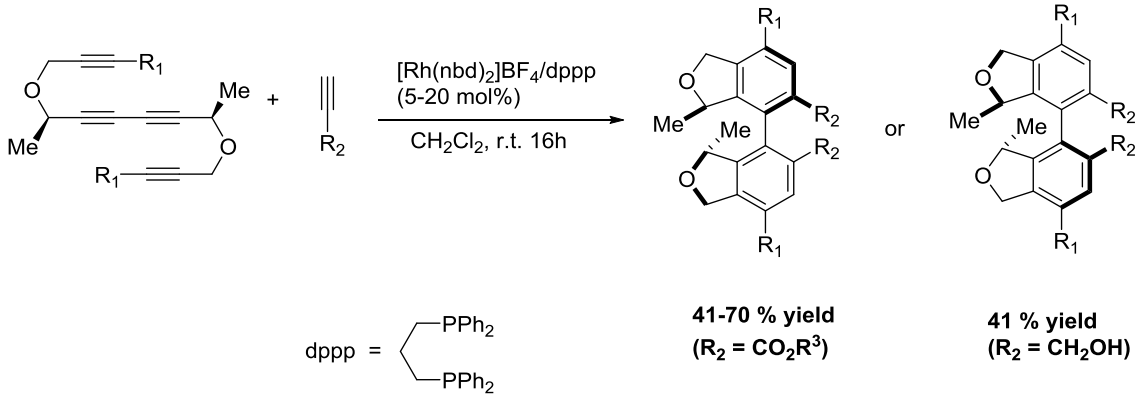

Scheme 4. 3 Substrate-controlled diastereoselective double [2+2+2] cycloaddition

Central to helical chirality induction was also demonstrated in several papers from the group of Stará and Starý.[80] They developed a highly stereoselective [2+2+2] cycloisomerization of optically pure aromatic triynes producing [7]helicene-like scaffolds in diastereoisomeric ratios up to 100:0. High diastereoselectivities were obtained when a Co(I) complex together with triphenylphosphine was used as catalytic system. The efficient central-to-axial chirality induction was controlled by the absolute configuration at the asymmetric centre and by the carbon substituents at the alkyne terminus.[80a,80b] The cobalt-catalysed diastereoselective [2+2+2] cycloaddition reaction was then effectively applied to the synthesis of functionalized penta-, hexa-, and heptacyclic helicenes in nonracemic form starting from optically pure triynes. They found out that theoretical techniques could be used to predict the stereochemical outcome of the reaction.[80c] In a further study they achieved the synthesis of

undecacyclic helicene, by a two-fold intramolecular [2+2+2] cycloisomerization of aromatic hexaynes under cobalt catalysis in a process in which the closing of six new cycles of a helicene backbone in a single operation was performed.[80d] Finally the same group reported the improvement of the selectivity of their methodology for the preparation of optically pure [5]-, [6]-, and [7]heterohelicenes for the first time. Theoretical calculations were used to determine suitable substituents on the terminus of the alkyne so that the cyclizations were highly diastereoselective and the helical compounds formed do not racemize (Scheme 4.4).[80e]

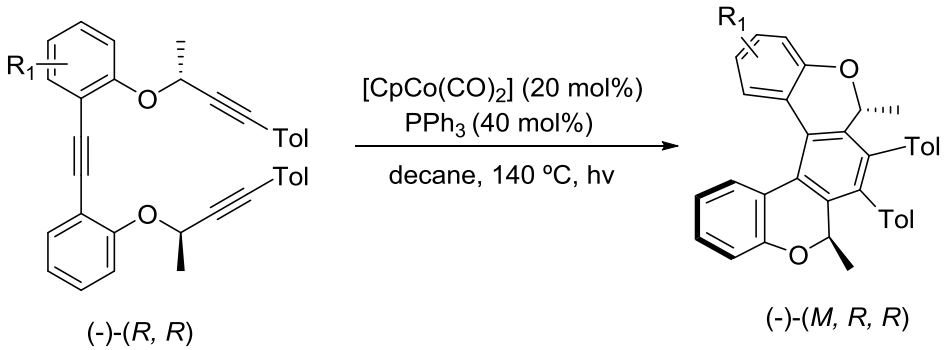

(-)-(*R, R*) (-)-(*M, R, R*)

57-88 % yield, 100:0 *dr*

R_1 = CH_3O, Br

Scheme 4. 4 Central-to-helical chirality induction in the formation of optically pure helicene-like scaffolds

Finally, Carbery et al. reported the synthesis of helicenoidal-DMAP organocatalysts upon diastereoselective [$RhCl(PPh_3)_3$]-catalysed [2+2+2] cycloisomerization on an optically pure triyne that had a stereogenic centre and that already contained a pyridine ring (Scheme 4.5).[81] They rationalized that the stereocontrol was founded upon minimalizing of A^{1-3}-like strain between the propargylic methyl group and the phenyl group during the construction of the central hexasubstituted aryl ring.

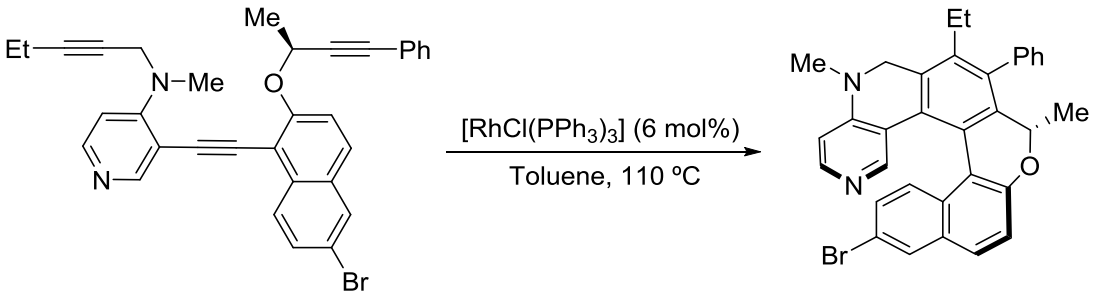

88 % yield, 95:5 *dr*

Scheme 4. 5 Selected example of central-to-helical chirality induction in the formation of helicenoidal-DMAP reported by Carbery et al.

We have described in chapter 3 the rhodium-catalyzed [2+2+2] cycloaddition of allene-ene/yne-allene systems. The Wilkinson's catalyst afforded the product diastereoselectively but when trying to obtain an enantiomerically pure compound by using combinations of a cationic rhodium source and biphosphine ligands, the diastereoselectivity of the process dramatically decreased. Therefore we set out the objective of this chapter which consisted on evaluating

the asymmetric synthesis of cyclohexanic and cyclohexenic scaffolds by chirality induction starting from an enantiomerically pure allene-ene/yne-allene substrate under [$RhCl(PPh_3)_3$] catalysis. This should allow us to determine if it is possible to induce chirality in the two or four stereogenic centers generated in the [2+2+2] cycloaddition reaction by the influence of two chiral centers already present in the substrate, i.e. to induce central chirality by the influence of a chiral center in a diastereoselective [2+2+2] cycloaddition reaction which contrary to the induction of axial and helical chirality has never been reported.

4.2. Results and discussion

4.2.1. Synthesis of the substrates

To perform the study on stereoselective [2+2+2] cycloaddition reaction with chiral bisallenic substrates, two model substrates bearing *N*-tosyl-linkage (*N*Ts) were designed which have a chiral centre next to the allene functionality (Figure 4.1). The substrates have either an alkene or an alkyne in the centre.

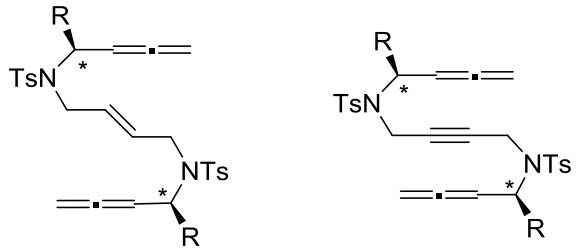

(*S*,*S*)-**13** (*S*,*S*)-**14**

R= C_5H_{11}

Figure 4. 1 The two model substrates tested on this study

The retrosynthetic analysis of the linear bisallenic substrates (*S*,*S*)-**13** and (*S*,*S*)-**14** is represented in scheme 4.6. The substrates for the cycloaddition could be obtained by reaction of (*S*)-4-methyl-*N*-(nona-1,2-dien-4-yl)benzenesulfonamide (*S*)-**15** and either (*E*)-1,4-dibromo-2-butene or 1,4-dibromobutyne. Intermediate (S)-**15** could be synthesized using a Mitsunobu reaction which allows the nucleophilic substitution in neutral reaction media and takes place with inversion of the configuration.

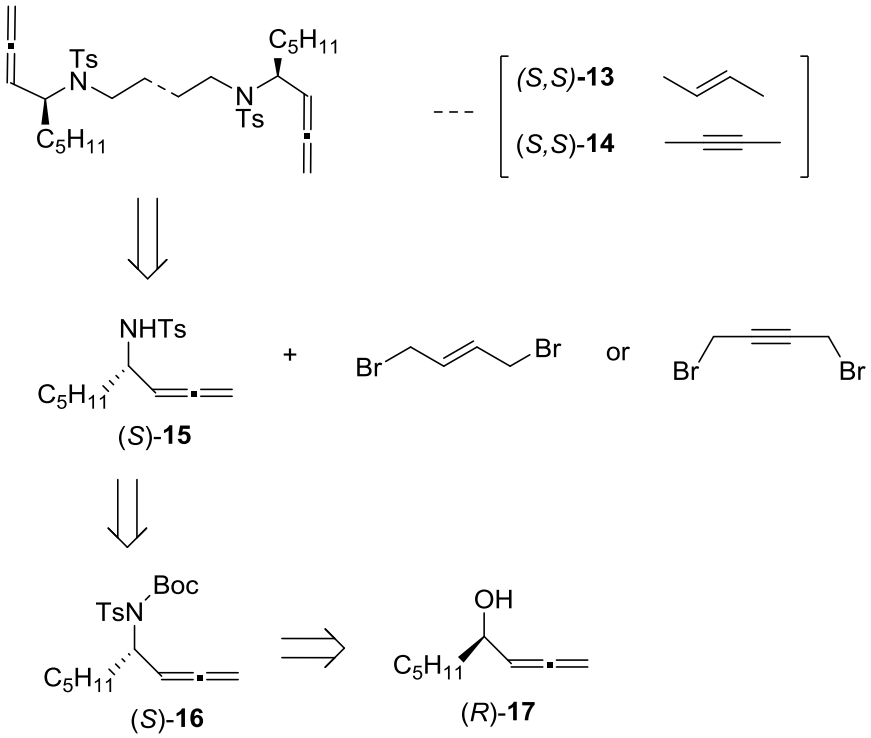

Scheme 4. 6 Retrosynthetic analysis of allene-ene-allene **13** and allene-yne-allene **14** substrates

4.2.1.1. Synthesis of allene-ene-allene substrate from racemic and optically pure allenol

Compound (*S*)-**15** was synthesised from (*R*)-nona-1,2-dien-4-ol (*R*)-**17**[82] in two steps. In the first one, *tert*-butyl tosylcarbamate was alkylated using a Mitsunobu reaction. This reaction allows the facile alkylation of an amine with an alcohol under neutral conditions. The Mitsunobu reaction permits C-O, C-S, C-N, or C-C bond formation by the condensation of an acidic component with a primary or a secondary alcohol. The hydroxyl group is converted into a potent leaving group which is then efficiently displaced by a wide variety of nucleophiles. The reaction is carried out in the presence of triphenylphosphine (or another suitable phosphine) and diisopropyl azadicarboxylate (DIAD) or diethyl azodicarboxylate (DEAD). The chiral secondary alcohols undergo a complete inversion of configuration.[83] Therefore, optically active allenol (*R*)-**17** was transformed into optically pure (*S*)-nona-1,2-dien-4-yl(tosyl)carbamate **16,** (S)-**16**, under Mitsunobu conditions, with the expected inversion of configuration. In a subsequent step, deprotection of the *tert*-butoxy group was accomplished using trifluoroacetic acid to give (*S)*-4-methyl-*N*-(nona-1,2-dien-4-yl)benzenesulfonamide **15** in very good yield (Scheme 4.7).

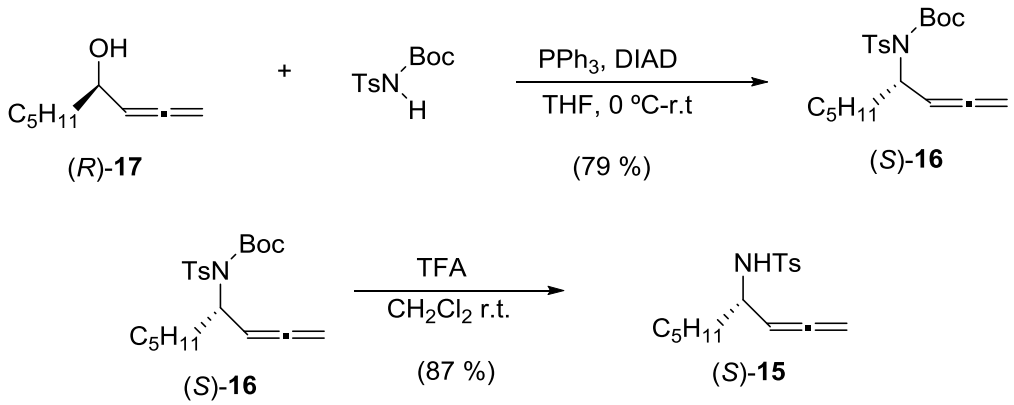

Scheme 4. 7 Synthesis of allenesulphonamide substrates (*S*)-**16** and (*S*)-**15**

The chiral allene-ene-allene substrate (*S*,*S*)-**13** was obtained by nucleophilic substitution of (*S*)-4-methyl-*N*-(nona-1,2-dien-4-yl)benzenesulfonamide (*S*)-**15** and (*E*)-1,4-dibromobutene. The reaction took place using cesium carbonate as a base affording a 72 % yield of the desired product together with an 18 % yield of the monosubstituted product which was separated by column chromatography (Scheme 4.8). Using potassium carbonate, the base which was used in all the other analogous alkylations, the reaction gave only a 54 % yield of the desired product. The process was optimized changing the base to cesium carbonate which effectively increased the product formation.

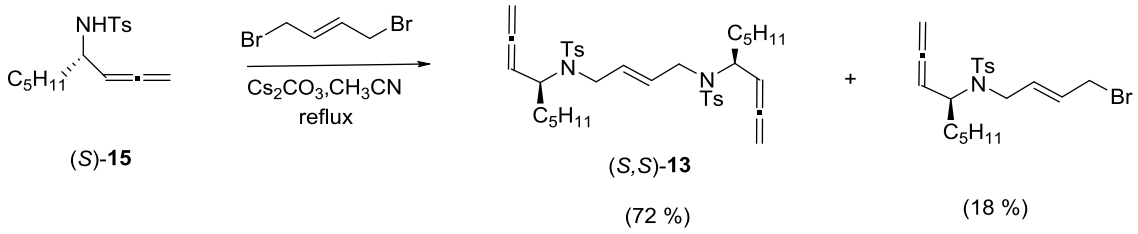

Scheme 4. 8 Synthesis of compound (*S*,*S*)-**13**

To evaluate the enantiomeric purity of the products obtained, model substrate **13** was synthesised starting both from the allenol as a racemic mixture and as an enantiomerically pure compound. The route of synthesis followed for the racemic one was identical to the one described above.

Along the synthesis, the products obtained with the racemic and chiral alcohol were analysed by HPLC to prove that the chirality was not erased. As an example, the results obtained for the final allene-ene-allene compound **13** are shown below. The HPLC chromatogram of the product obtained from optically pure alcohol shows only one signal at a retention time of 10.39 min which is assigned to optically pure compound (*S*,*S*)-**13** (Figure 4.2).

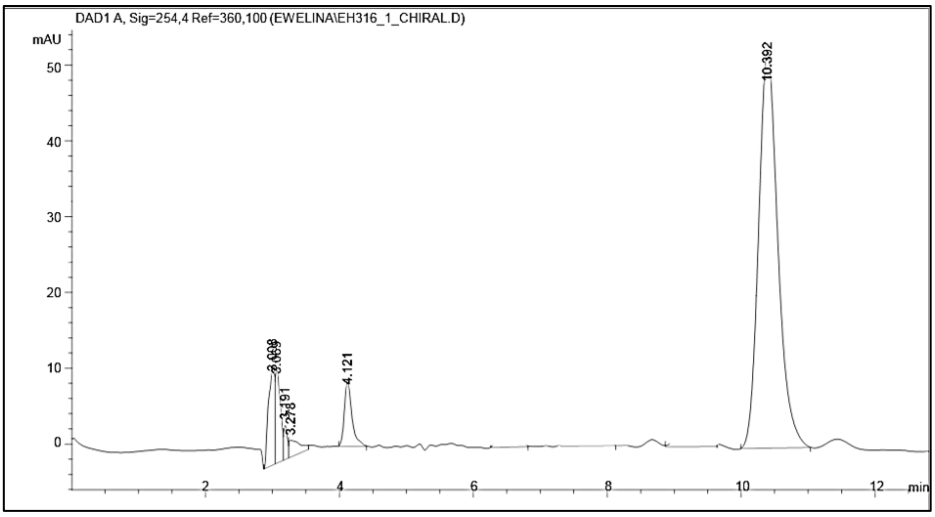

Figure 4. 2 HPLC chromatogram of enantiomerically pure compound (*S*,*S*)-**13**

When the route of synthesis was performed starting from racemic allenol **17**, a mixture of a *meso* form and a racemic mixture of two enantiomers was obtained. Taking into account the two stereogenic centres that bear the molecule, the equation 2^n would give us 4 stereoisomers, but due to the fact that there is presence of a symmetry centre an achiral *meso* form is obtained which only leaves three stereoisomers formed in result (Scheme 4.9).

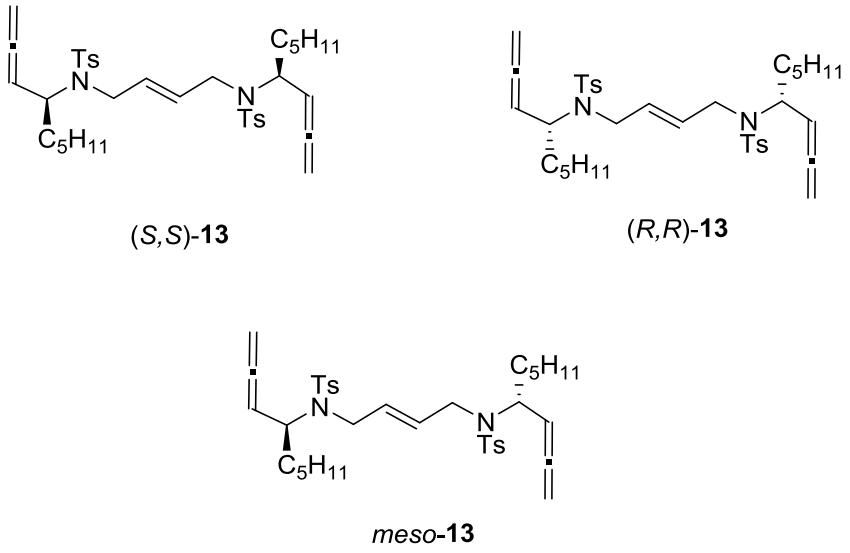

Scheme 4. 9 Stereoisomers of allene-ene-allene **13** obtained when it is synthesized starting from the racemic mixture of allenol **17**

The HPLC chromatogram of the product isolated at the end of the synthetic route very nicely shows the two peaks at retention times of 9.92 and 10.48 min. which correspond to the pair of enantiomers and a third peak at a retention time of 12.32 min. and double integration that corresponds to the *meso* form (Figure 4.3). The pair of enantiomers ((*S*,*S*)-**13** and (*R*,*R*)-**13**) and the *meso*-form (*meso*-**13**) are present in a 1:1 ratio in the mixture.

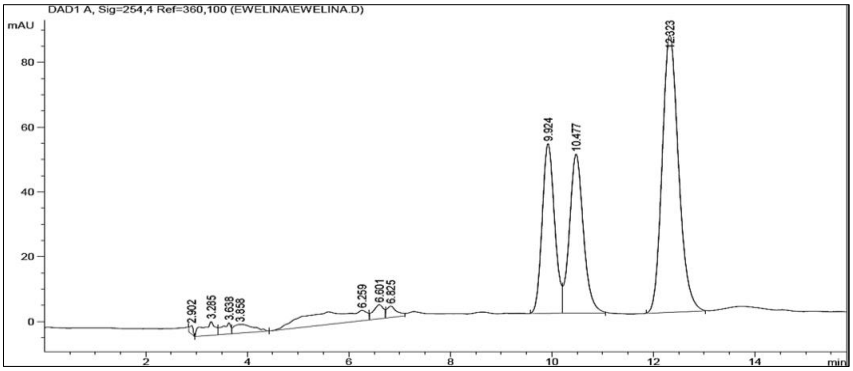

Figure 4. 3 HPLC chromatogram of stereoisomeric mixture of compound **13**

4.2.1.2. Synthesis of allene-yne-allene substrate from racemic and optically pure allenol

The allene-yne-allene (*S*,*S*)-**14** was prepared using 1,4-dibromobutyne instead of (*E*)-1,4-dibromo-2-butene in the last step of the synthetic route. The reaction was first carried out with potassium carbonate as a base affording only a 29 % yield of the desired product. The reaction was then carried out at 60˚C using cesium carbonate as the base forming the desired product (*S*,*S*)-**14** in an improved 56 % yield (Scheme 4.10) together with an 23 % yield of the monosubstituted product which was separated by column chromatography.

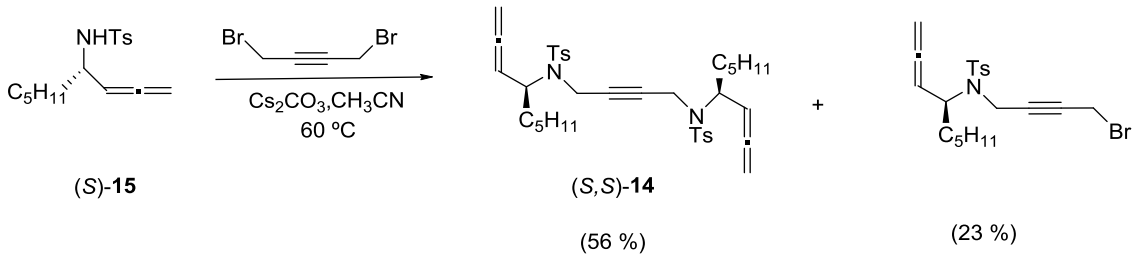

Scheme 4. 10 Synthesis of compound (*S*,*S*)-**14**

As in the former case, the synthesis was repeated starting from the racemic allenol **17** and HPLC was used to assure that no reaction racemizes the stereogenic centre when starting from chiral allenol (*R*)-**17**. The HPLC chromatogram of the products isolated at the end of the synthesis show only one signal at a retention time of 12.68 min. that corresponds to the optically pure compound (*S*,*S*)-**14** (Figure 4.4) when chiral allenol (*R*)-**17** was used as starting substrate, and a mixture of a *meso* form and a racemic mixture when starting from the racemic one (Figure 4.5). The pair of enantiomers ((*S*,*S*)-**14** and (*R*,*R*)-**14**) and the *meso*-form (*meso*-**14**) are present in a 1:1 ratio in the mixture.

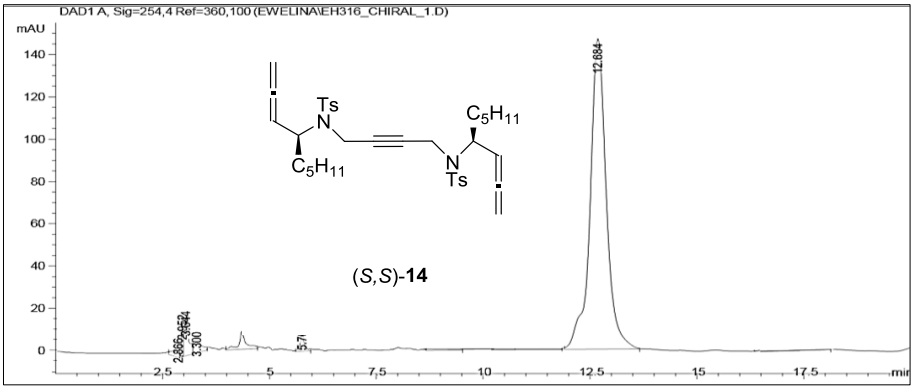

Figure 4. 4 HPLC chromatogram of enantiomerically pure compound (*S*,*S*)-**14**

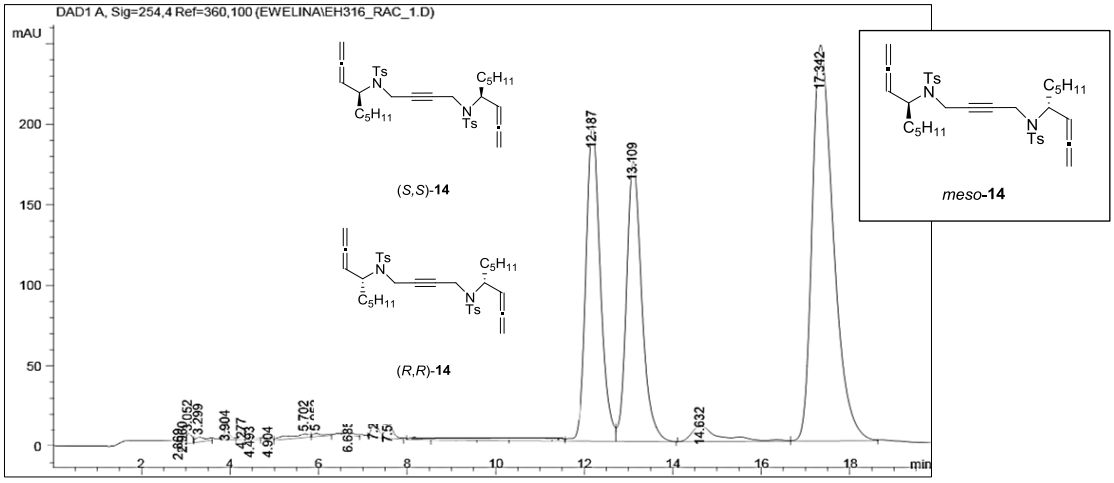

Figure 4. 5 HPLC chromatogram of stereoisomeric mixture of compound **14**

4.2.2. Reactivity studies of allene-ene-allene

After the preparation of the model substrates their reactivity in the [2+2+2] cycloaddition reaction was evaluated. The use of Wilkinson's catalyst and toluene as the solvent at 110˚C were chosen as reaction conditions based on the results obtained in chapter 3. We first investigated the reaction of allene-ene-allene **13** obtained from the racemic allenol. We were pleased to find that the reaction yielded only two diastereoisomeric products (see section 4.2.3.2) in 5:1 ratio in an overall 49 % yield. The cycloaddition products were isolated and purified by column chromatography. After running the complete set of 1D and 2D NMR spectra, diastereoisomers **18** and **19** were identified as the products formed in the reaction. The cycloaddition reaction that constructs four new stereogenic centers in the cycloadducts shows fairly good diastereoselectivity (Scheme 4.11).

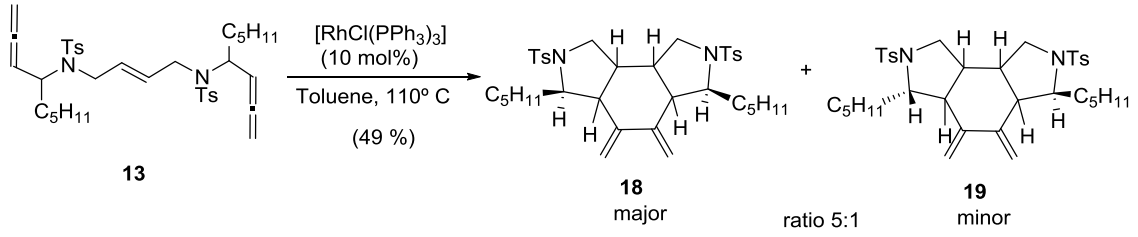

Scheme 4. 11 [2+2+2] cycloaddition reaction of substrate **13**

The HPLC shows four signals that belong to the racemic mixture of the two enantiomers for each of the two diastereisomers formed. The peaks corresponding to the major diastereoisomer (product **18**) are observed at retention times of 5.01 and 5.75 min. The other two signals at retention times of 6.75 and 8.90 min belong to the pair of enantiomers of the minor product **19** (Figure 4.6).

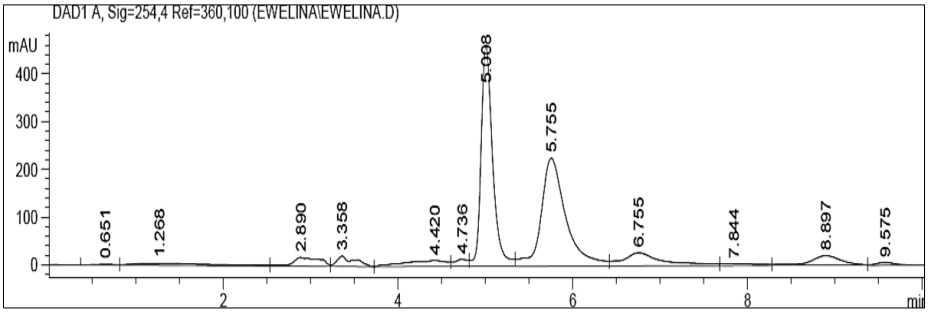

Figure 4. 6 HPLC chromatogram of the products mixture **18** and **19**

When the enantiomerically pure substrate (*S*,*S*)-**13** underwent the Rh-catalysed cycloaddition reaction, the stereogenic centers contained in the substrate induced a completely diastereoselective reaction that formed only one enantiomeric product (*S*,*S*)-**19**[84] in a 46 % yield (Scheme 4.12).

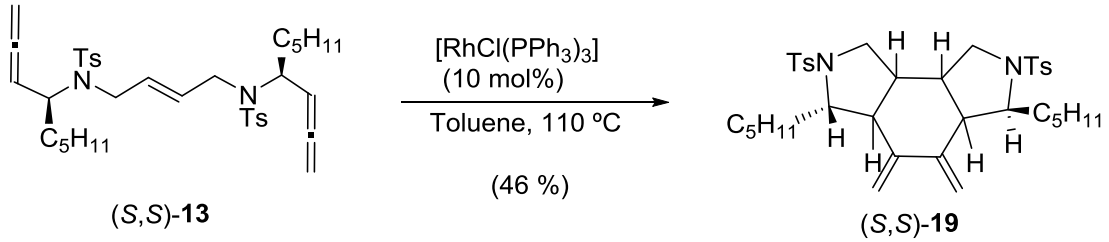

Scheme 4. 12 [2+2+2] cycloaddition reaction of optically pure substrate (*S*,*S*)-**13**

When the product obtained was injected into the HPLC only one peak at a retention time of 9.75 minutes was observed (Figure 4.7). Since the HPLC conditions were not identical for the two samples (Figures 4.6 and 4.7), we injected into the HPLC a mixture of the products of the two cycloaddition reactions (Scheme 4.11 and 4.12) in order to determine if the product obtained matched up with some of the stereoisomers already obtained in the cycloaddition of allene-ene-allene **13** obtained from the racemic allenol. The chromatogram showed only four peaks and the area of the peak corresponding to the enantiomer of lower retention time of the minor diastereoisomer (product **19**) increased. So we concluded that the only enantiomer formed in the cycloaddition reaction of the enatiomerically pure substrate (*S*,*S*)-**13** was the (*S*,*S*) enantiomer of the minor product **19** formed in cycloaddition reaction of **13**.

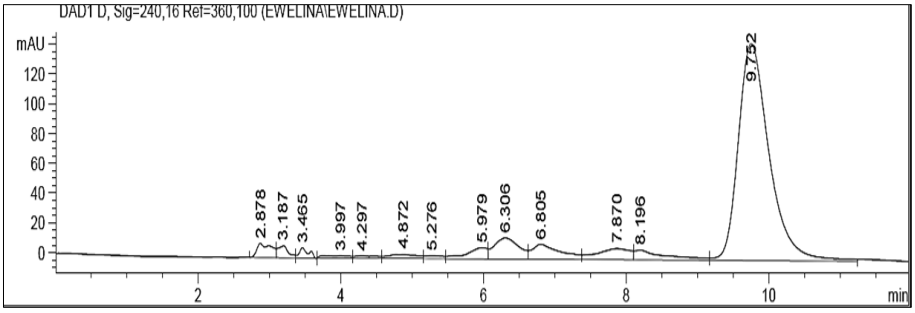

Figure 4. 7 HPLC chromatogram of the optically pure product (*S*,*S*)-**19**

4.2.3. Structural analysis by NMR

NMR spectroscopy allowed us to fully characterize the different diastereisomers formed in the reaction. The mixture of cycloadducts **18** and **19** obtained from the reaction of allene-ene-allene **13** synthesized from the racemic allenol was first analysed by ^{1}H-NMR. Analysis of the 4-6 ppm region of the spectra, where the protons of the exomethylenic protons appear, clearly indicated that cycloadduct **18** and **19** do not have symmetry. Two sets of four signals of different intensity were clearly observed. The four signals with higher intensity were assigned to the methylenic protons of the major diastereoisomer **18** (purple triangle), and were clearly differentiated from the four low intensity signals that belong to the methylenic protons of the minor diastereoisomer **19** (blue triangle) (Figure 4.8). Any symmetric diastereoisomer would have given only two signals for the chemically equivalent methylenic protons.

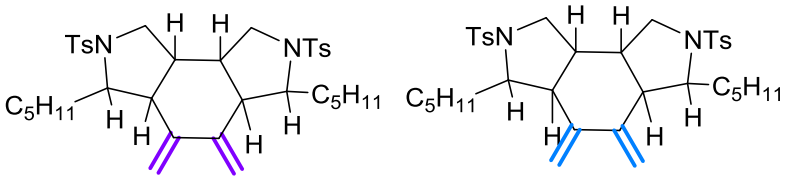

18
major

19
minor

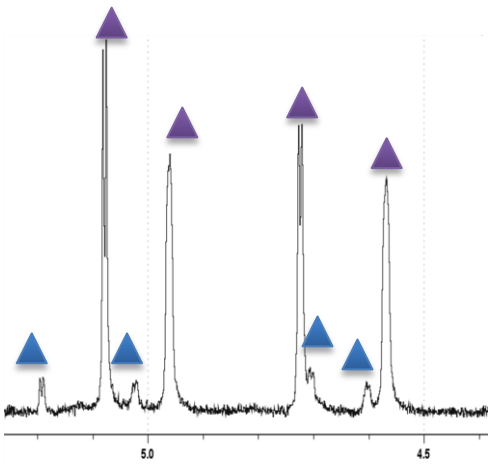

Figure 4. 8 Zoomed ^{1}H NMR spectrum of cycloadducts mixture **18** and **19**

The ^{1}H NMR spectra of the **18** and **19** cycloadducts mixture and the optically pure cycloadduct (*S*,*S*)-**19** obtained from the reaction of the enantiomerically pure substrate were then compared (Figure 4.9). The superposition of the olefinic region of the ^{1}H-NMR spectrum of the chiral product (*S*,*S*)-**19** (above spectrum, figure 4.9) and the diastereoisomeric mixture (spectrum below) showed that the methylenic proton signals (pink triangle) have the same shift as the minor cycloadduct product **19** (blue triangle) (below spectrum, figure 4.9). These data proved that minor cycloadduct **19** has the same configuration as optically pure cycloadduct (*S*,*S*)-**19** as had already been outlined by the HPLC analysis.

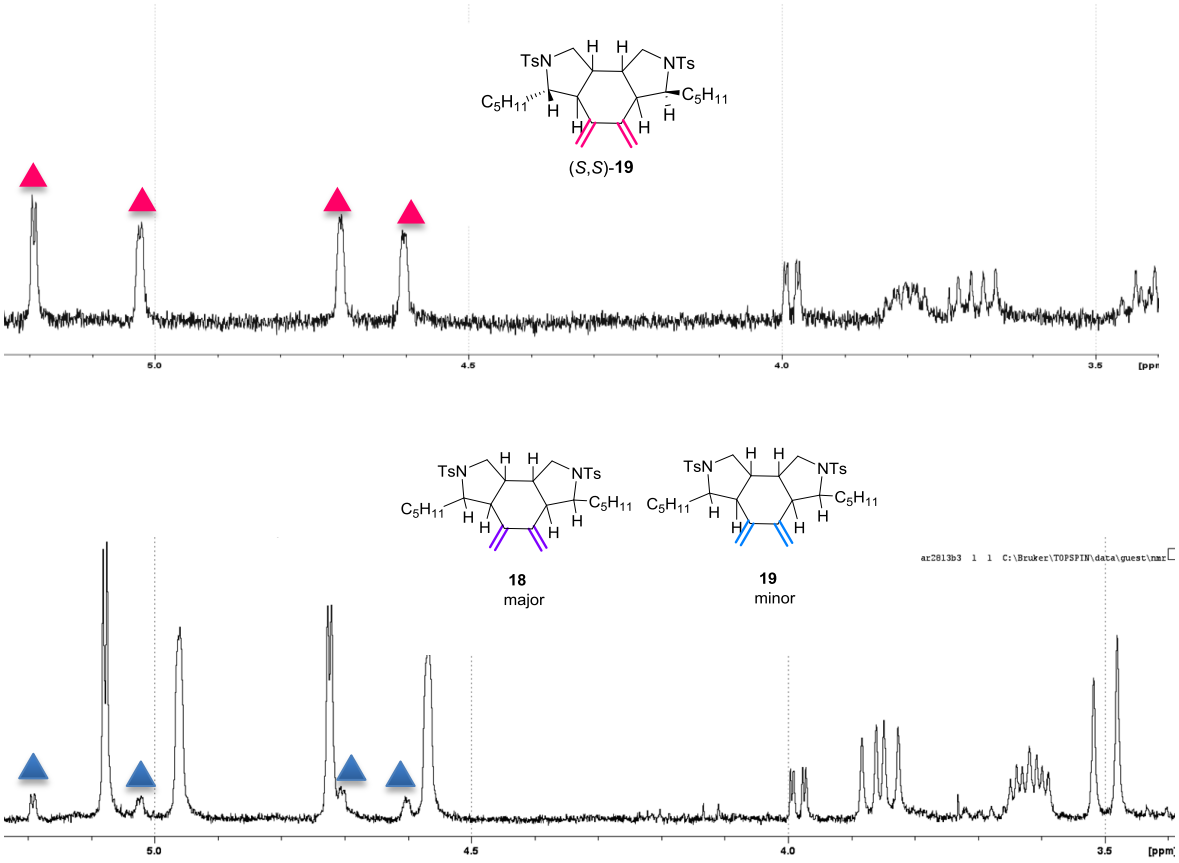

Figure 4. 9 Comparison of the ^{1}H NMR spectra of the cycloadducts mixture (**18** and **19**) and optically pure cycloadduct (*S*,*S*)-**19**

4.2.3.1. General model of stereoisomers for (S,S)-19

In order to determine the absolute configuration of the cycloadduct (*S*,*S*)-**19** formed in the [2+2+2] cycloaddition reaction of the enantiomerically pure substrate, an analysis of the possible stereosiomers that can be formed was made. The cycloadduct formed has six stereocenters. Four of them are new stereogenic centres formed in the reaction (the ones marked with an asterisk in Figure 4.10) whereas the other two are transferred from the substrate untouched and so have *S* absolute configuration (C4 and C9 on Figure 4.10).

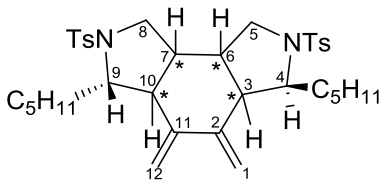

Figure 4. 10 General structure of cycloadduct (*S*,*S*)-**19**

Using the equation 2^n, where n is the number of stereocentres, to calculate the number of stereoisomers we arrive at 16 possible stereoisomers. Taking into account that the [2+2+2] cycloaddition is stereospecific, having started from a *trans* alkene the protons on C6 and C7 position will have a *trans* disposition. So the number of possible stereoisomers is reduced by half, and a further reduction of two enantiomers is obtained due to the symmetry of the substituents in the molecule, ending up with only six stereoisomers that could be formed upon cycloaddition of optically pure allene-ene-allene substrate (*S*,*S*)-**13**. The six possible stereoisomers with the absolute configuration of their stereocenters are listed in Figure 4.11.[85]

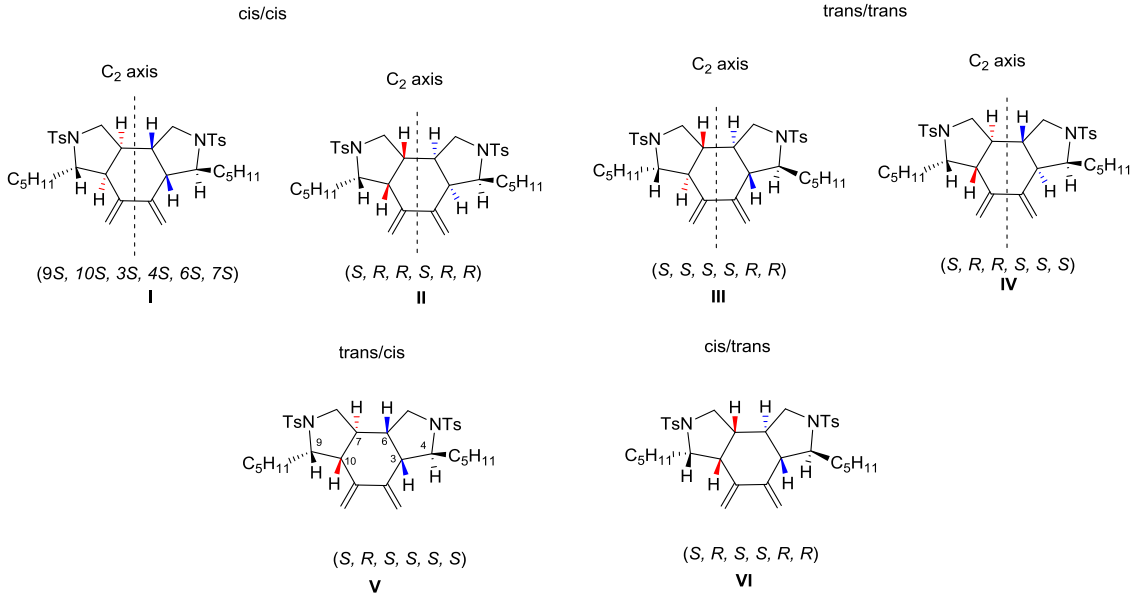

Figure 4. 11 Possible six stereoisomers that could be formed upon cyclization of (*S*,*S*)-**13**

Stereoisomers I and II which have the two *cis* 5,6-ring fusion and stereoisomers III and IV which have two *trans* 5,6-ring fusions are discarded as the products formed because they bear a C_2 axis of symmetry and as was abovementioned the cycloadduct formed is non-symmetrical. After the rational discussion we end up with only two stereoisomers, **V** and **VI**, that have a *cis* and a *trans* 5,6-ring fusion that could match the possible configuration of the searched product (Figure 4.12).

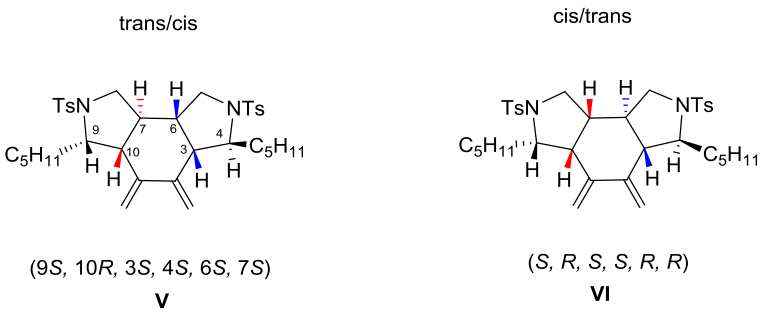

Figure 4. 12 Probable structures of the enantiomer formed upon [2+2+2] cycloaddition of optically pure allene-ene-allene substrate (*S*,*S*)-**13**

With this set of possible products a careful analysis of the 1D and 2D NMR spectroscopic data was undertaken to establish the structure of cycloadduct (*S*,*S*)-**19** formed in the [2+2+2] cycloaddition reaction. The first step was the chemical shift assignment of all the protons in the molecule and then the dipolar couplings observed in NOESY spectrum were analysed. Strong NOE cross-peaks were observed between H9 and both H10 and H7 protons confirming the *cis* ring fusion and the *cis* conformation of H9 with the two protons on the ring junction (green arrows). An intense dipolar coupling was observed between the proton on C4 and H6 that together with the absence of NOE contacts between H3 any of the H4 and H6 clearly indicate their *anti*-configuration (pink arrows). This set of evidences demonstrated that the cycloadduct bears a first *cis* 5,6-ring fusion which is in *cis* configuration with H9 proton and a second *trans* 5,6-ring fusion with the same *trans* configuration with H4 (Figure 4.13). On the other hand, the H7 proton shows strong NOE with the H3 and H10 indicating their relative cis relationship (blue arrows).

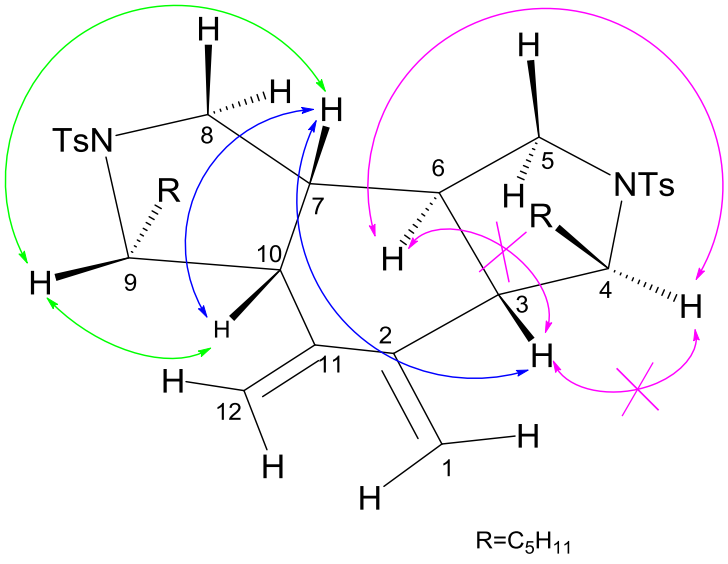

Figure 4. 13 The major NOESY correlations that were observed and help to confirm the proposed geometry of cycloadduct (*S*,*S*)-**19**

The configuration of the cycloadduct (*S*,*S*)-**19** determined by the NMR spectroscopic data represented on the figure 4.13 coincides with the proposed enantiomer **VI** listed on the figure 4.12.

4.2.3.2. General model of stereoisomers for racemic cyclodduct 18

The relative disposition of the diastereoisomer **18** formed in [2+2+2] cycloaddition reaction was next examined. Since the product was afforded from compound **13** obtained from the racemic allenol **17** the configuration on the position C4 and C9 remain unknown contrarily with what happened in the previous case (Figure 4.14).

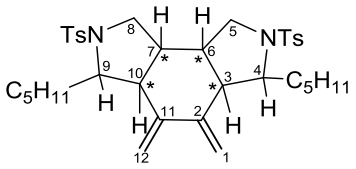

Figure 4. 14 General structure of diastereisomer **18**

A maximum of 64 possible stereoisomers are expected for a product containing six stereogenic centres. Taking into account the *trans* disposition coming from *trans* alkene (position C6 and C7 on figure 4.14) the number is reduced by half ending up with 32 stereoisomers that could be formed. The substrate in this cycloaddition consisted of a mixture of two diastereoisomeric forms, the racemic mixture of (*S,S*)-**13** and (*R,R*)-**13** and the *meso* form *meso*-**13**, and two different diastereoisomers **18** and **19** were obtained (equation b, Scheme 4.13). The minor diastereoisomer coincides with the product obtained from the cycloadditon of optically pure (*S*,*S*)-**13** (equation a, Scheme 4.13), so it was formed from the racemic mixture of (*R*,*R*)-**13** and (*S*,*S*)-**13** contained in the sample. We assumed at this point that the major diastereoisomer **18** was formed by cycloaddition of the *meso*-**13**. So the cycloadduct **18** isolated has (*R*,*S*) or (*S,R*) configuration on the C4 and C9 positions.

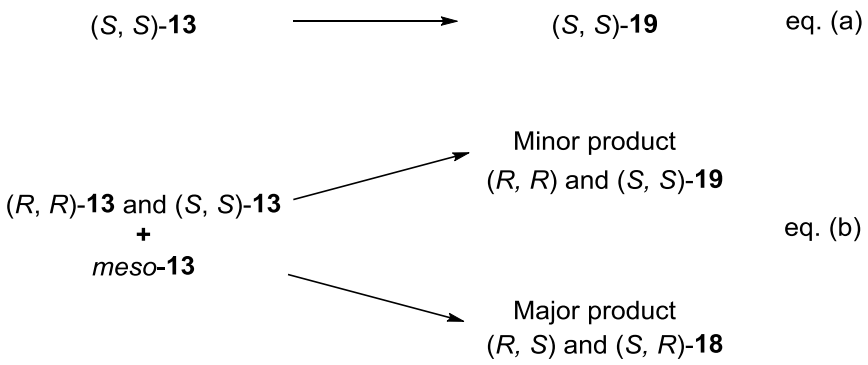

Scheme 4. 13 The absolute and relative configuration of substrates and cyclization products

The number of possible stereoisomers is reduced to four pairs of enantiomers where 5,6-ring fusions can be in *cis, trans* or *cis*/*trans* disposition as shown in figure 4.15. None of the stereoisomers is symmetric so all of them need to be considered as possible products of the cycloaddition reaction.

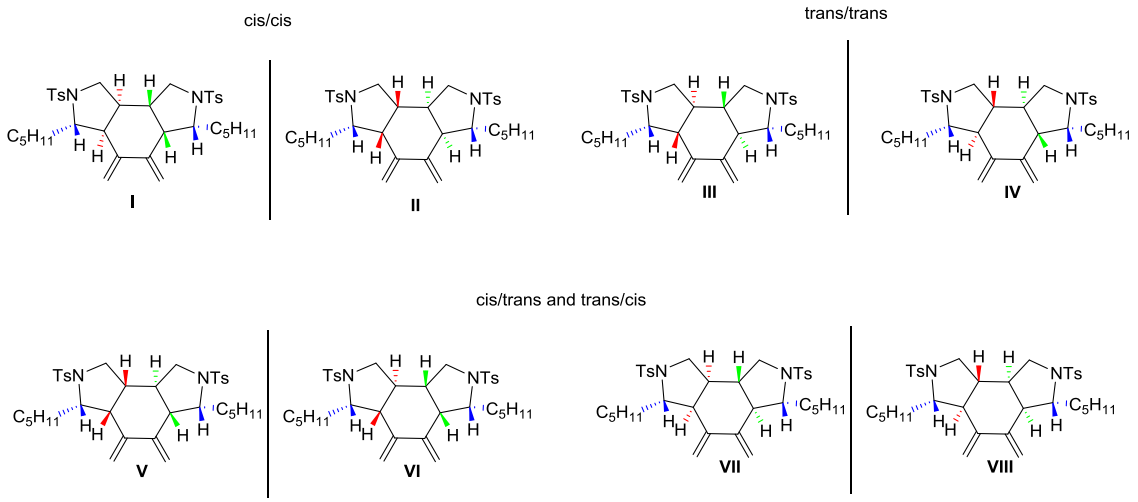

Figure 4. 15 The possible four pair of enantiomers of the diastereisomer **18**

The diastereoisomer formed was determined by analysing the 1D and 2D NMR data. After a complete chemical shift assignment, the dipolar couplings observed in the NOESY spectrum were analysed. An intense dipolar couplings was observed between the proton on C4 and H3 and H7 (green arrows), indicating their *cis* configuration. On the other hand, the absence of NOE cross-peak between H10 and any of the protons on positions 9 and 7 confirmed their *trans* disposition (pink arrows). The overlapping of the H6 and axial proton on the C8 prevented an unambigous analysis of the dipolar couplings for H6 to be done. However, the diastereoisomer could still be fully elucidated assuming that the H6 and H7 protons are in *trans* disposition due to the stereospecific nature of the reaction.

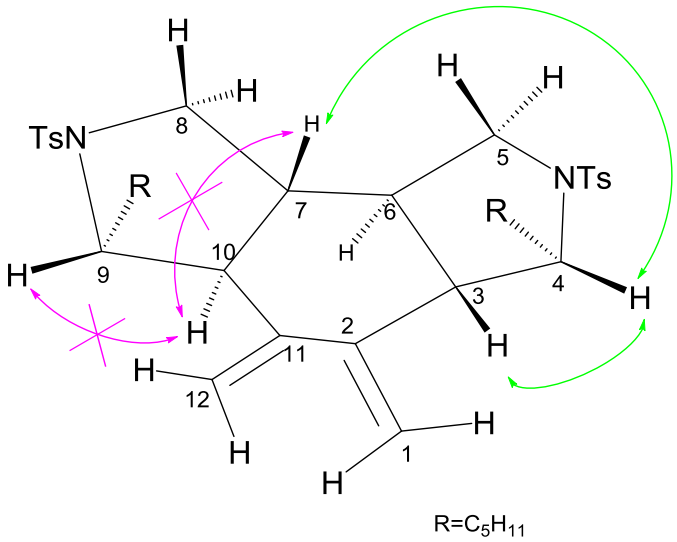

Figure 4. 16 The major NOESY correlations that were observed and help to confirm the proposed geometry of cycloadduct **18**

The structural study carried out led us to assign cycloadduct **18** to the racemic mixture of stereoisomers **III** and **IV** in Figure 4.15, that have both 5,6-ring fusions in *trans* configuration.

4.2.4. Reactivity studies of allene-yne-allene

After the preparation allene-yne-allene **14,** starting from the racemic and optically pure alcohol, their reactivity in the [2+2+2] cycloaddition using Wilkinson's catalyst and toluene as the solvent at 110˚C was evaluated. We first investigated the reaction of allene-yne-allene **14** obtained from the racemic alcohol. We were pleased to find that the reaction yields only two diastereoisomeric products (see section 1.2.5.2) in 2:1 ratio in an overall 48 % yield. The cycloaddition products could be isolated and purified by column chromatography. After running the complete set of 1D and 2D NMR spectra, the relative configuration of the different stereogenic carbons of compounds **20** and **21** was determined by NMR (study on NMR in the next section) (Scheme 4.14).

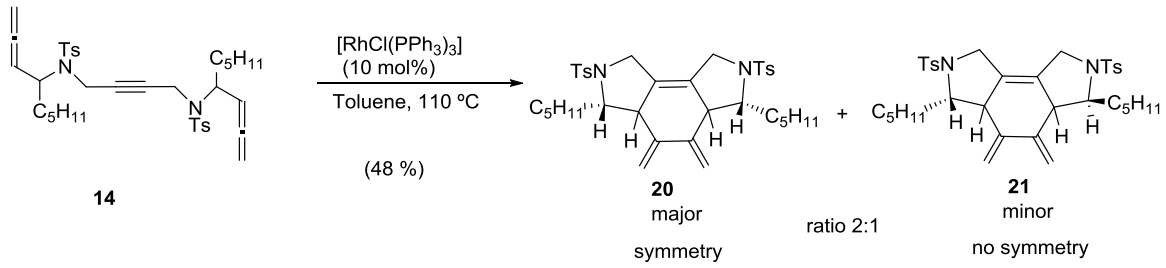

Scheme 4. 14 [2+2+2] cycloaddition reaction of substrate **14** obtained from the racemic allenol

The HPLC shows three signals that belong to the racemic mixture of the two enantiomers of the minor diastereoisomer and the major diastereoisomer which is a *meso* form. The peak corresponding to the major diastereoisomer (product **20**) is observed at a retention time of 12.44 min. The other two signals at retention times of 9.04 and 9.72 min belong to the pair of enantiomers of the minor product **21** (Figure 4.17).

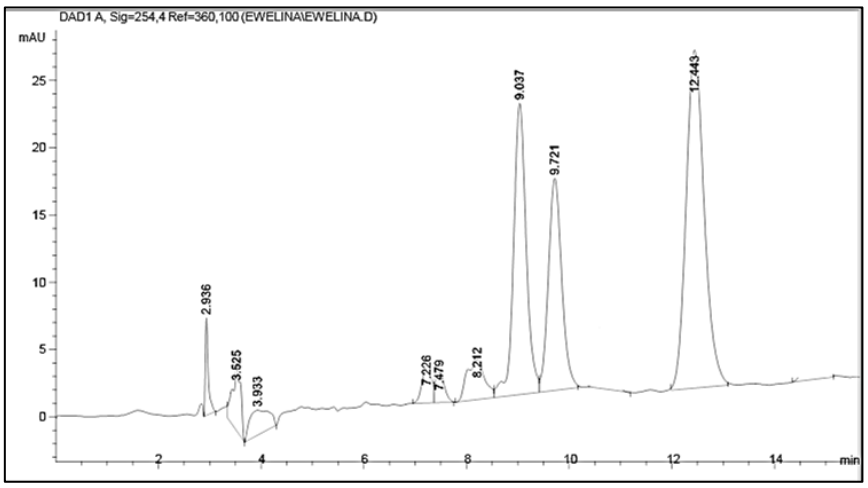

Figure 4. 17 HPLC chromatogram of the mixture of cycloadducts **20** and **21** obtained upon [2+2+2] cycloaddition

When the enantiomerically pure substrate (*S*,*S*)-**14** underwent the Rh-catalysed cycloaddition reaction, the stereogenic centers contained in the substrate induced a completely diastereoselective reaction that formed only one enantiomeric product (*S*,*S*)-**21** in a 46 % yield (Scheme 4.15).

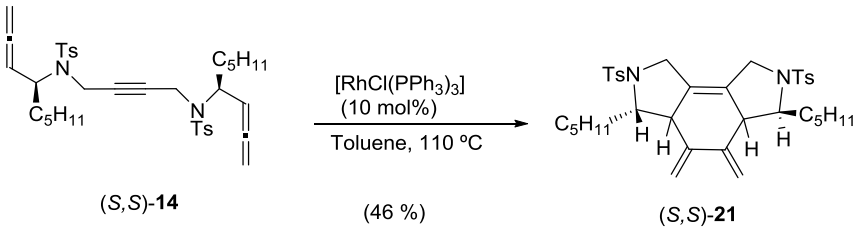

Scheme 4. 15 [2+2+2] cycloaddition reaction of optically pure substrate (*S*,*S*)-**14**

The HPLC shows one peak at a retention time of 9.81 min that nicely shows the only enantiomer formed in the cycloaddition reaction of the enatiomerically pure substrate (Figure 4.17). As in the case of the central alkene the product isolated corresponds to one of the enantiomers of the minor diastereoisomer obtained when the substrate obtained from the racemic alcohol is reacted.

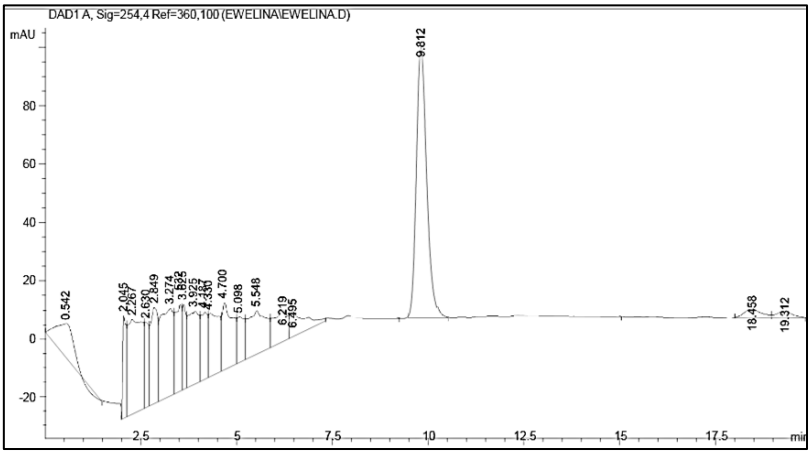

Figure 4. 18 HPLC chromatogram of the optically pure product (*S*,*S*)-**21**

4.2.5. Structural analysis by NMR

NMR spectroscopy allowed us to fully characterize the different stereoisomers formed in the reaction. The mixture of cycloadducts **20** and **21** obtained from the reaction of the allene-yne-allene **14** was first analysed by ^{1}H-NMR. Analysis of the 4-6 ppm region of the spectra, where the protons of the exomethylenic protons appear, clearly shows two sets of signals of different intensity. The two signals with higher intensity are assigned to the methylenic protons of the major diastereoisomer **20** (pink triangle). The presence of only two signals indicates that cycloadduct **20** is symmetric. Another set of four low intensity signals is clearly differentiated (although one of the signals is overlapped with one of the signals of **20**) that belong to the methylenic protons of the minor diastereoisomer **21** which is not symmetric (purple triangle) (Figure 4.19).

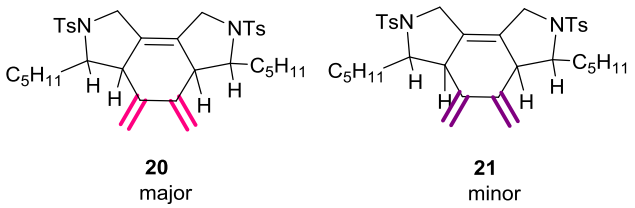

20
major

21
minor

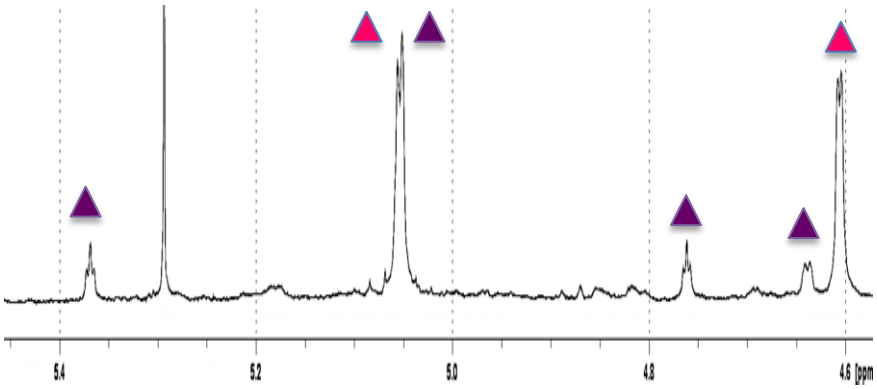

Figure 4. 19 Zoomed ^{1}H NMR spectrum of the mixture of cycloadducts **20** and **21**

The ^{1}H NMR spectra of the **20** and **21** cycloadducts mixture and the optically pure cycloadduct (*S*,*S*)-**21** obtained from the reaction of the enantiomerically pure substrate were then compared (Figure 4.20). The superposition of the olefinic region of the ^{1}H NMR spectrum of the chiral product (*S*,*S*)-**21** (above spectrum, figure 4.20) and the diastereoisomeric mixture (spectrum below) showed that the methylenic proton signals (green triangle) have the same shift as the minor cycloadduct product **21** (purple triangle) (below spectrum, figure 4.20). These data proved that minor cycloadduct **21** has the same configuration as optically pure cycloadduct (*S*,*S*)-**21** as had already been outlined by the HPLC analysis.

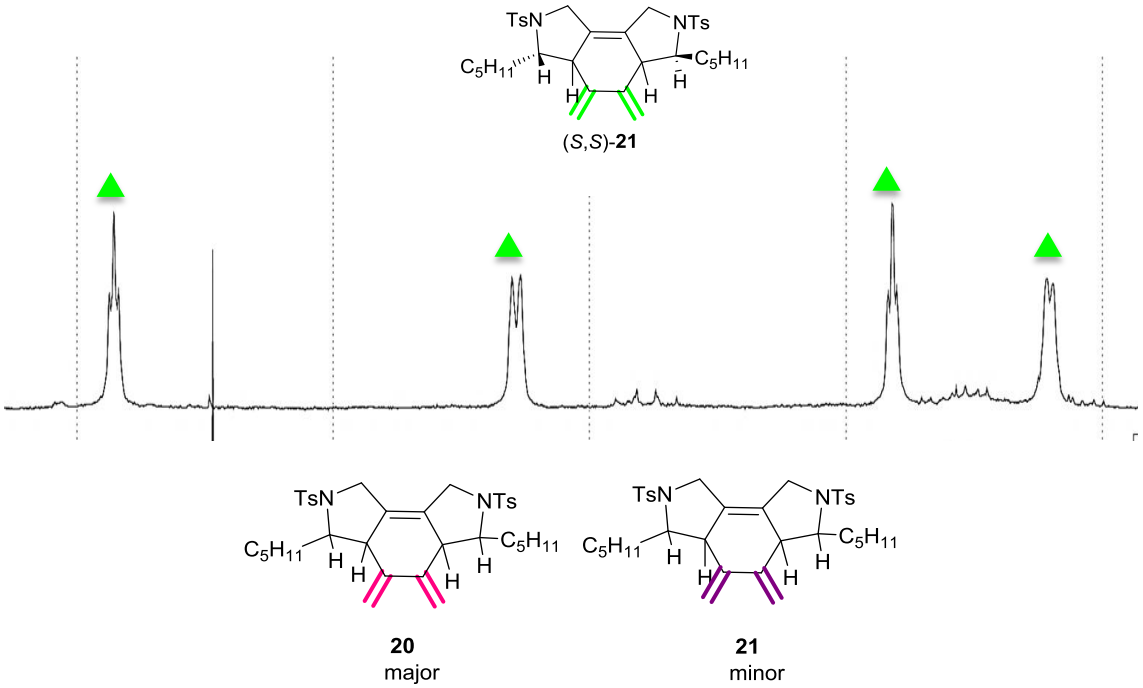

Figure 4. 20 Comparison of the ^{1}H NMR spectra of the optically pure cycloadduct (*S*,*S*)-**21** and cycloadducts mixture (**20** and **21**)

4.2.5.1. General model of stereoisomers for (S,S)-21

In order to determine the absolute configuration of the cycloadduct (*S*,*S*)-**21** formed in the [2+2+2] cycloaddition reaction of the enantiomerically pure substrate, an analysis of the possible stereosiomers that can be formed was made. The cycloadduct formed has four

stereocenters. Two of them are new stereogenic centres formed in the reaction (the ones marked with an asterisk in Figure 4.21) whereas the other two are transferred from the substrate untouched and so have *S* absolute configuration (C4 and C9 on Figure 4.21).

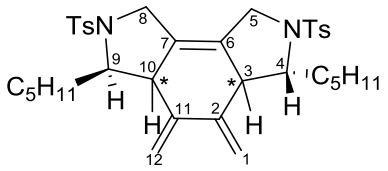

Figure 4. 21 General structure of cycloadduct (*S*,*S*)-**21**

The three possible stereoisomers that can be formed with the absolute configuration of the newly formed stereocenters are listed in figure 4.22.

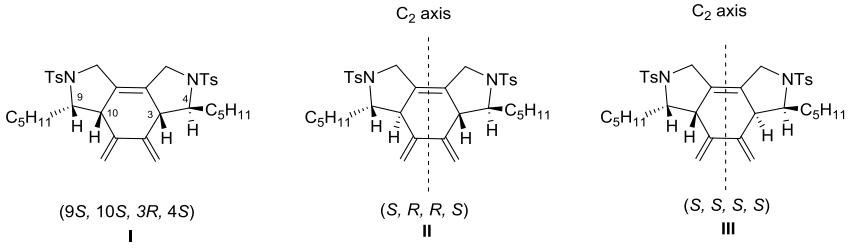

Figure 4. 22 The three possible stereoisomers that could be formed

Stereoisomers **II** and **III** are discarded as the products formed because they bear a C_2 axis of symmetry and as was abovementioned the cycloadduct formed is non-symmetrical. After the rational discussion we end up with only one stereoisomer and we proceed to analyse the NMR data to confirm its formation (Figure 4.23).

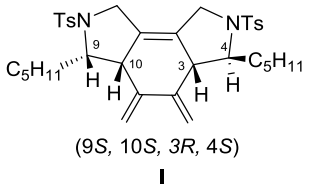

Figure 4. 23 The diastereisomer which is formed upon [2+2+2] cycloaddition of chiral allene-yne-allene substrate (*S*,*S*)-**14**

A careful analysis of the 1D and 2D NMR spectroscopic data was undertaken to establish the structure of cycloadduct (*S*,*S*)-**21** formed in [2+2+2] cycloaddition reaction. The first step was the assignment of signals and then the dipolar couplings observed in the NOESY spectrum were analysed (Figure 4.24). A strong dipolar couplings observed between H10 and the proton on C9 together with the absence of NOE contact between H10 and the protons on aliphatic groups on C9 (blue arrows) indicating their *cis* relationship. The presence in the NOESY spectrum of NOE cross-peaks between H3 and the protons on aliphatic groups on C4 together with the absence of dipolar coupling between H3 and H4 revealed the *trans* configuration on the other half of the cycloadduct. A NOE cross–peaks observed between H3 and H10

confirmed their *cis* configuration excluding possible structures **II** and **III** to be formed (Figure 4.22).

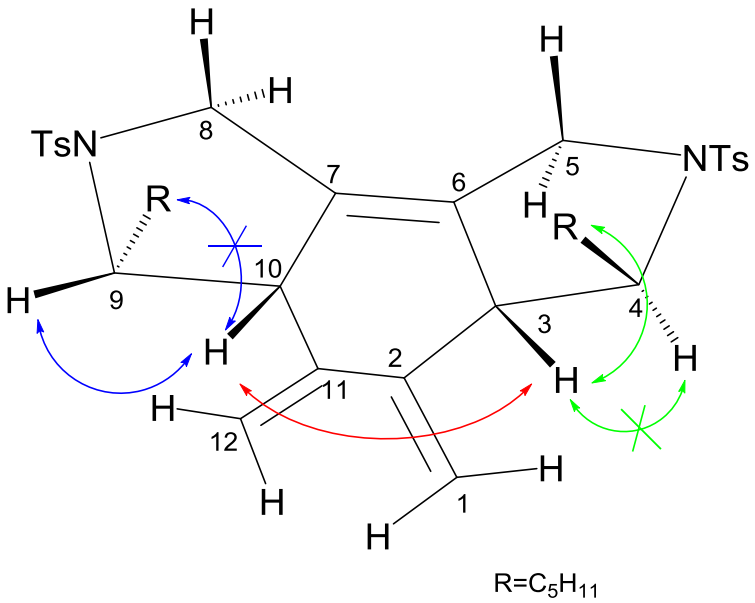

Figure 4. 24 The major NOESY correlations that were observed and help to confirm the proposed geometry of cycloadduct (*S*,*S*)-**21**

Figure 4.24 represented the absolute configuration of the cycloadduct (*S*,*S*)-**21** as determined by NMR spectroscopic data which coincides with the structure **I** on figure 4.22.

4.2.5.2. General model of stereoisomers for racemic cyclodduct 20a

The stereoisomers formed in the [$RhCl(PPh_3)_3$]-catalyzed [2+2+2] cycloaddition of the allene-yne-allene substrate synthesized form the racemic alcohol were then analysed. The minor diastereoisomer corresponds to a racemic mixture of the enantiomer obtained in the cycloaddition of the optically pure substrate and its enantiomer, as previously determined. The configuration of the major diastereoisomer **20** will be examined**.** The configuration on the position C4 and C9 remain unknown (Figure 4.25).

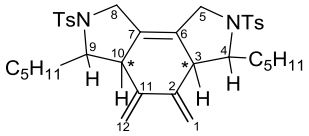

Figure 4. 25 General structure of diastereoisomer **20**

We assume that the major diastereoisomer **20** was formed from the *meso* compound comprised on the racemic mixture of substrate **14** (Scheme 4.16) as in the case of the cycloaddition of the allene-ene-allene.

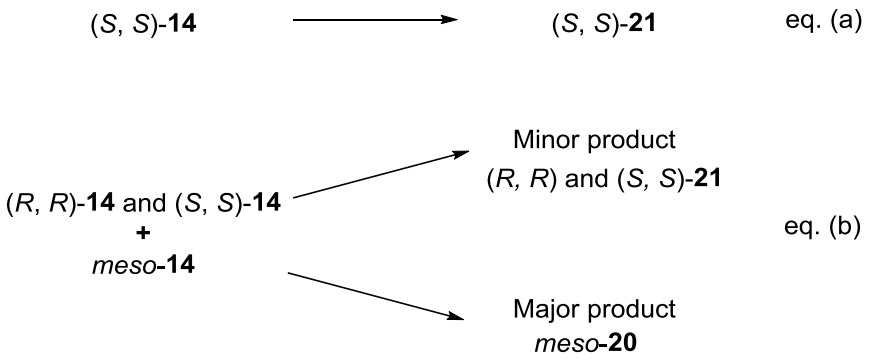

Scheme 4. 16 The absolute and relative configuration of substrates and cyclization products

So the structure that can be considered must have (*R*,*S*) configuration on the C4 and C9 position (Figure 4.25). Now, the numbers of possible structures is reduced to eight diastereisomers and a further reduction of four stereoisomers is obtained due to the symmetry of the substituents in the molecule. The four stereoisomers remaining are shown in Figure 4.26. **I** and **II** are *meso* forms and **III**, **IV** are a pair of enantiomers. Since the major product is symmetric as revealed by the ^{1}H NMR, the enantiomeric pair can be discarded.

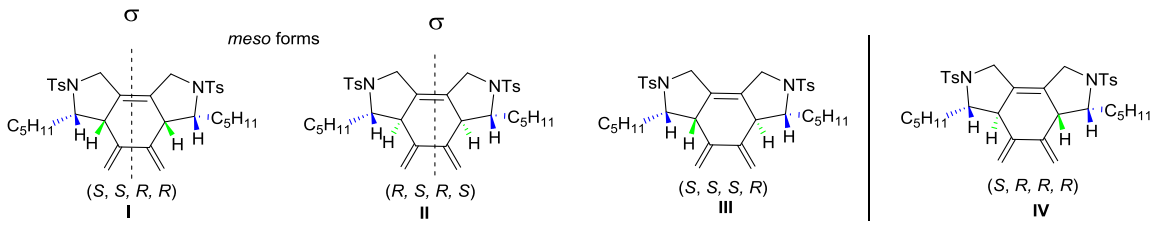

Figure 4. 26 The possible four structures of the diastereoisomer **20**

The structure of cycloadduct **20** formed in [2+2+2] cycloaddition reaction was then elucidated. After a complete chemical shift assignment of the signals, the dipolar couplings observed in the NOESY spectrum were analysed. The main difference between structure **I** and **II** is that protons H10 and H3 can be in a *cis* configuration with the protons on C9 and C4 (structure I on the Figure 4.27) or in a *trans* configuration (structure **II** on the Figure 4.27). The olefinic proton signals on C1 and C12 show dipolar coupling with the protons on C3 and C10, respectively (green arrows). The strong NOE cross-peak between H10 and H9, and between H3 and H4 (blue arrows) fully confirm the configuration of cycloadduct **20** that coincides with structure **I** in Figure 4.26.

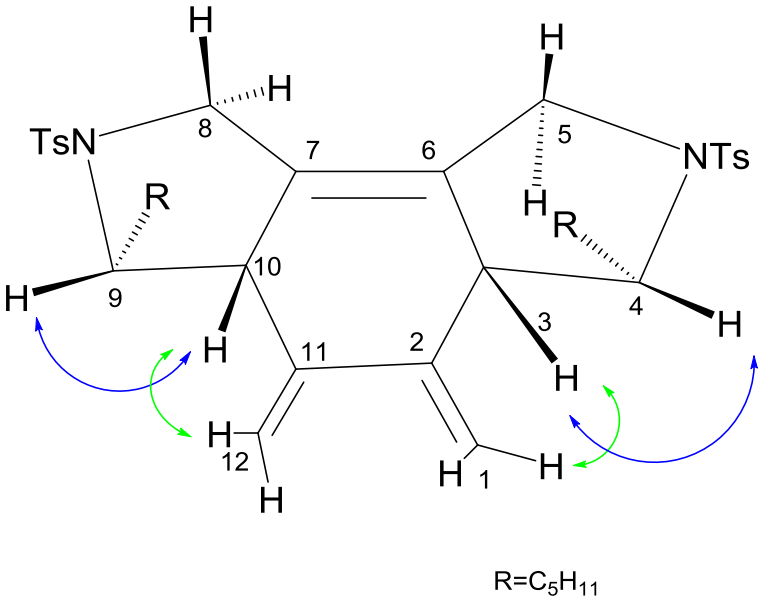

Figure 4. 27 The major NOESY correlations that were observed and help to confirm the proposed geometry of cycloadduct **20**

Chapter 5.

Dehydrogenative [2+2+2] cycloaddition of cyano-yne-allene substrates: convenient access to 2,6-napthyridine scaffolds

This chapter has been published in:

Haraburda, E.; Lledó, A.; Roglans, A.; Pla-Quintana, A. *Org. Lett.* **2015**, *17*, 2882.

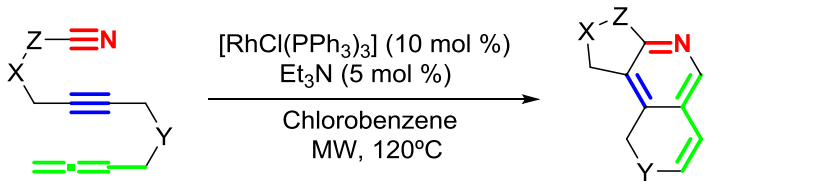

X, Y = NTs, $C(CO_2Et)_2$, O

Z = CH_2, $(CH_2)_2$,

5.1 Results and discussion

Encouraged with the results detailed in chapter 3, where allene-ene/yne-allene compounds were used as substrates affording exocyclic dienes in a completely intramolecular [2+2+2] cycloaddition reaction, we wanted to evaluate if it was possible to react an allene and a cyano group in a [2+2+2] cycloaddition reaction, as this has never been reported in the literature. Totally intramolecular reactions are entropically favoured so we decided that these at the outset would be the reactions of choice. So we designed substrates that have a cyano group, a terminal allene and either an alkene or alkyne as third insaturation in the central position to study their reactivity in the [2+2+2] cycloaddition reaction (Figure 5.1).

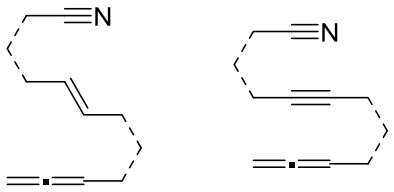

Figure 5. 1 Model substrates designed and tested in this study

5.1.1. Study of the intramolecular [2+2+2] cycloaddition of cyano-ene-allene systems

5.1.1.1. Synthesis of the cyano-ene-allene substrate

The synthesis of a cyano-ene-allene linear structure **22aa** that has *N*Ts-tethers, was defined as the first objective of this part of the thesis. The retrosynthesis of compound **22aa** is shown in Scheme 5.1.

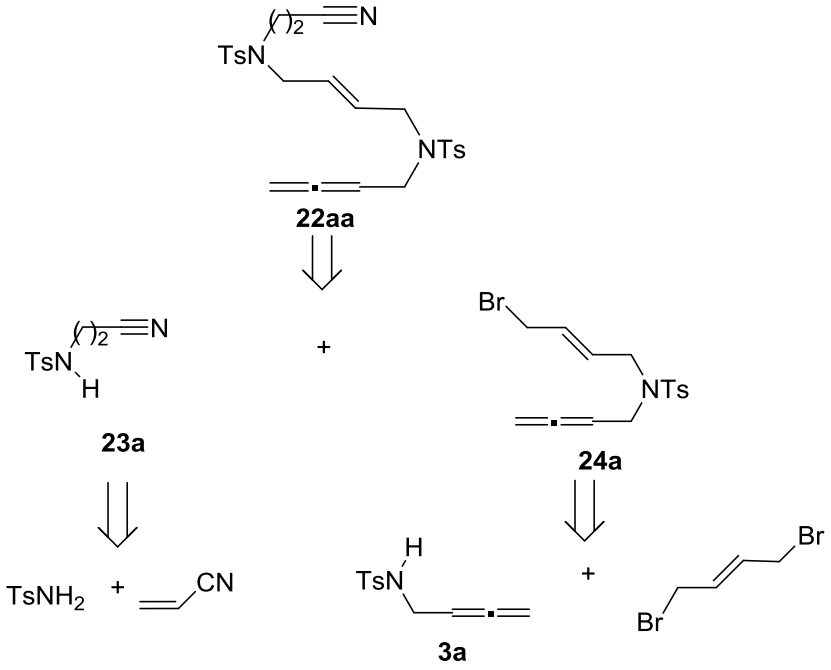

Scheme 5. 1 Retrosynthetic analysis of *N*Ts tethered cyano-ene-allene **22aa**

Cyano-ene-allene **22aa** could be prepared through the nucleophilic substitution of *N*-(cyanomethyl)-4-methylbenzenesulfonamide **23a**[17] and (*E*)-*N*-(4-bromobut-2-en-1-yl)-*N*-(buta-2,3-dien-1-yl)-4-methylbenzenesulfonamide **24a**.

Derivative **23a** was prepared by a Michael addition reaction of 4-methylbenzenesulfonamide and acrylonitrile in the presence of cesium carbonate as a base in toluene at 110˚C. The reaction yielded the product in 83 % yield (Scheme 5.2).

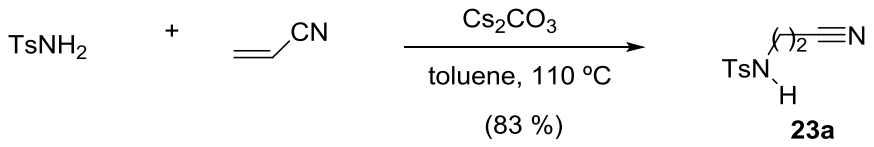

Scheme 5. 2 Synthesis of compound **23a**

Compound **24a** was prepared through the nucleophilic substitution of previously synthesised *N*-(buta-2,3-dien-1-yl)-4-methylbenzenesulfonamide **3a** (whose synthesis is detailed in chapter 3) with 4 equivalents of commercially available (*E*)-1,4-dibromobut-2-ene. The electrophile was used in excess to minimize the formation of the disubstituted product **1a**. The reaction took place affording a 60 % yield of the desired compound **24a** (Scheme 5.3) together with an 18 % yield of the disubstituted product **1a** which were separated by column chromatography.

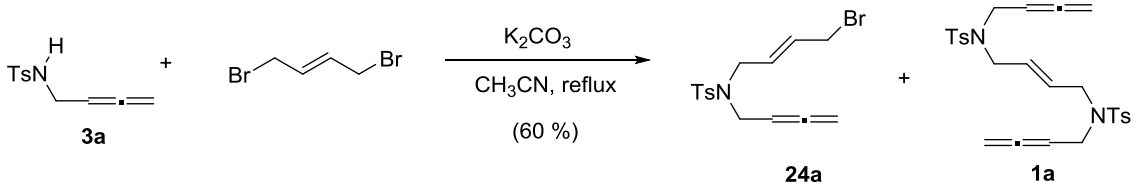

Scheme 5. 3 Synthesis of compound **24a**

To afford the desired linear cyano-ene-allene substrate **22aa**, bromo derivative **24a** was reacted with *N*-(2-cyanoethyl)-4-methylbenzenesulfonamide (**23a**). Using potassium carbonate as a base the reaction took place in 50 % yield (Scheme 5.4).

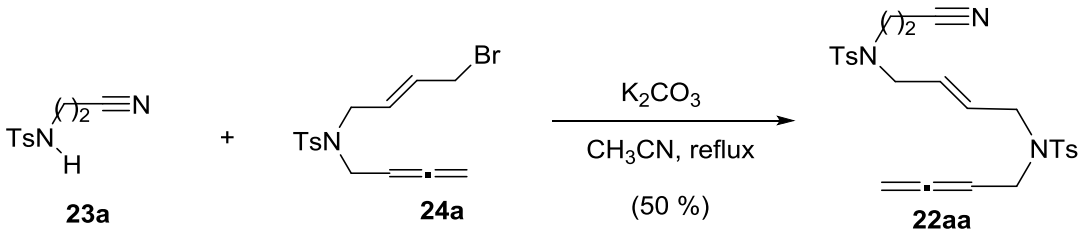

Scheme 5. 4 Synthesis of compound **22aa**

5.1.1.2. Reactivity study of cyano-ene-allene substrate

Before tackling the synthesis of other linear substrates we proceeded to evaluate the reactivity of compound **22aa** in the rhodium-catalysed [2+2+2] cycloaddition reaction. Wilkinson's catalyst was selected to start the process optimization. Two tests were carried out in toluene using either a 10 % or 20 % molar catalyst load. After one day at reflux the starting material

was consumed and a new product was formed which could be isolated and purified by column chromatography. ^{1}H NMR analysis of the isolated product showed no hint of cycloaddition product but only signals corresponding to compound **25aa** which was presumably formed by cleavage of the starting material (Scheme 5.5).

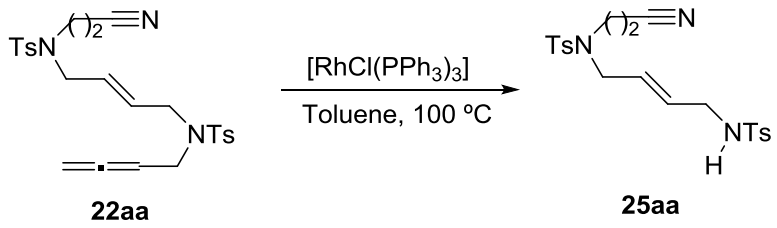

Scheme 5. 5 Reaction of cyano-ene-allene **22aa** using Wilkinson's catalyst

Formation of **25aa** was also confirmed by ESI-MS in the positive ion mode, which showed a peak at *m*/*z*=470.1 that corresponds to [**25aa**+Na]$^{+}$ adduct.

Figure 5. 2 ESI-MS of cyano-ene-allene reaction using Wilkinson's catalyst

After this unexpected results we proceeded to evaluate the linear cyano-ene-allene substrate in the [2+2+2] cycloaddition reaction using cationic rhodium(I) complexes as catalysts. The cyano-ene-allene substrate was treated with $[Rh(cod)_2]BF_4$ in combination with different biphosphines such as *Tol*-binap, (*R)*-binap, (*R)*-H_8-binap or Segphos. A set of experiments was run using different solvents such as dichloroethane, toluene and chlorobenzene. Reactions were carried out in different temperatures using either conventional or microwave heating. In every reaction a mixture of two products was obtained in different ratio depending on the reaction conditions used. These two products could be isolated and purified by column chromatography. Comparison of the proton spectra obtained for the two products (Figure 5.3 and Figure 5.4) with the spectra of the starting material showed that the signals which correspond to the methylene groups next to the cyano group remain at the same position (δ=2.61 and δ=3.27 ppm) and the alkene unit is unchanged as well (δ=5.56 ppm). The allene motif disappeared in the two products. Taken together these are clear evidences that the reaction did not proceed via a cycloaddition pathway. After a deeper analysis of the ^{1}H-NMR spectra, one of the products was assigned to the cleavage product **25aa** already obtained with the Wilkinson's catalyst (Scheme 5.6 and Figure 5.3).

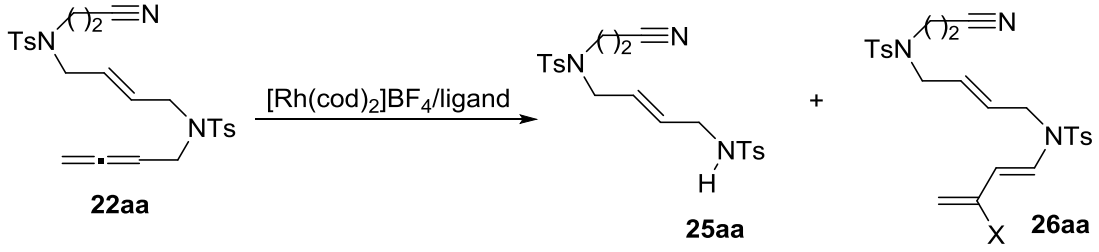

Scheme 5. 6 Reaction of cyano-ene-allene using $[Rh(cod)_2]BF_4$

Figure 5. 3 ^{1}H NMR spectrum of cleavage product **25aa** formed in reaction using $[Rh(cod)_2]BF_4$

The spectrum of the other product showed new signals in the olefinic region δ~4.8 ppm and δ~6.9 ppm (Figure 5.4). The product could not be fully elucidated but presumably an allene rearrangment occured[86] giving the diene motif that gives the characteristic signals marked with green squares in the 1H-NMR spectra (structure **26aa**, Scheme 5.6).

Figure 5. 4 ^{1}H NMR spectrum of isomerised product **26aa** formed in reaction using $[Rh(cod)_2]BF_4$

In summary, all the attempts made towards the [2+2+2] cycloaddition reaction of the cyano-ene-allene derivatives were unsuccessful. The allene motif was either cleaved or isomerized at the end of the reaction whereas the other unsaturations remained untouched. Therefore we decided to move forward to another objective.

5.1.2. Study of the intramolecular [2+2+2] cycloaddition of cyano-yne-allene systems

5.1.2.1. Synthesis of cyano-yne-allene substrates with NTs-tethers

Alkynes are more reactive than alkenes in the [2+2+2] cycloaddition reaction. Due to the lack of reactivity in the [2+2+2] cycloaddition reaction of the cyanoallene compound that has an alkene in the centre we decided to synthesise compounds which have an alkyne in the middle instead. The synthesis started with compounds that contain a sulphonamide in the linkage. The proposed retrosynthetic analysis for the preparation of linear cyano-yne-allenes that have *N*Ts-tether is represented in Scheme 5.7.

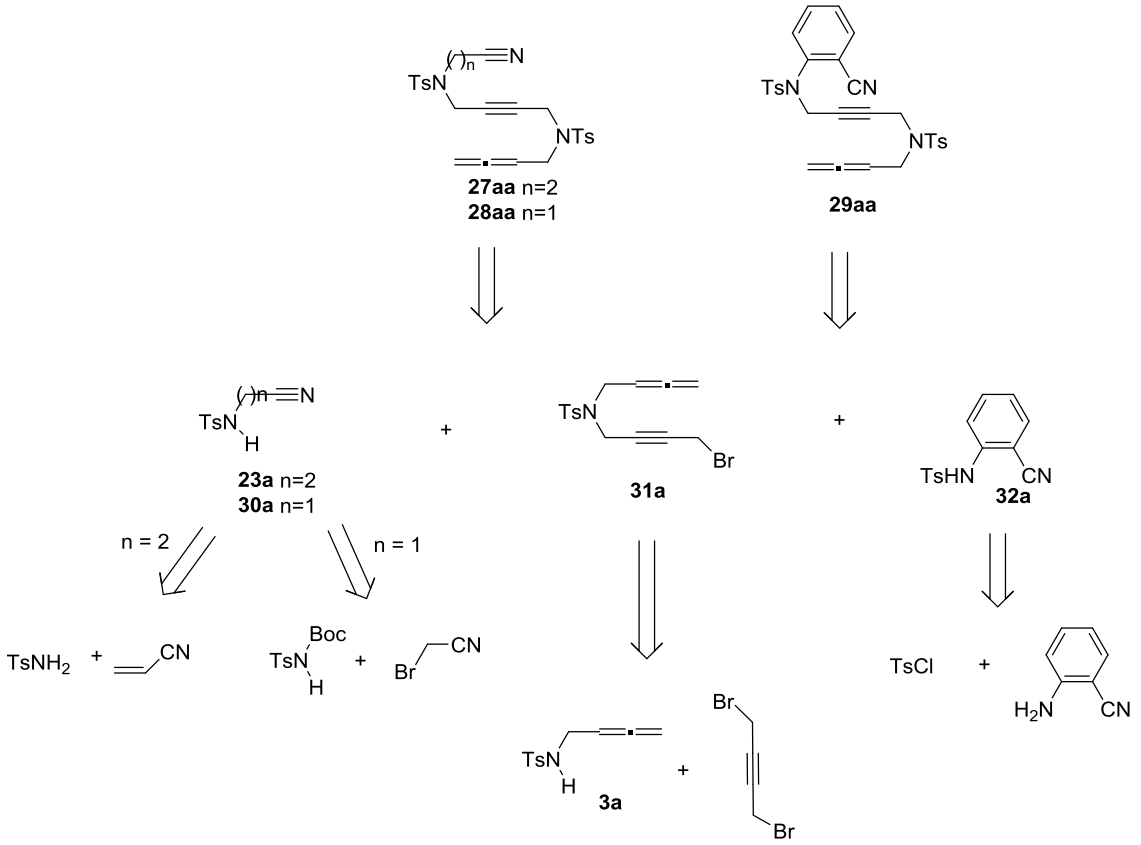

Scheme 5. 7 Retrosynthetic analysis of cyano-yne-allene compounds with *N*Ts tethers

*N*Ts-tethered linear cyano-yne-allene compounds **27aa**, **28aa** and **29aa** could be prepared through nucleophilic substitution of *N*-(cyanoethyl)-4-methylbenzenesulfonamide (**23a**), *N*-(cyanomethyl)-4-methylbenzenesulfonamide (**30a**) or *N*-(2-cyanophenyl)-4-methylbenzenesulfonamide (**32a**)[87] respectively with the bromo derivative intermediate **31a** which is a common intermediate in the synthesis of these three compounds. We have chosen different nitrilesulfonamide units to evaluate the possibility to form cycloadducts with different ring sizes. Among them, the incorporation of *N*-(2-cyanophenyl)-4-methylbenzenesulfonamide **32a** was planned to test the effect on the cycloaddition of a rigid aromatic ring in the tether and also to increase the complexity in the cycloadducts which could be formed.

The common intermediate **31a** was first synthesized as represented in Scheme 5.8.

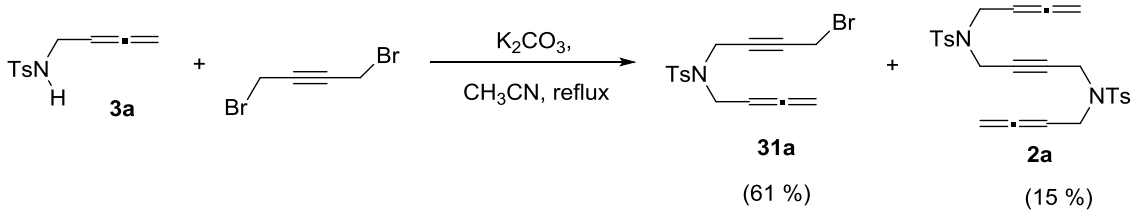

Scheme 5. 8 Synthesis of intermediate **31a**

Compound **31a** was prepared in accordance with the methods described in the literature for similar tosylamine compounds. *N*-(buta-2,3-dien-1-yl)-4-methylbenzenesulfonamide **3a** was reacted with 4 equivalents of 1,4-dibromobut-2-yne in acetonitrile at reflux with a high excess of potassium carbonate as a base. The electrophile was used in excess to minimize the formation of the disubstituted product **2a**. The reaction took place affording a 61 % yield of compound **31a** together with a 15 % yield of product **2a** which could be easily separated by column chromatography (Scheme 5.8).

In parallel, compound **30a** was prepared in two steps. In the first one, *tert*-butyl tosylcarbamate was reacted with 2-bromoacetonitrile using potassium carbonate as a base in acetonitrile at reflux. Boc-protected 4-methylbenzenesulfonamide was used to avoid the formation of the disubstitution product. The second step was the deprotection of the sulfonamide using trifluoroacetic acid in dichloromethane at room temperature. The overall yield of this reaction was 68 %. Finally, compound **32a** was prepared by reacting 2-aminobenzonitrile and 4-methylbenzenesulfonyl chloride in acetonitrile using potassium carbonate as a base. The reaction afforded the tosylated product **32a** in 70 % yield (Scheme 5.9).

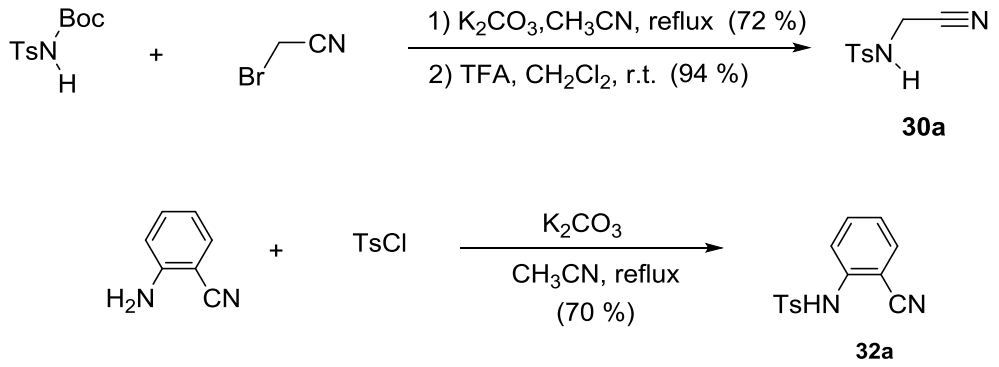

Scheme 5. 9 Synthesis of intermediates **30a** and **32a**

Once the reacting partners **23a** (whose synthesis is described in section 5.1.1), **30a** and **32a** were ready, compounds with *N*Ts-tethers could be prepared by reaction of the respective cyanosulfonamide with compound **31a**. In all cases using potassium carbonate as a base *N*Ts-linked cyano-yne-allene **27aa**, **28aa** and **29aa** were obtained in very good yields (Scheme 5.10).

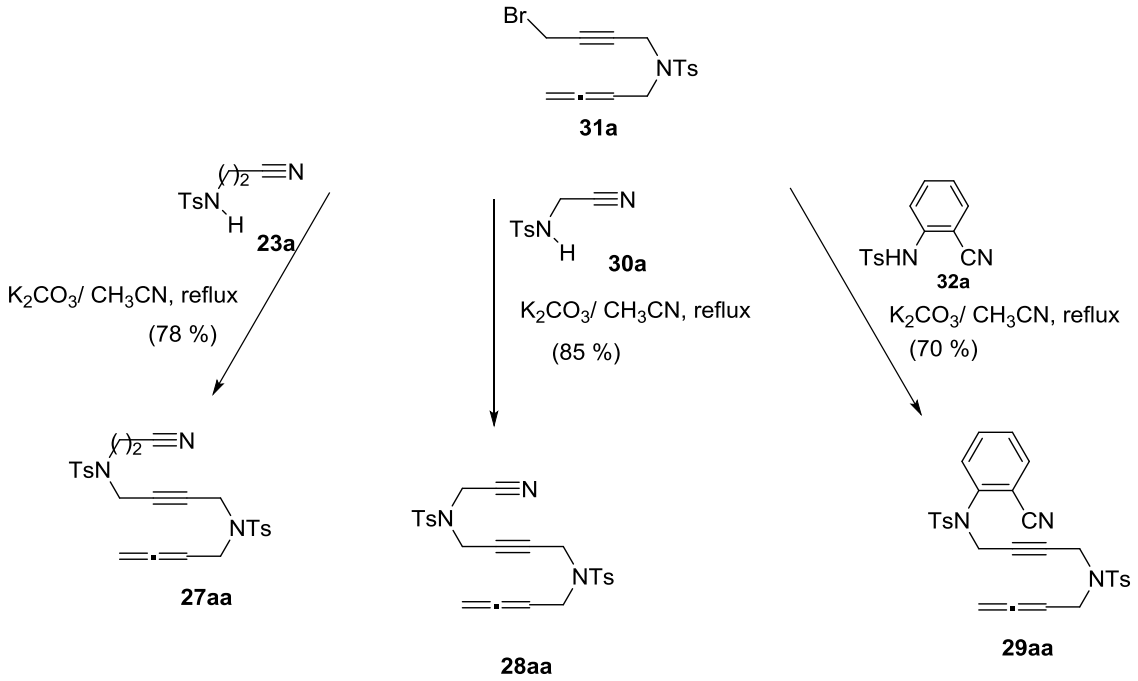

Scheme 5. 10 Synthesis of *N*Ts-linked cyano-yne-allene **27aa**, **28aa** and **29aa**

5.1.2.2. Synthesis of cyano-yne-allene substrates with malonate tether

To study the influence of the group that links the unsaturations in the cyano-yne-allene structure, it was decided to prepare analogous compounds in which either one or two of the tethers were replaced with malonates. The retrosynthetic analysis for the compounds which contain one malonate and one *N*Ts- linkage **27ba** or two malonates tethers **27bb** is detailed in Scheme 5.11.

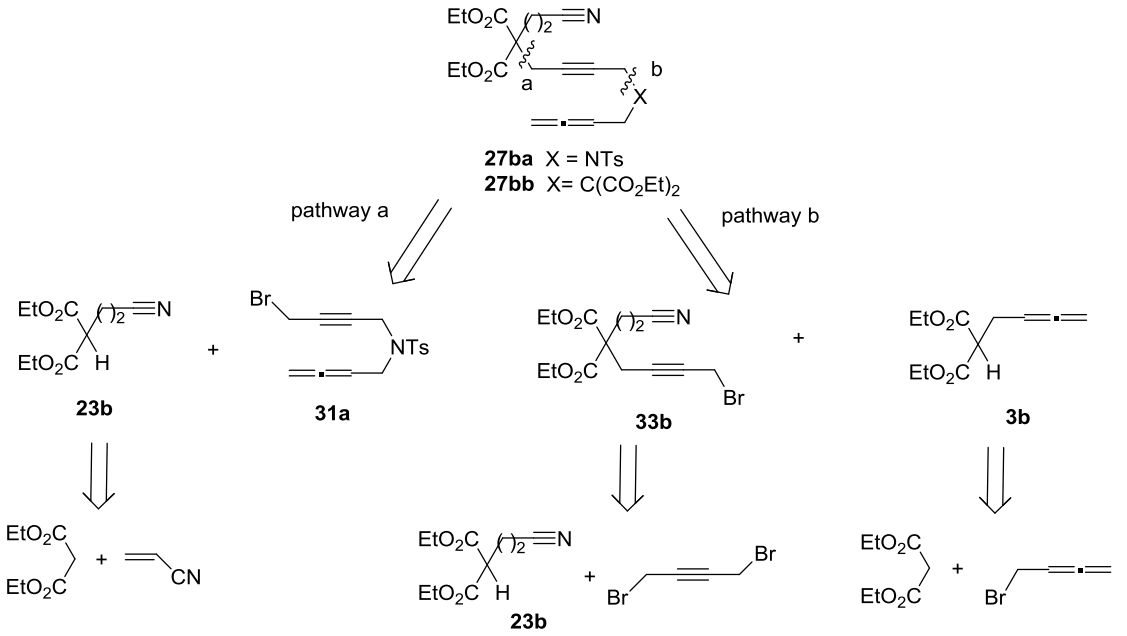

Scheme 5. 11 Retrosynthetic route of cyano-yne-allene **27ba** and **27bb**

The common intermediate **31a** (synthesis detailed in scheme 5.8) and diethyl 2-(2-cyanoethyl)malonate **23b**[88] were proposed as intermediates for the synthesis of ompound **27ba**. Cyanomalonate derivative **33b** and but-3,4-dienylmalonate **3b**[89] could be used to obtain compound **27bb**.

The malonate derivatives **23b**, **33b** and **3b** were prepared in accordance with the general method described in the literature for the synthesis of **23b**,[88] which consist on the reaction of diethyl malonate or diethyl malonate derivatives with high excess of the electrophile in the presence of a strong base. Using sodium hydride as a base in tetrahydrofuran, the reaction took place at low temperature affording the desired products in very good yields (Scheme 5.12).

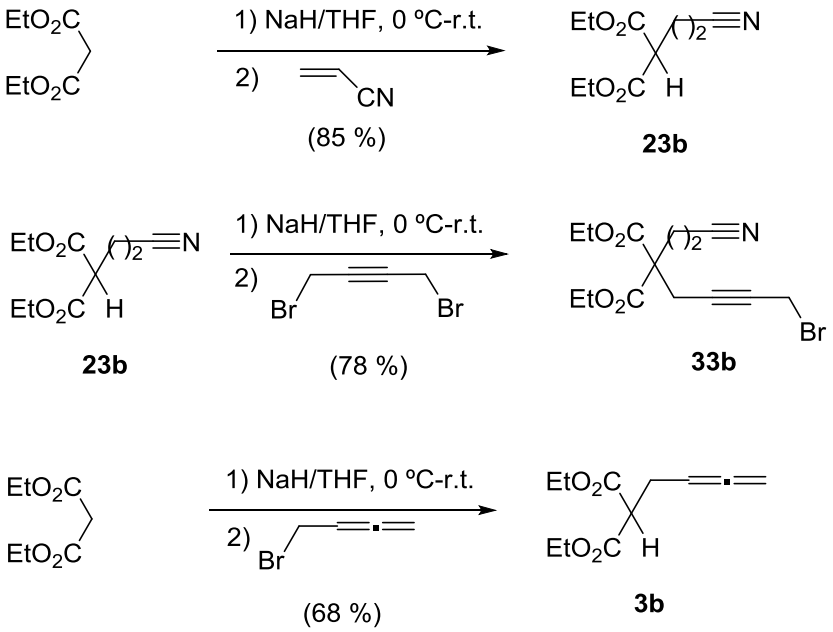

Scheme 5. 12 Synthesis of compounds **23b**, **33b** and **3b** by monoalkylation of malonate derivatives

The same alkylation method was used to obtain compounds **27ba** and **27bb**. The substitution reaction of cyanomalonate derivative **23b** or **33b** with allenic compounds **31a** or **3b**, respectively, in the present of sodium hydride at 0˚C efficiently yielded the desired products (Scheme 5.13).

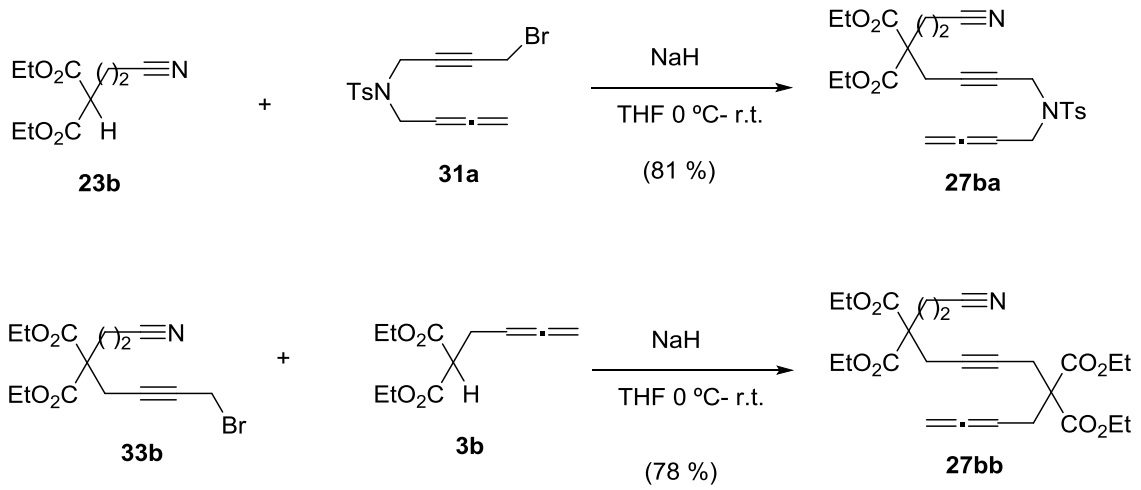

Scheme 5. 13 Synthesis of malonate-linked cyano-yne-allene **27ba** and **27bb**

5.1.2.3. Synthesis of cyano-yne-allene substrates with O-tether

In order to have more substrates to evaluate the influence of the tether, the synthesis of *O*-tethered compounds **27ac** and **29ac** (Scheme 5.14) and **28ca** (Scheme 5.17) was planned. *O*-tethered compounds **27ac** and **29ac** were planned to be prepared by Crabbé homologation of the corresponding cyanodyines **34ac** and **35ac**, compounds that have a terminal triple bond. Compounds **34ac** and **35ac** could be prepared by a Mitsunobu reaction of the common substrate 4-(prop-2-yn-1-yloxy)but-2-yn-1-ol **36c**[90] with the corresponding nitrolosulfonamides **23a** and **32a**, respectively (Scheme 5.14).

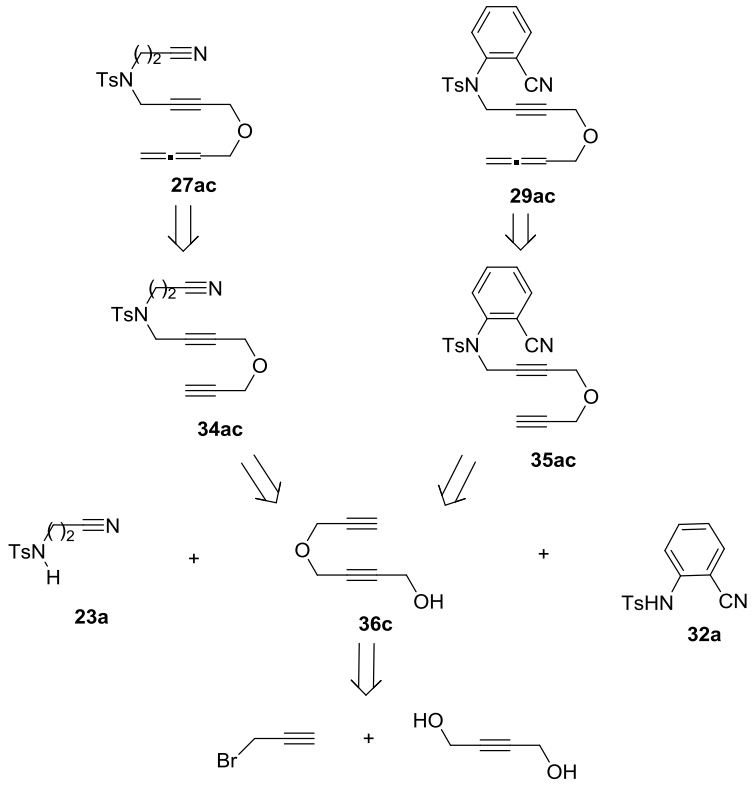

Scheme 5. 14 Retrosynthetic analysis of cyano-yne-allene **27ac** and **29ac**

Compounds **34ac** and **35ac** were prepared by a Mitsunobu reaction of 4-(prop-2-yn-1-yloxy)but-2-yn-1-ol **36c**[90] and either *N*-(cyanomethyl)-4-methylbenzenesulfonamide **23a** or *N*-(2-cyanophenyl)-4-methylbenzenesulfonamide **32a**. Using triphenylphosphine and DIAD, the reaction took place affording cyanodiyne **34ac** and benzocyanodiyne **35ac** in good 55 % and 85 % yield, respectively (Scheme 5.15).

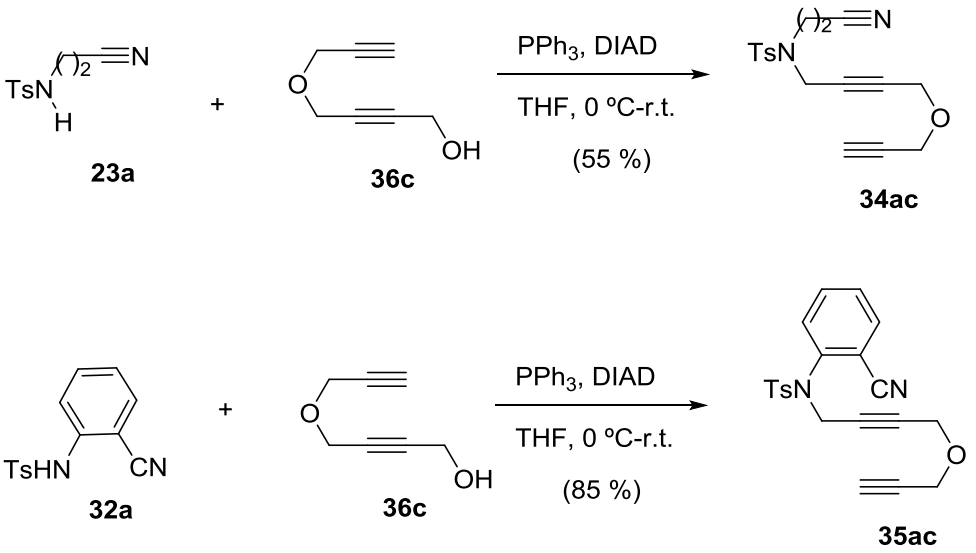

Scheme 5. 15 Synthesis of the substrate **34ac** and **35ac**

Terminal alkynes were converted to terminal allenes by Crabbé homologation. The reactions were performed using dicyclohexylamine, copper iodide and paraformaldehyde affording in good yields the allenic products **27ac** and **29ac** (Scheme 5.16).

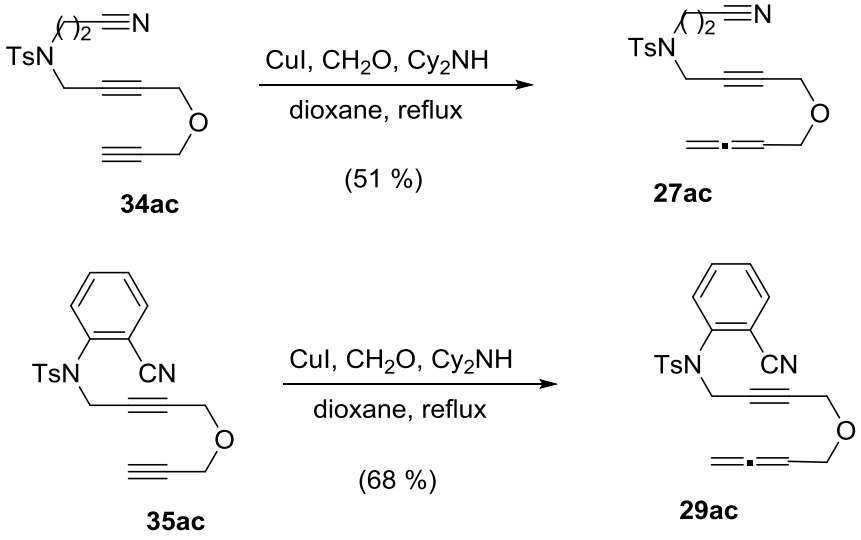

Scheme 5. 16 Synthesis of the substrate **27ac** and **29ac**

Finally, the synthesis of compound **28ca** was planned taking advantage of the already synthesised tosylallene **3a,** which through a Mitsunobu reaction with 2-((4-hydroxybut-2-yn-1-yl)oxy)acetonitrile **37c**[91] should afford the desired compound (Scheme 5.17).

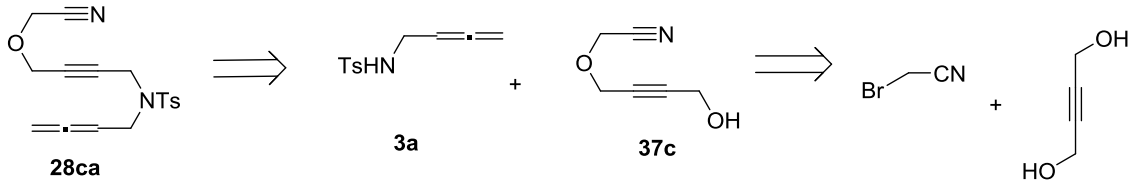

Scheme 5. 17 Retrosynthetic analysis of cyano-yne-allene **28ca**

Compound **37c** was prepared by a Williamson ether synthesis using commercially available 85 % KOH pellets as the base. Over the suspension of KOH and but-2-yne-1,4-diol in DMSO, 2-bromoacetonitrile was added. The reaction took place affording product **37c** in 47 % yield (Scheme 5.18).

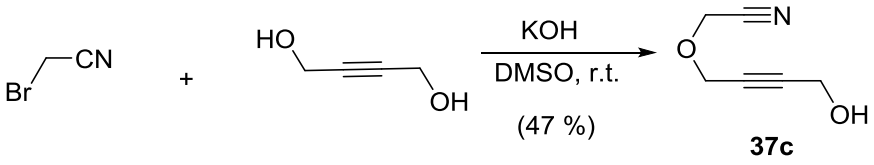

Scheme 5. 18 Synthesis of the compound **37c**

N-(buta-2,3-dien-1-yl)-4-methylbenzenesulfonamide **3a** and 2-((4-hydroxybut-2-yn-1-yl)oxy)acetonitrile **37c** were used to synthesise compound **28ca** in a Mitsunobu reaction. Using triphenylphosphine and DIAD the product was obtained in 72 % yield (Scheme 5.19).

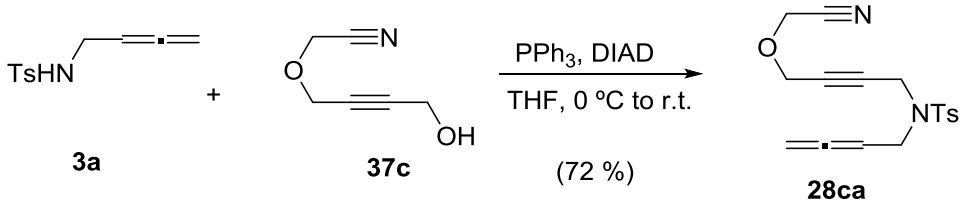

Scheme 5. 19 Synthesis of the substrate **28ca**

5.1.2.4. Reactivity study of cyano-yne-allene substrates

The study of the reactivity of linear cyano-yne-allene substrates was then undertaken using a cationic rhodium source, $[Rh(cod)_2]BF_4$, in combination with biphosphine ligands as the catalytic system of choice. The catalyst was generated *in situ* by hydrogenation of a mixture of $[Rh(cod)_2]BF_4$ and the corresponding biphosphine in dichloromethane. The substrate bearing *N*Ts-linkage was chosen to do the optimization study. Initially, the combination of *Tol*-binap with $[Rh(cod)_2]BF_4$ was tested. The reaction was carried out in dichloroethane as the solvent at reflux. After two hours, the starting material disappeared and two new products were formed in a 2:1 ratio as determined by ^1H NMR analysis of the crude reaction mixture (Scheme 5.20).

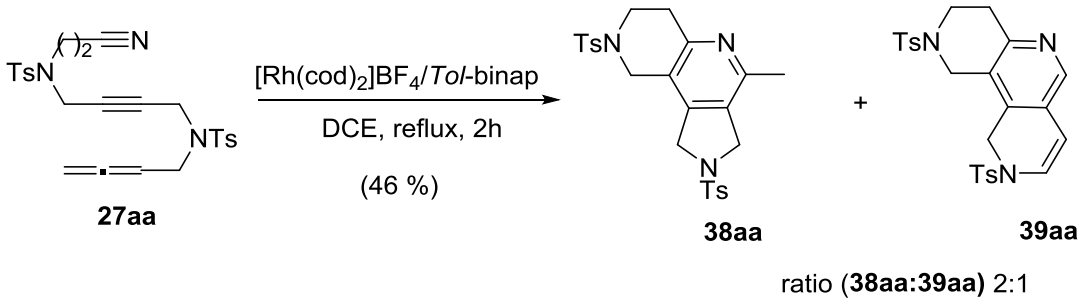

Scheme 5. 20 Reaction of cyano-yne-allene using $[Rh(cod)_2]BF_4$ and *Tol*-binap

Product **38aa** contains a pyridine ring which is presumably formed after [2+2+2] cycloaddition of the nitrile, the alkyne, and the internal double bond of the allene, and a subsequent tautomerization to gain aromaticity (Scheme 5.21). The same product **38aa** can be formed by reaction with a triple bond instead of the allene, as already shown in METSO group.[17] Highly functionalized pyridines were successfully obtained in a Wilkinson's catalyst catalysed [2+2+2] cycloaddition reaction of cyanodiynes run under microwave heating (Scheme 5.22). Whereas the formation of product **39aa** is interesting because it shows that the allene can participate together with a cyano group in the [2+2+2] cycloaddition reaction, the use of an allene moiety instead of an alkyne did not seem to have any advantage in the formation of the tricyclic pyridine scaffold.

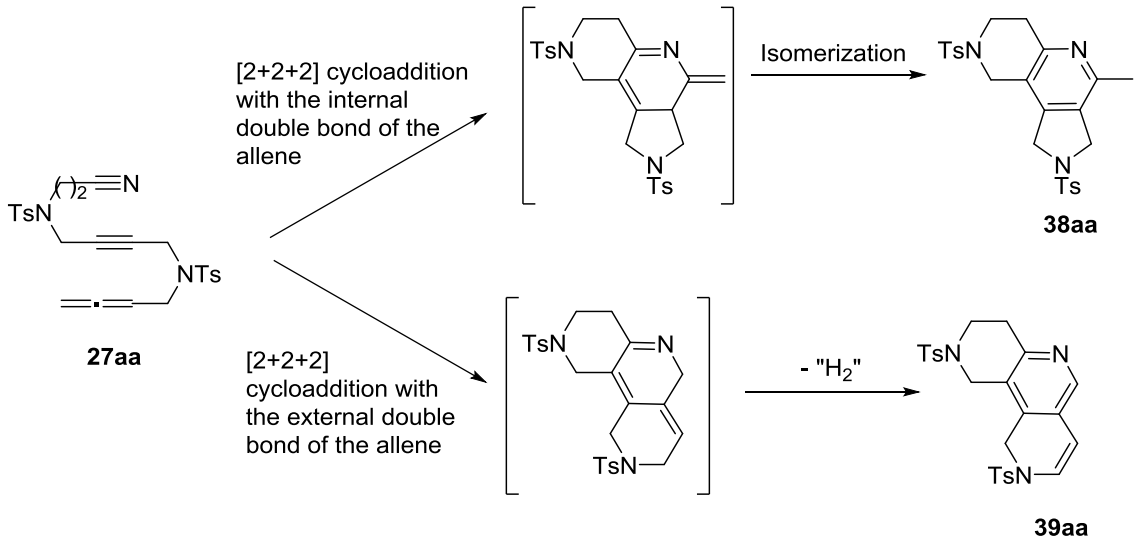

Scheme 5. 21 Different reaction pathway of cyano-yne-allene depending on which double bond is participating in the reaction

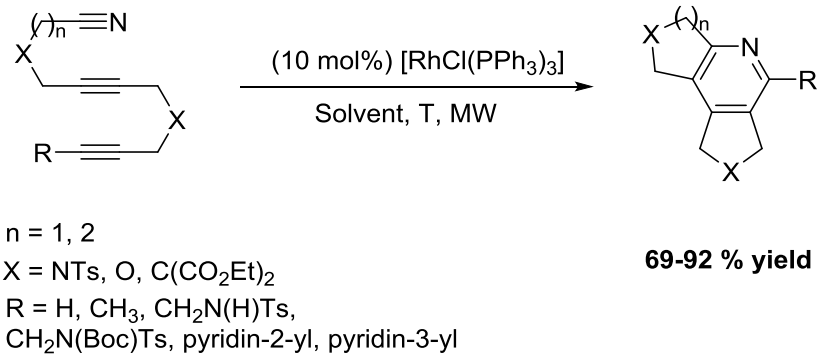

Scheme 5. 22 Pyridines products obtained in the [2+2+2] cycloaddition of cyanodiynes

Therefore we focused our interest on product **39aa**, which could be isolated as a pure fraction from the reaction mixture. On the ESI-MS spectrum a peak at m/z=496 was observed which shows a mass decrease of two mass units compared to the starting material **27aa**. This evidence clearly confirmed that product **39aa** had lost two hydrogen atoms with respect to the starting compound. After a detailed spectroscopic analysis, product **39aa** was identified to be a tricyclic adduct in which there was a central pyridine as indicated by the proton signal at δ=8.00 ppm in the ^{1}H NMR spectra (green rectangle in Figure 5.5), surrounded by two 6-membered aza rings, one of which had a double bond giving characteristic doublets signals at δ=5.79 and δ=6.83 ppm in the ^{1}H NMR spectra (blue rectangles in Figure 5.5). This product is postulated to be formed by a [2+2+2] cycloaddition reaction of the cyano, the alkyne and the external double bond of the allene, followed by a dehydrogenative isomerization (Scheme 5.21).

Figure 5. 5 ^{1}H NMR spectrum of the product **39aa**

In summary, this first reaction showed that allenes effectively react with nitriles in the [2+2+2] cycloaddition reaction but it also showed that the regioselectivity of the process regarding the double bond of the allene which participates in the process could not be controlled under the reaction conditions studied (Scheme 5.21).

The product **39aa** obtained can be viewed as a 2,6-naphthyridine derivative. The first naphthyridine derivative was obtained and named by Arnold Reissert in 1893 as the pyridine like analogue to naphthalene.[92] There are six isomeric naphthyridines which are defined through the position of the nitrogens in the bicyclic system. 2,6-Naphthyridine was independently reported by Giacomello et al. and Tan et al. in 1965.[93] Although the chemistry of 2,6-naphthyridines had attracted much less attention than that of the 1,5-, 1,6- or 1,7-naphthyridines, 2,6-naphthyridines derivatives show broad biological activities which have been found to have promising medicinal properties, including anti-HIV[94] and anticancer[95] (Figure 5.6).

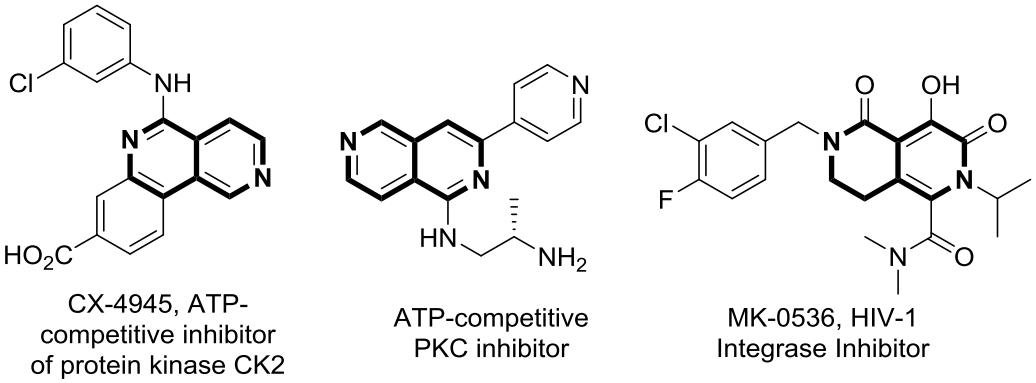

Figure 5. 6 Representative structures of biologically active 2,6-naphthyridine scaffolds

There are not many general methods reported in the literature for the synthesis of 2,6-naphthyridine scaffolds.[96] Rajamanickam and Shanmugam reported in 1985[97] the oxidative cyclization of 4-carbamoyl-3-(2-hydroxyethyl)quinolines **Ia-c** under CrO_3 in glacial acetic acid giving rise to benzo[*c*]2,6-naphthyridine-like derivatives **IIa-c**. The later were used in the synthesis of 2,6-naphthyridines **IIIa-c.** Further transformation lead to compound **IVa** or **Va** (Scheme 5.23).

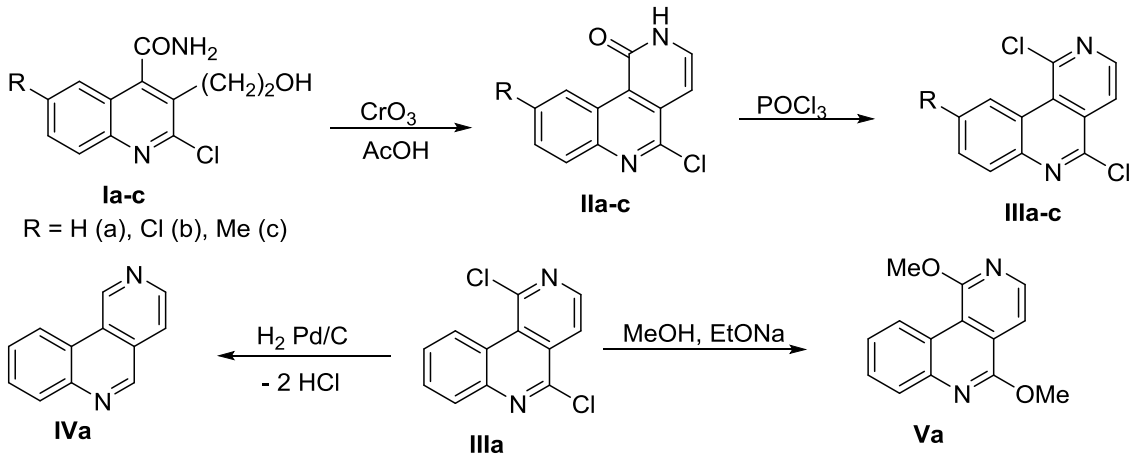

Scheme 5. 23 Synthetic route to obtain 2,6-naphthyridines through oxidative cyclization

The synthesis of the octahydro-2,6-naphthyridine scaffold **VII** used as a medicine or prophylaxis and treatment of schizophrenia and depressions was covered in a 1997 patent.[98] The bicyclic structure was constructed through a cyclization under Mitsunobu reaction conditions of 3-(2-hydroxyethyl)pyridine-2-carboxylic acid. Subsequent reaction of the resulting 2,6-naphtyridine **VI** with benzyl bromide and then with sodium borohydride afforded octahydro-2,6-naphthyridine **VII** (Scheme 5.24).

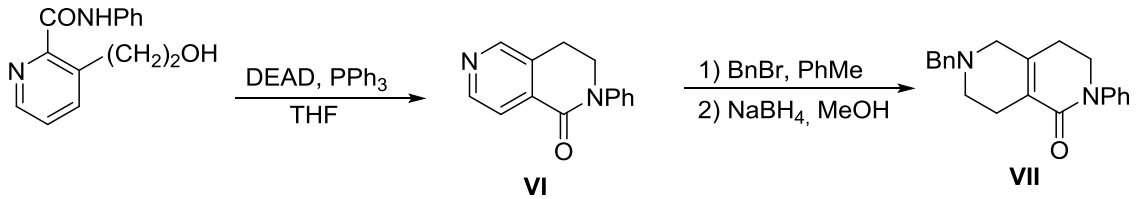

Scheme 5. 24 Synthetic route to obtain 2,6-naphthyridines through Mitsunobu reaction

The synthesis of a completely hydrogenated 2,6-naphthyridinetetrone was also reported by Elnagdi et al. in 1985.[99] The naphthyridine scaffold was obtained by treatment of toluidides of halogen-substituted acetoacetic acid with sodium hydride in dioxane which led to an intermolecular cyclization to form **VIII** (Scheme 5.25).

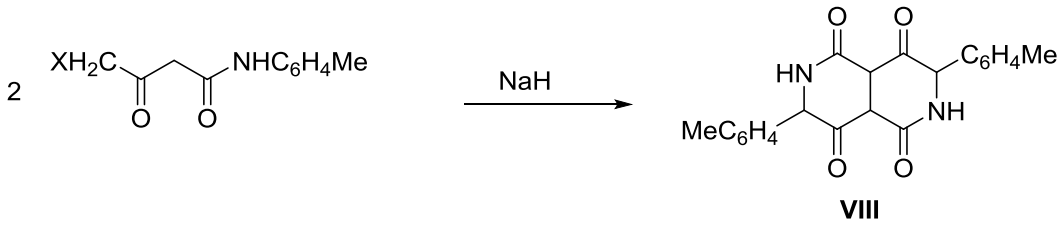

VIII

Scheme 5. 25 Synthetic route to obtain 2,6-naphthyridines through intermolecular cyclization

In summary, there are not many methods reported for the synthesis of 2,6-naphthyridines and most of them rely on reactions of amides that construct derivatives that contain a keto group in the scaffold. Since the cycloaddition of **27aa** could be a simple and straightforward route to new naphthyridine derivatives we decided to further develop the methodology.

In order to favour the formation of the desired product **39aa** different reaction conditions were tried. After the first attempt using $[Rh(cod)_2]BF_4$ and *Tol*-binap as catalytic system, a second trial was done in the same conditions but increasing the reaction time, unfortunately neither the regioselectivity nor the yield were improved (Entry 1-2, Table 5.1). Other biphosphine ligands such as (*R*)-H_8-binap and (*R*)-binap were then tried in dichloroethane at reflux. In the two cases the yield decreased and the use of (*R*)-H_8-binap favoured the formation of the undesired tricyclic pyridine **38aa** (Entry 3-4, Table 5.1). The use of microwave as heating source was also evaluated in an attempt to minimalize the formation of undesired product **38aa** but the yield worsen and the product ratio was maintained (Entry 5, Table 5.1). Finally, the reaction completely failed leading to the recovery of the starting material when Segphos was used as ligand (Entry 6, Table 5.1). Catalysts based on cobalt have shown great efficiency in the synthesis of pyridines through [2+2+2] cycloaddition reaction, therefore we decided to test the $[CpCo(CO)_2]$ complex. **27aa** was reacted with one equivalent of $[CpCo(CO)_2]$ in xylene at 140^0C under irradiation (330 W visible lamp). Unfortunately no cycloaddition was observed and only the starting material could be recovered.

Table 5. 1 [2+2+2] cycloaddition reaction on cyano-yne-allene using cationic Rh catalytic systems

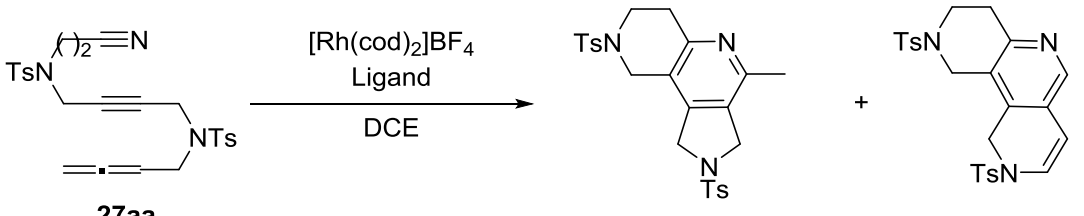

27aa **38aa** **39aa**

Entry	Ligand	Reaction time	38aa:39aa	Yield[b]

		/temperature	product ratio[a]	
1	*Tol*-binap	2h/reflux	2:1	46%
2	*Tol*-binap	3h/reflux	2:1	48%
3	(*R*)-H_8-binap	2h/reflux	3:1	34%
4	(*R*)-binap	5h/reflux	2:1	30%
5	(*R*)-binap	30min/80˚C[c]	2:1	10%
6	Segphos	24h/reflux	n.r.	n.r.

[a] Ratio of the regioisomers **38aa**:**39aa** calculated by ^{1}H-NMR analysis of the reaction mixture. [b] The yield refers to the mixture of the two regioisomeric products **38aa** and **39aa**. [c] Microwave heating.

In an attempt to find reaction conditions that selectively afford the dehydrogenative process, we proceeded to evaluate the reactivity of linear cyano-yne-allene using the Wilkinson's catalyst. Various reactions were performed using different solvents such as toluene, dichloroethane, chlorobenzene, 1,2-dichlorobenzene or even solvent mixtures (Table 5.2).

Table 5. 2 Optimization of the cycloaddition reaction using Wilkinson's catalyst

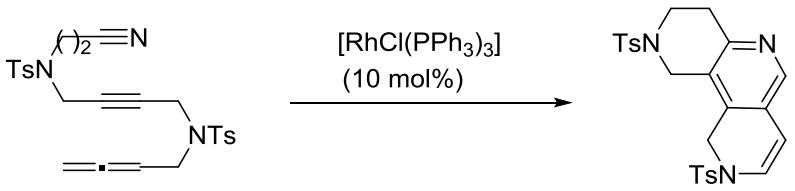

27aa **39aa**

Entry[a]	Solvent	Temp. (˚C)	Additive (eq.)	Reaction time (min.)	Yield (%)
1[b]	Toluene	reflux	-	240	48
2	Toluene	90	-	45	30
3	Chlorobenzene	120	-	30	50
4[c]	Chlorobenzene	120	-	30	40
5	1,2-dichlorobenzene	140	-	30	40
6	DMF:H_2O (1:1)	90	-	30	n.r.
7	Chlorobenzene	120	TFA (1)	30	30
8	Chlorobenzene	120	Et_3N (1)	10	54
9	Chlorobenzene	80	Et_3N (1)	10	46
10	Chlorobenzene	120	Et_3N (0.1)	10	64
11	Chlorobenzene	120	Et_3N (0.05)	10	66
12	Chlorobenzene	120	Cy_2NH (0.1)	20	40
13	Chlorobenzene	120	Quinuclidine (0.05)	30	41
14	Chlorobenzene	120	Hunig's base (0.05)	10	49
15	Chlorobenzene	120	2,6-di-*tert*-butylpyridine (0.05)	40	33

[a] A solution of **27aa** (0.05 M) and Wilkinson's catalyst (10 mol%) in the solvent noted was heated at the indicated temperature under microwave irradiation. [b] Reaction carried out under conventional heating. [c] Reaction carried out at a 0.025 M concentration of **27aa**.

When **27aa** was added to a hot solution of the Wilkinson's catalyst in toluene heated at reflux, only one product was formed which could be isolated in 48 % yield after column chromatography from a quite complex reaction mixture (Entry 1, Table 5.2). The result was confirmed by the ESI-MS spectrum showing only one peak at *m*/*z*=496 verifying the formation of the dehydrogenative product **39aa**.

In order to minimize the decomposition, the reaction was tested under microwave irradiation.[100] A first trial using toluene as the solvent at 90˚C for 45 min achieved the formation of a 30 % yield of the dehydrogenative cycloadduct in a process with only a 30 % of conversion (Entry 2, Table 5.2). In order to increase the conversion the solvent was switched to chlorobenzene and the temperature increased to 120˚C. The reaction leads to a 50 % yield in a process with full conversion (Entry 3, Table 5.2). Neither the dilution of the reaction mixture, nor an increased temperature or a change in the solvent system improved the reaction (Entries 4-6, Table 5.2). We next decide to test the effect of adding some additive to the reaction mixture. Whereas the addition of trifluoroacetic acid was detrimental to the reaction (Entry 7, Table 5.2), the addition of triethylamine allowed the cycloadduct to be obtained in an increased yield and a shorter reaction time (Entry 8, Table 5.2). It is important to note here that addition of triethylamine to rhodium(I)-catalysed reactions has already been shown to favour some reactions.[101] Corey et al. described that in the rhodium(I)-catalyzed addition of potassium isopropenyl trifluoroborate to enones, the addition of triethylamine not only inhibited the Lewis acid-induced hydrolysis of the substrate, but also greatly accelerated the conjugate addition reaction. Consequently the reaction could be carried out at room temperature.[101a] Tanaka et al. established that $[RhCl(PPh_3)_3]$ catalyzes the reaction of thiols with polychloroalkanes to form formaldehyde dithioacetals in the presence of triethylamine and claimed that the organic base helps in the product formation by a dehydrogenative process.[101b] On the other hand, Ikeda et al. reported that the [2+2+2] cycloaddition of diynes and α,β-enones in the presence of triethylamine and Ni(0) species initially generate a 1,3-diene which was easily dehydrogenated to give aromatized product.[101e]

The reaction was then evaluated with different amounts of triethylamine, and optimal results were obtained with a 5 % mol (Entries 9-11, Table 5.2). Finally the use of alternative nitrogenated bases such dicyclohexylamine, quinuclidine, Hunig's base and 2,6-di-*tert*-butylpyridine was examined, but the yield could not be improved (Entry 12-15, Table 5.2). Since best results are obtained when catalytical quantities of triethylamine are used we believe that the base might have an influence on the catalyst, either by stabilizing it or generating more reactive species.

Once, the best condition for the reaction on substrate **27aa** were found, we proceeded to evaluate the scope of the process on a series of cyano-yne-allene scaffolds having different tethers and number of methylenic units between the tether and the cyano group (Scheme 5.26).

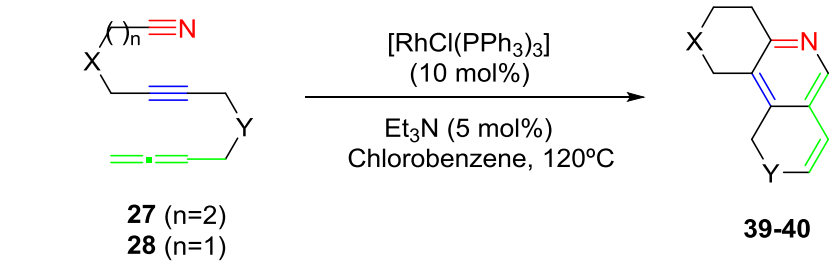

Scheme 5. 26 Scope of the intramolecular cycloaddition reaction

Figure 5.7 shows the different pyridine derivatives which have been formed from linear cyano-yne-allene substrates in the totally intramolecular dehydrogenative cycloaddition reactions. Cycloadducts having 6,6,6-tricyclic (**39aa**, **39ba** and **39bb**) and 5,6,6-tricyclic scaffolds (**40aa**, **39ac** and **40ca**) could be efficiently obtained. Although all substrates furnished the cycloadducts, those having two *p*-methylphenylsulfonamide (*N*Ts) in the tethers were the ones giving the corresponding cycloadducts in better yields and lower reaction times (**39aa** and **40aa**). For substrates bearing $C(CO_2Et)_2$ the reaction also work quite efficiently (48 % and 50 %) with slightly decreased yield compared to those having only *N*Ts-linkage. O-tether substrates gave the lowest yields of the series (**39ac** and **40ca**).

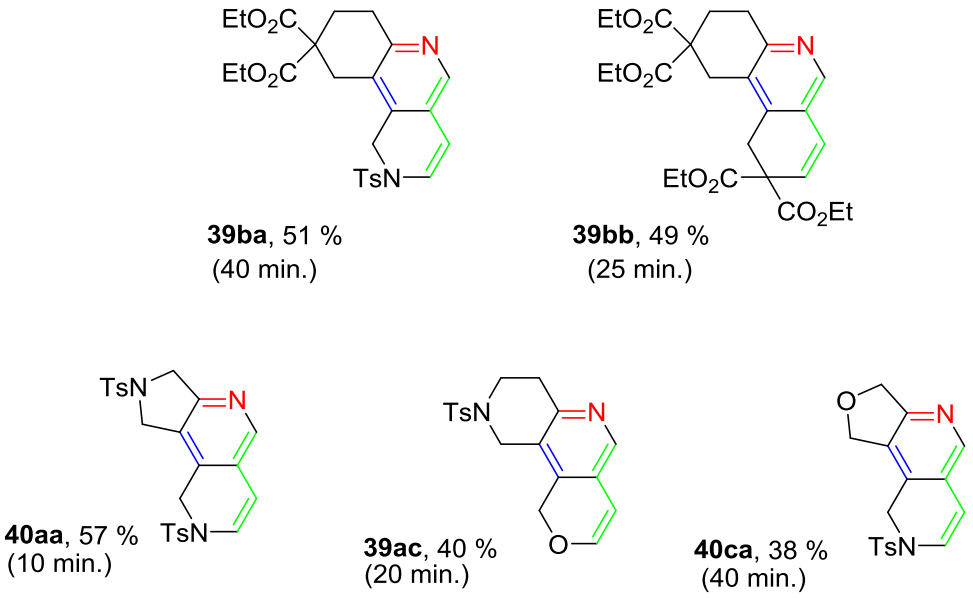

Figure 5. 7 Pyridines synthesis that have an aliphatic linker

Then the substrates that have a more rigid linker between the tether and the cyano group were reacted under the optimized conditions. Cycloadducts **41aa** and **41ac** were obtained in good yields, which prove that the rigid unit do not disturb the cycloadduct formation (Scheme 5.27).

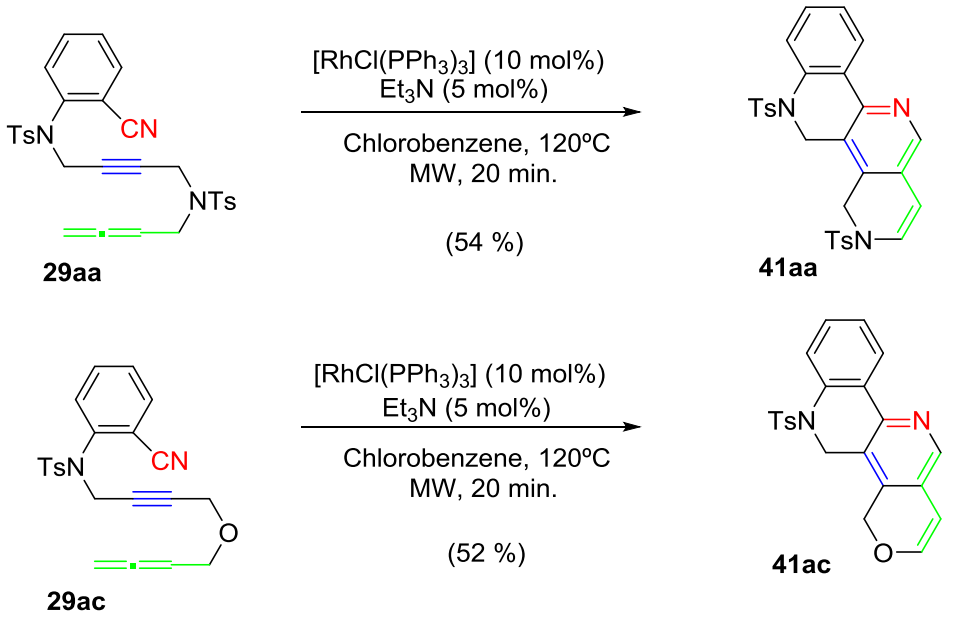

Scheme 5. 27 Tetracyclic scaffolds synthesised by microwave heating

As we can observed on figures 5.7 and scheme 5.27, pyridines derivatives have been successfully obtained with fairly good yield and short reaction times. The tricyclic and tetracyclic frameworks were regioselectively afforded in only one step reaction coming from linear cyano-yne-allene system.

As a last step we wanted to evaluate if the dihydronaphthyridine scaffolds obtained in the cycloaddition could be transformed to 2,6-naphthyridine containing structures. We found in the literature a method reported by Lamaty et al. that used potassium *tert*-butoxide in DMF to trigger the dehydrodesulfinylation/aromatization reaction of pyrrolynes to give pyrroles.[102] Cycloadduct **27aa** was subjected to the reactions reported by Lamaty et al. to afford the aromatized product **27a** in 87 % yield (Scheme 5.28), showing that the method developed is a convenient alternative for the synthesis of polycyclic naphthyridine molecules.

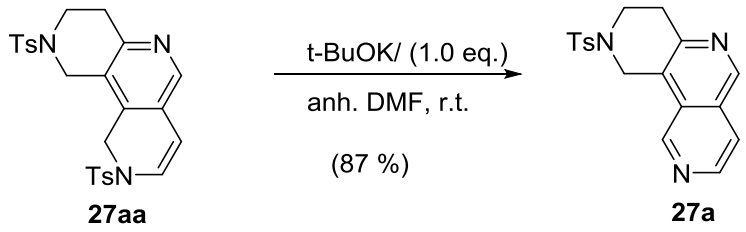

Scheme 5. 28 Deprotection of the tosyl group in **27aa** leading to the 2,6-naphthyridine derivative **27a**

5.1.3. Intramolecular study of yne-yne-allene system

5.1.3.1. Synthesis of diyneallene

In order to assess the generality of the dihydrogenative cycloaddition when other unsaturations were used, a diyneallene substrate was synthesised where the cyano motif was replaced by a terminal alkyne. A synthesis was planned that made use of the already synthesized intermediate **31a** and *N*-(but-3-yn-1-yl)-4-methylbenzenesulfonamide **44**.

Compound **44** was obtained in a two-step synthesis from *tert*-butyl tosylcarbamate. A Mitsunobu reaction of *tert*-butyl tosylcarbamate and but-3-yn-1-ol afforded in a 77 % yield compound **43**[103] (Scheme 5.29). Deprotection of the Boc group of compound **43** was achieved by using trifluoroacetic acid in dichloromethane at room temperature to afford in an 89 % yield the desired compound.

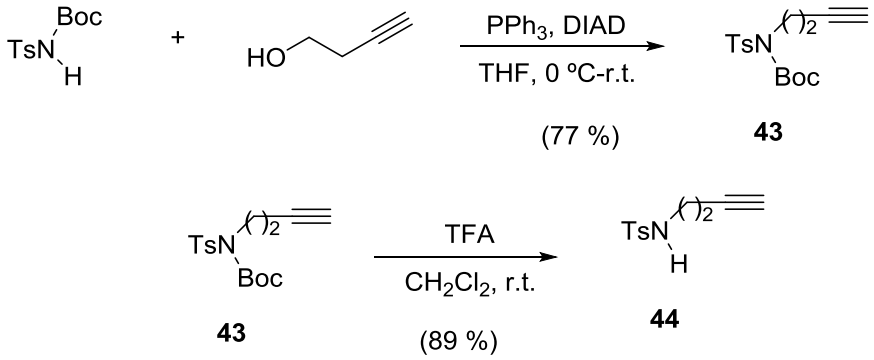

Scheme 5. 29 Synthesis of the compound **43** and **44**

Compound **44**[103] was reacted with bromo derivative **31a** (whose synthesis is detailed in scheme 5.8) in a nucleophilic substitution reaction. Potassium carbonate was used as a base affording product **45** in 93 % yield (Scheme 5.30).

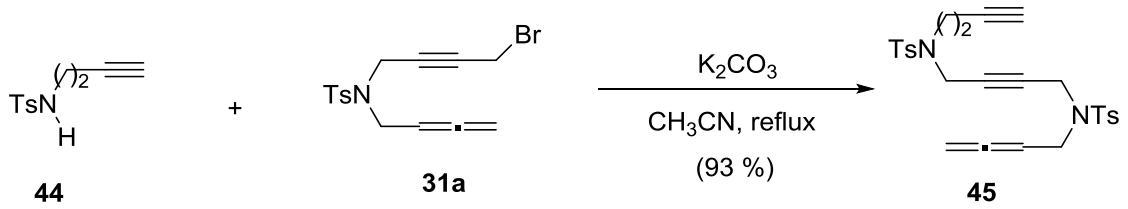

Scheme 5. 30 Synthesis of the compound **45**

5.1.3.2. Reactivity study on diyneallene substrate

The reactivity of diyneallene substrate **45** was tested under the optimized conditions (Scheme 5.31). The spectroscopic and spectrometric analysis of the product obtained clearly indicated that no atom was lost but a [2+2+2] cycloaddition reaction took place followed by an isomerization to furnish a tricyclic benzene scaffold **46**.[35,36,37] Noteworthy, the addition of triethylamine (5 mol %) greatly improves the reaction by almost doubling the yield (from 50 % to 95 % yield). It is of interest that the allene regioselectively reacts with its outer double bond, contrarily to what is most commonly found when terminal allenes are used, as is the case of the examples described in Chapter 3.

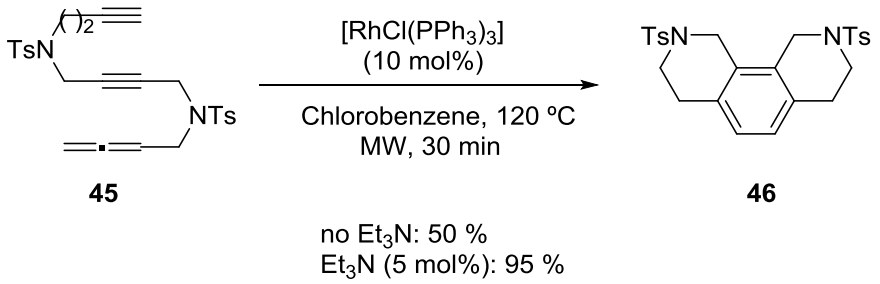

Scheme 5. 31 [2+2+2] cycloaddition of diyneallene substrate

5.1.4. Mechanistic study of the dehydrogenative reaction of cyano-yne-allene system

We tried then to shed some light to the mechanism through which the dehydrogenation takes place. Looking onto examples of dehydrogenative cycloaddition processes in the literature several conclusions can be drawn.

Some processes are favoured when a hydrogen scavenger is used. Porco Jr et. al. reported a biomimetic dehydrogenative Diels-Alder cycloaddition to synthesize natural products brosimones A and B.[104] They test various oxidants and hydrogen scavengers and found that the use of cyclopentene as hydrogen scavenger for transfer dehydrogenation afforded the best results. In the case of the nickel-catalysed dehydrogenative [4+2] cycloaddition of 1,3-dienes with nitriles described by Ogoshi et al.[105] hydrogen scavengers like styrene or norbornene were not hydrogenated. On the other hand, the formation of butenes in the reaction mixture suggested that the 1,3-butadiene reagents were hydrogenated and serve as hydrogen scavengers. Thus the reaction was carried out in the presence of a high excess of starting compound to avoid its shortage. An analogous behaviour was observed by Ikeda et. al. in the [2+2+2] cycloaddition of diynes with enones.[101e] The authors postulate that the obtained 1,3-cyclohexadiene is easily dehydrogenated in the presence of Ni(0) species and trimethylamine, and that the resulting nickel hydride reacts with the enone to produce a saturated ketone.

Oxidants are also commonly used to favour dehydrogenation processes. White et. al.[106] used 2,6-dimethyl-1,4-benzoquinone to accomplish the dehydrogenation of terminal olefins to 1,3-butadiene derivatives which were subsequently reacted in a Diels-Alder reaction. The addition of MnO_2 as an oxidant at the end of the reaction to favour the hydrogen elimination was observed to be efficient by Saito et al. in the intramolecular [2+2+2] cycloaddition of bis(propargylphenyl)carbodiimides.[107]

Also spontaneous loss of a hydrogen molecule was observed in several cases. Matsubara, Kurahashi et al.[108] described a dehydrogenative Diels-Alder reaction of dieneynes which possess a diene in the form of a styrene moiety and a dienophile in the form of an alkyne. They found that a key requirement for the dehydrogenative cycloaddition is the presence of a silyl group attached to alkyne moiety, which favours a fast *retro*-Diels-Alder that releases H_2 and forms the polyaromatic cycloadduct. In the dehydrogenative Diels-Alder reaction of styrenyl derivatives to provide cyclopenta[b]naphthalene substructures reported by Brummond et al.[109] dehydrogenation takes place spontaneously and addition of oxidants is found to be detrimental.

Taking into account the literature survey some more tests were done. The reaction mixture was thoroughly analysed by NMR to detect any hydrogenated starting material but no hint of hydrogenated product was observed. Then several reactions were carried out to test the effect of adding MnO_2 to favour the dehydrogenation step either with or without triethylamine but none of them proved to be beneficial (Table 5.3). We finally also tried to run the reaction under a flow of nitrogen to favour hydrogen elimination but this was not improving the outcome of the reaction either. So we conclude that the dehydrogenation takes place without the assistance of an oxidant and that the hydrogen released is not incorporated in the reagent.

Table 5. 3 Analysis of the dehydrogenation step

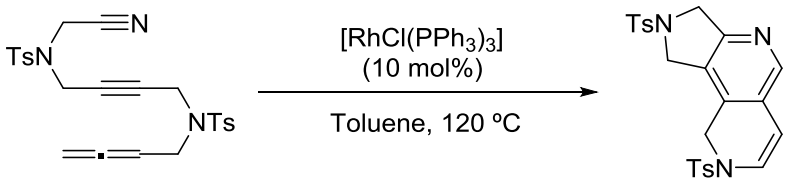

28aa **40aa**

Entry[a]	Additives	Reaction time (h.)	Yield (%)
1	5 % Et_3N	4	28
2	5 % Et_3N / MnO_2 (3 equiv.)	5	30
3	MnO_2 (3 equiv.)	4	24

[a] Reaction carried out under conventional heating.

Although the mechanism details are yet to be established, the plausible mechanistic cycle is sketched in scheme 5.32. Oxidative addition can take place between the alkyne and either the cyano group (intermediate **A**) or the allene (intermediate **C**). Subsequent insertion of the unsaturation which has not yet reacted delivers intermediates **B** and **D**, respectively. After reductive elimination, the cycloadduct **E** is obtained which is in a last step oxidized to the final product **39-40** without the need of addition of any oxidant.

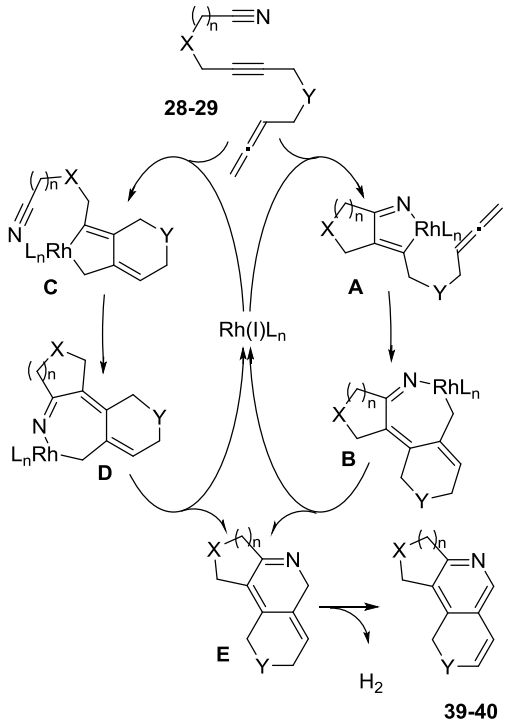

Scheme 5. 32 Plausible mechanistic cycle

5.1.5. Intermolecular study of yne-allene and nitrile

Next, the research focused on trying some intermolecular version of the [2+2+2] cycloaddition reaction. Among the different possibilities, we decided to try to react an yne-allene motif and nitriles. Such a selection of unsaturated partners was picked up because only in this way the dehydrogenation process could occur.

5.1.5.1. Synthesis of yne-allene substrate

First the yne-allene substrate was synthesised. Compound **47** was prepared by a nucleophilic substitution reaction of previously synthesised *N*-(buta-2,3-dien-1-yl)-4-methylbenzenesulfonamide **3a** with propargyl bromide in the presence of potassium carbonate. The reaction was carried out at reflux affording a 91 % yield of compound **47** (Scheme 5.33).

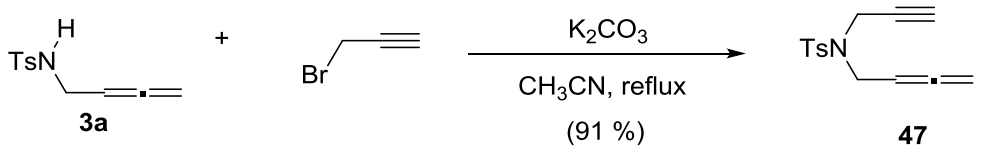

Scheme 5. 33 Synthesis of compound **47**

5.1.5.2. Reactivity study

The reactivity of substrate **47** was then evaluated in the conditions optimised for the cyano-yne-allene system. The yne-allene substrate was treated with Wilkinson's catalyst in the presence of a high excess of a nitrile (acetonitrile or benzonitrile). The reactions were carried out in toluene at 120˚C using microwave as the heating source. A product was formed which was isolated by column chromatography. Analysis of the isolated product showed that it

corresponds to a dimerization reaction of yne-allene substrate **47** indicating that the nitrile motif had not participated in the reaction. This was confirmed by ESI-MS in the positive ion mode which clearly showed a peak at *m*/*z*=523.1 that corresponds to $[2(\mathbf{47})+H]^+$ (Figure 5.8).

Figure 5. 8 ESI-MS spectrum of yne-allene and nitrile reaction

In summary, a novel type of rhodium-catalyzed [2+2+2] cycloaddition involving allenes and nitriles has been developed. Starting from linear substrates, the use of Wilkinson's catalyst allows the regioselective reaction of allenes through their external double bond to afford after a dehydrogenative step, unsaturated pyridine-containing scaffolds.

Chapter 6. General conclusions

In this thesis rhodium-catalysed [2+2+2] cycloaddition reactions have been studied and the following achievements from methodological and mechanistic point of view have been gained:

In Chapter 3 the reactivity of linear allene-ene-allene and allene-yne-allene substrates bearing either an *N*-tosyl or *O*-tether in the rhodium catalysed [2+2+2] cycloaddition reaction was optimized. Wilkinson's catalyst was able to promote the cycloaddition regioselectively involving the internal double bond of the allene allowing for the preparation of scaffolds featuring exocyclic dienes. Furthermore, the process is diastereoslective furnishing the cycloadduct with four contiguous stereocentres as only one diastereisomer for the allene-ene-allene substrates and two stereocentres in the case allene-yne-allene substrates. Pentacyclic scaffolds were obtained by react the cycloadducts with maleimide in a Diels-Alder reaction that also proved to be diastereoselective.

In Chapter 4 the same Wilkinson's catalyst was applied to the [2+2+2] cycloaddition reaction of allene-ene/yne-allene substrates bearing chiral centres. When an enantiomerically pure substrate was reacted, we were able to induce a completely diastereoselective reaction in which the product was isolated as only one optically pure enantiomer. Therefore, chiral scaffolds could be obtained from the cycloaddition of allene-ene/yne-allene systems by using the chiral pool strategy.

In Chapter 5 a novel type of rhodium-catalyzed [2+2+2] cycloaddition involving allenes and nitriles has been developed. Starting from linear cyano-yne-allene substrates, the use of Wilkinson's catalyst allows the regioselective reaction of allenes through their external double bond to afford after a dehydrogenative step, unsaturated pyridine-containing scaffolds. This study demonstrated the significant improvement in reaction times and yields of microwave irradiation comparing with conventional heating and presents a potentially useful and convenient method to form 2,6-naphthyridine core structures.

Chapter 7. Methods

7.1. General materials and instrumentation

7.1.1. General conditions

MATERIALS

Unless otherwise noted, materials were obtained from commercial suppliers and used without further purification. All reactions requiring anhydrous conditions were conducted in oven dried glassware under a dry nitrogen atmosphere. Dichloromethane and THF were degassed and anhydried under nitrogen atmosphere through solvent purification columns (MBraun, SPS-800). Toluene was distilled under nitrogen over sodium as a drying reagent. DMF was distilled under reduced pressure using molecular sieves as a drying reagent. Solvents were removed under reduced pressure with a rotary evaporator. Residues were chromatographed on a silica gel column (230-400 mesh) using a gradient solvent system (hexane/ethyl acetate or hexane/dichloromethane) as the eluent.

SPECTROSCOPY

NMR spectroscopy: ^{1}H and ^{13}C NMR spectra were measured on a Bruker Avance III 400 [^{1}H (400 MHz) and ^{13}C (100 MHz)] or Bruker DPX300 [^{1}H (300 MHz) and ^{13}C (75 MHz)] NMR spectrometers of the *Serveis Tècnics de Recerca* of the *Universitat de Girona*. Chemical shifts (δ) for ^{1}H and ^{13}C were referenced to internal solvent resonances and reported relative to $SiMe_4$.

IR spectroscopy: IR spectra were measured on a FT-IR spectrophotometer Mattson-Galaxy Satellite, using a MKII Golden Gate Single Reflection ATR System of the Chemistry Department of the Universitat de Girona.

SPECTROMETRY

Mass spectrometry: Electrospray Ionization Mass Spectra were registered in an Esquire 6000 Trap LC/MS (Bruker Daltonics) with an electrospray ionization source of the *Serveis Tècnics de Recerca* of the *Universitat de Girona*.
High Resolution Mass Sepectrometry (ESI-HRMS) spectra were registered in a Bruker Micro TOF-Q spectrometer with a quadrupole-Time-Of-Flight hybrid analyzer of the *Serveis Tècnics de Recerca* of the *Universitat de Girona.*

CHROMATOGRAPHY

Thin Layer Chromatography (TLC): were performed with pre-coated (0.20 mm width) chromatography plates Alugram Sil G/UV254.

Column chromatography: were performed using silica gel SDS with a size of 35-70 μm mesh particle size.
High Performance Liquid Chromatography (HPLC): HPLC analysis have been performed using a CHIRALPAK AD-H column (4.6 x 250 mm, 5 μm) on a Spectra System Thermo chromatograph (Shimadzu) equipped with a SN4000 connector, a SCM1000 degasser, a P2000 pump and a UV6000LP detector with a 20 μL loop.

ELEMENTAL ANALISIS

Elemental analisis: were registered on PerkinElmer type 2400 analyzer in the *Serveis Tècnics de Recerca* of the *Universitat de Girona.*
Melting points: were measured in a SMP10 apparatus from Stuart and were reported without any correction.

Microwaves heating: a CEM Discover S-Class microwave synthesizer was used (250 W/250 psi). Microwave heated reactions were performed in sealed vials in an Ethos SEL Lab station Milestone Inc.), a multimode microwave with a dual magnetron (1600 W). During the experiments, the time, temperature, and the power were measured with an "EasyControl" software package. The temperature was monitored and controlled throughout the reaction by an ATC-400FO Automatic Fiber Optic Temperature Control system. The wattage was automatically adjusted to maintain the desired temperature for the desired period of time.

7.2. Experimental procedure for the products synthesised in Chapter 3.

7.2.1. Synthesis of substrates

7.2.1.1. Synthesis of N-tosyl-prop-2-yn-1-amine

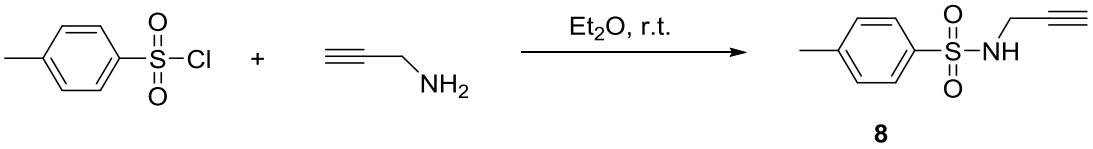

8

In a 50 mL 2-necked round bottom flask, a mixture of 4-toluenesulfonyl chloride, (4.09 g, 20.9 mmols) in 20 mL of diethyl ether was cooled down at 0˚C in an ice bath. Then a propargylamine was added dropwise (2.94 mL, 41.96 mmols). The mixture was stirred at room temperature for 2.5 h (TLC monitoring). The solvent was removed under reduced pressure and the residue was purified by column chromatography using a mixture of hexane:ethyl acetate (70:30) as the eluent to give *N*-tosyl-prop-2-yn-1-amine[110] (3.60 g, 82 % yield) as a colourless solid. **Molecular formula:** $C_{10}H_{11}NSO_2$ **MW:** 209.20 g/mol; **^{1}H NMR (300 MHz, $CDCl_3$) δ(ppm):** 2.10 (t, $^4J_{H\text{-}H}$ = 2.6 Hz ,1H), 2.43 (s, 3H), 3.80-3.85 (m, 2H), 4.56 (br. s, 1H), 7.31 (d, $^3J_{H\text{-}H}$ = 8.4 Hz, 2H), 7.77 (d, $^3J_{H\text{-}H}$ = 8.4 Hz, 2H).

7.2.1.2. Synthesis of N-(buta-2,3-dien-1-yl)-4-methylbenzenesulfonamide

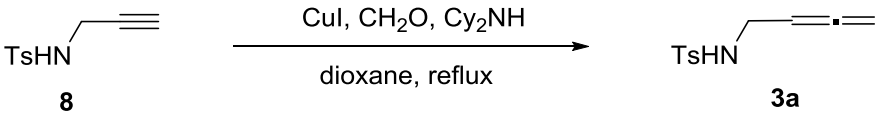

8 **3a**

In a 50 mL 2-necked round bottom flask, a mixture of *N*-tosyl-prop-2-yn-1-amine (0.42 g, 1.61 mmols), formaldehyde (0.12 g, 4.04 mmols) and copper(I) iodide (0.16 g, 0.81 mmols) in 20 mL of dioxane was heated up to reflux. Then dicyclohexylamine (0.60 mL, 2.92 mmols) was added slowly to the reaction mixture. The mixture was stirred for 3 h (TLC monitoring). The insoluble salts were filtered off and solvent was removed under reduce pressure. Reaction crude was purified by column chromatography using a mixture of hexane:ethyl acetate (90:10) as the eluent to give *N*-(buta-2,3-dien-1-yl)-4-methylbenzenesulfonamide[66] (0.38 g, 84 % yield) as yellow oil. **Molecular formula:** $C_{11}H_{13}NO_2S$; **MW:** 223.29 g/mol; **^{1}H NMR (300 MHz, $CDCl_3$) δ(ppm):** 2.43 (s, 3H), 4.45 (dt, $^5J_{H\text{-}H}$ = 2.5 Hz, $^3J_{H\text{-}H}$ = 7.0 Hz, 2H), 4.79 (dt, $^5J_{H\text{-}H}$ = 2.5 Hz, $^4J_{H\text{-}H}$ = 7.0 Hz, 2H), 5.29 (dq, $^4J_{H\text{-}H}$ = 7.0 Hz,$^3J_{H\text{-}H}$ = 7.0 Hz, 1H), 7.30 (d, $^3J_{H\text{-}H}$ = 8.4 Hz, 2H), 7.82 (d, $^3J_{H\text{-}H}$ = 8.4 Hz, 2H).

7.2.1.3. Synthesis of 1,4-dibromobut-2-yne

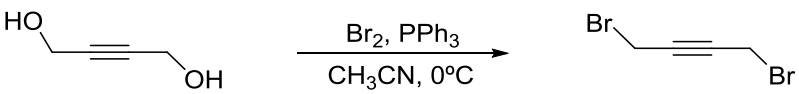

In a 100 mL 2-necked round bottom flask, a suspention of triphenylphosphine (5.10 g, 19.51 mmols) and acetonitrile (50 mL) was cooled down to 0˚C in nitrogen atmosphere. The bromine (1.0 mL, 19.51 mmols) was added slowly over the suspention. Then, a solution of but-2-yne-1,4-diol (0.84 g, 9.76 mmols) in 10 mL acetonitrile was added dropwise over the reaction mixture, which was allowed to warm up to room temperature and was stirred for 2.5 h (TLC monitoring). The solvent was evaporated and the residue was purified by column chromatography using a hexane as the eluent to give 1,4-dibromobut-2-yne[72] (1.50 g, 73 % yield) as a colourless oil. **Molecular formula:** $C_4H_4Br_2$; **MW:** 211.88 g/mol; **^{1}H NMR (300 MHz, $CDCl_3$) δ (ppm):** 3.95 (s, 4H).

7.2.1.4. Synthesis of (E)-N,N-di(buta-2,3-dienyl)-N,N-ditosylbut-2-ene-1,4-diamine

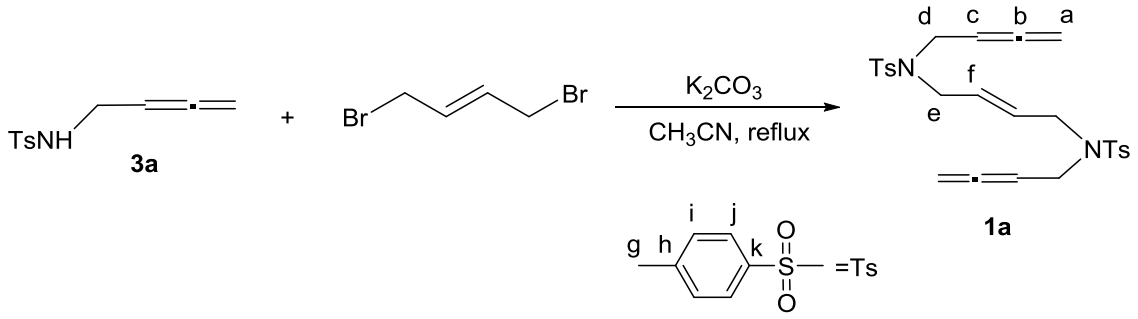

In a 50 mL 2-necked round bottom flask, a mixture of *N*-tosylbuta-2,3-dien-1-amine, **1** (0.30 g, 1.34 mmols) and potassium carbonate (0.44 g, 3.20 mmols) in 20 mL of acetonitrile was heated up to reflux. Then a mixture of (*E*)-1,4-dibromobut-2-ene, (0.14 g, 0.67 mmol) in 3 mL of acetonitrile was added slowly to the reaction mixture. The mixture was stirred for 6 h (TLC monitoring). The insoluble salts were filtered off and solvent was removed under reduced pressure. Reaction crude was purified by column chromatography using a mixture of hexane:ethyl acetate (80:20) as the eluent to give the product, **1a**, (0.22 g, 56 % yield) as a white solid. **MW:** 498.66 g/mol; **m.p.:** 88-90˚C; **IR (ATR) ν (cm^{-1}):** 2922, 1952, 1334, 1153; **^{1}H NMR (300 MHz, $CDCl_3$) δ(ppm):** 2.46 (s, 6H, **g**), 3.77-3.81 (m, 8H, **d-e**), 4.69 (dt, $^5J_{Ha\text{-}Hd}$ = 2.5 Hz, $^4J_{Ha\text{-}Hc}$ = 6.9 Hz, 4H, **a**), 4.79 (dq, $^3J_{Hc\text{-}Hd}$ = 6.0 Hz, $^3J_{Hc\text{-}Hd}$ = 6.9 Hz, $^4J_{Ha\text{-}Hc}$ = 6.9 Hz, 2H, **c**), 5.47 (m, 2H, **f**), 7.31 (d, $^3J_{Hi\text{-}Hj}$ = 8.1 Hz, 4H, **i**), 7.67 (d, $^3J_{Hi\text{-}Hj}$ = 8.1 Hz, 4H, **j**); **^{13}C NMR (75 MHz, $CDCl_3$) δ (ppm):** 21.5 (C**g**), 45.7 (C**d**), 47.8 (C**e**), 76.6 (C**a**), 85.4 (C**c**), 127.1 (C**i**), 129.3 (C**f**), 129.6 (C**j**), 137.3 (C**h**), 143.4 (C**k**), 209.5 (C**b**). **ESI-HRMS (m/z):**calcd. for $[C_{26}H_{30}N_2O_4S_2 + Na]^+$: 521.1539. Found: 521.1557

7.2.1.5. Synthesis of N,N-di(buta-2,3-dienyl)- N^1,N^4 -ditosylbut-2-yne-1,4-diamine

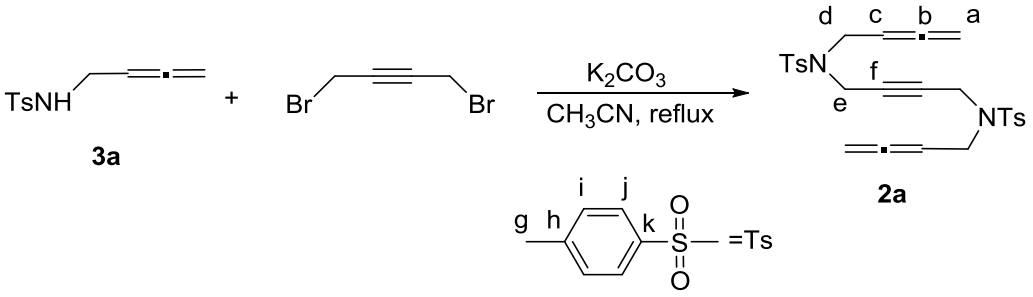

In a 50 mL 2-necked round bottom flask, a mixture of *N*-tosylbuta-2,3-dien-1-amine, **3a**, (0.23 g, 1.04 mmols) and potassium carbonate (0.33 g, 2.36 mmols) in 20 mL of acetonitrile was heated up to reflux. Then a mixture of 1,4-dibromobut-2-yne, (0.10 g, 0.47 mmols) in 3 mL of acetonitrile was added slowly to the reaction mixture. The mixture was stirred for 20 h (TLC monitoring). The insoluble salts were filtered off and solvent was removed under reduce pressure. Reaction crude was purified by column chromatography using a mixture of hexane:ethyl acetate (80:20) as the eluent to give the product, **2a**, (0.81 g, 35 % yield) as a white solid. **MW:** 496.64 g/mol; **m.p.:** 86-88˚C; **IR (ATR) ν (cm^{-1}):** 2917, 1945, 1340, 1157; **^{1}H NMR (300 MHz, $CDCl_3$) δ(ppm):** 2.43 (s, 6H, **g**), 3.68 (dt, $^5J_{Ha\text{-}Hd}$ =2.5 Hz, $^3J_{Hc\text{-}Hd}$ = 6.9 Hz, 4H, **d**), 3.94 (s, 4H, **e**), 4.72 (dt, $^5J_{Ha\text{-}Hd}$ = 2.5 Hz, $^4J_{Ha\text{-}Hc}$ = 6.0 Hz, 4H, **a**), 4.90 (dq, $^3J_{Hc\text{-}Hd}$ = 6.9 Hz, $^4J_{Ha\text{-}Hc}$ = 6.9 Hz, $^4J_{Ha\text{-}Hc}$ = 6.0 Hz, 2H, **c**), 7.29 (d, $^3J_{Hi\text{-}Hj}$ = 8.4 Hz, 4H, **i**), 7.65 (d, $^3J_{Hi\text{-}Hj}$ = 8.4 Hz, 4H, **j**); **^{13}C NMR (75 MHz, $CDCl_3$) δ (ppm):** 21.5 (C**g**), 35.9 (C**e**), 45.5 (C**d**), 76.5 (C**a**), 78.3 (C**f**), 85.3 (C**c**), 127.1 (C**i**), 129.6 (C**j**), 136.2 (C**h**), 143.7 (C**k**), 209.7 (C**b**). **ESI-HRMS (m/z):**calcd. for $[C_{26}H_{28}N_2O_4S_2 + Na]^+$: 519.1383. Found: 519.1401.

7.2.1.6. Synthesis of (E)-1,4-bis(prop-2-yn-1-yloxy)but-2-ene

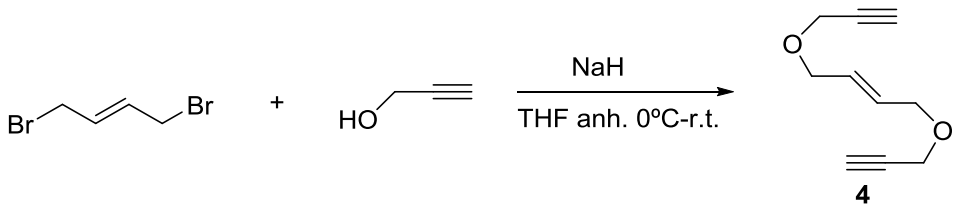

4

In a 50 mL 2-necked round bottom flask, a mixture of sodium hydride in 60% oil dispersion (1.12 g, 28.05 mmols of pure NaH) and prop-2-yn-1-ol (2.45 mL, 42.07 mmols) in ahydrous THF (20 mL) was cooled down to 0˚C. The mixture was stirred at this temparature for 1 h under nitrogen atmosphere. (*E*)-1,4-dibromo-2-butene (3.0 g, 14.02 mmols) in THF (7 mL) was added dropwise at 0˚C and then, the mixture was allowed to warm up to room temperature. The reaction was stirred for 6 h (TLC monitoring). The residue was quenched with saturated solution of ammonium chloride (30 mL) and extracted with ethyl acetate (3 x 30 mL). The organic phase was dried over anhydrous sodium sulfate and the solvent was evaporated. The residue was purified by column chromatography using a mixture of hexane:ethyl acetate (90:10) as the eluent to give (*E*)-1,4-bis(prop-2-yn-1-yloxy)but-2-ene[68a], **4** (1.32 g, 58 % yield) as a yellow oil. **Molecular formula:** $C_{10}H_{12}O_2$; **MW:** 162.20 g/mol; **^{1}H NMR (400 MHz, $CDCl_3$) δ (ppm):** 2.43 (t, $^4J_{H\text{-}H}$ =2.4 Hz, 2H), 4.08 (d, $^3J_{H\text{-}H}$ = 1.2 Hz, 4H), 4.14 (d, $^4J_{H\text{-}H}$ =2.4 Hz, 4H), 5.83 (t, $^3J_{H\text{-}H}$ = 1.2 Hz, 2H).

7.2.1.7. Synthesis of 4-((E)-4-(buta-2,3-dienyloxy)but-2-enyloxy)buta-1,2-diene

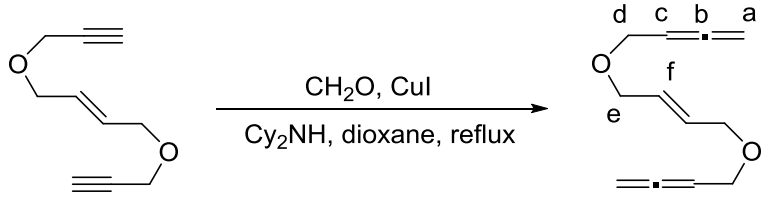

4 **1b**

In a 50 mL 2-necked round bottom flask, a mixture of *(E)*-1,4-bis(prop-2-ynyloxy)but-2-ene, **4**, (1.00 g, 6.09 mmols), formaldehyde (0.46 g, 15.23 mmols) and copper(I) iodide (0.58 g, 3.05 mmols) in 30 mL of dioxane was heated up to reflux. Then dicyclohexylamine (2.18 mL, 10.96 mmols) was added slowly to the reaction mixture. The mixture was stirred for 3 h (TLC monitoring). The insoluble salts were filtered off and solvent was removed under reduce pressure. Reaction crude was purified by column chromatography using a mixture of hexane:ethyl acetate (80:20) as the eluent to give the product, **1b**, (0.68 g, 58 % yield) as a yellow oil. **MW:** 192.25 g/mol; **IR (ATR) ν (cm^{-1}):** 2954, 1956, 1723, 1033; **^{1}H NMR (300 MHz, $CDCl_3$) δ(ppm):** 4.01 (m, 8H, **d**-**e**), 4.78 (dt, $^5J_{Ha\text{-}Hd}$ = 2.5 Hz, $^4J_{Ha\text{-}Hc}$ = 6.6 Hz, 4H, **a**), 5.23 (dq, $^4J_{Ha\text{-}Hc}$ = 6.6 Hz, $^3J_{Hc\text{-}Hd}$ = 6.6 Hz, $^3J_{Hc\text{-}Hd}$ = 6.0 Hz, 2H, **c**), 5.80 (m, 2H, **f**); **^{13}C NMR (75 MHz, $CDCl_3$) δ (ppm):** 67.9 (C**d**), 69.7 (C**e**), 75.7 (C**a**), 87.7 (C**c**), 129.5 (C**f**), 209.3 (C**b**)**; ESI-HRMS (m/z):**calcd. for $[C_{12}H_{16}O_2 + Na]^+$: 215.1043 Found: 215.1053.

7.2.1.8. Synthesis of 1,4-bis(prop-2-yn-1-yloxy)but-2-yne

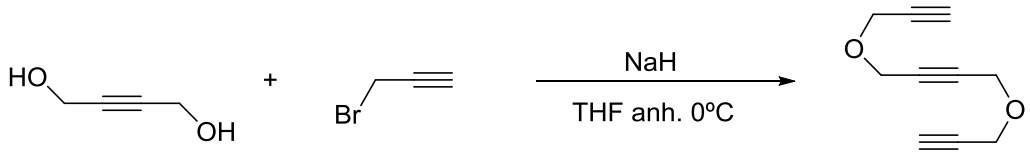

5

In a 50 mL 2-necked round bottom flask, a mixture of sodium hydride in 60% oil dispersion (0.56 g, 23.20 mmols of pure NaH) and but-2-yne-1,4-diol (0.50 g, 5.80 mmols) in ahydrous THF (20 mL) was cooled down to 0˚C. The mixture was stirred at this temparature for 1h under nitrogen atmosphere. 3-bromoprop-1-yne (1.50 mL, 16.26 mmols) in THF (7 mL) was added dropwise at 0˚C and then, the mixture was allowed to warm up to room temperature. The reaction was stirred for 24 h (TLC monitoring). The residue was quenched with saturated solution of ammonium chloride (30 mL) and extracted with ethyl acetate (3 x 30 mL). The organic phase was dried over anhydrous sodium sulfate and the solvent was evaporated. The residue was purified by column chromatography using a mixture of hexane:ethyl acetate (90:10) as the eluent to give 1,4-bis(prop-2-yn-1-yloxy)but-2-yne[68b], **5** (0.96 g, 54 % yield) as a yellow oil. **Molecular formula:** $C_{10}H_{10}O_2$; **MW:** 162.07 g/mol; **^{1}H NMR (400 MHz, $CDCl_3$) δ (ppm):** 2.46 (t, $^4J_{H\text{-}H}$ = 2.4 Hz, 2H), 4.25 (d, $^4J_{H\text{-}H}$ =2.4 Hz, 4H), 4.32 (s, 4H).

7.2.1.9. Synthesis of of 4-(4-(buta-2,3-dienyloxy)but-2-ynyloxy)buta-1,2-diene

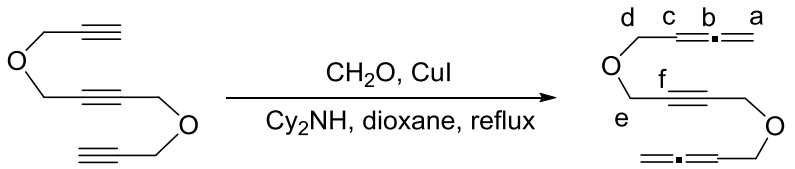

5 **2b**

In a 50 mL 2-necked round bottom flask, a mixture of 1,4-bis(prop-2-ynyloxy)but-2-yne, **5**, (0.32 g, 41.97 mmols), formaldehyde (0.15 g, 4.93 mmols) and copper(I) iodide (0.19 g, 0.99 mmols) in 20 mL of dioxane was heated up to reflux. Then dicyclohexylamine (0.70 mL, 3.55

mmols) was added slowly to the reaction mixture. The mixture was stirred for 4 h (TLC monitoring). The insoluble salts were filtered off and solvent was removed under reduce pressure. Reaction crude was purified by column chromatography using a mixture of hexane:ethyl acetate (90:10) as the eluent to give the product, **2b**, (0.30 g, 51 % yield) as a yellow oil. **MW:** 190.24 g/mol; **IR (ATR) ν (cm^{-1}):** 2921, 1954, 1074. **^{1}H NMR (400 MHz, $CDCl_3$) δ(ppm):** 4.10 (dt, $^5J_{Ha\text{-}Hd}$ =2.5 Hz, $^3J_{Hc\text{-}Hd}$ = 6.9 Hz, 4H, **d**), 4.22 (s, 4H, **e**), 4.81 (dt, $^5J_{Ha\text{-}Hd}$ = 2.5 Hz, $^4J_{Ha\text{-}Hc}$ = 6.6 Hz, 4H, **a**), 5.23 (dq, $^4J_{Ha\text{-}Hc}$ = 6.6 Hz, $^4J_{Ha\text{-}Hc}$ = 6.9 Hz, $^3J_{Hc\text{-}Hd}$ = 6.9 Hz, 2H, **c**); **^{13}C NMR (75 MHz, $CDCl_3$) δ (ppm):** 57.1 (C**d**), 67.4 (C**e**), 75.9 (C**a**), 82.2 (C**f**), 87.1 (C**c**), 209.6 (C**b**). **ESI-HRMS (m/z):**calcd. for $[C_{12}H_{14}O_2 + Na]^+$: 213.0886. Found:213.0899.

7.2.2. Preparation and characterization data for cycloisomerized derivatives catalysed by rhodium

7.2.2.1. General procedure for the [$RhCl(PPh_3)_3$]-catalysed [2+2+2] cycloaddition reaction of allene-ene-allene 1a and characterization data for 9a

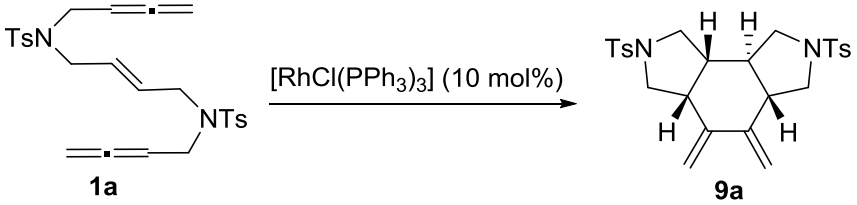

In a 10 mL 2-necked round bottom flask, a mixture of (*E*)-*N*,*N*-di(buta-2,3-dienyl)-*N*,*N* ditosylbut-2-ene-1,4-diamine, **1a**, (0.10 g, 0.20 mmols) and tris(triphenylphosphine)rhodium(I) chloride (0.018 g, 0.020 mmols) was purged with nitrogen and dissolved in the indicated solvent (3 mL). The mixture was stirred at the indicated temperature for the stated time (TLC monitoring). The solvent was removed and the crude was purified by column chromatography using mixture of hexane:ethyl acetate (90:10) as the eluent to give cycloisomerised product **9a** as a colourless solid.

Specific data for the reactions listed in Table 3.2 (Chapter 3):

Entry	Solvent	Reaction temp. (^{0}C)	Reaction time (h)	Isolated **9a** (g)	Yield of **9a (%)**
1	DCE	40	8	0.030	30
2	Methanol	40	8	0.035	35
3	Toluene	40	8	0.032	32
4	Methanol	65	2.5	0.038	38
5	Toluene	100	6.5	0.041	41

MW: 498.66g/mol; **m.p.:** 181-183˚C; **IR (ATR) ν (cm^{-1}):** 2925, 1336, 1157; **^{1}H NMR (300 MHz, $CDCl_3$) δ(ppm):** 0.94-1.07 (m, 2H), 1.92-2.02 (m, 2H), 2.44 (s, 3H), 2.48 (s, 3H), 2.69 (dd, $^5J_{H\text{-}H}$ =1.5 Hz, 1H), 2.85-2.93 (m, 1H), 3.03 (t, $^5J_{H\text{-}H}$ =1.5 Hz, 1H), 3.20-2.56 (m, 4H), 3.53 (dd, $^5J_{H\text{-}H}$ =1.5 Hz, 1H), 4.51 (d, ^5J = 1.5Hz, 1H), 4.81 (d, $^5J_{H\text{-}H}$ = 1.5 Hz, 1H), 5.07 (dd, ^5J = 1.5 Hz, 1H), 5.11 (d, $^5J_{H\text{-}H}$ = 1.5 Hz, 1H), 7.34 (t, $^3J_{H\text{-}H}$ = 8.1 Hz, 4H), 7.70 (d, $^3J_{H\text{-}H}$ = 8.1 Hz, 4H); **^{13}C NMR (75 MHz, $CDCl_3$) δ (ppm):** 21.9, 21.9, 42.3, 43.0, 46.5, 46.6, 49.8, 50.7, 52.2, 52.5, 109.0, 114.7, 127.5, 130.2,

133.8, 134.8, 143.9, 144.3, 144.4, 144.5; **ESI-HRMS (m/z):**calcd. for $[C_{26}H_{30}N_2O_4S_2 + Na]^+$: 521.1545. Found: 521.1538.

7.2.2.2. General procedure for the $[Rh(cod)_2]BF_4$/BINAP-catalysed [2+2+2] cycloaddition reaction of allene-ene-allene 1a

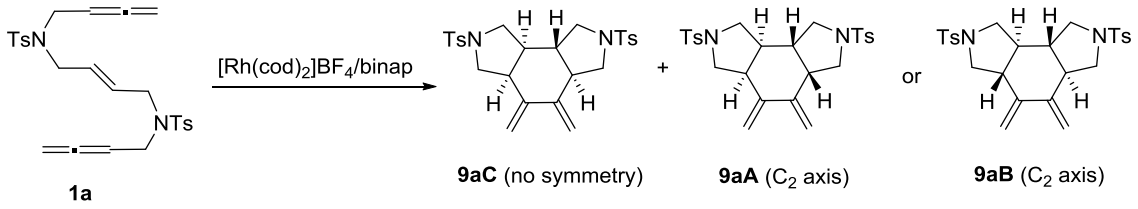

In a 10 mL flast, a mixture of (*R*)-H_8-binap (6.30 mg, 0.01 mmol) or (*R*)-binap (6.30 mg, 0.01 mmol) and rhodium complex $[Rh(cod)_2]BF_4$ (4.06 mg, 0.010 mmol) or $[RhCl(C_2H_4)_2]_2$ (3.88 mg, 0.010 mmol) was dissolved in dichloromethane (3 mL) under N_2. Hydrogen gas was bubbled to the stirred catalyst solution for 30 minutes. The resulting mixture was then concentrated to dryness. The reaction solvent (5 mL) was added and the solution was stirred under a N_2 atmosphere. In the indicated cases $AgBF_4$ (1.95 mg, 0.01 mmol) was added to the catalyst mixture. A solution of compound **1a** (0.05 g, 0.10 mmol) in the reaction solvent (3 mL) was then added and the reaction was stirred at the indicated temperature for the stated reaction time (TLC monitoring). The solvent was removed and the crude was purified by column chromatography using a mixture of hexane:ethyl acetate (90:10) as the eluent to give a mixture of products **9a** as a colourless solid (Entry 1). The ratio of stereoisomers was determinaed from the mixture by ^{1}H-NMR.

Specific data for the reactions listed in Table 3.5 (Chapter 3):

Entry	Rh source	L / additive	Solvent / Reaction temp. (^{0}C)	Reaction time (h)	Isolated **9a** (g)/Yield of **9a (%)**	Product ratio
1	$[Rh(cod)_2]BF_4$	(*R*)-H_8-binap/-	MeOH/r.t.	72	0.018/35	4:1
2	$[Rh(cod)_2]BF_4$	(*R*)-H_8-binap/-	DCE/r.t.	42	0.023/46	1:1
3	$[Rh(cod)_2]BF_4$	(*R*)-H_8-binap/-	Toluene/r.t.	18	0.017/34	3:1
4	$[Rh(cod)_2]BF_4$	(*R*)-binap/-	DCE/r.t.	72	0.018/35	4:1
5	$[Rh(cod)_2]BF_4$	(*R*)-binap/-	Toluene/r.t.	72	0.016/32	2:1
6	$[RhCl(C_2H_4)_2]_2$	(*R*)-H_8-binap/$AgBF_4$	Toluene/50^{0}C	24	0.012/24	2:1
7	$[RhCl(C_2H_4)_2]_2$	(*R*)-H_8-binap/ $AgBF_4$	Toluene/100^{0}C	19	0.024/47	2:1

7.2.2.3. Synthesis of cycloisomerized derivative 10a

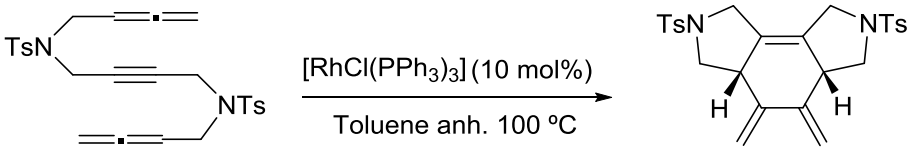

2a **10a**

In a 10 mL 2-necked round bottom flask, a mixture of (*E*)-*N*,*N*-di(buta-2,3-dienyl)-*N*,*N*-ditosylbut-2-yne-1,4-diamine, **2a**, (0.05 g, 0.10 mmols) and tris(triphenylphosphine)rhodium(I) chloride (0.009 g, 0.010 mmols) was purged with nitrogen and dissolved in anhydrous toluene (3 mL). The mixture was stirred at 100˚C for 2 h (TLC monitoring). The solvent was removed and the crude was purified by column chromatography using mixture of hexane:ethyl acetate (90:10) as the eluent to give the cycloisomerised product **10a** (0.016 g, 32 % yield), as a colourless solid. **MW:** 496.15g/mol; **m.p.:** 185-187˚C (dec.); **IR (ATR) ν (cm^{-1}):** 2921, 1340, 1154, 1090. **^{1}H NMR (400 MHz, $CDCl_3$) δ(ppm):** 2.43 (s, 6H), 2.72 (t, 2H), 3.28 (m, 2H), 3.49 (dd, 3H), 3.93 (m, 4H), 4.70 (d, 2H), 5.38 (d, 2H), 7.32 (d, $^{3}J_{H\text{-}H}$ = 8.1 Hz, 4H), 7.70 (d, $^{3}J_{H\text{-}H}$ = 8.1 Hz, 4H); **^{13}C NMR (100 MHz, $CDCl_3$) δ (ppm):** 21.6, 43.0, 49.0, 52.2, 110.6, 127.7, 128.2, 129.9, 132.9, 142.3, 143.9. **ESI-HRMS (m/z):**calcd. for $[C_{26}H_{28}N_2O_4S_2 + Na]^+$: 519.1383. Found: 519.1400.

7.2.2.4. Synthesis of cycloisomerized derivative 9b

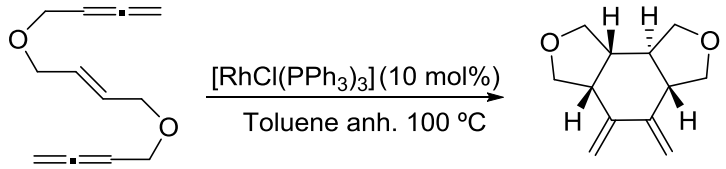

1b **9b**

In a 10 mL 2-necked round bottom flask, a mixture of 4-((*E*)-4-(buta-2,3-dienyloxy)but-2-enyloxy)buta-1,2-diene, **1b**, (0.050 g, 0.260 mmols) and tris(triphenylphosphine)rhodium(I) chloride (0.024 g, 0.026 mmols) was purged with nitrogen and dissolved in toluene anh. (3 mL).The mixture was stirred at 100˚C for 2.2 h (TLC monitoring). The solvent was removed and the crude was purified by column chromatography using mixture of hexane:ethyl acetate (90:10) as the eluent to give cycloisomerised product **9b** (0.022 g, 44 % yield) as a yellow oil. **MW:** 192.25g/mol; **IR (ATR) ν (cm^{-1}):** 2925, 1639, 1038; **^{1}H NMR (300 MHz, $CDCl_3$) δ(ppm):** 1.93-2.03 (m, 1H), 2.22-2.28 (m, 1H), 2.41-2.48 (m, 1H), 3.17-3.24 (m, 1H), 3.40-3.56 (m, 2H), 3.71-3.78 (m, 2H), 3.87-3.96 (m, 2H), 4.07-4.14 (m, 2H), 4.55 (d, $^{3}J_{H\text{-}H}$ = 1.2 Hz, 1H), 4.91 (q, $^{5}J_{H\text{-}H}$ = 1.2 Hz, 1H), 5.16 (q, $^{5}J_{H\text{-}H}$ = 1.2 Hz, 1H), 5.26 (d, $^{3}J_{H\text{-}H}$ = 1.2 Hz, 1H); **^{13}C NMR (75 MHz,**

$CDCl_3$) δ (ppm): 42.7, 44.9, 47.1, 48.1, 69.3, 70.9, 71.9, 73.0, 107.1, 113.4, 145.3; **ESI-HRMS (m/z):** calcd. for $[C_{12}H_{16}O_2 + Na]^+$: 215.1043. Found: 215.1027.

7.2.2.5. Synthesis of cycloisomerized derivative 10b

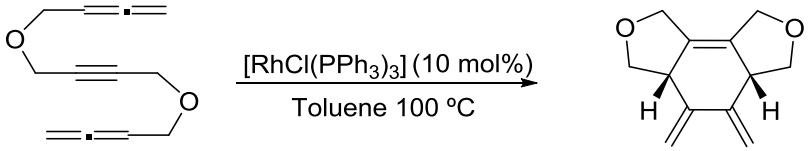

2b **10b**

In a 10 mL 2-necked round bottom flask, a mixture of 4-(4-(buta-2,3-dienyloxy)but-2-ynyloxy)buta-1,2-diene, **2b**, (0.048 g, 0.252 mmols) and tris(triphenylphosphine)rhodium(I) chloride (0.024 g, 0.026 mmols) was purged with nitrogen and dissolved in toluene anh. (2 mL).The mixture was stirred at reflux for 1 h (TLC monitoring). The solvent was removed and the crude was purified by column chromatography using mixture of hexane:ethyl acetate (90:10) as the eluent to give the cycloisomerised product **10b** (0.010 g, 27 % yield), as a yellow oil. **MW:** 190.24g/mol; **IR (ATR) ν(cm^{-1}):** 2925, 2854, 1726, 1039; **^{1}H NMR (300 MHz, $CDCl_3$) δ(ppm):** 3.46-3.52 (m, 4H), 4.23 (dt, $^5J_{H\text{-}H}$ = 1.2 Hz, $^3J_{H\text{-}H}$ = 12.9 Hz, 2H), 4.33-4.40 (m, 4H), 4.74 (d, $^5J_{H\text{-}H}$ = 1.2 Hz, 2H), 5.47 (d, $^5J_{H\text{-}H}$ = 1.2 Hz, 2H); **^{13}C NMR (75 MHz, $CDCl_3$) δ (ppm):** 44.8, 68.3, 72.1, 109.7, 129.2, 143.7; **ESI-HRMS (m/z):** calcd. for $[C_{12}H_{14}O_2 + Na]^+$: 213.0886. Found: 213.0879.

7.2.2.6. Synthesis of cycloisomerized derivative 11a

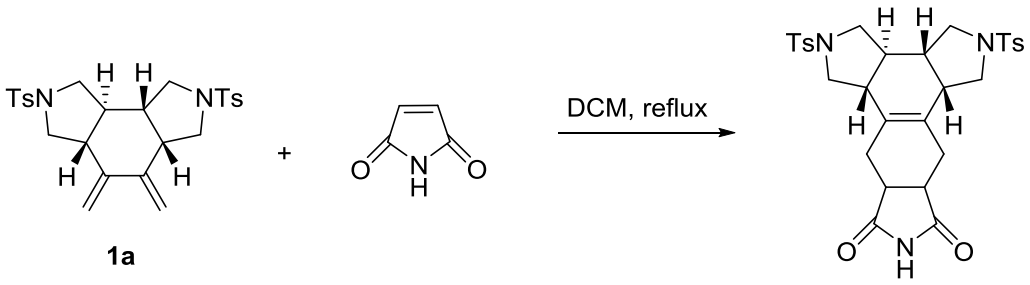

1a **11a**

In a 10 mL 2-necked round bottom flask, a mixture of cycloisomerised deivative **1a**, (0.020 g, 0.040 mmols) and maleimide (0.004 g, 0.040 mmols) was purged with nitrogen and dissolved in DCM (3 mL).The mixture was stirred at reflux for 4 h (TLC monitoring). The solvent was removed and the crude was purified by column chromatography using mixture of hexane:ethyl acetate (90:10) as the eluent to give the cycloisomerised product **11a** (0.022 g, 92 % yield), as a colourless solid. **MW:** 595.73 g/mol; **IR (ATR) ν(cm^{-1}):** 2921, 1716, 1338, 1158; **^{1}H NMR (400 MHz, $CDCl_3$) δ(ppm):** 1.38-1.45 (m, 1H), 2.06-2.23 (m, 4H), 2.30-2.50 (m, 9H), 2.55-2.64 (m, 1H), 2.74-2.87 (m, 3H), 3.08-3.16 (m, 3H), 3.21 (dd, $^4J_{H\text{-}H}$ = 6.2 Hz, 1H), 3.44-3.50 (m, 2H), 3.67 (dd, $^4J_{H\text{-}H}$ = 7.4 Hz, 1H), 7.34 (dd, $^3J_{H\text{-}H}$ = 8.1 Hz, 4H), 7.68 (dd, $^3J_{H\text{-}H}$ = 8.1 Hz, 4H), 8.14 (s, 1H); **^{13}C NMR (100 MHz, $CDCl_3$) δ (ppm):** 21.6, 21.6, 25.7, 27.2, 39.8, 40.3, 40.7, 42.9, 44.4, 44.7, 50.0, 50.9, 51.0, 51.5, 127.1, 127.5, 129.9, 123.0, 130.4, 131.1, 132.7, 134.8, 143.7, 144.2, 179.2, 179.3; **ESI-HRMS (m/z):**calcd. for $[C_{30}H_{33}N_3O_6S_2 + Na]^+$: 618.1703. Found: 618.1684.

7.2.2.7. Synthesis of cycloisomerized derivative 12a

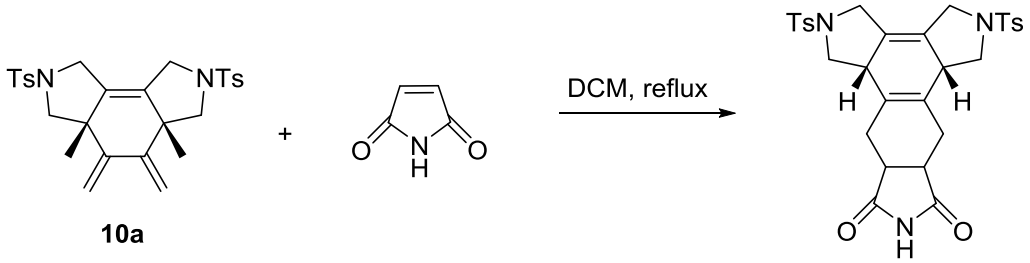

In a 10 mL 2-necked round bottom flask, a mixture of cycloisomerised deivative **10a**, (0.012 g, 0.024 mmols) and maleimide (0.002 g, 0.024 mmols) was purged with nitrogen and dissolved in DCM (3 mL).The mixture was stirred at reflux for 1 h (TLC monitoring). The solvent was removed and the crude was purified by column chromatography using mixture of hexane:ethyl acetate (90:10) as the eluent to give the cycloisomerised product **12a** (0.010 g, 75 % yield), as a colourless solid. **MW:** 593.71 g/mol; **IR (ATR) ν(cm^{-1}):** 2918, 1707, 1337, 1156, 1091; **^{1}H NMR (400 MHz, $CDCl_3$) δ(ppm):** 2.11-2.17 (m, 2H), 2.44 (s, 6H), 2.46-2.48 (m, 2H), 2.58 (dd, $^{4}J_{H\text{-}H}$ = 2.4 Hz, $^{2}J_{H\text{-}H}$ = 11.6 Hz, 2H), 3.04 (br. s, 2H), 3.15 (t, $^{3}J_{H\text{-}H}$ = 4.0 Hz, 2H), 3.64 (d, $^{2}J_{H\text{-}H}$ = 16.4 Hz, 2H), 3.81-3.81 (m, 4H), 7.33 (t, $^{3}J_{H\text{-}H}$ = 8.1 Hz, 4H), 7.70 (d, $^{3}J_{H\text{-}H}$ = 8.1 Hz, 4H); **^{13}C NMR (100 MHz, $CDCl_3$) δ (ppm):** 21.6, 26.1, 40.7, 43.5, 48.6, 51.0, 127.5, 127.7, 127.7, 129.1, 123.0, 133.7, 144.0, 178.8. **ESI-HRMS (m/z):**calcd. for $[C_{30}H_{31}N_3O_6S_2 + Na]^+$: 616.1546 Found: 616.1531.

7.3. Experimental procedure for the products synthesised in Chapter 4.

7.3.1. Synthesis of substrates

7.3.1.1. Synthesis of tert-butyl (S)-nona-1,2-dien-4-yl(tosyl)carbamate

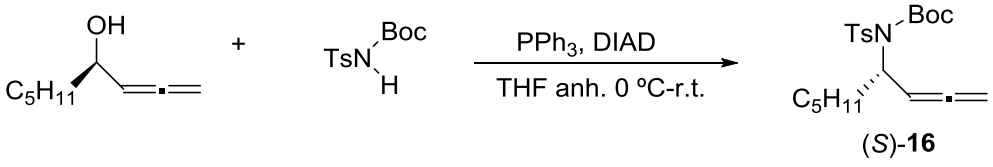

In a 50 mL two-necked round bottom flask, a mixture of (*R*)-nona-1,2-dien-4-ol (0.25 g, 1.78 mmols), *tert*-butyl tosylcarbamate (0.48 g, 1.78 mmols) and triphenylphosphine (1.17 g, 4.45 mmols) in anhydrous and degassed tetrahydrofuran (10 mL) was stirred and cooled to 0˚C. Diisopropyl azodicarboxylate (0.87 mL, 4.45 mmols) was added dropwise to this solution and the mixture was stirred at room temperature for 1 h (TLC monitoring). The solvent was removed under reduced pressure and the crude reaction mixture was purified by column chromatography using a mixture of hexane: ethyl acetate (90:10) as the eluent to afford product (*S*)-**16** (0.55 g, 79 % yield) as a yellow oil. **MW:** 393.54 g/mol; **IR (ATR) ν (cm^{-1}):** 2930, 1725, 1246, 1148; **^{1}H NMR (300 MHz, $CDCl_3$) δ(ppm):** 0.91 (t, 3H), 1.35-1.37 (m, 15H), 1.88-2.05 (m, 2H), 2.45 (s, 3H), 4.81 (dd, $^{4}J_{H\text{-}H}$ =8.8 Hz, $^{5}J_{H\text{-}H}$ =2.1 Hz, 2H), 5.01-5.10 (m, 1H), 5.46 (q,

$^{3}J_{H\text{-}H}$ = 8.8 Hz, $^{4}J_{H\text{-}H}$ = 8.8 Hz, 1H), 7.29 (d, $^{3}J_{H\text{-}H}$ = 8.2 Hz, 2H), 7.81 (d, $^{3}J_{H\text{-}H}$ = 8.2 Hz, 2H). **^{13}C NMR (75 MHz, $CDCl_3$) δ (ppm):** 14.0, 21.6, 22.5, 26.4, 27.9, 31.4, 34.0, 58.4, 74.4, 84.0, 91.1, 128.1, 129.1, 137.7, 143.8, 150.5, 208.7. **ESI-MS (m/z):** 416.1 $[M+Na]^+$; **AE:** calcd for $[C_{21}H_{31}NO_4S]$: C, 64.09; H, 7.94; N, 3.56. Found: C, 64.63; H, 7.82; N, 3.71. **$[\alpha]^{20}_D$** +34.4 (*c* 1.4, $CHCl_3$).

7.3.1.2. Synthesis of (S)-4-methyl-N-(nona-1,2-dien-4-yl)benzenesulfonamide

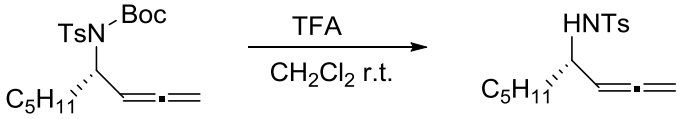

(*S*)-**16** (*S*)-**15**

In a 50 mL two-necked round bottom flask, a mixture of *tert*-butyl (*S*)-nona-1,2-dien-4-yl(tosyl)carbamate, (*S*)-**16**, (0.55 g, 1.78 mmols) and trifluoroacetic acid (1.5 mL, 17.82 mmols) in 20 mL of dichloromethane was stirred at room temperature for 4 h (TLC monitoring). The solvent was removed under reduced pressure and the residue was purified by column chromatography using a mixture of hexane:ethyl acetate (90:10) as the eluent to give product (*S*)-**15** (0.45 g, 87 % yield) as a yellow oil. **MW:** 293.43 g/mol; **IR (ATR) ν (cm^{-1}):** 2929, 1323, 1157; **^{1}H NMR (300 MHz, $CDCl_3$) δ(ppm):** 0.85 (t, $^{3}J_{H\text{-}H}$ = 6.9 Hz, 3H), 1.12-1.38 (m, 6H), 1.40-1.59 (m, 2H), 2.43 (s, 3H), 3.79 (m, 1H), 4.43 (d, $^{3}J_{H\text{-}H}$ = 8.7 Hz, 1H), 4.58-4.76 (m, 2H), 4.95 (m, 1H), 7.29 (d, $^{3}J_{H\text{-}H}$ = 8.4 Hz, 2H), 7.74 (d, $^{3}J_{H\text{-}H}$ = 8.4 Hz, 2H). **^{13}C NMR (75 MHz, $CDCl_3$) δ (ppm):** 14.0, 21.5, 22.5, 24.9, 31.3, 36.1, 52.1, 78.4, 92.4, 127.2, 129.5, 138.0, 143.2, 206.8. **ESI-MS (m/z):** 294.1 $[M + H]^+$, 316.1 $[M + Na]^+$; **AE:** calcd for $[C_{16}H_{23}NO_2S]$: C, 65.49; H, 7.90; N, 4.77. Found: C, 65.28; H, 7.85; N, 4.99. **$[\alpha]^{20}_D$** -18.9 (*c* 1.0, $CHCl_3$).

The enantiomeric excess was determined by HPLC analysis (Daicel Chiralpak column (4.6 x 250 mm, 5 μm); 1 mL/min flow rate of a 2 % 2-propanol: 98 % heptane mobile phase during 12 min.; λ = 254 nm.; R_t = 9.78 min. and R_t = 10.38 min. for the two enantiomers in the racemic mixture; R_t= 9.99 min. for the enantiomerically pure product).

7.3.1.3. Synthesis of compound (S,S)-13

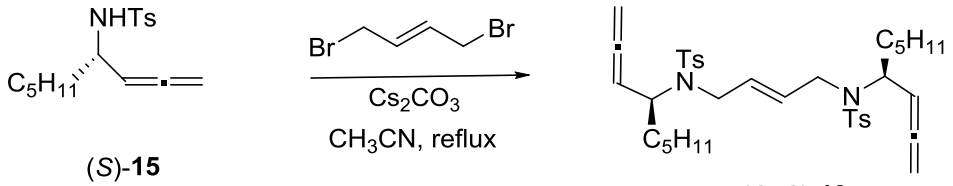

(*S*)-**15** (*S, S*)-**13**

In a 25 mL two-necked round bottom flask, a mixture of *(S)*-4-methyl-*N*-(nona-1,2-dien-4-yl)benzenesulfonamide, (*S*)-**15**, (0.11 g, 0.394 mmols), *(E)*-1,4-dibromobut-2-ene (0.04 g, 0.197 mmols) and cesium carbonate (0.32 g, 0.984 mmols) in 10 mL of acetonitrile was heated at reflux for 4 h (TLC monitoring). The insoluble salts were filtered off and the solvent was removed under reduced pressure. The crude reaction mixture was purified by column chromatography using a mixture of hexane: ethyl acetate of increasing polarity (100:0-90:10)

as the eluent to give product (*S,S*)-**13** (0.09 g, 73 % yield) as a white solid. **MW:** 638.93 g/mol; **m.p.:** 115-117^{0}C; **IR (ATR) ν (cm^{-1}):** 2926, 1955, 1338, 1158; **^{1}H NMR (300 MHz, $CDCl_3$) δ(ppm):** 0.83-0.89 (m, 6H), 1.15-1.37 (m, 12H), 1.42-1.57 (m, 4H), 2.42 (s, 6H), 3.53-3.81 (m, 4H), 4.31-4.41 (m, 2H), 4.67-4.72 (m, 4H), 4.76-4.87 (m, 2H), 5.63-5.69 (m, 2H), 7.27 (d, $^3J_{H\text{-}H}$ = 8.4 Hz, 4H), 7.70 (d, $^3J_{H\text{-}H}$ = 8.4 Hz, 4H). **^{13}C NMR (75 MHz, $CDCl_3$) δ (ppm):** 14.1, 21.5, 22.6, 25.9, 31.4, 32.8, 45.0, 56.7, 77.1, 90.0, 127.3, 129.6, 130.5, 137.8, 143.1, 208.6. **ESI-MS (m/z):** 661.4 [M + Na]$^+$. **AE:** calcd for [$C_{36}H_{50}N_2O_4S_2$] : C, 67.68; H, 7.89; N, 4.38. Found: C, 67.81 and 67.85; H, 8.04 and 7.97; N, 4.27 and 4.27. **[α]$^{20}_D$** -89.7 (*c* 4.0, $CHCl_3$).

The enantiomeric excess was determined by HPLC analysis (Daicel Chiralpak column (4.6 x 250 mm, 5 μm); 1 mL/min flow rate of a 10 % 2-propanol: 90 % heptane mobile phase during 15 min.; λ = 254 nm.; R_t = 9.92 min and R_t = 10.48 min for the two enantiomers and R_t = 12.32 min for *meso* form in the racemic mixture; R_t = 10.39 min for the enantiomerically pure product).

7.3.1.4. Synthesis of compound (S,S)-14

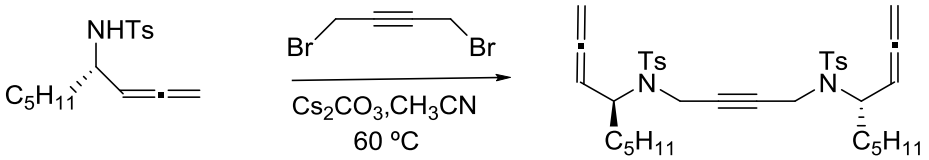

(*S*)-**15** (*S,S*)-**14**

In a 25 mL two-necked round bottom flask, a mixture of *(S)*-4-methyl-*N*-(nona-1,2-dien-4-yl)benzenesulfonamide, (*S*)-**15**, (0.11 g, 0.394 mmols), 1,4-dibromobut-2-yne (0.04 g, 0.197 mmols) and cesium carbonate (0.32 g, 0.984 mmols) in 10 mL of acetonitrile was heated at 60 ˚C for 4 h (TLC monitoring). The insoluble salts were filtered off and the solvent was removed under reduced pressure. The crude reaction mixture was purified by column chromatography using a mixture of hexane: ethyl acetate of increasing polarity (100:0-90:10) as the eluent to give product (*S,S*)-**14** (0.05 g, 53 % yield) as a yellow oil. **MW:** 636.91 g/mol; **IR (ATR) ν (cm^{-1}):** 2926, 1955, 1338, 1158; **^{1}H NMR (300 MHz, $CDCl_3$) δ(ppm):** 0.78-0.93 (m, 6H), 1.12-1.36 (m, 12H), 1.48-1.61 (m, 4H), 2.42 (s, 6H), 3.83-4.02 (m, 4H), 4.31-4.35 (m, 2H), 4.69-4.74 (m, 4H), 4.88-4.98 (m, 2H), 7.30 (d, $^3J_{H\text{-}H}$ = 8.0 Hz, 4H), 7.76 (d, $^3J_{H\text{-}H}$ = 8.0 Hz, 4H). **^{13}C NMR (75 MHz, $CDCl_3$) δ (ppm):** 14.0, 21.5, 22.6, 25.9, 29.7, 31.4, 32.3, 32.4, 56.4, 77.3, 79.7, 79.7, 90.0, 127.5, 129.4, 137.7, 143.3, 208.6. **ESI-MS (m/z):** 637.3 [M + H]$^+$, 654.3 [M + Na]$^+$; **ESI-HRMS (m/z):**calcd. for [$C_{36}H_{48}N_2O_4S_2$ + Na]$^+$:659,2948 found 659,2971. **[α]$^{20}_D$** -36.2 (*c* 1.0, $CHCl_3$).

The enantiomeric excess was determined by HPLC analysis (Daicel Chiralpak column (4.6 x 250 mm, 5 μm); 1 mL/min flow rate of a 8 % 2-propanol: 92 % heptane mobile phase during 20 min.; λ = 254 nm.; R_t = 12.19 min and R_t = 13.11 min for the two enantiomers and R_t = 17.34 min for *meso* form in the racemic mixture; R_t = 12.68 min for the enantiomerically pure product).

7.3.2. Rh-catalysed [2+2+2] cycloaddition reactions of allene-ene/yne-allene

7.3.2.1. Synthesis of racemic cycloadducts 18 and 19

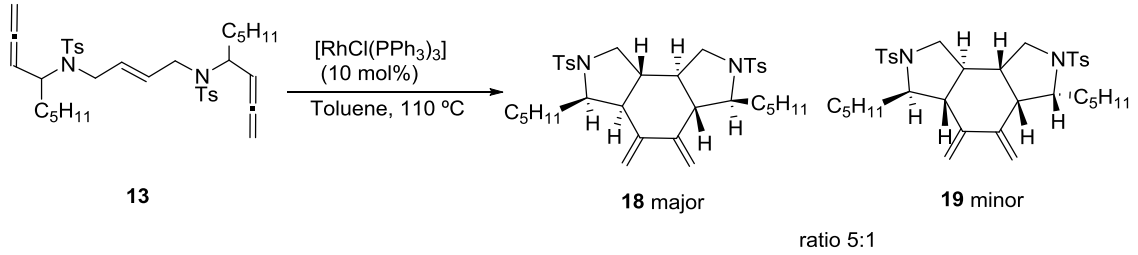

13 **18** major **19** minor

ratio 5:1

In a 10 mL two-necked round bottom flask, a mixture of compound **13** (0.066 g, 0.103 mmols) and tris(triphenylphosphine)rhodium(I)chloride (0.010 g, 0.010 mmols) was purged with nitrogen and dissolved in anhydrous toluene (3 mL). The mixture was stirred at reflux for 2h (TLC monitoring). The solvent was removed and the crude was purified by column chromatography using a mixture of hexane:ethyl acetate (80:20) as the eluent to give products **18** and **19** (0.032 g, 49 % combined yield, in 5:1 ratio) as a colourless solid. **MW:** 638.93 g/mol; **IR (ATR) ν (cm^{-1}):** 2920, 2852, 1339, 1146, 1088; **ESI-HRMS (m/z):**calcd. for [$C_{36}H_{50}N_2O_4S_2$ + Na]$^+$: 661.3104, found 661.3093.

Characterization of cycloadduct **18**

^{1}H NMR (400 MHz, $CDCl_3$) δ(ppm): 0.80 (m, 1H), 1.89-1.94 (quint, $^3J_{H\text{-}H}$ = 5.52 Hz, 1H), 2.01-2.07 (m, 1H), 2.41 (s, 3H), 2.46 (s, 3H), 2.78-2.83 (m, 2H), 3.23 (dd, $^3J_{H\text{-}H}$ = 4.7 Hz, $^2J_{H\text{-}H}$ = 11.1 Hz, 1H), 3.30 (ddd, $^4J_{H\text{-}H}$ = 1.9 Hz, $^3J_{H\text{-}H}$ = 5.1 Hz, $^2J_{H\text{-}H}$ = 9.8 Hz, 1H), 3.50 (d, $^2J_{H\text{-}H}$ = 11.1 Hz, 1H), 3.62 (ddd, $^4J_{H\text{-}H}$ = 3.0 Hz, $^3J_{H\text{-}H}$ = 5.8 Hz, $^2J_{H\text{-}H}$ = 9.1 Hz, 1H), 3.86 (dd, $^4J_{H\text{-}H}$ = 6.7 Hz, $^2J_{H\text{-}H}$ = 10.5 Hz, 1H), 4.57 (brs, 1H), 4.72 (d, $^2J_{H\text{-}H}$ = 1.7 Hz, 1H), 4.96 (brs, 1H), 5.08 (d, $^2J_{H\text{-}H}$ = 1.8 Hz, 1H), 7.33 (dd, $^3J_{H\text{-}H}$ = 8.2 Hz, $^3J_{H\text{-}H}$ = 8.4 Hz, 4H), 7.68 (dd, $^3J_{H\text{-}H}$ = 8.2 Hz, $^3J_{H\text{-}H}$ = 8.4 Hz, 4H); **^{13}C NMR (100 MHz, $CDCl_3$) δ (ppm):** 14.0, 21.5, 21.5, 22.3, 22.6, 22.6, 23.6, 29.7, 30.1, 31.9, 32.0, 32.9, 42.0, 42.7, 50.6, 51.1, 52.4, 53.0, 61.0, 61.1, 107.6, 114.0, 126.5, 126.8, 129.8, 129.9, 136.9, 136.9, 143.3, 143.6. 145.6, 146.7.

The enantiomeric excess was determined by HPLC analysis (Daicel Chiralpak column (4.6 x 250 mm, 5 µm); 1 mL/min flow rate of a 15 % 2-propanol: 85 % heptane mobile phase during 10 min.; λ = 254 nm.; R_t = 5.01 min and R_t = 5.75 min for major diastereoisomer **18** and R_t = 6.75 min and R_t = 8.90 min for minor diastereoisomer **19** in racemic mixture).

7.3.2.2. Synthesis of chiral cycloadduct (S,S)-19

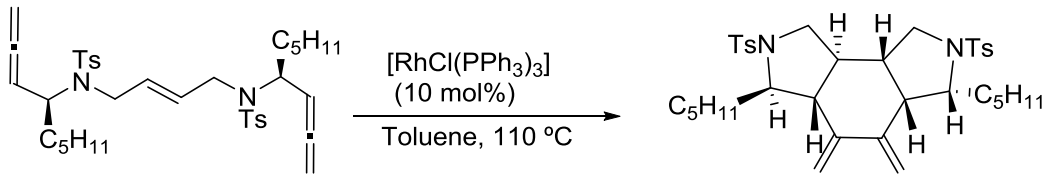

(*S*,*S*)**-13** (*S*,*S*)**-19**

In a 10 mL 2-necked round bottom flask, a mixture of compound (*S*,*S*)-**13** (0.020 g, 0.031 mmols) and tris(triphenylphosphine)rhodium(I)chloride (0.003 g, 0.003 mmols) was purged with nitrogen and dissolved in anhydrous toluene (3 mL). The mixture was stirred at reflux for 2h (TLC monitoring). The solvent was removed and the crude was purified by column chromatography using mixture of hexane:ethyl acetate (90:10) as the eluent to give cycloisomerised product (*S,S*)-**19** (0.009 g, 46% yield) as a colourless solid. **MW:** 638.93 g/mol; **$[\alpha]^{20}_{D}$** +23.4 (*c* 1.0, $CHCl_3$).

Characterization of cycloadduct **(*S,S*)-19**

^{1}H NMR (400 MHz, $CDCl_3$) δ(ppm): 0.86-0.91 (m, 7H), 1.81-1.83 (m, 1H), 1.92-1.97 (m, 1H), 2.41 (s, 3H), 2.43 (s, 3H), 2.47-2.51 (m, 1H), 2.73 (t, $^2J_{H\text{-}H}$ = 12.0 Hz, 1H), 3.00 (dd, $^2J_{H\text{-}H}$ = 11.2 Hz, $^3J_{H\text{-}H}$ = 1.9 Hz, 1H), 3.25 (dd, $^2J_{H\text{-}H}$ = 11.2 Hz, $^3J_{H\text{-}H}$ = 7.5 Hz, 1H), 3.43 (m, 1H), 3.68 (dd, $^2J_{H\text{-}H}$ = 11.5 Hz, $^3J_{H\text{-}H}$ = 6.5 Hz, 1H), 3.80 (m, 1H), 4.60 (brs, 1H), 4.70 (d, $^2J_{H\text{-}H}$ = 1.7 Hz, 1H), 5.02 (brs, 1H), 5.19 (d, $^2J_{H\text{-}H}$ = 1.7 Hz, 1H), 7.32 (d, $^3J_{H\text{-}H}$ = 8.2 Hz, 4H), 7.69 (dd, $^3J_{H\text{-}H}$ = 8.2 Hz, 4H); **^{13}C NMR (100 MHz, $CDCl_3$) δ (ppm):** 14.1, 14.1, 21.5, 21.6, 22.61, 22.6, 24.1, 27.4, 29.7, 30.9, 31.9, 32.1, 33.0, 35.1, 40.5, 45.4, 48.2, 51.4, 51.5, 53.3, 61.6, 64.6, 106.3, 116.1, 127.2, 127.5, 129.7, 130.0, 134.4, 134.8, 143.6, 143.9, 145.1, 147.5.

The enantiomeric excess was determined by HPLC analysis (Daicel Chiralpak column (4.6 x 250 mm, 5 μm); 1 mL/min flow rate of a 15 % 2-propanol: 85 % heptane mobile phase during 10 min.; λ = 254 nm.; R_t = 9.75 min for a single enantiomer.

7.3.2.3. Synthesis of racemic cycloadducts 20 and 21

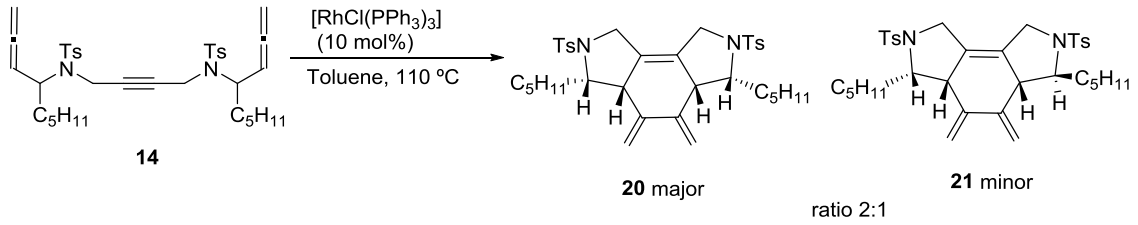

In a 10 mL 2-necked round bottom flask, a mixture of compound **14** (0.056 g, 0.088 mmols) and tris(triphenylphosphine)rhodium(I)chloride (0.008 g, 0.009 mmols) was purged with nitrogen and dissolved in anhydrous toluene (3 mL). The mixture was stirred at reflux for 2h (TLC monitoring). The solvent was removed and the crude was purified by column chromatography using mixture of hexane:ethyl acetate (80:20) as the eluent to give a mixture of cycloisomerised products **20** and **21** (0.027 g, 48 % combined yield in 2:1 ratio) as a colourless solid. **MW:** 636.91 g/mol; **IR (ATR) ν (cm^{-1}):** 320, 2922, 2854, 1342, 1150, 1090; **ESI-HRMS (m/z):**calcd. for $[C_{36}H_{48}N_2O_4S_2 + Na]^+$: 659.2948, found 659.2944.

Characterization of cycloadduct **20** and **21**

^{1}H NMR (400 MHz, $CDCl_3$) δ(ppm): 0.86-0.91 (m, 9H, **20** + **21**), 1.01-1.43 (m, 24H, **20** + **21**), 2.37 (s, 9H, **20** +**21**), 2.93 (br s, 1H, **20**), 3.55 (m, 3H, **20** + **21**), 3.83 (m, 3H, **20** + **21**), 4.06 (m, 3H, **20** + **21**), 4.60 (d, $^5J_{H\text{-}H}$ = 1.6 Hz, 2H, **20**), 4.65 (s, 1H, **21**), 4.76 (t, $^5J_{H\text{-}H}$ = 1.3 Hz, 1H, **21**), 5.05 (d, $^5J_{H\text{-}H}$

= 1.6 Hz, 3H, **20** + **21**), 5.37 (t, $^{5}J_{H\text{-}H}$ = 1.3 Hz,1H), 7.12 (d, $^{3}J_{H\text{-}H}$ = 8.4 Hz, 6H, **20** + **21**), 7.60 (d, $^{3}J_{H\text{-}H}$ = 8.2 Hz, 6H, **20** + **21**); **^{13}C NMR (100 MHz, $CDCl_3$) δ (ppm):** 14.1, 21.4, 22.6, 24.1, 31.9, 34.6, 48.0, 49.8, 63.7, 109.2, 127.3, 127.8, 129.7, 135.5, 143.5, 144.1.

The enantiomeric excess was determined by HPLC analysis (Daicel Chiralpak column (4.6 x 250 mm, 5 µm); 1 mL/min flow rate of a 10 % 2-propanol: 90 % heptane mobile phase during 15 min.; λ = 254 nm.; R_t = 9.04 min and R_t = 9.72 min for minor diastereoisomer **21** and R_t = 12.44 min for major diastereoisomer **20** (*meso* form) in racemic mixture).

7.3.2.4. Synthesis of chiral cycloadduct (S,S)-21

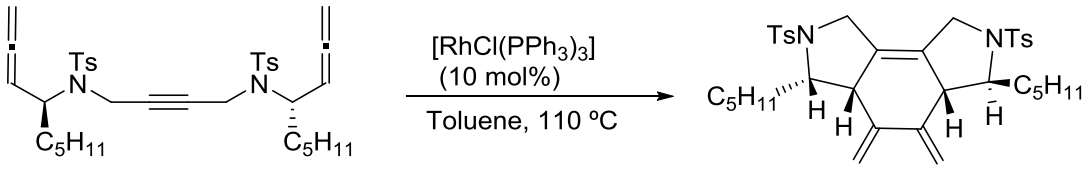

(*S,S*)-**14** (*S,S*)-**21**

In a 10 mL 2-necked round bottom flask, a mixture of compound (*S,S*)-**14**, (0.020 g, 0.031 mmols) and tris(triphenylphosphine)rhodium(I)chloride (0.003 g, 0.003 mmols) was purged with nitrogen and dissolved in anhydrous toluene (3 mL). The mixture was stirred at reflux for 2 h (TLC monitoring). The solvent was removed and the crude was purified by column chromatography using mixture of hexane:ethyl acetate (90:10) as the eluent to give cycloisomerised product (*S,S*)-**21** (0.009 g, 46 % yield) as a colourless solid. **MW:** 636.91 g/mol; **[α]**$^{20}_{D}$ -24.7 (*c* 0.9, $CHCl_3$).

Characterization of cycloadduct (*S,S*)-**21**

^{1}H NMR (400 MHz, $CDCl_3$) δ(ppm): 0.86-0.91 (m, 6H), 1.01-1.43 (m, 16H), 2.37 (s, 3H), 2.43 (s, 3H), 2.74(br s, 1H), 2.93 (br s, 1H), 3.56 (m, 2H), 3.80 (m, 2H), 3.84-4.01 (m, 2H), 4.60 (d, $^{5}J_{H\text{-}H}$ = 2.0 Hz, 1H), 4.76 (t, $^{5}J_{H\text{-}H}$ = 1.3 Hz, 1H), 5.05 (d, $^{5}J_{H\text{-}H}$ = 2.0 Hz, 1H), 5.37 (t, $^{5}J_{H\text{-}H}$ = 1.3 Hz,1H), 7.22 (d, $^{3}J_{H\text{-}H}$ = 8.4 Hz, 2H), 7.32 (d, $^{3}J_{H\text{-}H}$ = 8.4 Hz, 2H), 7.62 (d, $^{3}J_{H\text{-}H}$ = 8.2 Hz, 2H), 7.72 (d, $^{3}J_{H\text{-}H}$ = 8.2 Hz, 2H); **^{13}C NMR (100 MHz, $CDCl_3$) δ (ppm):** 14.0, 14.1, 21.5, 21.5, 22.6, 22.7, 24.1, 25.6, 31.6, 31.9, 36.2, 38.7, 47.0, 47.4, 48.3, 49.7, 62.6, 63.7, 107.6, 115.5, 127.1, 127.3, 127.4, 127.7, 129.61, 129.63, 129.9, 130.5, 135.0, 135.8, 143.3, 145.1.

The enantiomeric excess was determined by HPLC analysis (Daicel Chiralpak column (4.6 x 250 mm, 5 µm); 1 mL/min flow rate of a 10 % 2-propanol: 90 % heptane mobile phase during 15 min.; λ = 254 nm.; R_t = 9.81 min for a single enantiomer.

7.4. Experimental procedure for the products synthesised in Chapter 5.

7.4.1. Synthesis of substrates

7.4.1.1. Synthesis of N-(cyanoethyl)-4-methylbenzenesulfonamide

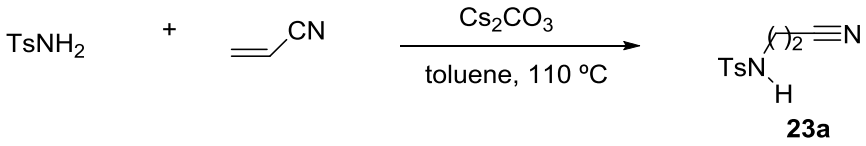

In a 100 mL sealable Shlenk tube, a mixture of *N*-tosylamine, (2.07 g, 12.11 mmols), acrylonitrile (1.6 mL, 24.30 mmols) and cesium carbonate (7.89 g, 24.21 mmols) in 80 mL of toluene was heated at 110˚C. The mixture was stirred for 12 h (TLC monitoring). The solvent was removed under reduced pressure and residue dissolved in 50 mL of dichloromethane was extracted with water (3 x 30 mL). Organic phases were joined together and dried over sodium sulphate anhydrous. The salts were filtered off and solvent was remove under reduced pressure and give the product, **23a**, (2.2 g, 83 % yield) as a brown solid, which is characterized by ours spectroscopic data. **MW:** 224.28 g/mol; **^{1}H NMR (400 MHz, $CDCl_3$) δ(ppm):** 2.46 (s, 3H), 2.60 (t, $^3J_{H\text{-}H}$ = 8.8 Hz, 2H), 3.28 (t, $^3J_{H\text{-}H}$ = 8.8 Hz, 2H), 5.04 (br s, 1H), 7.37 (d, $^3J_{H\text{-}H}$ = 8.1 Hz, 2H), 7.76 (d, $^3J_{H\text{-}H}$ = 8.1 Hz, 4H).

7.4.1.2. Synthesis of 24a

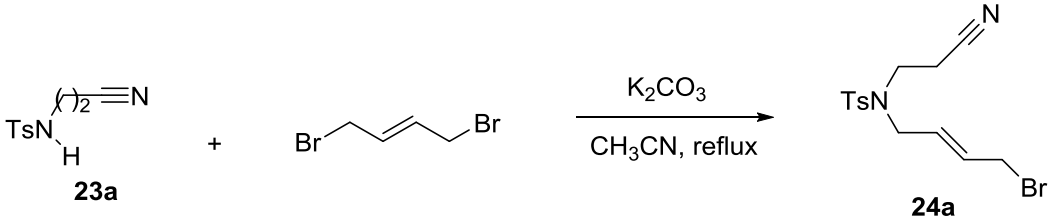

In a 100 mL two-necked round bottom flask, a mixture of *N*-(2-cyanoethyl)-4-methylbenzenesulfonamide **23a** (2.0 g, 8.92 mmols), (*E*)-1,4-dibromobut-2-ene (7.63 g, 35.67 mmols) and potassium carbonate (6.16 g, 44.58 mmols) in acetonitrile (50 mL) was heated at reflux. The mixture was stirred for 4 h until completion (TLC monitoring). The salts were filtered off and the solvent was removed under reduced pressure. The reaction crude was purified by column chromatography using a mixture of hexane: ethyl acetate (90:10) as the eluent to give compound **24a** (1.91 g, 60 % yield) as a colourless solid. **MW:** 357.26 g/mol; **m.p.:** 88-90^{0}C; **^{1}H NMR (400 MHz, $CDCl_3$) δ (ppm):** 2.45 (s, 3H), 2.69 (t, $^3J_{H\text{-}H}$ = 7.2 Hz, 2H), 3.36 (t, $^3J_{H\text{-}H}$ = 7.2 Hz, 2H), 3.88 (m, 4H), 5.76 (m, 2H), 7.33 (d, $^3J_{H\text{-}H}$ = 8.4 Hz, 2H), 7.72 (d, $^3J_{H\text{-}H}$ = 8.4 Hz, 2H). **^{13}C NMR (75 MHz, $CDCl_3$) δ (ppm):** 18.9, 21.6, 30.8, 43.4, 50.5, 117.5, 127.2, 127.3, 129.1, 130.1, 131.7, 131.7, 135.5, 144.3. **ESI-MS (m/z):** 379-381 $[M + Na]^+$.

7.4.1.3. Synthesis of 22aa

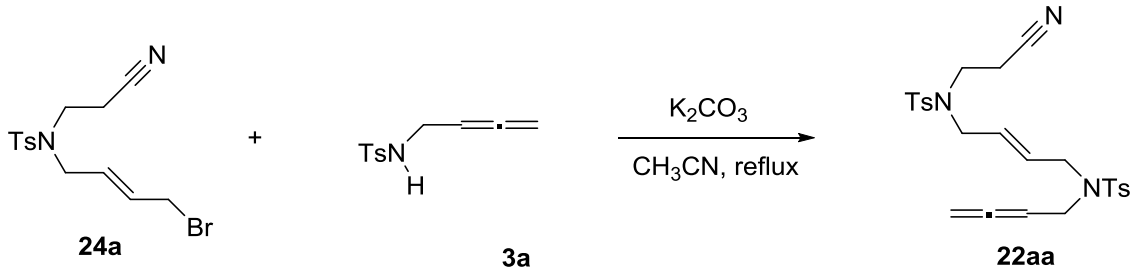

In a 100 mL two-necked round bottom flask, a mixture of (*E*)-*N*-(4-bromobut-2-en-1-yl)-*N*-(2-cyanoethyl)-4-methylbenzenesulfonamide, **24a**, (1.00 g, 2.80 mmols), *N*-(buta-2,3-dien-1-yl)-4-methylbenzenesulfonamide, **3a,** (0.70 g, 2.80 mmols) and potassium carbonate (3.67 g, 26.60 mmols) in acetonitrile (50 mL) was heated at reflux. The mixture was stirred for 6h until completion (TLC monitoring). The salts were filtered off and the solvent was removed under reduced pressure. The reaction crude was purified by column chromatography using a mixture of hexane: ethyl acetate (80:20) as the eluent to give compound **22aa** (0.60 g, 50% yield) as a colourless solid. **MW:** 499.65 g/mol; **m.p.:** 108-110˚C; **^{1}H NMR (300 MHz, $CDCl_3$) δ (ppm):** 2.43 (s, 3H), 2.45 (s, 3H), 2.66 (t, $^{3}J_{H\text{-}H}$ = 6.9 Hz, 2H), 3.32 (t, $^{3}J_{H\text{-}H}$ = 6.9 Hz, 2H), 3.78 (m, 6H), 4.70 (dt, $^{4}J_{H\text{-}H}$ = 6.6 Hz, $^{5}J_{H\text{-}H}$ = 2.4 Hz, 2H), 4.85 (dq, $^{3}J_{H\text{-}H}$ = 7.2 Hz, $^{4}J_{H\text{-}H}$ = 6.6 Hz, 1H), 5.56 (m, 2H), 7.33 (d, $^{3}J_{H\text{-}H}$ = 8.1 Hz, 2H), 7.69 (d, $^{3}J_{H\text{-}H}$ = 8.2 Hz, 2H), 7.67 (d, $^{3}J_{H\text{-}H}$ = 8.2 Hz, 4H). **^{13}C NMR (100 MHz, $CDCl_3$) δ (ppm):** 18.8, 21.5, 21.6, 43.2, 46.4, 47.9, 50.7, 76.4, 85.6, 117.6, 127.2, 127.3, 128.3, 129.8, 130.1, 130.9, 135.5, 136.9, 143.6, 144.2, 209.5. **ESI-MS (m/z):** 500.1 $[M + H]^+$.

7.4.1.4. Synthesis of N-(cyanomethyl)-4-methylbenzenesulfonamide

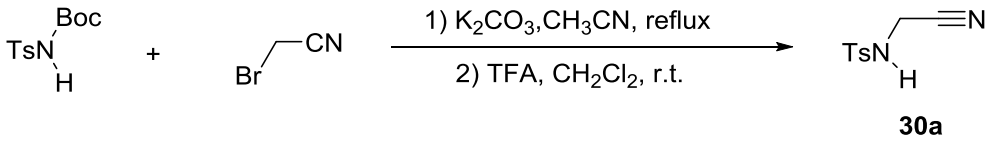

In a 100 mL two-necked round bottom flask, a mixture of *tert*-butyl tosylcarbamate, (1.00 g, 3.68 mmols), 2-bromoacetonitrile, (0.26 mL, 3.68 mmols) and potassium carbonate (2.54 g, 18.40 mmols) in acetonitrile (50 mL) was heated at reflux. The mixture was stirred for 5 h until completion (TLC monitoring). The salts were filtered off and the solvent was removed under reduced pressure. Then, the reaction was dissolved in dichloromethane (30 mL) and trifluoroacetic acid (2.80 mL, 36.80 mmols) was added and stirred for 2 h. The reaction crude was purified by column chromatography using a mixture of hexane: ethyl acetate (80:20) as the eluent to give compound **30a** (0.53 g, 68 % yield) as a colourless solid. **MW:** 210.25 g/mol; **^{1}H NMR (300 MHz, $CDCl_3$) δ (ppm):** 2.46 (s, 3H), 4.02 (d, $^{3}J_{H\text{-}H}$ = 6.0 Hz, 2H), 5.00 (t, $^{3}J_{H\text{-}H}$ = 6.0 Hz, 1H), 7.37 (d, $^{3}J_{H\text{-}H}$ = 8.4 Hz, 2H), 7.79 (d, $^{3}J_{H\text{-}H}$ = 8.4 Hz, 2H).

7.4.1.5. Synthesis of 31a

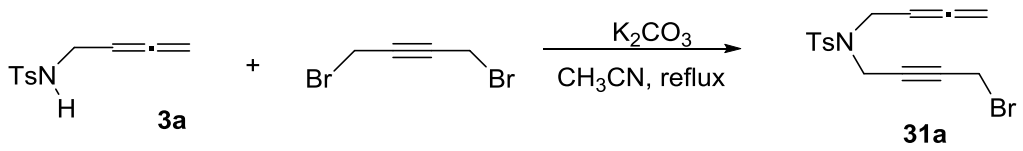

In a 100 mL two-necked round bottom flask, a mixture of *N*-4-tosylbuta-2,3-dien-1-amine **3a** (1.0 g, 4.48 mmols), 1,4-dibromo-2-butyne (3.05 g, 14.39 mmols) and potassium carbonate (2.51 g, 18.16 mmols) in acetonitrile (50 mL) was heated at reflux. The mixture was stirred for 6 h until completion (TLC monitoring). The salts were filtered off and the solvent was removed under reduced pressure. The reaction crude was purified by column chromatography using a mixture of hexane:ethyl acetate (80:20) as the eluent to give compound **31a** (0.97 g, 61 % yield) as a yellow oil. **MW:** 354.26 g/mol; **IR (ATR) ν (cm^{-1}):** 1344, 1210, 1156, 1091; **^{1}H NMR (400 MHz, $CDCl_3$) δ (ppm):** 2.43 (s, 3H), 3.64 (t, $^{5}J_{H\text{-}H}$ = 2.0 Hz, 2H), 3.83 (dt, $^{3}J_{H\text{-}H}$ = 7.0 Hz, $^{5}J_{H\text{-}H}$ = 2.4 Hz, 2H), 4.19 (t, $^{5}J_{H\text{-}H}$ = 2.0 Hz, 2H), 4.79 (dt, $^{4}J_{H\text{-}H}$ = 7.0 Hz, $^{5}J_{H\text{-}H}$ = 2.4 Hz, 2H), 5.04 (quint., $^{3}J_{H\text{-}H}$ = 7.0 Hz, 1H), 7.33 (d, $^{3}J_{H\text{-}H}$ = 8.4 Hz, 2H), 7.72 (d, $^{3}J_{H\text{-}H}$ = 8.4 Hz, 2H). **^{13}C NMR (75 MHz, $CDCl_3$) δ (ppm):** 13.7, 21.6, 36.3, 45.9, 76.6, 79.6, 80.5, 85.4, 127.6, 129.6, 135.8, 143.7, 209.8. **ESI-MS (m/z):** 376.0-378.0 $[M + Na]^+$: **AE:** calcd. for $[C_{15}H_{16}BrNO_2S]$: C, 49.60; H, 4.72; N, 3.86. Found: C, 49.80; H, 4.61; N, 3.77.

7.4.1.6. Synthesis of N-(2-cyanophenyl)-4-methylbenzenesulfonamide

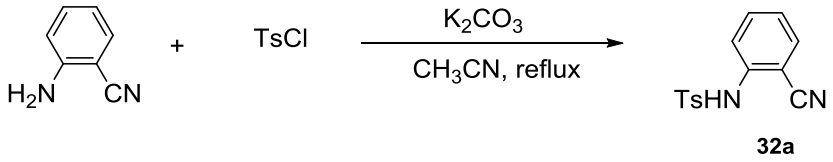

In a 100 mL two-necked round bottom flask, a mixture of 2-aminobenzonitrile (1.0 g, 8.46 mmols), 4-methylbenzenesulfonyl chloride (1.61 g, 8.46 mmols) and potassium carbonate (5.85 g, 42.30 mmols) in acetonitrile (50 mL) was heated at reflux. The mixture was stirred for 8h until completion (TLC monitoring). The salts were filtered off and the solvent was removed under reduced pressure. The reaction crude was purified by column chromatography using a mixture of hexane:ethyl acetate (90:10) as the eluent to give compound **32a** (1.61 g, 70 % yield) as a yellow solid. **MW:** 272.32 g/mol; **^{1}H NMR (400 MHz, $CDCl_3$) δ (ppm):** 2.39 (s, 3H), 7.17 (dt, $^{5}J_{H\text{-}H}$ = 1.0 Hz, $^{3}J_{H\text{-}H}$ = 7.7 Hz, 1H), 7.26 (d, $^{3}J_{H\text{-}H}$ = 8.4 Hz, 2H), 7.46 (m, 1H), 7.54 (m, 1H), 7.72 (m, 3H).

7.4.1.7. Synthesis of 27aa

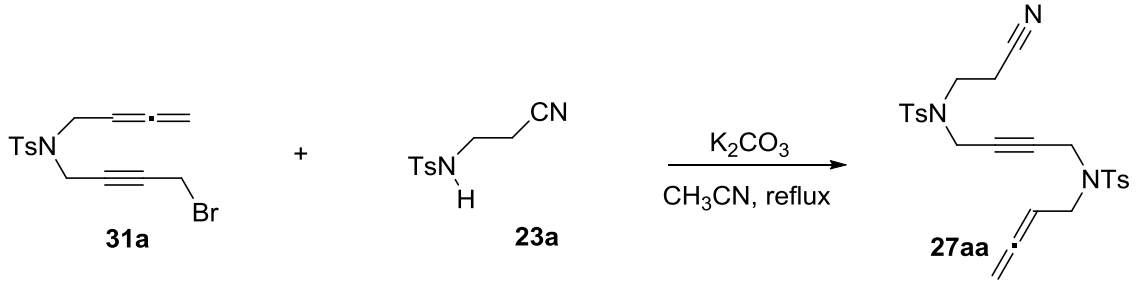

In a 50 mL two-necked round bottom flask, a mixture of *N*-(2-cyanoethyl)-4-methylbenzenesulfonamide **23a** (0.50 g, 2.25 mmols), *N*-(4-bromobut-2-yn-1-yl)-*N*-(buta-2,3-dien-1-yl)-4-methylbenzenesulfonamide **31a** (0.80 g, 2.25 mmols) and potassium carbonate (1.55 g, 11.25 mmols) in acetonitrile (50 mL) was heated at reflux. The mixture was stirred for 6h until completion (TLC monitoring). The salts were filtered off and the solvent was removed under reduced pressure. The reaction crude was purified by column chromatography using a mixture of hexane:ethyl acetate (80:20) as the eluent to give compound **27aa** (0.95 g, 85 % yield) as a colourless solid. **MW:** 497.63 g/mol; **m.p.:** 115-117˚C; **IR (ATR) ν (cm^{-1}):** 2248, 1338, 1158, 1003. **^{1}H NMR (300 MHz, $CDCl_3$) δ (ppm):** 2.44 (s, 3H), 2.45 (s, 3H), 2.63 (t, $^{3}J_{H\text{-}H}$ = 6.9 Hz, 2H), 3.29 (t, $^{3}J_{H\text{-}H}$ = 6.9 Hz, 2H), 3.69 (dt, $^{3}J_{H\text{-}H}$ = 7.2 Hz, $^{5}J_{H\text{-}H}$ = 2.4 Hz, 2H), 3.96 (t, $^{5}J_{H\text{-}H}$ = 1.8 Hz, 2H), 3.99 (t, $^{5}J_{H\text{-}H}$ = 1.8 Hz, 2H), 4.74 (dt, $^{4}J_{H\text{-}H}$ = 6.6 Hz, $^{5}J_{H\text{-}H}$ = 2.4 Hz, 2H), 4.91 (dq, $^{3}J_{H\text{-}H}$ = 7.2 Hz, $^{4}J_{H\text{-}H}$ = 6.6 Hz, 1H), 7.31 (d, $^{3}J_{H\text{-}H}$ = 8.2 Hz, 2H), 7.33 (d, $^{3}J_{H\text{-}H}$ = 8.2 Hz, 2H), 7.67 (d, $^{3}J_{H\text{-}H}$ = 8.2 Hz, 4H). **^{13}C NMR (75 MHz, $CDCl_3$) δ (ppm):** 18.3, 21.5, 21.6, 35.8, 38.2, 42.9, 45.7, 77.8, 79.4, 85.3, 117.3, 127.5, 127.6, 129.6, 129.9, 135.0, 136.1, 143.9, 144.5, 209.7. **ESI-MS (m/z):** 498.1 [M + H]$^{+}$. **AE:** calcd. for [$C_{25}H_{27}N_3O_4S_2$] : C, 60.34; H, 5.47; N, 8.44. Found: C, 59.93; H, 4.99; N, 8.63.

7.4.1.8. Synthesis of 28aa

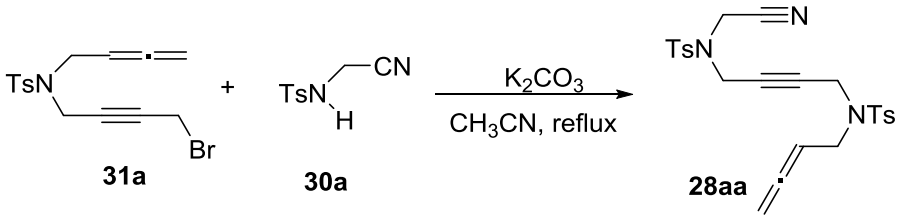

In a 50 mL two-necked round bottom flask, a mixture of *N*-(cyanomethyl)-(4-methylphenyl)sulfonamide **30a** (0.10 g, 0.48 mmols), bromo derivative **31a** (0.17 g, 0.48 mmols) and potassium carbonate (0.33 g, 2.39 mmols) in acetonitrile (30 mL) was heated at reflux. The mixture was stirred for 4h until completion (TLC monitoring). The salts were filtered off and the solvent was removed under reduced pressure. The reaction crude was purified by column chromatography using a mixture of hexane:ethyl acetate (80:20) as the eluent to give compound **28aa** (0.18 g, 78 % yield) as a yellow oil. **MW:** 483.60 g/mol; **IR (ATR) ν (cm^{-1}):** 1596, 1342, 1157. **^{1}H NMR (300 MHz, $CDCl_3$) δ (ppm):** 2.44 (s, 3H), 2.45 (s, 3H), 3.76 (dt, $^{3}J_{H\text{-}H}$ = 7.0 Hz, $^{5}J_{H\text{-}H}$ = 2.5 Hz, 2H), 3.90 (t, $^{5}J_{H\text{-}H}$ = 1.8 Hz, 2H), 4.05 (t, $^{5}J_{H\text{-}H}$ = 1.8 Hz, 2H), 4.09 (s, 2H), 4.77 (dt, $^{4}J_{H\text{-}H}$ = 7.0 Hz, $^{5}J_{H\text{-}H}$ = 2.5 Hz, 2H), 4.97 (q, $^{4}J_{H\text{-}H}$ = 7.0 Hz, 1H), 7.30-7.40 (m, 4H), 7.65-7.78 (m, 4H). **^{13}C NMR (75 MHz, $CDCl_3$) δ (ppm):** 21.5, 21.7, 34.7, 35.9, 37.4, 42.9, 76.5, 80.46, 80.5, 85.3, 85.3, 113.2, 127.6, 129.7, 130.1, 133.7, 135.9, 144.0, 145.2, 209.8. **ESI-MS (m/z):** 506.1 [M + Na]$^{+}$. **AE:** calcd. for [$C_{24}H_{25}N_3O_4S_2.1.5H_2O$] : C, 56.45; H, 5.53; N, 8.23. Found: C, 56.86; H, 5.00; N, 7.97.

7.4.1.9. Synthesis of 29aa

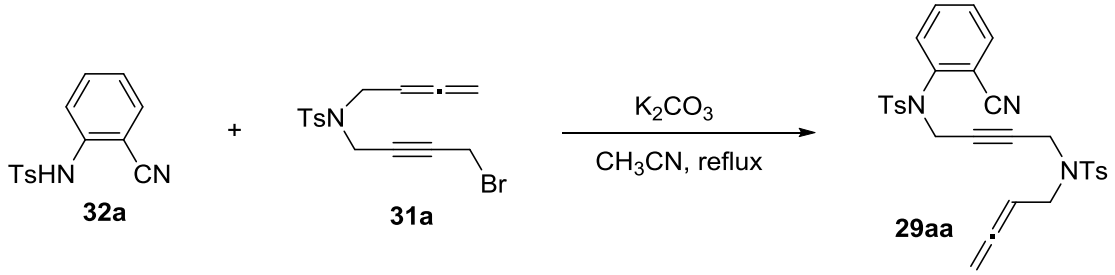

In a 50 mL two-necked round bottom flask, a mixture of *N*-tosyl-2-aminobenzonitrile **32a** (0.05 g, 0.23 mmols), bromo derivative **31a** (0.08 g, 0.23 mmols) and potassium carbonate (0.16 g, 1.13 mmols) in acetonitrile (30 mL) was heated at reflux. The mixture was stirred for 5 h until completion (TLC monitoring). The salts were filtered off and the solvent was removed under reduced pressure. The reaction crude was purified by column chromatography using a mixture of hexane:ethyl acetate (90:10) as the eluent to give compound **29aa** (0.08 g, 70 % yield) as a colourless solid. **MW:** 545.67 g/mol; **m.p.:** 120-122˚C; **IR (ATR) ν (cm^{-1}):** 2920, 2236, 1347, 1159, 1088. **^{1}H NMR (400 MHz, $CDCl_3$) δ (ppm):** 2.43 (s, 3H), 2.44 (s, 3H), 3.61 (dt, $^{3}J_{H\text{-}H}$ = 7.0 Hz, $^{5}J_{H\text{-}H}$ = 2.5 Hz, 2H), 3.99 (t, $^{5}J_{H\text{-}H}$ = 1.9 Hz, 2H), 4.26 (t, $^{5}J_{H\text{-}H}$ = 1.9 Hz, 2H), 4.73 (dt, $^{4}J_{H\text{-}H}$ = 6.6 Hz, $^{5}J_{H\text{-}H}$ = 2.5 Hz, 2H), 4.91 (q, $^{4}J_{H\text{-}H}$ = 6.6 Hz, 1H), 7.27-7.31 (m, 5H), 7.45 (dt, $^{3}J_{H\text{-}H}$ = 7.8 Hz, $^{4}J_{H\text{-}H}$ = 1.5 Hz, 1H), 7.55 (dd, $^{3}J_{H\text{-}H}$ = 7.8 Hz, $^{4}J_{H\text{-}H}$ = 1.5 Hz, 1H), 7.57-7.66 (m, 5H). **^{13}C NMR (75 MHz, $CDCl_3$) δ (ppm):** 21.6, 21.7, 35.0, 36.0, 40.7, 45.6, 78.6, 79.3, 85.3, 114.8, 115.9, 127.6, 128.2, 129.5, 129.8, 131.5, 134.9, 136.0, 140.8, 143.8, 144.7, 209.6. **ESI-MS (m/z):** 546.1 $[M + H]^+$, 568.2 $[M + Na]^+$. **AE:** calcd. for $[C_{29}H_{27}N_3O_4S_2]$: C, 63.83; H, 4.99; N, 7.70. Found: C, 64.04; H, 5.26; N, 7.21.

7.4.1.10. Synthesis of 23b

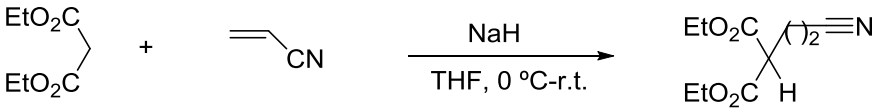

23b

In 50 mL 2-neck round bottom flask, a mixture of diethyl malonate (0.20 g, 1.25 mmols) in anhydrous THF (5 mL) was added to a solution of NaH (60 % in mineral oil, 0.04 g, 1.73 mmols) in 10 mL of anhydrous THF at 0˚C and stirred for 1 h. A solution of acrylonitrile (0.07 g, 1.25 mmols) in anhydrous THF (5 mL) was added at 0˚C and the resulting mixture was stirred overnight at room temperature. The reaction mixture was poured onto ice-water (10 mL) and extracted with ether (3 × 5 mL). The combined organic layer was dried over Na_2SO_4 and concentrated in vacuum conditions. The reaction crude was purified by column chromatography using a mixture of hexane:ethyl acetate (90:10) as the eluent to give the product **23b** (0.38 g, 81 % yield) as a yellow oil. **MW:** 199.21 g/mol; **^{1}H NMR (400 MHz, $CDCl_3$) δ (ppm):** 1.29 (t, $^{3}J_{H\text{-}H}$ = 7.2 Hz, 6H), 2.25 (dt, $^{3}J_{H\text{-}H}$ = 7.2 Hz, $^{3}J_{H\text{-}H}$ = 7.2 Hz, 2H), 2.51 (t, $^{3}J_{H\text{-}H}$ = 7.2 Hz 2H), 3.51 (t, $^{3}J_{H\text{-}H}$ = 7.2 Hz, 1H), 4.20-4.26 (m, 4H).

7.4.1.11. Synthesis of 27ba

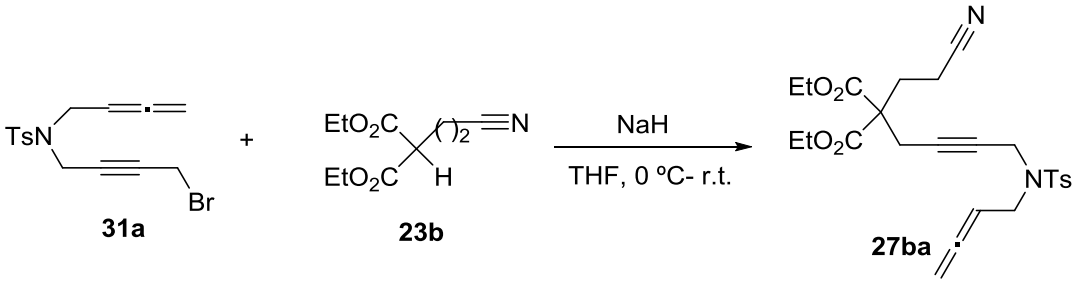

In 50 mL 2-neck round bottom flask, a mixture of diethyl 2-(2-cyanoethyl)malonate **23b** (0.20 g, 0.96 mmols) in anhydrous THF (5 mL) was added to a solution of NaH (60 % in mineral oil, 0.04 g, 1.73 mmols) in 10 mL of anhydrous THF at 0˚C and stirred for 1 h. A solution of bromo derivative **31a** (0.41 g, 1.15 mmols) in anhydrous THF (5 mL) was added at 0˚C and the resulting mixture was stirred overnight at room temperature. The reaction mixture was poured onto ice-water (10 mL) and extracted with ether (3 × 5 mL). The combined organic layer was dried over Na_2SO_4 and concentrated in vacuum conditions. The reaction crude was purified by column chromatography using a mixture of hexane:ethyl acetate (80:20) as the eluent to give the product **27ba** (0.38 g, 81 % yield) as a yellow oil. **MW:** 486.58 g/mol; **IR (ATR) ν (cm^{-1}):** 2921, 2250, 1729, 1347, 1191, 1158. **^{1}H NMR (300 MHz, $CDCl_3$) δ (ppm):** 1.25 (t, $^3J_{H\text{-}H}$ = 7.2 Hz, 6H), 2.15-2.23 (m, 2H), 2.27- 2.35 (m, 2H), 2.45 (s, 3H), 2.63 (t, $^5J_{H\text{-}H}$ = 2.4 Hz, 2H), 3.83 (dt, $^3J_{H\text{-}H}$ = 7.0 Hz, $^3J_{H\text{-}H}$ = 2.5 Hz, 2H), 4.10 (t, $^5J_{H\text{-}H}$ = 2.4 Hz, 2H), 4.19 (q, $^3J_{H\text{-}H}$ = 7.2 Hz, 4H), 4.80 (dt, $^4J_{H\text{-}H}$ = 7.0 Hz, $^5J_{H\text{-}H}$ = 2.5 Hz, 2H), 4.90 (quint. $^3J_{H\text{-}H}$ = 7.0 Hz, 1H), 7.32 (d, $^3J_{H\text{-}H}$ = 8.4 Hz, 2H), 7.67 (d, $^3J_{H\text{-}H}$ = 8.4 Hz, 2H). **^{13}C NMR (75 MHz, $CDCl_3$) δ (ppm):** 12.8, 13.9, 21.6, 23.6, 28.4, 36.0, 45.6, 55.4, 62.2, 76.5, 79.1, 85.3, 118.7, 127.6, 129.6, 129.7, 136.3, 143.6, 168.9, 209.7. **ESI-MS (m/z):** 487.1 $[M + H]^+$. **AE:** calcd. for $[C_{25}H_{30}N_2O_6S]$: C, 61.71; H, 6.21; N, 5.76. Found: C, 61.31; H, 6.16; N, 5.65.

7.4.1.12. Synthesis of 33b

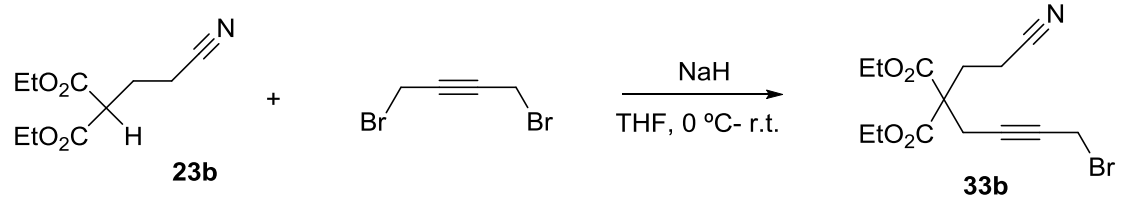

In a 50 mL 2-neck round bottom flask, a mixture of diethyl 2-(2-cyanoethyl)malonate **23b** (0.50 g, 2.34 mmols) in anhydrous THF (5 mL) was added to a solution of NaH (60 % in mineral oil, 0.13 g, 5.62 mmols) in 10 mL of anhydrous THF at 0˚C and stirred for 1 h. A solution of 1,4-dibromo-2-butyne (1.98 g, 9.38 mmols) in anhydrous THF (5 mL) was added at 0˚C and the resulting mixture was stirred overnight at room temperature. The reaction mixture was poured onto ice-water (10 mL) and extracted with ether (3 × 5 mL). The combined organic layer was dried over Na_2SO_4 and concentrated in vacuum conditions. The reaction crude was purified by column chromatography using a mixture of hexane:ethyl acetate (80:20) as the eluent to give the product **33b** (0.63 g, 78 % yield) as a yellow oil. **MW:** 344.20 g/mol; **IR (ATR) ν (cm^{-1}):** 2917, 2248, 1728, 1203. **^{1}H NMR (300 MHz, $CDCl_3$) δ (ppm):** 1.30 (t, $^3J_{H\text{-}H}$ = 7.2 Hz, 6H), 2.39-2.52 (m,

4H), 2.91 (d, $^{5}J_{H\text{-}H}$ = 2.4 Hz, 2H), 3.88 (d, $^{5}J_{H\text{-}H}$ = 2.4 Hz, 2H), 4.26 (q, $^{3}J_{H\text{-}H}$ = 7.2 Hz, 4H). **^{13}C NMR (75 MHz, $CDCl_3$) δ (ppm):** 13.0, 14.0, 14.1, 14.3, 24.0 28.7, 55.7, 62.3, 79.2, 81.0, 118.8, 169.0. **HRMS** calcd. for $[C_{14}H_{18}NO_4Br + Na]^+$: 366.0311. Found: 366.0309.

7.4.1.13. Synthesis of 3b

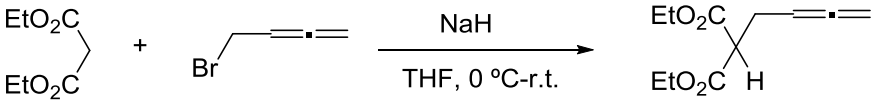

3b

In a 50 mL 2-neck round bottom flask, a mixture of diethyl malonate (0.50 mL, 3.31 mmols) in anhydrous THF (5 mL) was added to a solution of NaH (60 % in mineral oil, 0.1 g, 4.16 mmols) in 15 mL of anhydrous THF at 0˚C and stirred for 1 h. A solution of 4-bromobuta-1,2-diene (0.46 g, 3.50 mmols) in anhydrous THF (10 mL) was added at 0˚C and the resulting mixture was stirred overnight at room temperature. The reaction mixture was poured onto ice-water (10 mL) and extracted with ether (3 × 10 mL). The combined organic layer was dried over Na_2SO_4 and concentrated in vacuum conditions. The reaction crude was purified by column chromatography using a mixture of hexane:ethyl acetate (90:10) as the eluent to give the product **3b** (0.48 g, 68 % yield) as a yellow oil. **MW:** 212.24 g/mol; **^{1}H NMR (400 MHz, $CDCl_3$) δ (ppm):** 1.26 (t, $^{3}J_{H\text{-}H}$ = 8.0 Hz, 6H), 2.56-2.61 (m, 2H), 3.46 (t, $^{3}J_{H\text{-}H}$ = 7.6 Hz, 1H), 4.17-4.22 (m, 4H), 4.71 (dt, $^{4}J_{H\text{-}H}$ = 7.2 Hz, $^{5}J_{H\text{-}H}$ = 3.2 Hz, 2H), 5.13 (quint., $^{4}J_{H\text{-}H}$ = 6.4 Hz, 1H).

7.4.1.14. Synthesis of 27bb

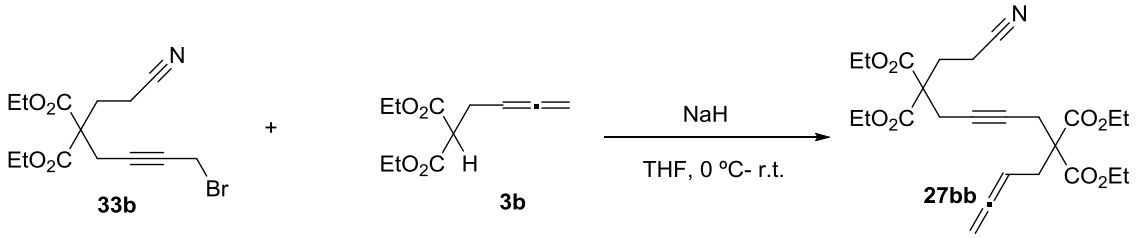

In a 50 mL 2-neck round bottom flask, a mixture of diethyl 2-(4-bromobut-2-yn-1-yl)-2-(2-cyanoethyl)malonate **33b** (0.51 g, 1.48 mmols) in anhydrous THF (5 mL) was added to a solution of NaH (60 % in mineral oil, 0.06 g, 2.50 mmols) in 10 mL of anhydrous THF at 0˚C and stirred for 1 h. A solution of diethyl 2-(buta-2,3-dien-1-yl)malonate **3b** (0.24 g, 1.21 mmols) in anhydrous THF (5 mL) was added at 0˚C and the resulting mixture was stirred overnight at room temperature. The reaction mixture was poured onto ice-water (10 mL) and extracted with ether (3 × 5 mL). The combined organic layer was dried over Na_2SO_4 and concentrated in vacuum conditions. The reaction crude was purified by column chromatography using a mixture of hexane:ethyl acetate (90:10) as the eluent to give the product **27bb** (0.50 g, 86 % yield) as a yellow oil. **MW:** 475.54 g/mol; **IR (ATR) ν (cm^{-1}):** 2923, 2248, 1726, 1443, 1280, 1185. **^{1}H NMR (400 MHz, $CDCl_3$) δ (ppm):** 1.23-1.28 (m, 12H), 2.35-2.46 (m, 4H), 2.70 (dt, $^{3}J_{H,H}$ = 8.0 Hz, $^{5}J_{H,H}$ = 2.5 Hz, 2H), 2.77-2.80 (m, 4H), 4.20-4.26 (m, 8H), 4.69 (dt, $^{4}J_{H,H}$ = 6.6 Hz, $^{5}J_{H,H}$ = 2.5 Hz, 2H), 4.91 (m, 1H). **^{13}C NMR (100 MHz, $CDCl_3$) δ (ppm):** 14.0, 14.1, 22.7, 23.6, 28.4, 31.5, 55.8, 57.0, 61.6, 62.1, 74.8, 78.8, 83.8, 118.9, 169.1, 169.6, 210.2. **HRMS** calcd. for $[C_{25}H_{33}NO_8 + Na]^+$: 498.2098. Found: 498.2115.

7.4.1.15. Synthesis of 34ac

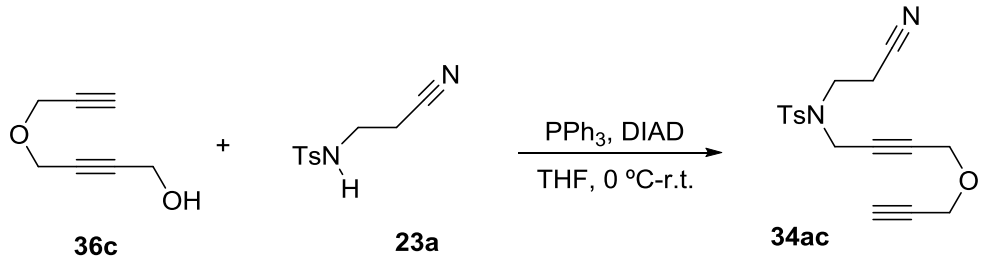

36c **23a** **34ac**

In a 50 mL two-necked round bottom flask, a mixture 4-(prop-2-yn-1-yloxy)but-2-yn-1-ol **36c** (0.30 g, 2.42 mmols), *N*-(2-cyanoethyl)-4-methylbenzenesulfonamide **23a** (0.54 g, 2.41 mmols) and triphenylphosphine (1.58 g, 6.05 mmols) in anhydrous and degassed tetrahydrofuran (30 mL) was stirred and cooled to 0˚C in an ice-water bath. Diisopropyl azodicarboxylate (1.20 mL, 6.02 mmols) was added dropwise to this solution and the resulting mixture was stirred at room temperature for 20 h (TLC monitoring). The solvent was removed under reduced pressure and the reaction crude was purified by column chromatography using a mixture of hexane:ethyl acetate (90:10) as the eluent to afford compound **34ac** (0.44 g, 55 % yield) as a yellow oil. **MW:** 330.40 g/mol; **IR (ATR) ν (cm^{-1}):** 2250, 1344, 1158, 1077. **^{1}H NMR (400 MHz, $CDCl_3$) δ(ppm):** 2.44 (s, 3H), 2.46 (t, $^{4}J_{H\text{-}H}$ = 2.4 Hz, 1H), 2.74 (t, $^{3}J_{H\text{-}H}$ = 7.2 Hz, 2H), 3.47 (t, $^{3}J_{H\text{-}H}$ = 7.2 Hz, 2H), 4.04 (d, $^{4}J_{H\text{-}H}$ = 2.4 Hz, 2H), 4.06 (t, $^{5}J_{H\text{-}H}$ = 2.0 Hz, 2H), 4.23 (t, $^{5}J_{H\text{-}H}$ = 2.0 Hz, 2H), 7.34 (d, $^{3}J_{H\text{-}H}$ = 8.4 Hz, 2H), 7.73 (d, $^{3}J_{H\text{-}H}$ = 8.4 Hz, 2H). **^{13}C NMR (75 MHz, $CDCl_3$) δ (ppm):** 18.4, 21.6, 38.4, 43.1, 56.4, 56.5, 75.3, 78.6, 79.3, 81.4, 117.4, 127.7, 129.8, 135.0, 144.5. **ESI-MS (m/z):** 353.1 $[M + H]^+$. **HRMS** calcd. for $[C_{17}H_{18}N_2O_3S + Na]^+$: 353.0947. Found: 353.0930.

7.4.1.16. Synthesis of 27ac

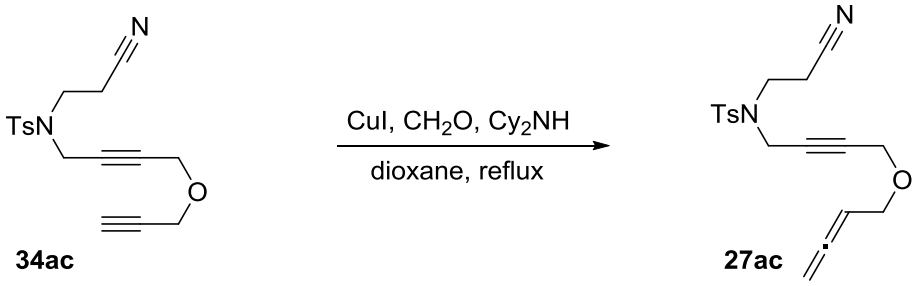

34ac **27ac**

In a 50 mL two-necked round bottom flask, a mixture of **34ac** (0.17 g, 0.51 mmols), formaldehyde (0.03 g, 1.29 mmols) and copper(I) iodide (0.05 g, 0.26 mmols) in dioxane (20 mL) was heated to reflux. Dicyclohexylamine (0.2 mL, 1.00 mmols) was then added dropwise to the reaction mixture and was stirred for 4 h until completion (TLC monitoring). The salts were filtered off and the solvent was removed under reduced pressure. The reaction crude was purified by column chromatography using a mixture of hexane:ethyl acetate (90:10) as the eluent to afford derivative **27ac** (0.09 g, 51 % yield) as a yellow oil. **MW:** 344.43 g/mol; **IR (ATR) ν (cm^{-1}):** 2916, 2250, 1347, 1159, 1101; **^{1}H NMR (300 MHz, $CDCl_3$) δ(ppm):** 2.44 (s, 3H), 2.74 (t, $^{3}J_{H\text{-}H}$ = 7.5 Hz, 2H), 3.47 (t, $^{3}J_{H\text{-}H}$ = 7.5 Hz, 2H), 3.90 (dt, $^{3}J_{H\text{-}H}$ = 7.0 Hz, $^{5}J_{H\text{-}H}$ = 2.5 Hz, 2H), 3.98 (t, $^{5}J_{H\text{-}H}$ = 2.1 Hz, 2H), 4.23 (t, $^{5}J_{H\text{-}H}$ = 2.1 Hz, 2H), 4.82 (dt, $^{4}J_{H\text{-}H}$ = 7.0 Hz, $^{5}J_{H\text{-}H}$ = 2.5 Hz, 2H), 5.15 (quint. $J_{H\text{-}H}$ = 7.0 Hz, 1H), 7.33 (d, $^{3}J_{H\text{-}H}$ = 8.4 Hz), 7.73 (d, $^{3}J_{H\text{-}H}$ = 8.4 Hz). **^{13}C NMR (75 MHz, $CDCl_3$) δ (ppm):** 18.4, 21.9, 38.4, 43.1, 56.7, 67.4, 76.0, 78.7, 82.2, 86.8, 117.3, 127.7, 129.8, 135.0,

144.3, 209.5. **GC-MS (m/z):** 344.3 $[M]^+$. **AE:** calcd. for $[C_{18}H_{20}N_2O_3S.1.5H_2O]$: C, 61.17; H, 5.99; N, 7.93. Found: C, 61.47; H, 6.25; N, 7.70.

7.4.1.17. Synthesis of 35ac

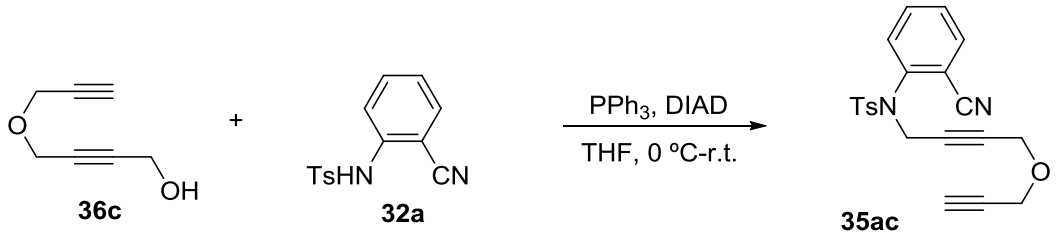

In a 100 mL two-necked round bottom flask, a mixture of 4-(prop-2-yn-1-yloxy)but-2-yn-1-ol **36c** (0.40 g, 3.23 mmols), *N*-(2-cyanophenyl)-4-methylbenzenesulfonamide **32a** (0.76 g, 3.23 mmols) and triphenylphosphine (2.12 g, 8.06 mmols) in anhydrous and degassed tetrahydrofuran (40 mL) was stirred and cooled to 0˚C in an ice-water bath. Diisopropyl azodicarboxylate (1.60 mL, 8.06 mmols) was added dropwise to this solution and the resulting mixture was stirred at room temperature for 2 h (TLC monitoring). The solvent was removed under reduced pressure and the reaction crude was purified by column chromatography using a mixture of hexane:dichloromethane (70:30) as the eluent to afford compound **35ac** (1.04 g, 85 % yield) as a yellow oil. **MW:** 378.45 g/mol; **IR (ATR) ν (cm^{-1}):** 3276, 2919, 2231, 1348, 1159, 1083. **^{1}H NMR (400 MHz, $CDCl_3$) δ(ppm):** 2.42 (t, $^4J_{H\text{-}H}$ = 2.4 Hz, 1H), 2.44 (s, 3H), 4.03 (d, $^4J_{H\text{-}H}$ = 2.4 Hz, 2H), 4.12 (t, $^5J_{H\text{-}H}$ = 1.9 Hz, 2H), 4.51 (t, $^5J_{H\text{-}H}$ = 1.9 Hz, 2H), 7.31 (d, $^3J_{H\text{-}H}$ = 8.3 Hz, 2H), 7.42-7.49 (m, 2H), 7.60 (dt, $^3J_{H\text{-}H}$ = 7.8 Hz, $^4J_{H\text{-}H}$ = 1.5 Hz, 1H), 7.68-7.70 (m, 3H). **^{13}C NMR (100 MHz, $CDCl_3$) δ (ppm):** 21.7, 41.2, 56.2, 56.4, 75.1, 78.7, 80.3, 81.6, 115.2, 116.1, 128.2, 129.2, 129.8, 131.3, 133.3, 133.9, 135.2, 141.2, 144.6. **HRMS** calcd. for $[C_{21}H_{18}N_2O_3S + Na]^+$: 401.0930. Found: 401.0947.

7.4.1.18. Synthesis of 29ac

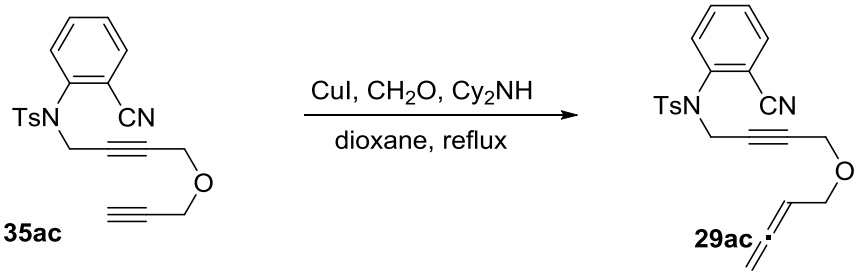

In a 50 mL two-necked round bottom flask, a mixture of **35ac** (0.53 g, 1.40 mmols), formaldehyde (0.10 g, 2.80 mmols) and copper(I) iodide (0.15 g, 0.70 mmols) in dioxane (20 mL) was heated to reflux. Dicyclohexylamine (0.5 mL, 2.52 mmols) was then added dropwise to the reaction mixture and stirred for 5 h until completion (TLC monitoring). The salts were filtered off and the solvent was removed under reduced pressure. The reaction crude was purified by column chromatography using a mixture of hexane: dichloromethane (70:30) as the eluent to afford derivative **29ac** (0.37 g, 68 % yield) as a yellow oil. **MW:** 392.47 g/mol; **IR (ATR) ν (cm^{-1}):** 2918, 2231, 1349, 1155, 1074.; **^{1}H NMR (400 MHz, $CDCl_3$) δ(ppm):** 2.44 (s, 3H), 3.87

(dt, $^{3}J_{H\text{-}H}$ = 6.8 Hz, $^{5}J_{H\text{-}H}$ = 2.4 Hz, 2H), 4.03 (t, $^{3}J_{H\text{-}H}$ = 2.0 Hz, 2H), 4.51 (t, $^{5}J_{H\text{-}H}$ = 2.0 Hz, 2H), 4.78 (dt, $^{4}J_{H\text{-}H}$ = 6.8 Hz, $^{5}J_{H\text{-}H}$ = 2.4 Hz, 2H), 5.15 (quint., $J_{H\text{-}H}$ = 7.0 Hz, 1H), 7.31 (d, $^{3}J_{H\text{-}H}$ = 8.3 Hz, 2H), 7.39 (dd, $^{3}J_{H\text{-}H}$ = 8.1 Hz, $^{4}J_{H\text{-}H}$ = 1.0 Hz, 1H), 7.47 (dt, $^{3}J_{H\text{-}H}$ = 7.8 Hz, $^{4}J_{H\text{-}H}$ = 1.3 Hz, 1H), 7.59 (dt, $^{3}J_{H\text{-}H}$ = 7.8 Hz, $^{4}J_{H\text{-}H}$ = 1.5 Hz, 1H), 7.66-7.70 (m, 3H). **^{13}C NMR (100 MHz, $CDCl_3$) δ (ppm):** 21.6, 41.2, 56.7, 67.1, 75.8, 79.5, 82.3, 86.9, 115.2, 116.0, 128.2, 129.1, 129.7, 131.1, 133.2, 133.8, 135.1, 141.1, 144.5, 209.4. **HRMS** calcd. for $[C_{22}H_{20}N_2O_3S + Na]^+$: 415.1087. Found: 415.1095.

7.4.1.19. Synthesis of 37c

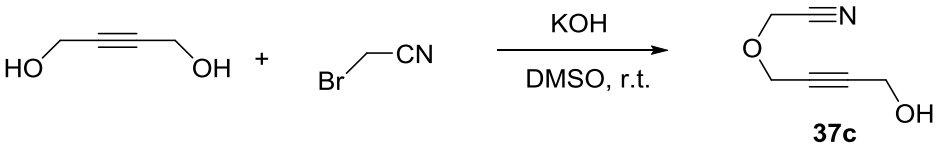

37c

In a 100 mL two-necked round bottom flask, a mixture of potassium hydroxide (4.02 g, 71.64 mmol) and 2-butyne-1,4-diol (6.20 g, 72.02 mmol) in DMSO (60 mL) was stirred at room temperature. 2-Bromoacetonitrile (1.0 mL, 14.33 mmol) was then added dropwise and the resulting mixture was stirred for 2 h (TLC monitoring). Water (20 mL) was added and the mixture was extracted with dichloromethane (3 x 40 mL). The aqueous phase was then acidified with aqueous HCl 3N (10 mL) and further extracted with dichloromethane (3 x 40 mL). The combined organic phases were washed with H_2O (3 x 30 mL), dried over anhydrous Na_2SO_4 and evaporated under reduced pressure. The residue was purified by column chromatography using a mixture of hexane:ethyl acetate (60:40) as the eluent to give compound **37c** (0.86 g, 47 % yield) as a colourless oil. **MW:** 125.13 g/mol; **^{1}H NMR (400 MHz, $CDCl_3$) δ (ppm):** 2.41 (t, $^{3}J_{H\text{-}H}$ = 5.4 Hz, 1H), 4.31-4.35 (m, 2H), 4.37 (t, $^{5}J_{H\text{-}H}$ = 1.8 Hz, 2H), 4.38 (s, 2H).

7.4.1.20. Synthesis of 28ca

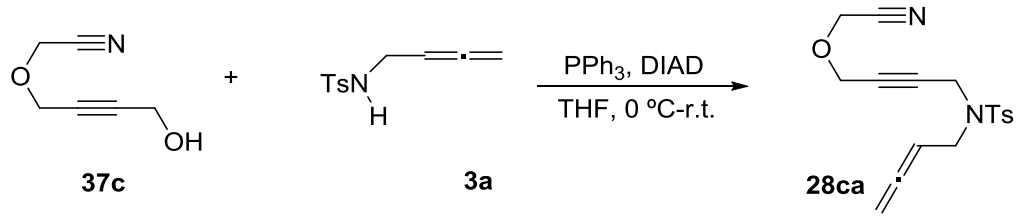

37c **3a** **28ca**

In a 50 mL two-necked round bottom flask, a mixture of 2-(4-hydroxybut-2-ynyloxy)acetonitrile **37c** (0.20 g, 1.60 mmols), *N*-tosylbuta-2,3-dien-1-amine **3a** (0.36 g, 1.60 mmols) and triphenylphosphine (1.05 g, 4.00 mmols) in anhydrous and degassed tetrahydrofuran (30 mL) was stirred and cooled to 0˚C in an ice-water bath. Diisopropyl azodicarboxylate (0.8 mL, 4.06 mmols) was added dropwise to this solution and the resulting mixture was stirred at room temperature for 20 h (TLC monitoring). The solvent was removed under reduced pressure and the reaction crude was purified by column chromatography using a mixture of hexane:ethyl acetate (90:10) as the eluent to afford product **28ca** (0.38 g, 72 % yield) as a yellow oil. **MW:** 330.40 g/mol; **IR (ATR) ν (cm^{-1}):** 1343, 1158, 1088. **^{1}H NMR (400 MHz, $CDCl_3$) δ (ppm):** 2.44 (s, 3H), 3.86 (dt, $^{3}J_{H\text{-}H}$ = 7.2 Hz, $^{5}J_{H\text{-}H}$ = 2.5 Hz , 2H), 4.08 (t, $^{5}J_{H\text{-}H}$ = 1.8 Hz, 2H), 4.14 (s, 2H), 4.20 (t, $^{5}J_{H\text{-}H}$ = 1.8 Hz, 2H), 4.80 (dt, $^{4}J_{H\text{-}H}$ = 6.8 Hz, $^{5}J_{H\text{-}H}$ = 2.5 Hz, 2H), 5.05 (dq, $^{3}J_{H\text{-}H}$ = 7.2 Hz, $^{4}J_{H\text{-}H}$ = 6.8 Hz, 1H), 7.34 (d, $^{3}J_{H\text{-}H}$ = 8.4 Hz, 2H), 7.73 (d, $^{3}J_{H\text{-}H}$ = 8.4 Hz, 2H). **^{13}C NMR (100 MHz, $CDCl_3$) δ (ppm):** 21.7, 36.0, 46.0, 53.8, 57.9, 76.6, 78.7, 81.8, 85.4, 115.2, 127.7, 129.6, 136.0, 143.9,

209.8. **GS-MS (m/z):** 330.1 $[M]^+$. **HRMS** calcd. for $[C_{17}H_{18}N_2O_3S + Na]^+$: 353.0930. Found: 353.0938.

7.4.1.21. Synthesis of tert-butyl prop-2-yn-1-yl(tosyl)carbamate 43

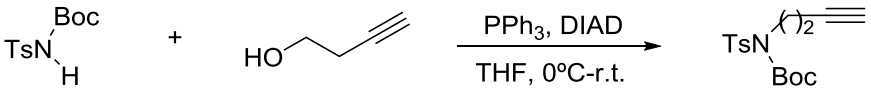

42 **43**

In a 100 mL two-necked round bottom flask, a mixture of but-3-yn-1-ol (0.56 mL, 3.68 mmols), *tert*-butyl tosylcarbamate **42** (2.0 g, 3.68 mmols) and triphenylphosphine (2.50 g, 9.20 mmols) in anhydrous and degassed tetrahydrofuran (50 mL) was stirred and cooled to 0˚C in an ice-water bath. Diisopropyl azodicarboxylate (2.0 mL, 9.20 mmols) was added dropwise to this solution and the resulting mixture was stirred at room temperature for 20h (TLC monitoring). The solvent was removed under reduced pressure and the reaction crude was purified by column chromatography using a mixture of hexane:ethyl acetate (90:10) as the eluent to afford product **43** (0.88 g, 77 % yield) as colourless solid. **MW:** 309.38 g/mol; **^{1}H NMR (400 MHz, $CDCl_3$) δ (ppm):** 1.35 (s, 9H), 2.02 (t, $^4J_{H\text{-}H}$ = 2.7 Hz ,1H), 2.45 (s, 3H), 2.66 (dt, $^3J_{H\text{-}H}$ = 7.2 Hz, $^5J_{H\text{-}H}$ = 2.4 Hz , 2H), 4.01 (t, $^3J_{H\text{-}H}$ = 7.2 Hz, 2H), 7.32 (d, $^3J_{H\text{-}H}$ = 8.4 Hz, 2H), 7.80 (d, $^3J_{H\text{-}H}$ = 8.4 Hz, 2H).

7.4.1.22. Synthesis of 4-methyl-N-(prop-2-yn-1-yl)benzenesulfonamide 44

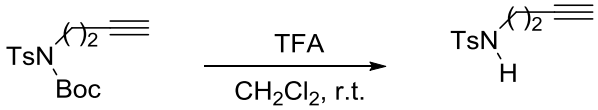

43 **44**

In a 100 mL two-necked round bottom flask, a mixture of *tert*-butyl prop-2-yn-1-yl(tosyl)carbamate **43** (0.92 g, 2.84 mmols) and trifluoroacetic acid (4.35 mL, 56.80 mmols) in dichloromethane (40 mL) was stirred at room temperature for 2 h (TLC monitoring). The solvent was removed under reduced pressure and solution of sodium bicarbonate (15 mL) was the reaction crude. The mixture was extracted with dichloromethane (3 x 20 mL). The combined organic phases were washed with H_2O (3 x 10 mL), dried over anhydrous Na_2SO_4 and evaporated under reduced pressure. The residue was purified by column chromatography was purified by column chromatography using a mixture of hexane:ethyl acetate (60:40) as the eluent to afford product **43** (0.56 g, 89 % yield) as colourless solid. **MW:** 309.38 g/mol; **^{1}H NMR (400 MHz, $CDCl_3$) δ (ppm):** 2.01 (t, $^4J_{H\text{-}H}$ = 2.7 Hz ,1H), 2.35 (dt, $^3J_{H\text{-}H}$ = 6.6 Hz, $^5J_{H\text{-}H}$ = 2.4 Hz , 2H), 2.44 (s, 3H), 3.12 (q, $^3J_{H\text{-}H}$ = 6.6 Hz, 2H), 4.75 (t, $^3J_{H\text{-}H}$ = 7.6 Hz , 1H), 7.32 (d, $^3J_{H\text{-}H}$ = 8.4 Hz, 2H), 7.75 (d, $^3J_{H\text{-}H}$ = 8.4 Hz, 2H).

7.4.1.23. Synthesis of 45

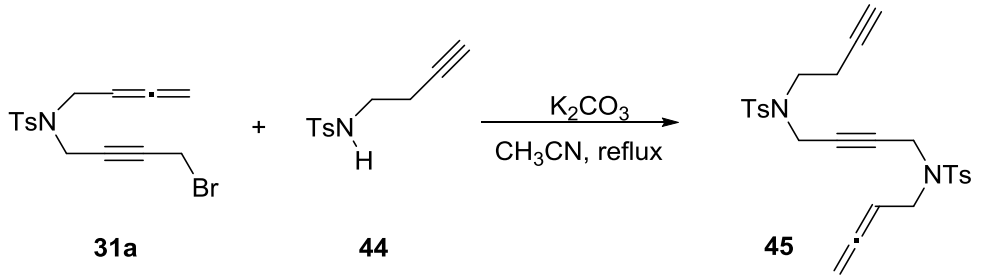

31a **44** **45**

In a 50 mL two-necked round bottom flask, a mixture of bromo derivative **31a** (0.10 g, 0.27 mmols), *N*-but-3-ynyl-4-methylbenzenesulfonamide **44** (0.06 g, 0.28 mmols) and potassium carbonate (0.19 g, 1.37 mmols) in acetonitrile (30 mL) was heated at reflux. The mixture was stirred for 3 h until completion (TLC monitoring). The salts were filtered off and the solvent was removed under reduced pressure. The reaction crude was purified by column chromatography using a mixture of hexane:ethyl acetate (80:20) as the eluent to give compound **45** (0.13 g, 93 % yield) as a colourless solid. **MW:** 496.64 g/mol; **m.p.:** 86-88˚C; **IR (ATR) ν (cm^{-1}):** 1327, 1156, 1090. **^{1}H NMR (400 MHz, $CDCl_3$) δ (ppm):** 2.01 (t, $^{4}J_{H\text{-}H}$ = 2.7 Hz, 1H), 2.40 (dt, $^{4}J_{H\text{-}H}$ = 2.7 Hz, $^{3}J_{H\text{-}H}$ = 7.2 Hz, 2H), 2.40 (s, 3H), 2.44 (s, 3H), 3.17 (t, $^{3}J_{H\text{-}H}$ = 7.2 Hz, 2H), 3.66 (dt, $^{3}J_{H\text{-}H}$ = 7.0 Hz, $^{5}J_{H\text{-}H}$ = 2.5 Hz, 2H), 3.94-3.98 (m 4H), 4.74 (dt, $^{4}J_{H\text{-}H}$ = 7.0 Hz, $^{5}J_{H\text{-}H}$ = 2.5 Hz, 2H), 4.91 (quint., $J_{H\text{-}H}$ = 7.0 Hz, 1H), 7.28-7.32 (m, 4H), 7.62-7.67 (m, 4H). **^{13}C NMR (75 MHz, $CDCl_3$) δ (ppm):** 18.9, 21.6, 35.9, 37.3, 45.3, 45.6, 70.5, 78.4, 78.5, 80.6, 85.2, 127.5, 127.6, 129.6, 129.7, 135.8, 136.0, 143.8, 143.9, 209.6. **ESI-MS (m/z):** 497.1 $[M + H]^+$. **AE:** calcd. for $[C_{26}H_{28}N_2O_4S_2.1.5H_2O]$: C, 59.63; H, 5.97; N, 5.35. Found: C, 60.03; H, 5.41; N, 5.38.

7.4.1.24. Synthesis of 47

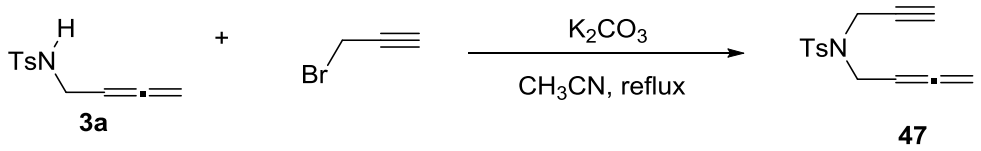

3a **47**

In a 50 mL two-necked round bottom flask, a mixture of *N*-(buta-2,3-dien-1-yl)-4-methylbenzenesulfonamide **3a** (0.50 g, 1.81 mmols), propargyl bromide (0.16 mL, 1.81 mmols) and potassium carbonate (1.25 g, 9.05 mmols) in acetonitrile (30 mL) was heated at reflux. The mixture was stirred for 6 h until completion (TLC monitoring). The salts were filtered off and the solvent was removed under reduced pressure. The reaction crude was purified by column chromatography using a mixture of hexane:ethyl acetate (80:20) as the eluent to give compound **47** (0.43 g, 91 % yield) as a colourless solid. **MW:** 261.34 g/mol; **^{1}H NMR (300 MHz, $CDCl_3$) δ (ppm):** 2.04 (t, $^{4}J_{H\text{-}H}$ = 2.7 Hz, 1H), 2.44 (s, 3H), 3.89 (dt, $^{3}J_{H\text{-}H}$ = 4.8 Hz, $^{5}J_{H\text{-}H}$ = 2.4 Hz, 2H), 4.17 (d, $^{4}J_{H\text{-}H}$ = 2.7 Hz, 2H), 4.80 (dt, $^{4}J_{H\text{-}H}$ = 4.8 Hz, $^{5}J_{H\text{-}H}$ = 2.4 Hz, 2H), 4.91 (quint., $^{3}J_{H\text{-}H}$ = 4.8 Hz, 1H), 7.31 (d, $^{3}J_{H\text{-}H}$ = 8.4 Hz, 2H), 7.75 (d, $^{3}J_{H\text{-}H}$ = 8.4 Hz, 2H).

7.4.2. Rh(I)-catalysed [2+2+2] cycloaddition reaction of cyano-yne-allene

7.4.2.1. General procedure for $[Rh(cod)_2]BF_4$-catalysed [2+2+2] cycloaddition reaction of cyano-yne-allene 27aa described in Table 5.1 (Chapter 5)

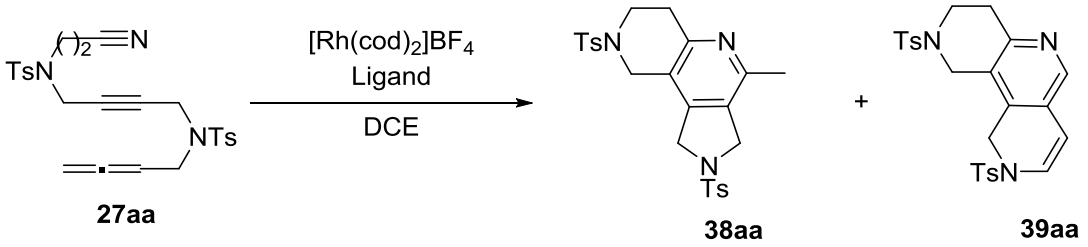

27aa **38aa** **39aa**

In a 10 mL flask, a mixture of the indicated biphosphine (0.010 mmol) and rhodium complex $[Rh(cod)_2]BF_4$ (4.06 mg, 0.010 mmol) was dissolved in dichloromethane (3 mL) under nitrogen. Hydrogen gas was introduced to the catalyst solution and stirred for 30 minutes. The resulting mixture was then concentrated to dryness. 1,2-dichloroethane (5 mL) was added and the solution was stirred under N_2 atmosphere. Compound **27aa** (0.050 mg, 0.100 mmol) in 1,2-dichloroethane (3 mL) was then added and the reaction was stirred for the indicated time at the stated temperature (TLC monitoring). The solvent was removed and the crude was purified by column chromatography using mixtures of hexane:ethyl acetate (60:40) as the eluent to give mixture of products **38aa** and **39aa** (the product ratio was determined by ^{1}H NMR) as a yellow oil.

Specific data for the reactions listed in Table 5.1 (Chapter 5):

Entry	Biphosphine	Reaction temp. (^{0}C)	Reaction time (h)	Isolated **38aa**+**39aa** (g)	Combined yield of **38aa**+**39aa** **(%)**	**38aa**:**39aa** ratio
1	*Tol*-binap (6.80 mg)	reflux	2	0.023	46	2:1
2	*Tol*-binap (6.80 mg)	reflux	3	0.024	48	2:1
3	(*R*)-H_8-binap (6.30 mg)	reflux	2	0.017	34	3:1
4	(*R*)-binap (6.30 mg)	reflux	5	0.015	30	2:1
5	(*R*)-binap (6.30 mg)	80	0.5	0.005	10	2:1
6	Segphos (6.10 mg)	reflux	24	n.r.	-	-

7.4.2.2. General procedures for $[RhCl(PPh_3)_3]$-catalysed [2+2+2] cycloaddition reaction of cyano-yne-allene 27aa

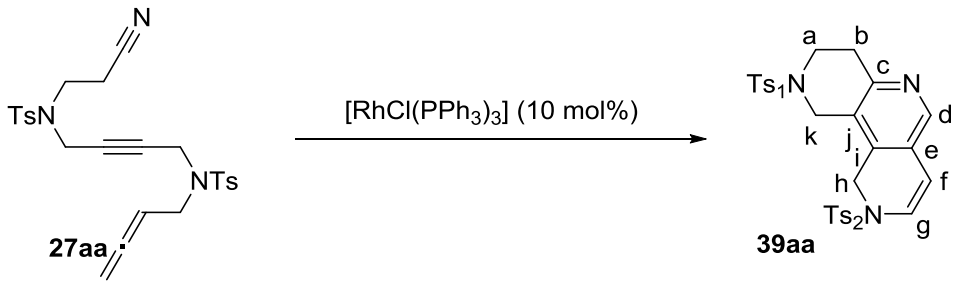

Conventional heating (entry 1, Table 5.2, Chapter 5): A mixture of chlorotris(triphenylphosphine)rhodium(I) (9.3 mg, 0.010 mmol), cyano-yne-allene derivative **27aa** (50 mg, 0.100 mmol) was dissolved in toluene (5 mL) under N_2 and heated at reflux for 4h (TLC monitoring). Upon completion, the solvent was evaporated under reduced pressure and the residue was purified by column chromatography using a mixture of hexane:ethyl acetate (40:60) as the eluent to give compound **39aa** (22 mg, 44 % yield) as a colourless solid (Entry 1).

Microwave heating (entries 2-15, Table 5.2, Chapter 5): A mixture of chlorotris(triphenylphosphine)rhodium(I) (9.3 mg, 0.010 mmol), cyano-yne-allene derivative **27aa** (50 mg, 0.100 mmol) and the additive if appropriate were dissolved in the indicated solvent (2 mL (or 5 mL for entry 4)) under N_2 and heated in a sealed 10 mL septum-containing, screw-capped vial for the stated time at the indicated temperature under microwave irradiation (TLC monitoring). Upon completion, the solvent was evaporated under reduced pressure and the residue was purified by column chromatography using a mixture of hexane:ethyl acetate (40:60) as the eluent to give compound **39aa** as a colourless solid.

Specific data for the reactions listed in Table 5.2 (entries 2-15) (Chapter 5):

Entry	Solvent[a]	Reaction temp. (^{0}C)	Reaction time (h)	Additive	Isolated **39aa** (g)	Yield of **39aa (%)**
2	Toluene	90	45	-	0.015	30
3	MCB	120	30	-	0.025	50
4	MCB	120	30	-	0.020	40
5	DCB	140	30	-	0.020	40
6	DMF:H_2O (1:1)	90	30	-	n.r.	-
7	MCB	120	30	TFA (8 µL, 0.10 mmol)	0.015	30
8	MCB	120	10	Et_3N (14 µL, 0.10 mmol)	0.026	54
9	MCB	80	10	Et_3N (14 µL, 0.10 mmol)	0.023	46
10	MCB	120	10	Et_3N (1 µL, 0.010 mmol)	0.032	64
11	MCB	120	10	Et_3N (0.5 µL, 0.005 mmol)	0.033	66
12	MCB	120	20	Cy_2NH (2 µL, 0.010 mmol)	0.020	40

13	MCB	120	30	Quinuclidine (0.5 µL, 0.005 mmol)	0.020	41
14	MCB	120	10	Hünig's base (0.8 µL, 0.005 mmol)	0.024	49
15	MCB	120	40	2,6-di-*tert*-butylpyridine (11 µL, 0.010 mmol)	0.017	33

[a]MCB = chlorobenzene / DCB = 1,2-dichlorobenzene

7.4.2.3. Synthesis of compound 39aa

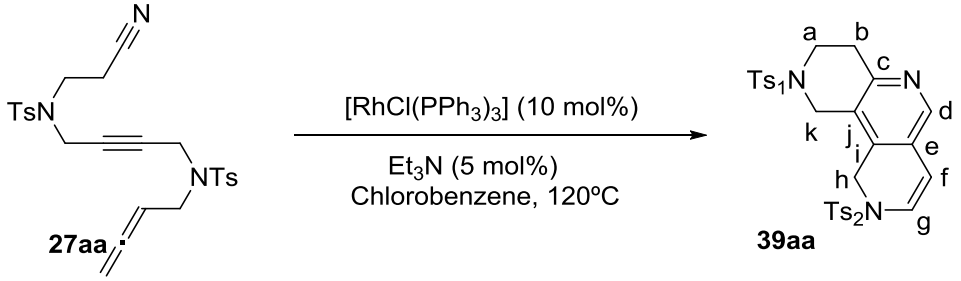

A degassed solution of chlorotris(triphenylphosphine)rhodium(I) (9.3 mg, 0.010 mmol), cyano-yne-allene derivative **27aa** (0.050 g, 0.100 mmol) and triethylamine (0.0007 mL, 0.005 mmol) in chlorobenzene (2 mL) was heated in a sealed 10 mL septum-containing, screw-capped vial for 10 min. at 120˚C under microwave irradiation (TLC monitoring). Upon completion, the solvent was evaporated under reduced pressure and the residue was purified by column chromatography using a mixture of hexane:ethyl acetate (40:60) as the eluent to give compound **39aa** (33 mg, 66 % yield) as a colourless solid. **MW:** 495.61 g/mol; **IR (ATR) ν (cm^{-1}):** 2918, 1436, 1338, 1158. **^{1}H NMR (300 MHz, $CDCl_3$) δ(ppm):** 2.43 (s, 3H, Ts_2), 2.47 (s, 3H, Ts_1), 3.01 (t, $^3J_{H\text{-}H}$ = 5.8 Hz, 2Hb), 3.39 (t, $^3J_{H\text{-}H}$ = 5.8 Hz, 2Ha), 4.11 (s, 2Hk), 4.50 (s, 2Hh), 5.79 (d, $^3J_{H\text{-}H}$ = 8.0 Hz, 1Hf), 6.83 (d, $^3J_{H\text{-}H}$ = 8.0 Hz, 1Hg), 7.33 (d, $^3J_{H\text{-}H}$ = 8.3 Hz, 2HTs_2), 7.39 (d, $^3J_{H\text{-}H}$ = 8.0 Hz, 2HTs_1), 7.73 (d, $^3J_{H\text{-}H}$ = 8.3 Hz, 2HTs_2), 7.76 (d, $^3J_{H\text{-}H}$ = 8.0 Hz, 2HTs_1), 8.00 (s, 1Hd). **^{13}C NMR (75 MHz, $CDCl_3$) δ (ppm):** 21.5 (CH_3-Ts), 21.6 (CH_3-Ts), 32.1 (Cb), 42.6 (Ch), 43.2 (Ca), 44.0 (Ck), 105.7 (Cf), 122.9 (Cj), 124.0 (Ce), 127.1 (Ts), 127.5 (Cg), 127.7 (Ts), 130.0 (Ts), 130.1 (Ts), 132.6 (Ci), 133.0 (Ts), 133.9 (Ts), 143.4 (Cd), 144.2 (Ts), 144.8 (Ts), 152.5 (Cc). **ESI-MS (m/z):** 496.1 $[M+ H]^+$. **HRMS** calcd. for $[C_{25}H_{25}N_3O_4S_2 + Na]^+$: 518.1179. Found: 518.1183.

7.4.2.4. Synthesis of compound 39ba

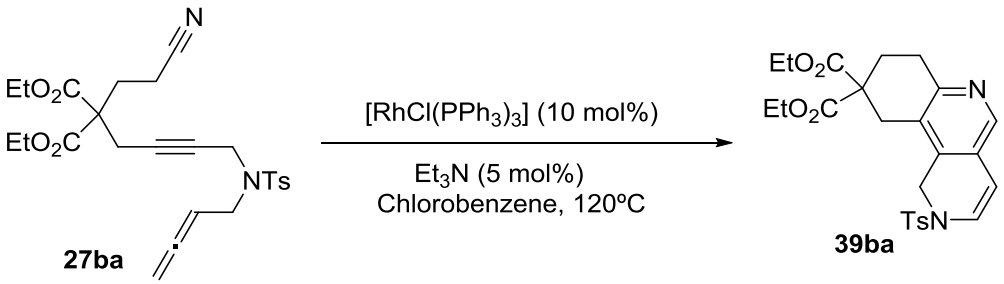

A degassed solution of chlorotris(triphenylphosphine)rhodium(I) (9.3 mg, 0.010 mmol), cyano-yne-allene derivative **27ba** (0.050 g, 0.103 mmol) and triethylamine (0.0007 mL, 0.005 mmol)

in chlorobenzene (2 mL) was heated in a sealed 10 mL septum-containing, screw-capped vial for 40 min. at 120˚C under microwave irradiation (TLC monitoring). Upon completion, the solvent was evaporated under reduced pressure and the residue was purified by column chromatography using a mixture of hexane:ethyl acetate (40:60) as the eluent to give compound **39ba** as a yellow oil (25 mg, 51 % yield). **MW:** 484.61 g/mol; **IR (ATR) ν (cm^{-1}):** 2922, 1725, 1350, 1161; **^{1}H NMR (300 MHz, $CDCl_3$) δ(ppm):** 1.27 (t, $^3J_{H-H}$ = 7.2 Hz, 6H), 2.36 (t, $^3J_{H-H}$ = 6.8 Hz, 2H), 2.41 (s, 3H), 2.89 (t, $^3J_{H-H}$ = 6.8 Hz, 2H), 3.04 (s, 2H), 4.15-4.28 (m, 4H), 4.64 (s, 2H), 5.77 (d, $^3J_{H-H}$ = 7.8 Hz, 1H), 6.80 (d, $^3J_{H-H}$ = 7.8 Hz, 1H), 7.32 (d, $^3J_{H-H}$ = 8.4 Hz, 4H), 7.70 (d, $^3J_{H-H}$ = 8.4 Hz, 4H), 7.97 (s, 1H). **^{13}C NMR (75 MHz, $CDCl_3$) δ (ppm):**14.0, 14.1, 21.6, 34.0, 38.7, 43.3, 53.0, 61.9, 106.1, 120.2, 127.0, 127.2, 129.7, 130.0, 134.1, 142.1, 144.5, 154.1, 162.2, 170.7. **ESI-MS (m/z):** 485.1 [M+ H]$^+$. **HRMS** calcd. for $[C_{25}H_{28}N_2O_6S + H]^+$: 485.1741. Found: 485.1747.

7.4.2.5. Synthesis of compound 39bb

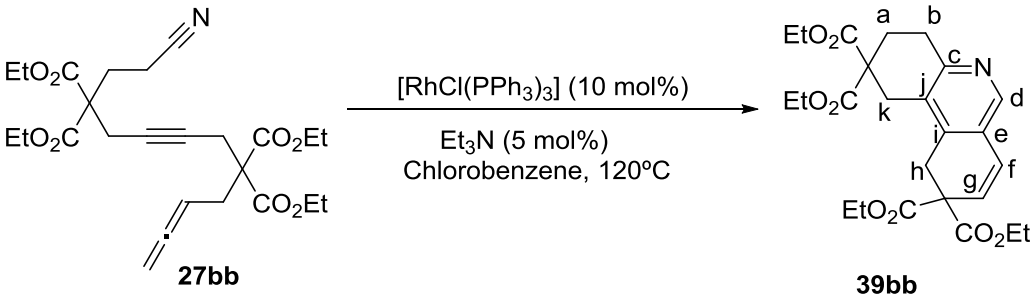

27bb **39bb**

A degassed solution of chlorotris(triphenylphosphine)rhodium(I) (9.3 mg, 0.010 mmol), cyano-yne-allene derivative **27aa** (0.050 g, 0.106 mmol) and triethylamine (0.0007 mL, 0.005 mmol) in chlorobenzene (2 mL) was heated in a sealed 10 mL septum-containing, screw-capped vial for 25 min. at 120˚C under microwave irradiation (TLC monitoring). Upon completion, the solvent was evaporated under reduced pressure and the residue was purified by column chromatography using a mixture of hexane:ethyl acetate (40:60) as the eluent to give compound **39bb** as a yellow oil (24 mg, 49 % yield). **MW:** 473.52 g/mol; **IR (ATR) ν (cm^{-1}):** 2917, 2247, 1726, 1444, 1187, 1026. **^{1}H NMR (400 MHz, $CDCl_3$) δ(ppm):** 1.23-1.27 (m, 12H, CH_3CH_2O), 2.40 (t, $^3J_{H-H}$ = 6.8 Hz, 2Ha), 2.93 (t, $^3J_{H-H}$ = 6.8 Hz, 2Hb), 3.25 (s, 2Hk,h), 3.35 (s, 2Hk,h), 4.16-4.25 (m, 8H, CH_3CH_2O), 6.21 (d, $^3J_{H-H}$ = 9.4 Hz, 1Hf,g), 6.60 (d, $^3J_{H-H}$ = 9.4 Hz, 1Hf,g), 8.10 (s, 1Hd). **^{13}C NMR (75 MHz, $CDCl_3$) δ (ppm):** 13.9, 14.0, 14.1, 14.2, 27.3 (Cb), 29.3 (Ch), 29.5 (Ca,k), 30.9 (Ca,k), 53.3, 54.5, 61.7, 62.1, 124.9 (Ci), 125.1 (Cf), 126.4 (Ce), 126.1 (Cg), 139.4 (Cj), 144.8 (Cd), 155.0 (Cc), 169.8 (C=O), 171.0 (C=O). **HRMS** calcd. for $[C_{25}H_{31}NO_8 + H]^+$: 474.2122 Found: 474.2123.

7.4.2.6. Synthesis of compound 40aa

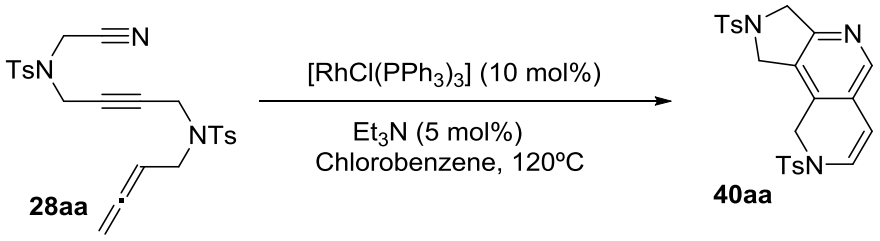

A degassed solution of chlorotris(triphenylphosphine)rhodium(I) (9.3 mg, 0.010 mmol), cyano-yne-allene derivative **27aa** (0.050 g, 0.104 mmol) and triethylamine (0.0007 mL, 0.005 mmol) in chlorobenzene (2 mL) was heated in a sealed 10 mL septum-containing, screw-capped vial for 10 min. at 120˚C under microwave irradiation (TLC monitoring). Upon completion, the solvent was evaporated under reduced pressure and the residue was purified by column chromatography using a mixture of hexane:ethyl acetate (40:60) as the eluent to give compound **40aa** as a yellow oil (28 mg, 57 % yield). **MW:** 481.59 g/mol; **IR (ATR) ν (cm^{-1}):** 2920, 1594, 1342, 1161; **^{1}H NMR (300 MHz, $CDCl_3$) δ(ppm):** 2.43 (s, 3H), 2.44 (s, 3H), 4.46 (s, 2H), 4.50 (s, 2H), 4.54 (s, 2H), 5.78 (d, $^{3}J_{H\text{-}H}$ = 7.8 Hz, 1H), 6.84 (d, $^{3}J_{H\text{-}H}$ = 7.8 Hz, 1H), 7.31-7.39 (m, 4H), 7.69 (d, $^{3}J_{H\text{-}H}$ = 8.4 Hz, 2H), 7.79 (d, $^{3}J_{H\text{-}H}$ = 8.1 Hz, 2H), 8.01 (s, 1H). **^{13}C NMR (75 MHz, $CDCl_3$) δ (ppm):** 21.5, 43.5, 50.4, 53.6, 105.1, 125.2, 125.9, 127.2, 127.6, 128.0, 130.0, 130.1, 130.8, 133.2, 133.7, 144.2, 144.8, 144.9, 156.1. **ESI-MS (m/z):** 482.1 $[M+ H]^+$. **HRMS** calcd. for $[C_{24}H_{23}N_3O_4S_2 + Na]^+$: 482.1203. Found: 482.1220.

7.4.2.7. Synthesis of compound 39ac

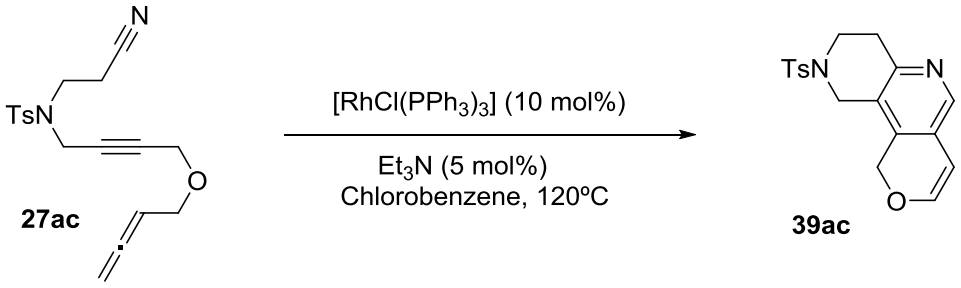

A degassed solution of chlorotris(triphenylphosphine)rhodium(I) (9.3 mg, 0.010 mmol), cyano-yne-allene derivative **27aa** (0.050 g, 0.146 mmol) and triethylamine (0.0007 mL, 0.005 mmol) in chlorobenzene (2 mL) was heated in a sealed 10 mL septum-containing, screw-capped vial for 20 min. at 120˚C under microwave irradiation (TLC monitoring). Upon completion, the solvent was evaporated under reduced pressure and the residue was purified by column chromatography using a mixture of hexane:ethyl acetate (40:60) as the eluent to give compound **39ac** as a yellow oil (20 mg, 40 % yield). **MW:** 342.41 g/mol; **IR (ATR) ν (cm^{-1}):** 2921, 1331, 1155. **^{1}H NMR (300 MHz, $CDCl_3$) δ(ppm):** 2.44 (s, 3H), 3.04 (t, $^{3}J_{H\text{-}H}$ = 6.0 Hz, 2H), 3.42 (t, $^{3}J_{H\text{-}H}$ = 6.0 Hz, 2H), 4.11 (s, 2H), 5.00 (s, 2H), 5.75 (d, $^{3}J_{H\text{-}H}$ = 5.7 Hz, 1H), 6.83 (d, $^{3}J_{H\text{-}H}$ = 5.7 Hz, 1H), 7.36 (dd, $^{3}J_{H\text{-}H}$ = 8.1 Hz, 2H), 7.73 (d, $^{3}J_{H\text{-}H}$ = 8.1 Hz, 2H), 8.02 (s, 1H). **^{13}C NMR (75 MHz, $CDCl_3$) δ (ppm):** 21.6, 32.2, 43.4, 43.9, 63.1, 101.5, 121.7, 123.7 127.7, 129.9, 132.7, 132.9,

142.1, 144.1, 146.8, 151.9. **ESI-MS (m/z):** 343.1 $[M + H]^+$. **HRMS** calcd. for $[C_{18}H_{18}N_2O_3S + H]^+$: 343.1111. Found: 343.1106.

7.4.2.8. Synthesis of compound 40ca

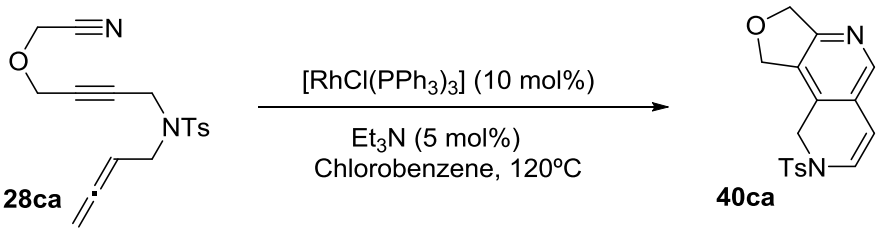

A degassed solution of chlorotris(triphenylphosphine)rhodium(I) (9.3 mg, 0.010 mmol), cyano-yne-allene derivative **27aa** (0.050 g, 0.152 mmol) and triethylamine (0.0007 mL, 0.005 mmol) in chlorobenzene (2 mL) was heated in a sealed 10 mL septum-containing, screw-capped vial for 40 min. at 120˚C under microwave irradiation (TLC monitoring). Upon completion, the solvent was evaporated under reduced pressure and the residue was purified by column chromatography using a mixture of hexane:ethyl acetate (40:60) as the eluent to give compound **40ca** as a colourless solid (19 mg, 38 % yield). **MW:** 328.38 g/mol; **m.p.:** 234-236^{0}C; **IR (ATR) ν (cm^{-1}):** 2921, 1570, 1346, 1160. **^{1}H NMR (300 MHz, $CDCl_3$) δ(ppm):** 2.42 (s, 3H), 4.50 (s, 2H), 4.98 (s, 2H), 5.05 (s, 2H), 5.85 (d, $^3J_{H\text{-}H}$ = 7.8 Hz, 1H), 6.84 (d, $^3J_{H\text{-}H}$ = 7.8 Hz, 1H), 7.33 (d, $^3J_{H\text{-}H}$ = 8.1 Hz, 2H), 7.70 (d, $^3J_{H\text{-}H}$ = 8.1 Hz, 2H), 8.06 (br s, 1H). **^{13}C NMR (75 MHz, $CDCl_3$) δ (ppm):** 21.6, 43.8, 70.5, 72.8, 105.7, 124.6, 127.1, 127.6, 128.2, 129.8, 130.1, 133.9, 144.7, 144.8, 160.0. **ESI-MS (m/z):** 329.1 $[M+ H]^+$. **AE:** calcd. for $[C_{17}H_{16}N_2O_3S]$: C, 62.18; H, 4.91; N,8.53. Found: C, 61.64; H, 4.92; N, 7.97.

7.4.2.9. Synthesis of compound 41aa

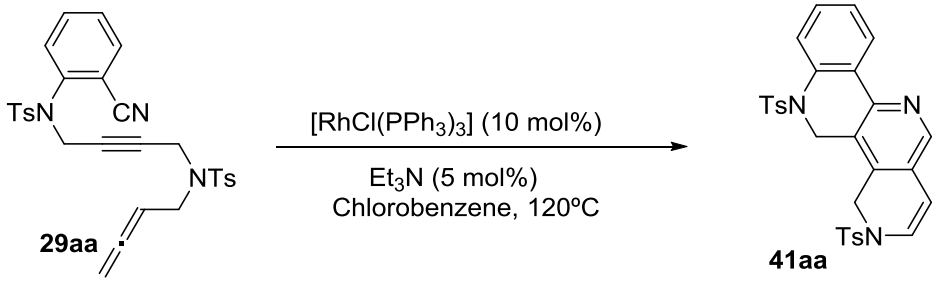

A degassed solution of chlorotris(triphenylphosphine)rhodium(I) (9.3 mg, 0.010 mmol), cyano-yne-allene derivative **27aa** (0.050 g, 0.092 mmol) and triethylamine (0.0007 mL, 0.005 mmol) in chlorobenzene (2 mL) was heated in a sealed 10 mL septum-containing, screw-capped vial for 20 min. at 120˚C under microwave irradiation (TLC monitoring). Upon completion, the solvent was evaporated under reduced pressure and the residue was purified by column chromatography using a mixture of hexane:ethyl acetate (40:60) as the eluent to give compound **41aa** as a yellow oil (27 mg, 54 % yield). **MW:** 543.66 g/mol; **IR (ATR) ν (cm^{-1}):** 2920, 2253, 1343, 1154, 1087. **^{1}H NMR (400 MHz, $CDCl_3$) δ(ppm):** 2.12 (s, 3H), 2.40 (s, 3H), 4.57 (s, 2H), 4.74 (s, 2H), 5.71 (d, $^3J_{H\text{-}H}$ = 7.8 Hz, 1H), 6.69 (d, $^3J_{H\text{-}H}$ = 7.8 Hz, 2H), 6.89-6.92 (m,3H), 7.36-7.46 (m, 4H), 7.46 (dt, $^3J_{H\text{-}H}$ = 1.5 Hz, $^4J_{H\text{-}H}$ = 7.5 Hz, 1H), 7.74 (dd, $^3J_{H\text{-}H}$ = 1.3 Hz, $^4J_{H\text{-}H}$ = 8.0 Hz, 1H),

7.83 (d, $^{3}J_{H\text{-}H}$ = 8.2 Hz, 2H), 7.88 (s, 1H), 8.04 (dd, $^{3}J_{H\text{-}H}$ = 1.5 Hz, $^{4}J_{H\text{-}H}$ = 7.5 Hz, 1H), **^{13}C NMR (100 MHz, $CDCl_3$) δ (ppm):** 21.3, 21.6, 42.7, 44.7, 104.8, 122.0, 125.0, 125.2, 126.7, 127.3, 127.6, 127.7, 128.9, 130.1, 130.3, 134.1, 134.7, 136.9, 143.5, 143.8, 144.9, 146.8, 148.4. **HRMS** calcd. for $[C_{29}H_{25}N_3O_4S_2 + H]^+$: 544.1359. Found: 544.1371.

7.4.2.10. Synthesis of compound 41ac

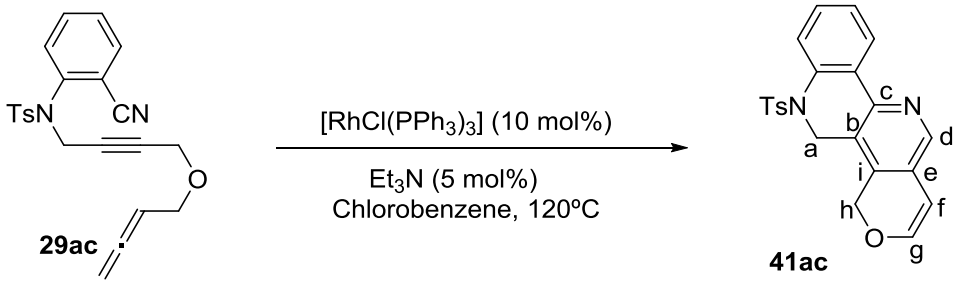

A degassed solution of chlorotris(triphenylphosphine)rhodium(I) (9.3 mg, 0.010 mmol), cyano-yne-allene derivative **27aa** (0.050 g, 0.128 mmol) and triethylamine (0.0007 mL, 0.005 mmol) in chlorobenzene (2 mL) was heated in a sealed 10 mL septum-containing, screw-capped vial for 20 min. at 120˚C under microwave irradiation (TLC monitoring). Upon completion, the solvent was evaporated under reduced pressure and the residue was purified by column chromatography using a mixture of hexane:ethyl acetate (40:60) as the eluent to give compound **41ac** as a yellow oil (26 mg, 52 % yield). **MW:** 390.46 g/mol; **IR (ATR) ν (cm^{-1}):** 2919, 1338, 1158, 1069. **^{1}H NMR (400 MHz, $CDCl_3$) δ(ppm):** 2.16 (s, 3H, Ts), 4.77 (s, 2Ha,h), 5.10 (s, 2Ha,h), 5.74 (d, $^{3}J_{H\text{-}H}$ = 5.6 Hz, 1Hf), 6.64 (d, $^{3}J_{H\text{-}H}$ = 5.6 Hz, 1Hg), 6.82 (d, $^{3}J_{H\text{-}H}$ = 8.7 Hz, 2H, Ts), 6.84 (d, $^{3}J_{H\text{-}H}$ = 8.7 Hz, 2H, Ts), 7.40 (dt, $^{3}J_{H\text{-}H}$ = 7.7 Hz, $^{4}J_{H\text{-}H}$ = 1.3 Hz, 1H, Ar), 7.46 (dt, $^{3}J_{H\text{-}H}$ = 8.0 Hz, $^{4}J_{H\text{-}H}$ = 1.7 Hz, 1H, Ar), 7.76 (dd, $^{3}J_{H\text{-}H}$ = 8.0 Hz, $^{4}J_{H\text{-}H}$ = 1.3 Hz 1H, Ar), 7.90 (s, 1Hd), 8.07 (dd, $^{3}J_{H\text{-}H}$ = 7.7 Hz, $^{4}J_{H\text{-}H}$ = 1.7 Hz, 1H, Ar). **^{13}C NMR (100 MHz, $CDCl_3$) δ (ppm):** 21.3 (Ts), 44.7 (Ca), 63.4 (Ch), 101.7 (Cf), 120.9 (Ce), 124.8 (Cg), 124.9 (Ci), 126.7 (Ts), 127.6 (Ar), 127.7 (Ar), 128.9 (Ts), 129.1 (Ar), 129.7 (Ar), 129.8 (Ts), 131.3 (Ar), 134.7 (Ar), 136.8 (Cb), 142.1 (Ts), 143.8 (Cd), 147.3 (Cc). **HRMS** calcd. for $[C_{22}H_{18}N_2O_3S + H]^+$: 391.1111. Found: 391.1106.

7.4.2.11. Procedures for the Rh(I)-catalysed [2+2+2] cycloaddition reaction of cyano-yne-allene 27aa described in Table 5.3 (Chapter 5)

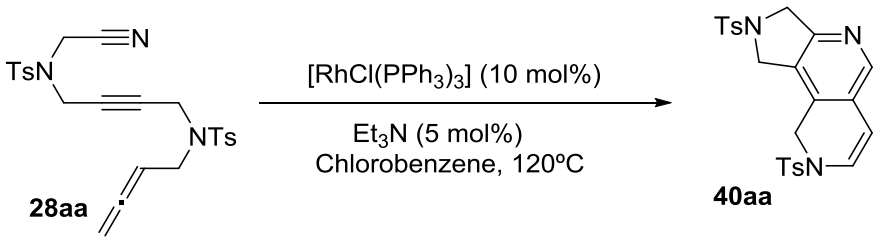

A degassed solution of chlorotris(triphenylphosphine)rhodium(I) (9.3 mg, 0.010 mmol), cyano-yne-allene derivative **28aa** (0.050 g, 0.104 mmol) and triethylamine (0.0007 mL, 0.005 mmol) in toluene (5 mL) was heated at reflux for 4 h (TLC monitoring). Upon completion, the solvent

was evaporated under reduced pressure and the residue was purified by column chromatography using a mixture of hexane:ethyl acetate (40:60) as the eluent to give compound **40aa** (14 mg, 28 % yield) as a colourless solid (Entry 1).

A degassed solution of chlorotris(triphenylphosphine)rhodium(I) (9.3 mg, 0.010 mmol), cyano-yne-allene derivative **28aa** (0.050 g, 0.104 mmols) and triethylamine (0.0007 mL, 0.005 mmol) in toluene (5 mL) was heated at reflux for 4 h (TLC monitoring). Upon completion, MnO_2 (26 mg, 0.300 mmol) was added to the reaction mixture and stirred for 1 h. The solvent was evaporated under reduced pressure and the residue was purified by column chromatography using a mixture of hexane:ethyl acetate (40:60) as the eluent to give compound **40aa** (15 mg, 30 % yield) as a colourless solid (Entry 2).

A degassed solution of chlorotris(triphenylphosphine)rhodium(I) (9.3 mg, 0.010 mmol), cyano-yne-allene derivative **28aa** (0.050 g, 0.104 mmols) in toluene (5 mL) was heated at reflux for 3 h (TLC monitoring). Upon completion, MnO_2 (26 mg, 0.300 mmol) was added to the reaction mixture and stirred for 1 h. The solvent was evaporated under reduced pressure and the residue was purified by column chromatography using a mixture of hexane:ethyl acetate (40:60) as the eluent to give compound **40aa** (12 mg, 24 % yield) as a colourless solid (Entry 3).

7.4.2.12. Synthesis of compound 46

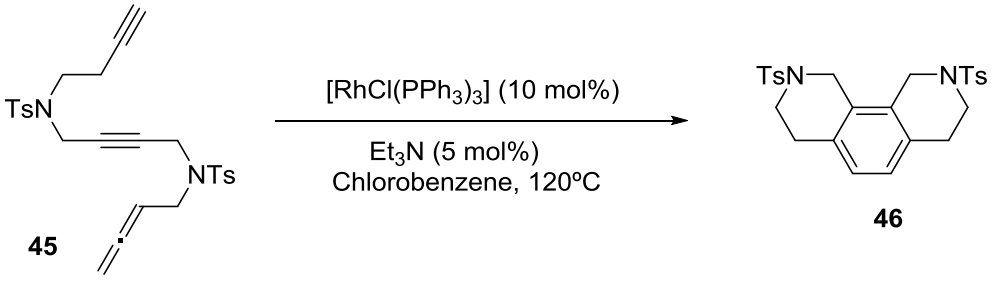

A degassed solution of chlorotris(triphenylphosphine)rhodium(I) (9.3 mg, 0.010 mmol), cyano-yne-allene derivative **27aa** (0.050 g, 0.104 mmol) and triethylamine (0.0007 mL, 0.005 mmol) in chlorobenzene (2 mL) was heated in a sealed 10 mL septum-containing, screw-capped vial for 40 min. at 120˚C under microwave irradiation (TLC monitoring). Upon completion, the solvent was evaporated under reduced pressure and the residue was purified by column chromatography using a mixture of hexane:ethyl acetate (40:60) as the eluent to give compound **46** as a colourless solid (45 mg, 90 % yield). **MW:** 496.64 g/mol; **m.p.:** 255-257^{0}C. **IR (ATR) ν (cm^{-1}):** 2920, 1336, 1158; **^{1}H NMR (400 MHz, $CDCl_3$) δ(ppm):** 2.43 (s, 6H, Ts), 2.88 (t, $^3J_{H\text{-}H}$ = 6.0 Hz, 4H), 3.31 (t, $^3J_{H\text{-}H}$ = 6.0 Hz, 4H), 4.04 (s, 4H), 6.90 (s, 2H), 7.38 (d, $^3J_{H\text{-}H}$ = 8.1 Hz, 4H), 7.75 (d, $^3J_{H\text{-}H}$ = 8.1 Hz, 4H). **^{13}C NMR (75 MHz, $CDCl_3$) δ (ppm):** 21.6, 29.1, 43.1, 44.5, 127.3, 127.7, 128.2, 129.9, 131.3, 133.2, 143.9. **ESI-MS (m/z):** 497.1 $[M+ H]^+$. **HRMS** calcd. for $[C_{26}H_{28}N_2O_4S + Na]^+$: 519.1383. Found: 519.1409.

7.4.2.13. Synthesis of the compound 27a

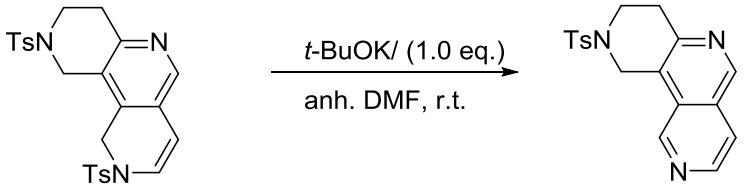

27aa **27a**

In 10mL 2-neck round bottom flask, to the mixture of potassium *tert*-butoxide (5 mg, 0.04 mmols) in anhydrous DMF (1 mL) was added a solution of **27aa** (20 mg, 0.04 mmols) in 1 mL of anhydrous DMF at 0˚C. The reaction was stirred for 10 min (TLC monitoring). The ethyl acetate (2 mL) was added to the reaction mixture and washed with water (3 × 2 mL). The organic layer was dried over Na_2SO_4 and concentrated in vacuum conditions. The reaction crude was purified by column chromatography using a mixture of hexane:ethyl acetate (20:80) as the eluent to give the product **27a** (11.8 mg, 87 % yield) as a yellow oil. **MW:** 339.41 g/mol; **^{1}H NMR (400 MHz, $CDCl_3$) δ (ppm):** 2.43 (s, 3H), 3.28 (t, $^3J_{H\text{-}H}$ = 5.6 Hz, 2H), 3.57 (t, $^3J_{H\text{-}H}$ = 5.6 Hz, 2H), 4.78 (s, 2H), 7.36 (d, $^3J_{H\text{-}H}$ = 8.0 Hz, 2H), 7.74 (d, $^3J_{H\text{-}H}$ = 5.6 Hz, 2H) 7.80 (d, $^3J_{H\text{-}H}$ = 8.0 Hz, 2H), 8.74 (d, $^3J_{H\text{-}H}$ = 5.6 Hz, 2H), 9.16 (s, 1H), 9.33 (s, 1H). **^{13}C NMR (100 MHz, $CDCl_3$) δ (ppm):** 21.6, 32.1, 43.5, 44.0, 119.7, 120.0, 127.2, 127.8, 130.0, 133.1, 144.2, 144.7, 146.6, 148.6, 150.9. **ESI-MS (m/z):** 340.1 $[M + H]^+$, **HRMS** calcd. for $[C_{18}H_{17}N_3O_2S + Na]^+$: 362.0925. Found: 362.0934.

Suplementary data

^{1}H NMR (300MHz, $CDCl_3$)

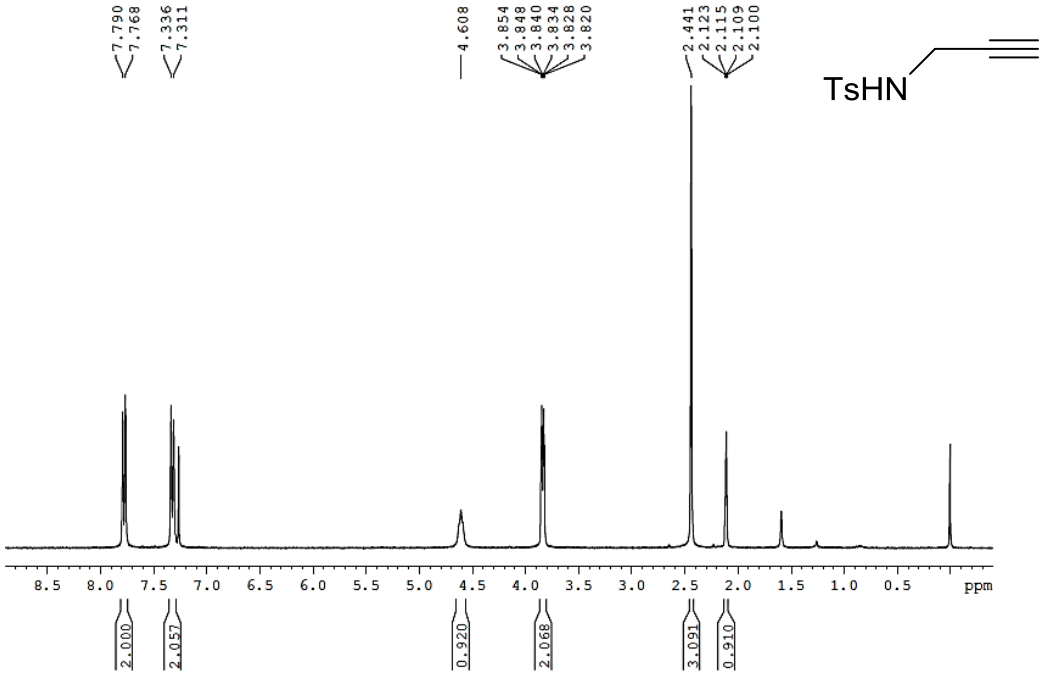

^{1}H NMR (300MHz, $CDCl_3$)

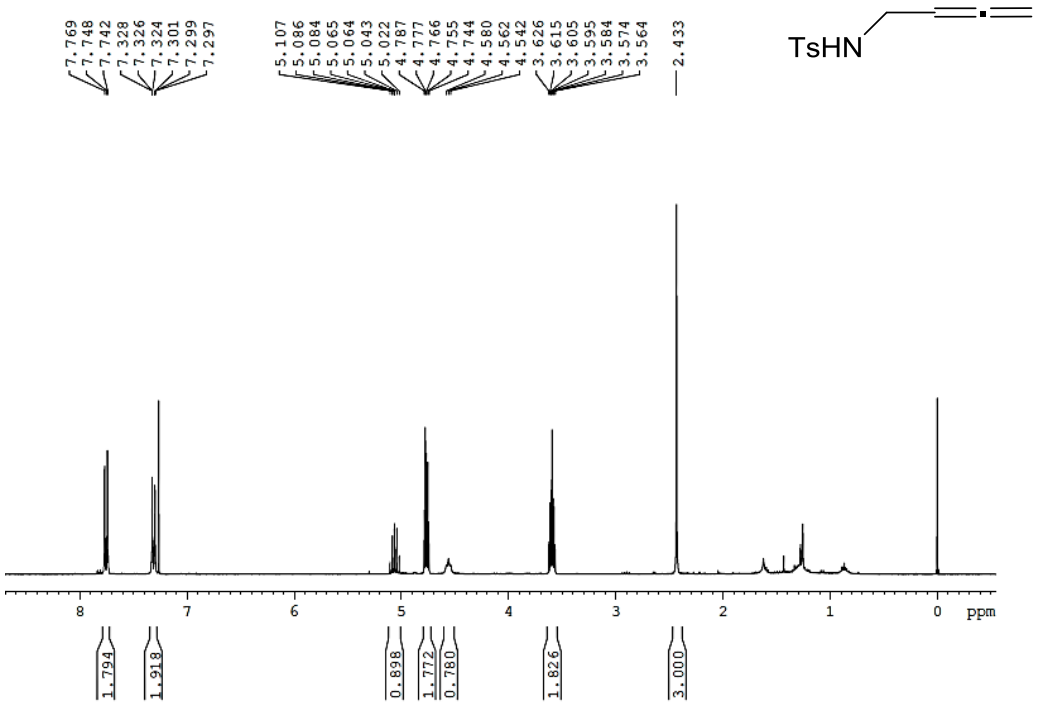

^{1}H NMR (300MHz, $CDCl_3$)

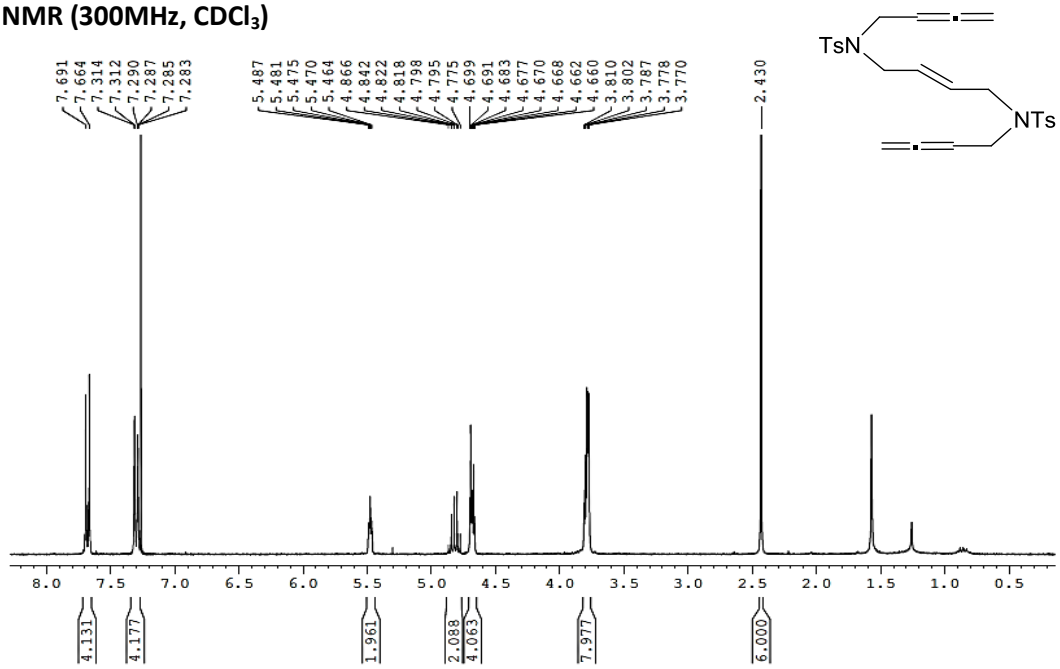

^{13}C NMR (75 MHz, $CDCl_3$)

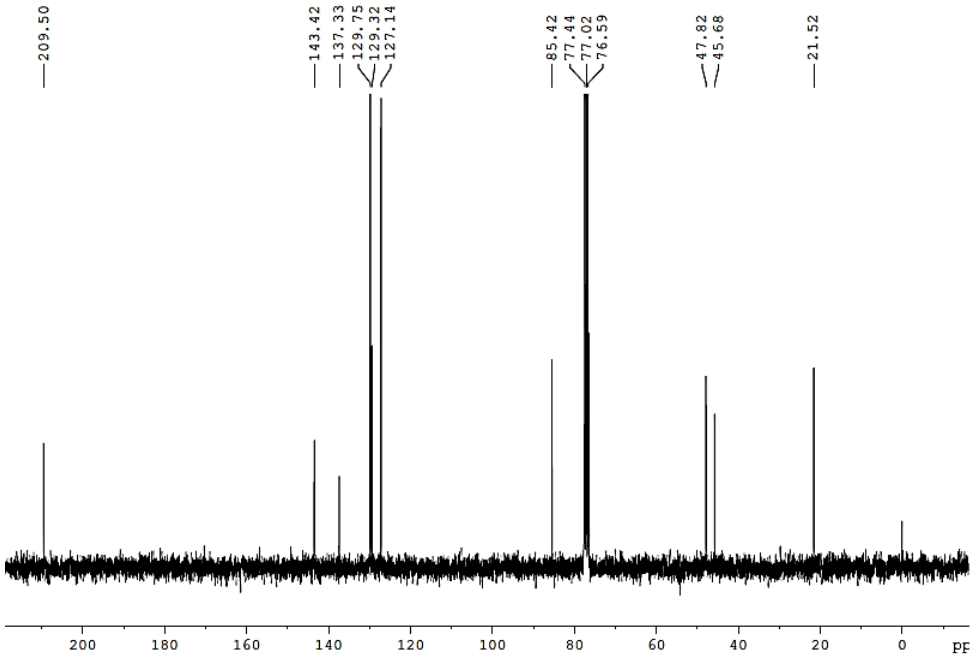

ESI-HRMS (+)

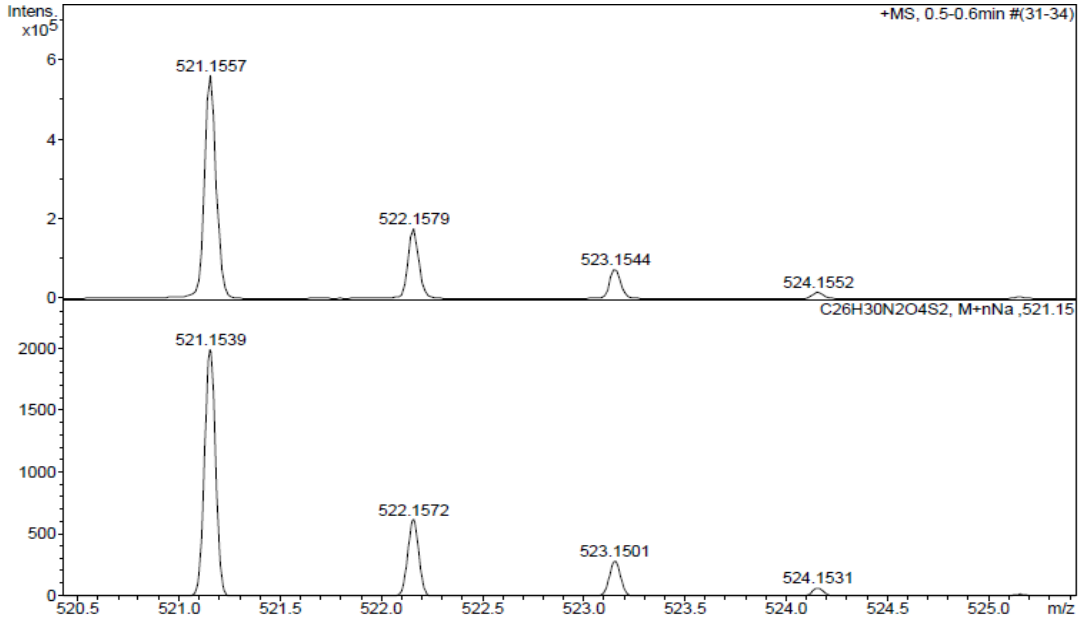

IR (ATR)

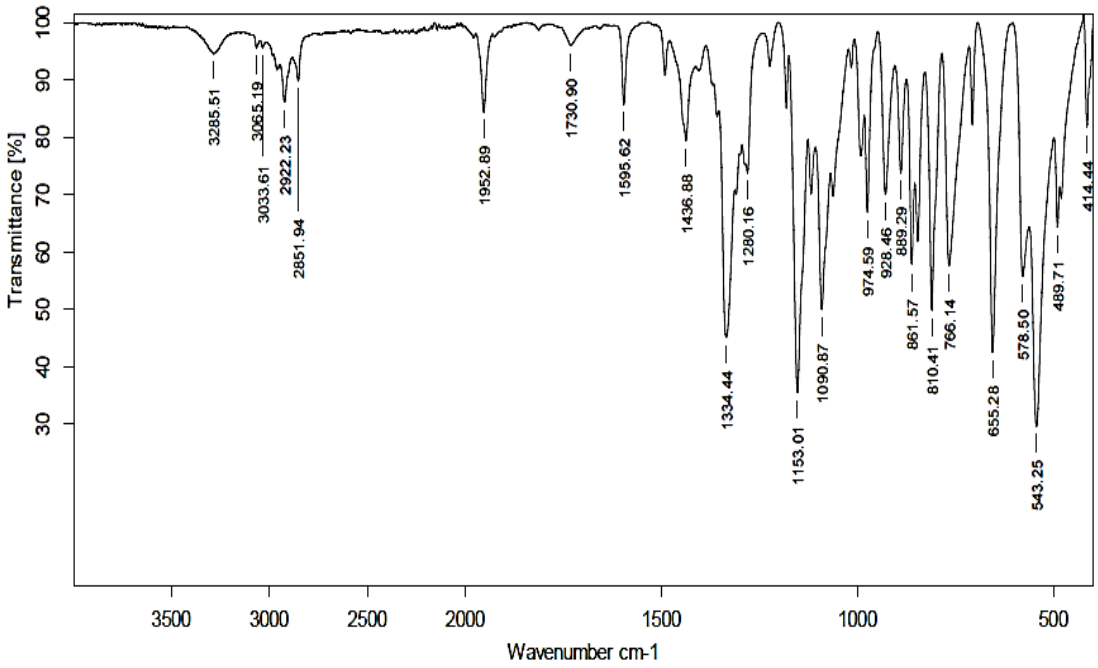

^{1}H NMR (300MHz, $CDCl_3$)

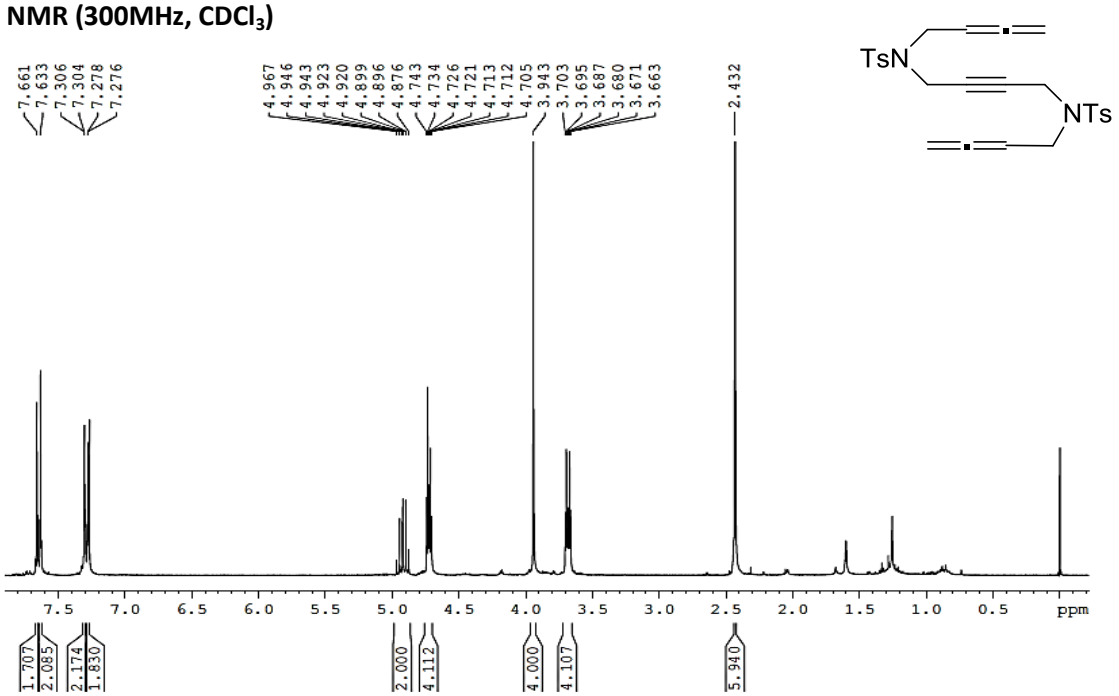

^{13}C NMR (75 MHz, $CDCl_3$)

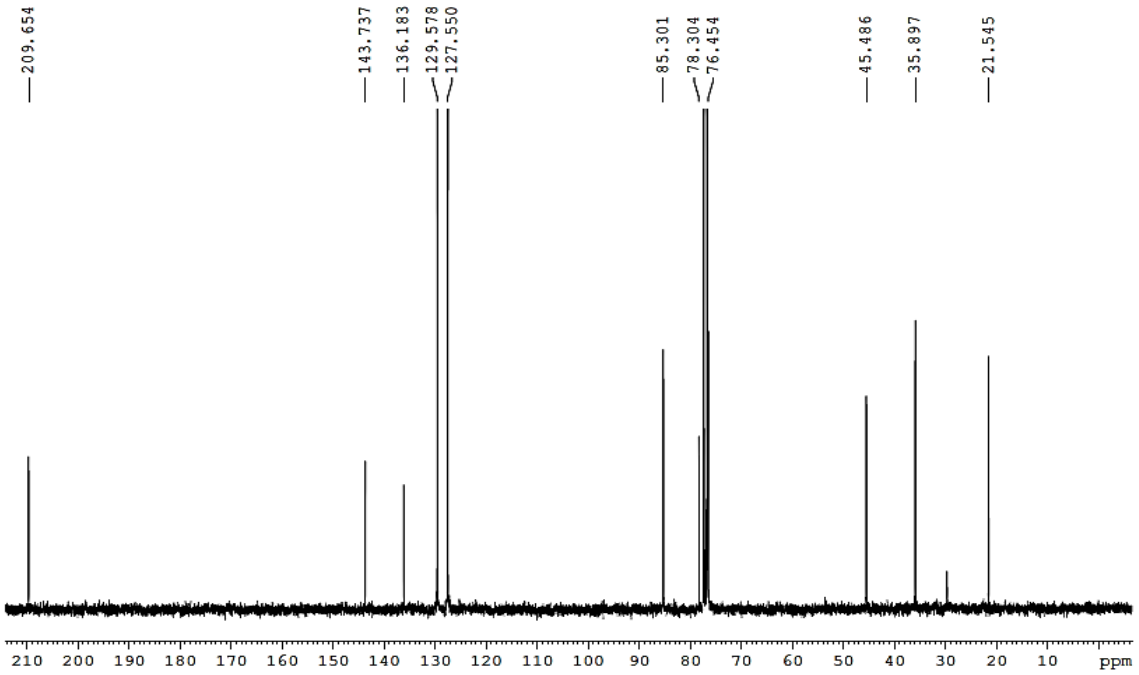

ESI-HRMS (+)

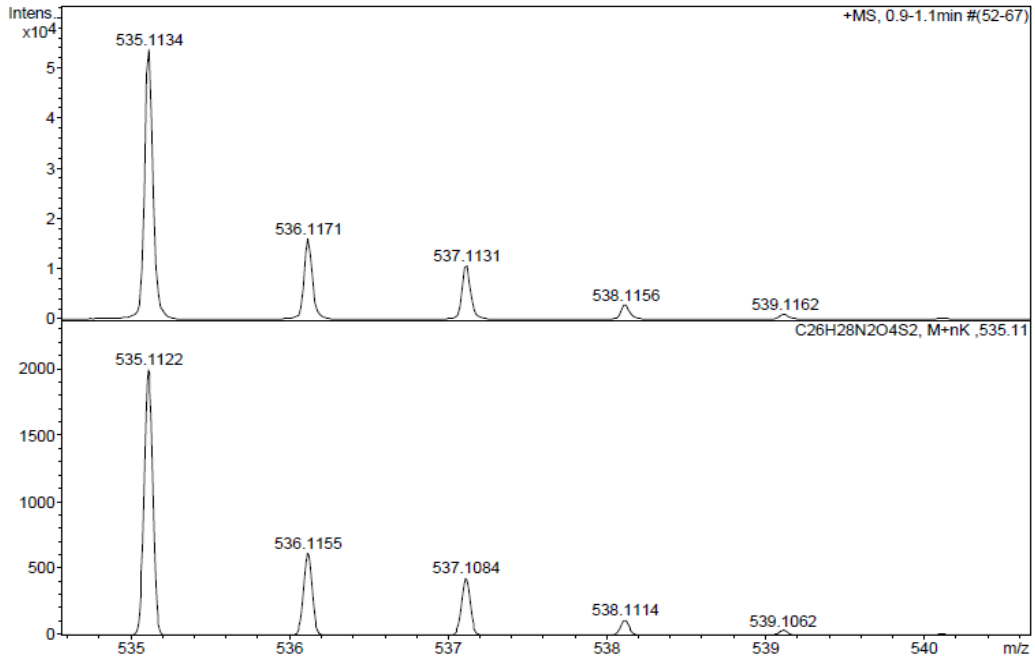

IR (ATR)

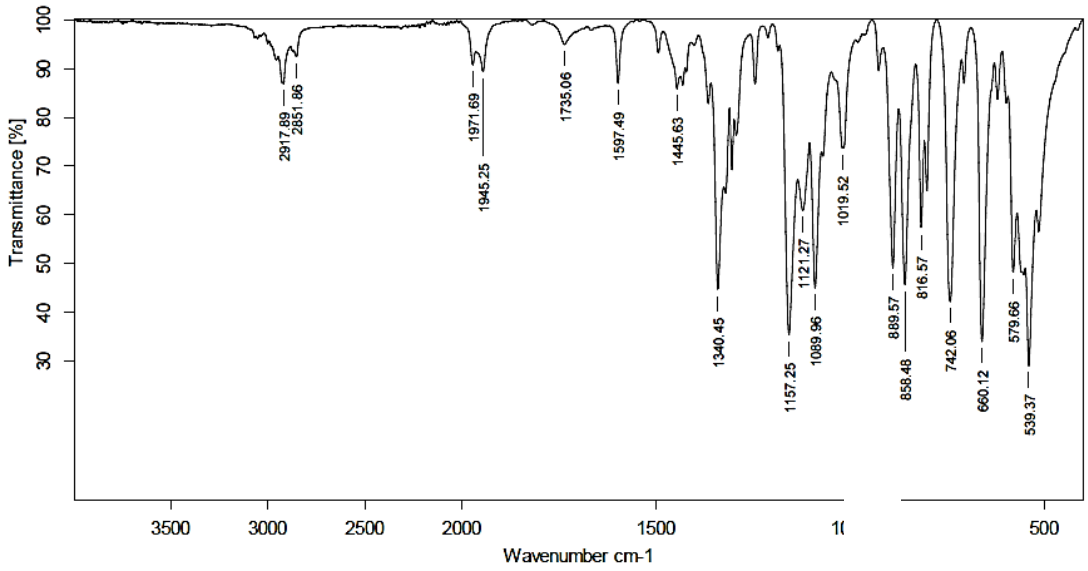

^{1}H NMR (300MHz, $CDCl_3$)

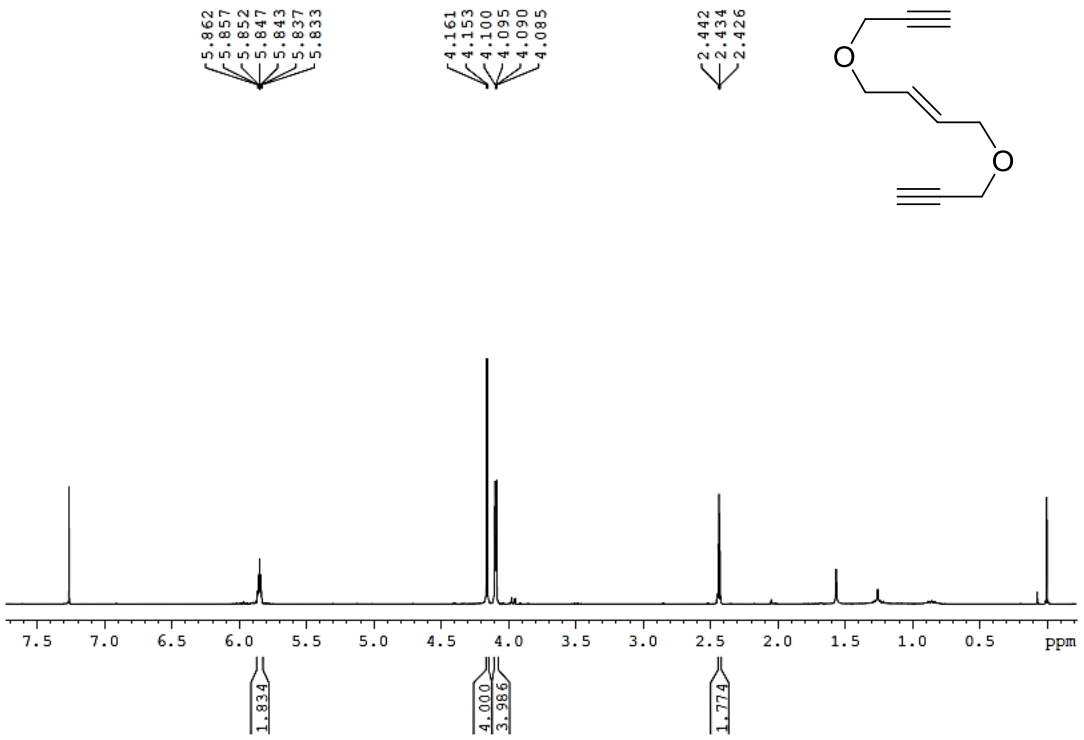

^{1}H NMR (300MHz, $CDCl_3$)

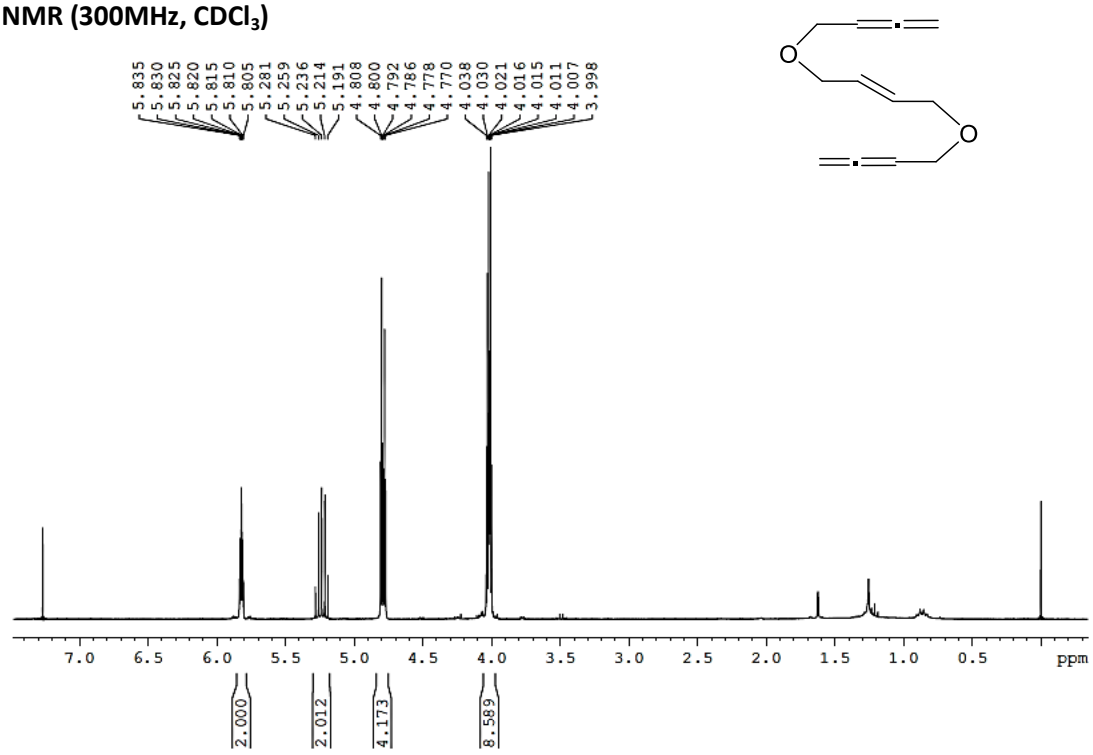

^{13}C NMR (100 MHz, $CDCl_3$)

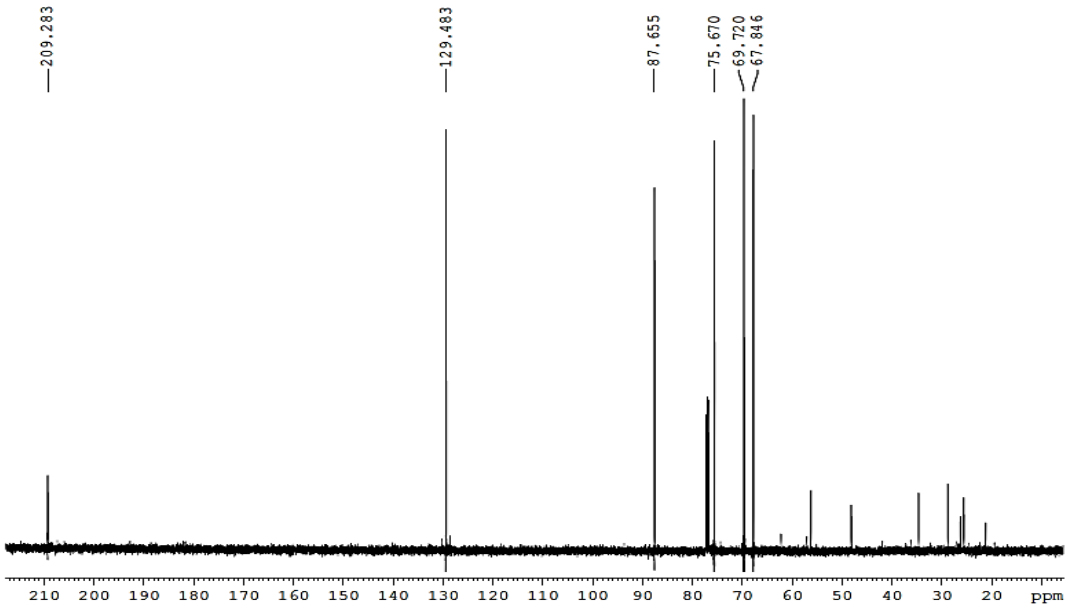

ESI-HRMS (+)

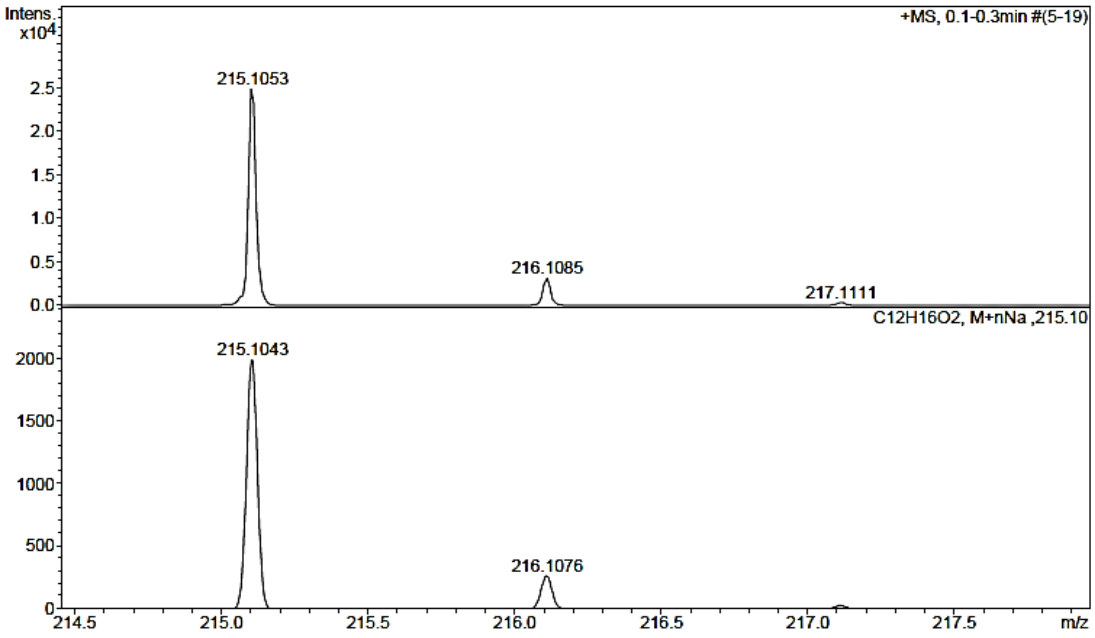

IR (ATR)

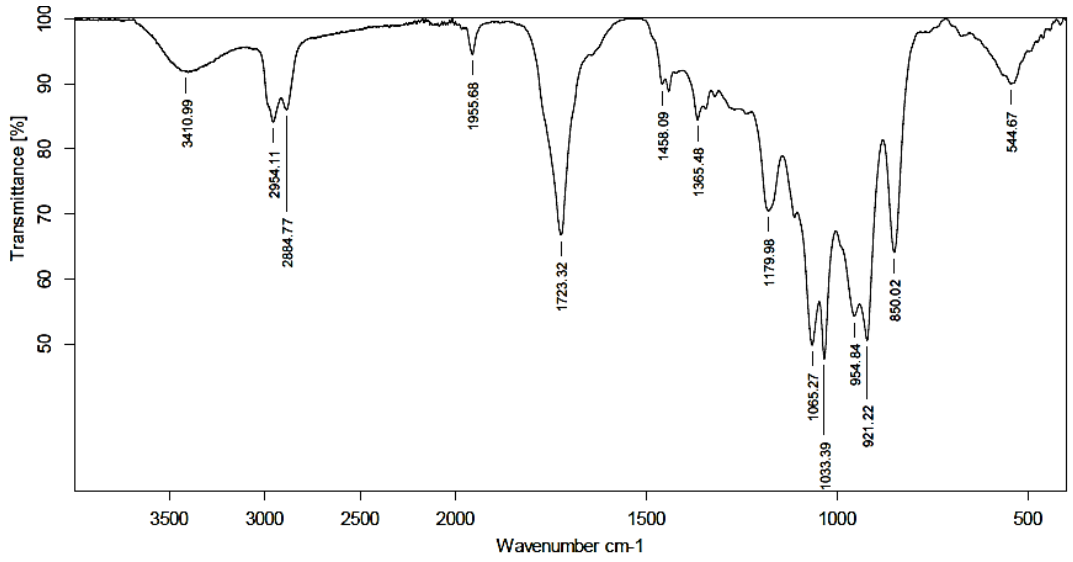

^{1}H NMR (300MHz, $CDCl_3$)

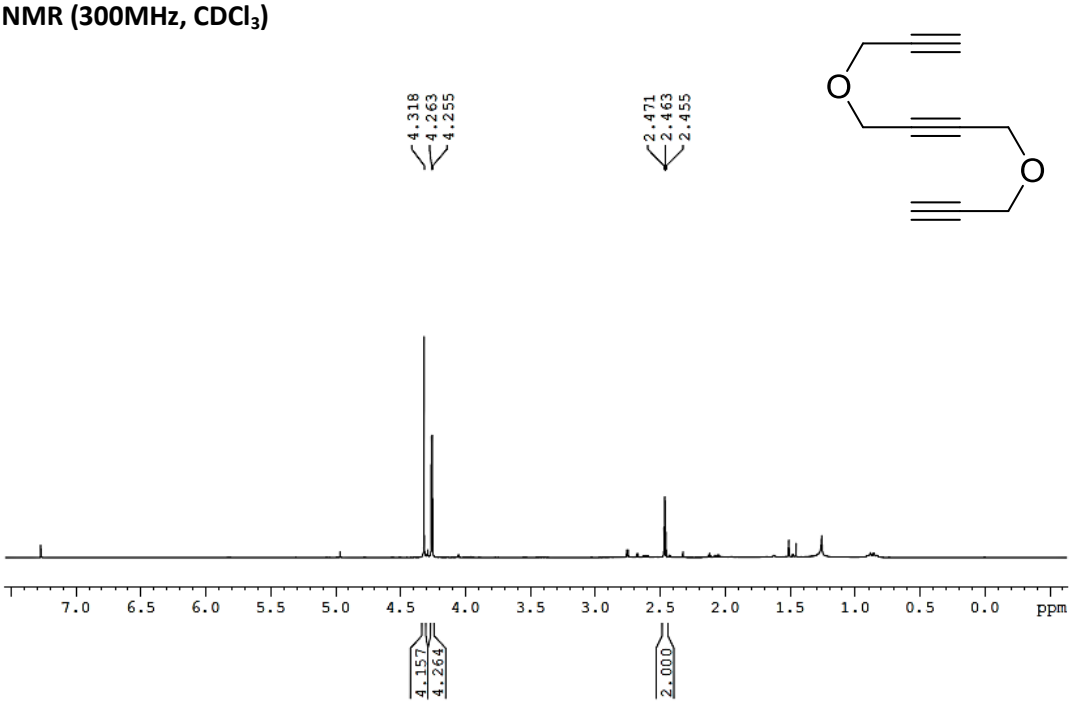

^{1}H NMR (300MHz, $CDCl_3$)

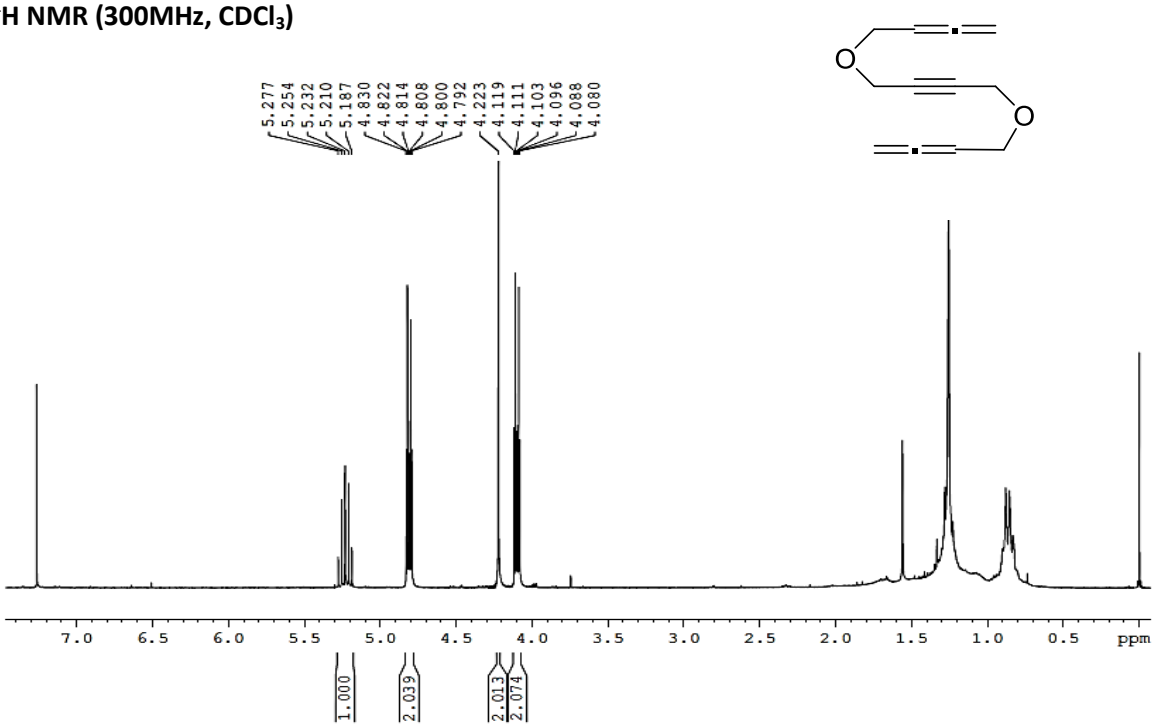

^{13}C NMR (100 MHz, $CDCl_3$)

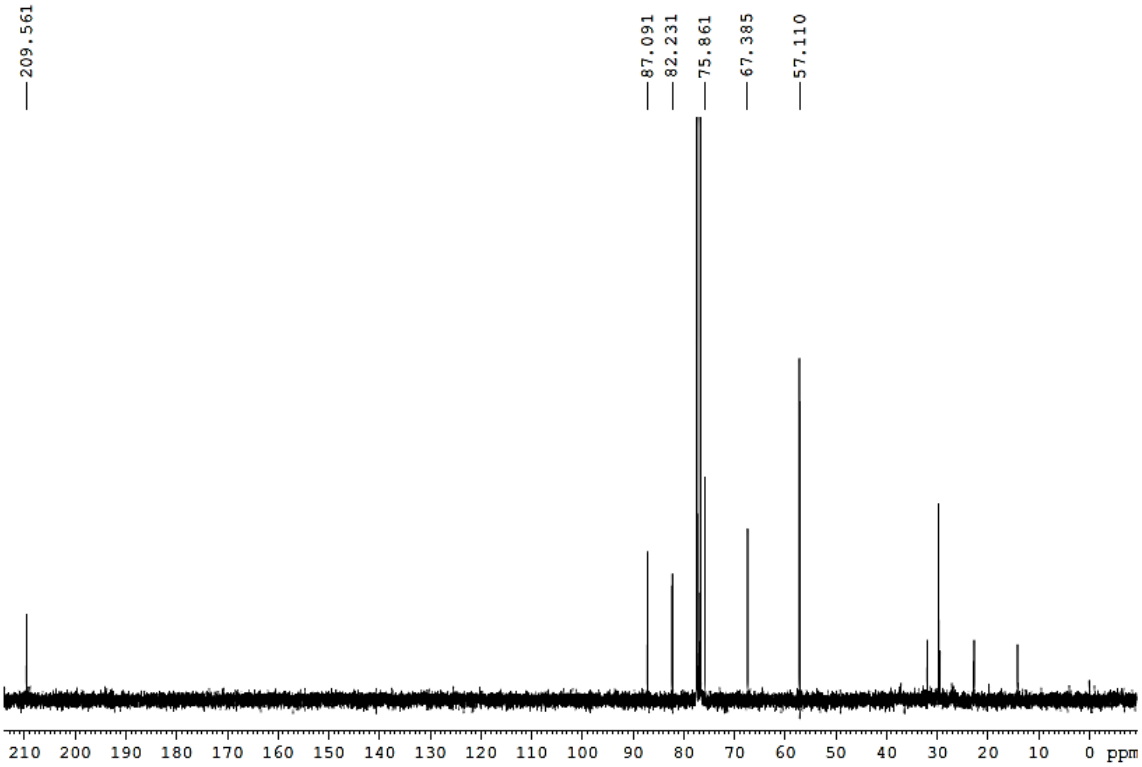

ESI-HRMS (+)

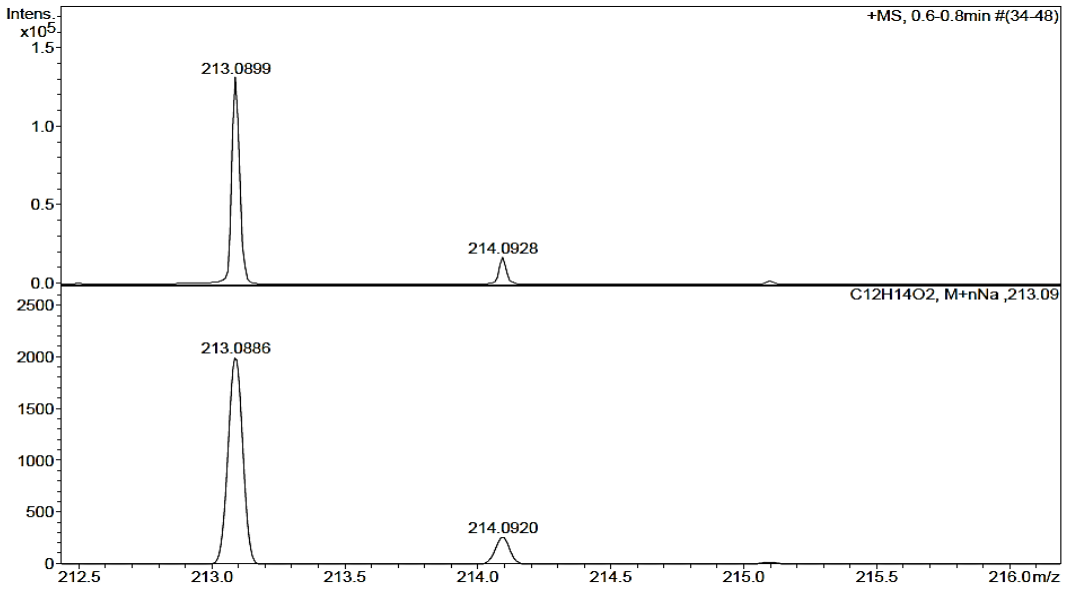

IR (ATR)

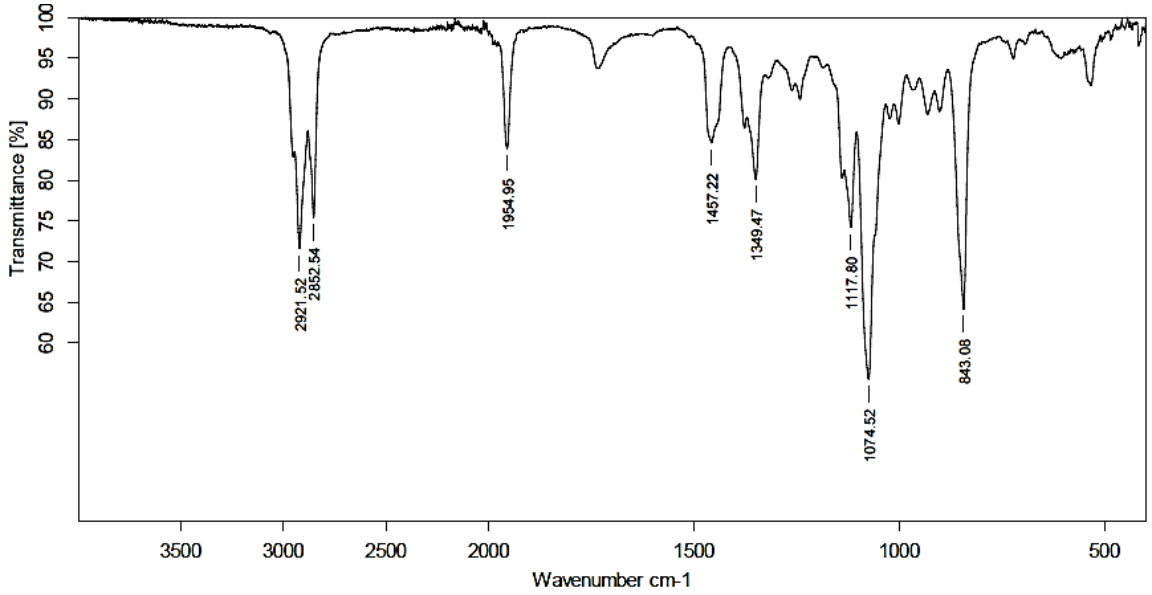

^{1}H and ^{13}C NMR chemical shift assignment

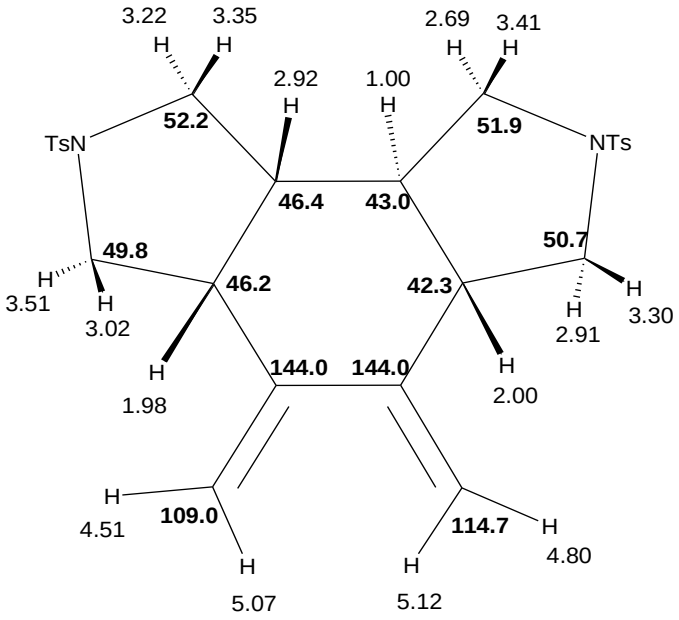

^{1}H NMR (300MHz, $CDCl_3$)

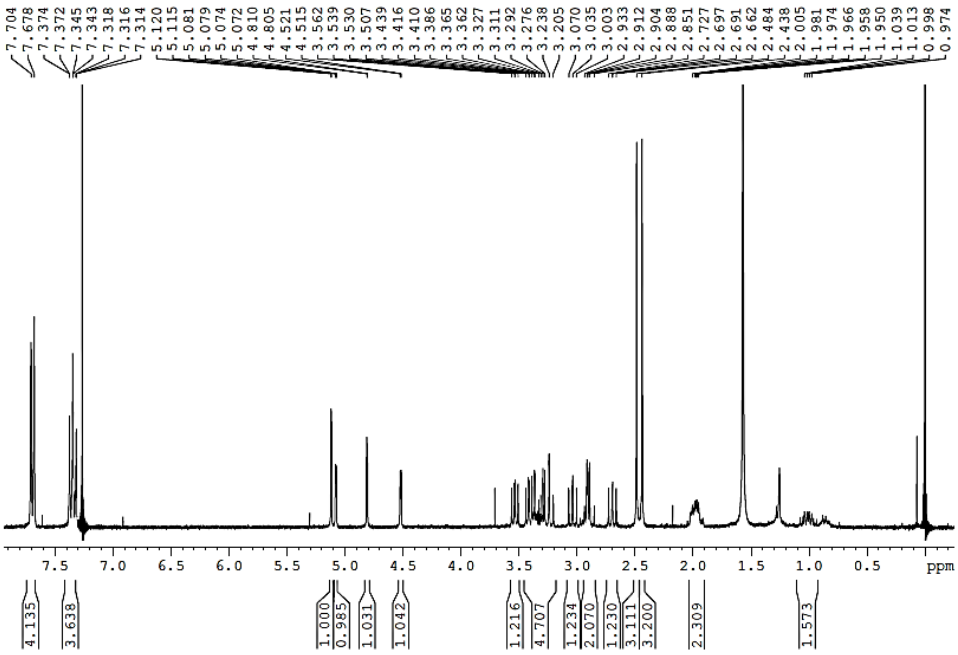

^{13}C NMR (75 MHz, $CDCl_3$)

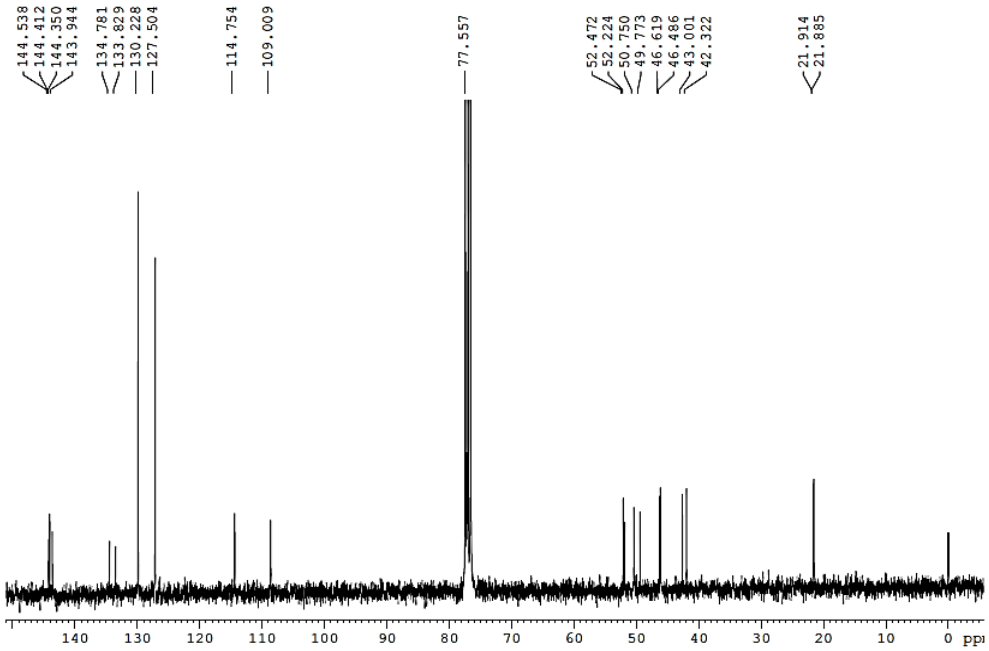

2D 1H-1H NOESY ($CDCl_3$)

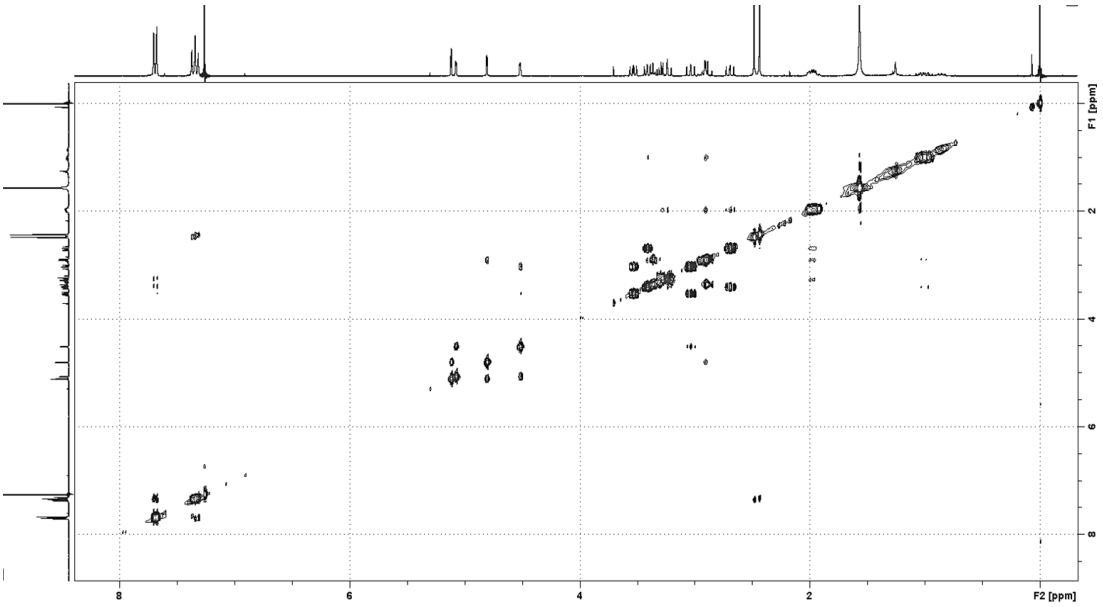

2D ^{1}H-^{1}H COSY ($CDCl_3$)

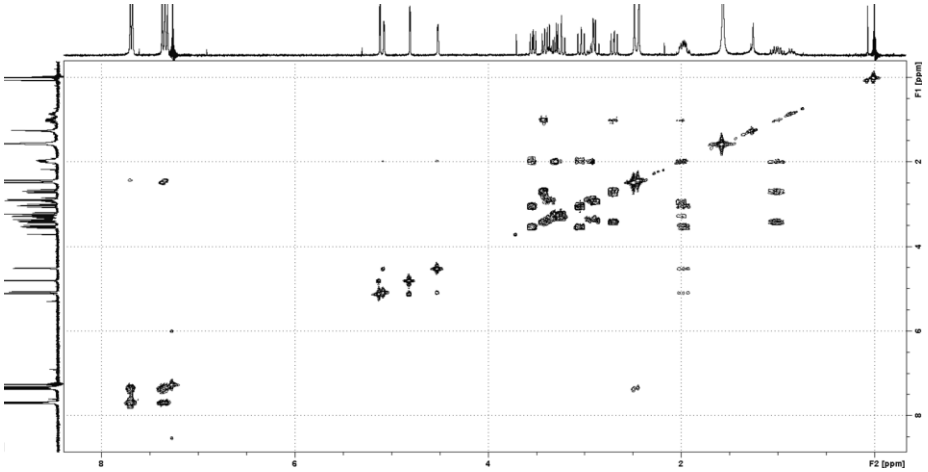

2D ^{1}H-^{13}C HSQC

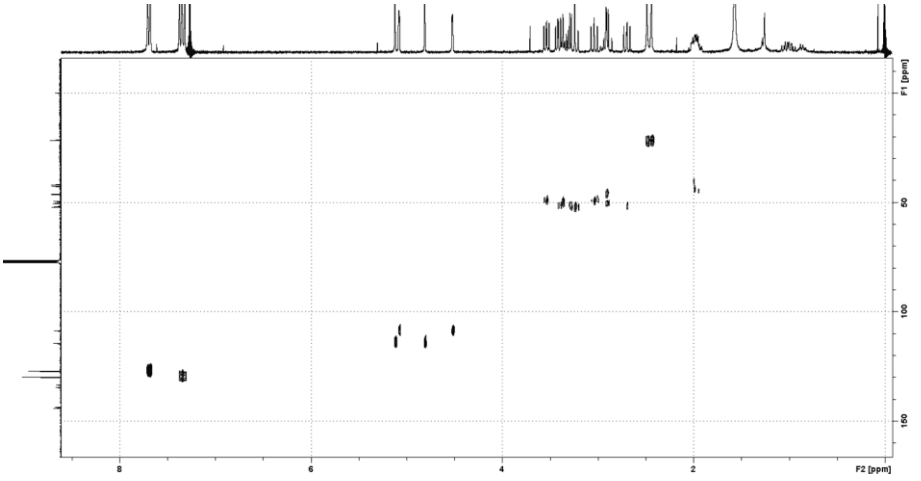

2D ^{1}H-^{13}C HMBC ($CDCl_3$)

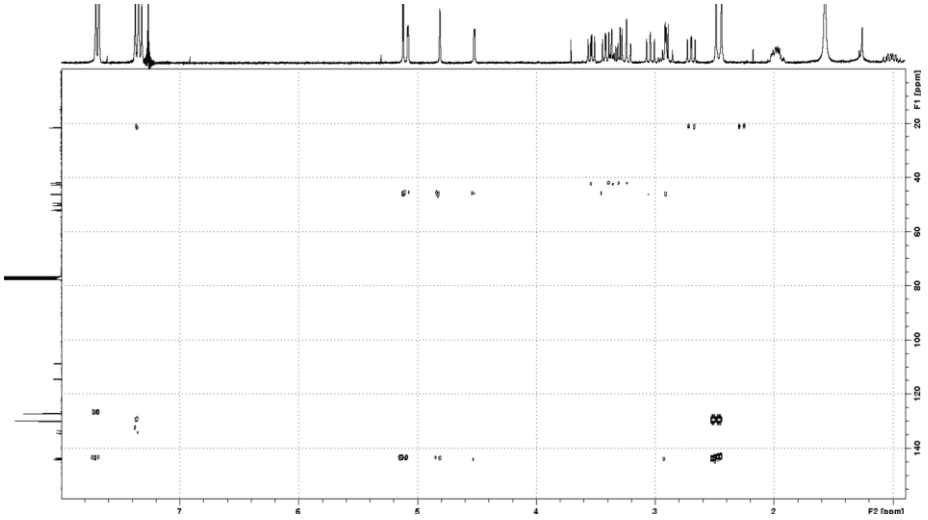

ESI-HRMS (+)

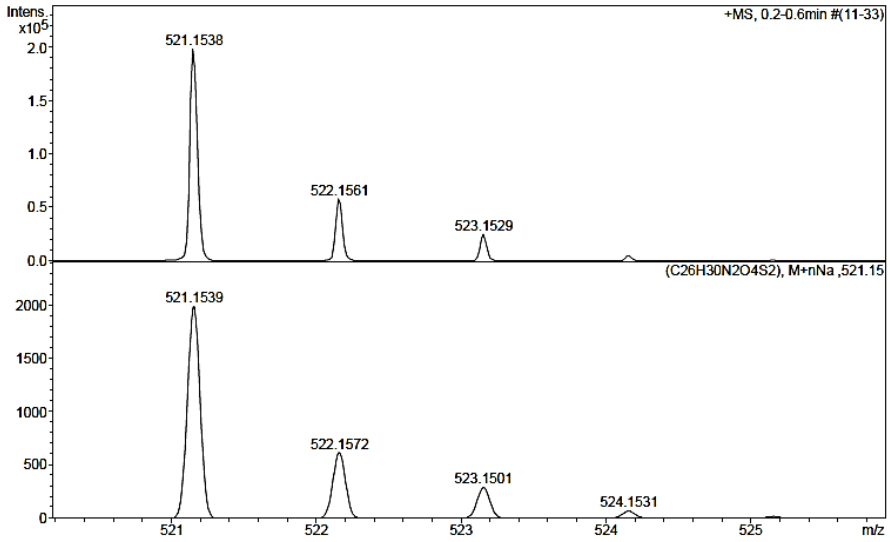

IR (ATR)

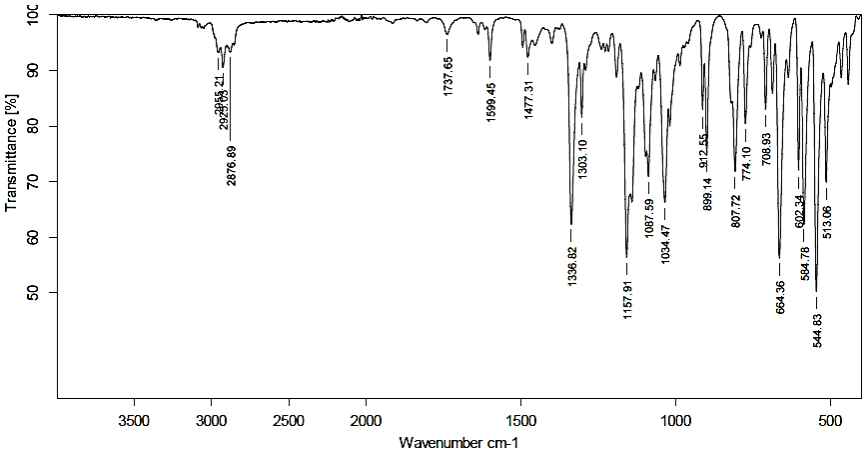

^{1}H and ^{13}C NMR chemical shift assignment

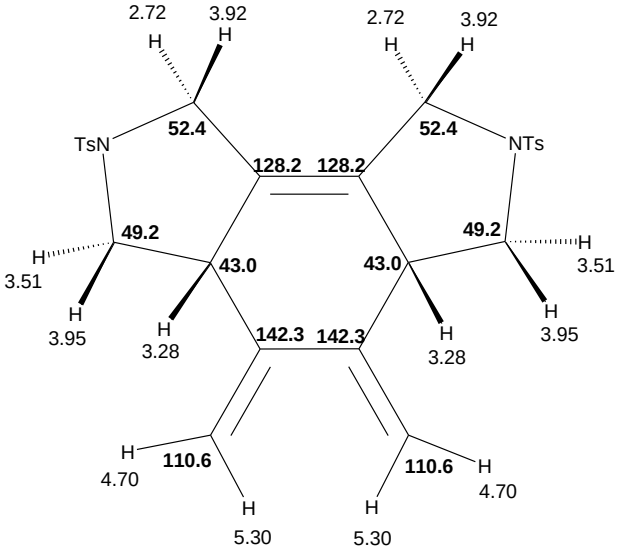

^{1}H NMR (400MHz, $CDCl_3$)

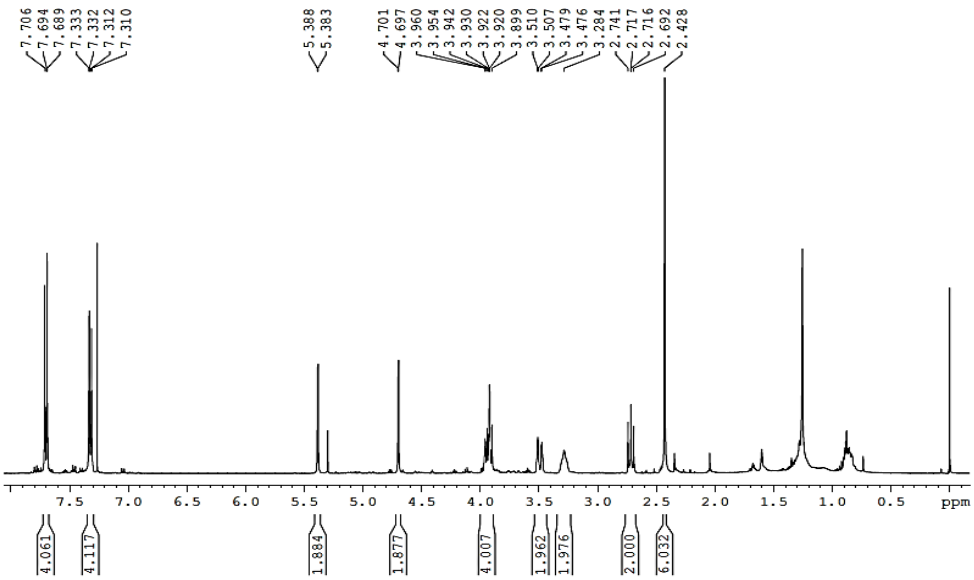

^{13}C NMR (100 MHz, $CDCl_3$)

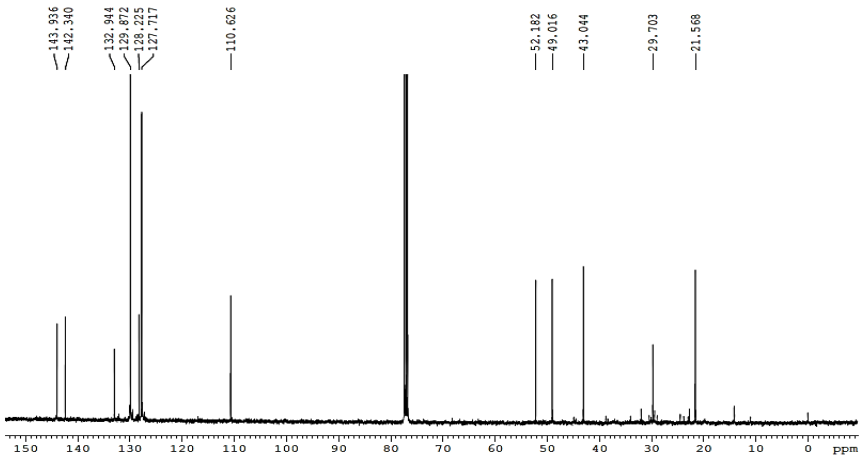

ESI-HRMS (+)

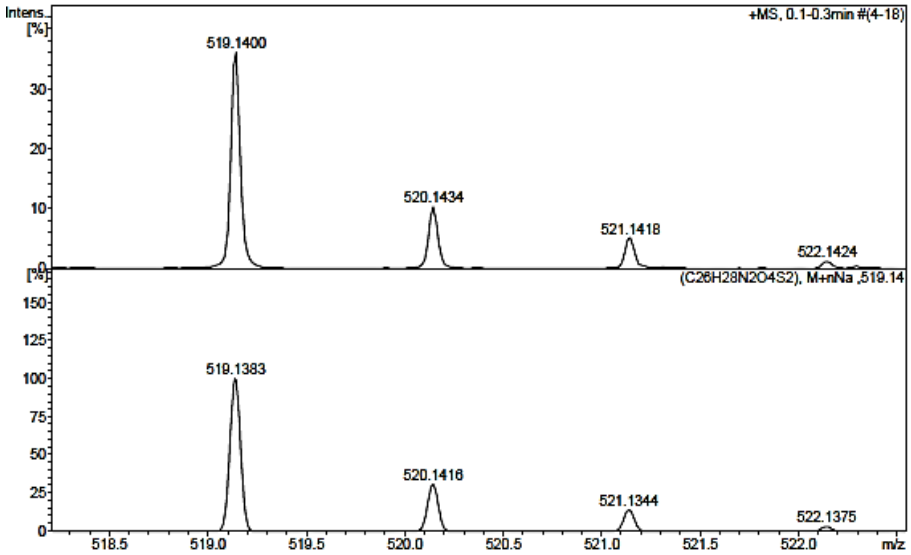

IR (ATR)

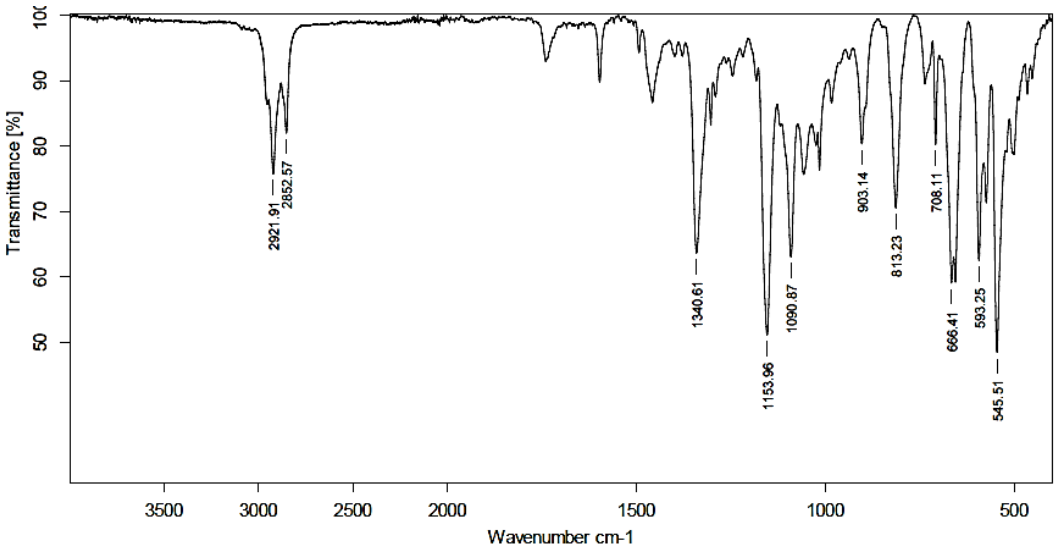

^{1}H and ^{13}C NMR chemical shift assignment

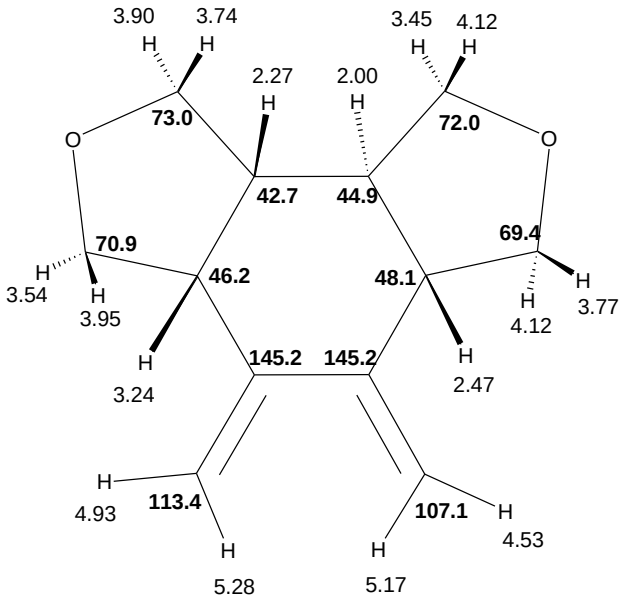

^{1}H NMR (400MHz, $CDCl_3$)

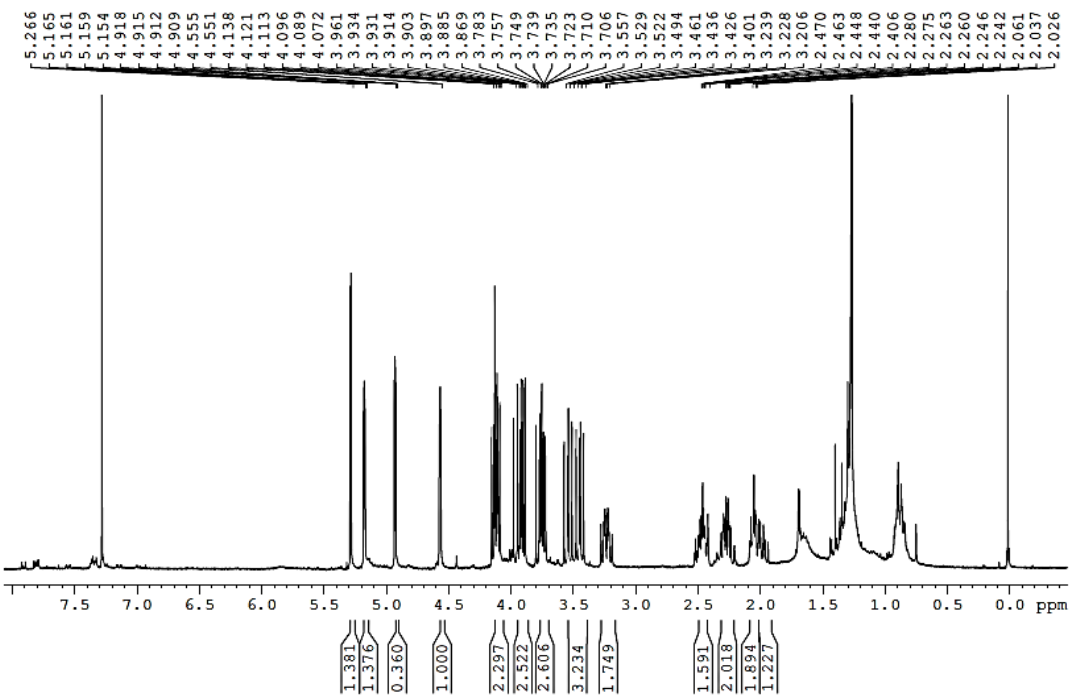

^{13}C NMR (75 MHz, $CDCl_3$)

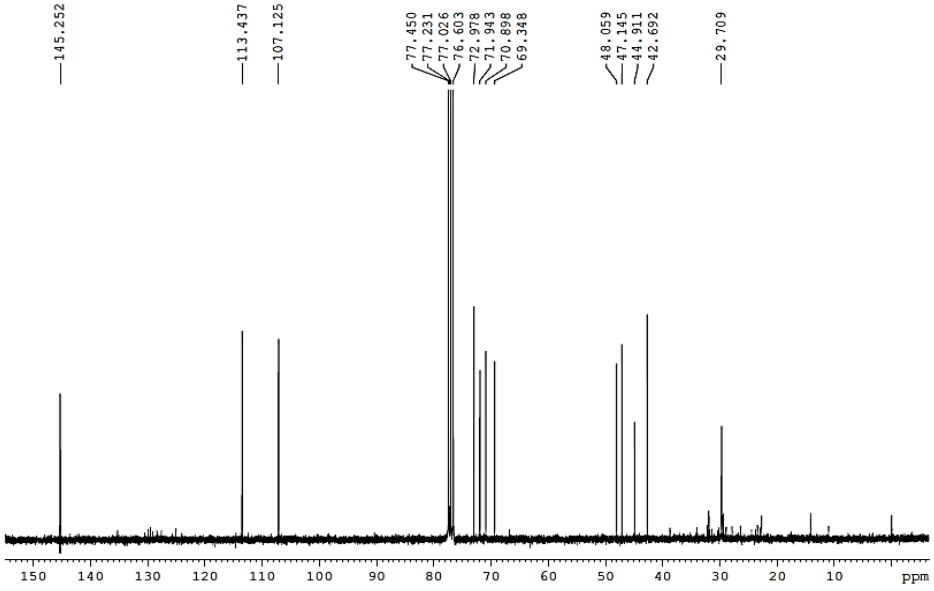

2D 1H-1H NOESY

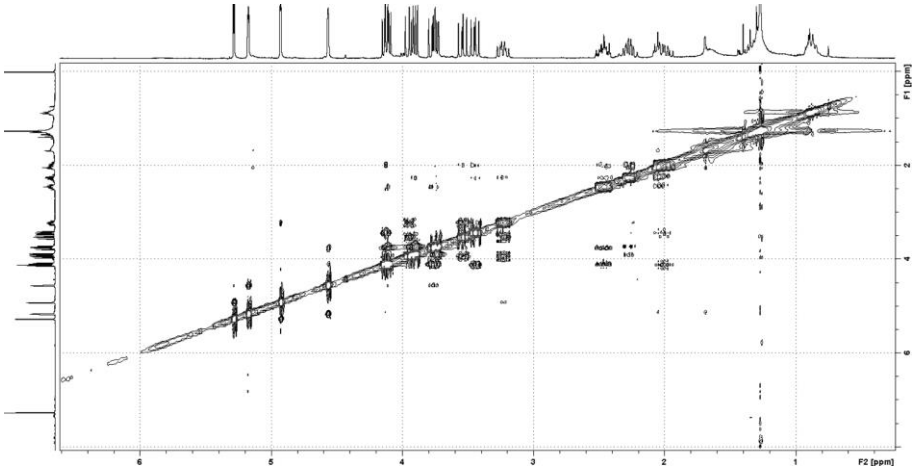

2D ^{1}H-^{1}H COSY

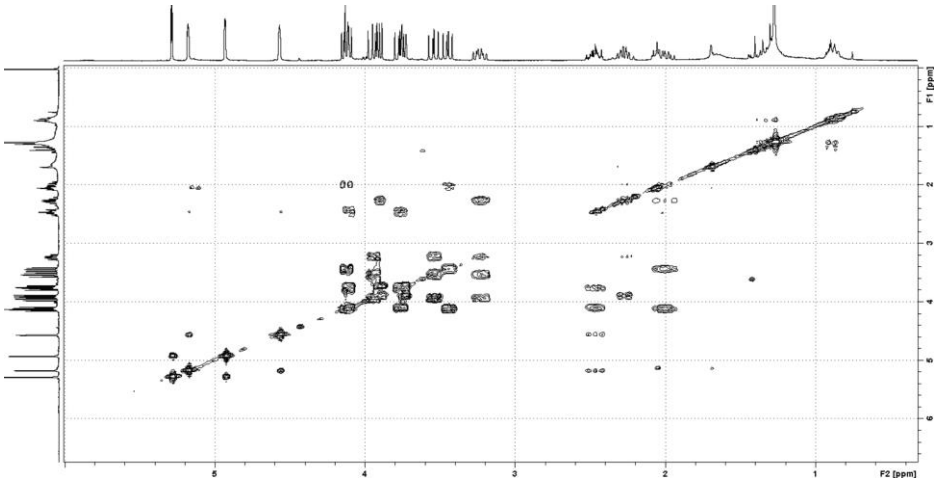

2D ^{1}H-^{13}C HSQC

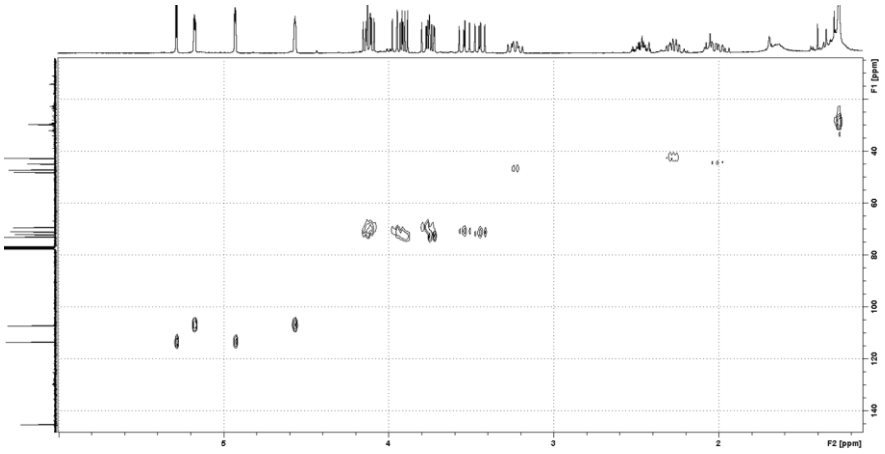

2D ^{1}H-^{13}C HMBC

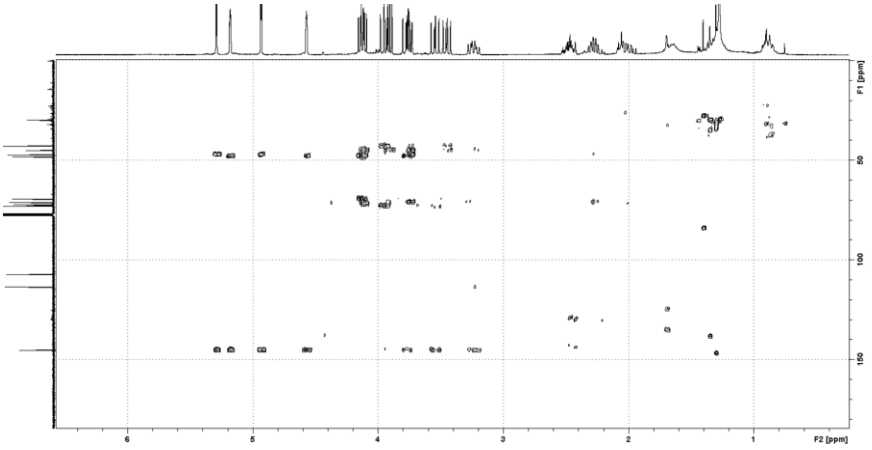

ESI-HRMS (+)

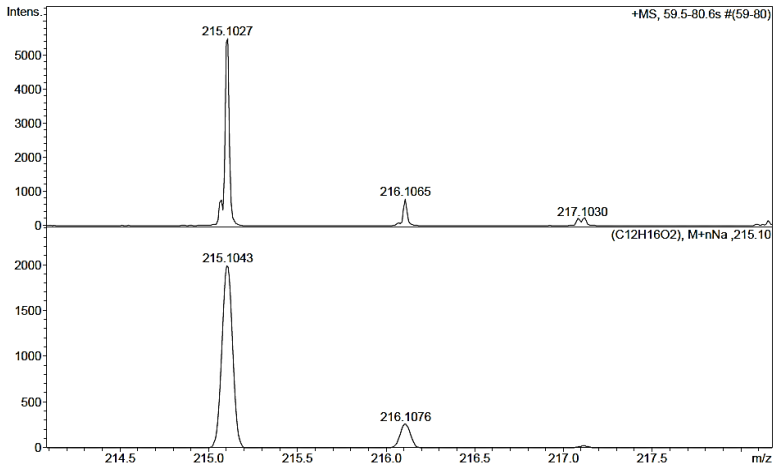

IR (ATR)

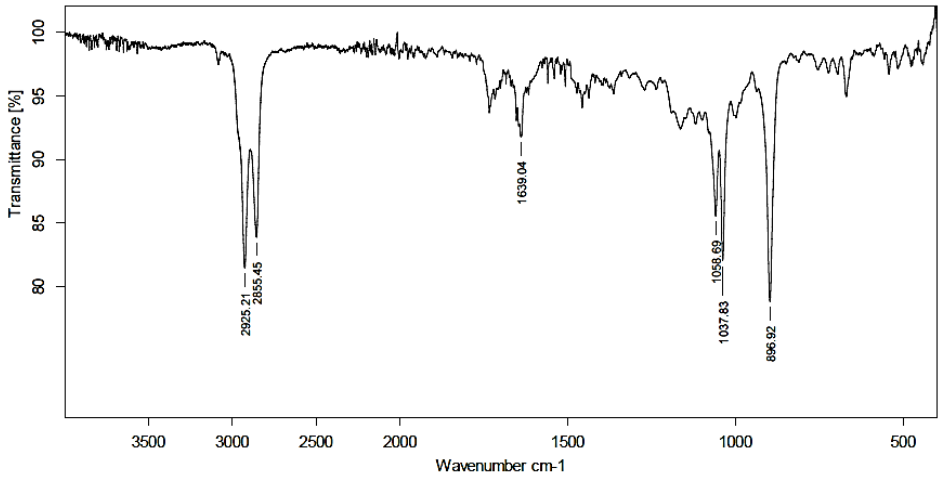

^{1}H and ^{13}C NMR chemical shift assignment

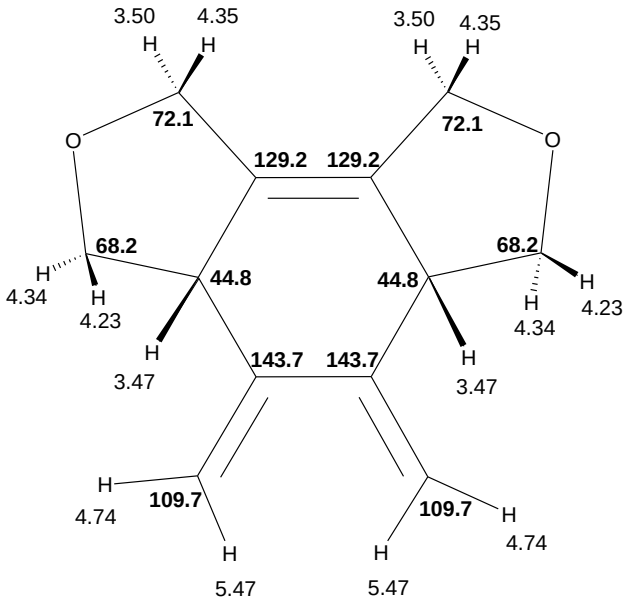

^{1}H NMR (300 MHz, $CDCl_3$)

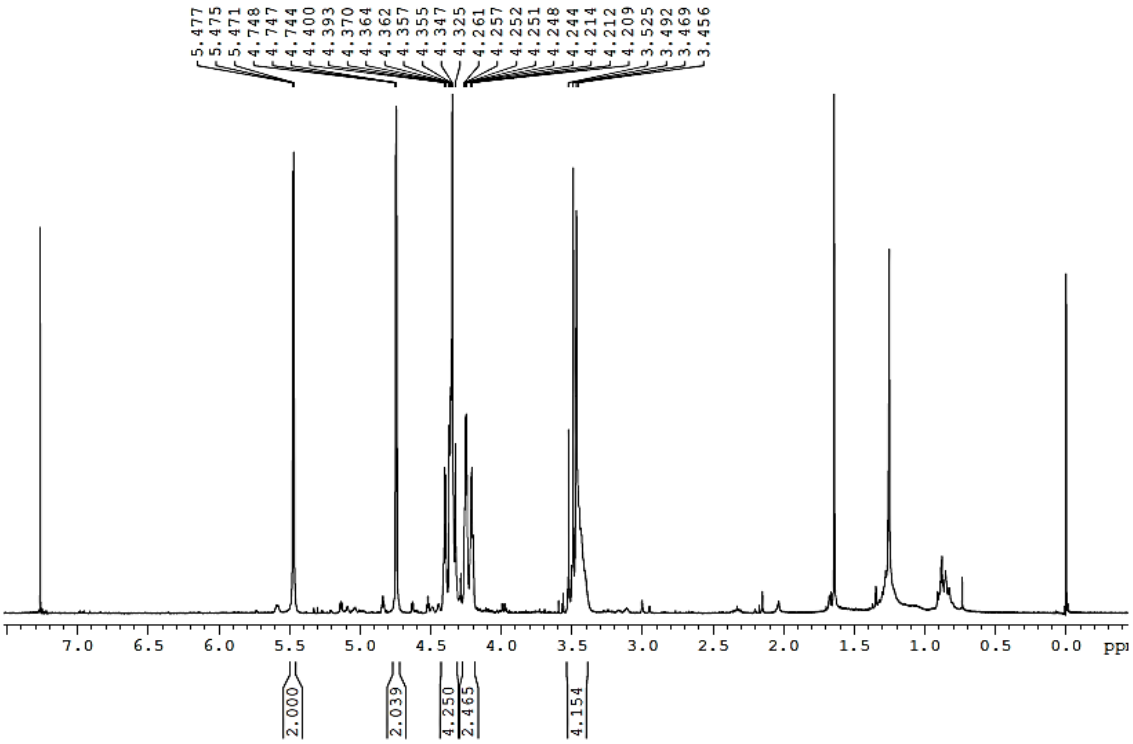

^{13}C NMR (75 MHz, $CDCl_3$)

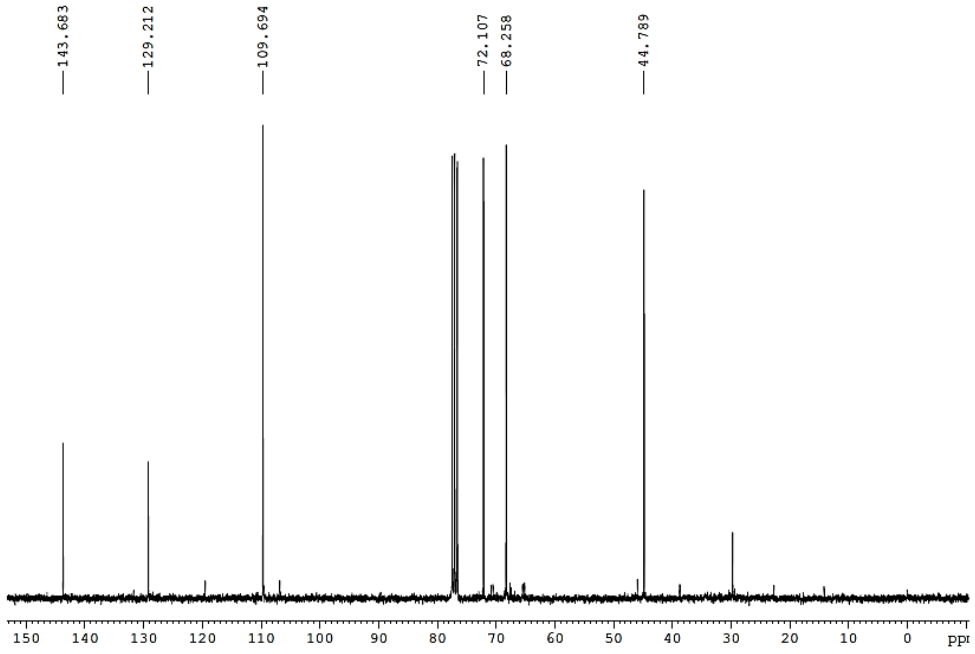

2D ^{1}H-^{1}H COSY

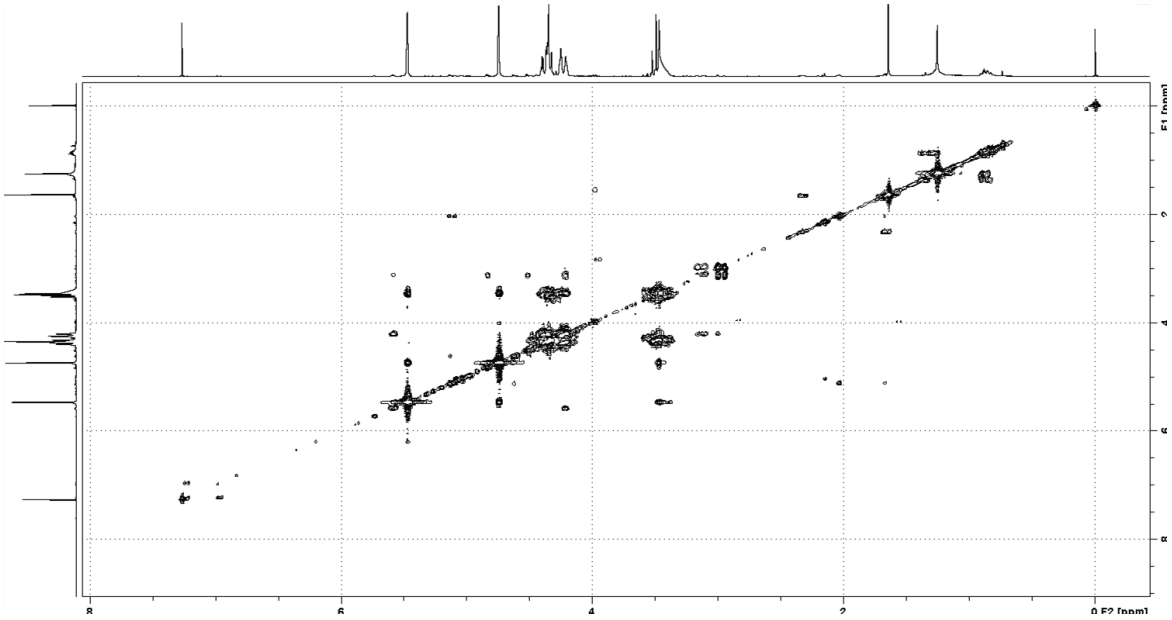

2D ^{1}H-^{1}H NOESY

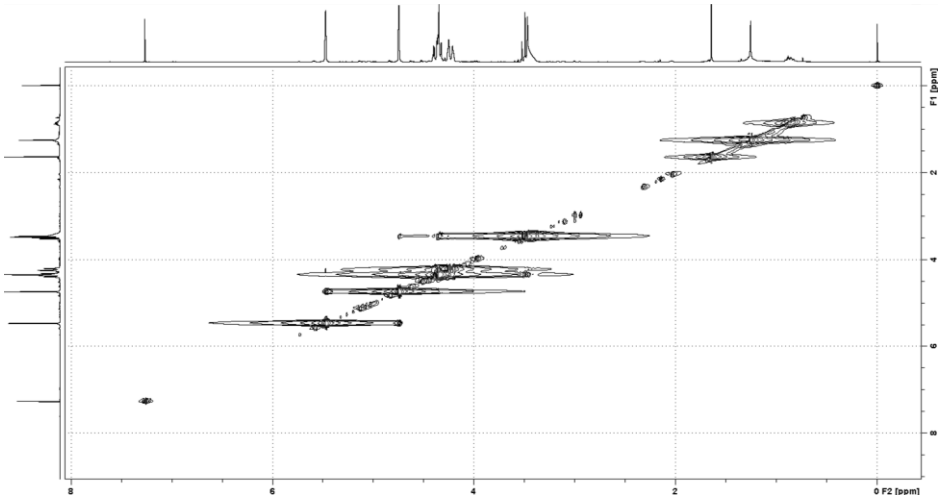

2D ^{1}H-^{13}C HSQC

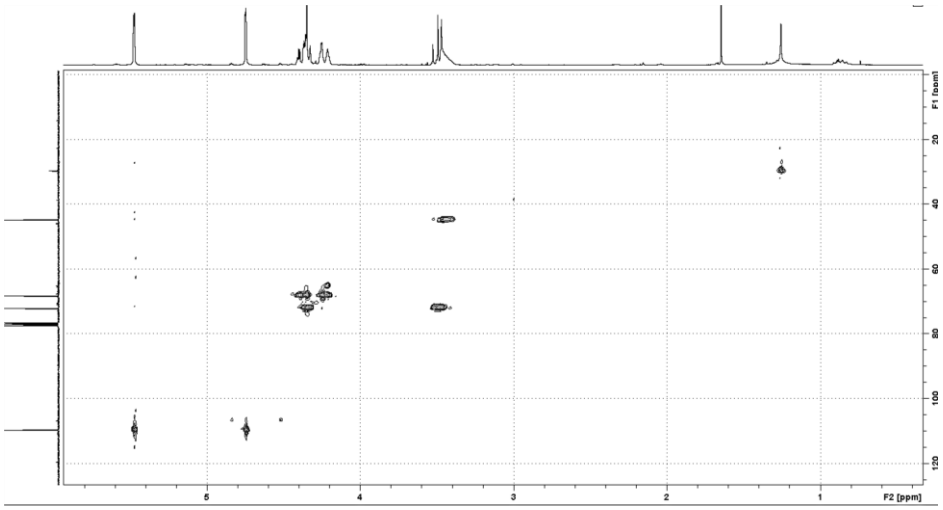

2D ^{1}H-^{13}C HMBC

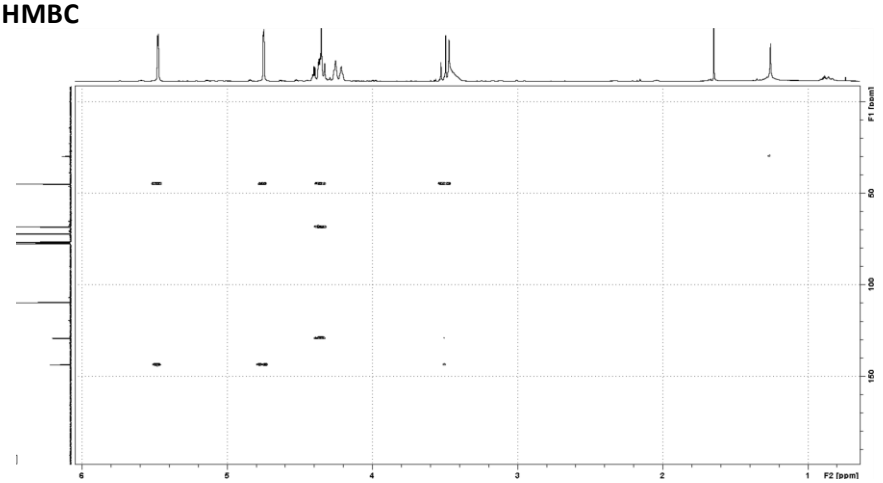

ESI-HRMS (+)

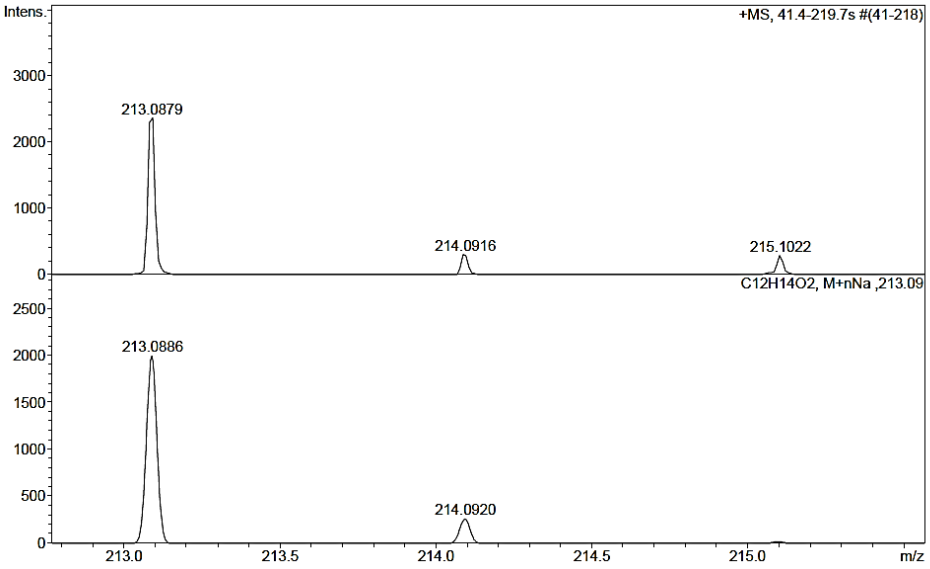

IR (ATR)

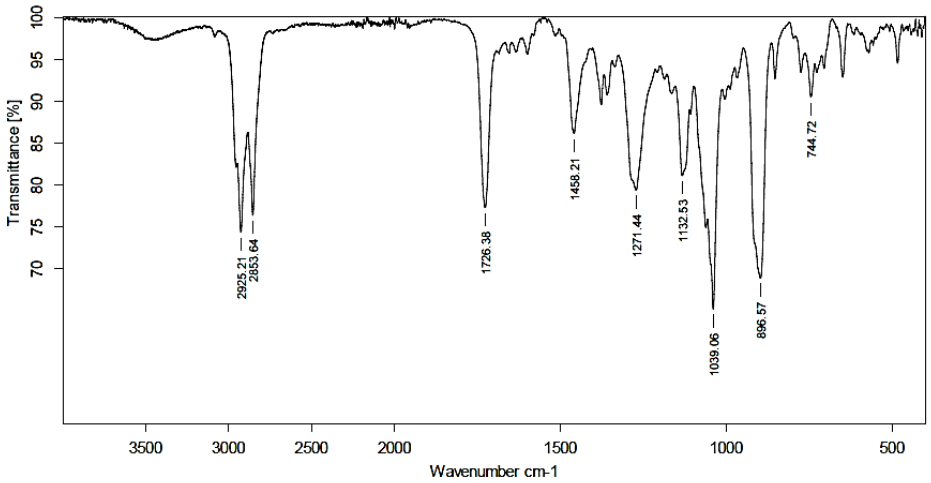

^{1}H and ^{13}C NMR chemical shift assignment

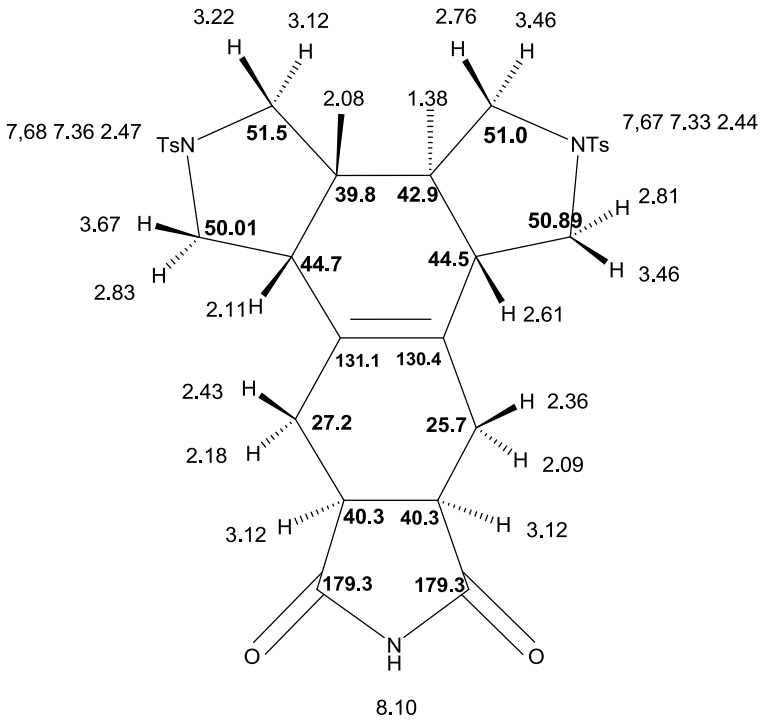

^{1}H NMR (400 MHz, $CDCl_3$)

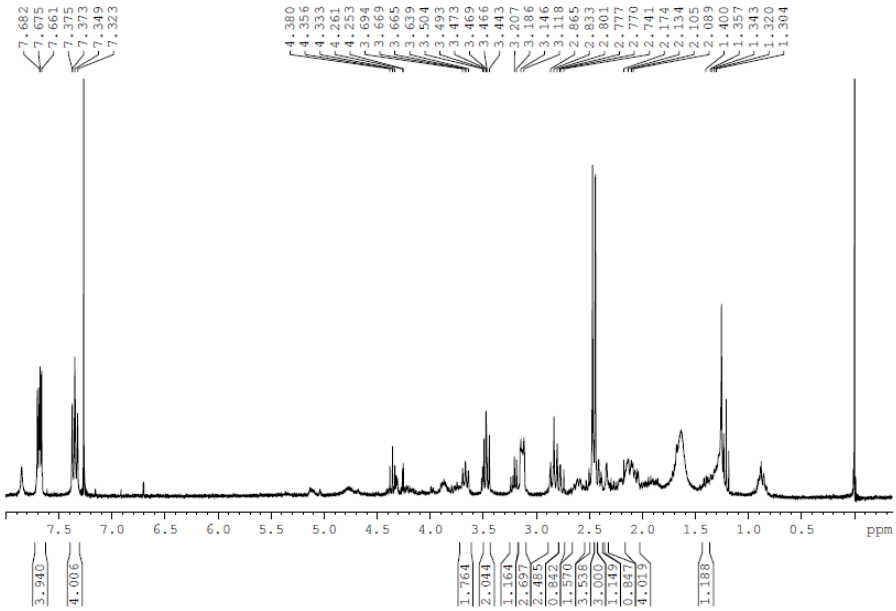

^{13}C NMR (100 MHz, $CDCl_3$)

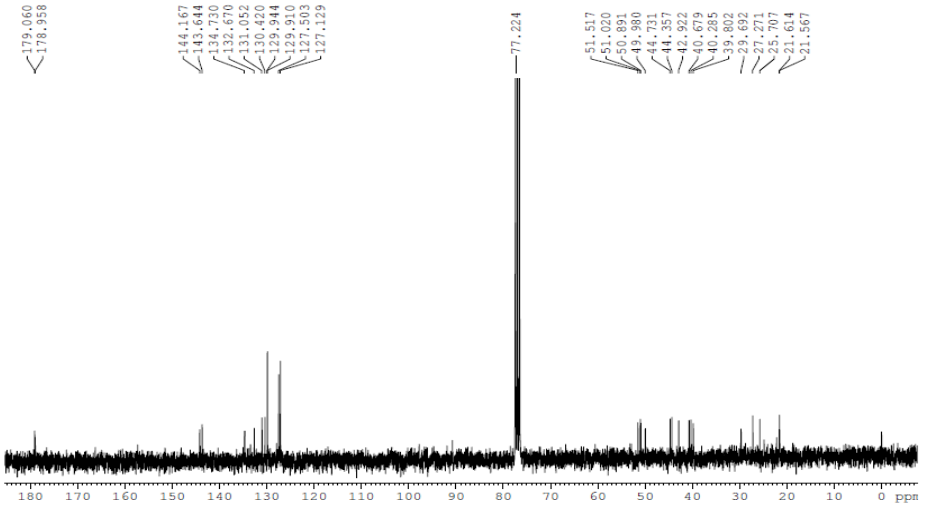

2D ^{1}H-^{1}H NOESY

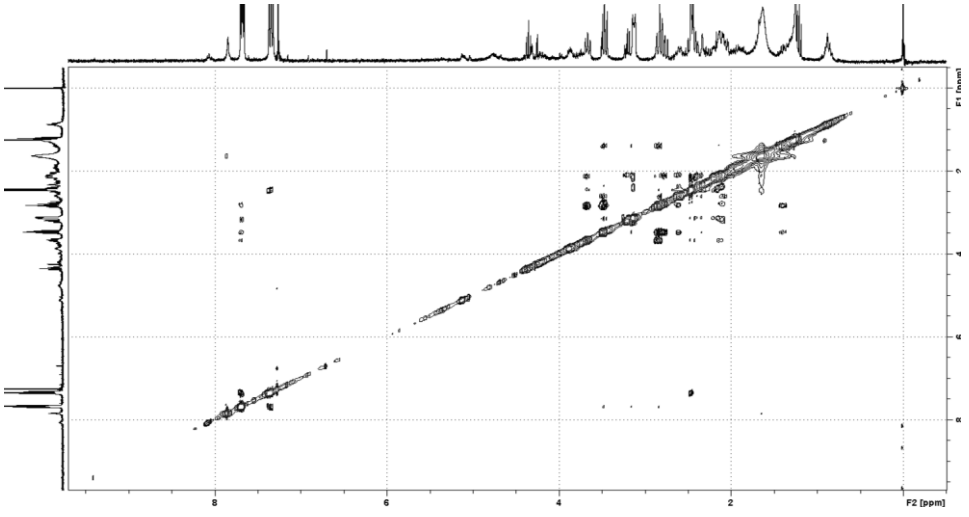

2D ^{1}H-^{1}H COSY

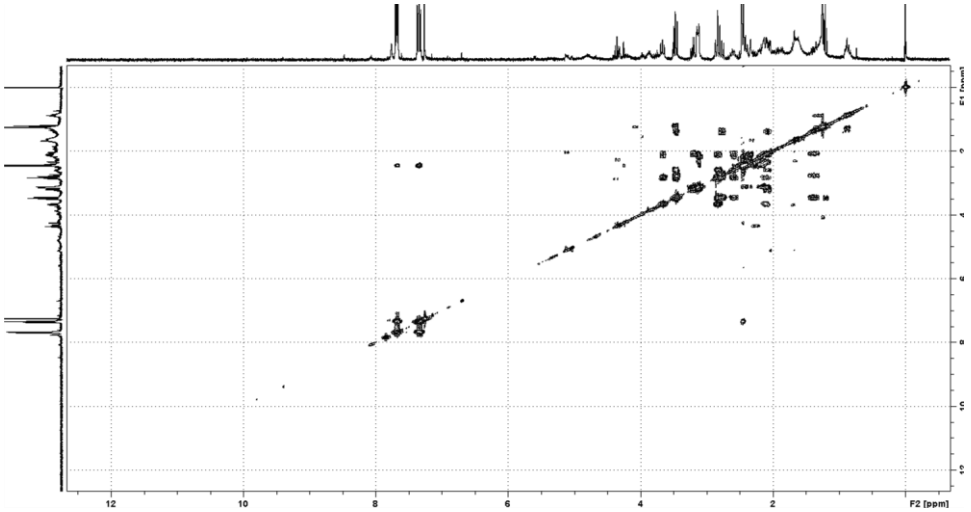

2D ^{1}H-^{13}C HSQC

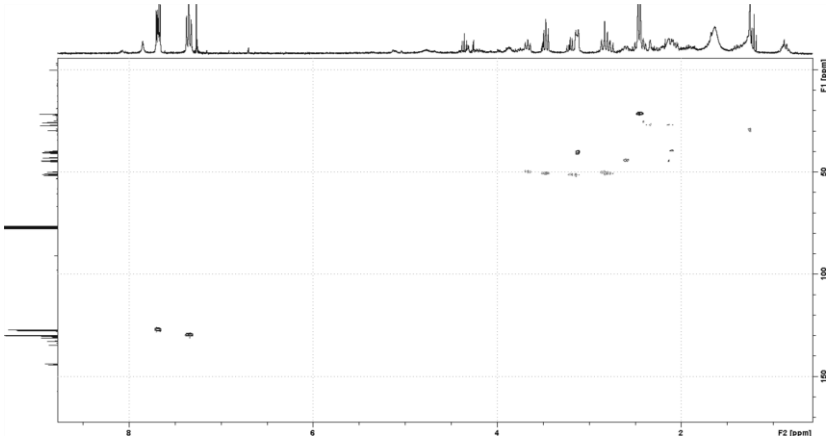

2D ^{1}H-^{13}C HMBC

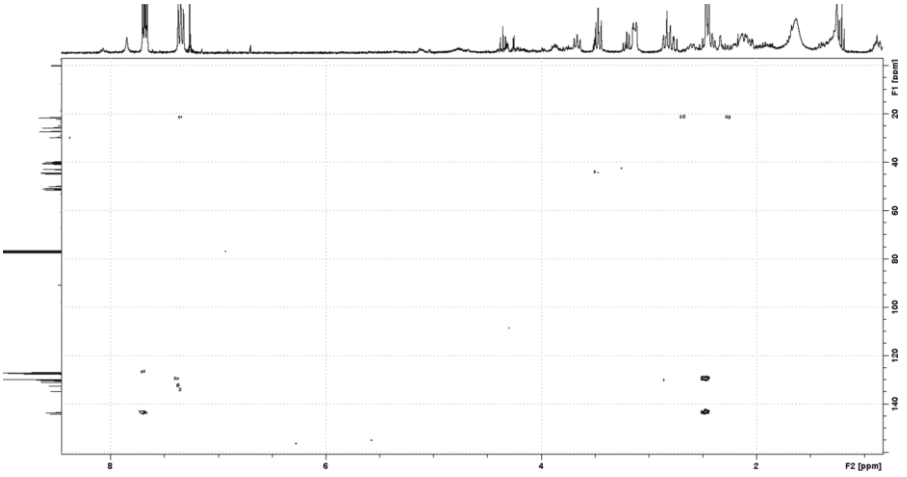

ESI-HRMS (+)

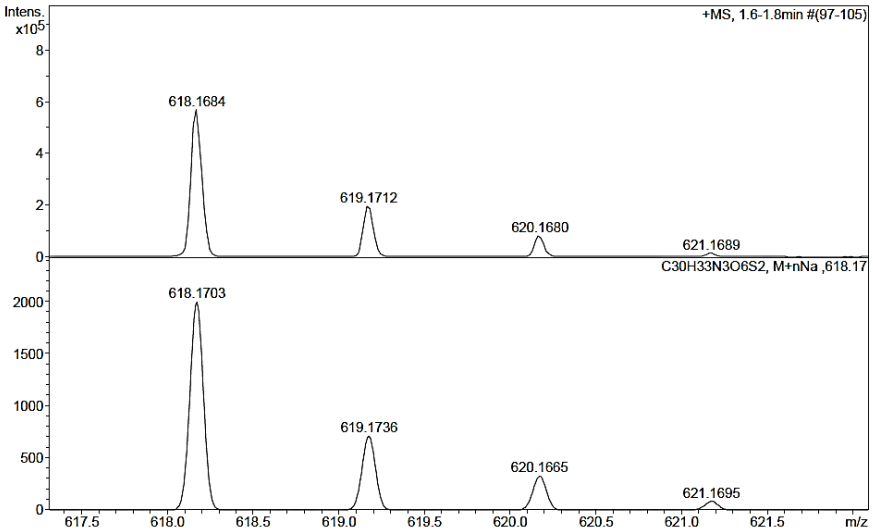

IR (ATR)

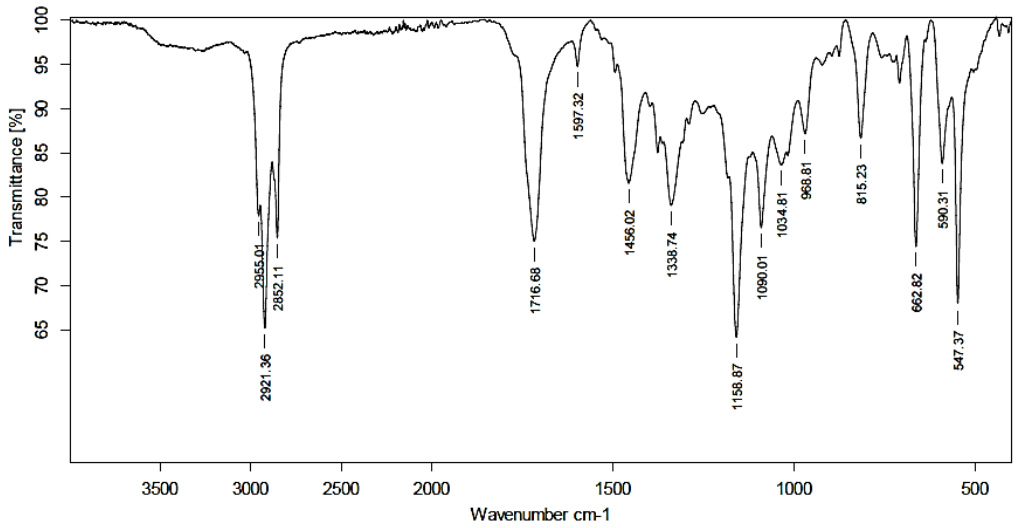

^{1}H and ^{13}C NMR chemical shift assignment

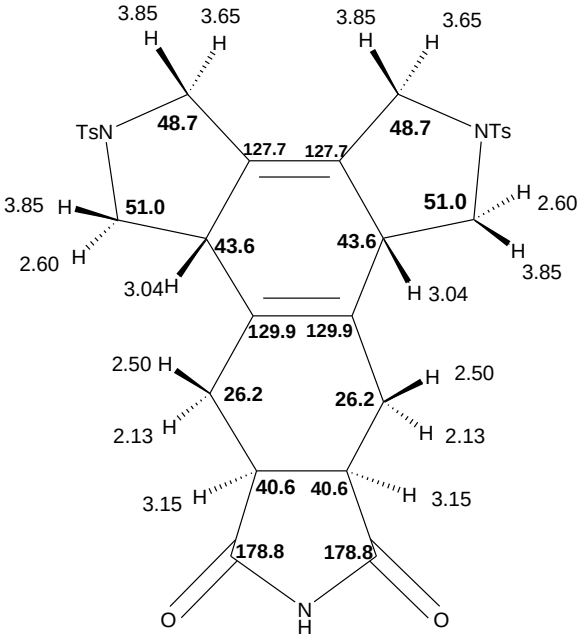

7,96

^{1}H NMR (400 MHz, $CDCl_3$)

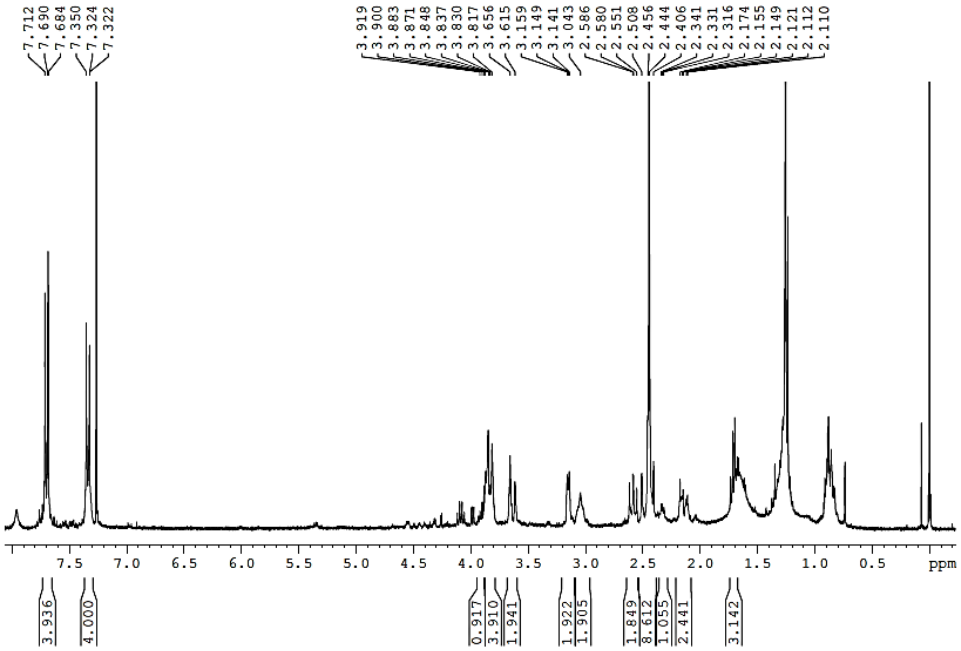

^{13}C NMR (100 MHz, $CDCl_3$)

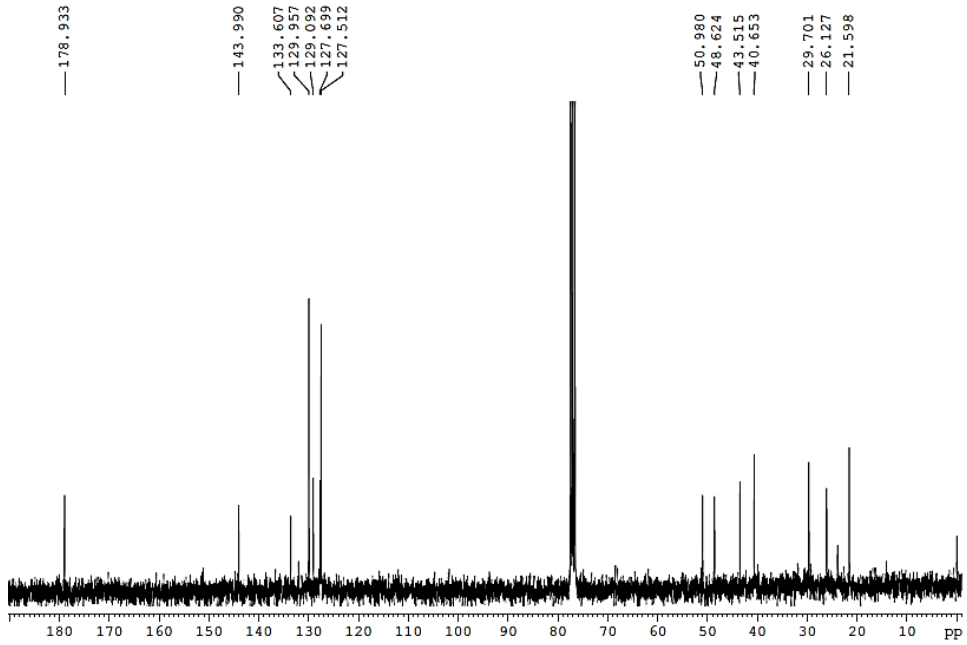

2D ^{1}H-^{1}H COSY

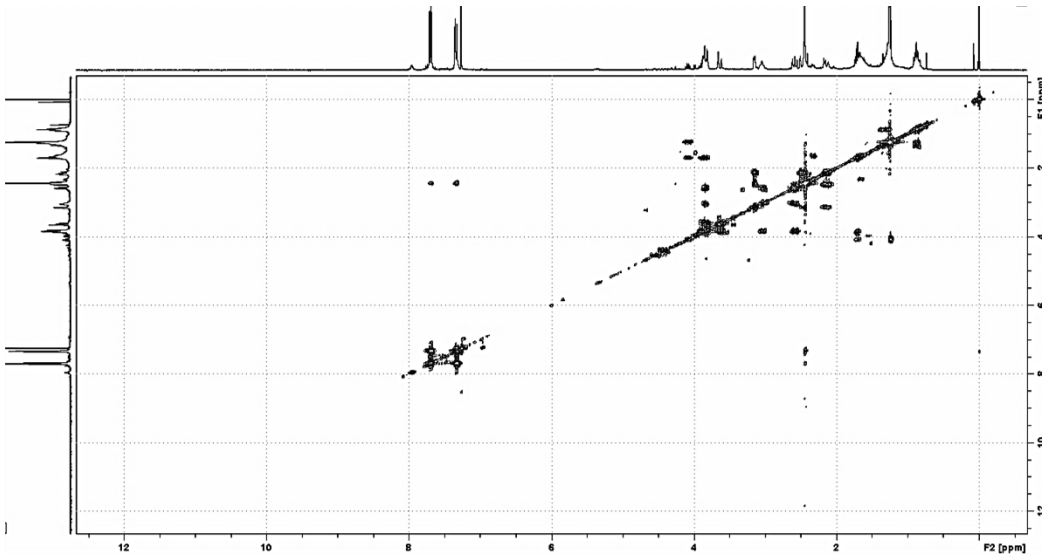

2D ^{1}H-^{1}H NOESY

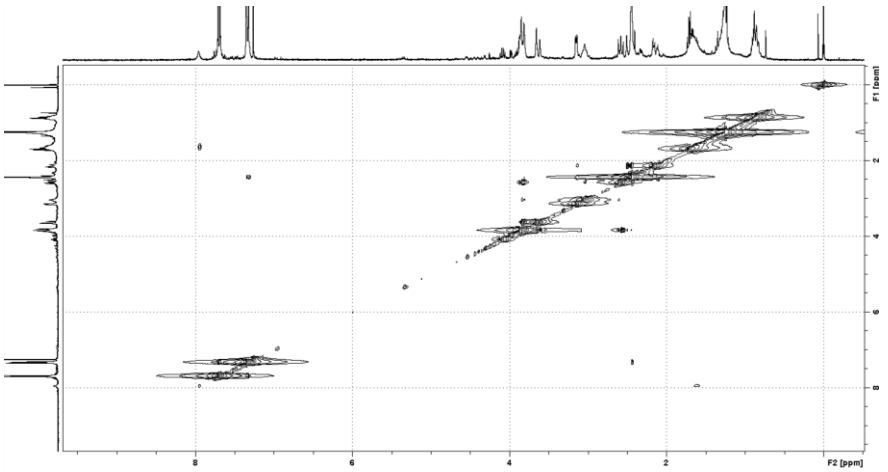

2D ^{1}H-^{13}C HSQC

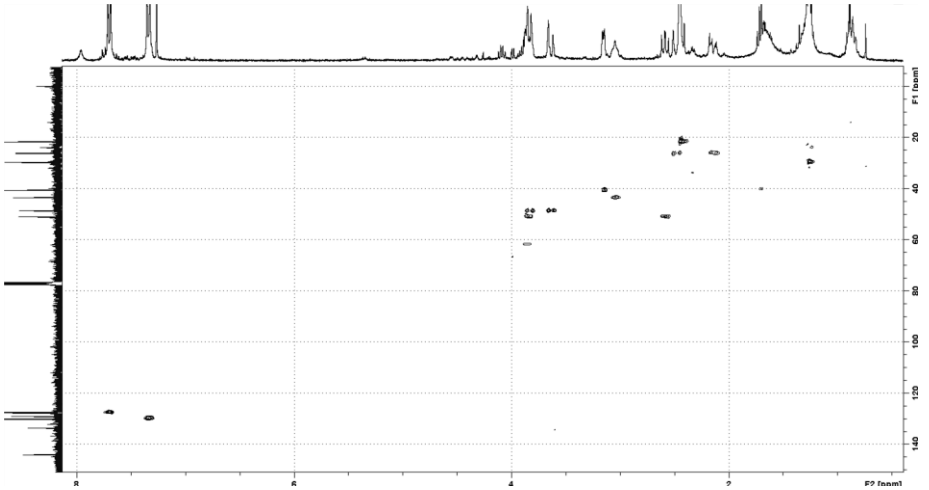

2D ^{1}H-^{13}C HMBC

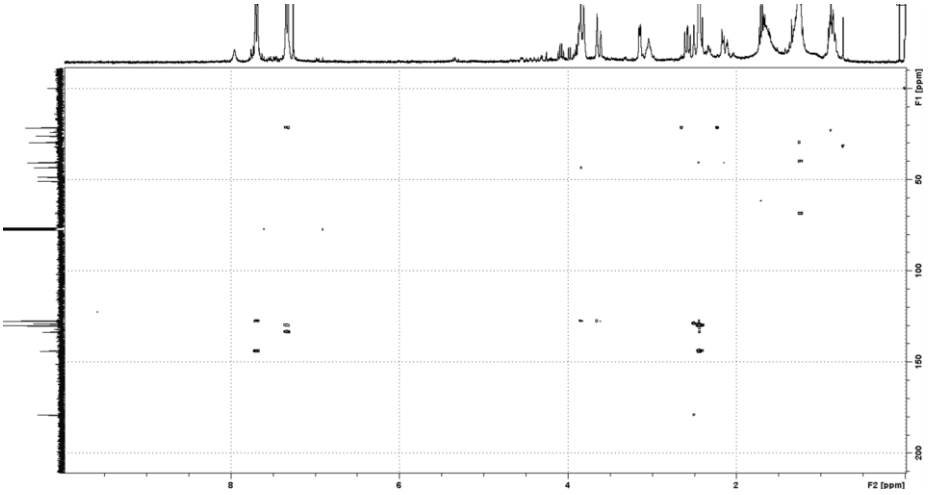

ESI-HRMS (+)

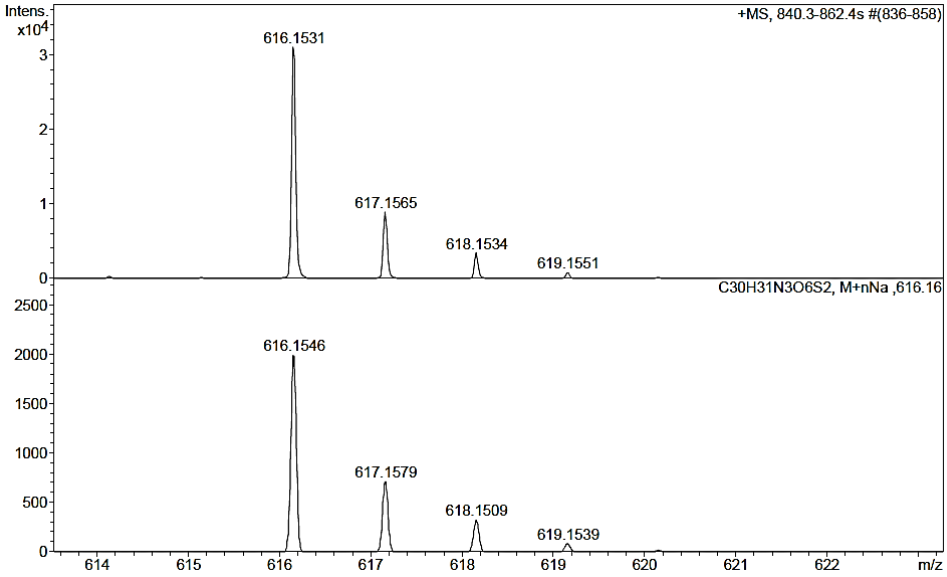

IR (ATR)

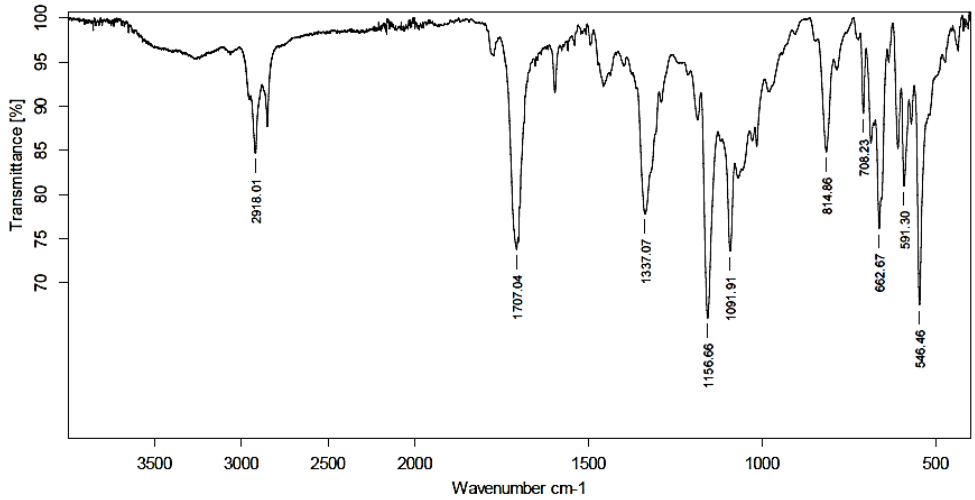

^{1}H NMR (400 MHz, $CDCl_3$)

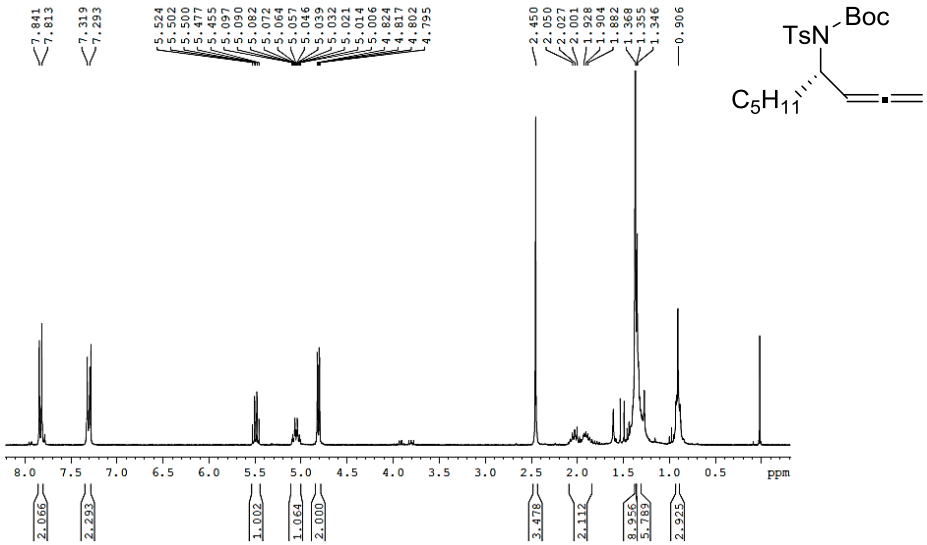

^{13}C NMR (100 MHz, $CDCl_3$)

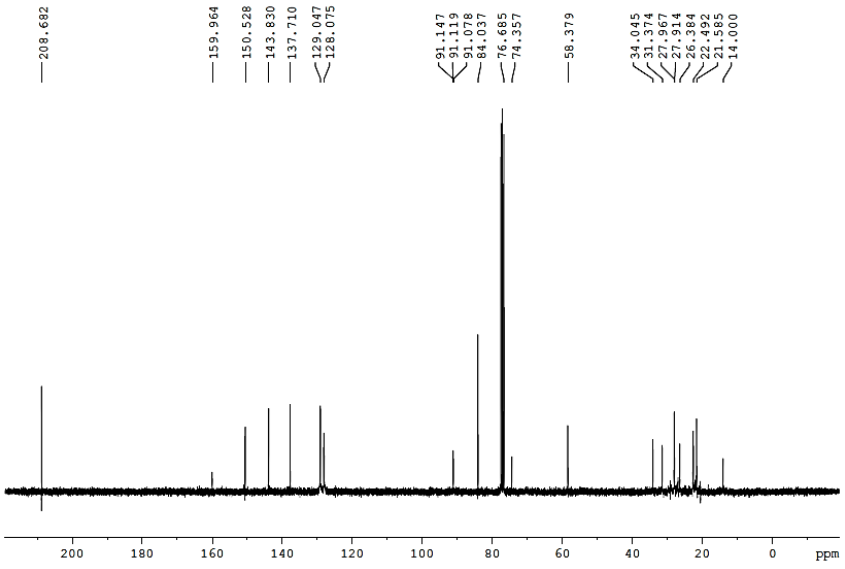

ESI-MS (+)

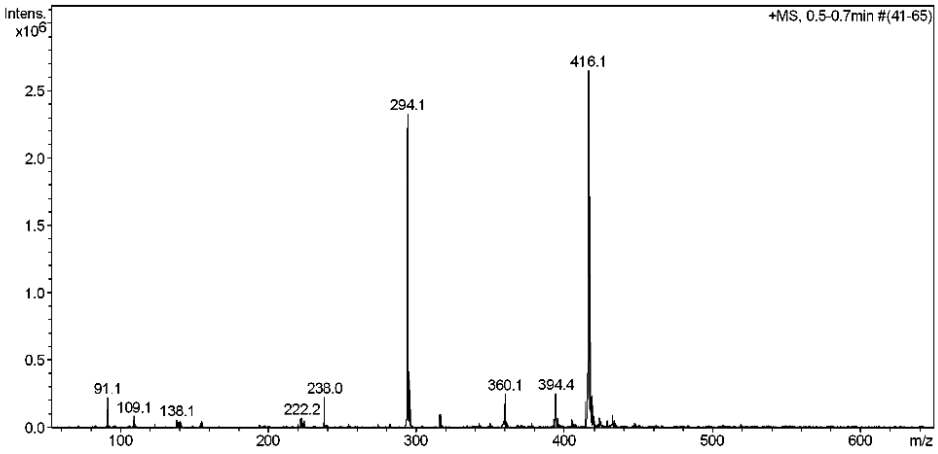
Intens.
x10^6
+MS, 0.5-0.7min #(41-65)
416.1
294.1
91.1
109.1
138.1
222.2
238.0
360.1
394.4
m/z

IR (ATR)

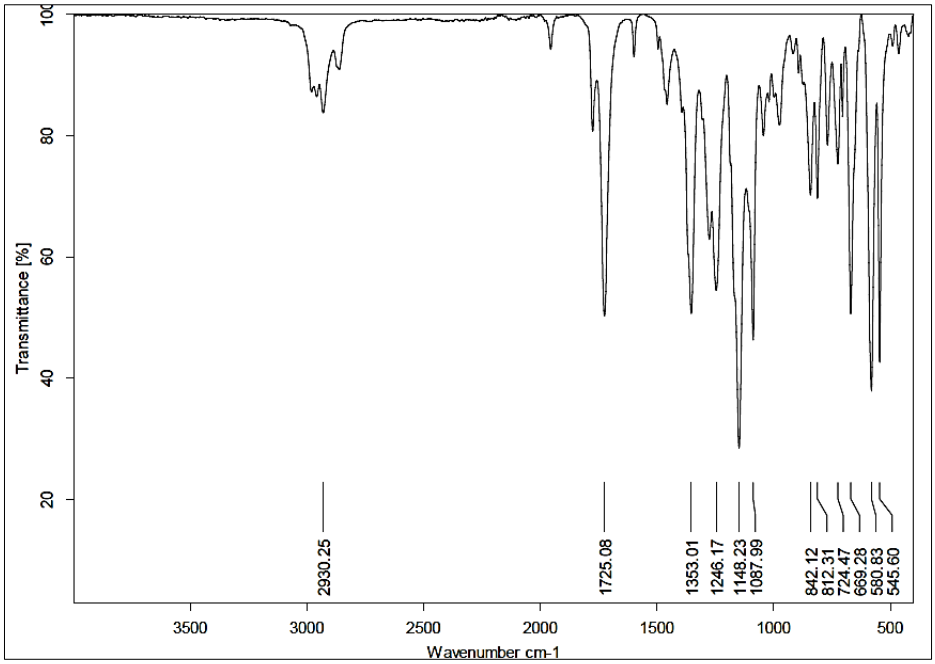
Transmittance [%]
2930.25
1725.08
1353.01
1246.17
1148.23
1087.99
842.12
812.31
724.47
669.28
580.83
545.60
Wavenumber cm-1

^{1}H NMR (300 MHz, $CDCl_3$)

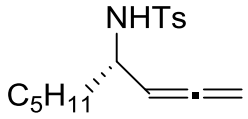

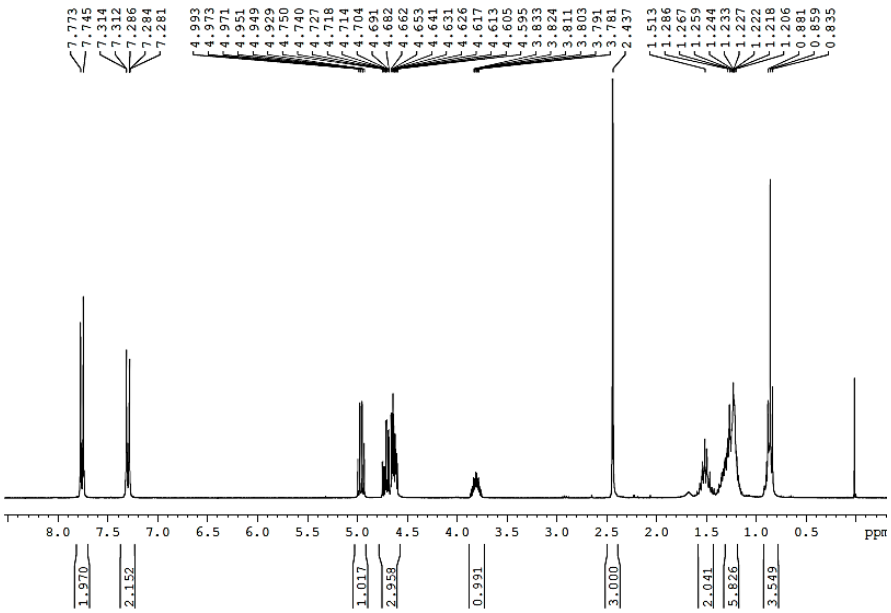

^{13}C NMR (75 MHz, $CDCl_3$)

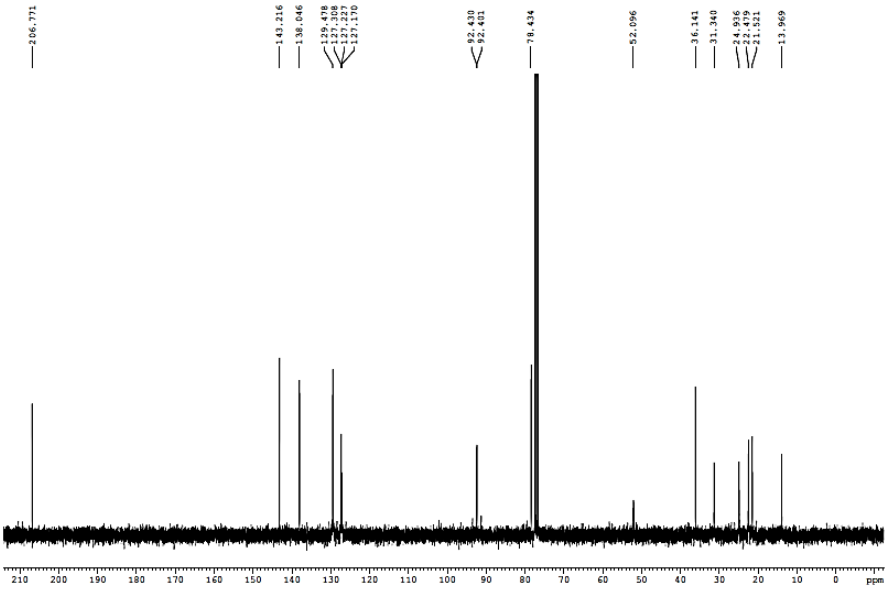

IR (ATR)

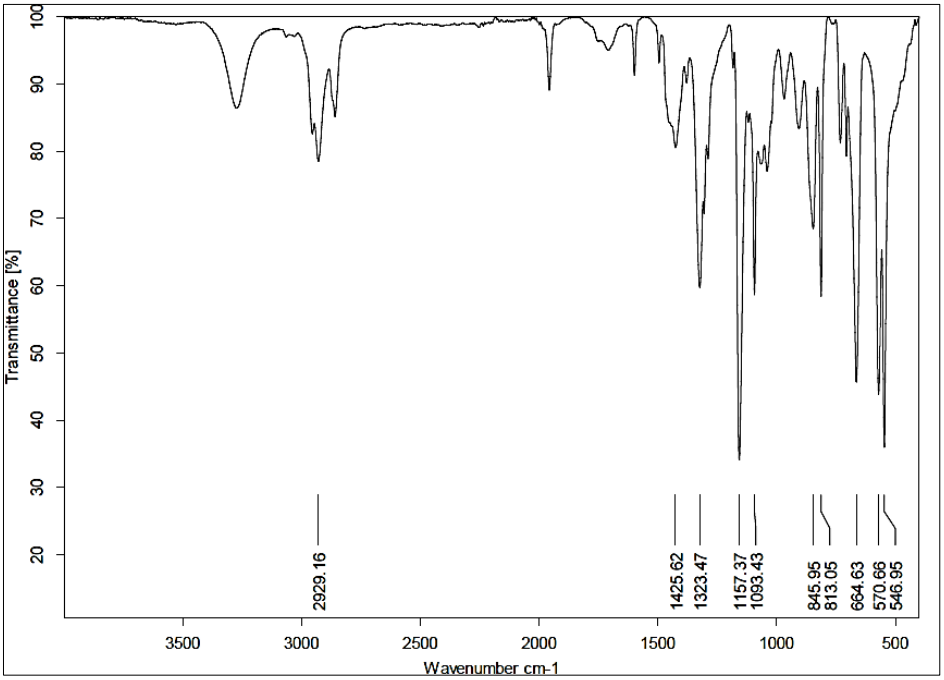
Transmittance [%]
100
90
80
70
60
50
40
30
20
2929.16
1425.62
1323.47
1157.37
1093.43
845.95
813.05
664.63
570.66
546.95
3500
3000
2500
2000
1500
1000
500
Wavenumber cm-1

ESI-MS (+)

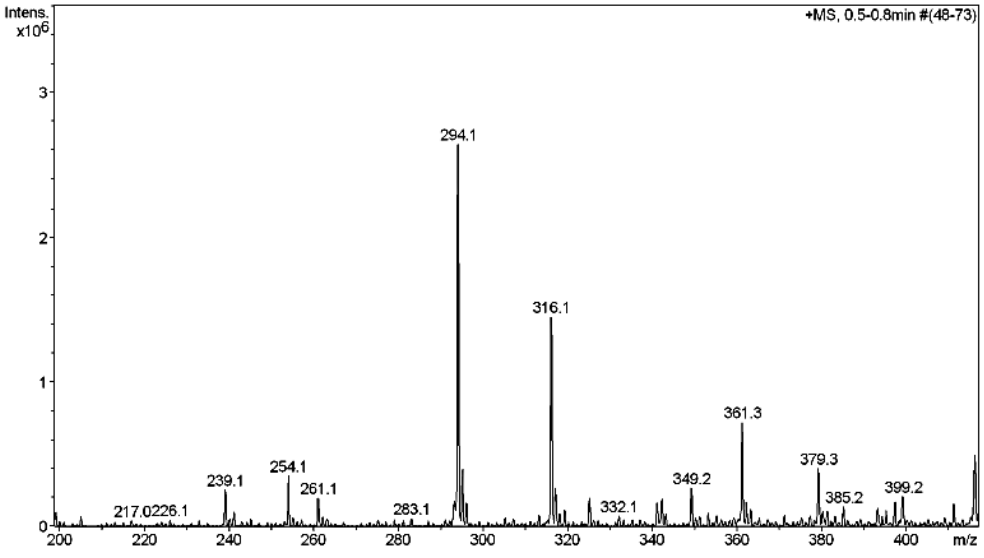
Intens.
x10^6
+MS, 0.5-0.8min #(48-73)
3
2
1
0
294.1
316.1
361.3
379.3
254.1
239.1
261.1
349.2
399.2
385.2
217.0226.1
283.1
332.1
200
220
240
260
280
300
320
340
360
380
400
m/z

^{1}H NMR (300 MHz, $CDCl_3$)

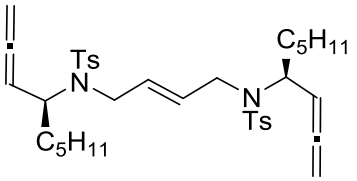

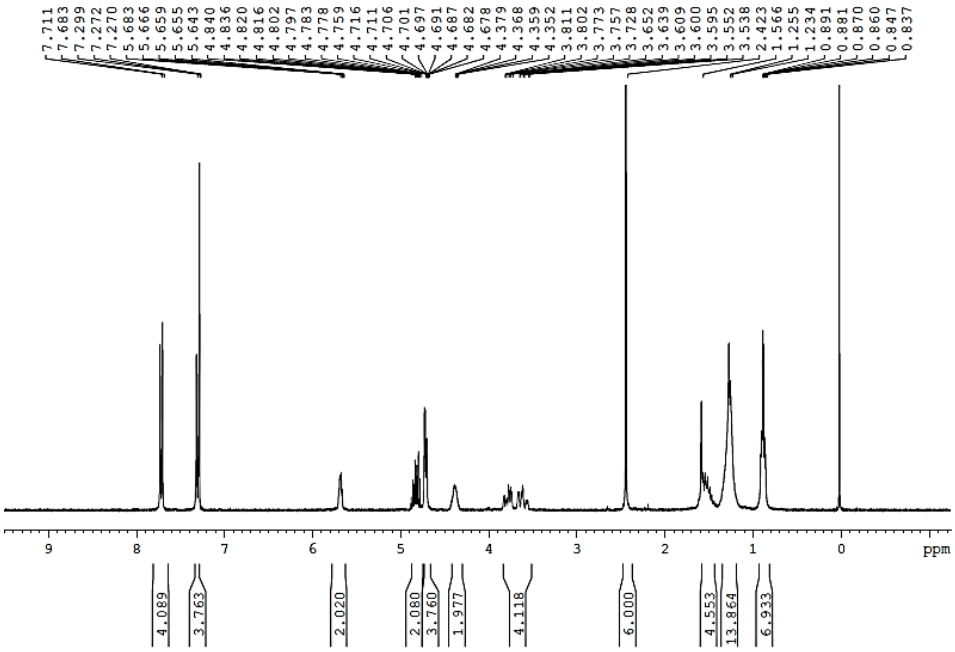

^{13}C NMR (75 MHz, $CDCl_3$)

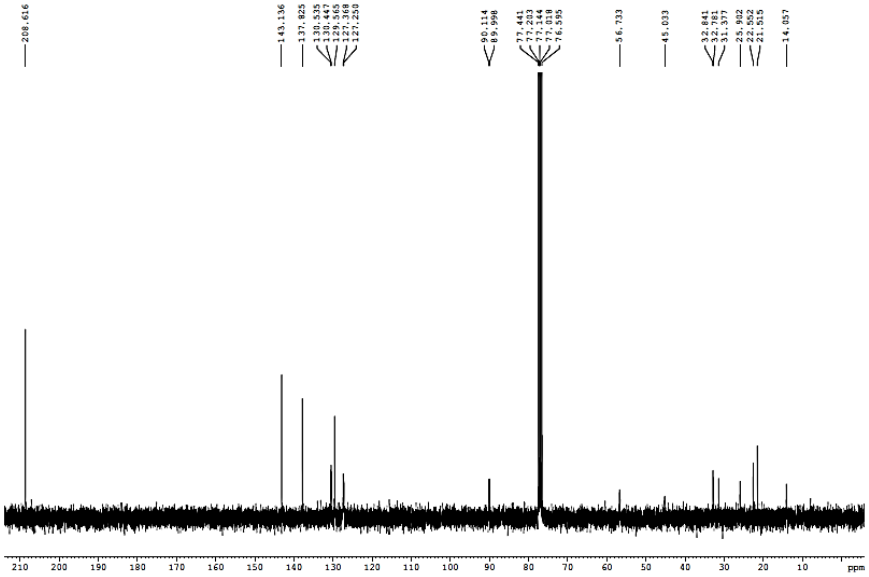

ESI-MS (+)

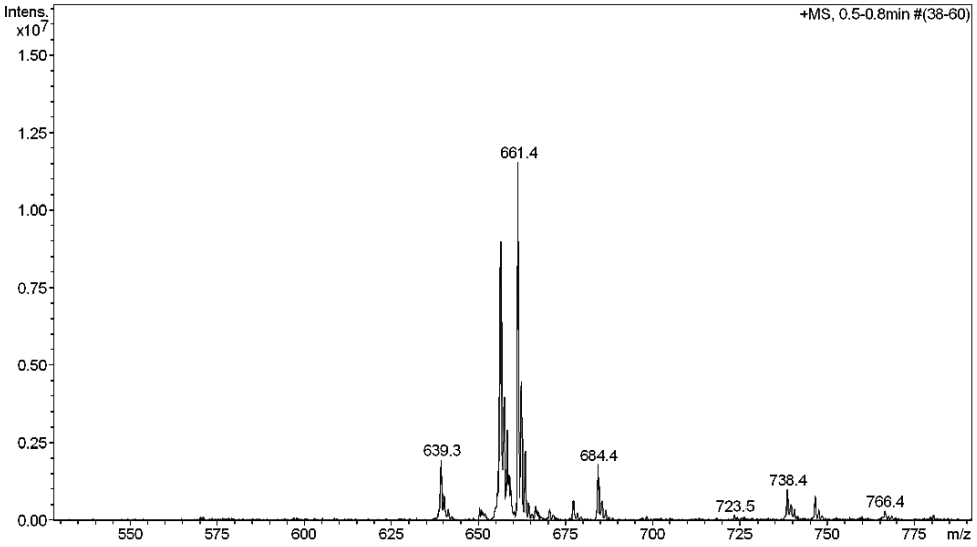
Intens.
x10^7
+MS, 0.5-0.8min #(38-60)
1.50
1.25
1.00
0.75
0.50
0.25
0.00
661.4
639.3
684.4
738.4
723.5
766.4
550
575
600
625
650
675
700
725
750
775
m/z

IR (ATR)

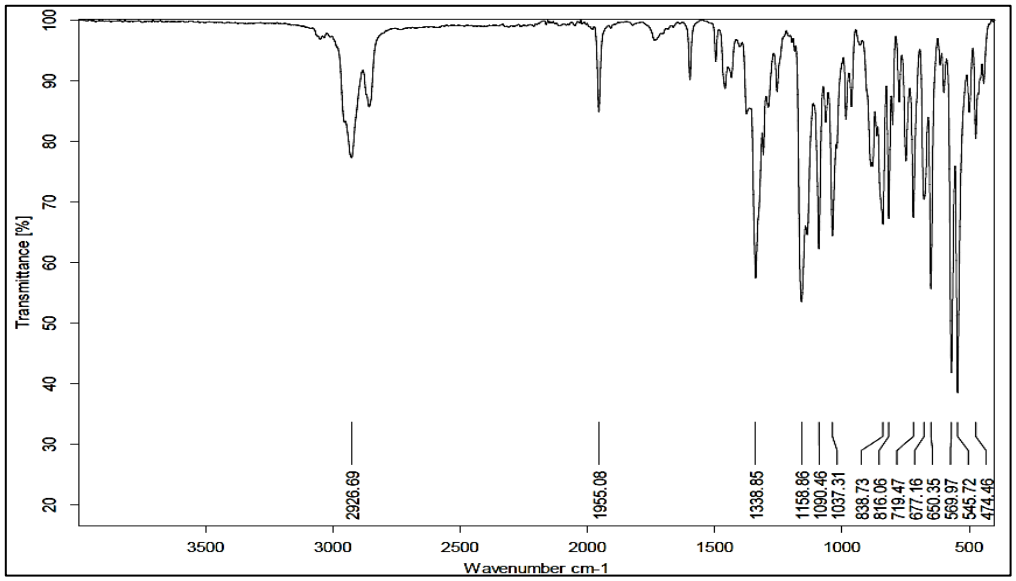
Transmittance [%]
100
90
80
70
60
50
40
30
20
2926.69
1955.08
1338.85
1158.86
1090.46
1037.31
838.73
816.06
719.47
677.16
650.35
569.97
545.72
474.46
3500
3000
2500
2000
1500
1000
500
Wavenumber cm-1

^{1}H NMR (300 MHz, $CDCl_3$)

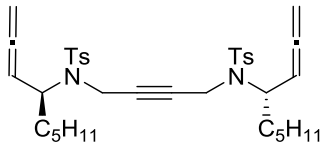

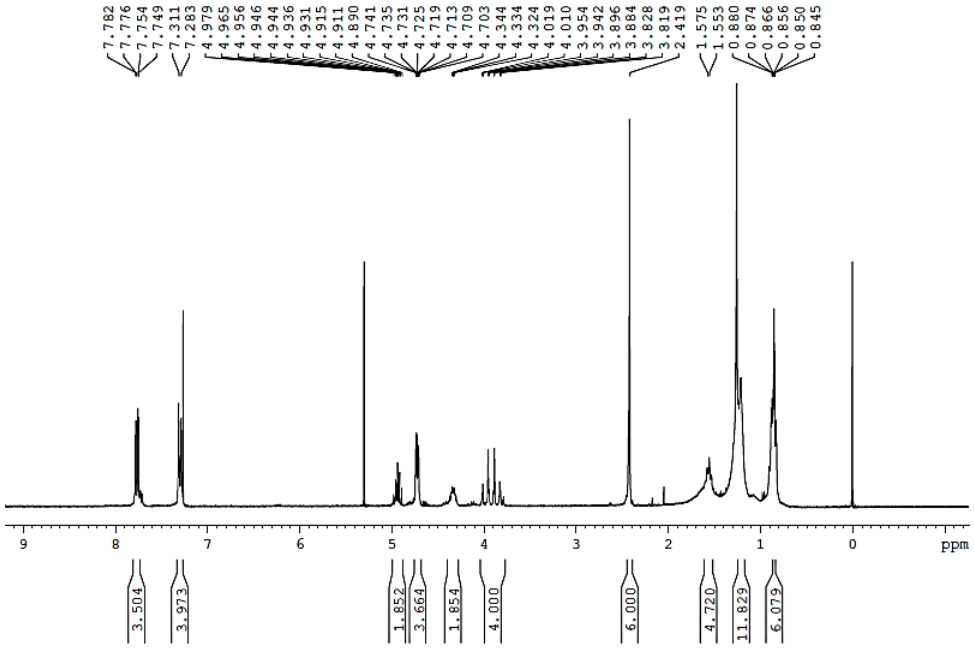

^{13}C NMR (100 MHz, $CDCl_3$)

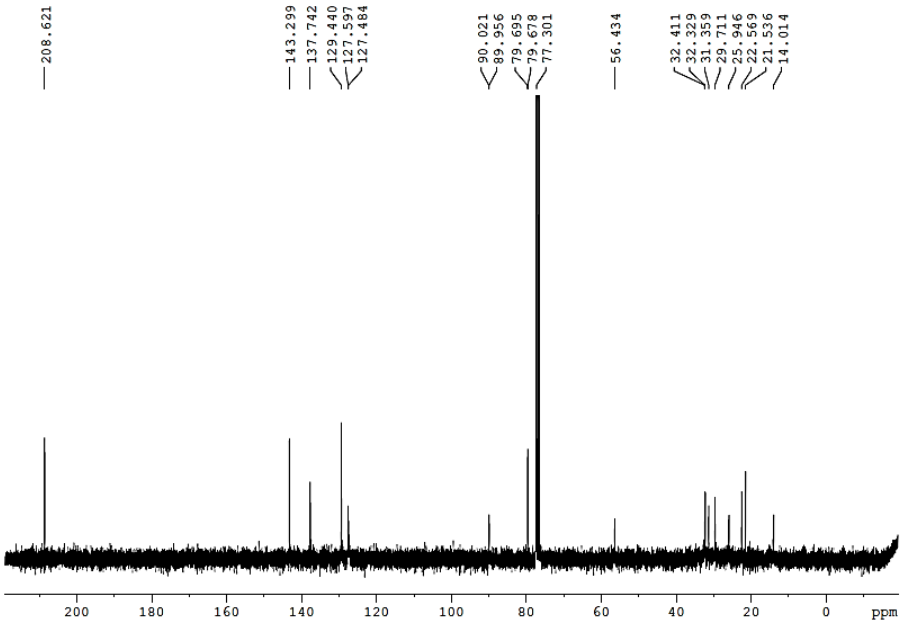

ESI-HRMS (+)

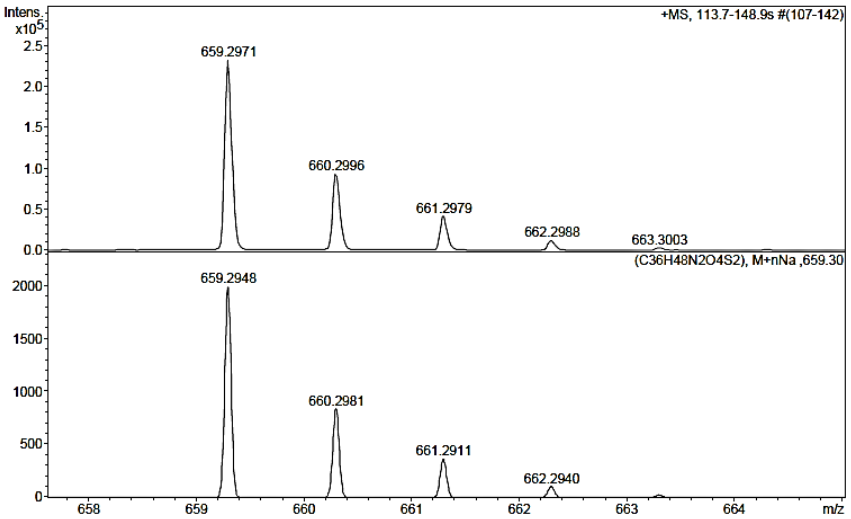

IR (ATR)

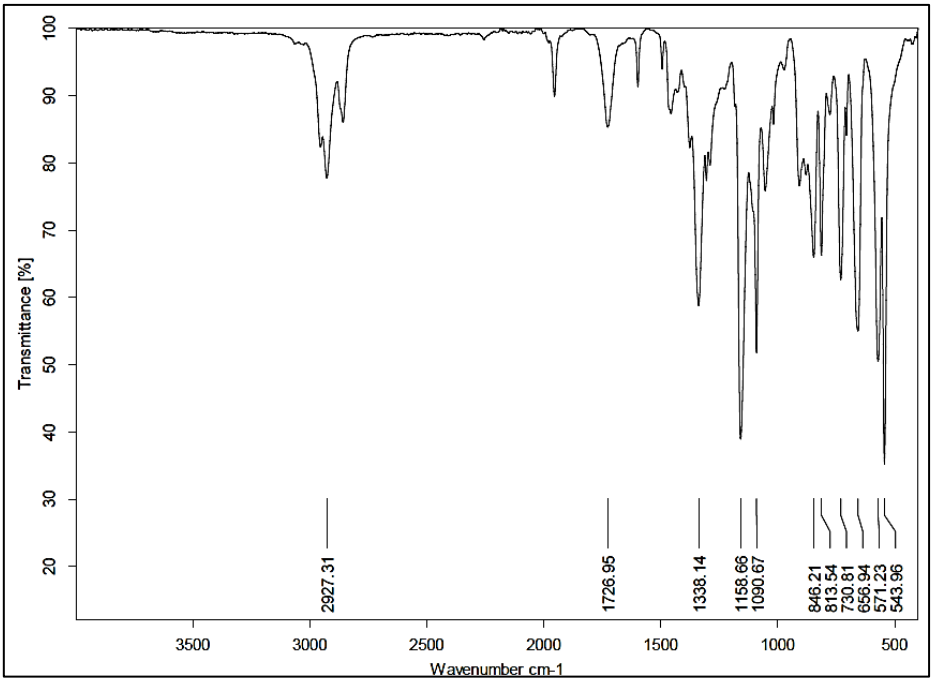

^{1}H NMR (300 MHz, $CDCl_3$)

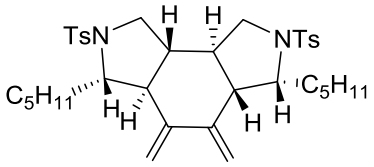

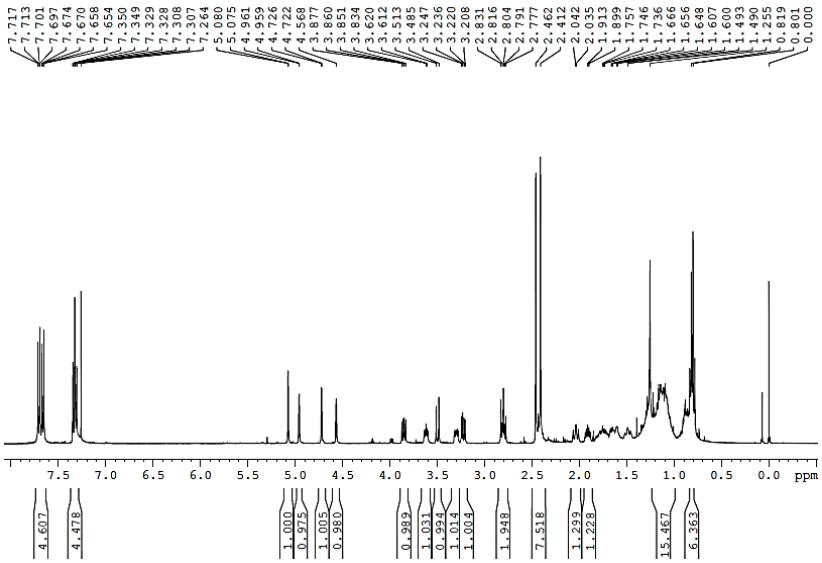

^{13}C NMR (75 MHz, $CDCl_3$)

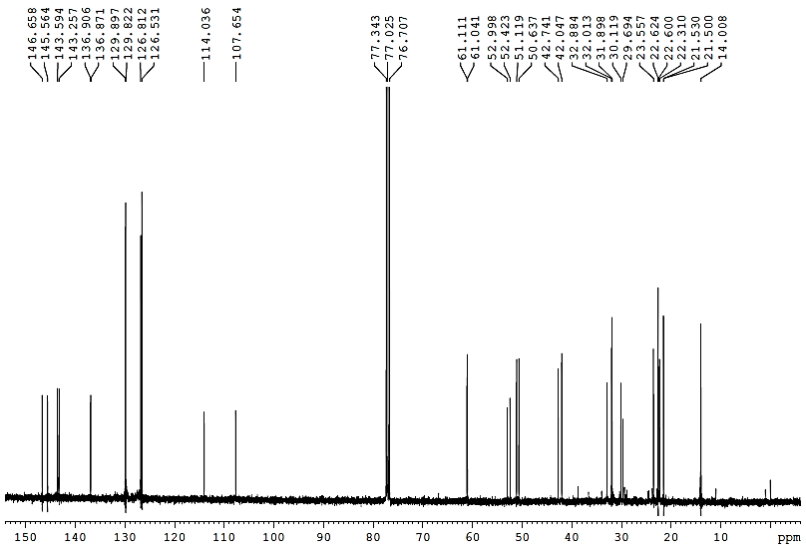

2D ^{1}H - ^{13}C HSQC

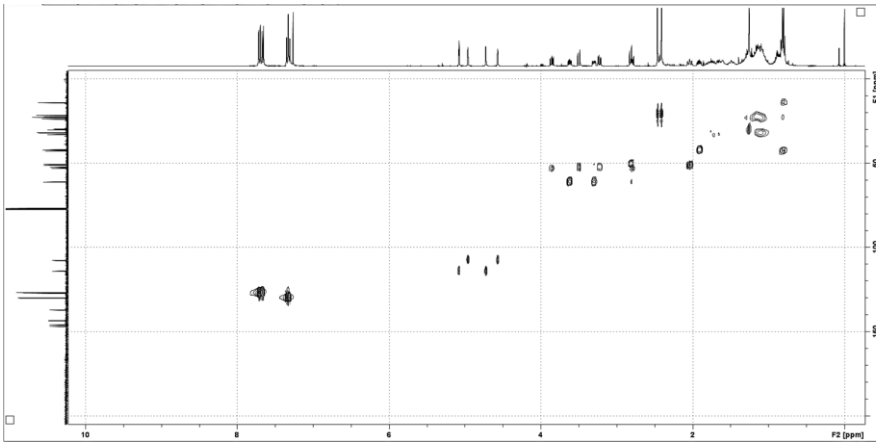

2D ^{1}H - ^{13}C HMBC

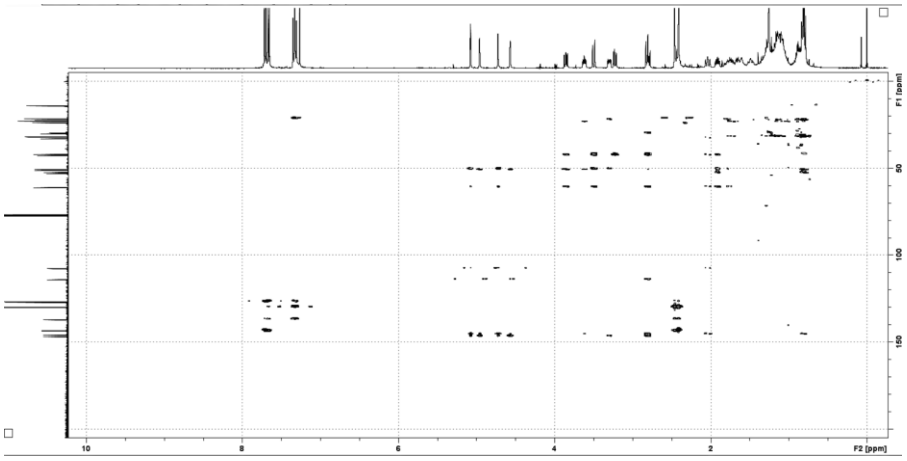

2D ^{1}H – ^{1}H COSY

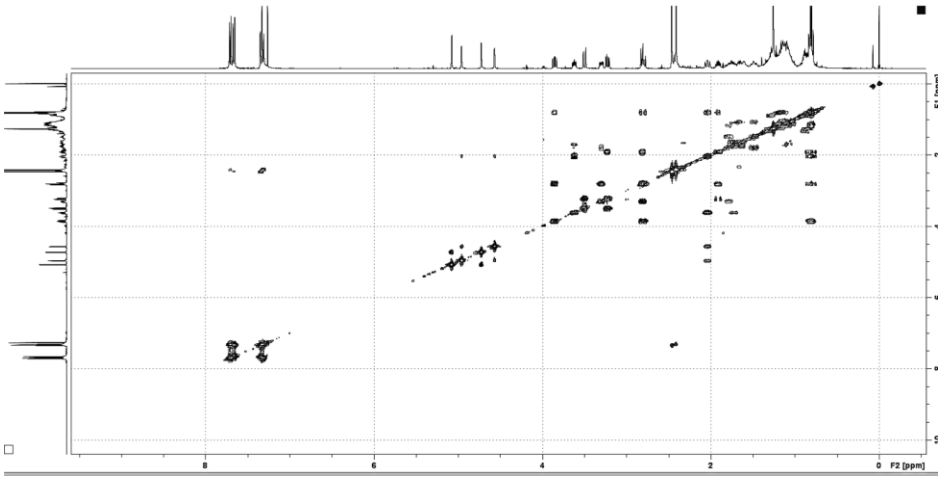

2D $^{1}H - {}^{1}H$ NOESY

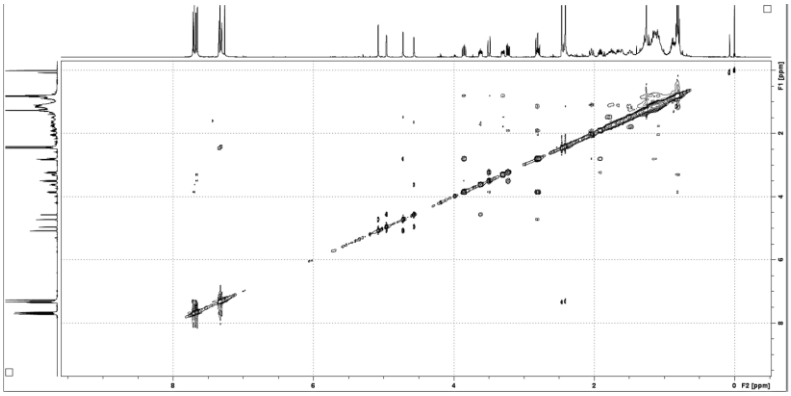

ESI-HRMS (+)

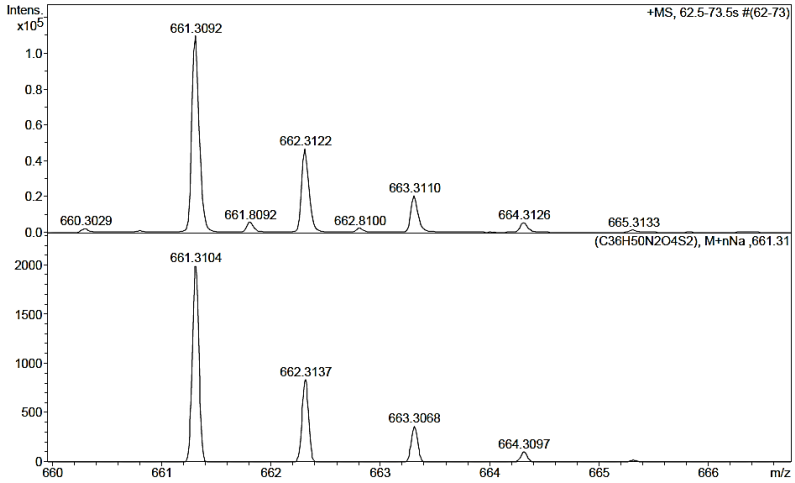

IR (ATR)

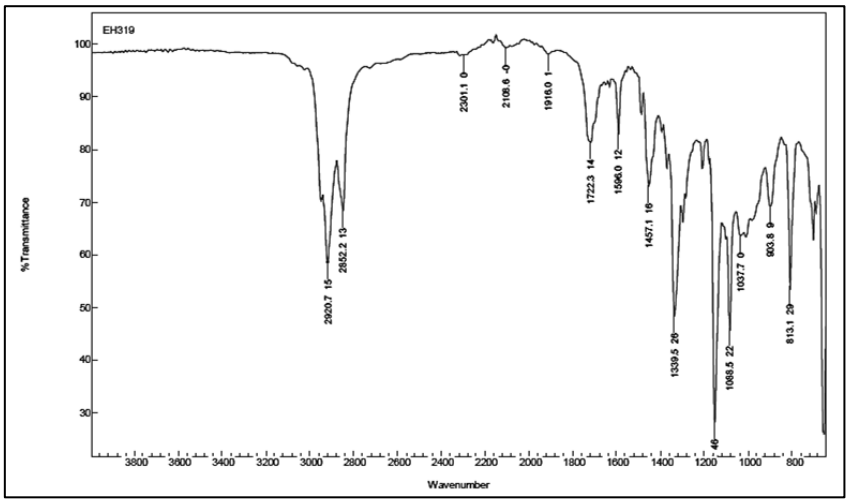

^{1}H NMR (300 MHz, $CDCl_3$)

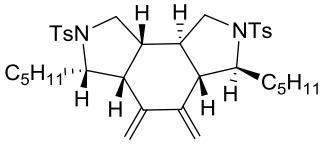

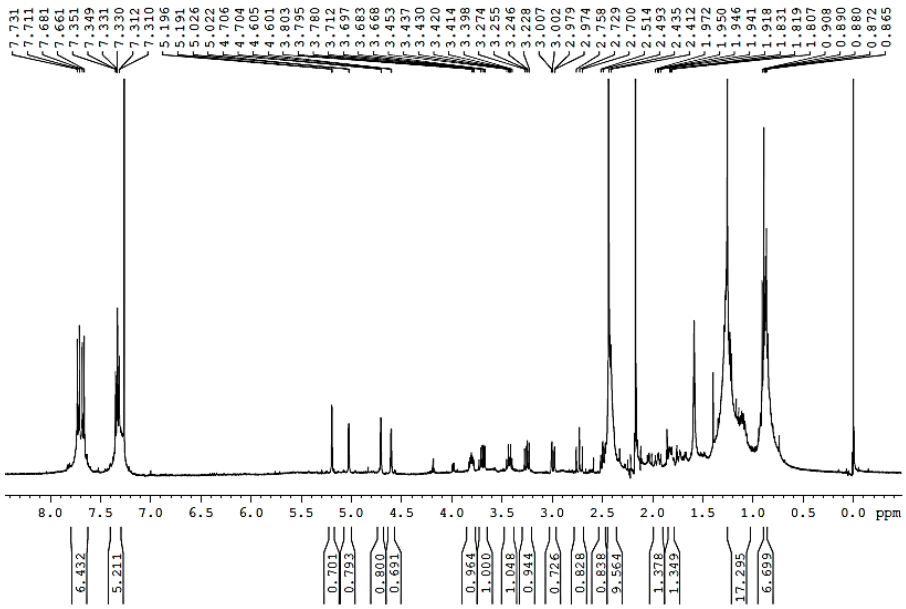

^{13}C NMR (75 MHz, $CDCl_3$)

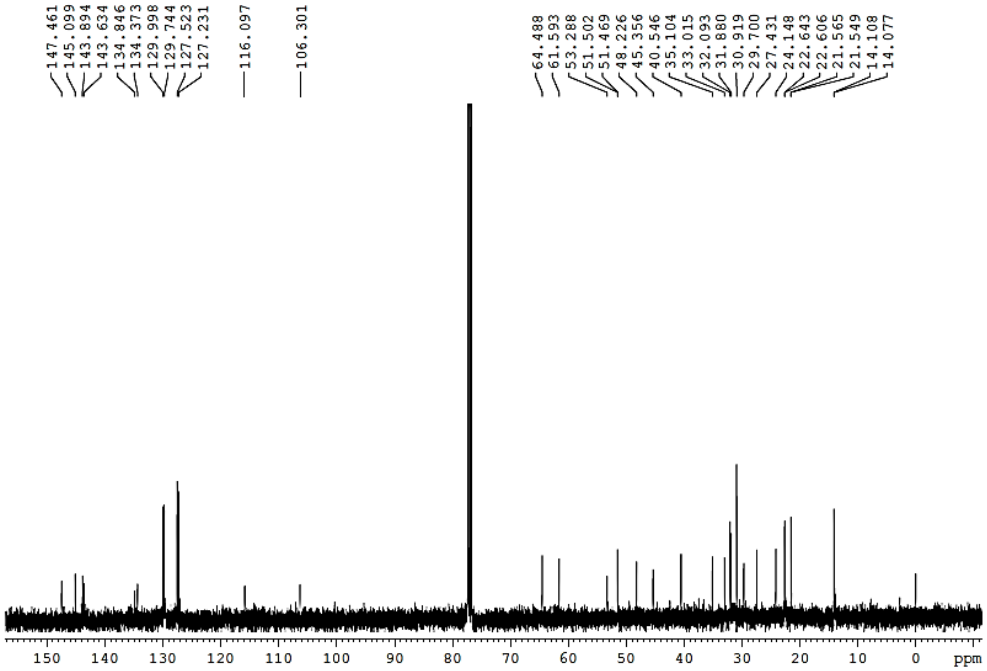

2D $^{1}H - ^{13}C$ HSQC

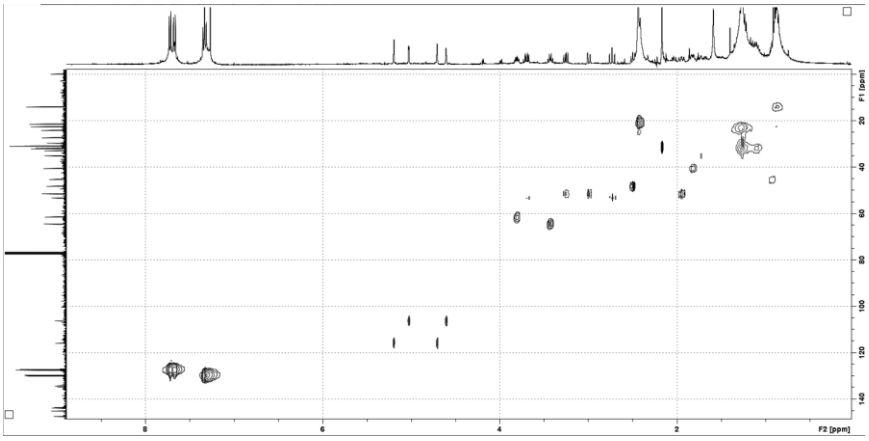

2D $^{1}H - ^{13}C$ HMBC

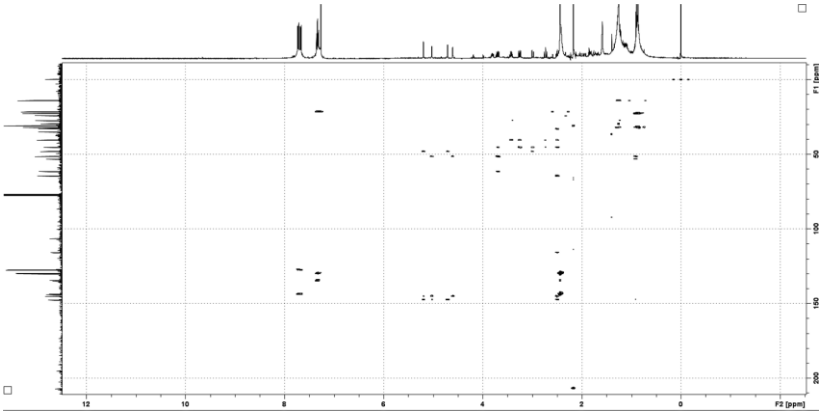

2D $^{1}H - ^{1}H$ COSY

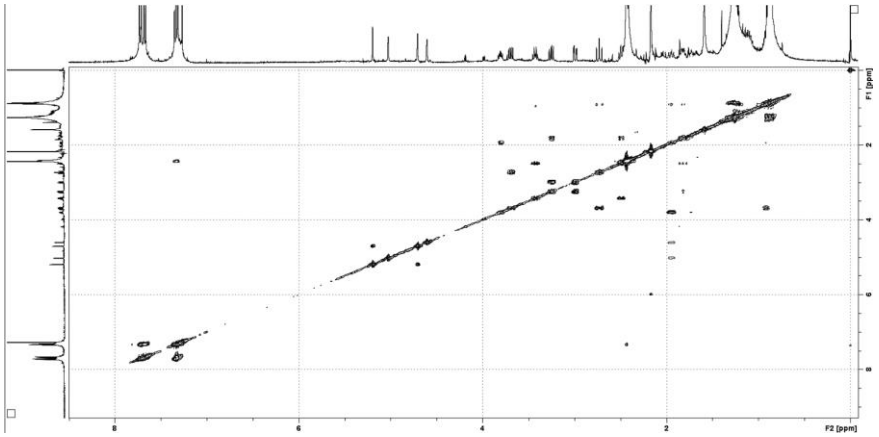

2D ^{1}H – ^{1}H NOESY

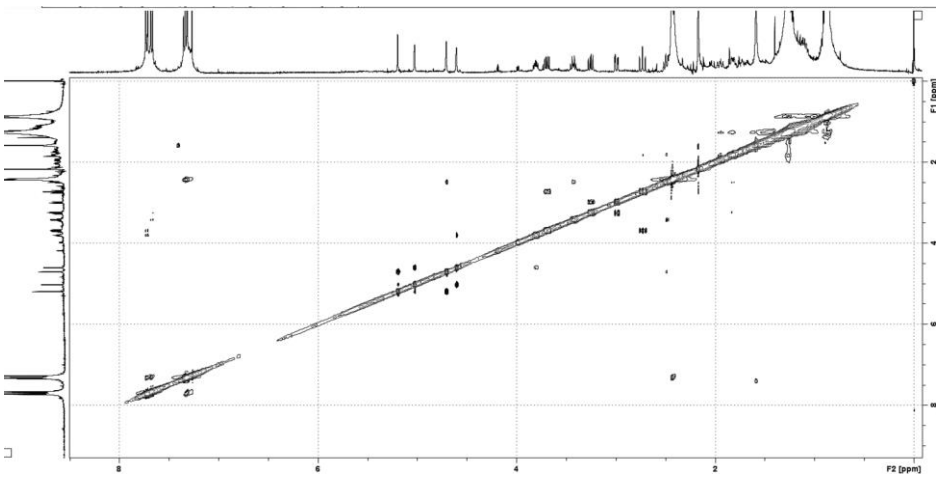

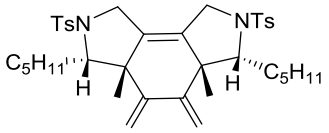

^{1}H NMR (300 MHz, $CDCl_3$)

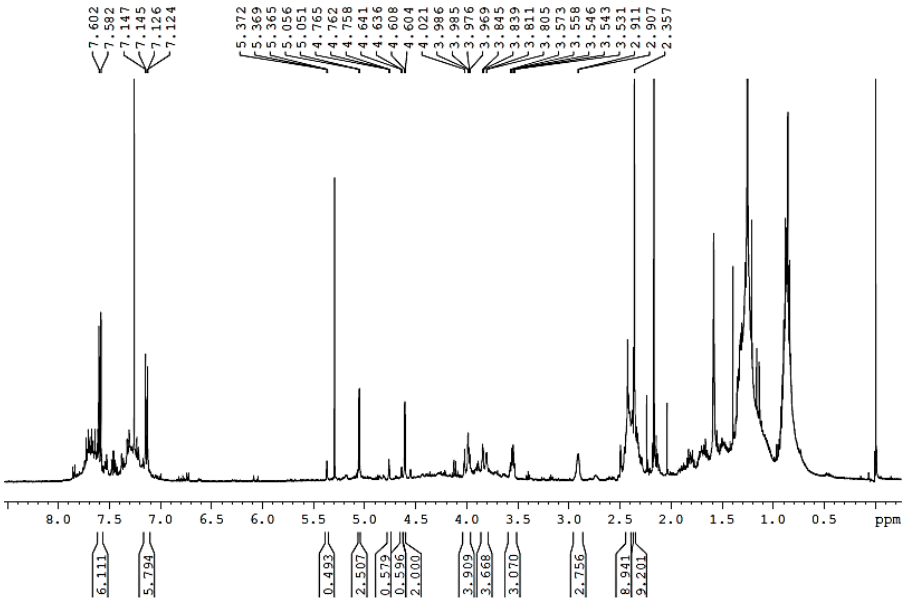

^{13}C NMR (75 MHz, $CDCl_3$)

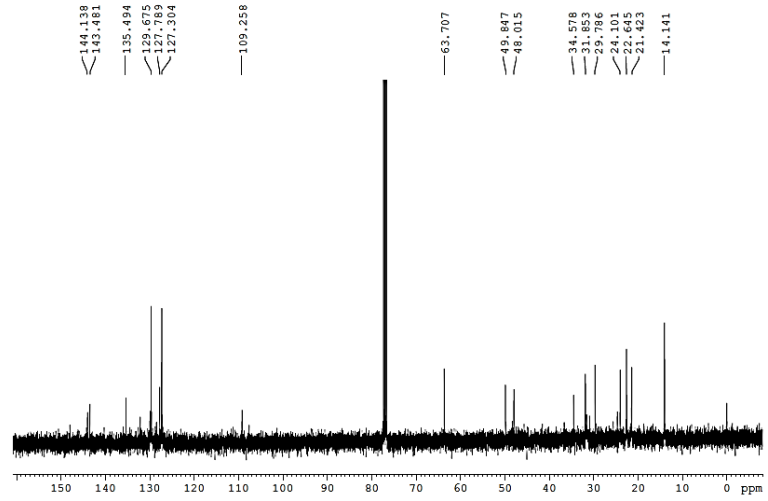

ESI-HRMS (+)

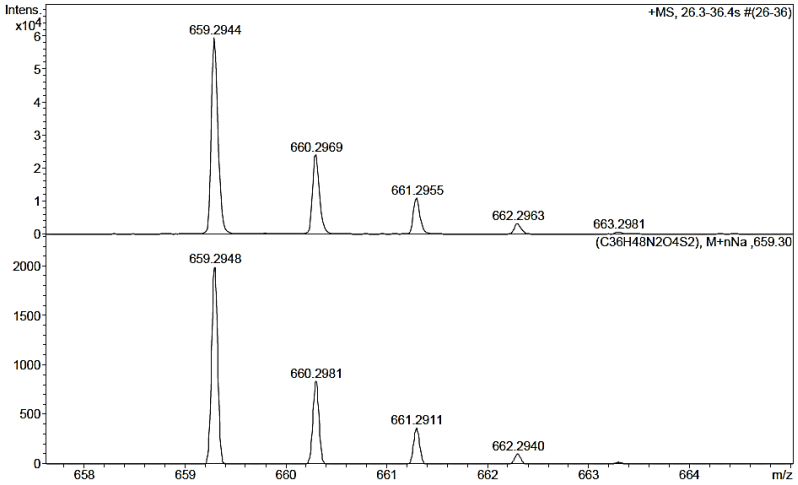

IR (ATR)

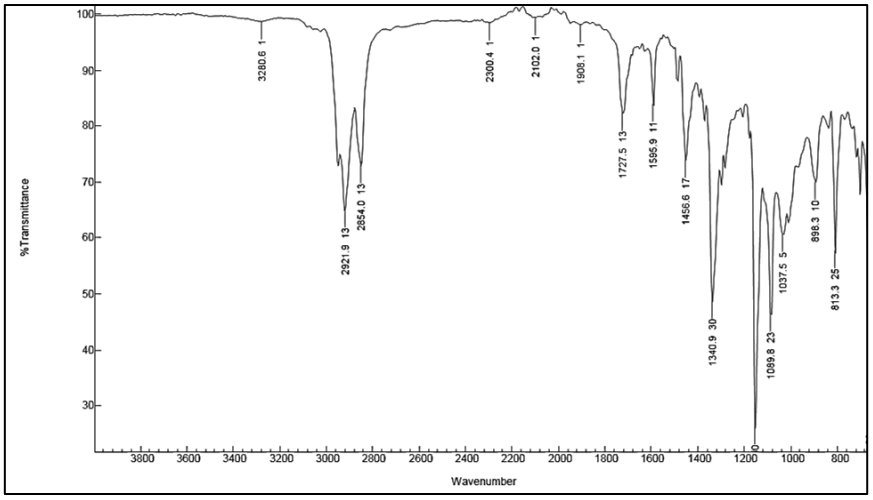

2D ^{1}H – ^{1}H NOESY

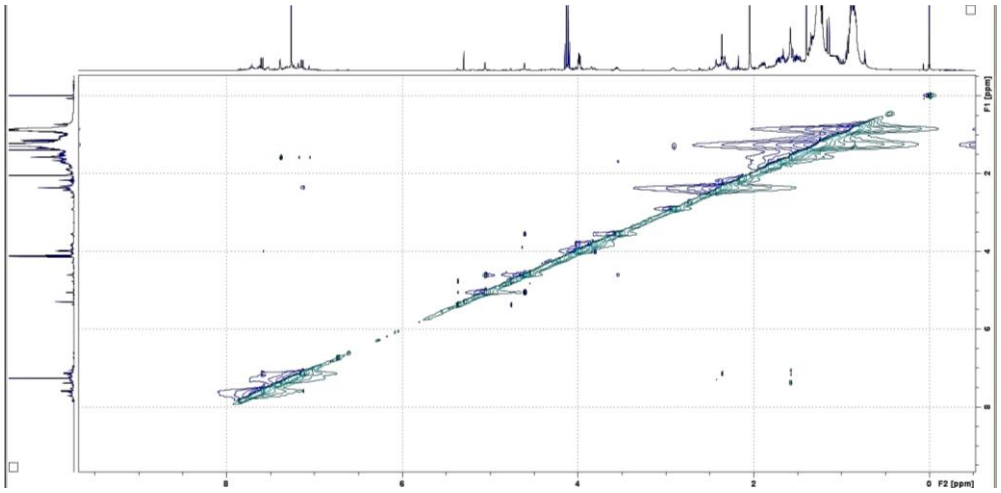

2D ^{1}H – ^{1}H COSY

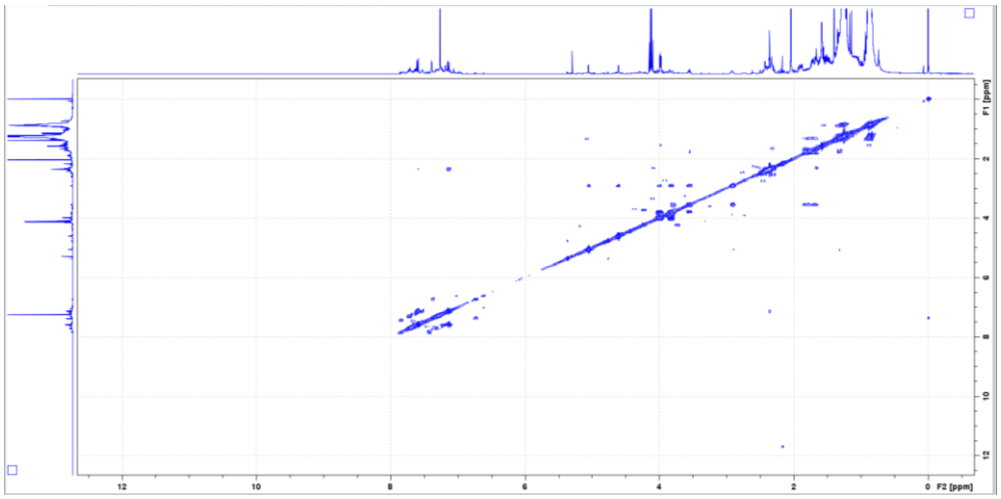

2D ^{1}H – ^{13}C HSQC

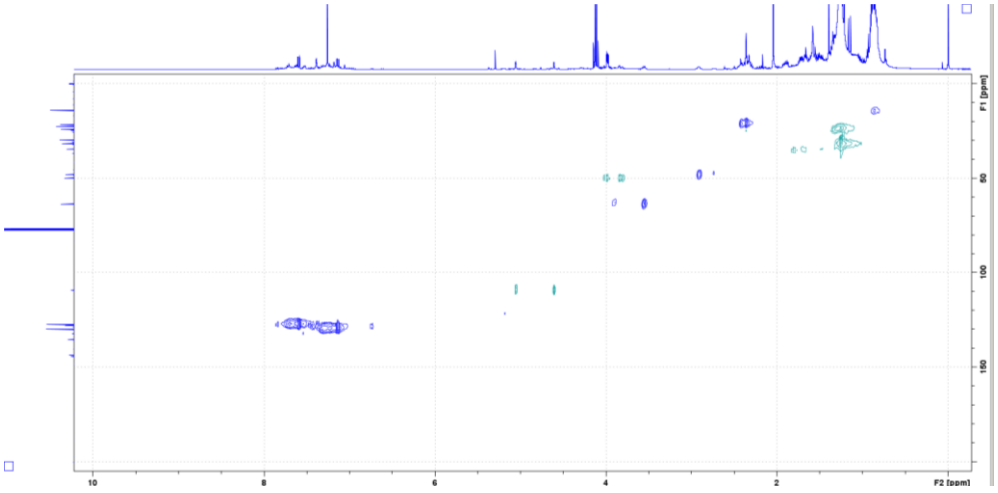

^{1}H NMR (300 MHz, $CDCl_3$)

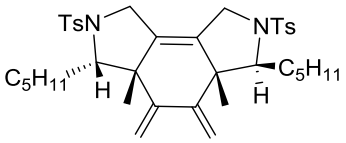

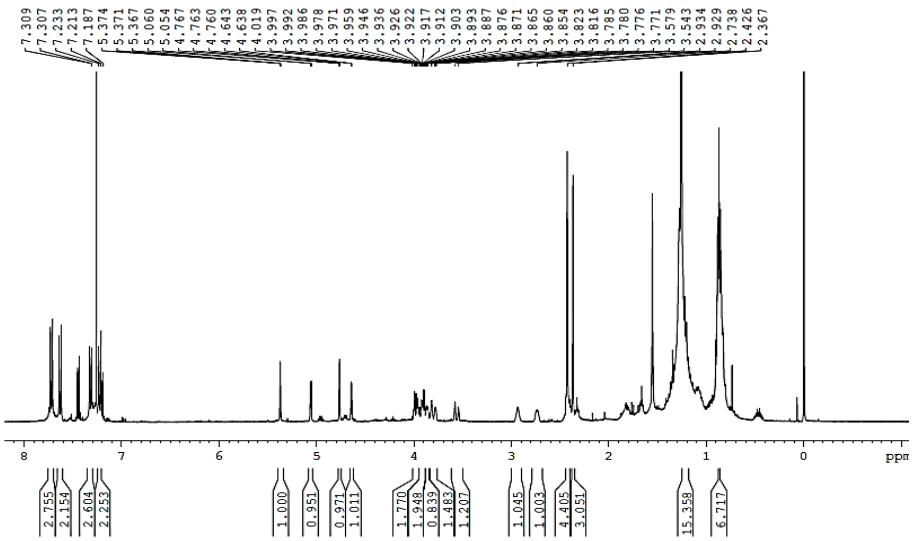

^{13}C NMR (100 MHz, $CDCl_3$)

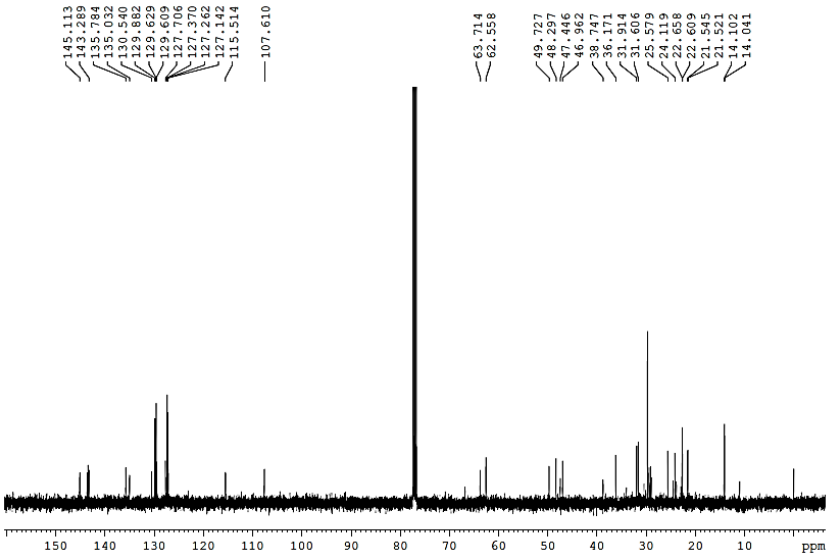

2D ^{1}H – ^{13}C HSQC

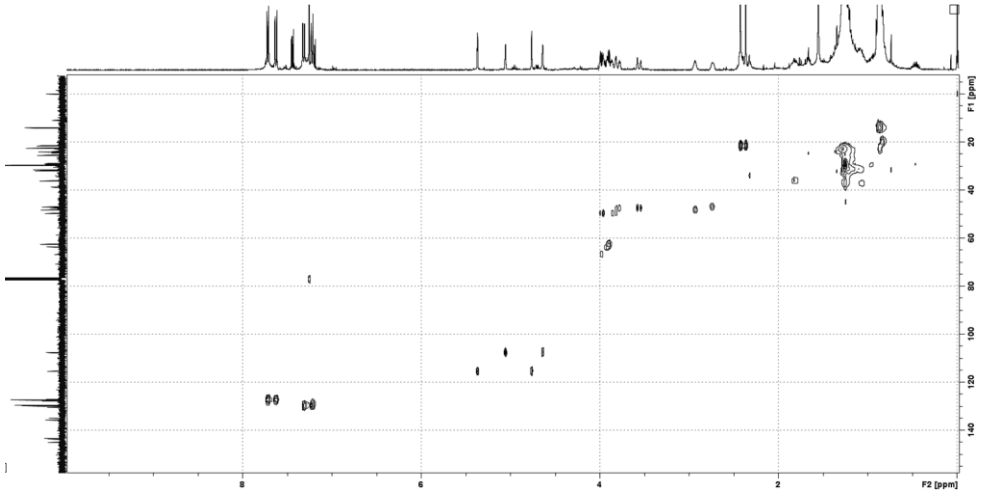

2D ^{1}H – ^{13}C HMBC

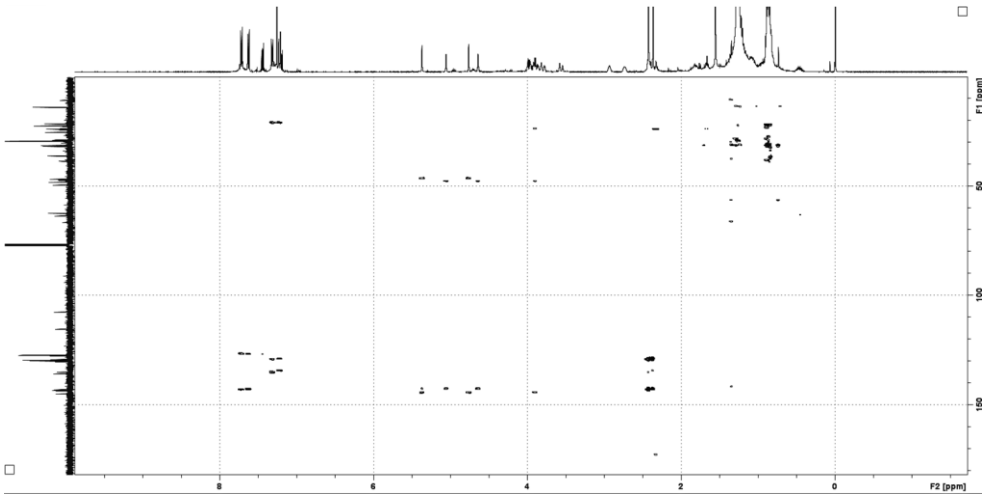

2D $^{1}H - ^{1}H$ COSY

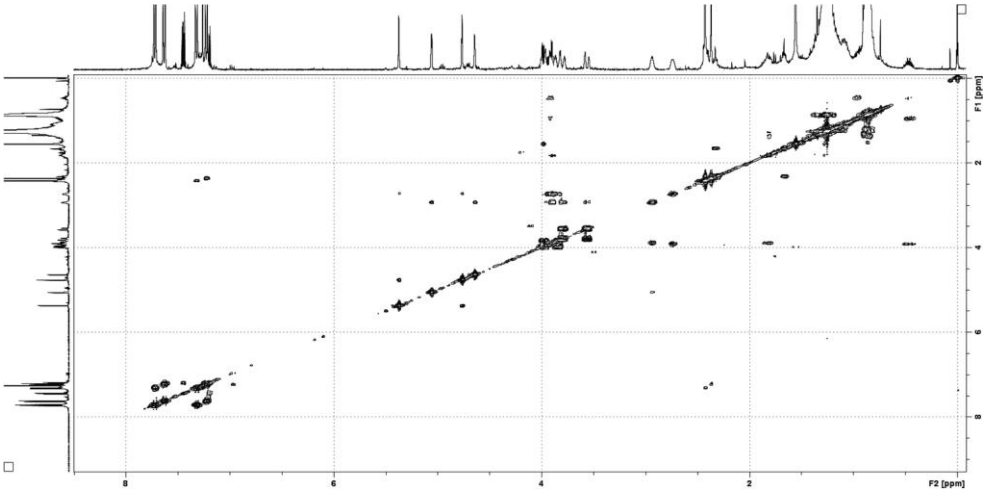

2D $^{1}H - ^{1}H$ NOESY

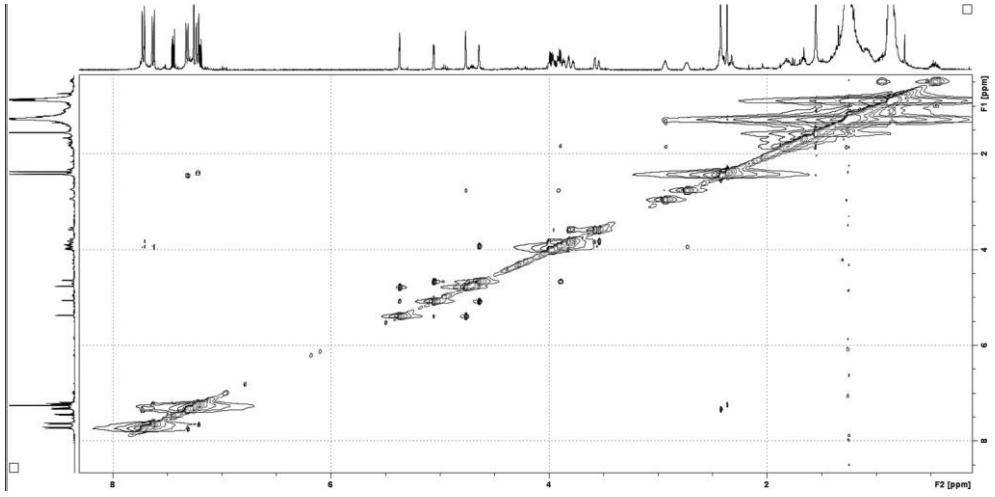

Figure 1. Chromatogram of (*S,S*)-**15** (using IPA/Heptane 2:98 as a eluent)

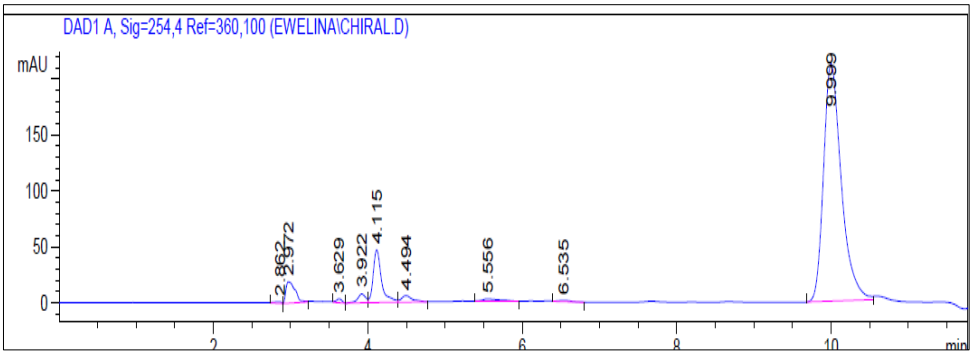

Figure 2. Chromatogram of **15** (using IPA/Heptane 2:98 as a eluent)

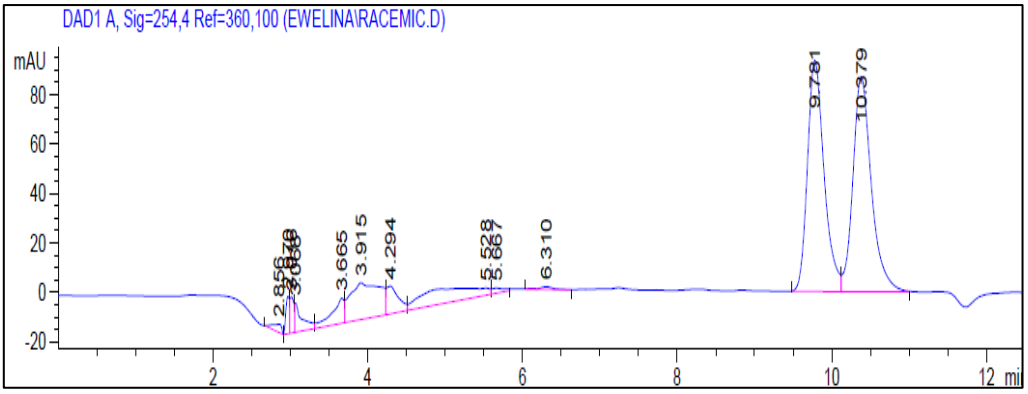

Figure 3. Chromatogram of (*S,S*)-**13** (using IPA/Heptane 10:90 as a eluent)

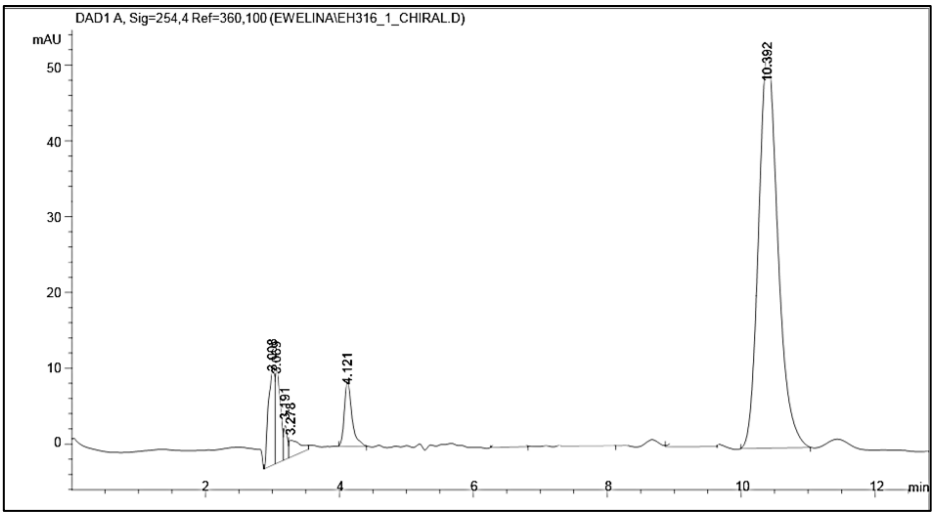

Figure 4. Chromatogram of **13** (using IPA/Heptane 10:90 as a eluent)

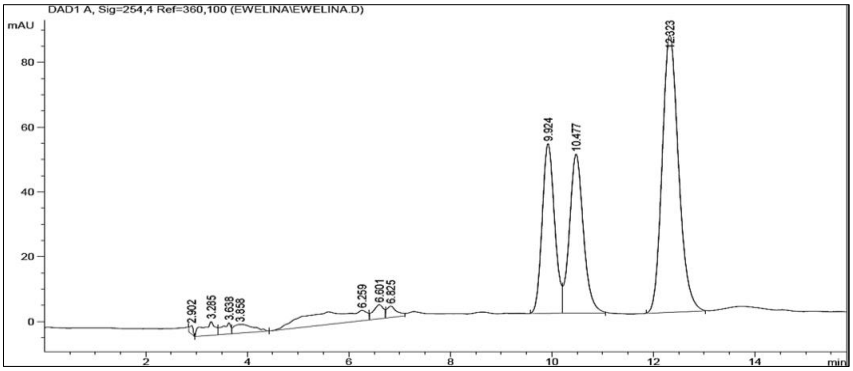

Figure 5. Chromatogram of (*S,S*)-**14** (using IPA/Heptane 8:92 as a eluent)

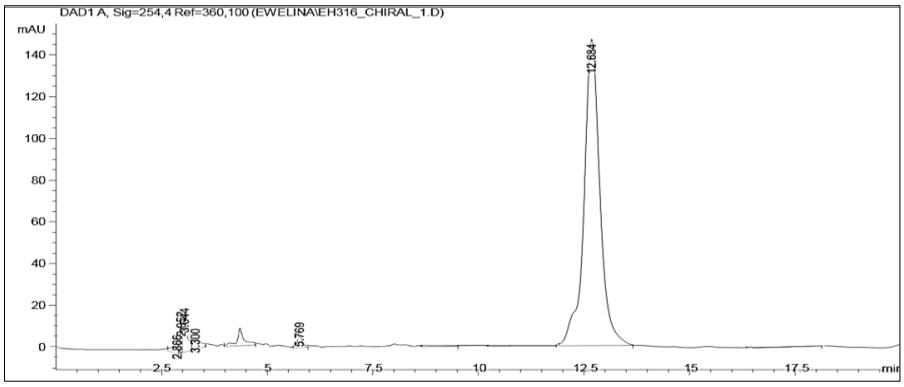

Figure 6. Chromatogram of **14** (using IPA/Heptane 8:92 as a eluent)

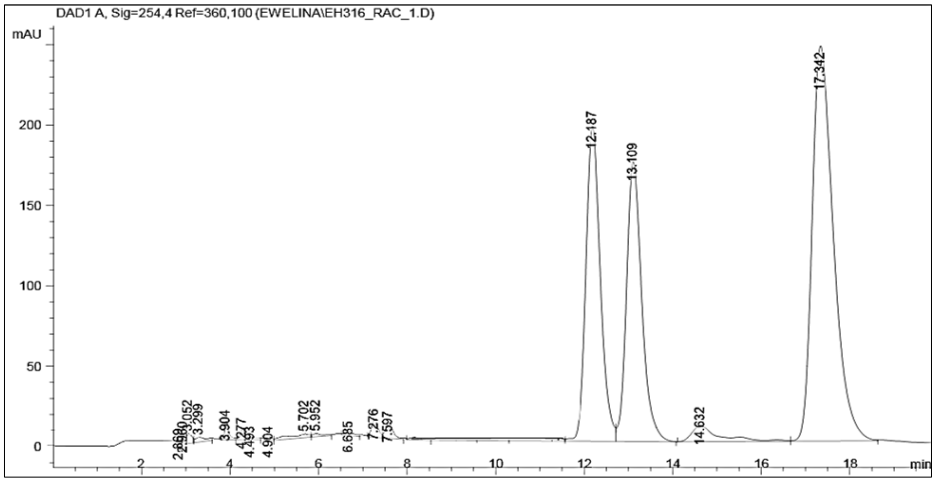

Figure 7. Chromatogram of the products mixture **18** and **19** (using IPA/Heptane 15:85 as a eluent)

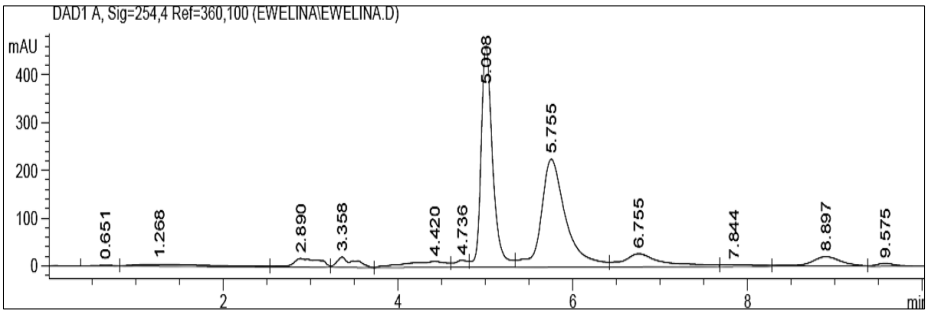

Figure 8. Chromatogram of the product (*S,S*)-**19** (using IPA/Heptane 8:92 as a eluent)

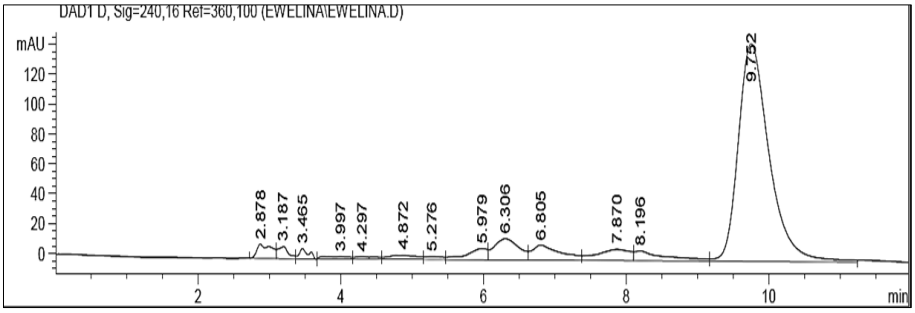

Figure 9. Chromatogram of the products mixture **20** and **21** (using IPA/Heptane 10:90 as a eluent)

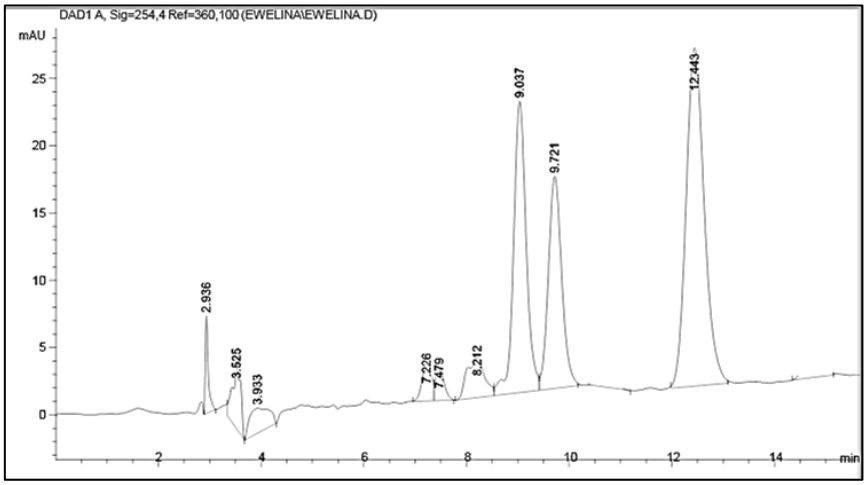

Figure 10. Chromatogram of the product (*S,S*)-**21** (using IPA/Heptane 10:90 as a eluent)

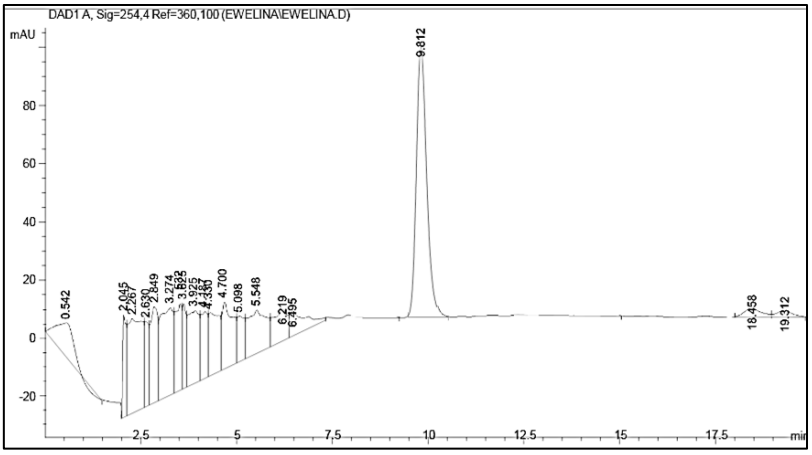

^{1}H NMR (400 MHz, $CDCl_3$)

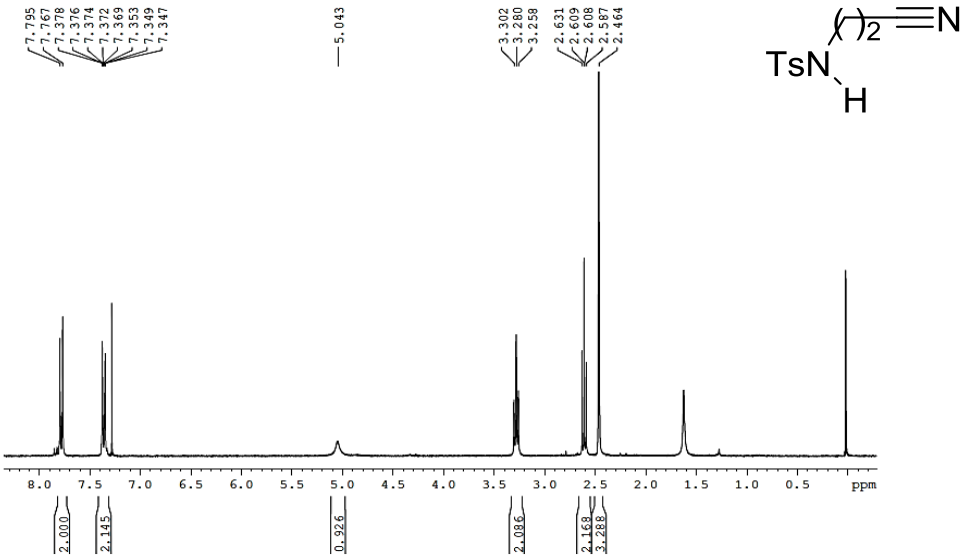

^{1}H NMR (300 MHz, $CDCl_3$)

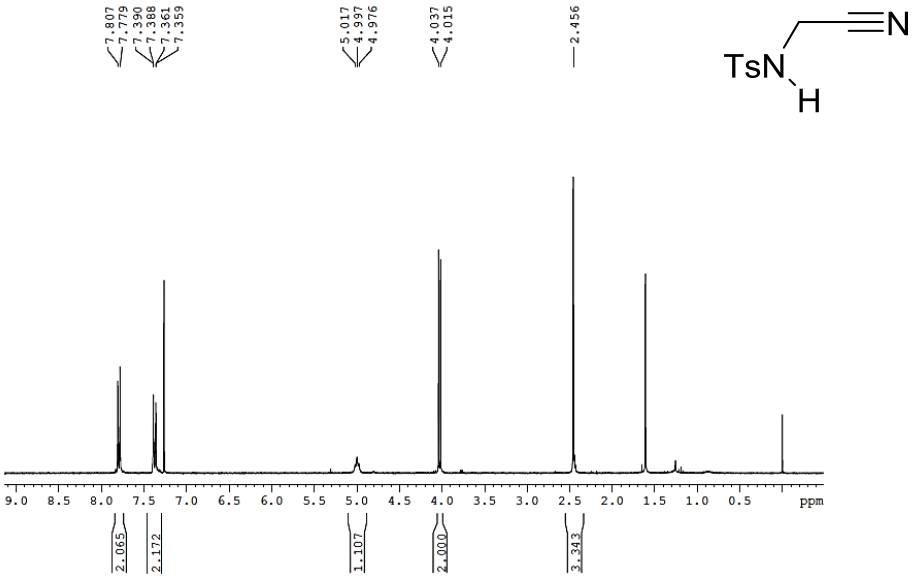

^{1}H NMR (400 MHz, $CDCl_3$)

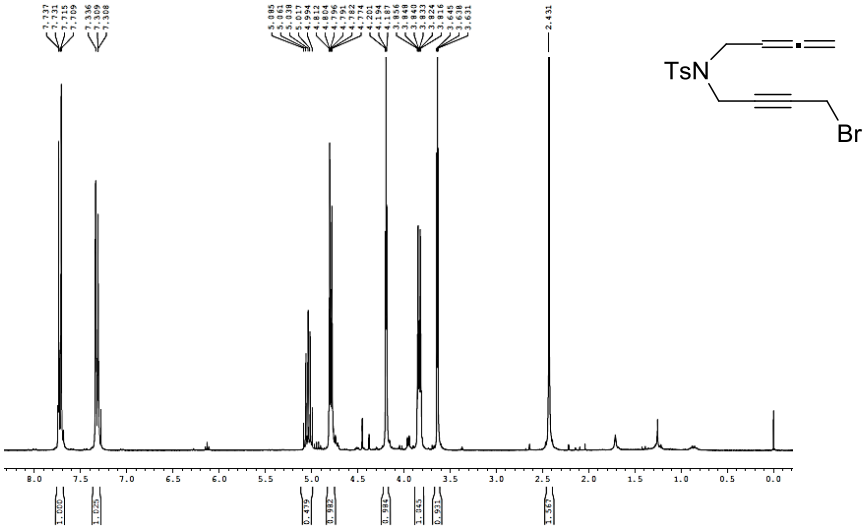

^{13}C NMR (75 MHz, $CDCl_3$)

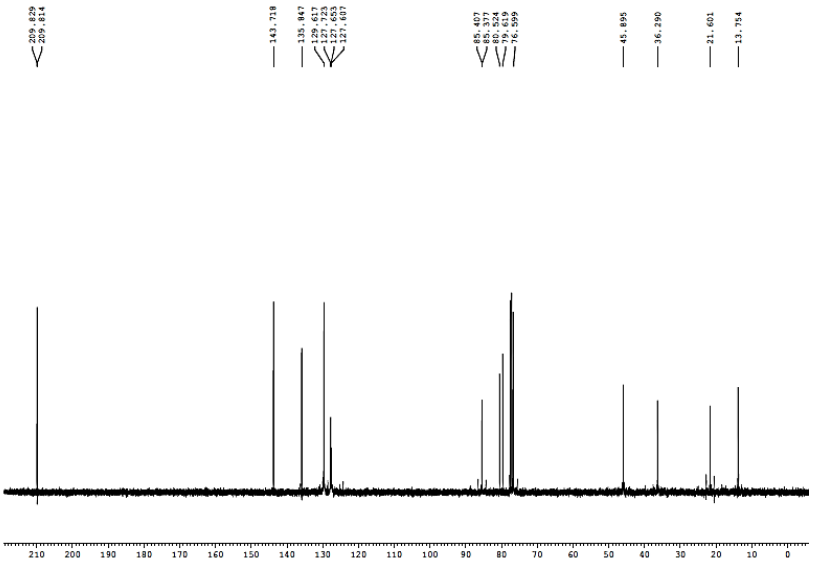

ESI-MS (+)

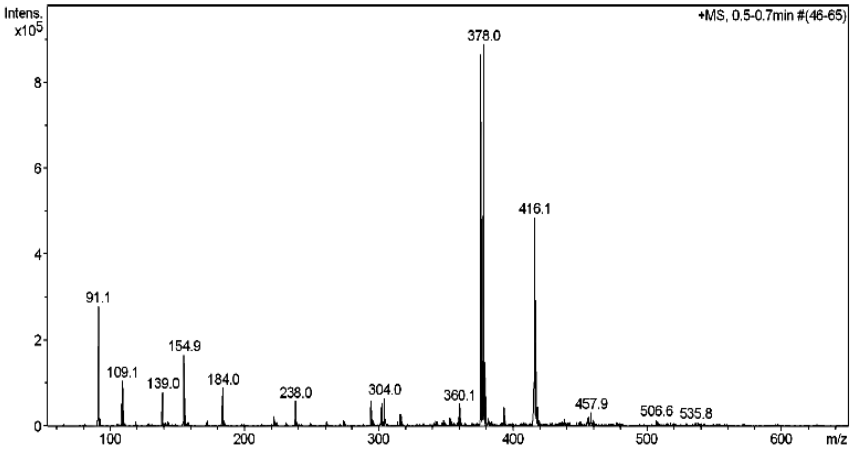

IR (ATR)

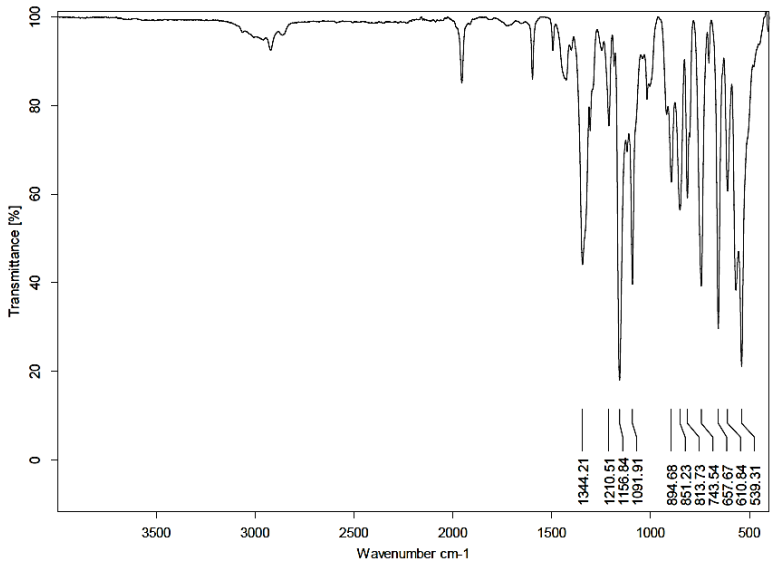

^{1}H NMR (400 MHz, $CDCl_3$)

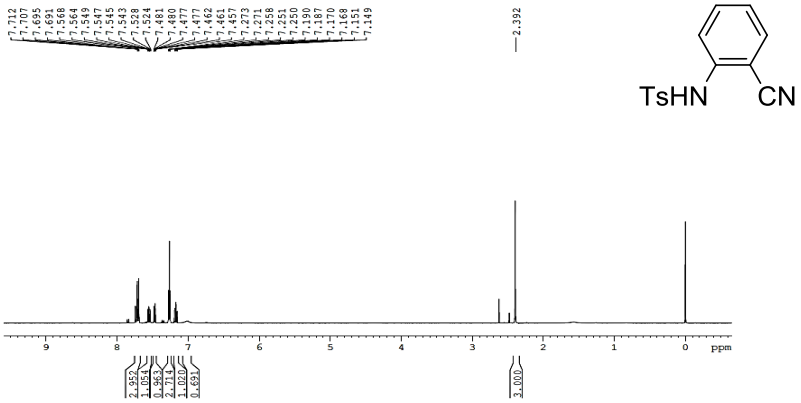

^{1}H NMR (400 MHz, $CDCl_3$)

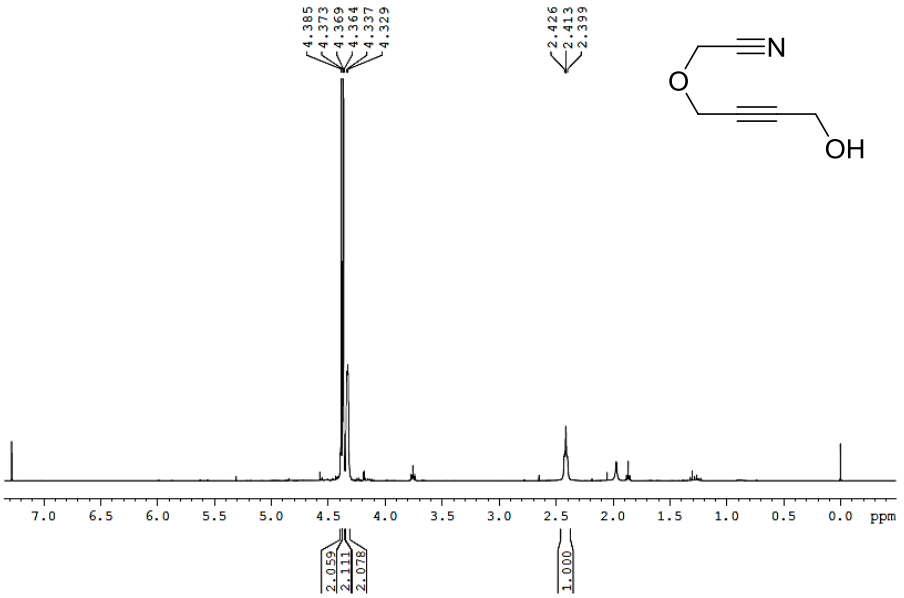

^{1}H NMR (400 MHz, $CDCl_3$)

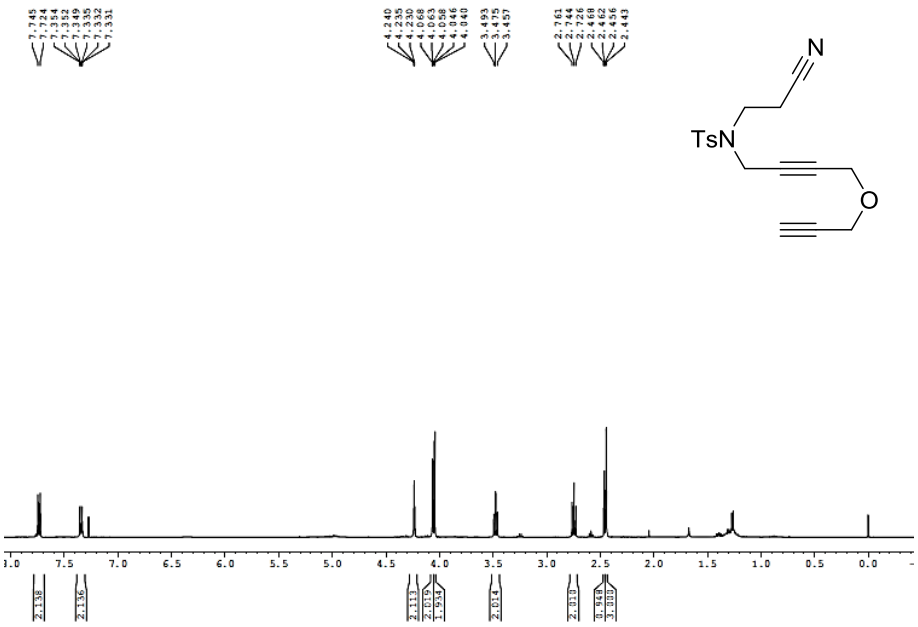

^{13}C NMR (75 MHz, $CDCl_3$)

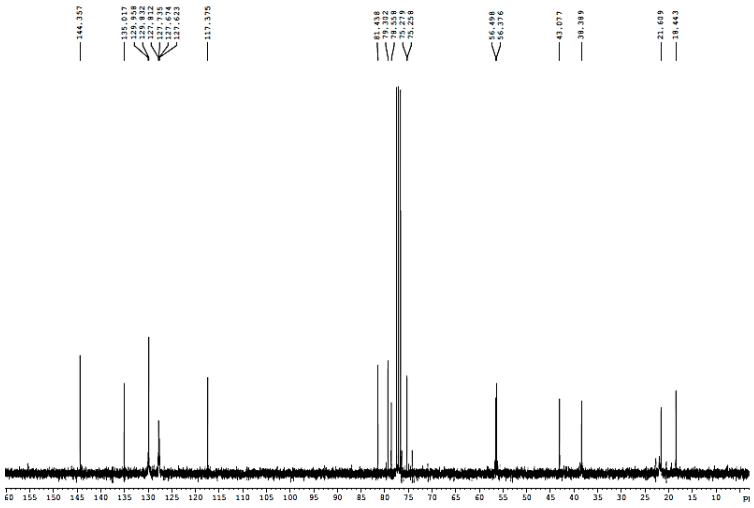

ESI-MS (+)

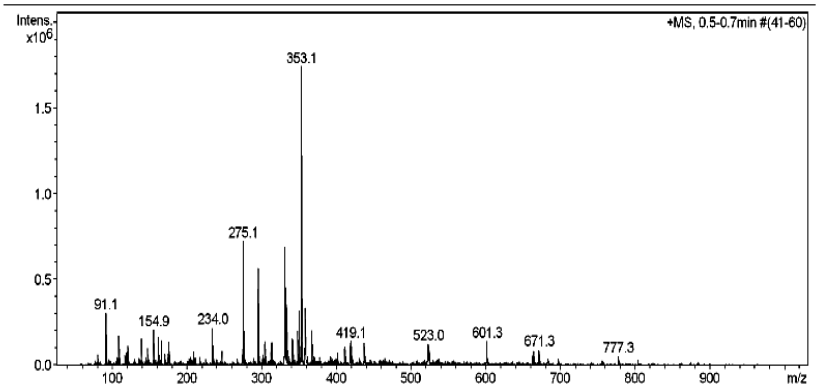

ESI-HRMS (+)

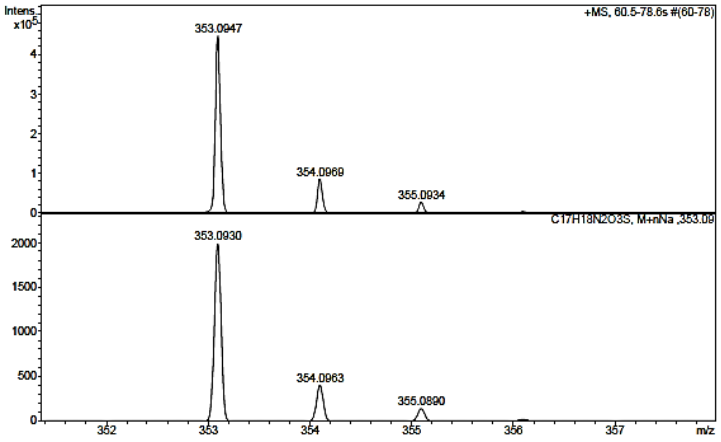

IR (ATR)

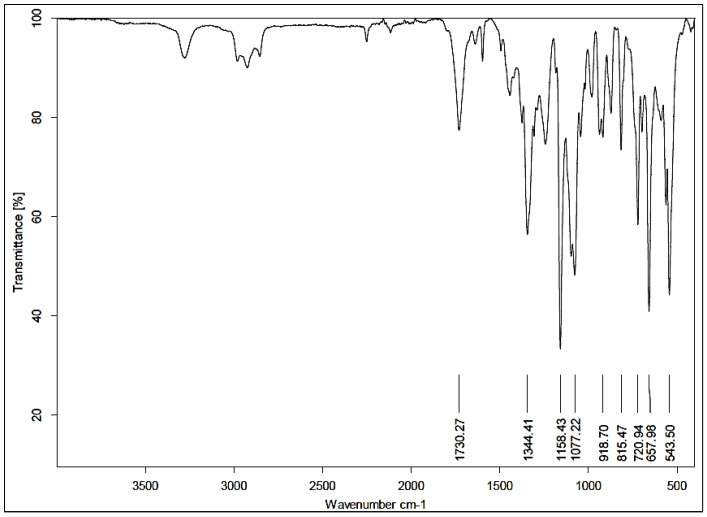

^{1}H NMR (400 MHz, $CDCl_3$)

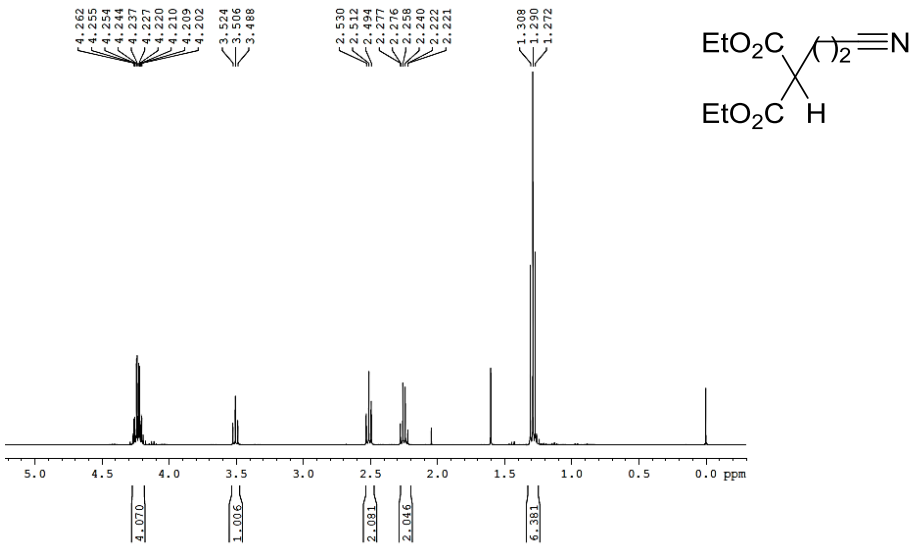

^{1}H NMR (300 MHz, $CDCl_3$)

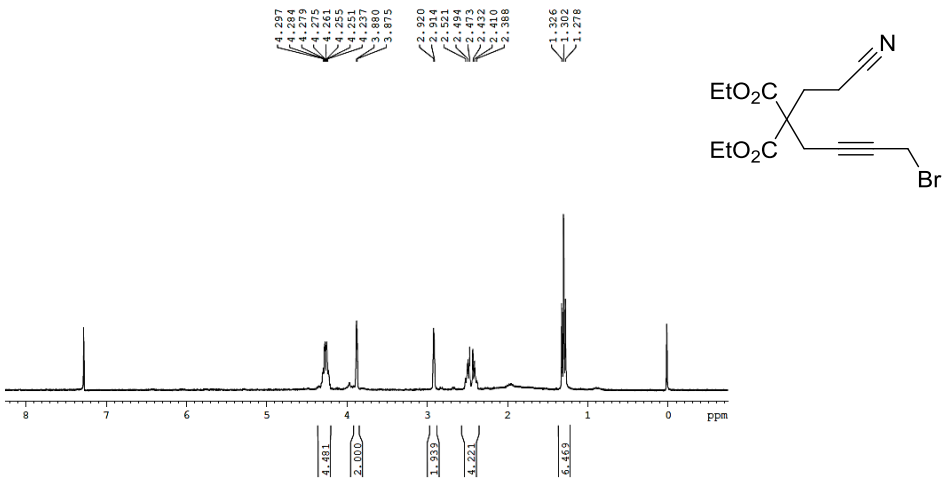

^{13}C NMR (75 MHz, $CDCl_3$)

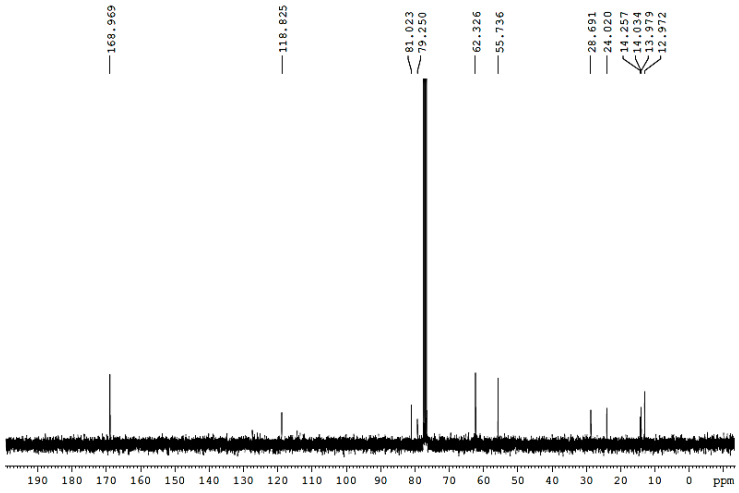

IR (ATR)

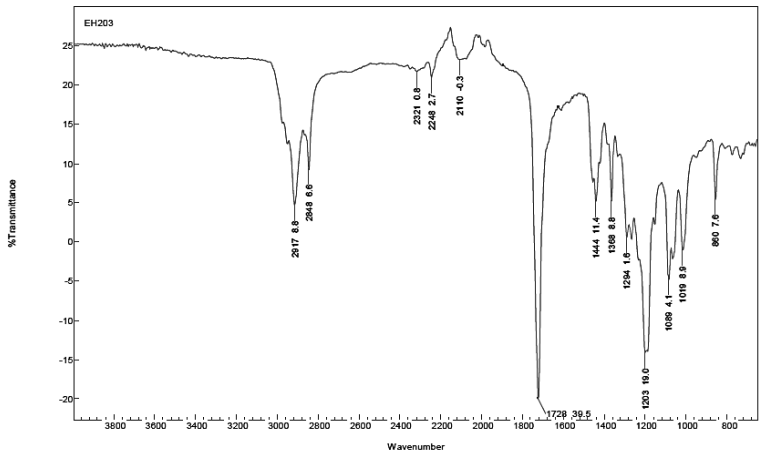

ESI-HRMS (+)

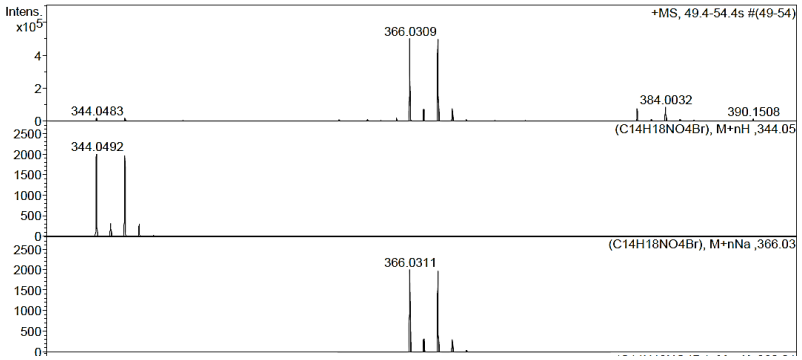

^{1}H NMR (400 MHz, $CDCl_3$)

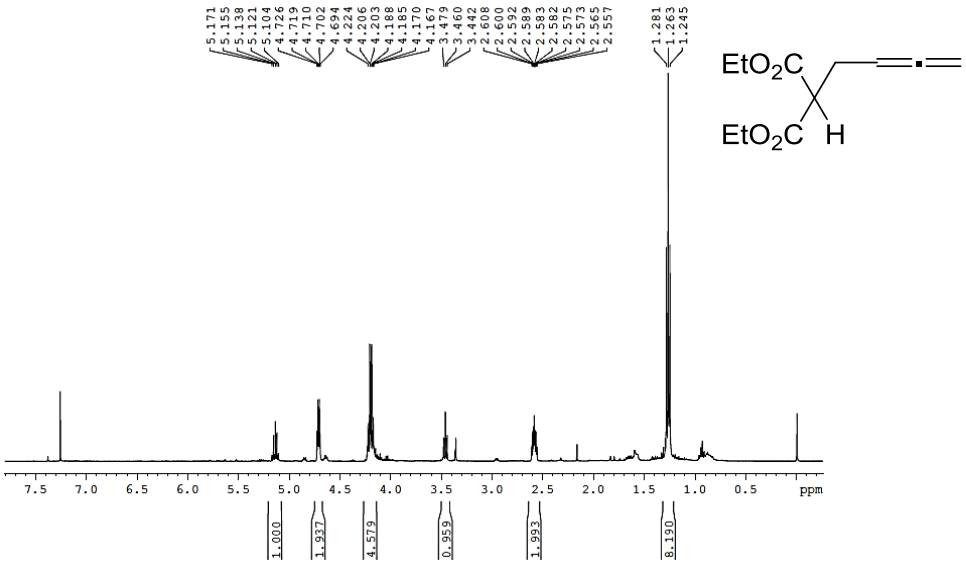

^{1}H NMR (400 MHz, $CDCl_3$)

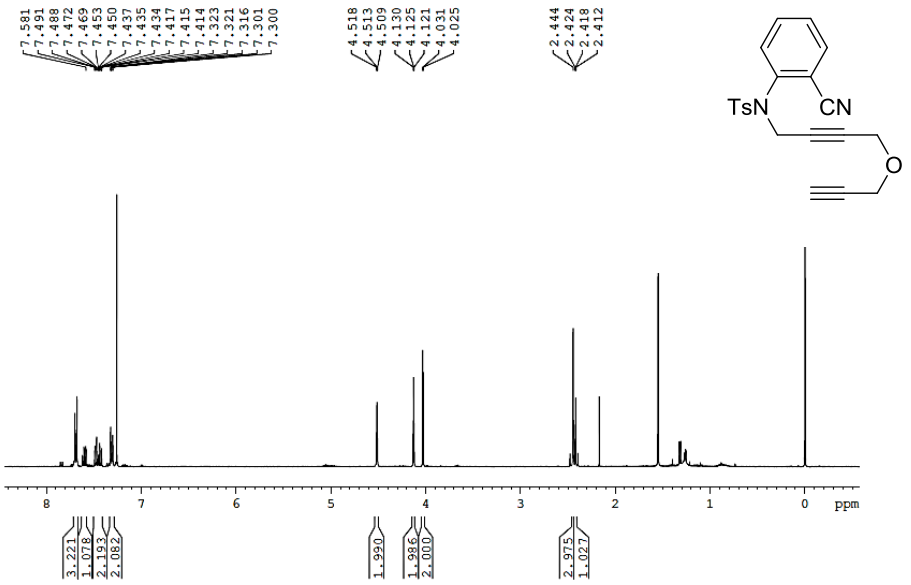

^{13}C NMR (100 MHz, $CDCl_3$)

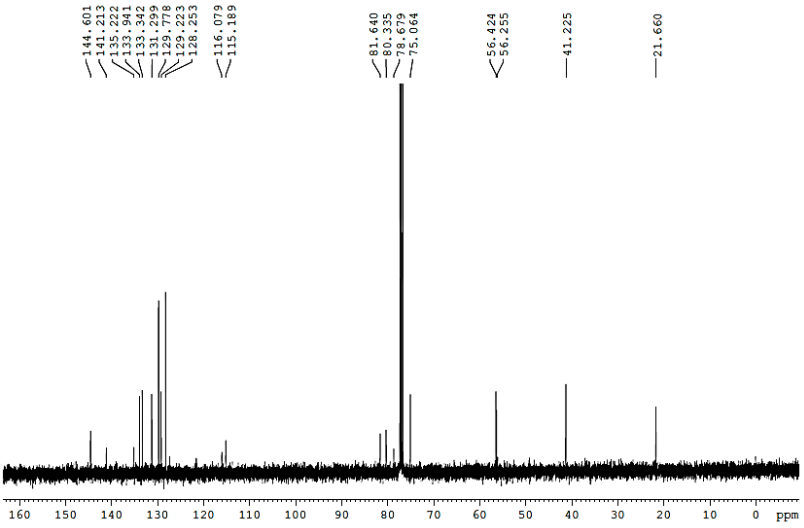

IR (ATR)

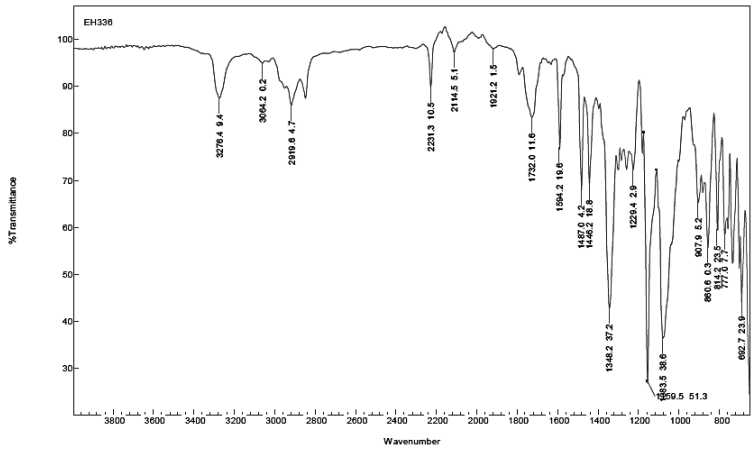

ESI-MS (+)

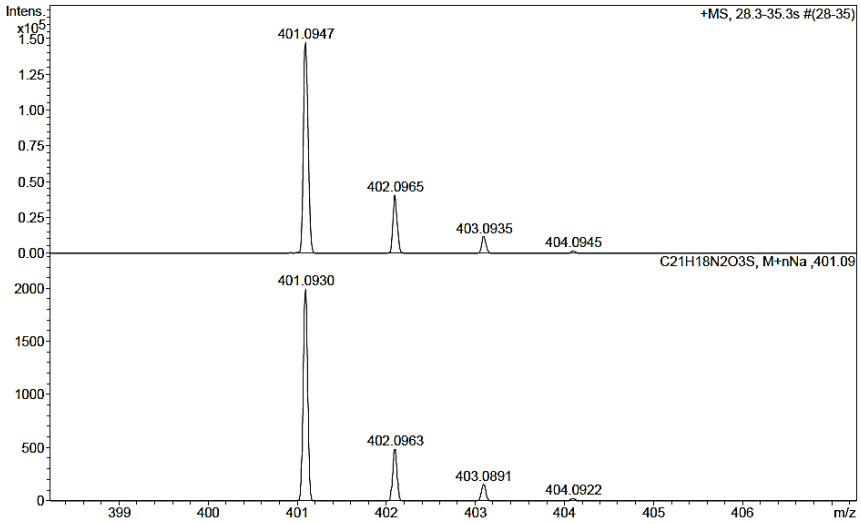

^{1}H NMR (300 MHz, $CDCl_3$)

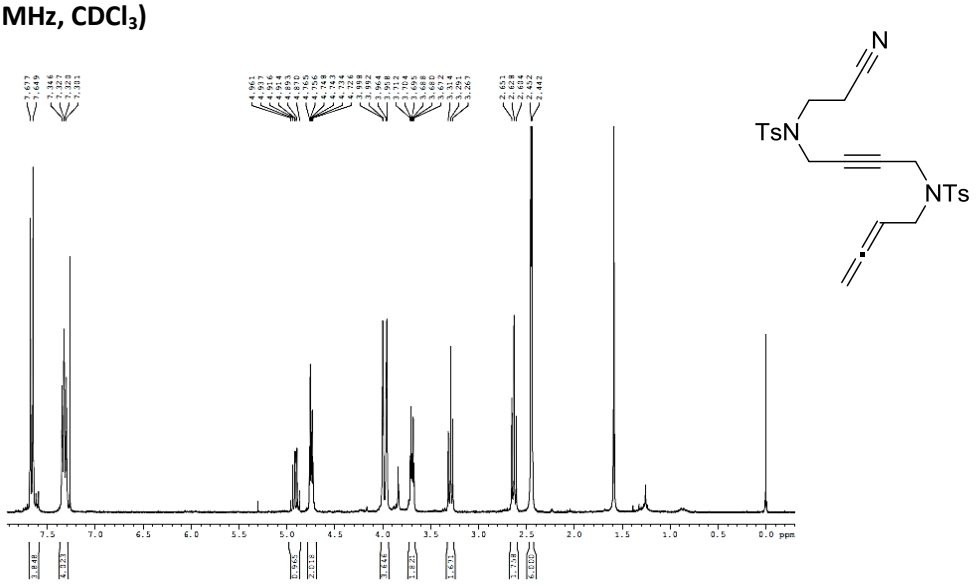

^{13}C NMR (75 MHz, $CDCl_3$)

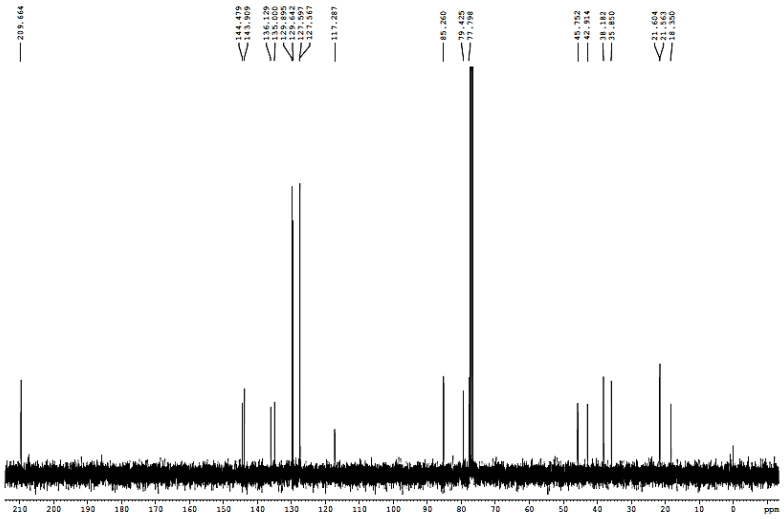

ESI-MS (+)

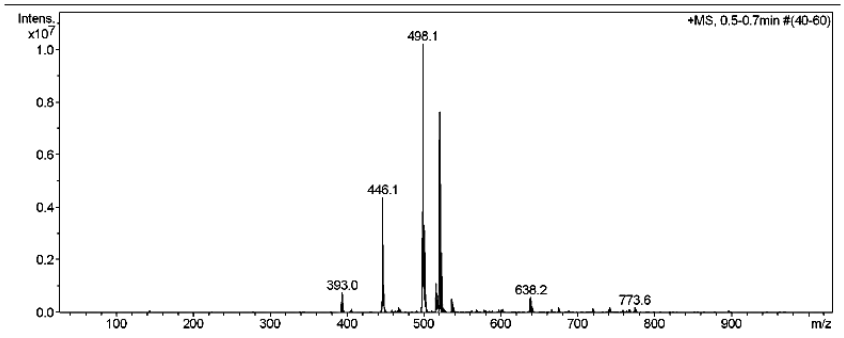

IR (ATR)

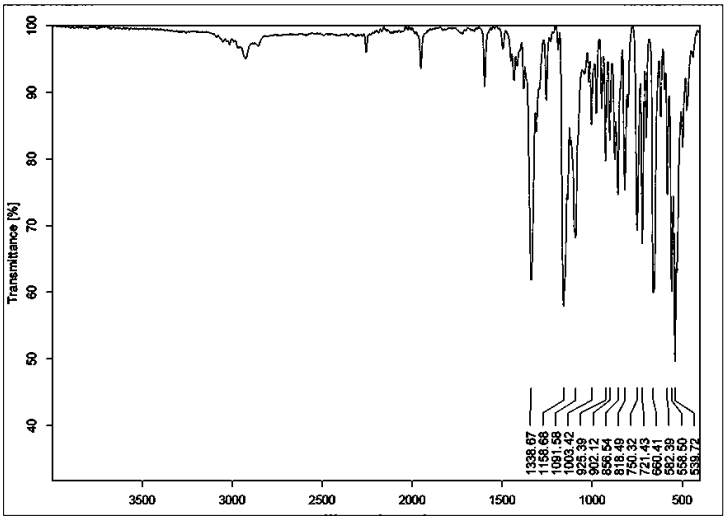

^{1}H NMR (300 MHz, $CDCl_3$)

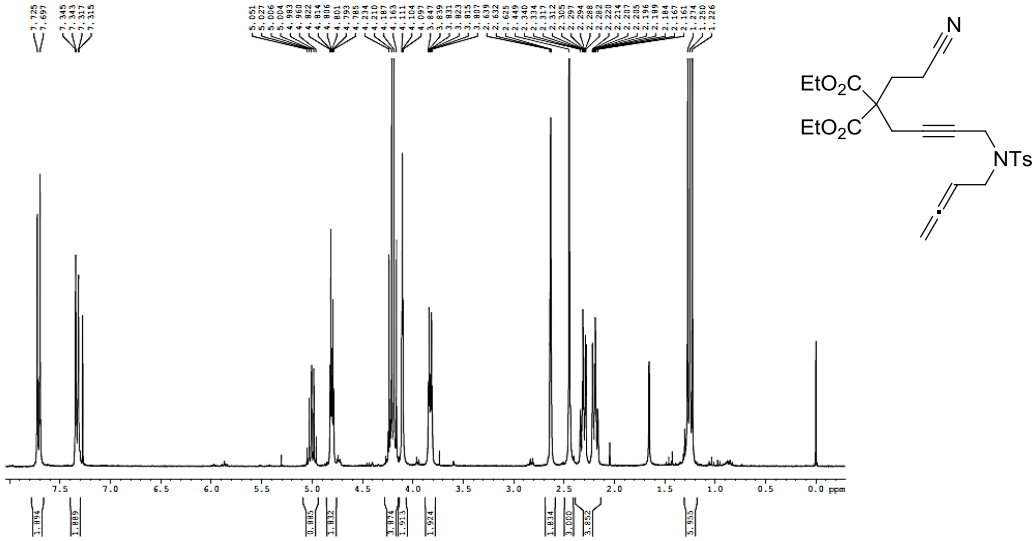

^{13}C NMR (75 MHz, $CDCl_3$)

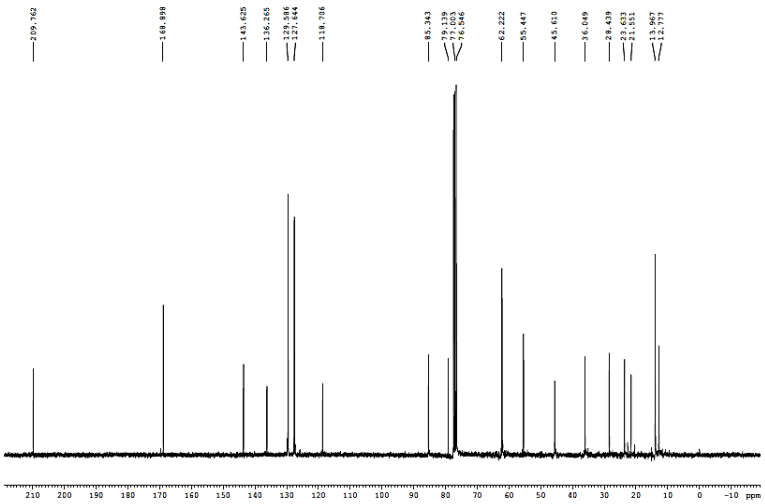

ESI-MS (+)

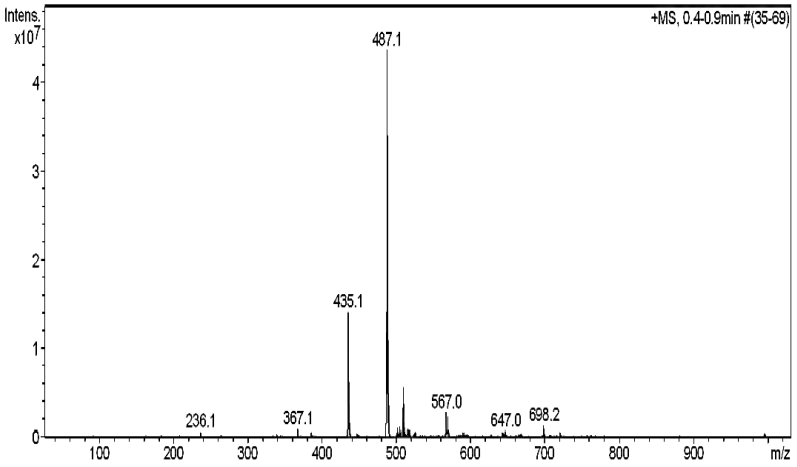
Intens.
x10^7
+MS, 0.4-0.9min #(35-69)
487.1
435.1
236.1
367.1
567.0
647.0
698.2
m/z

IR (ATR)

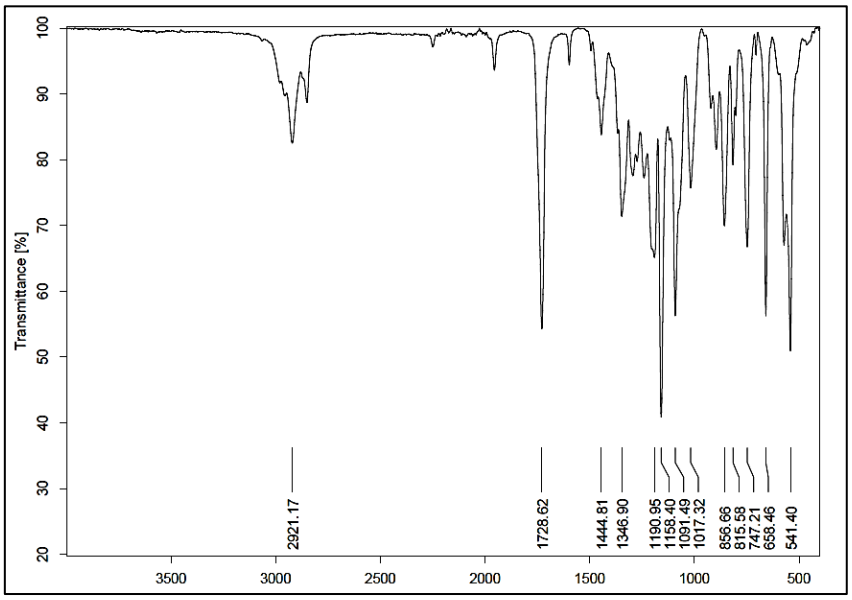
Transmittance [%]
2921.17
1728.62
1444.81
1346.90
1190.95
1158.40
1091.49
1017.32
856.66
815.58
747.21
658.46
541.40

^{1}H NMR (300 MHz, $CDCl_3$)

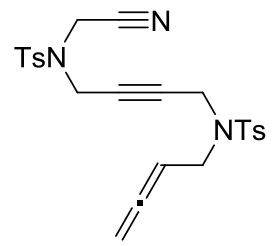

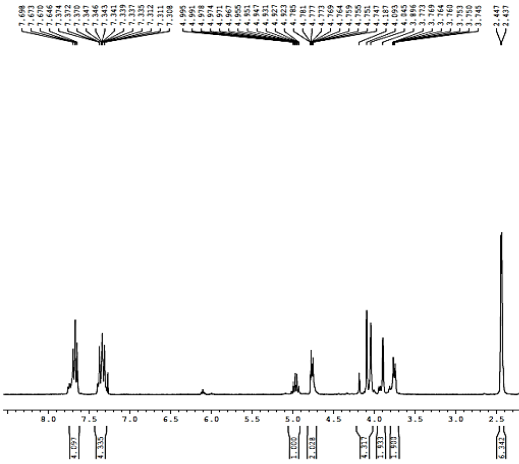

^{13}C NMR (75 MHz, $CDCl_3$)

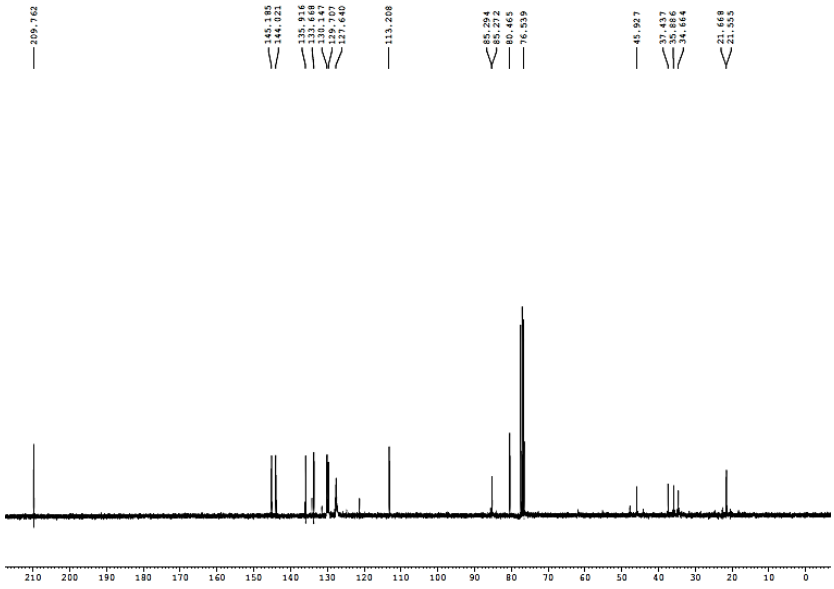

ESI-MS (+)

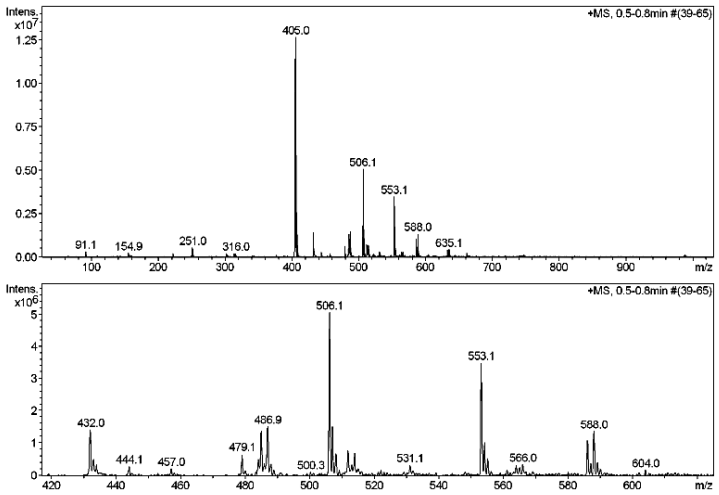
Intens.
x10^7
+MS, 0.5-0.8min #(39-65)
405.0
506.1
553.1
588.0
635.1
91.1
154.9
251.0
316.0
m/z
Intens.
x10^6
+MS, 0.5-0.8min #(39-65)
506.1
553.1
432.0
486.9
588.0
444.1
457.0
479.1
500.3
531.1
566.0
604.0
m/z

IR (ATR)

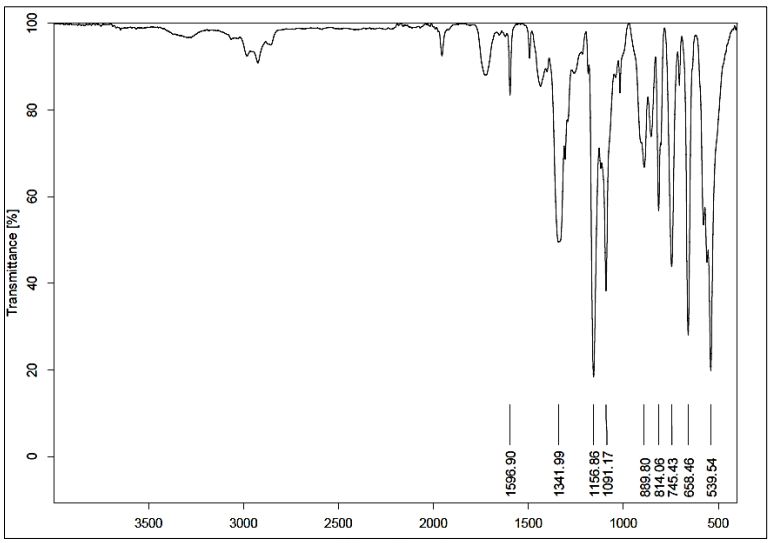
Transmittance [%]
1596.90
1341.99
1156.86
1091.17
889.80
814.06
745.43
658.46
539.54

^{1}H NMR (400 MHz, $CDCl_3$)

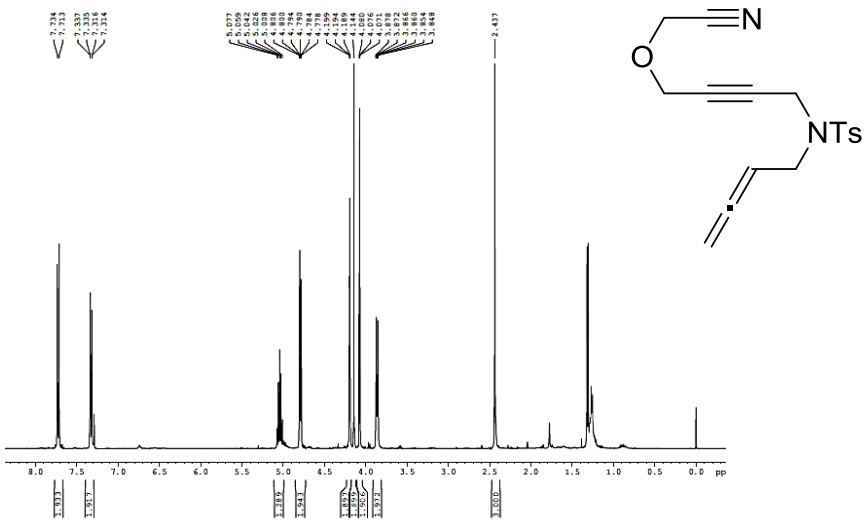

^{13}C NMR (100 MHz, $CDCl_3$)

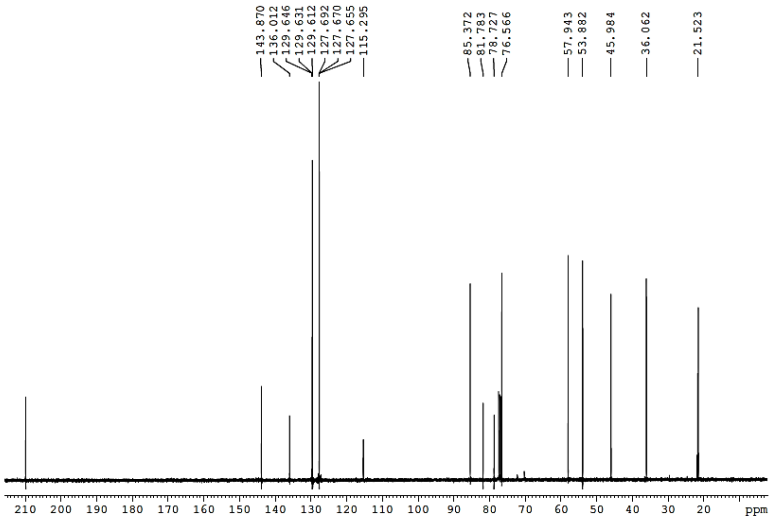

GC-MS

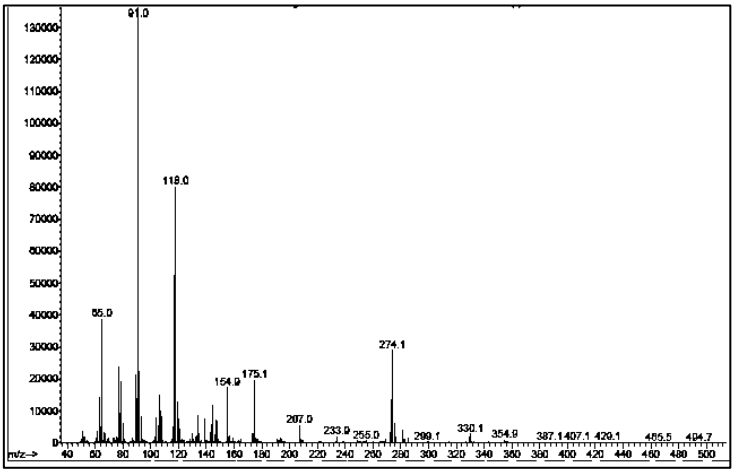
91.0
118.0
55.0
274.1
175.1
154.9
287.0
233.9
255.0
299.1
330.1
354.9
387.1
407.1
429.1
455.5
494.7
m/z-->

IR (ATR)

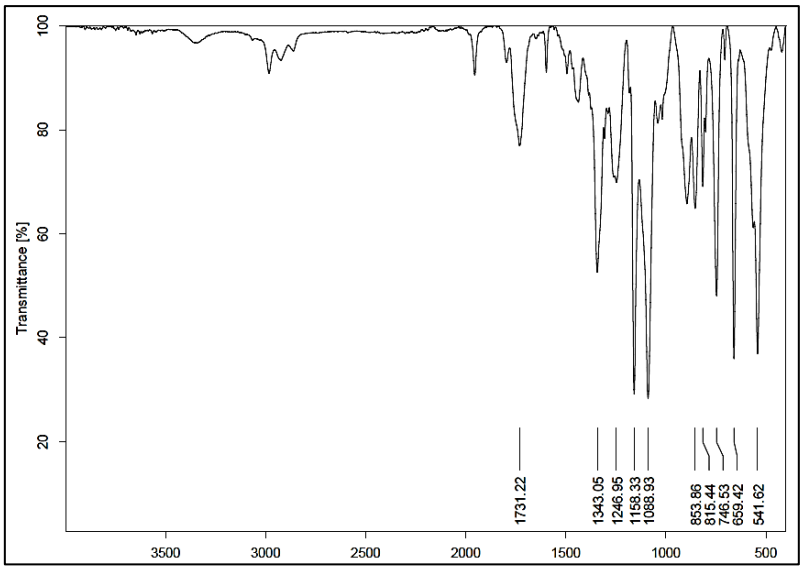
Transmittance [%]
100
80
60
40
20
3500
3000
2500
2000
1500
1000
500
1731.22
1343.05
1246.95
1158.33
1088.93
853.86
815.44
746.53
659.42
541.62

^{1}H NMR (300 MHz, $CDCl_3$)

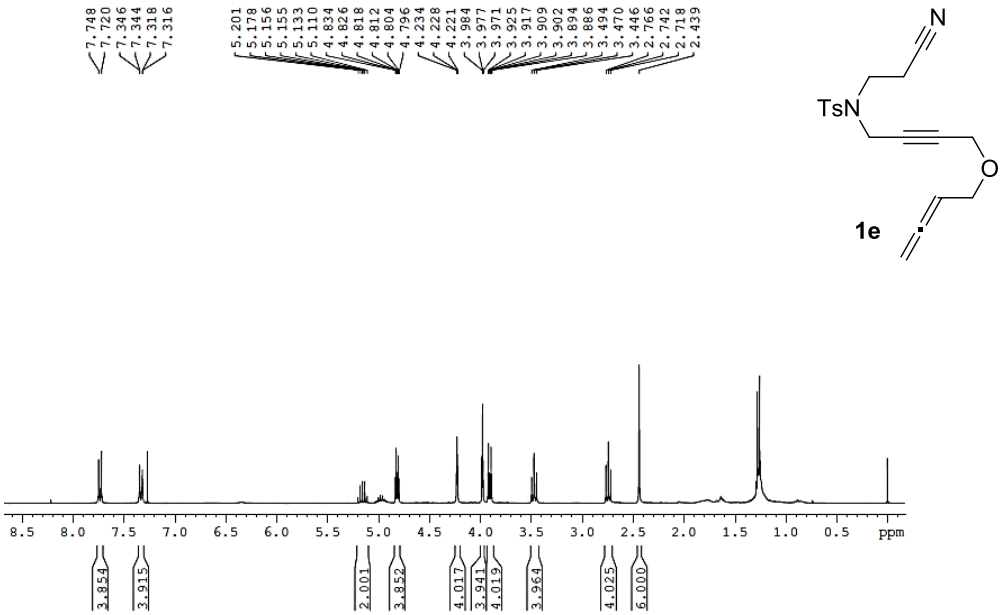

^{13}C NMR (75 MHz, $CDCl_3$)

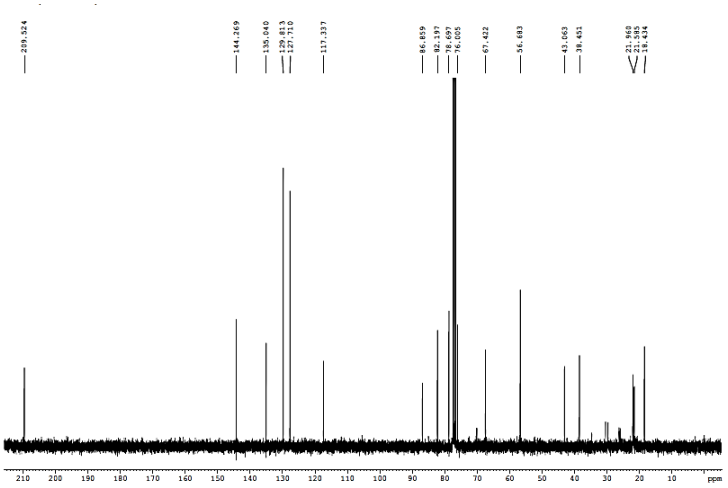

GC-MS

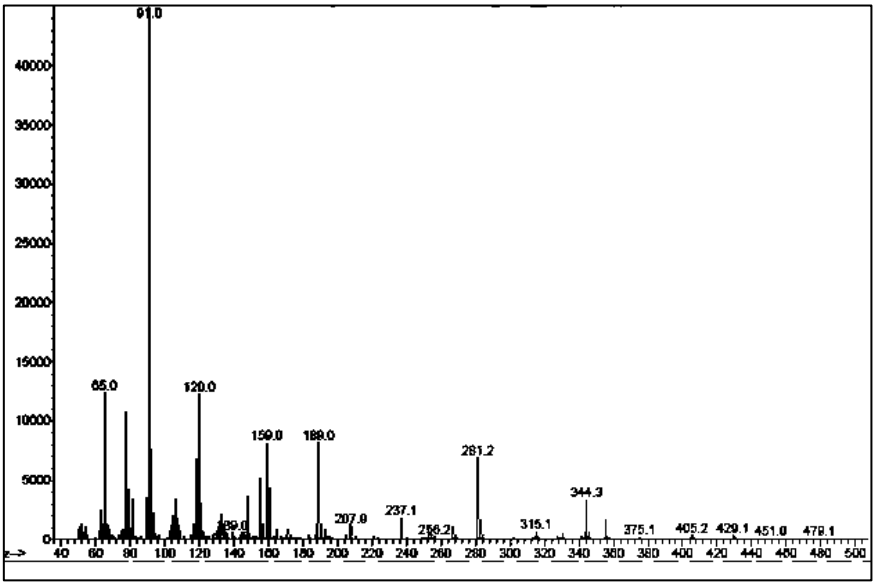
91.0
65.0
120.0
159.0
189.0
281.2
344.3
237.1
207.0
315.1
375.1
405.2
429.1
451.0
479.1

IR (ATR)

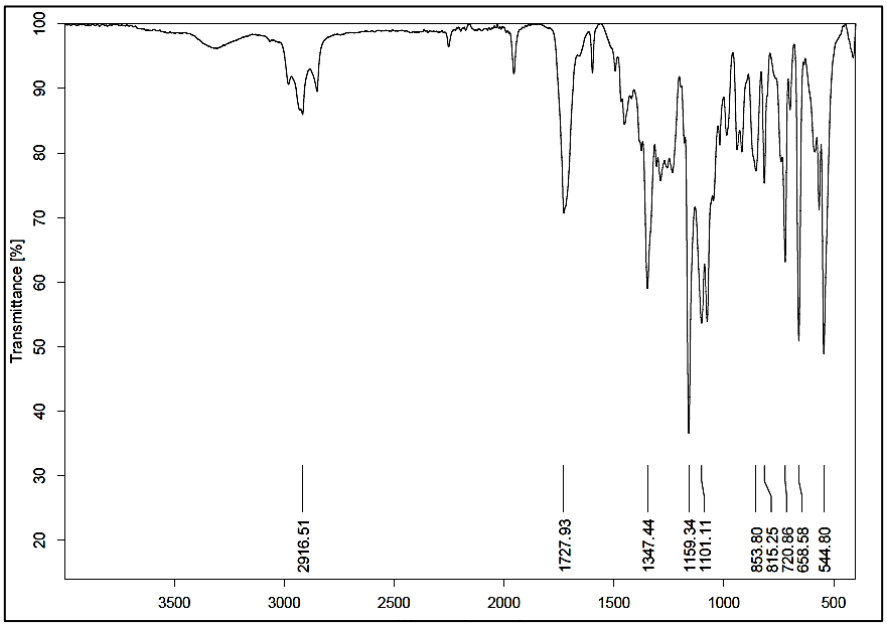
Transmittance [%]
2916.51
1727.93
1347.44
1159.34
1101.11
853.80
815.25
720.86
658.58
544.80

^{1}H NMR (400 MHz, $CDCl_3$)

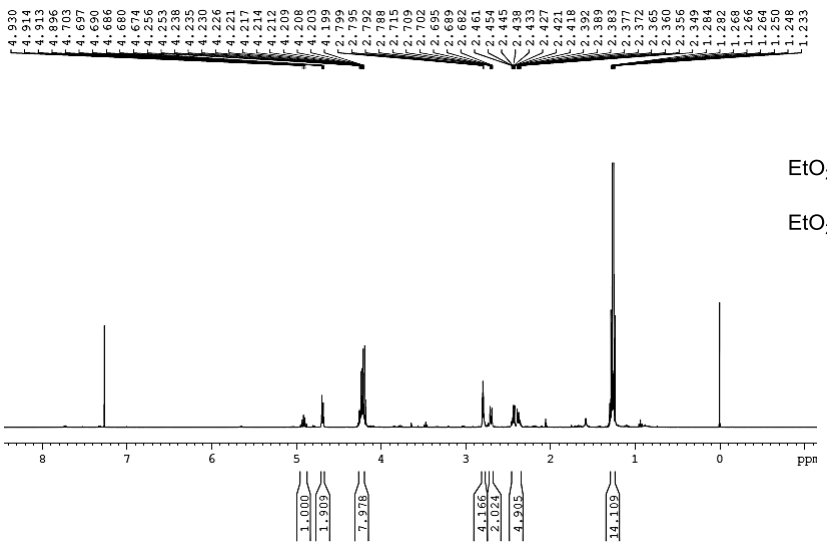

^{13}C NMR (100 MHz, $CDCl_3$)

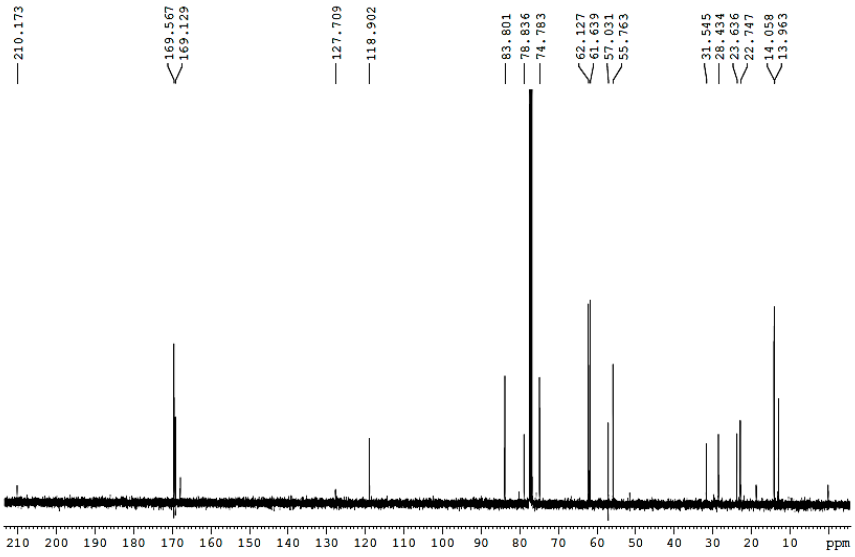

IR (ATR)

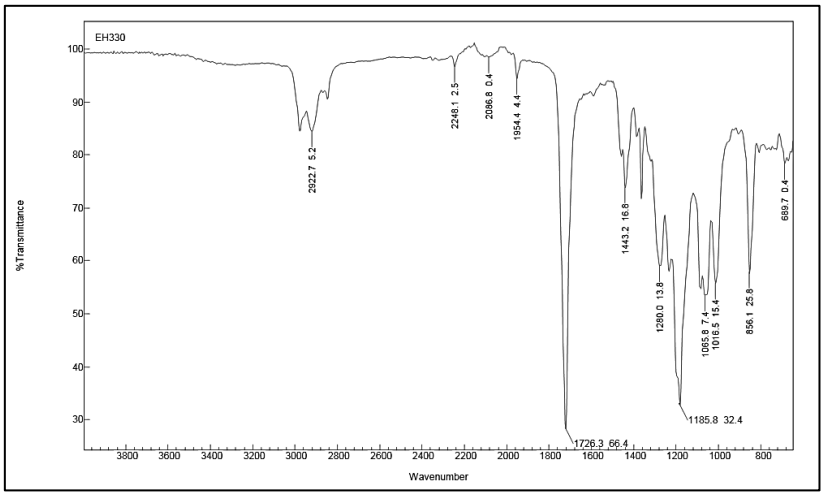

ESI-HRMS (+)

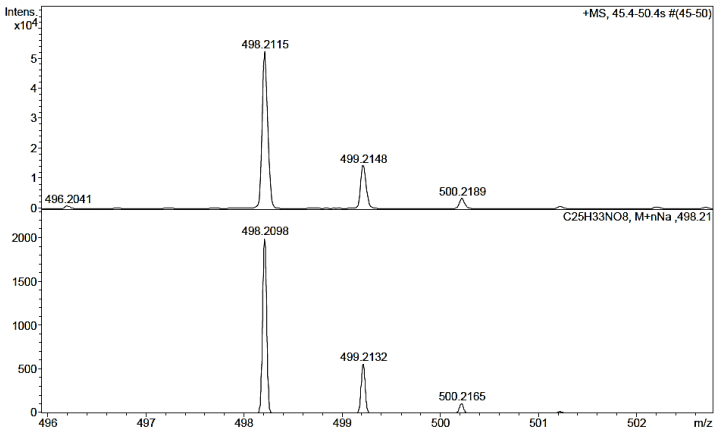

^{1}H NMR (400 MHz, $CDCl_3$)

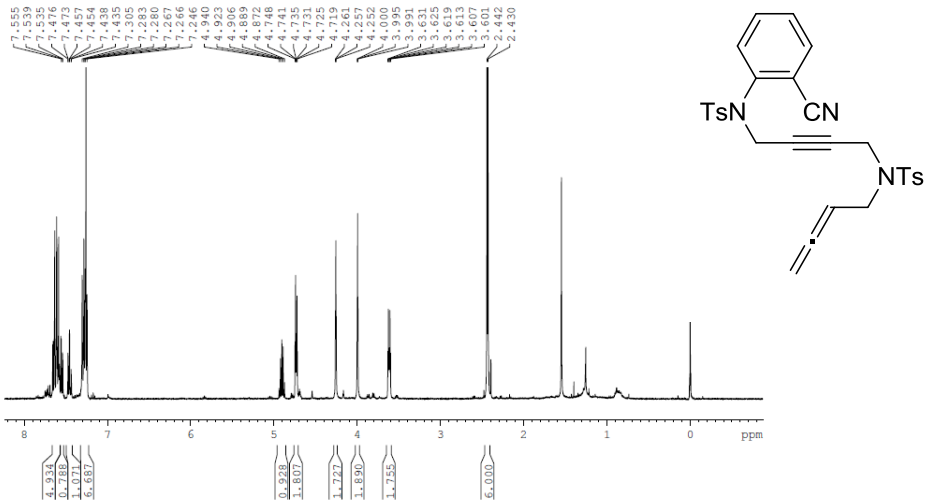

^{13}C NMR (75 MHz, $CDCl_3$)

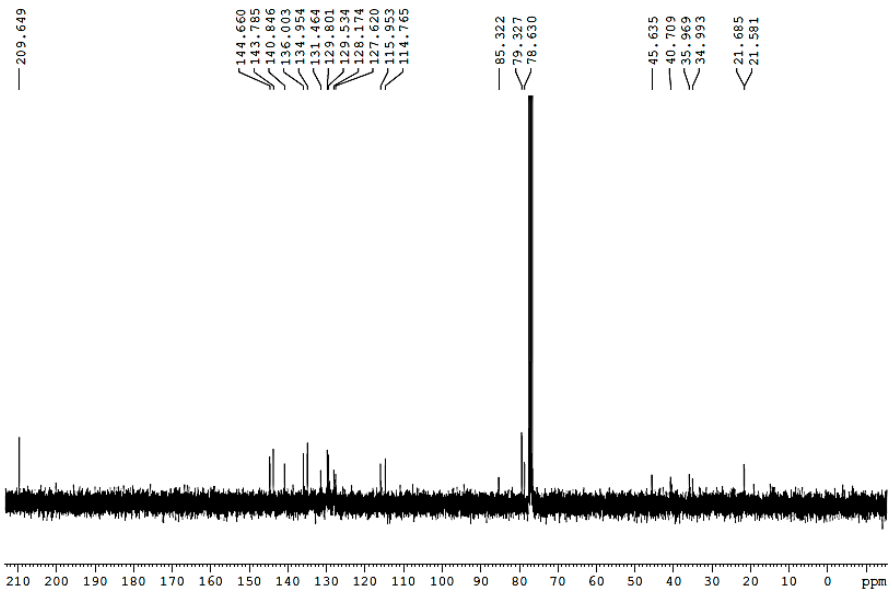

ESI-MS (+)

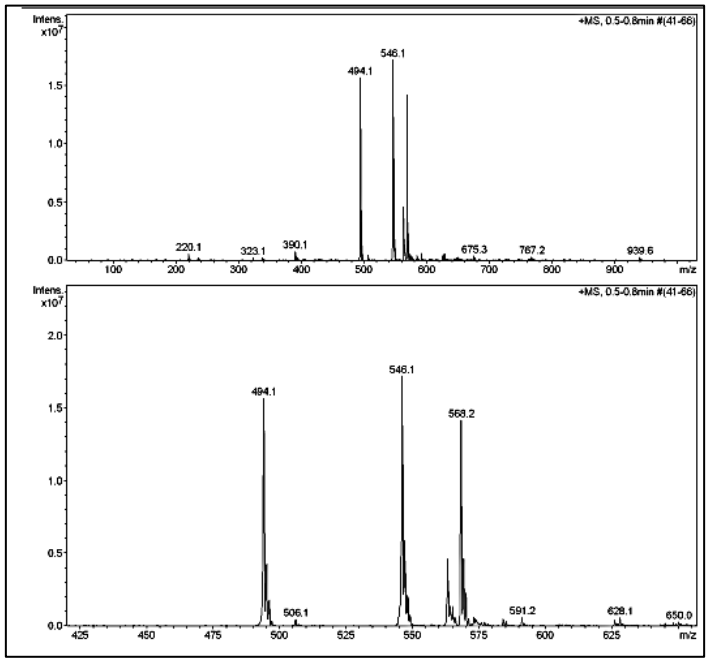

IR (ATR)

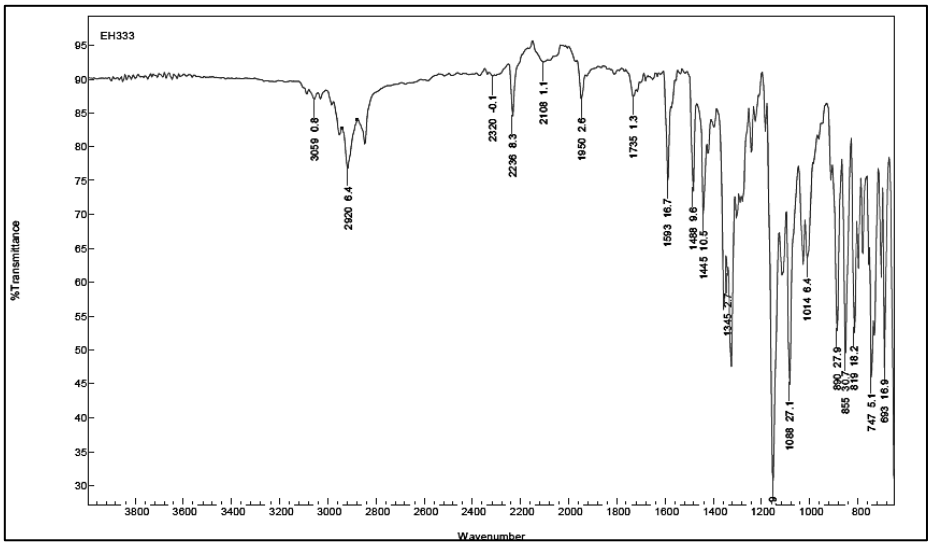

^{1}H NMR (400 MHz, $CDCl_3$)

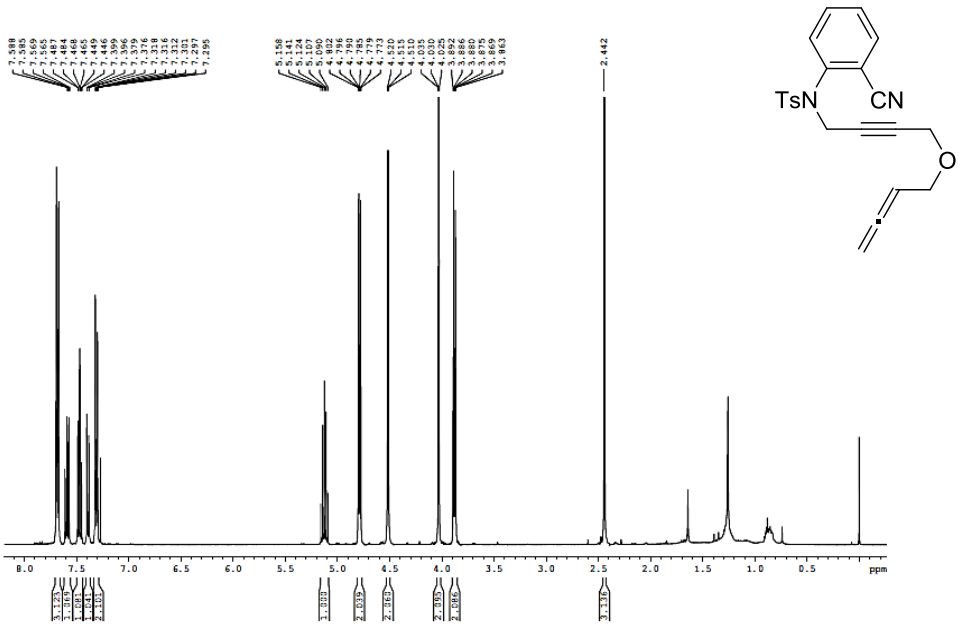

^{13}C NMR (100 MHz, $CDCl_3$)

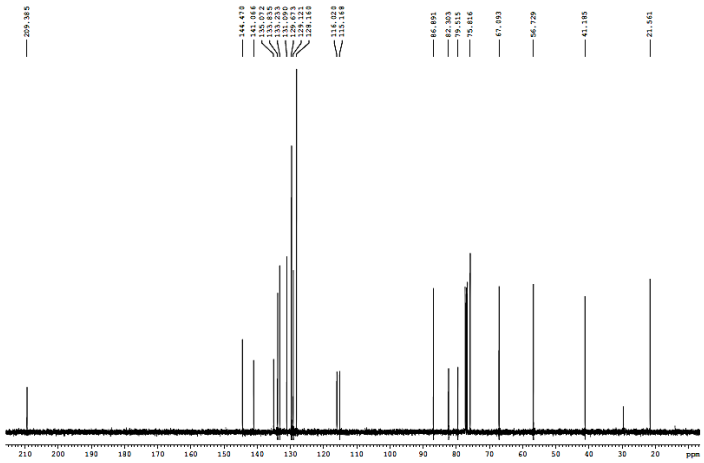

IR (ATR)

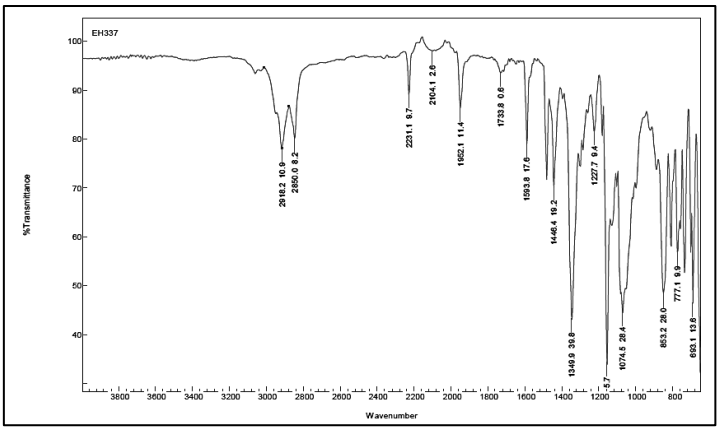

ESI-HRMS (+)

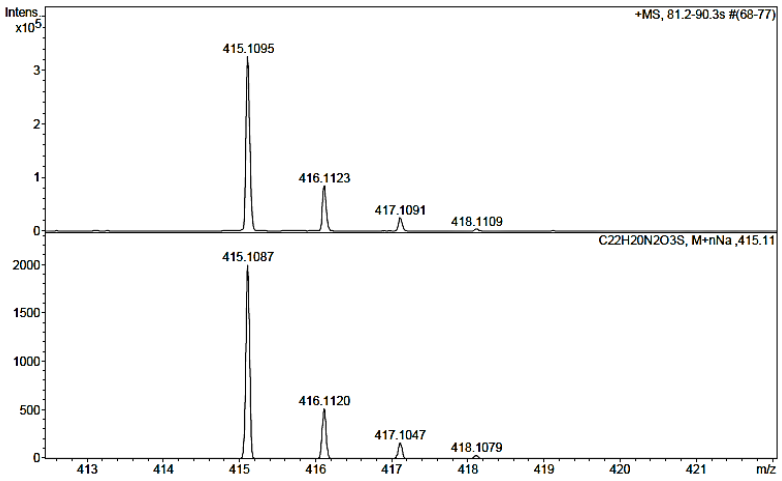

^{1}H NMR (400 MHz, $CDCl_3$)

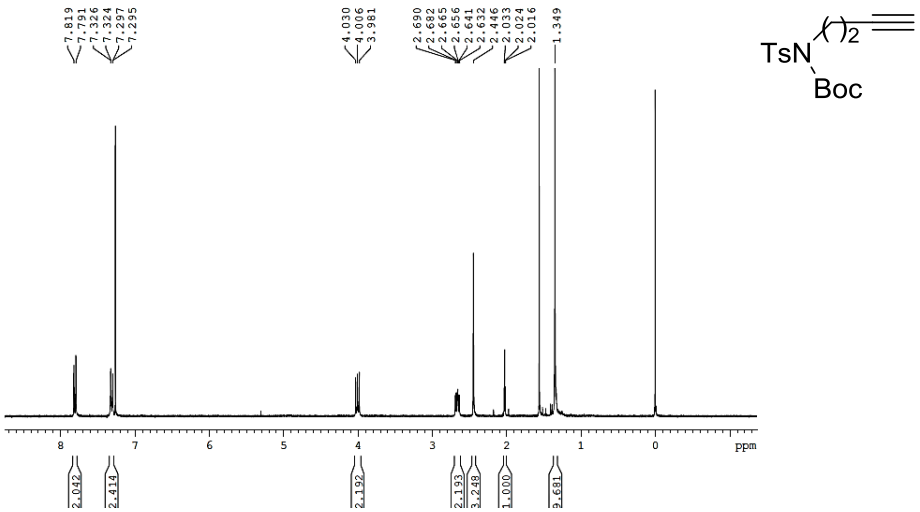

^{1}H NMR (400 MHz, $CDCl_3$)

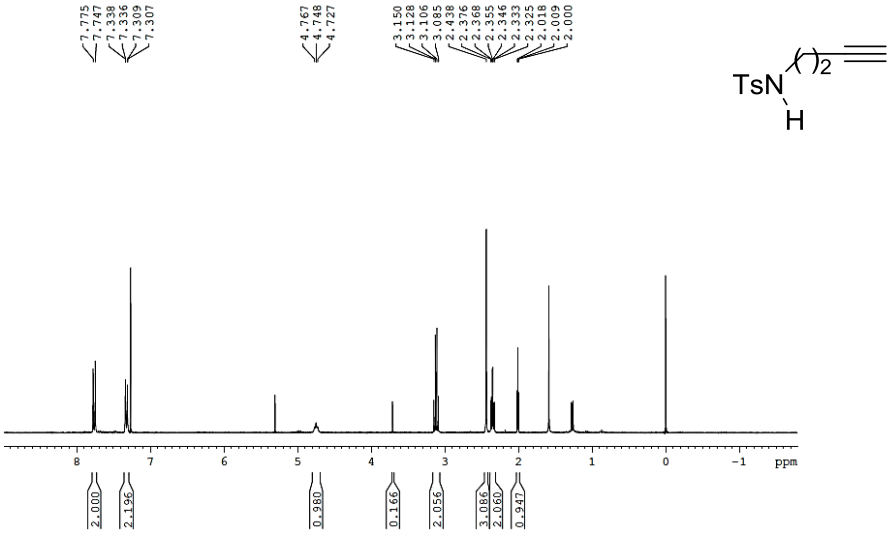

^{1}H NMR (400 MHz, $CDCl_3$)

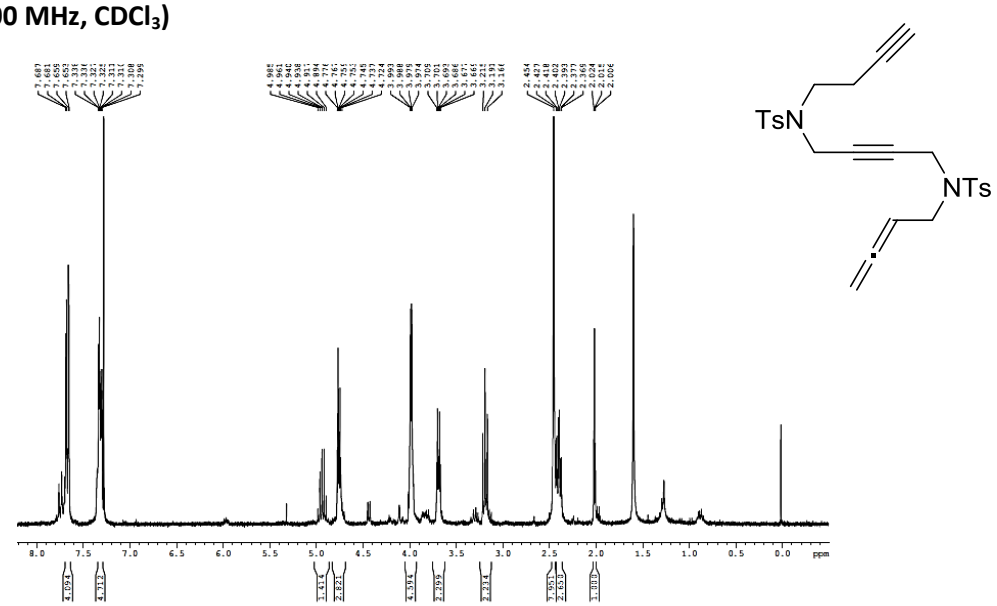

^{13}C NMR (75 MHz, $CDCl_3$)

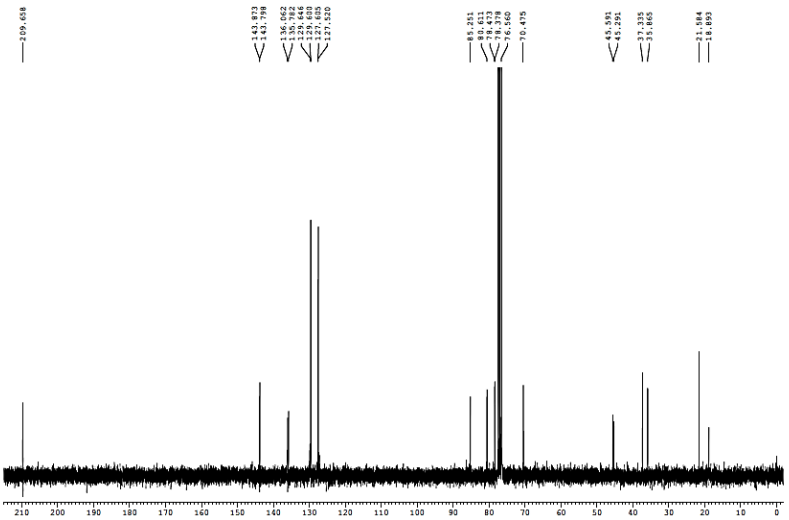

ESI-MS (+)

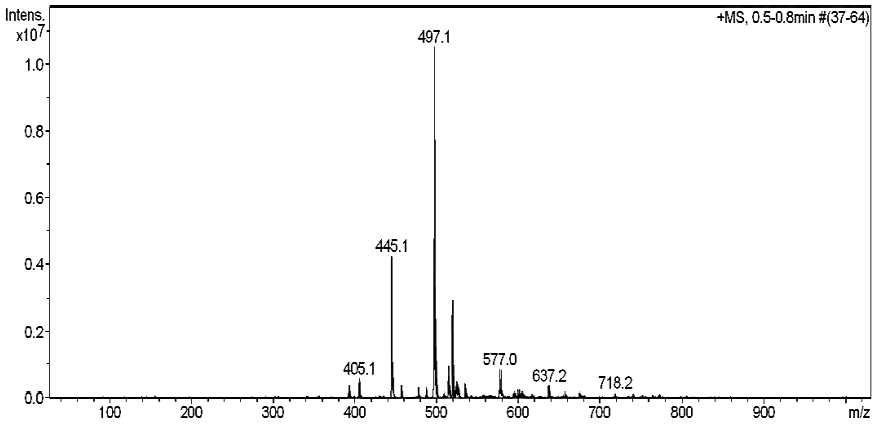

IR (ATR)

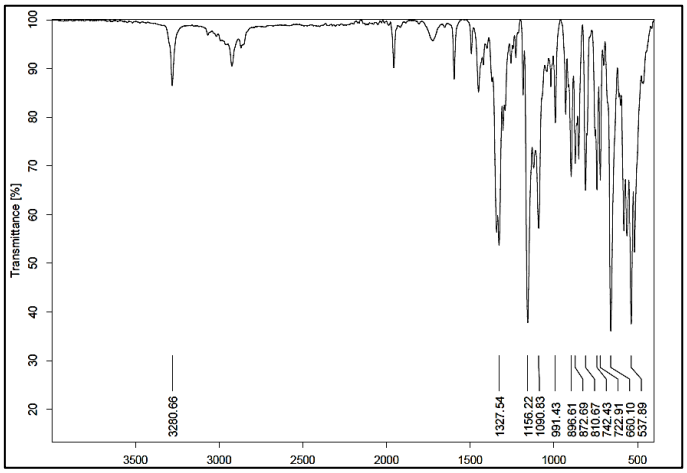

^{1}H NMR (300 MHz, $CDCl_3$)

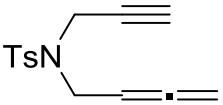

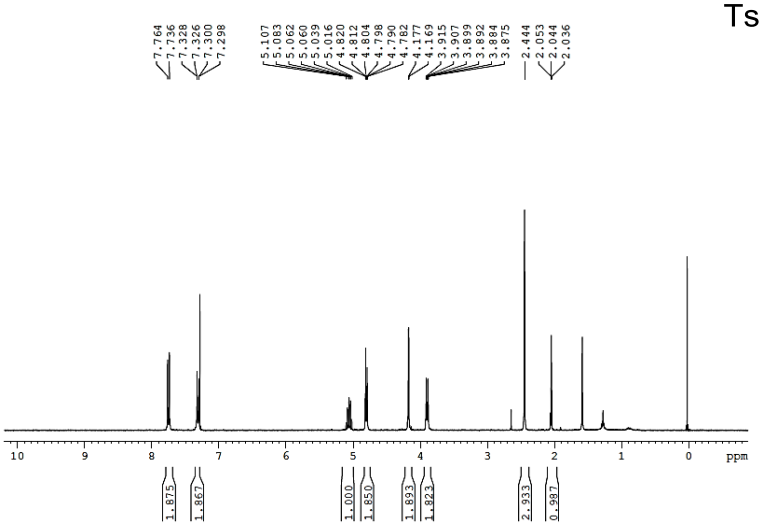

^{1}H NMR (300 MHz, $CDCl_3$)

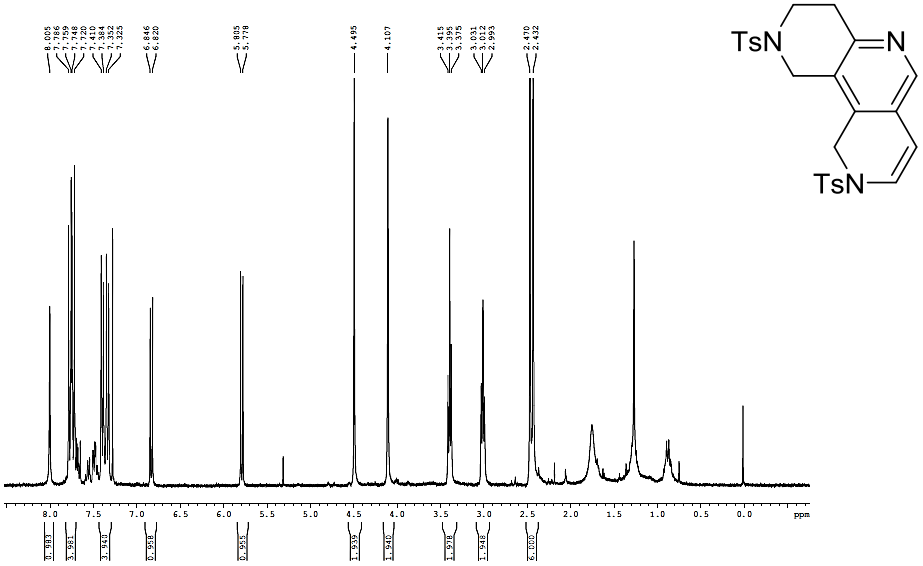

^{13}C NMR (75 MHz, $CDCl_3$)

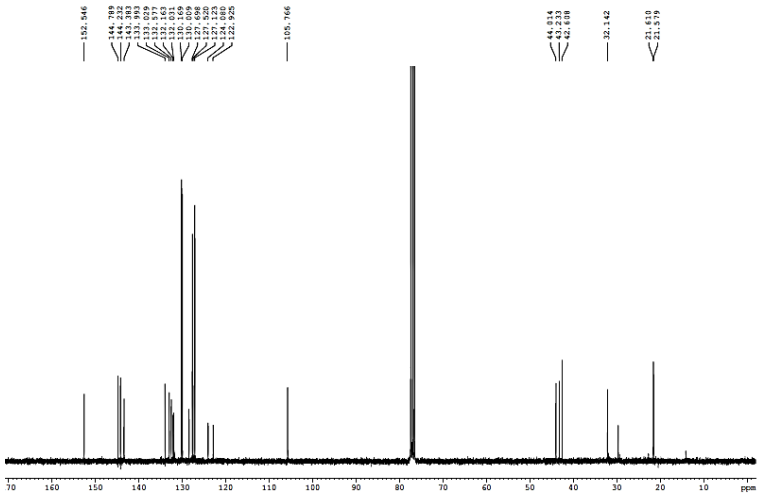

2D ^{1}H-^{13}C HSQC

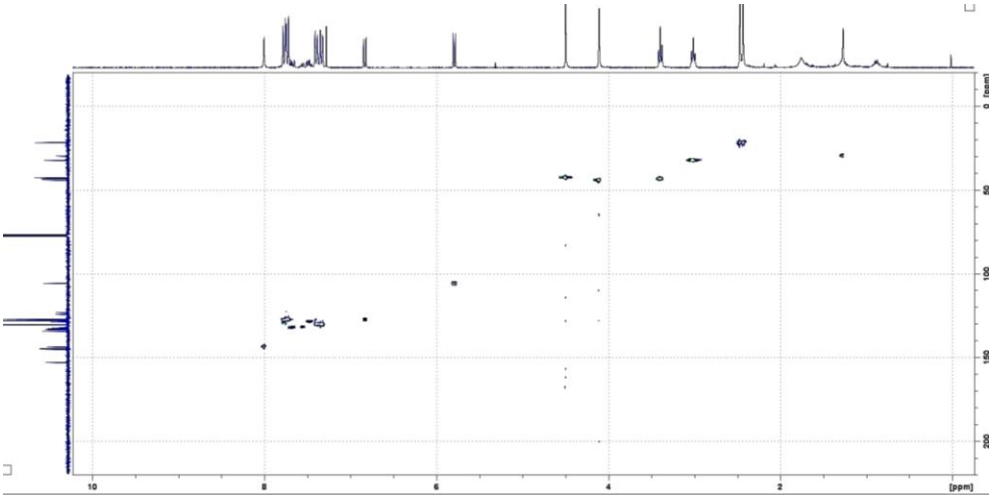

2D ^{1}H-^{13}C HMBC

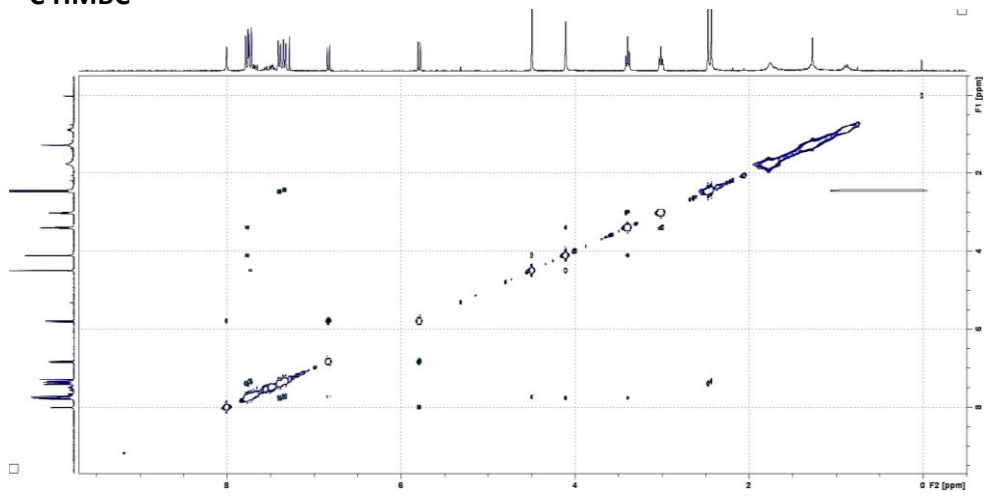

2D ^{1}H-^{1}H COSY

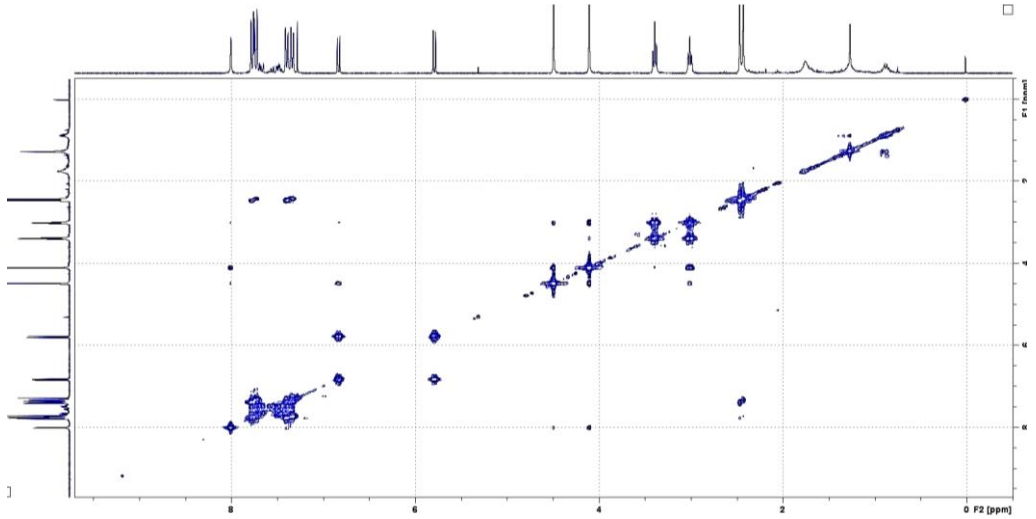

2D 1H-1H NOESY.

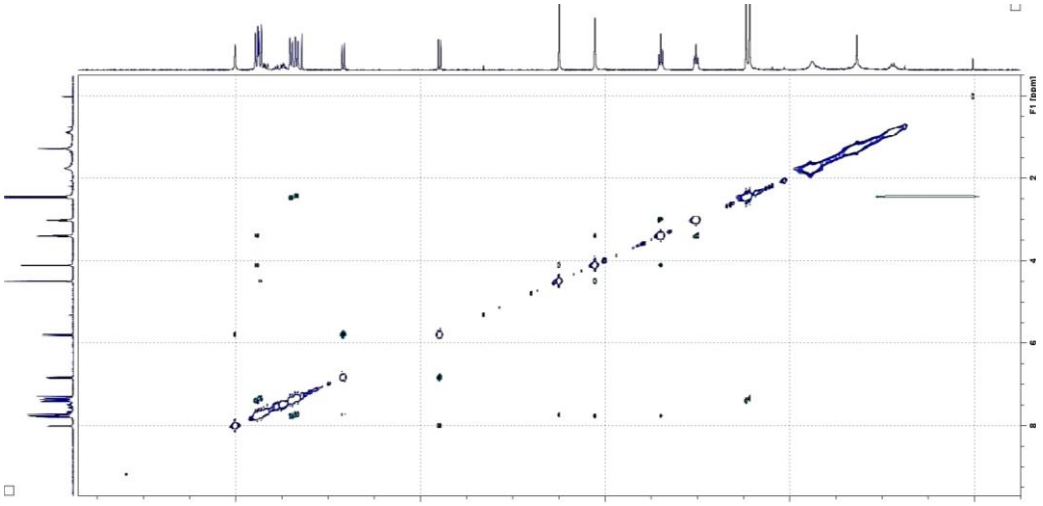

ESI-MS (+)

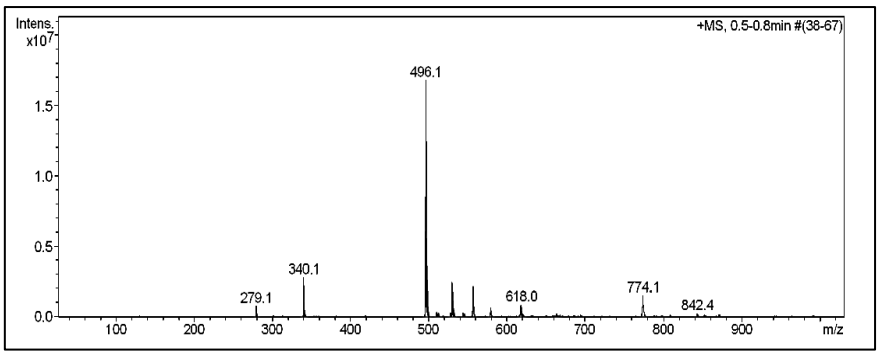

IR (ATR)

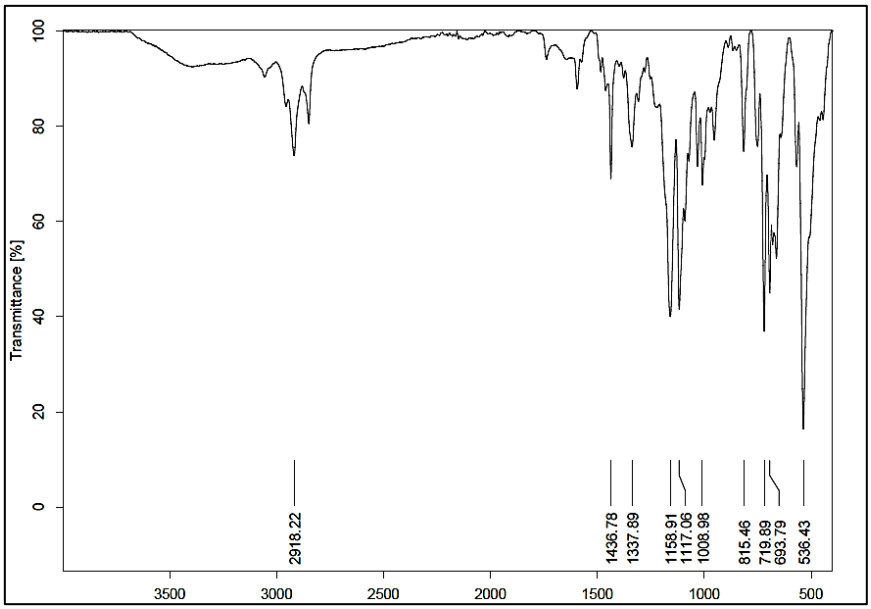

ESI-HRMS (+)

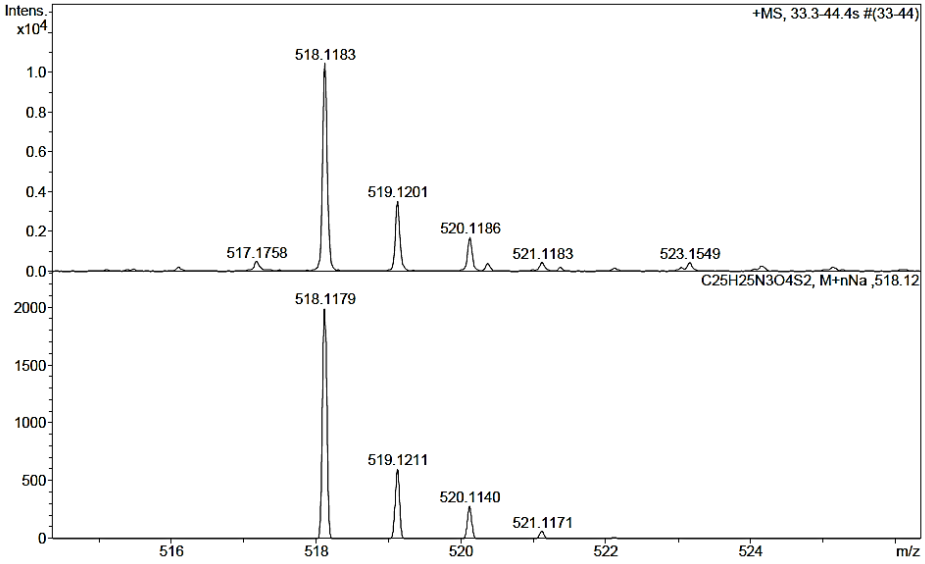

^{1}H NMR (300 MHz, $CDCl_3$)

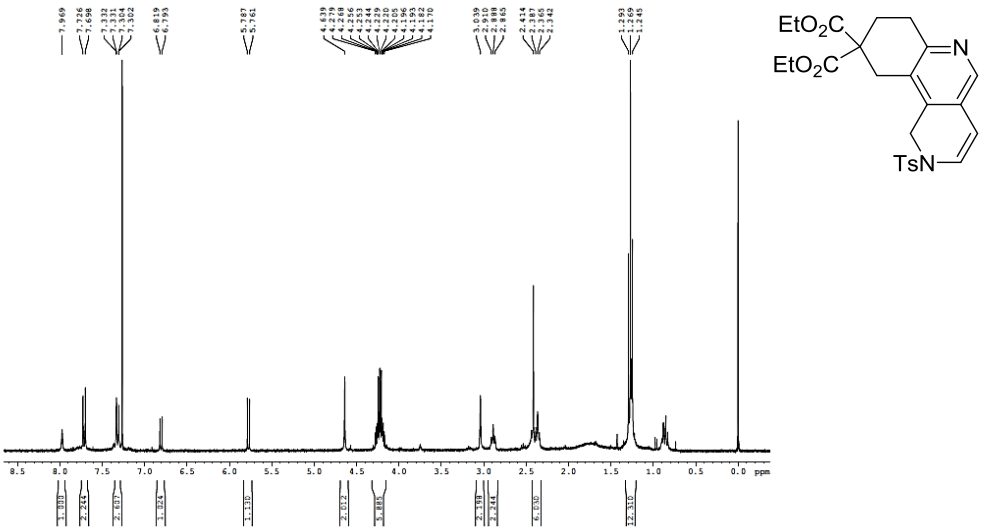

^{13}C NMR (75 MHz, $CDCl_3$)

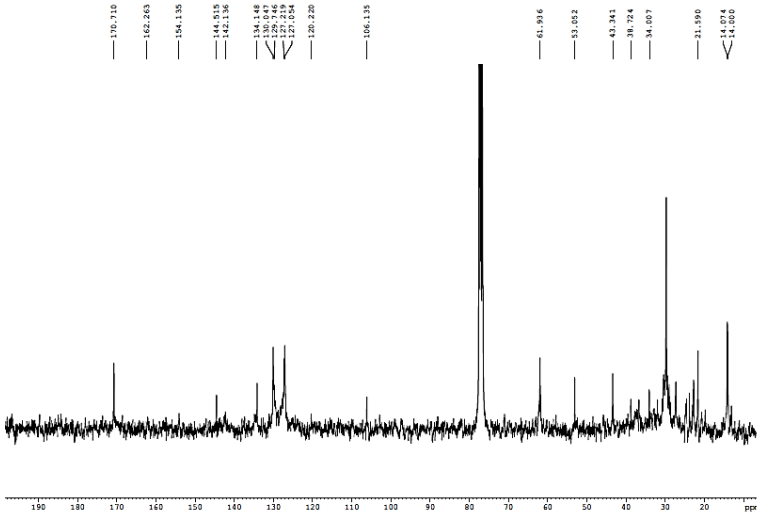

ESI-MS (+)

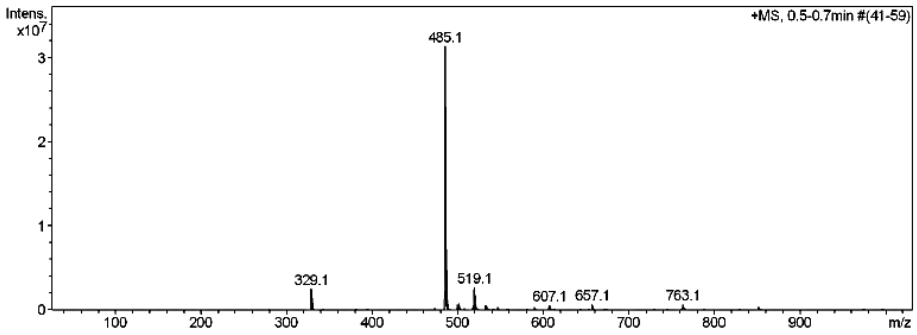

IR (ATR)

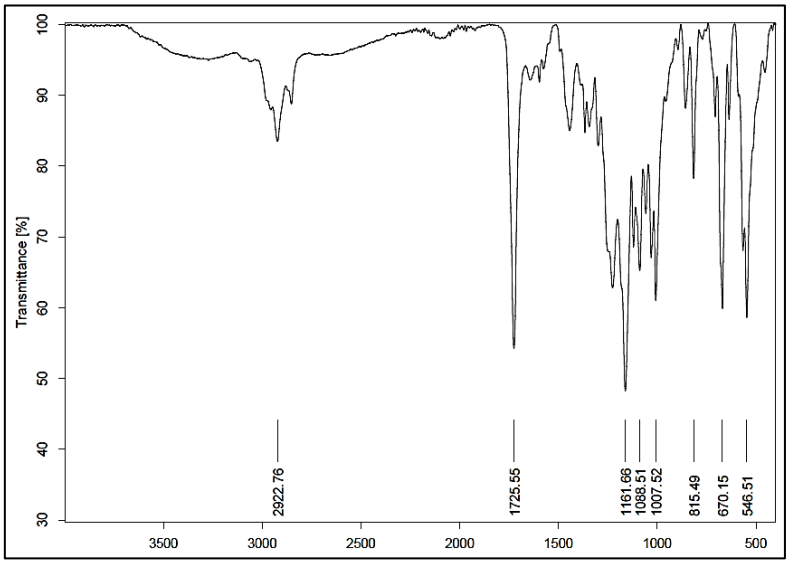

ESI-HRMS (+)

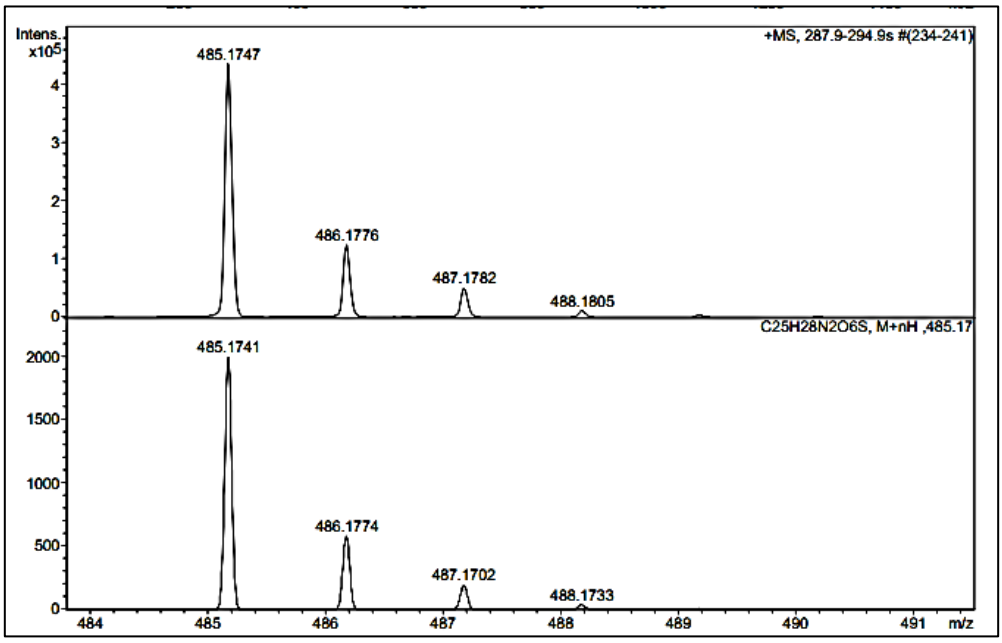

^{1}H NMR (300 MHz, $CDCl_3$)

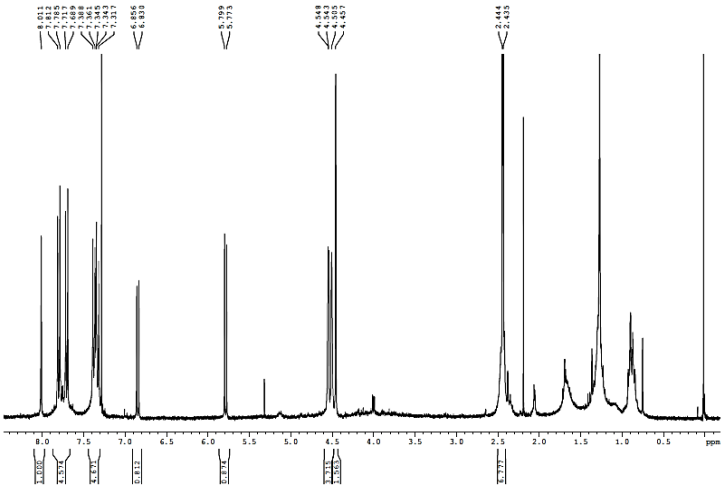

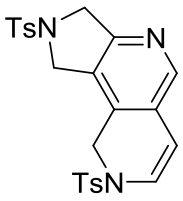

^{13}C NMR (75 MHz, $CDCl_3$)

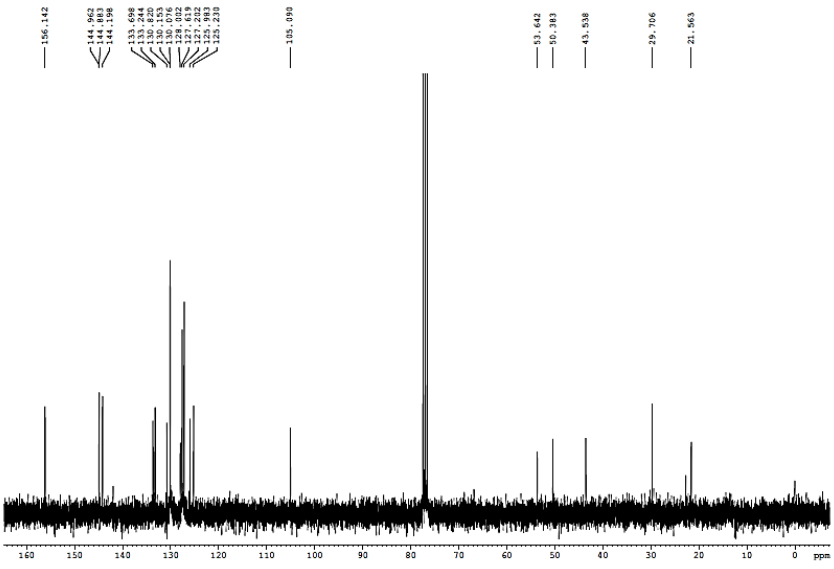

ESI-MS (+)

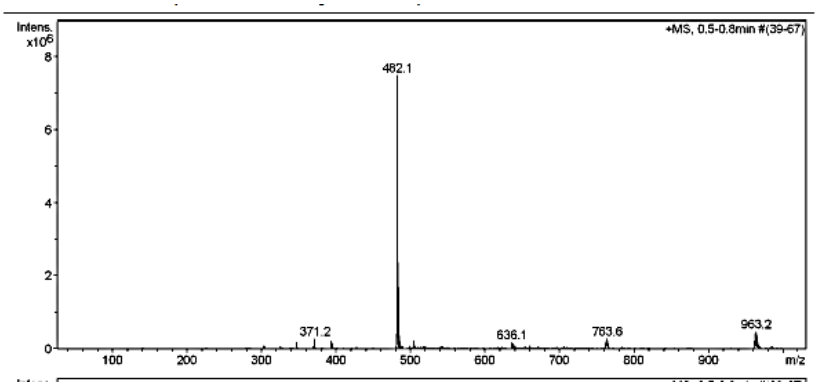

IR (ATR)

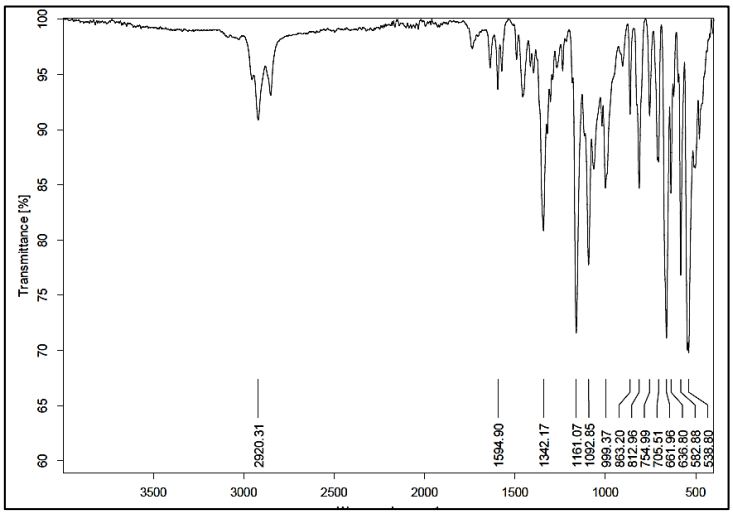

ESI-HRMS (+)

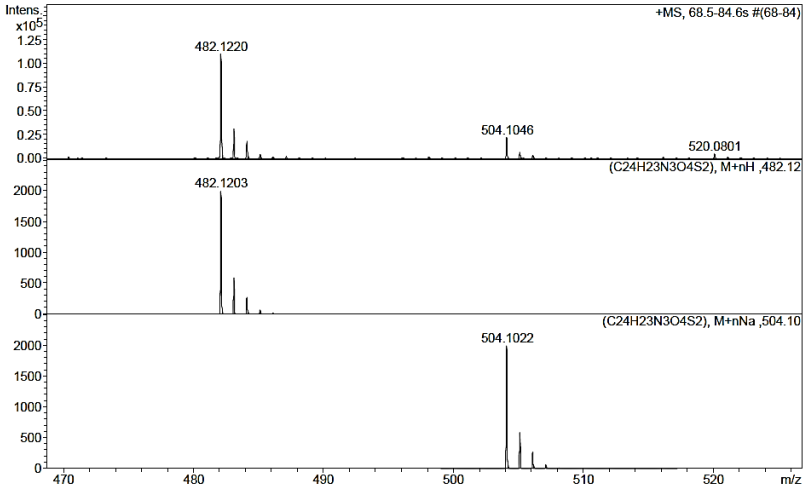

^{1}H NMR (300 MHz, $CDCl_3$)

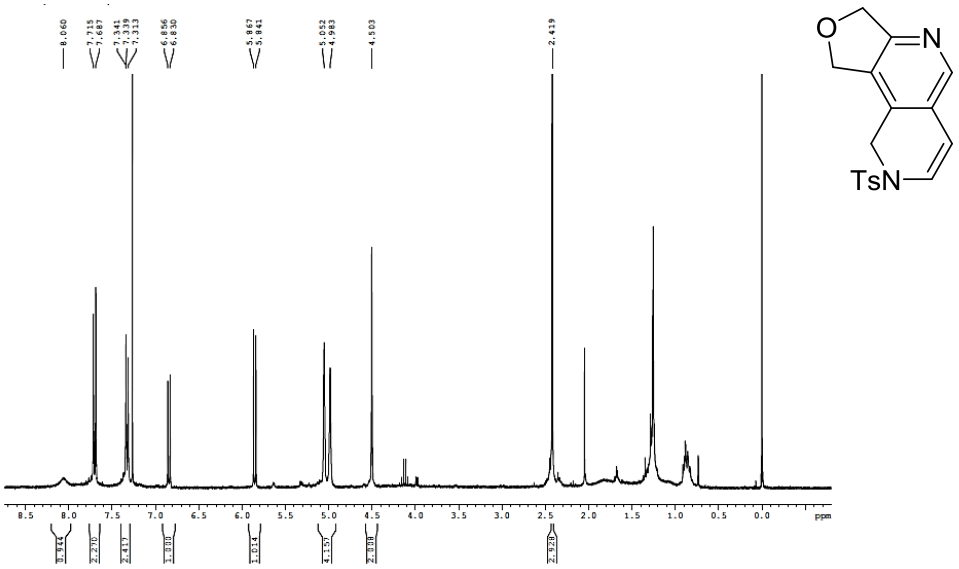

^{13}C NMR (75 MHz, $CDCl_3$)

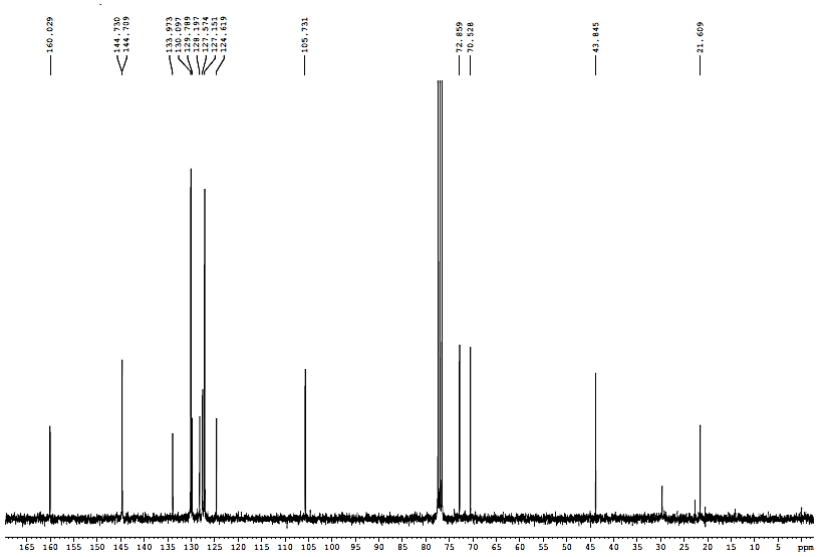

ESI-MS (+)

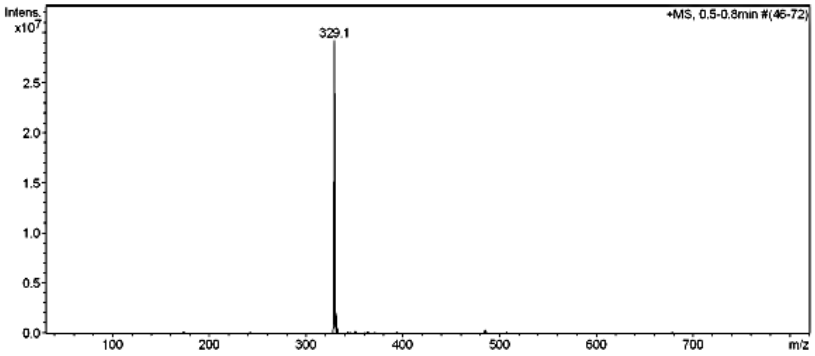

IR (ATR)

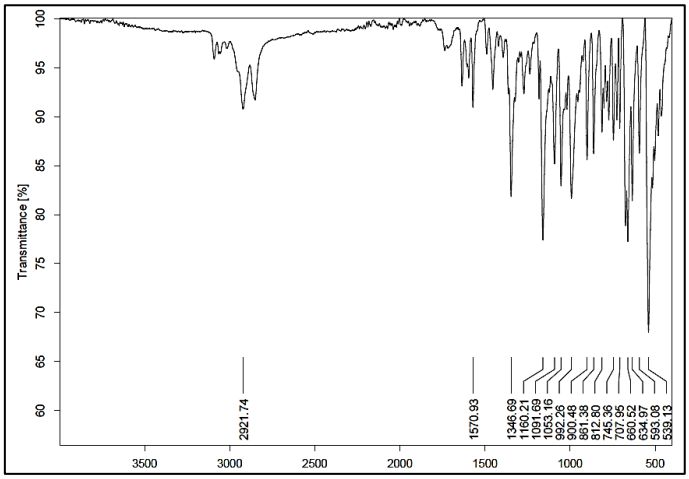

^{1}H NMR (300 MHz, $CDCl_3$)

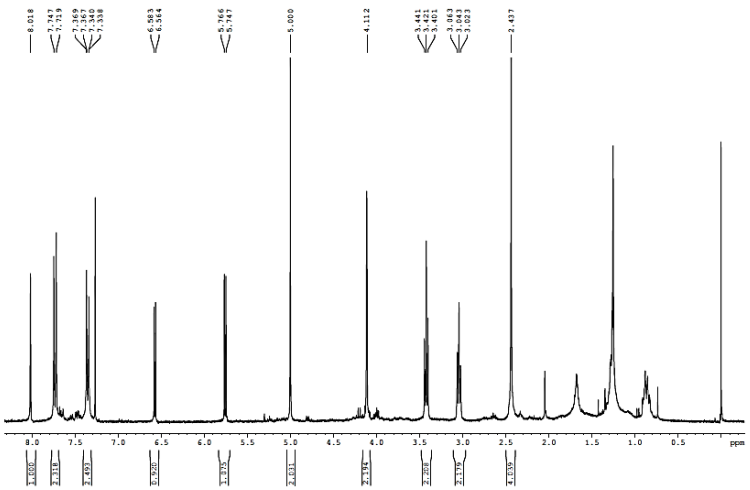

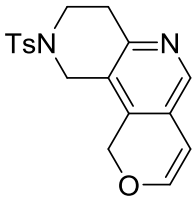

^{13}C NMR (75 MHz, $CDCl_3$)

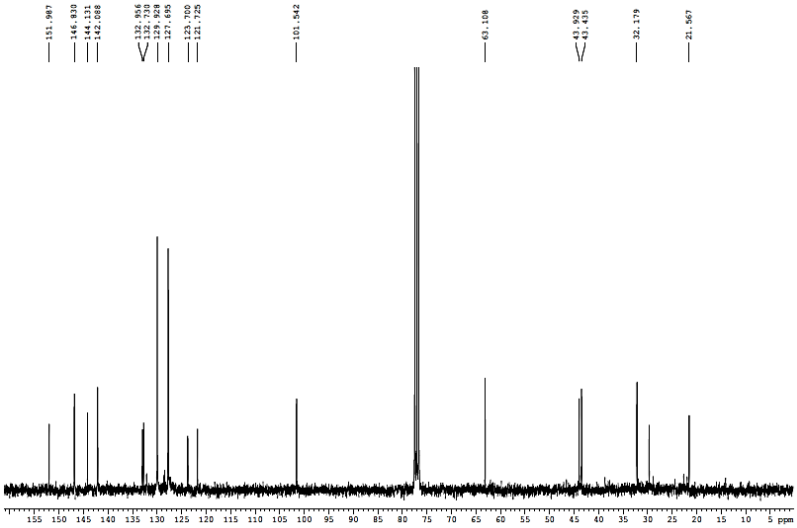

ESI-MS (+)

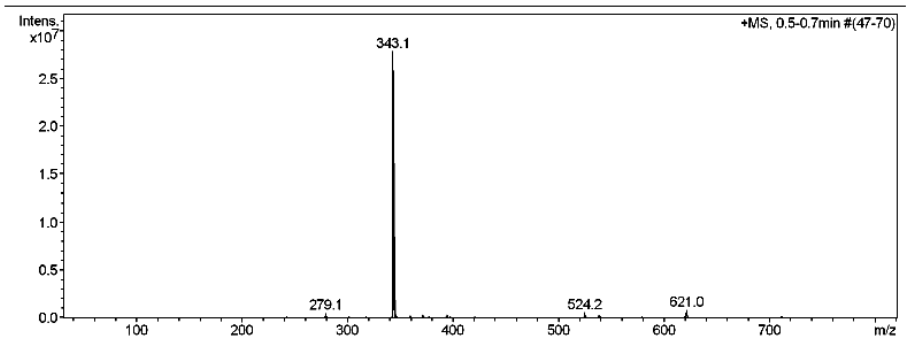

IR (ATR)

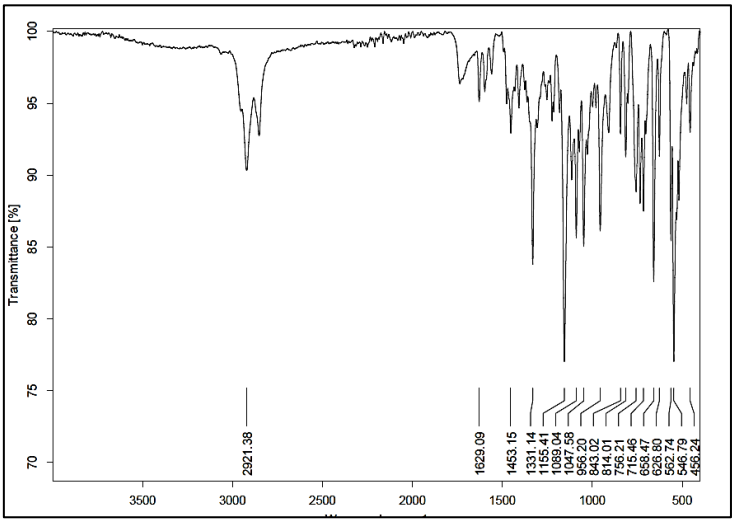

ESI-HRMS (+)

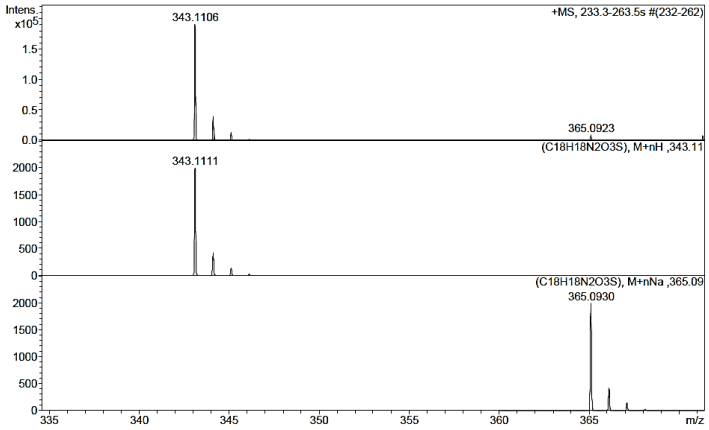

^{1}H NMR (400 MHz, $CDCl_3$)

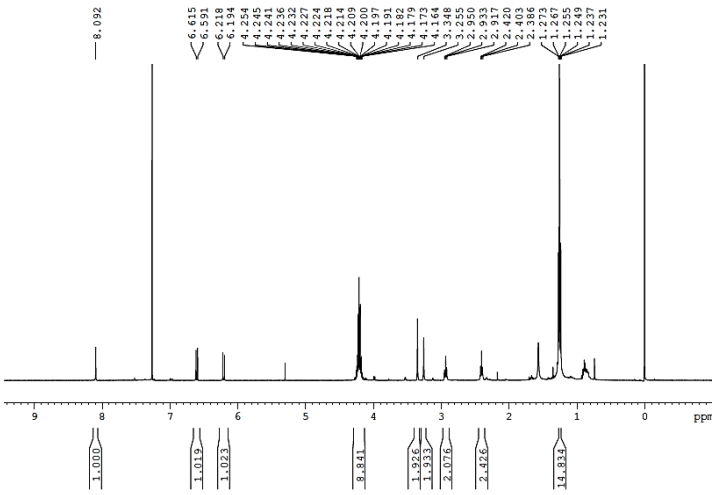

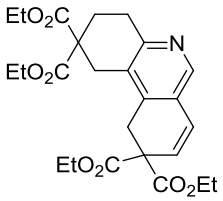

^{13}C NMR (75 MHz, $CDCl_3$)

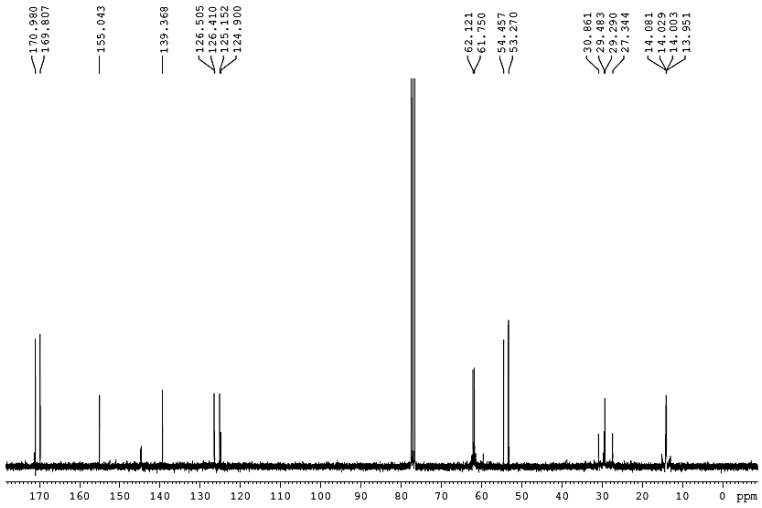

2D ^{1}H-^{1}H COSY.

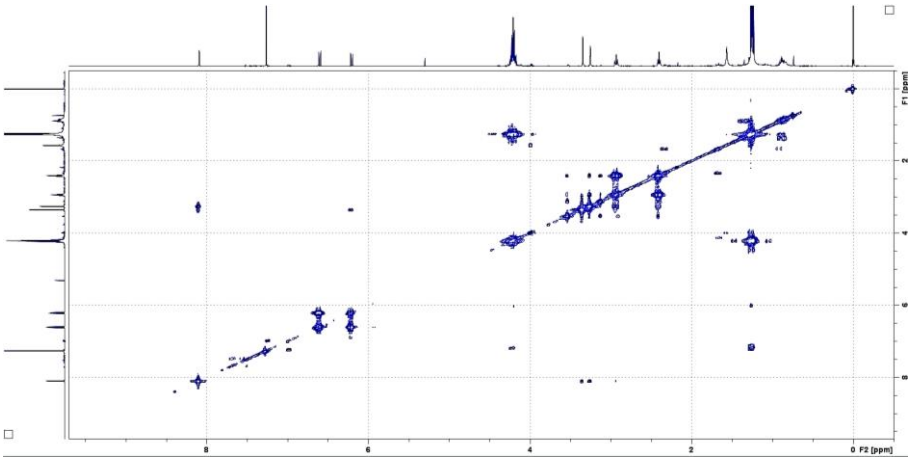

2D ^{1}H-^{13}C HSQC

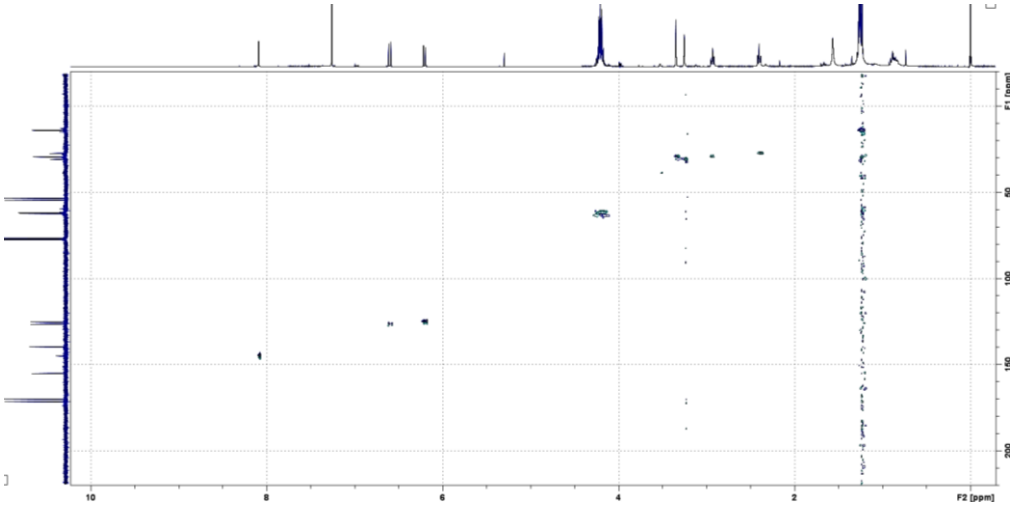

IR (ATR)

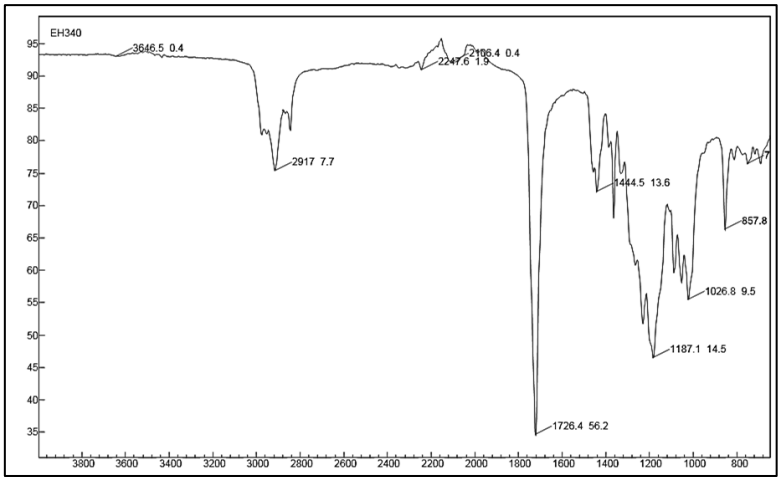

ESI-HRMS (+)

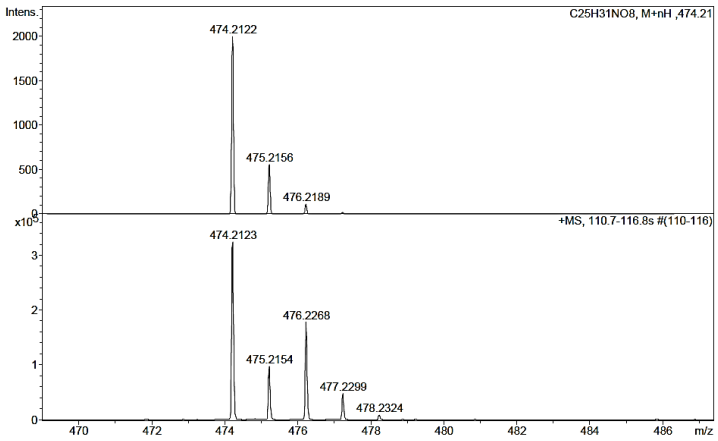

^{1}H NMR (400 MHz, $CDCl_3$)

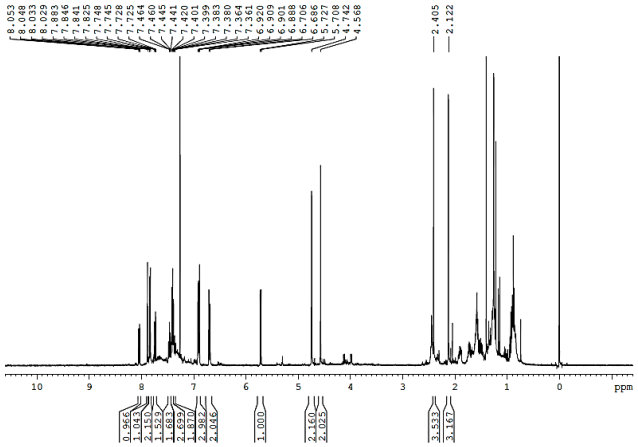

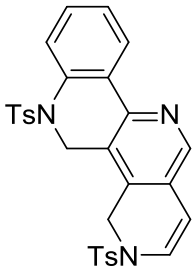

^{13}C NMR (100 MHz, $CDCl_3$)

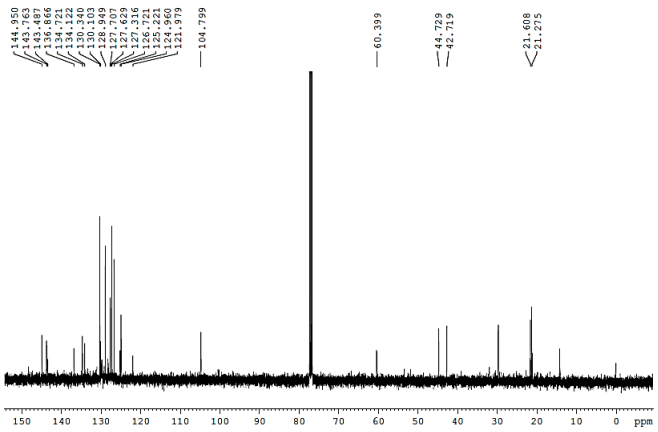

IR (ATR)

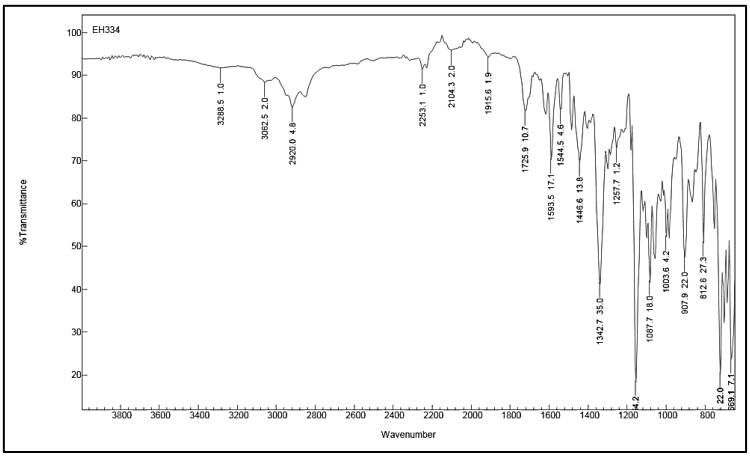

ESI-HRMS (+)

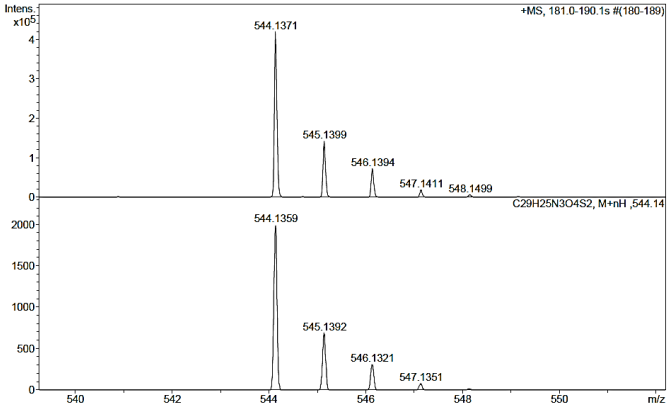

^{1}H NMR (400 MHz, $CDCl_3$)

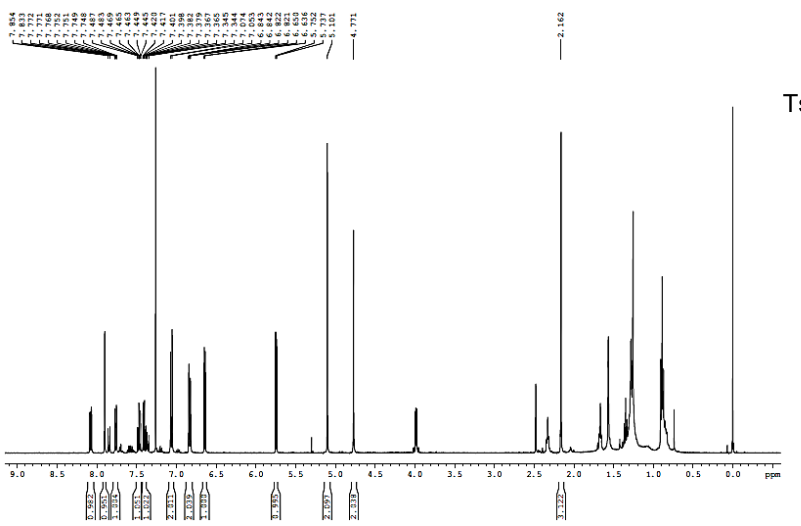

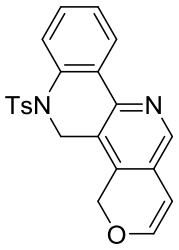

^{13}C NMR (100 MHz, $CDCl_3$)

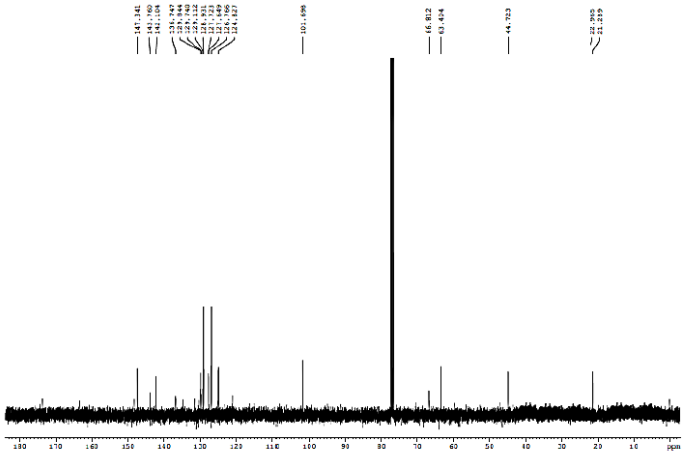

IR (ATR)

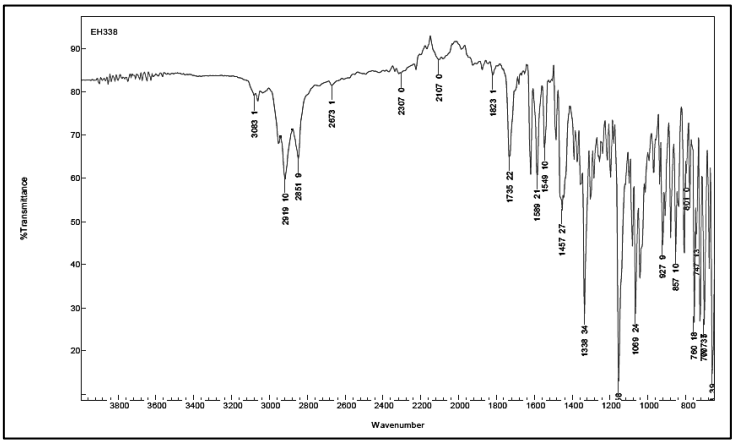

ESI-HRMS (+)

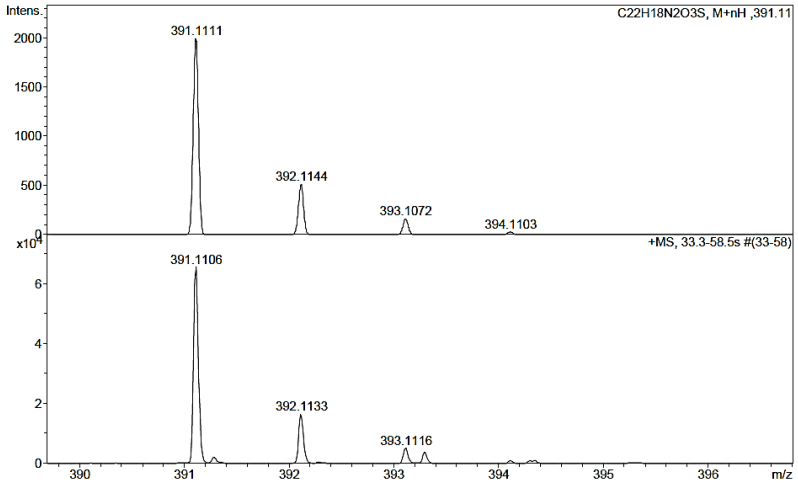

^{1}H NMR (300 MHz, $CDCl_3$)

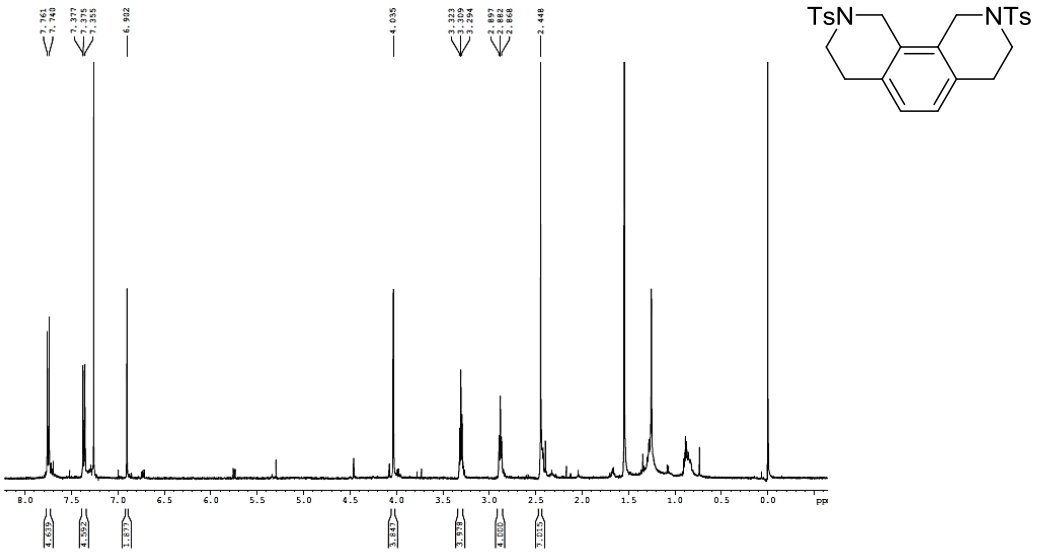

^{13}C NMR (75 MHz, $CDCl_3$)

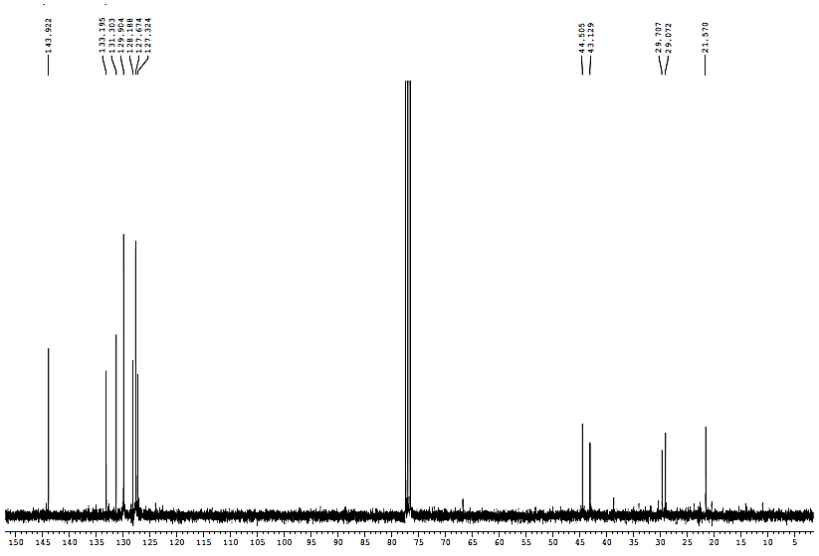

ESI-MS (+)

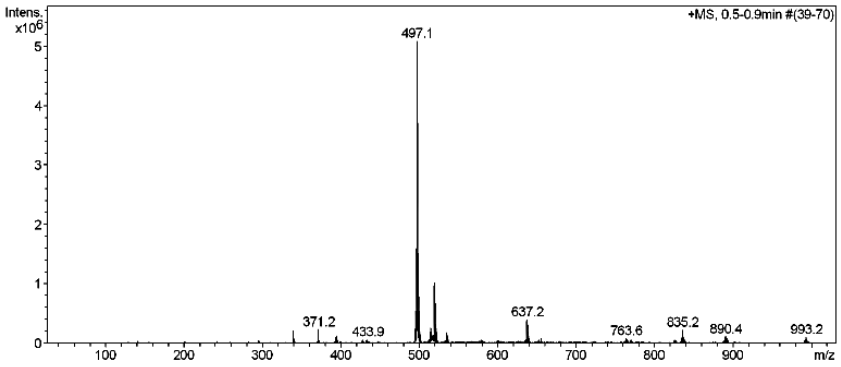

IR (ATR)

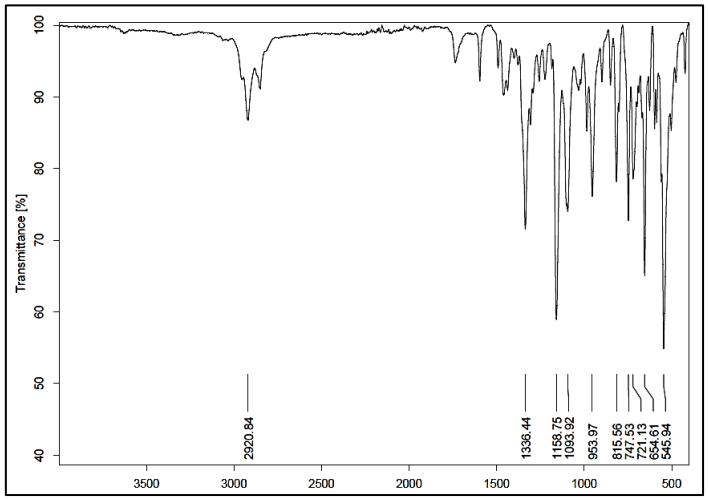

ESI-HRMS (+)

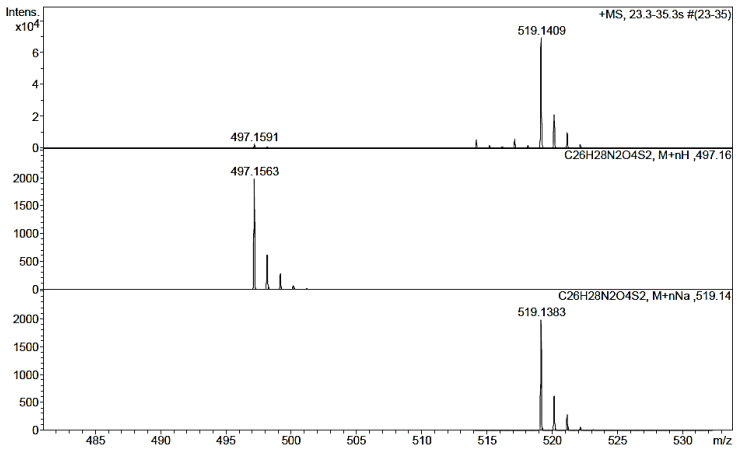

^{1}H NMR (400 MHz, $CDCl_3$)

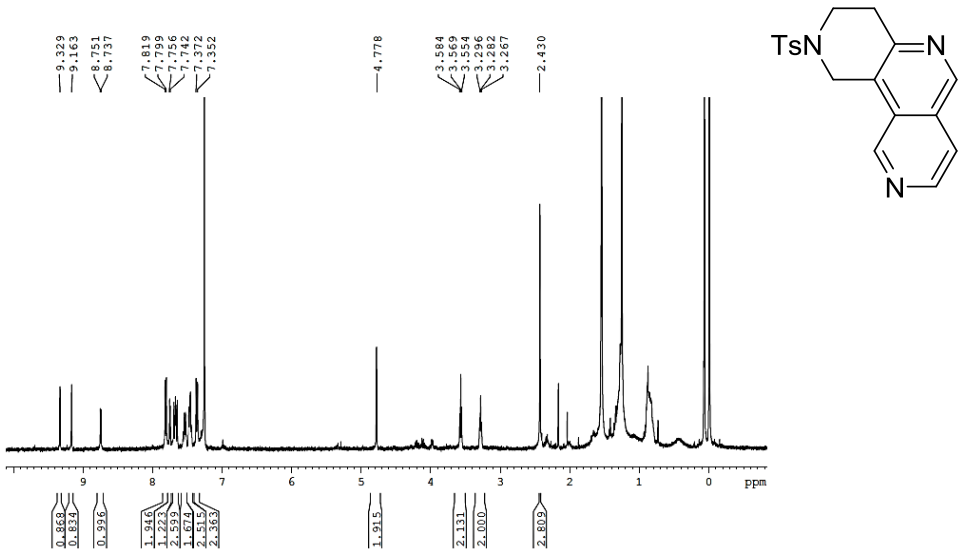

^{13}C NMR (100 MHz, $CDCl_3$)

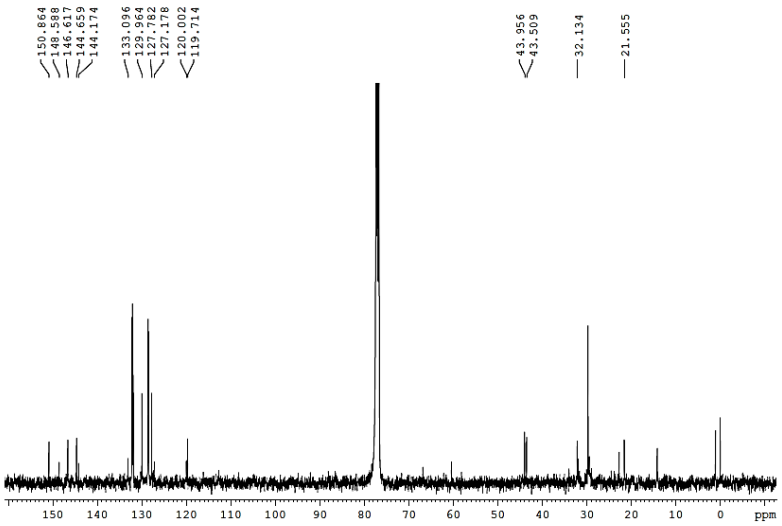

ESI-MS (+)

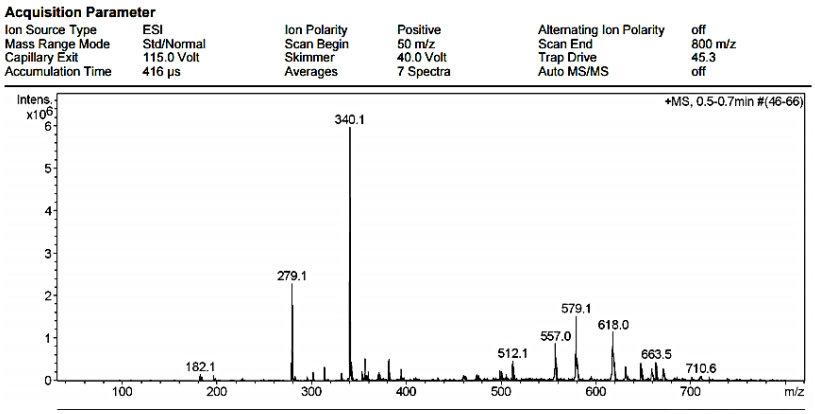

ESI-HRMS (+)

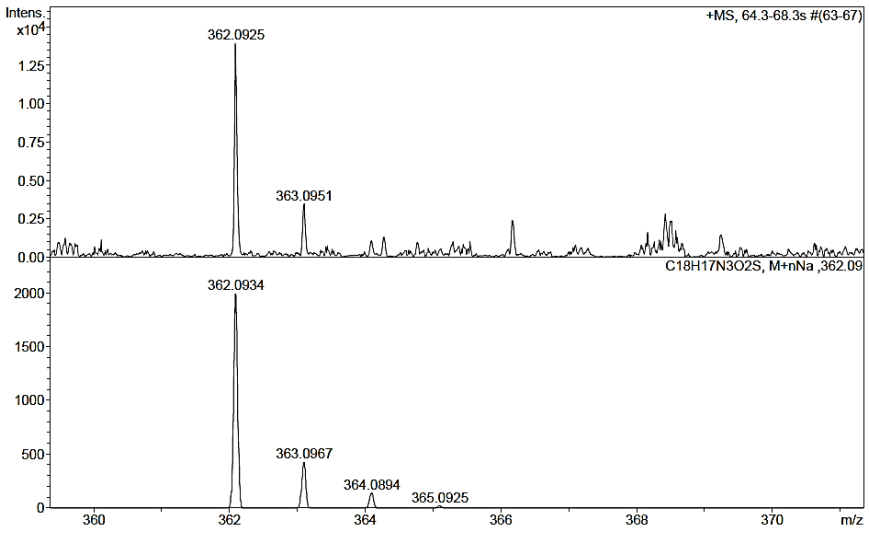

Bibliography

[1] a) Ma, S. *Chem. Rev.* **2005**, *105*, 2829; b) Krause, N.; Hashmi, A. S. K. *Modern Allene Chemistry*, Wiley-VCH, Weinheim, **2004**; c) Schuster, H. F.; Coppola, G. M. *Allenes in Organic Synthesis*, Wiley-Interscience, New York, **1984**.

[2] Hoffman-Röder, A.; Krause, N. *Angew.Chem., Int. Ed.* **2004**, *43*, 1196.

[3] a) Neff, R. K.; Frantz, D. E. *Tetrahedron,* **2015**, *71*, 7; b) Aubert, C.; Fensterbank, L.; Garcia, P.; Malacria, M.; Simonneau, A. *Chem. Rev.* **2011**, *111*, 1954; c) Bates, R. W.; Satcharoen, V.; *Chem. Soc. Rev*. **2002**, *31*, 12; d) Stephen, A.; Hashmi, K. *Angew. Chem. Int. Ed.* **2000**, *39*, 3590.

[4] Reppe, W.; Schweckendiek, W. J. *Justus Liebigs Ann. Chem*. **1948**, *560*, 104.

[5] For a monograph of [2+2+2] cycloadditions, see: Tanaka, K. *Transition-Metal-Mediated Aromatic Ring Construction*, Wiley, John & Sons, Inc., **2013**. For selected reviews, see: a) Shibata, Y; Tanaka, K. *Synthesis* **2012**, 323; b) Marinetti, A.; Jullien, H.; Voituriez, A. *Chem. Soc. Rev,* **2012**, *41,* 4884; c) Tanaka, K. *Heterocycles* **2012**, *85*, 1017; d) Okamoto, S. *Heterocycles* **2012**, *85*, 1579; e) Hua, R.; Abrenica, M. V. A.; Wang, P. *Curr. Org. Chem.* **2011**, *15*, 712; f) Inglesby, P. A.; Evans, P. A. *Chem. Soc. Rev.* **2010**, *39*, 2791; g) Pla-Quintana, A.; Roglans, A.; *Molecules* **2010**, *15*, 9230; h) Tanaka, K. *Chem. Asian J.* **2009**, *4*, 508; i) Galan, B. R.; Rovis, T. *Angew. Chem. Int. Ed.* **2009**, *48*, 2830; j) Shibata, T.; Tsuchikama, K. *Org. Biomol. Chem.* **2008**, *6*, 1317; k) Tanaka, K. *Synlett.* **2007**, 1977; l) Chopade, P. R.; Louie, J. *Adv. Synth. Catal.* **2006**, *348*, 2307; m) Gandon, V.; Aubert, C.; Malacria, M. *Chem. Commun.* **2006**, 2209; n) Yamamoto, Y. *Curr. Org. Chem.* **2005**, *9*, 503; o) Kotha, S.; Brahmachary, E.; Lahiri, K. *Eur. J. Org. Chem.* **2005**, 4741; p) Varela, J. A.; Saá, C.; *Chem. Rev.* **2003**, *103*, 3787; r) Saito, S.; Yamamoto, Y. *Chem. Rev.* **2000**, *100*, 2901; s) Lautens, M.; Klute, W.; Tam, W. *Chem. Rev.* **1996**, *96*, 49.

[6] For selected references, see: a) Orian, L.; Swart, M.; Bickelhaupt, F. M. *ChemPhysChem*. **2014**, *15*, 219; b) Orian, L.; Wolters, L. P.; Bickelhaupt, F. M. *Chem. Eur. J.* **2013**, *19,* 13337; c) Calhorda, M. J.; Costa, P. J.; Kirchner, K. *Inorg. Chim. Acta* **2011**, *374*, 24; d) Li, X.; Xu, J. *Org. Biomol. Chem.* **2011**, *9*, 5997; e) Varela, J. A.; Saá, C. *J. Organomet. Chem.* **2009**, *694*, 143; f) Orian, L.; van Stralen, J. N. P.; Bickelhaupt, F. M. *Organometallics* **2007**, *26*, 3816; g) Agenet, N.; Gandon, V.; Vollhardt, K. P. C.; Malacria, M.; Aubert, C. *J. Am. Chem. Soc.* **2007**, *129*, 8860; h) Yamamoto, Y.; Kinpara, K.; Ogawa, R.; Itoh, K. *Chem. Eur. J.* **2006**, *12*, 5618. For contributions of our group on mechanistic DFT calculations on Rh-catalysed [2+2+2] cycloadditions: i) Dachs, A.; Roglans, A.; Solà, M. *Organometallics* **2011**, *30*, 3151; j) Dachs, A.; Pla-Quintana, A.; Parella, T.; Solà, M.; Roglans, A. *Chem. Eur. J.* **2011**, *17*, 14493; k) Dachs, A.; Osuna, S.; Roglans, A.; Solà, M. *Organometallics* **2010**, *29*, 562; l) Dachs, A.; Torrent, A.; Roglans, A.; Parella, T.; Osuna, S.; Solà, M. *Chem. Eur. J.* **2009**, *15*, 5289.

[7] Selected references: a) Parera, M.; Dachs, A.; Solà, M.; Pla-Quintana, A.; Roglans, A. *Chem. Eur. J.* **2012**, *18*, 13097, b) Dachs, A.; Torrent, A.; Pla-Quintana, A.; Roglans, A.; Jutand, A. *Organometallics* **2009**, *28*, 6063; c) Uchimura, H.; Ito, J. I.; Iwasa, S.; Nishiyama, H. *J. Organomet. Chem.* **2007**, *692*, 481; d) Xue, P.; Sung, H. S. Y.; Williams, I. D.; Jia, G. *J. Organomet. Chem.* **2006**, *691*, 1945; e) Nishiyama, H.; Niwa, E.; Inoue, T.; Ishima, Y.; Aoki, K. *Organometallics* **2002**, *21*, 2572; f) Rourke, J. P.; Batsanov, A. S.; Howard, J. A. K.; Marder, T. B. *Chem. Commun.* **2001**, 2626; g) Bianchini, C.; Meli, A.; Peruzzini, M.; Vacca, A.; Vizza, F. *Organometallics* **1991**, *10*, 645; h) Bianchini, C.; Caulton, K. G.; Chardon, C.; Eisenstein, O.; Folting, K.; Johnson, T. J.; Meli, A.; Peruzzini, M.; Tauscher, D. J.; Streib, W. E.; Vizza, F. *J. Am. Chem. Soc.* **1991**, *113*, 5127; i) Iglesias, M.; del Pino, C.; Ros, J.; García Blanco, S.; Carrera, S. M. *J. Organomet. Chem.* **1988**, *338*, 38; j) Gastinger, R. G.; Rausch, M. D.; Sullivan, D. A.; Palenik, G. J. *J. Organomet. Chem.* **1976**, *117*, 355; k) Müller, E. *Synthesis* **1974**, 761; l) Mague, J. T. *Inorg. Chem.* **1973**, *12*, 2649; m) Mague, J. T. *Inorg. Chem.* **1970**, *9*, 1610.

[8] Schore, N. E. *Chem. Rev.* **1988**, *88*, 1081.

[9] a) Santos, J. C.; Polo, V.; Andrés, J. *Chem. Phys. Lett.* **2005**, *406*, 393; b) Ioffe, A.; Shaik, S. *J. Chem. Soc. Perkin Trans. 2,* **1992**, 2101.

[10] For reviews on pyridine synthesis by transition metal-catalysed [2+2+2] cycloaddition, see: a) Broere, D. L. J.; Ruijter, E. *Synthesis* **2012**, 2639; b) Tanaka, K. *Heterocycles* **2012**, *85*, 1017; c) Domínguez, G.; Pérez-Castells, J. *Chem. Soc. Rev.* **2011**, *40*, 3430; d) Weding, N.; Hapke, M. *Chem. Soc. Rev*. **2011**, *40*, 4525; e) Sugiyama, Y.-K.; Okamoto, S. *Synthesis* **2011,** 2247; f) Shaaban, M. R.; El-Sayed, R.; Elwahy, A. H. M. *Tetrahedron* **2011**, *67*, 6095; g) Varela, J. A.; Saá, C. *Synlett.* **2008**, 2571; h) Heller, B.; Hapke, M. *Chem. Soc. Rev*. **2007**, *36*, 1085. For applications of the metal-catalysed [2+2+2] cycloaddition reaction in natural product synthesis, see: i) Witulski, B.; Grand, J. *Application to the Synthesis of Natural Products, in Transition-Metal-Mediated Aromatic Ring Construction*, ed. K. Tanaka, John Wiley & Sons, Inc., Hoboken, NJ, USA, 2013.

[11] Wakatsuki, Y.; Yamazaki, H. *Tetrahedron Lett.* **1973**, *14*, 3383.

[12] Brien, J. D.; Naiman, A.; Vollhardt, K. P. C. *J. Chem. Soc., Chem. Commun.* **1982**, 133.

[13] a) Garcia, P.; Evanno, Y.; George, P.; Sevrin, M.; Ricci, G.; Malacria, M.; Aubert, C.; Gandon, V. *Chem. Eur. J*. **2012**, *18*, 4337; b) Garcia, P.; Evanno, Y.; George, P.; Sevrin, M.; Ricci, G.; Malacria, M.; Aubert, C.; Gandon, V. *Org. Lett*. **2011**, *13*, 2030; c) Yuan, C.; Chang, C.-T.; Axelrod, A.; Siegel, D. *J. Am. Chem. Soc*. **2010**, *132*, 5924; d) Gray, B. L.; Wang, X.; Brown, W. C.; Kuai, L.; Schreiber, S. L. *Org. Lett*. **2008**, *10*, 2621; e) Boñaga, L. V. R.; Zhang, H.-C.; Moretto, A. F.; Ye, H.; Gauthier, D. A.; Li, J.; Leo, G. C.; Maryanoff, B. E. *J. Am. Chem. Soc*. **2005**, *127*, 3473; f) Varela, J. A.; Castedo, L.; Saá, C. *Org. Lett*. **1999**, *1*, 2141.

[14] a) Yamamoto, Y.; Kinpara, K.; Ogawa, R.; Nishiyama, H.; Itoh, K. *Chem. Eur. J.* **2006**, *12*, 5618; b) Yamamoto, Y.; Kinpara, K.; Saigoku, T.; Takagishi, H.; Okuda, S.; Nishiyama, H.; Itoh, K. *J. Am. Chem. Soc.* **2005**, *127*, 605; c) Varela, J. A.; Castedo, L.; Saá, C. *J. Org. Chem*. **2003**, *68*, 8595; d) Yamamoto, Y.; Ogawa, R.; Itoh, K. *J. Am. Chem. Soc.* **2001**, *123*, 6189; e) Yamamoto, Y.; Okuda, S.; Itoh, K. *Chem. Commun.* **2001**, 1102.

[15] a) Komine, Y.; Tanaka, K. *Org. Lett*. **2010**, *12*, 1312; b) Shibata, T.; Uchiyama, T.; Endo, K. *Org. Lett.* **2009**, *11*, 3906; b) Tanaka, K.; Hara, H.; Nishida, G.; Hirano, M. *Org. Lett*. **2007**, *9*, 1907; c) Wada, A.; Noguchi, K.; Hirano, M.; Tanaka, K.; *Org. Lett*. **2007**, *9*, 1295; d) Tanaka, K.; Suzuki, N.; Nishida, G. *Eur. J. Org. Chem.* **2006**, 3917.

[16] a) Richard, V.; Ipouck, M.; Mérel, D.; Gaillard, S.; Whitby, R. J.; Witulski, B.; Renaud, J.-L. *Chem. Commun*. **2014**, *50*, 593; b) Wang, C.; Wang, D.; Xu, F.; Pan, B.; Wan, B. *J. Org. Chem*. **2013**, *78*, 3065;

[17] Garcia, L.; Pla-Quintana, A.; Roglans, A.; Parella, T. *Eur. J. Org. Chem.* **2010**, 3407.

[18] Lane, T. K.; Nguyen, H. M.; D'Souza, B. R.; Spahn, N. A.; Louie, J. *Chem. Commun*. **2013**, *49*, 7735.

[19] Narayan, S.; Liu, R. S. *Angew. Chem. Int. Ed*. **2014**, *53*, 9072.

[20] a) Brun, S.; Garcia, L.; González, I.; Torrent, A.; Dachs, A.; Pla-Quintana, A.; Parella, T.; Roglans, A. *Chem. Commun*. **2008**, 4339; b) González, I.; Bouquillon, S.; Roglans, A.; Muzart, J. *Tetrahedron Lett.* **2007**, *48,* 6425; c) Torrent, A.; González, I.; Pla-Quintana, A.; Roglans, A. *J. Org. Chem*. **2005**, *70*, 2033; d) Pla-Quintana, A.; Roglans, A.; Torrent, A.; Moreno-Mañas, M.; Benet-Buchholz, J. *Organometallics*, **2004**, *23*, 2762.

[21] a) Welsch, T.; Tran, H.-A.; Witulski, B. *Org. Lett.* **2010**, *12*, 5644; b) Zou, Y.; Deiters, A. *J. Org. Chem.* **2010**, *75*, 5355; c) Kesenheimer, C.; Kalogerakis, A.; Meiβner, A.; Groth, U. *Chem. Eur. J.* **2010**, *16*, 8805; d) Nicolaus, N.; Strauss, S.; Neudörfl, J.-M.; Prokop, A.; Schmalz, H.-G. *Org. Lett.* **2009**, *11*, 341; e) Anderson, E. A.; Alexanian, E. J.; Sorensen, E. J. *Angew. Chem. Int. Ed*. **2004**, *43*, 1998; f) Witulski, B.; Zimmermann, A. *Synlett.* **2002**, 1855.

[22] Witulski, B.; Zimmermann, H.; Gowans, N. D. *Chem. Commun*. **2002**, 2984.

[23] Saito, N.; Ichimaru, T.; Sato, Y. *Org. Lett*. **2012**, *14*, 1914.

[24] For selected references of Rh-catalysed [2+2+2] cycloadditions between diynes and monoynes, see: a) Araki, T.; Noguchi, K.; Tanaka, K. *Angew. Chem. Int. Ed.* **2013**, *52*, 5617; b) Murayama, K.; Sawada, Y.; Noguchi, K.; Tanaka, K. *J. Org. Chem.* **2013**, *78*, 6202; c) Li, Y.; Zhu, J.; Zhang, L.; Wu, Y.; Gong, Y. *Chem. Eur. J.* **2013**, *19*, 8294; d) Garcia, L.; Roglans, A.; Laurent, R.; Majoral, J.-P.; Pla-Quintana, A.; Caminade, A.-M. *Chem. Commun*. **2012**, 9248; e) Cízková, M.; Kolivoska, V.; Cisarová, I.; Saman, D.; Pospisil, L.; Teplý, F. *Org. Biomol. Chem*. **2011**, *9*, 450; f) Suryawanshi, S. B.; Dushing, M. P.; Gonnade, R. G.; Ramana, C. V. *Tetrahedron* **2010**, *66*, 6085; g) Sedlák, D.; Novák, P.; Kotora, M.; Bartunek, P. *J. Med. Chem*. **2010**,

53, 4290; h) Wu, W.; Zhang, X. Y.; Kang, S. X. *Chin*. *Chem. Lett*. **2010**, *21*, 18; i) Tanaka, K.; Sawada, Y.; Aida, Y.; Thammathevo, M.; Tanaka, R.; Sagae, H.; Otake, Y. *Tetrahedron* **2010**, *66*, 1563; j) Young, D. D.; Teske, J. A.; Deiters, A. *Synthesis* **2009**, 3785; k) Garcia, L.; Pla-Quintana, A.; Roglans, A. *Org. Biomol. Chem.* **2009**, *7*, 5020; l) Komine, Y.; Kamisawa, A.; Tanaka K. *Org. Lett.* **2009**, *11*, 2361; m) Suda, T.; Noguchi, K.; Hirano, M.; Tanaka, K. *Chem. Eur. J.* **2008**, *14*, 6593; n) Novák, P.; Cíhalová, S.; Otmar, M.; Hocek, M.; Kotora, M. *Tetrahedron* **2008**, *64*, 5200; o) Nishida, G.; Noguchi, K.; Hirano, M.; Tanaka, K. *Angew. Chem. Int. Ed*. **2007**, *46*, 3951.

[25] a) Vollhardt, K. P. C. *Angew. Chem. Int. Ed. Engl.* **1984**, *23*, 539; b) Sternberg, E. D.; Vollhardt, K. P. C. *J. Org. Chem.* **1982**, *47*, 3447; c) Vollhardt K. P. C. *Chem. Res.* **1977**, *10*, 1; d) Funk, R. L.; Vollhardt, K. P. C. *J. Am. Chem. Soc.* **1980**, *102*, 5253; e) Vollhardt, K. P. C. *Ann. N. Y. Acad. Sci.* **1980**, *333*, 241.

[26] For selected references see: a) Hara, H.; Hirano, M.; Tanaka, K. *Org. Lett.* **2008**, *10*, 2537; b) Yoshida, K.; Morimoto, I.; Mitsudo, K.; Tanaka, H. *Tetrahedron* **2008**, *64*, 5800; c) Tanaka, K.; Toyoda, K.; Wada, A.; Shirasaka, K.; Hirano, M. *Chem. Eur. J.* **2005**, *11*, 1145; d) Tanaka, K.; Shirasaka, K. *Org. Lett.* **2003**, *5*, 4697.

[27] a) Sripada, L.; Teske, J. A.; Deiters, A. *Org. Biomol. Chem*. **2008**, *6*, 263; b) Yamamoto, Y.; Ishii, J.; Nishiyama, H.; Itoh, K. *J. Am. Chem. Soc*. **2005**, *127*, 9625; c) Yamamoto, Y.; Ishii, J.; Nishiyama, H.; Itoh, K. *J. Am. Chem. Soc.* **2004**, *126*, 3712.

[28] a) Llerena, D.; Buisine, O.; Aubert, C.; Malacria, M. *Tetrahedron* **1998**, *54*, 9373; b) Aubert, C.; Llerena, D.; Malacria, M. *Tetrahedron Lett.* **1994**, *35*, 2341.

[29] a) Slowinski, F.; Aubert, C.; Malacria, M. *J. Org. Chem.* **2003**, *68*, 378; b) Slowinski, F.; Aubert, C.; Malacria, M. *Tetrahedron Lett.* **1999**, *40*, 707; c) Slowinski, F.; Aubert, C.; Malacria, M. *Tetrahedron Lett.* **1999**, *40*, 5849.

[30] Buisine, O.; Aubert, C.; Malacria, M. *Synthesis* **2000**, 985.

[31] a) Petit, M.; Aubert, C.; Malacria, M. *Tetrahedron* **2006**, *62*, 10582; b) Petit, M.; Aubert, C.; Malacria, M. *Org. Lett.* **2004**, *6*, 3937.

[32] Saito, N.; Ichimaru, T.; Sato, Y. *Chem. Asian J.* **2012**, *7*, 1521.

[33] Oonishi, Y.; Kitano, Y.; Sato, Y. *Tetrahedron* **2013**, *69,* 7713.

[34] Sakashita, K.; Masutomi, K.; Noguchi, K.; Tanaka, K. *Chem. Lett.* **2014**, *43*, 1260.

[35] Shanmugasundaram, M.; Wu, M.-S.; Jeganmohan, M.; Huang, C.-W.; Cheng, C.-H. *J. Org. Chem.* **2002**, *67*, 7724.

[36] Wu, M. S.; Shanmugasundaram, M.; Cheng. C.-H. *Chem. Commun.* **2003**, 718.

[37] Shanmugasundaram, M.; Wu M.-S.; Cheng, C.-H. *Org. Lett.* **2001**, *3*, 4233.

[38] Hsieh, J.-C.; Kumar Rayabarapu, D.; Cheng, C.-H. *Chem. Commun.* **2004**, 532.

[39] Faustino, H.; Varela, I.; Mascareñas, J. L.; López, F. *Chem. Sci.* **2015**, *6*, 2903.

[40] For monographs and general reviews of asymmetric organometallic catalysis, see: a) Aubert, C.; Amatore, M. *Eur. J. Org. Chem.* **2015**, 265; b) Christmann, M.; Bräse, S. *Asymmetric Synthesis*: *The Essentials*, Shibasaki, M.; Matsunaga, S. "*Part II, Metal Catalysed Asymmetric Synthesis*", **2007**, Wiley-VCH, Weinheim; c) Ma, J.-A.; Cahard, D. *Angew. Chem. Int. Ed.* **2004**, *43*, 4566; d) Beller, M.; Bolm, C. *Transition Metals for Organic Synthesis* **2004**, 2nd edition, Wiley- VCH, Weinheim; e) Ojima, I. *Catalytic Asymmetric Synthesis* **2000**, 2nd edition, Wiley-VCH, New York; f) Special number "*Catalytic Asymmetric Synthesis*", *Acc. Chem. Res*. **2000**, *33*, 323; g) Jacobsen, E. N.; Pfaltz, A.; Yamamoto, H. *Comprehensive Asymmetric Catalysis* **1999**, Springer, (vol. I-III), Berlin; h) Noyori, R. *Asymmetric Catalysis in Organic Synthesis* **1994**, Wiley, New York.

[41] Eliel, E. L.; Wilen, S. H. Doyle, M. P. *Separation of Stereoisomers, Resolution, and Racemisation in Basic Organic Stereochemistry,* Wiley, New York, **2001**, 608.

[42] Sato, Y.; Nishimata, T.; Mori, M. *J. Org. Chem.* **1994**, *59*, 6133.

[43] a) Shibata, T.; Tahara, Y.; Tamura, K.; Endo, K. *J. Am. Chem. Soc.* **2008**, *130*, 3451; b) Shibata, T.; Kurokawa, H.; Kanda, K. *J. Org. Chem.* **2007**, *72*, 6521.

[44] a) León, T.; Parera, M.; Roglans, A.; Riera, A. Verdaguer, X. *Angew. Chem. Int. Ed*. **2012**, *51*, 6951; b) Brun, S.; Parera, M.; Pla-Quintana, A.; Roglans, A.; León, T.; Achard, T.; Solà, J.; Verdaguer, X.; Riera, A. *Tetrahedron* **2010**, *66*, 9032.

[45] a) Sagae, H.; Noguchi, K.; Hirano, M.; Tanaka, K. *Chem. Commun.* **2008**, 3804; b) Tanaka, K.; Nishida, G.; Sagae, H.; Hirano, M. *Synlett.* **2007**, *167*, 1426.

[46] b) Shibata, T.; Otomo, M.; Endo, K. *Synlett.* **2010**, 1235; b) Shibata, T.; Tahara, Y. *J. Am. Chem. Soc.* **2006**, *128*, 11766.

[47] Tanaka, K.; Nishida, G.; Sagae, H.; Hirano, M. *Synlett.* **2010**, 1426.

[48] Tanaka, K.; Takahashi, M.; Imase, H.; Osaka, T.; Noguchi, K. *Tetrahedron* **2008**, *64*, 6289.

[49] Amatore, M.; Leboeuf, D.; Malacria, M.; Gandon, V.; Aubert, C. *J. Am. Chem. Soc.* **2013**, *135*, 4576.

[50] Yu, R. T.; Rovis, T. *J. Am. Chem. Soc.* **2006**, *128*, 12370.

[51] Hara, J.; Ishida, M.; Kobayashi, M.; Noguchi, K.; Tanaka, K., *Angew. Chem. Int. Ed.* **2014**, *53*, 2956.

[52] Sato, Y.; Ohashi, K.; Mori, M. *Tetrahedron Lett.* **1999**, *40*, 5231.

[53] Mori, F.; Fukawa, N.;Noguchi, K.; Tanaka, K. *Org. Lett.* **2011**, *13*, 362.

[54] a) Doherty, S.; Smyth, C. H.; Harrington, R. W.; Clegg, W. *Organometallics* **2008**, *27*, 4837; b) Nishida, G.; Ogaki, S.; Yusa, Y.; Yokozawa, T.; Noguchi, K.; Tanaka, K. *Org. Lett.* **2008**, *10*, 2849; c) Nishida, G.; Noguchi, K.; Hirano, M.; Tanaka, K. *Angew. Chem. Int. Ed.* **2007**, *46*, 3951; d) Doherty, S.; Knight, J. G.; Smyth, C. H.; Harrington, R. W.; Clegg, W. *Org. Lett.* **2007**, *9*, 4925.

[55] Cahn, R. S.; Ingold, C.; Prelog, V. *Angew. Chem. Int. Ed. Engl.* **1966**, *5*, 385.

[56] Tanaka, K.; Kamisawa, A.; Suda, T.; Noguchi, K.; Hirano, M. *J. Am. Chem. Soc.* **2007**, *129*, 12078.

[57] Tanaka, K.; Fukawa, N.; Suda, T.; Noguchi, K. *Angew. Chem. Int. Ed.* **2009**, *48*, 5470.

[58] Fukawa, N.; Osaka, T.; Noguchi, K.; Tanaka, K. *Org. Lett.* **2010**, *12*, 1324.

[59] Sawada, Y.; Furumi, S.; Takai, A.; Takeuchi, M.; Noguchi, K.; Tanaka, K. *J. Am. Chem. Soc.* **2012**, *134*, 4080.

[60] a) *Modern Cyclophane Chemistry* (Eds.: R. Gleither, H. Hopf), Wiley, Chichester, UK, **2004**; b) *Cyclophane Chemistry* (Ed.: F. Vögtle), Wiley, Chichester, UK, **1993**.

[61] Tanaka, K.; Sagae, H.; Toyoda, K.; Noguchi, K.; Hirano, M. *J. Am. Chem. Soc.* **2007**, *129*, 1522.

[62] Tanaka, K.; Sagae, H.; Toyoda, K.; Hirano, M. *Tetrahedron* **2008**, *64*, 831.

[63] a) Lu, P.; Ma, S. *Chem. Lett.* **2010**, *39*, 78; b) Lu, P.; Ma, S. *Org. Lett.* **2007**, *9*, 5319; c) Ma, S.; Lu, L. *Chem. –Asian J.* **2007**, *2*, 199; d) Jiang, X.; Ma, S. *J. Am. Chem. Soc.* **2007**, *129*, 11600; e) Ma, S.; Lu, P.; Lu, L.; Hou, H.; Wei, J.; He, Q.; Gu, Z.; Jiang, X.; Jin, X. *Angew. Chem. Int. Ed.* **2005**, *44*, 5275.

[64] a) Noucti, N. N.; Alexanian, E. J. *Angew. Chem. Int. Ed.* **2013**, *52*, 8424; b) Brusoe, A. T.; Edwankar, R. V.; Alexanian, E. J. *Org. Lett.* **2012**, *14*, 6096; c) Brusoe, A. T.; Alexanian, E. J. *Angew. Chem. Int. Ed.* **2011**, *50*, 6596.

[65] Miura, T.; Morimoto, M.; Murakami, M. *J. Am. Chem. Soc.* **2010**, *132*, 15836.

[66] Ohno, H.; Mizutani, T.; Kadoh, Y.; Aso, A.; Miyamura, K.; Fujii, N.; Tanaka, T. *J. Org. Chem.* **2007**, *72*, 4378.

[67] a) Crabbé, P., André, D., Fillion H. *Tetrahedreon Lett.* **1979**, *10*, 893; b) Crabbé, P.; Fillion H.; André, D.; Luche, J.-L. *J. Chem. Soc. Chem.Commun.* **1979**, 859; c) Rona, P.; Crabbé, P. *J. Am. Chem. Soc*. **1969**, *91*, 3289.

[68] For our group reports describing the synthesis of **4** and **5**, see reference 44; For the first reports describing these molecules, see: a) Grigg, R.; Scott, R.; Stevenson, P. *J. Chem. Soc. Perkin Trans. 1,* **1988**, 1365; b) Grigg, R.; Scott, R.; Stevenson, P. *J. Chem. Soc., Perkin Trans. 1,* **1988**, 1357.

[69] Brandsma, L. *Synthesis of Acetylenes, Allenes and Cumulenes. Methods and Techniques.* (Ed. Elsevier Ltd), Oxford, UK, **2004**.

[70] González, M.; Rodríguez, R. Á.; Cid, M. M.; López, C. S. *J. Comput. Chem.,* **2012**, *33*, 1236.

[71] Kuang, J.; Ma, S. *J. Org. Chem*. **2009**, *74*, 1763.

[72] Machinek, R.; Luttke, W.; *Synthesis* **1975**, *4*, 255.

[73] Sir Geoffrey Wilkinson and Ernst Otto Fischer received the Nobel Prize in Chemistry in 1973 for their pioneering work on the chemistry of organometallic sandwich compounds.

[74] For examples of axial chirality, see: a) Sakiyama, N.; Hojo, D.; Noguchi, K.; Tanaka, K. *Chem. Eur. J*. **2011**, *17*, 1428; b) Ogaki, S.; Shibata, Y.; Noguchi, K.; Tanaka, K. *J. Org. Chem*. **2011**, *76*, 1926; c) Nishida, G.; Ogaki, S.; Yusa, Y.; Yokozawa, T.; Noguchi, K.; Tanaka, K. *Org. Lett.* **2008**, *10*, 2849; d) Suda, T.; Noguchi, K.; Hirano, M.; Tanaka, K. *Chem Eur. J.* **2008**, *14,* 6593; e) Tanaka, K.; Suda, T.; Noguchi, K.; Hirano, M. *J. Org. Chem.* **2007**, *72*, 2243.

[75] For examples of other types of chirality, see: a) Tanaka, K.; Sagae, H.; Toyoda, K.; Hirano, M. *Tetrahedron* **2008**, *64*, 831; b) Nishida, G.; Noguchi, K.; Hirano, M.; Tanaka, K. *Angew. Chem. Int. Ed*. **2008,** *47,* 3410; c) Tanaka, K.; Sagae, H.; Toyoda, K.; Noguchi, K.; Hirano, M. *J. Am. Chem. Soc*. **2007**, *129*, 1522; d) Tanaka, K.; Osaka, T.; Noguchi, K.; Hirano, M. *Org. Lett.,* **2007**, *9*, 1307; e) Tanaka, K.; Wada, A.; Noguchi, K. *Org. Lett.* **2006**, *8*, 907; f) Tanaka, K.; Suzuki, N.; Nishida, G. *Eur. J. Org. Chem.* **2006**, 3917.

[76] a) Kozuch, S.; Shaik, S. *J. Am. Chem. Soc.* **2006**, *128*, 3855; b) Kozuch, S.; Shaik, S. *J. Phys. Chem. A.* **2008**, *112*, 6032; c) Kozuch, S.; Shaik, S. *Acc. Chem. Res.* **2011**, *44*, 101.

[77] Campolo, D.; Gastaldi, S.; Roussel, C.; Bertrand, M. P.; Nechab, M. *Chem. Soc. Rev.* **2013**, *42*, 8434.

[78] Fischer, F.; Jungk, P.; Weding, N.; Spannenberg, A.; Ott, H.; Hapke, M. *Eur. J. Org. Chem.* **2012**, *29*, 5828.

[79] Mori, A.; Araki, T.; Miyauchi, Y.; Noguchi, K.; Tanaka, K. *Eur. J. Org. Chem.* **2013**, 6774.

[80] a) Stará, I. G.; Alexandrová, Z.; Teplý, F.; Sehnal, P.; Starý, I.; Šaman, D.; Budešínský, M.; Cvacka, J. *Org. Lett*. **2005**, *13*, 2547. b) Starý, I.; Stará, I. G.; Alexandrová, Z.; Sehnal, P.; Teplý, F.; Šaman, D.; Rulíšek, L. *Pure Appl. Chem*. **2006**, *78*, 495. c) Sehnal, P.; Krausová, Z.; Teplý, F.; Stará, I. G.; Starý, I.; Rulíšek, L.; Šaman, D.; Císařová, I. *J. Org. Chem.* **2008**, *73*, 2074. d) Sehnal, P.; Stará, I. G.; Šaman, D.; Tychý, M.; Mísek, J.; Cvacka, J.; Rulíšek, L.; Chocholoušová, J.; Vacek, J.; Goryl, G.; Szymonski, M.; Císařová, I.; Starý, I. *Proc. Natl. Acad. Sci.* **2009**, *106*, 13169. e) Žádný, J.; Jančařík, A.; Andronova, A.; Šámal, M.; Chocholoušová, J.; Vacek, J.; Pohl, R.; Šaman, D.; Císařová, I.; Stará, I. G.; Starý, I. *Angew. Chem. Int. Ed.* **2012**, *51*, 5857.

[81] Crittall, M. R.; Fairhurst N. W. G.; Carbery, D. R. *Chem.Comm*. **2012**, *48*, 11181.

[82] (*R*)-nona-1,2-dien-4-ol (*R*)-**17** was synthesised in Prof. Jordi Garcia laboratory at the Universitat de Barcelona using a Crabbé homologation from the corresponding acetylenic alcohol which is commercially available both in the racemic and enantiopure forms.

[83] Kumara Swamy, K. C.; Bhuvan Kumar, N. N.; Balaraman, E.; Pavan Kumar, K. V. P. *Chem. Rev*. **2009**, 109, 2551.

[84] The (*S,S*) configuration is referred to the configuration which is transferred from starting material.

[85] The numbering of the positions marked for structure **I** is maintained in all possible stereoisomers on the chapter 4 but the numbering in labels and structures are removed for the clarity.

[86] Huntsman, W. D. *Rearrangements Involving Allenes, in Ketenes, Allenes and Related Compounds: Volume 2*, **1980** (ed S. Patai), John Wiley & Sons, Ltd., Chichester, UK.

[87] Okuda, K.; Zhang, Y-X.; Hirota, T.; Sasaki, K. *J. Heterocyclic Chem.* **2012**, *49*, 755.

[88] Koelsch, C. F. *J. Am. Chem. Soc.* **1943**, *65*, 2458.

[89] Bennecer, B.; Fujiwara, M.; Lee, S. Y.; Ojima, I. *J. Am. Chem. Soc.* **2005**, *127*, 17756.

[90] Iafe, R. G.; Kuo, J. L.; Hochstatter, D. G.; Saga, T.; Turner, J. W.; Merlic, C. A. *Org. Lett.* **2013**, *15*, 582.

[91] Nicolaus, N.; Strauss, S.; Neudörfl, J.-M.; Prokop, A.; Schmalz, H.-G. *Org. Lett.* **2009**, *11*, 341.

[92] Reissert, A. *Berichte,* **1893**, *26*, 2137.

[93] a) Giacomello, G.; Gualteri, F.; Ricceri, F. M.; Stein, M. L. *Tetrahedron Lett*. **1965**, 1117; b) Tan, R.; Taurins, A. *Tetrahedron Lett.* **1965**, 2737.

[94] a) Egbertson, M. S.; Wai, J. S.; Cameron, M.; Hoerrner, R. S. *Discovery of MK-0536: A Potential Second-Generation HIV-1 Integrase Strand Transfer Inhibitor with a High Genetic Barrier to Mutation, in Antiviral Drugs: From Basic Discovery through Clinical Trials* (Ed.: Kazmierski, W. M.), **2011**, John Wiley & Sons, Inc., Hoboken, NJ, USA; b) Métifiot, M.; Johnson, B.; Smith, S.; Zhao, X. Z.; Marchand, C.; Burke, T.; Hughes, S.; Pommier, Y. *Antimicrob. Agents Chemother.* **2011**, *55*, 5127.

[95] For selected examples, see: a) Pierre, F.; Chua, P. C.; O'Brien, S. E.; Siddiqui-Jain, A.; Bourbon, P.; Haddach, M.; Michaux, J.; Nagasawa, J.; Schwaebe, M. K.; Stefan, E.; Vialettes, A.; Whitten, J. P.; Chen, T.

K.; Darjania, L.; Stansfield, R.; Anderes, K.; Bliesath, J., Drygin, D.; Ho, C.; Omori, M.; Proffitt, C.; Streiner, N.; Trent, K.; Rice, W. G.; Ryckman, D. M. *J. Med. Chem.* **2011**, *54*, 635; b) van Eis, M. J.; Evenou, J.-P.; Floersheim, P.; Gaul, C.; Cowan-Jacob, S. W.; Monovich, L.; Rummel, G.; Schuler, W.; Stark, W.; Strauss, A.; von Matt, A.; Vangrevelinghe, E.; Wagner, J.; Soldermann, N. *Bioorg. Med. Chem. Lett.* **2011**, *21*, 7367.

[96] a) Litvinov, V. P. *Adv. Heterocycl. Chem*. **2006**, *91*, 189; b) Litvinov, V. P.; Roman, S. V.; Dyachenko, V. D. *Russ. Chem. Rev.* **2000**, *69*, 201.

[97] Rajamanickam, P.; Shanmugam, P. *Synthesis* **1985**, 541.

[98] Br. Pat. 2299582, *Ref. Zh. Khim*, 12 (O), 64 (P), **1997**.

[99] Ibrahim, N. S.; Sadek, K. U.; Aziz, S. I.; Elnagdi, M. H. *Naturforsch. B. Chem. Sci*. **1985**, *40*, 129.

[100] For a monography about Microwave-Assisted Organic Synthesis see: a) *Microwave-Assisted Organic Synthesis*; Lidström, P.; Tierney, J. P. Eds.; Blackwell Scientific: Oxford, **2004**. For reviews, see: b) Kappe, C. O.; Dallinger, D. *Nature Rev.* **2006**, 5, 51; c) de la Hoz, A.; Díaz-Ortiz, A.; Moreno, A. *Chem. Soc. Rev.* **2005**, 34, 164; d) Kappe, C. O. *Angew. Chem. Int. Ed.* **2004**, 43, 6250.

[101] For selected references, see: a) Lalic, G.; Corey, E.J. *Tetrahedron Lett.* **2008**, *49*, 4894; b) Tanaka, K.; Ajiki, K. *Org. Lett.* **2005**, *7*, 1537; c) Musolino, M. G.; Apa, G.; Donato, A.; Pietropaolo, R. *Catalysis Today* **2005**, *100*, 467; d) Itooka, R.; Iguchi, Y.; Miyaura, N. *J. Org. Chem.* **2008**, *68*, 6000; e) Ikeda, S.; Watanabe, H.; Sato, Y. *J. Org. Chem.* **1998**, *63*, 7026.

[102] Declerck, V.; Allouchi, H.; Martinez, J.; Lamaty, F. *J. Org. Chem*. **2007**, *72*, 1518.

[103] Garcia, P.; Evanno, Y.; George, P.; Sevrin, M.; Ricci, G.; Malacria, M.; Aubert, C.; Gandon, V. *Org. Lett.* **2011**, *13*, 2030-2033.

[104] Qi, C.; Cong, H.; Cahill, K. J.; Müller, P.; Johnson, R. P.; Porco Jr., J. A. *Angew. Chem. Int. Ed.* **2013**, *52*, 8345.

[105] Ohashi, M.; Takeda, I.; Ikawa, M.; Ogoshi, S. *J. Am. Chem. Soc.* **2011**, *133*,18018.

[106] Stang, E. M.; White, M. C. *J. Am. Chem. Soc.* **2011**, *133*, 14892.

[107] Otani, S.; Saito, T.; Sakamoto, R.; Osada, H.; Hirahara, A.; Furukawa, N.; Kutsumura, N.; Matsuo, T.; Tamao, K. *Chem. Commun.* **2013**, *49*, 6206.

[108] Ozawa, T.; Kurahashi, T.; Matsubara, S. *Org. Lett.* **2011**, *13*, 5390.

[109] Kocsis, L. S.; Benedetti, E.; Brummond, K. M. *Org. Lett.* **2012**, *14*, 4430.

[110] Deng, J.; Tabei, J; Shiotsuki, M.; Sanda, F.; Matsuda, T. *Macromolecules* **2004**, *37*, 5538.